

Alma Mater Studiorum – Università di Bologna

DOTTORATO DI RICERCA IN

Scienze Farmaceutiche

Ciclo XXV

Settore Concorsuale di afferenza: 03/D1

Settore Scientifico disciplinare: CHIM/08

**DESIGN AND SYNTHESIS OF MULTIPOTENT DRUGS:
APPLICATION TO ALZHEIMER'S DISEASE AND BENIGN PROSTATIC
HYPERPLASIA**

Presentata da: Valentina Maestri

Coordinatore Dottorato

Relatore

Prof.- Maurizio Recanatini

Prof. Carlo Melchiorre

Esame finale anno 2013

Our greatest weakness is giving up.
The most certain way to succeed is always to try just one more time
-Thomas Edison-

During my PhD, I was involved in three different projects. The first and the second one concern the design and synthesis of potential drugs for the treatment of two diseases involving elderly people such as Alzheimer's disease (**Chapter 1**) and benign prostatic hyperplasia (**Chapter 2**). They have been developed at the Department of Pharmacy and Biotechnology in Bologna under the supervision of Prof. C. Melchiorre.

Chapter 3 treats the development of new isocyanide multicomponent reactions. The research project was developed at the University College of London (UCL) under the supervision of Dr. T. Sheppard during my second year of PhD.

OUTLINES OF THE THESIS

Chapter 1	Synthesis and biological evaluation of memoquin analogs as potential muscarinic M ₁ receptor allosteric modulators: a challenge for the treatment of Alzheimer's disease.....	7
Chapter 2	Design and synthesis of quinazoline derivatives as novel and multipotent drugs for the treatment of benign prostatic hyperplasia (BPH)	132
Chapter 3	Development of new isocyanide multicomponent reactions	183
Acknowledgements	252
References	253

Abbreviations

5 α -DHT: 5 α -dihydrotestosterone

5 α -R: 5 α -reductase

5-HT: 5-hydroxytryptamine or serotonin

α_1 -AR: α_1 -adrenoreceptor

A β : amyloid- β peptide

A β 40: amyloid- β peptide constituted by 40 aminoacids.

A β 42: amyloid- β peptide constituted by 42 aminoacids.

ACh: acetylcholine

AChE: acetylcholinesterase

AD: Alzheimer's disease

ADAM: A disintegrin and metalloprotease

AChEI: AChE inhibitor

APOE4: apolipoprotein E 4

APP: amyloid precursor protein

α -APPs: α -APP soluble fragment

β -APPs: β -APP soluble fragment

BACE: β -secretase

BBB: blood–brain barrier

BuChE: butyrylcholinesterase

BPH: benign prostatic hyperplasia

CCh: carbachol

ChAT: choline acetyltransferase

CHO: Chinese hamster ovary

CNS: central nervous system

CoQ10: coenzyme Q10

CQ: clioquinol

DAG: diacylglycerol

DCE: dichloroethane

DCM: dichloromethane

DHP: dihydropyridine

DS: Down syndrome

DR6: death receptor 6

ETC: electron transport chain
FAD: early-onset Alzheimer's disease
GABA: γ -aminobutyric acid
GPCRs: G protein-coupled receptors
GSK3 β : glycogen synthase kinase 3 β
KGDHC: α -ketoglutarate–dehydrogenase complex
KPI: Kunitz-type protease inhibitor domain
[³H]NMS= [³H]-N-methyl scopolamine
IMCR: isocyanide-based multicomponent reactions
IP3: inositol trisphosphate
LUTS= lower urinary tract symptoms
mAChR: muscarinic acetylcholine receptor
MAPK: mitogen-activated protein kinase
MAO: monoamine oxidase
MAOI: monoamine oxidase inhibitor
MCR: multicomponent reaction
MTDL: multitarget-directed ligand
nAChR: nicotinic acetylcholine receptor
NFTs neurofibrillary tangles
NMDAR: N-methyl D-aspartate receptor
NSAID: Non-steroidal anti-inflammatory drug
NOS: nitric oxide synthase
NQO1: NAD(P)H:quinone oxidoreductase 1
OXO-M: oxotremorine
OXPHOS: oxidative phosphorylation
P-3CR: Passerini three-component reaction
PAM: positive allosteric modulator
PAS: peripheral anionic site
PDHC: pyruvate–dehydrogenase complex
PI3K: phosphatidyl inositol 3-kinase
PKC: protein kinase C
PLC: phospholipase C
PS: presenilin
ROS: reactive oxygen species

SAR: structure activity relationship

TGF- β : transforming growth factor- β

TOSMIC: tosylmethyl isocyanides

TURP: transurethral resection of the prostate

U-4CR: Ugi four-component reaction

vL-3CR: van Leusen multicomponent reaction

Chapter 1

SYNTHESIS AND BIOLOGICAL EVALUATION OF MEMOQUIN ANALOGS AS POTENTIAL MUSCARINIC M₁ RECEPTOR ALLOSTERIC MODULATORS: A CHALLENGE FOR THE TREATMENT OF ALZHEIMER'S DISEASE

OUTLINES

Chapter 1	7
1 Introduction.....	9
1.1 Amyloidogenesis	9
1.1.1 Proteolytic processing of APP.....	10
1.1.2 α -secretase	14
1.1.3 β -secretase	15
1.1.4 γ -secretase	17
1.2 Neurofibrillar tangles and tau	21
1.3 The cholinergic hypothesis.....	25
1.3.1 Acetylcholinesterase.....	27
1.4 Role of ApoE	29
1.5 The role of metallobiology in AD	32
1.5.1 Metals in AD	33
1.5.2 A β binding to metals	34
1.5.3 Metal homeostatic therapy	35
1.6 Role of oxidative stress in AD.....	36
1.6.1 Contribution of ROS	37
1.6.2 Mitochondrial dysfunction	38
1.7 Inflammation and AD.....	41
1.8 The glutamatergic hypothesis.....	42
1.8.1 Memantine: a NMDA receptor uncompetitive fast off-rate inhibitor.....	46

1.9	The role of G protein-coupled receptors in AD.....	48
1.9.1	Metabotropic glutamate receptors.....	48
1.9.2	5-Hydroxytryptamine receptors.....	50
1.9.3	β_2 -adrenergic receptors.....	51
1.9.4	Adenosine A _{2A} receptors.....	51
1.9.5	M ₁ muscarinic receptors.....	52
1.10	Multitarget-Directed-Ligand approach for the treatment of Alzheimer's disease.	67
1.10.1	Dual binding site AChE inhibitors.....	68
1.10.2	AChEIs Targeting Other Neurotransmitter Systems.....	71
1.10.3	AChEIs with Antioxidant Properties.....	75
1.10.4	Development of Memoquin.....	76
2	Aim of the project.....	78
3	Chemistry.....	84
4	Results and Discussion.....	93
4.1	Compounds 1-11.....	93
4.2	Compounds 12 and 13.....	109
4.3	Compounds 14-17.....	110
5	Conclusions and Future Works.....	111
6	Experimental section.....	113
6.1	Chemistry.....	113
6.2	Biology.....	129

1 Introduction

Alzheimer's disease (AD) is an irreversible, multi-factorial neurodegenerative disorder that occurs gradually, and results in memory loss, unusual behaviour, personality changes, and decline in thinking abilities. It constitutes the most common and fatal form of dementia in adults.¹ Therefore, the incidence of AD is expected to double every 20 years and it is predicted that over 100 million individuals will have AD in 2050.² AD is named from Dr. Alois Alzheimer,³ a German doctor who in 1907 noticed changes in the brain tissue of a woman who had died of an unusual mental illness. He observed post mortem two characteristic pathological features: amyloid plaques and neurofibrillary tangles (NFTs) in the cerebral cortex and limbic system.

So far, the main neuropathological hallmarks of AD are identified as: diffusive loss of neurons, dysfunctional cholinergic system, intracellular protein deposits termed NFTs consisting of hyperphosphorylated tau protein and extracellular protein deposits termed amyloid or senile plaques.^{4, 5, 6} AD exists in a genetically determined form, known as the familial form (with an autosomal dominant character), and a sporadic form.

Disease-modifying drugs are not available yet because the nature and the exact role of biological molecules involved in AD physiopathology are not clearly understood. Thus, the elucidation of the molecular mechanisms, which cause AD, would greatly help the design of drugs able to interfere with neurotoxic processes. In this section the main molecular mechanisms that cause AD are reviewed.

1.1 Amyloidogenesis

According to this hypothesis, neuronal degeneration in the brain of AD patients is the direct consequence of amyloid β -peptide ($A\beta$) hyperproduction.⁷ This causes the formation of amyloid plaques which consequently induces dendrite and axon retraction and neuronal death.⁸ The peptide $A\beta$ is derived from the amyloid precursor protein (APP).⁹ The APP gene is localized on chromosome 21 which is triplicated in trisomy 21 Down syndrome (DS). In fact, most patients who have DS manifest also AD by the age of 50. Post-mortem analysis of their brains showed diffusive intraneuronal deposits of $A\beta$ ¹⁰ in the absence of any tau pathology, suggesting that $A\beta$ deposition might be the primary cause of a feed-forward cycle, which results in AD.

1.1.1 Proteolytic processing of APP

APP is a 770 residue transmembrane glycoprotein possessing a large extracellular amino-terminal domain and a small intracellular cytoplasmic domain. It is expressed not only in the brain but also throughout the body.¹¹ APP is processed post-translationally by glycosylation and proteolytic cleavage producing different isoforms in specific tissue types.^{12, 13} There are several APP isoforms arising from the alternative splicing of its pre-mRNA and ranging from 365 to 770 aminoacids residue. The most important isoforms are those with 695, 751 and 770 aminoacids residue. The most important isoforms are those with 695, 751 and 770 aminoacids residue (referred to as APP695, APP751 and APP770). APP695 isoform is predominately expressed in the central nervous system (CNS).¹⁴ Different subdomains can be identified in the extracellular sequence of APP, based on its primary sequences and structural studies (**Fig 1**).^{15, 16} These include the E1 domain, which consists of the N-terminal growth factor like domain and the metal (copper and zinc) binding motif, the Kunitz-type protease inhibitor (KPI) domain present in APP751 and APP770 isoforms, the E2 domain which include the sequence that promotes fibroblast growth and the extracellular binding sites for heparin, collagen, and laminin. The biological properties of APP have been extensively studied since its identification nearly 20 years ago. It demonstrates a number of interesting putative physiological roles. In fact, it seems to participate in synaptic formation and repair,¹⁷ in adhesion, intercellular communication and membrane-to-nucleus signaling.¹⁸

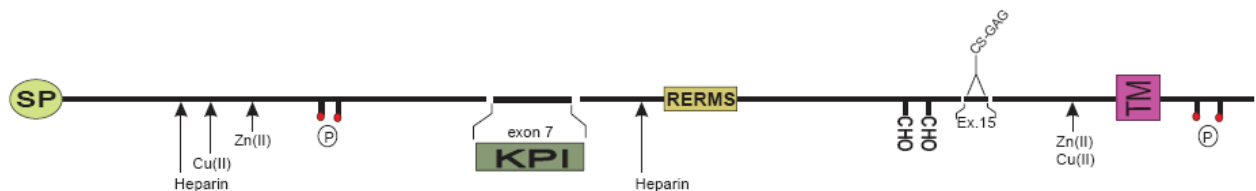


Figure 1: Domain structure of APP695. SP: signal peptide; TM: transmembrane peptide; KPI: Kunitz-type protease inhibitor; P: phosphorylation sites; CHO: glycosylation sites; RERMS: sequence that promotes fibroblast growth.¹⁹

The production of A β is dependent upon the activities of two proteases: β -secretase (BACE) and γ -secretase.²⁰ The cleavage of APP can follow an amyloidogenic or a nonamyloidogenic pathway (**Fig. 2**). The first one starts by α -secretase, the second by β -secretase; two different proteases which cleave at different position within APP molecule leading to the release of the large soluble N-terminal fragments α -APPs and β -APPs, respectively. Cleavage by α -secretase occurs within the region containing A β (between Lys₁₆ and Leu₁₇), precluding A β formation. α -APPs has been suggested to exhibit neuroprotective and synapse-promoting activities,²¹ but the exact mechanism or the receptor mediating these effects have not been identified yet. On the

other hand, β -APPs is further processed by an unknown protease, producing a 35-kDa amino-terminal domain fragment that binds to the death receptor DR6. This interaction to DR6 triggers activation of caspase-6 and mediates axonal pruning during embryogenesis.²²

Two C-terminal fragments C83 and C99 are also produced by α -secretase and BACE respectively. Both C83 and C99 can be further cleaved by γ -secretase, within the APP transmembrane domain which leads to the formation of A β from C99 and of p3, a shorter, presumably non pathogenic A β from C83. The release of the free N-terminus of A β is therefore considered the first critical step in amyloid formation.²³ The majority of secreted A β peptides are constituted by 40 aminoacids in length (A β 40), although the longer species, 42 aminoacids in length (A β 42), have received greater attention due to its propensity to nucleate and produce insoluble β sheets that are neurotoxic.²⁴

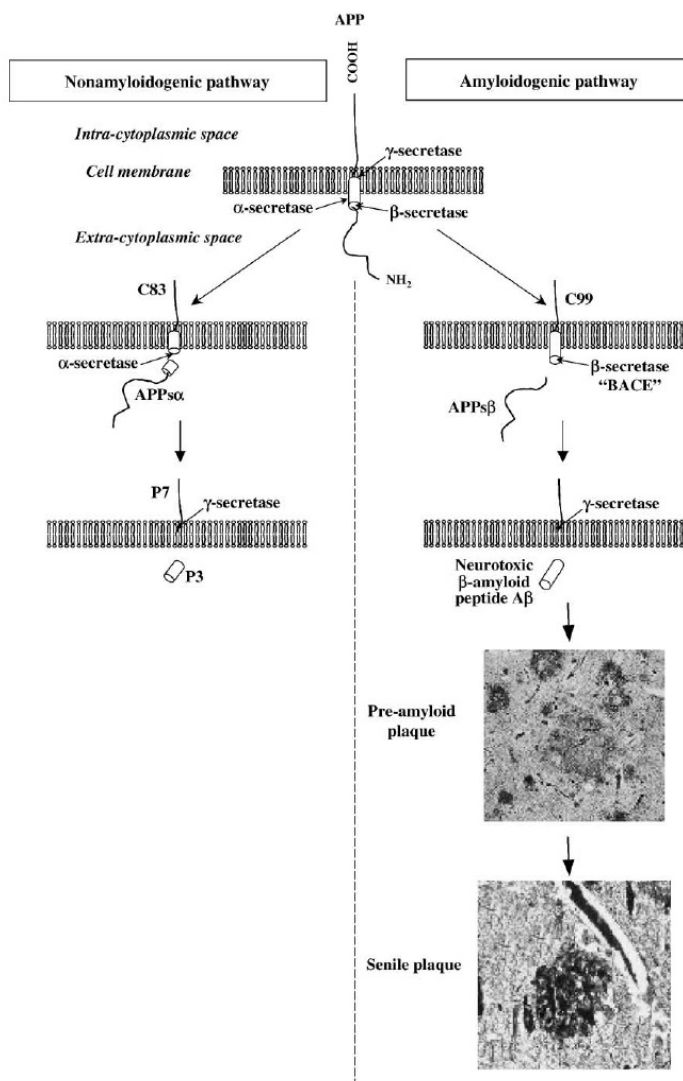


Figure 2: Schematic description of the amyloidogenic and nonamyloidogenic pathways of APP cleavage.²⁵

Amyloids from AD and in other degenerative disorders, may share a common pathway for fibrils formation and accumulation in plaques. The initiating event is protein misfolding or denaturation, which results in the acquisition of the ability to aggregate in an infinitely propagating way.²⁶ In AD, A β monomers can aggregate into oligomeric assemblies or soluble spherical aggregates of approximately 3-10 nm (**Fig. 3**). Small nuclei of such aggregates can induce protofibril and amyloid fibril formation. Amyloid fibrils have a “cross β ” structure. It is a double β -sheet, with each sheet formed from parallel segments, stacked in-register.^{27, 28} This structural motif of amyloid fibrils is not commonly present in native protein structure and the formation of protein aggregates is related to the onset and/or progression of the disease. A β -induced neurodegeneration appears to result, at least in part, from the activation of apoptotic pathways,^{29, 30} including caspases^{31, 32, 33} and Jun N-terminal kinase³⁴ which consequently induce neuronal death.

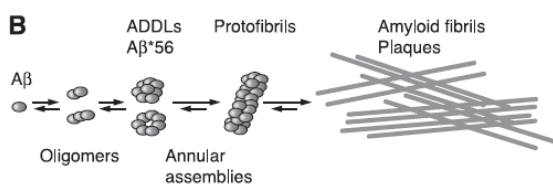


Figure 3: Pathway of amyloid fibril formation.³⁵

However, a body of evidence suggests that soluble amyloid oligomers may primary be involved in the mechanism of pathogenesis. Indeed, it is shown that amyloid oligomers can form pores or channels in cell membranes increasing permeability and intracellular calcium concentration.^{36, 37} The increase of Ca⁺² may be the initiator of many pathogenic pathways; reactive oxygen species (ROS) production,³⁸ altered signalling pathway,^{39, 40} mitochondrial dysfunction⁴¹ and cell death⁴² (**Fig. 4**). The accumulation of autophagosomes and autolysosomes has been recognized as a common component of AD and other neurodegenerative disorders.⁴³ The up-regulations of these defensive mechanisms may be a protective response to the enhanced A β deposition. The fact that amyloid aggregates and autophagics vesicles continue to accumulate suggests that this response is not entirely successful. The failure to clear amyloid plaques may also contribute to pathogenesis and neuronal loss.⁴⁴

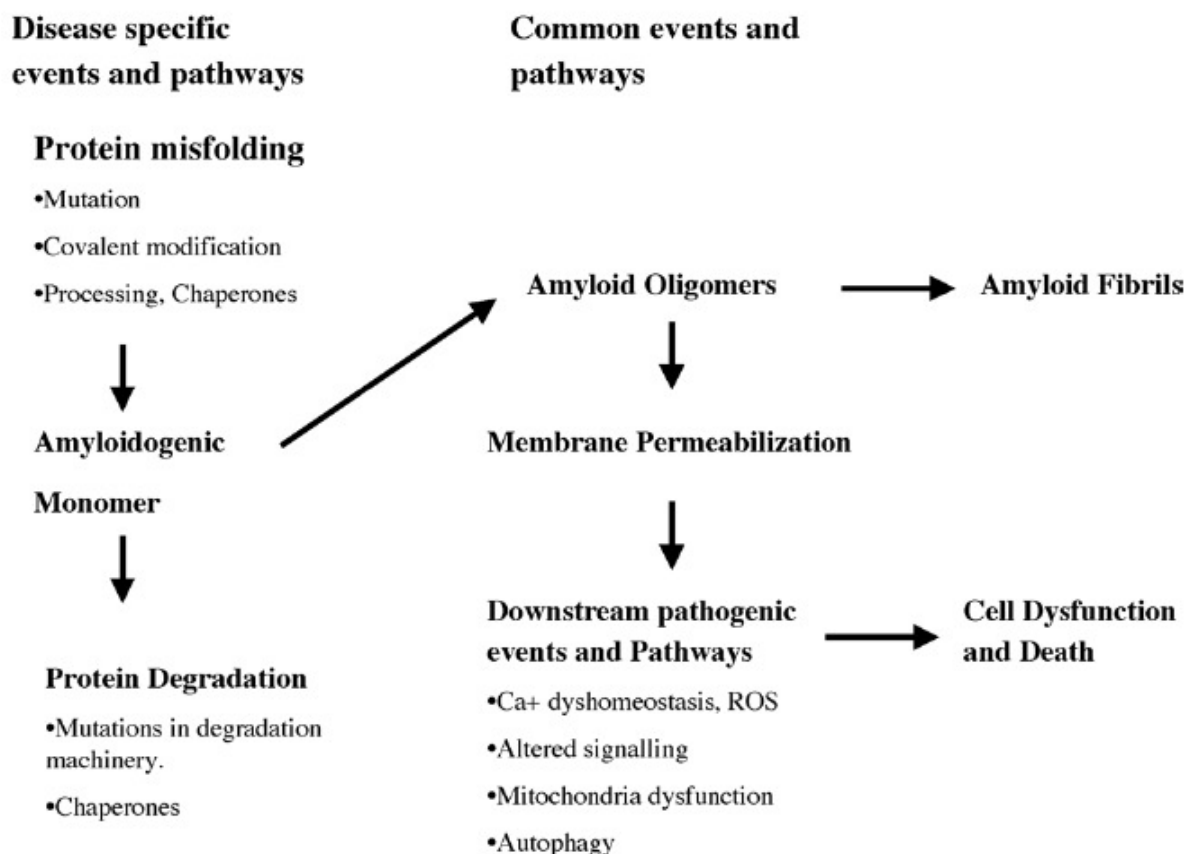


Figure 4: Common and disease-specific pathways in degenerative diseases.⁴⁵

Although the neurotoxic properties of A β have been described for over a decade,⁴⁶ it is still not known how A β participates in a pathologic cascade that causes progressive cognitive decline. It is also not well-known if A β , which is detected in both cerebrospinal fluid and plasma in healthy individuals,⁴⁷ is fundamental in normal physiology. Initially, it was believed that the cleavage of APP by BACE was pathological, while the cleavage by α -secretase was physiological. In reality, β - and γ -secretase processing of APP also occurs under physiological conditions. This suggests that all fragments of APP, including the A β peptide, are essential for normal physiology.^{48, 49} Interestingly, deficiencies for presenilin 1 and especially presenilins 1 and 2 (catalytic subunits of γ -secretase, see 1.1.4) abolished γ -secretase activity causing disastrous effects in many tissues, leading to prenatal death of the embryos in all animals investigated so far.^{50, 51} Similar data were shown for the α -secretase isoforms ADAM 10 and ADAM 17/TACE (see 1.1.2). Indeed, ADAM17/TACE null mice or mice carrying mutation inactivating the active site of the enzyme die during late fetal period with hypoplastic lungs and defective development of eyes and skin.⁵²

These data clearly suggest that α - and γ -secretase have other functions apart from APP processing.

The abnormal processing of APP by α -, β -, and γ -secretase is a key step in AD pathogenesis.⁵³ More than 30 mutations in APP gene have been identified which affect the production and/or aggregation of the A β peptide. These missense mutations were found in patients with early-onset AD (FAD), i.e. familial cases with Mendelian inheritance. They account for about 0.5% of all AD cases. In particular, the cleavage of APP770 is facilitated by the mutations **K670M671**→**N670L671** near the BACE cleavage site.⁵⁵ These mutations are referred to as the “Swedish mutations” and they leads to an increase of BACE cleavage and a 6-7 fold A β peptide production, and a decrease of the α -secretase product p3.⁵⁶ Other FAD mutations have been identified near the γ -secretase site, and these increase the generation of the more toxic A β 42.⁵⁷ Moreover, FAD mutations near the α -secretase site appear to reduce the efficiency of α -secretase activity, thus providing more APP substrate for BACE cleavage, increasing the production of A β .

1.1.2 α -secretase

α -secretase is a membrane-bound metalloprotease involved in the non-amyloidogenic pathway of APP processing. It cleaves APP between Lys₁₆ and Leu₁₇ in the A β sequence and the subsequent membrane-bound carboxy-terminal fragment (C83) is further processed by γ -secretase leading to the p3 fragment. Very little is known about the toxicity or functions of these p3 fragments. However, evidence suggests that α -secretase-mediated cleavage of APP is the nonamyloidogenic pathway and it is thought that increasing α -secretase activity could be beneficial in AD. Stimulation of α -secretase can be accomplished by the activation of protein kinase C (PKC), which can be stimulated by M₁ and M₃ muscarinic receptors agonist, and such agents are considered reasonable candidates for AD therapy.⁵⁸

Many members of the “A disintegrin and metalloprotease” or ADAM family have been implicated as α -secretase. The most important are ADAM10 and ADAM17/TACE. ADAM10 is the major constitutive α -secretase in many cell types. Overexpression of ADAM10 in the brain lowers the number of A β plaques and leads to an improvement of cognitive performance in mouse AD model.⁵⁹ ADAM 17 is another α -secretase expressed in neuronal cells. It has also a crucial role in the release of a series of membrane-bound proteins, such as transforming growth factor- α and tumor necrosis factor- α .⁶⁰

1.1.3 β -secretase

Human β -secretase or BACE (for beta-site APP-cleaving enzymes) is a type I integral membrane aspartic protease. It is also known as Asp2 (for novel aspartic protease 2) and memapsin2 (for membrane aspartic protease/pepsin 2). BACE catalyzes the internal cleavage of APP at Asp₁ residue of the A β sequence, producing a secreted ectodomain of APP, called β -APPs and the C99 fragment, the membrane bound C-terminal 99 amino acids that is the substrate of γ -secretase. Two β -secretases were identified: BACE-1 and BACE-2. BACE-1 is the major β -secretase. It has a rather broad tissue distribution, but it is enriched in brain and in neuronal cells, consistent with the finding that A β is normally produced and released in patients with AD and in normal individuals.^{61, 62} BACE hydrolyzes APP specifically at the Met-Asp site and an acidic pH is optimum for its activity. The gene that encodes for BACE is located on chromosome 11, but no AD-causing mutation in this gene has been identified yet.

This protease was identified in 1999^{63, 64, 65} and in 2000 its crystal structure was obtained in a peptide mimetic inhibitor complex (**Fig. 5**).⁶⁶

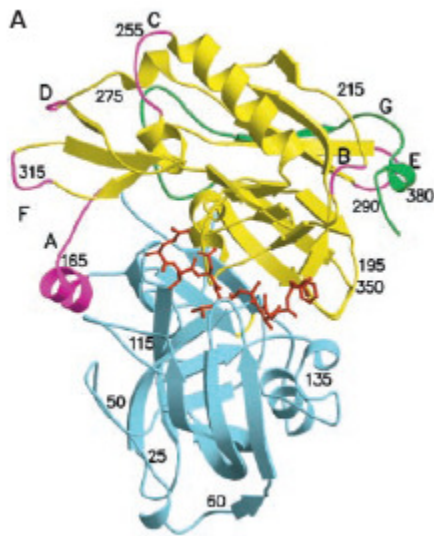


Figure 5: The crystal structure of memapsin 2 complexed to inhibitor OM99-2. The N-lobe and C-lobe are blue and yellow, respectively. The inhibitor bound between the lobes is shown in red.⁶⁶

Hussain et al. showed that transfection of BACE-1 in cells expressing APP, causes an increase in secretion of β -secretase-derived fragments. Mutation of either of the putative catalytic aspartyl residues (Asp₉₃ and Asp₂₈₉) abrogates its activity. On the other hand, genetic inactivation of BACE-1 causes a decrease in A β deposition in different APP-overexpressing mouse AD models.^{67, 68, 69, 70}

Several publications have documented increased BACE-1 protein and activity in the brain of AD patients. In fact, BACE-1 expression is under a complex regulation. It is affected by many stress factors associated with neurodegenerative disease such as oxidative stress,⁷¹ ischemia,⁷² hypoxia⁷³ and traumatic brain injury.⁷⁴ The human BACE-1 promoter contains binding sites for several putative transcription factors like for example the nuclear factor κ B (NF- κ B).⁷⁵ The activation of this transcription factor is associated with chronic stress and inflammation in macrophages, astrocytes, and microglia in the CNS, where it has been found to mediate different responses to trauma in neurons and glia. Bourne et al.⁷⁶ suggested that NF- κ B acts as an activator of BACE1 transcription in activated astrocytes, a feature present in the AD brain. In the aged and AD brain, NF- κ B transcription factor-mediated responses to stress are attenuated,^{77, 78} and there is an increase of NF- κ B activity⁷⁹ which may be a significant contributor to increase A β levels.

Soon after the discovery of BACE-1, an homologous novel aspartic protease was discovered, BACE-2.^{80, 81} BACE-1 and BACE-2 share ~64% amino acid similarity, and both have two aspartic protease residues, six conserved luminal cysteine residues, a C-terminal transmembrane domain and other similar structural characteristics. The high degree of similarity between BACE-1 and BACE-2 suggests that BACE-2 might also function as β -secretase. BACE-2 gene is localized on chromosome 21 in the DS region. Consequently, a third copy of the BACE-2 gene (and the APP gene) is present in DS and this suggests a potential role of BACE-2 in the FAD syndrome found in DS patients. In fact, cell transfection studies demonstrate that BACE-2 cuts APP at the BACE site⁸² and the Flemish FAD mutation of APP (Ala \rightarrow Gly at position 21 of A β) causes an increase in A β production that is mediated by BACE-2 but not BACE-1.⁸³ Thus, BACE-2 may play an important role in the pathogenesis of Flemish FAD. However, BACE-2 cleaves at two other positions (Phe₁₉ and Phe₂₀) within the A β domain near the α -secretase cleavage site.⁸⁴ Interestingly, BACE-2 may also function like an alternative α -secretase, so that the processing of APP by BACE-2 leads to a reduction of A β production in cells.

BACE is a particularly attractive drug target because it initiates A β formation and is the rate-limiting enzyme for A β production in cells. For example knockout of BACE1 in mice drastically reduces A β production and reduces amyloid plaque and AD symptoms in AD mouse model.^{69, 70}

The advantage of inhibiting BACE-1 instead of γ -secretase is that this does not result in blocking Notch signaling which is fundamental for cell life (see 1.1.4). Several factors must be taken into consideration for the development of new BACE-1 inhibitors. Since its catalytic site is exceptionally long, it is very difficult to develop small compounds targeting BACE-1. The compound should have low molecular weight and high lipophilicity to cross the blood-brain barrier (BBB) and achieve high concentrations in the brain. In addition, since it is not known yet

whether BACE-2 is dispensable *in vivo*, it may be necessary to design BACE-1-selective drug that do not exhibit inhibition of BACE-2 or other aspartic proteases. Because of the high degree of homology between BACE-1 and BACE-2, the design of new BACE-1 selective-drugs could be very difficult.

1.1.4 γ -secretase

γ -secretase is a type I membrane-spanning protein composed by 19 transmembrane domains. It was identified in 1993 as the protease responsible of the cleavage of APP releasing the A β peptide.⁸⁵

Presenilin 1 (PS1) was later identified as the major constituent of its proteolytic activity. The remainder of the γ -secretase activity is mediated by presenilin 2 (PS2), a close homolog of PS1.⁸⁶ PS is an aspartyl protease with eight transmembrane segments.⁸⁷ Two transmembrane aspartates, Asp₂₅₇ and Asp₃₈₅ in TM6 and TM7 respectively, are essential for γ -secretase activity. In fact, mutations of these aminoacids abolished completely its activity. Moreover, γ -secretase activity is diminished in cells derived from PS knockout mice.⁸⁸ This result confirms that PS is the catalytic subunit of γ -secretase.⁸⁹

PS requires the association of three additional subunits: nicastrin, aph-1 and pen-2 to become proteolytically active. The reason(s) why PS requires these proteins for its activity remains unclear. It has been suggested that the single transmembrane domain nicastrin is a “gate-keeper” restricting access of substrates to the catalytic site.⁹⁰ However, up to now less is known about aph-1 and pen-2 functions.

In the human genome, two PS genes (PS1 and PS2) and two aph-1 genes (aph-1a and aph-1b), have been identified. It was shown that either PS1 or PS2 and either aph-1a or aph-1b are incorporated into the mature γ -secretase tetrameric complex. Thus, a minimum of four different γ -secretase complexes may exist with potentially different biological functions.⁹¹

A structure at 12-Å resolution of the complex PS1/Aph1a/Pen2/Nicastrin with cryoelectron microscopy revealed a globular and porous structure with a smooth cytosolic side and a larger irregular extracellular surface (**Fig. 6**).⁹² At the cytosolic side there is a sizable pore that reaches halfway into the membrane region and, at the extracellular space, other two large cavities are present. Cysteine scanning studies demonstrated that the aspartate-containing active site, presumably located within the transmembrane domain, is water accessible.⁹³ Thus it appears that γ -secretase, similar to other intramembrane cleaving proteases, sequesters its substrate from the hydrophobic lipid bilayer of the membrane in a structure that allows entrance of water molecules that are necessary for its hydrolysis activity.

The majority of FAD cases are caused by mutations within the PS genes. More than 150 mutations were identified in the gene for PS1, and only 10 for PS2.⁹⁴ PS2 containing γ -secretase complexes do not have the major role in A β production and, therefore, this is the reason why there are fewer PS2 mutations that lead to FAD.⁹⁵ The effect of PS mutations is represented by a gain of toxic functions of γ -secretase; they shift the preferred site of γ -cleavage from position 40 to 42 of APP, leading to an increase of the more amyloidogenic form of A β in cultured cells and in the brain of transgenic mice.⁹⁶ Given that PS1 and PS2 inactivation completely prevents A β formations, it means that these mutations cause an “incomplete digestion” of APP substrate, generating fewer but longer A β peptides.^{97, 98}

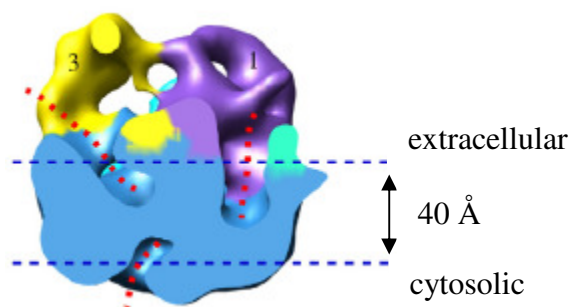


Figure 6: Structure of the complex PS1/Aph1a/Pen2/Nicastrin with cryoelectron microscopy.⁹²

Other proteins that have been shown to be substrates for γ -secretase cleavage include Notch⁹⁹ and the Notch ligands Delta1 and Jagged2,¹⁰⁰ ErbB4,¹⁰¹ CD44,¹⁰² and E-cadherin.¹⁰³ Current data also indicate that two members of the α -secretase family ADAM, i.e. ADAM17/TACE and ADAM 10, may be involved in the cleavage of Notch.^{104, 105, 106}

Notch is a cell-surface receptor that mediates signal transduction between the cell surface and the nucleus. Four Notch genes (Notch 1–4) and five ligands (Jagged 1 and 2; Delta 1, 2 and 3) have been identified in vertebrates.¹⁰⁷ Notch-1 (commonly referred to as Notch) has been widely investigated, while other Notch genes have been studied minimally. Notch proteins contain on the extracellular sequence an epidermal growth factor domain. Activation of Notch by ligand binding causes a proteolytic cleavage at site2 near to the membrane surface¹⁰⁸, creating the ‘Notch Extracellular Truncated’ derivative (NEXT). NEXT is then cleaved by a second protease at site3 within the transmembrane domain near to the inner membrane surface, releasing the intracellular domain, which enters the cell nucleus to modify gene expression (**Fig. 7**).

The site2 cleavage appears to be the key step in the Notch activation and it is regulated by ligand binding. Current data indicate that ADAM17/TACE and ADAM 10 may be involved in this

ligand-regulated cleavage. However, it seems that ADAM17/TACE is the major site2 protease.¹⁰⁸ On the other hand, cleavage of Notch at site3 depends on PS activity. The involvement of the PS in the site3 of Notch receptors has been established from several lines of evidence. In fact, small animals with loss of function in PS genes show a Notch signaling deficient phenotype. For example, mice with PS 1 deficiency display a complex pathological morphology affecting mesoderm segmentation, cardiovascular, and nervous system.^{109, 110} Because of the essential role of γ -secretase in the generation of A β peptides, γ -secretase inhibitors may be useful in the treatment of AD. Many γ -secretase inhibitors have been identified that lower A β production in AD models.¹¹¹ Nevertheless, recent studies showed that inhibition of γ -secretase has the expected benefit of reducing A β , but has undesirable biological effects as well, because of the inhibition of Notch processing.¹¹² For example, blocking Notch signaling in the crypts of the intestinal epithelium induces differentiation into goblet cells and interferes with the normal replacement of the epithelium, explaining the gastrointestinal toxicity of γ -secretase inhibitors.^{113, 114} In addition, immune suppression or autoimmune disorders might be caused by Notch deficiency.^{115, 116}

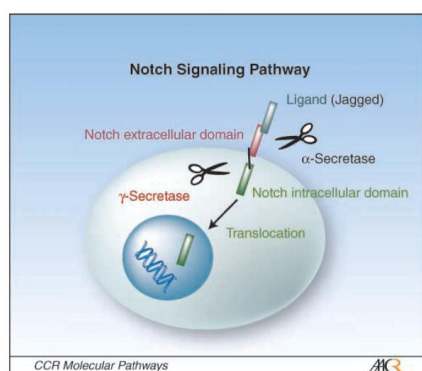


Figure 7: Notch cleavage pathway.¹¹⁷

Several approaches to increase the therapeutic window, i.e., to find compounds that efficiently block A β generation without affecting Notch signaling, have been explored. For example γ -secretase modulators have attracted much attention in the last years because they would shift the production of amyloid peptides in favour of shorter forms of A β . Recent study suggested that A β 40, compared to A β 42, seems to be benign and may even be protective presumably because A β 40 suppresses the deposition of A β 42.¹¹⁸ A subset of non-steroidal anti-inflammatory drugs (NSAIDs), such as ibuprofen, sulindac sulfide and indomethacin, are able to reduce the ratio A β 42/A β 40 without affecting the amount of A β 40 and, most importantly, Notch cleavage.¹¹⁹ The decrease of A β 42 was accompanied by an increase in the production of shorter A β 38 peptides.

The mechanism of action is independent from their anti-inflammatory action but it is not fully understood. It seems that NSAIDs could reduce secretion of A β 42 by shifting γ -secretase activity towards production of A β 38. However, future studies need to be conducted to understand this complex mechanism. Furthermore, Netzer et al.¹²⁰ observed that *in vitro* generation of A β by γ -secretase ATP dependent. In addition, they showed that the tyrosine-kinase inhibitor imatinib mesylate (Gleevec) is able to reduce A β production *in vitro* and *in vivo* without influencing Notch cleavage. Gleevec is a useful drug for chronic myelogenous leukemia. Its activity depends on the interaction with the ATP-binding site of Abl tyrosine-kinase. It does not appear that Abl kinase is required for A β production or for A β inhibition by Gleevec. Because Gleevec targets several other tyrosine-kinases (e.g. ARG, platelet-derived growth factor receptor (PDGFR), Src, c-kit), it is possible that its activity on A β production depends upon inactivation of one of these other enzymes. Indeed, in support to this hypothesis, it has been reported that the activation of PDGFR-Src-Rac1 cascade induces cleavage of APP through activation of β and γ -secretase.¹²¹ Nowadays, masitinib, a tyrosine-kinase inhibitor used in the treatment of mast cell tumors in dogs, is in Phase II clinical trials as potential drug for AD.¹²²

In 2009, G protein-coupled receptors (GPCRs) have been proposed as a target for drugs that selectively block APP processing and do not affect Notch signaling.¹²³ G protein-coupled receptor 3 (GPR3), an active orphan receptor, is constitutively expressed in areas of the normal brain implicated in AD and it is increased in patients with sporadic AD. It seems a regulator of A β production. In fact in AD mice models, overexpression of GPR3 caused an increase of A β 40 and A β 42 without affecting γ -secretase expression, whereas genetic ablation caused a decrease of accumulation of A β peptide. Thus, the expression of GPR3 is involved in assembly of γ -secretase complex affecting APP processing, in the absence of any effect of Notch processing. This finding suggests that GPR3 represents a potential therapeutic target for the treatment of AD.

1.2 Neurofibrillar tangles and tau

Tau is a member of the microtubule associated protein family widely expressed in the brain. Its primary function is to maintain microtubule stability.¹²⁴ This protein contains several phosphorylation sites and in its hyperphosphorylated form is the major component of neurofibrillar tangles (NFTs) found in AD brains. The tau hypothesis argues that in AD, phosphorylation of tau reduces its ability to bind microtubules and indeed, in diseased neurons, tau aggregates into polymers that constitute the intracellular neurofibrillary lesions of AD.^{125, 126, 127} Similar inclusions are found in a number of other neurodegenerative diseases, where they are found in the absence of A β deposits. These diseases include, for example, Pick's disease and Parkinson disease.

The longest version of tau proteins contains 441 aminoacids. Alternative splicing generates six major isoforms in the adult brain. Tau is post-translationally modified by phosphorylation, glycosylation, glycation, ubiquitination and proteolytic processing.¹²⁸ Some researchers support the hypothesis that the dementia symptoms in AD correlate to a greater extent with the gradual appearance and spread of tangles throughout the brain, than with the deposition of A β in senile plaques.^{129, 130}

Tau aggregation is a multistep process which starts with a nucleation step, followed by the progressive addition of tau proteins in an elongation process which induces pretangles, paired helical filaments and finally, neurofibrillar tangles (**Fig. 8**). Tau bound to microtubule (Tau_{MT}) can be displaced into cytoplasm (Tau_{cyt}) by various factors. Mutations,¹³¹ proteolysis or the presence of polyanionic structures^{132, 133, 134} probably play a crucial role in the aggregation of the nuclei and may be, therefore, therapeutic targets.

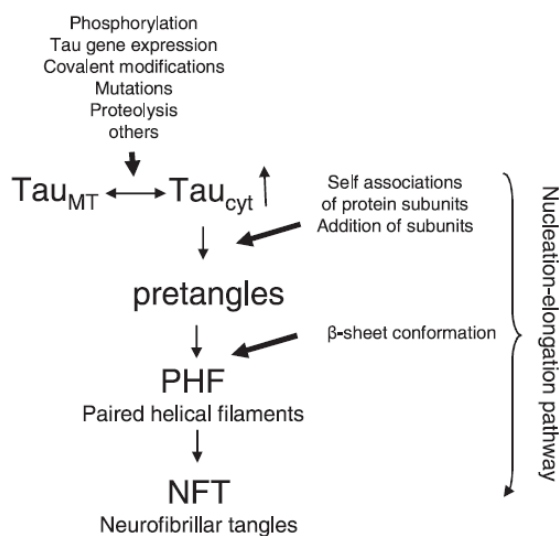


Figure 8: Nucleation-elongation pathway in tangles formation.³⁵

Tau mutations are all clustered in the microtubule-binding region and in the carboxy-terminal part of the protein. The pathway leading from a mutation in tau to neurodegeneration is still unknown. It is supposed that the primary effect of most missense mutations is a change in the conformation of tau that results in a minor ability to interact with microtubules, as reflected by a reduction of mutant tau to promote microtubule assembly.^{135, 136} Thus, microtubules will be destabilized with resultant deleterious effects on cellular processes and rapid axonal transport (Fig. 9).

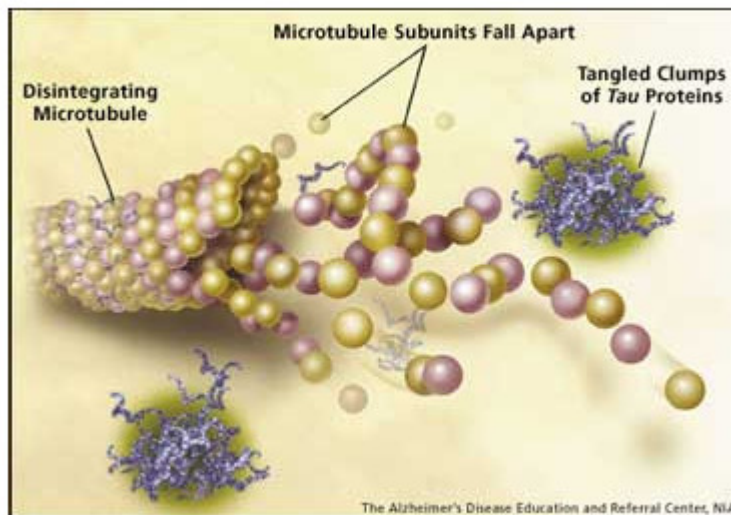


Figure 9: NFTs formation and microtubules disintegration.

The hypothesis that tau proteolysis contributes to tangle formation *in vivo* has been known for a long time.¹³⁷ An important fraction of tau found in the brain of AD patients is truncated at position Glu₃₉₁ and Asp₄₂₁ (numbering referred for the longest form of tau). Removal of the carboxy-terminal part of tau enhances neurofibrillary nucleation *in vitro*.¹³⁸ This indicates that in sporadic AD, truncated tau species might play an important role. Both amino- and carboxy-terminal parts of tau appear to have an inhibitory effect on the aggregation of tau. They fold back in a “hairpin” conformation on the central domain which contains the microtubule-binding portions (R) (Fig. 10).¹³⁹ In repeats R2 and R3 there are two peptide motifs with a high propensity to form β -sheet structures.¹⁴⁰ In fact, a synthetic 4R tau construct, truncated at both the amino and carboxy terminus, showed to have a high tendency to form intracellular tau aggregates.¹⁴¹

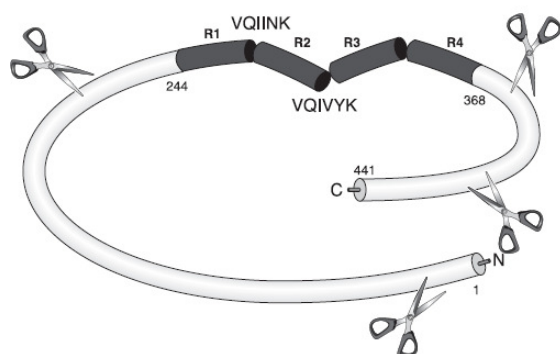


Figure 10: “Hairpin” conformation of tau.³⁵

Tau is phosphorylated by several protein kinases; cyclic AMP-dependent protein kinase (PKA),¹⁴² calmodulin-dependent protein kinase II (CaMKII),¹⁴³ glycogen synthase kinase-3 β (GSK-3 β)^{144, 145, 146} and cyclin-dependent protein kinase 5 (cdk5). Glycogen synthase kinase-3 was discovered over 20 years ago as a regulator of glycogen metabolism.¹⁴⁷ It is a serine–threonine kinase and a well-established component of the *Wnt signalling pathway*, which is essential during embryonic development. It also plays important roles in protein synthesis, cell proliferation, cell differentiation, microtubule dynamics, cell motility and neuronal development by phosphorylating initiation factors, transcription factors and proteins involved in microtubule functions and cell adhesion.^{148, 149} There are two isoforms of the protein, GSK-3 α and GSK-3 β . They share 98% of homology, but they are not functionally identical, although both have been suggested to be involved in AD pathogenesis.¹⁴⁹ GSK-3 α has been implicated in the amyloidogenic processing of APP to yield A β peptides,¹⁵⁰ while GSK-3 β has been implicated in the tau-related pathogenesis of AD by phosphorylating tau.¹⁵¹ GSK itself is also regulated by phosphorylation. Phosphorylation at Ser₉ of GSK-3 β and the equivalent Ser₂₁ of GSK-3 α by PKC inhibits its activity. On the other hand, phosphorylation at Tyr₂₁₆/Tyr₂₇₉ of GSK-3 β and GSK-3 α , respectively, increases its activity.¹⁵²

In the last few years, the interest for GSK-3 increased because it may offer an attractive target for drugs aimed at ameliorating AD. This is supported by the hypothesis that there is a correlation between A β accumulation and hyperphosphorylation of tau protein. Indeed, A β increases the phosphorylation of tau by activation of GSK-3. Wang et al.¹⁵³ suggested that A β causes a reduction in PKC activity and, the subsequent inhibitory phosphorylation at Ser₉, may be a crucial mechanism for the activation of GSK-3. More recently, it was shown that GSK-3 regulates A β 42 toxicity *in vivo* in a *Drosophila* model of AD overexpressing A β 42. Inhibition of GSK-3 by lithium chloride, a direct inhibitor of GSK-3 α and GSK-3 β ,¹⁵⁴ rescued A β 42 toxicity,

suppressing the locomotor dysfunction caused by expression of the peptide in flies' neurons. GSK-3 effects on A β 42 toxicity appear to be mediated by a tau-independent mechanism; it is suggested that inhibition of GSK-3 may increase A β degradation or clearance by enhancing the expression of A β -degrading enzymes.¹⁵⁵ On the contrary, increased GSK-3 activity reduces A β -degrading enzymes activity with subsequent amyloidosis.¹⁵⁶

Finally, Phiel et al.¹⁵⁰ proposed that GSK-3 α itself regulates production of A β . They showed that lithium chloride is able to block the production of A β 40 and A β 42 in cultured cells and in the brain of mice that overproduce amyloid peptides by interfering with APP cleavage at γ -secretase cleavage site. Furthermore, overexpression of GSK-3 α increases A β production. Interestingly, lithium chloride does not inhibit Notch processing indicating that lithium is not a direct inhibitor of γ -secretase. It means that GSK-3 α might regulate γ -secretase activity by regulating the access of substrate to γ -secretase complex.

In conclusion, GSK-3 offers an attractive target for drugs aimed at reducing the formation of amyloid plaques and neurofibrillary tangles, the pathological hallmarks of AD. Thus, Abbott has identified potential inhibitors of GSK-3 β , one of these (ABT-3174919) is now in preclinical trials for AD.¹²² Moreover, AL-108/davunetide is in Phase II for the treatment of mild cognitive impairment and AD. Davunetide seems to protect microtubules against hyperphosphorylated tau-induced damage and it seems to have protective and cognition-enhancing properties.¹²²

1.3 The cholinergic hypothesis

The cholinergic hypothesis is the first theory proposed to explain AD. It states that a loss of cholinergic function in the CNS contributes to the cognitive decline associated with AD.¹⁵⁷ The neuronal damage and death encompass regions critical for learning and memory, including the neocortex, hippocampus, amygdala, anterior thalamus and basal forebrain.^{158, 159} The key role of the acetylcholine system (choline acetyltransferase [ChAT], acetylcholine [ACh], acetylcholinesterase [AChE], muscarinic and nicotinic ACh receptors) in normal brain functions and in the memory impairment in AD, have been known for a long time.^{157, 160, 161, 162}

The cholinergic system uses ACh as neurotransmitter which is synthesized in neurons by action of ChAT, then concentrated in vesicles, and released from the pre-synaptic cell following depolarization. ACh, after interaction with receptors in the synaptic cleft, is hydrolyzed by action of AChE (**Fig. 11**).

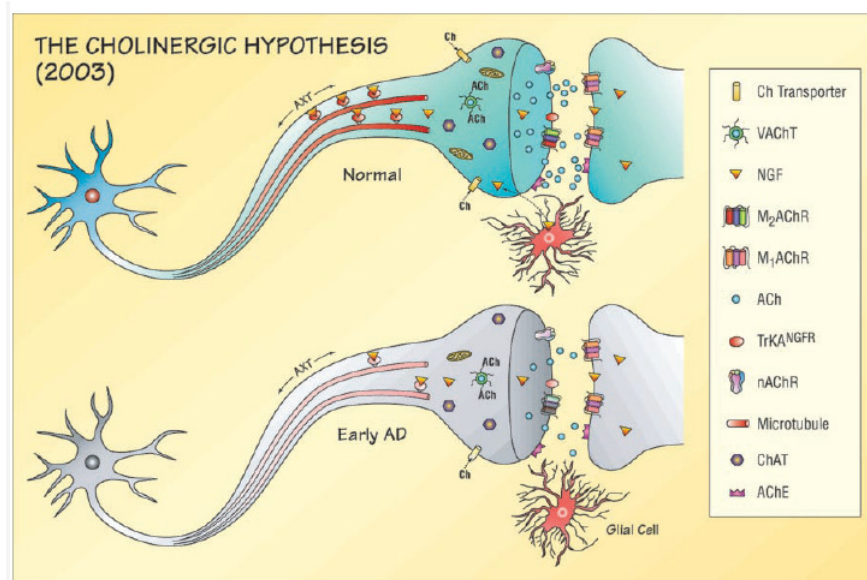


Figure 11: Schematic representation of the alterations that occur in cholinergic system in early AD brain compared with healthy young neurons.¹⁶³

The cholinergic hypothesis was developed a little earlier than the amyloid hypothesis of AD. In fact, the first finding in this field emerged in 1976 when it was found a significant loss of ChAT activity in different parts of the AD brain.^{164, 165, 166} This discovery was soon confirmed with the finding that neurons in the basal part of the brain were selectively degenerated in AD,¹⁶⁷ which explained the reduction in ChAT activity in the cortex and hippocampus.

The cholinergic neurons release ACh, which can bind two different receptor subtypes: the nicotinic receptors (nAChRs) and the muscarinic receptors (mAChRs). nAChRs are ligand-gated-ion-channels composed of different subunits assembled in pentameric structures.

Differently, mAChRs are metabotropic receptors that use G proteins as signal transducing molecules. M₁, M₃ and M₅ receptor subtypes couple to Gq family G proteins, which activate phospholipase C (PLC), releasing inositol trisphosphate (IP₃) and intracellular calcium. M₂ and M₄ mAChRs couple to Gi proteins which inhibit adenylate cyclase, decreasing the production of cAMP from ATP and inhibiting voltage-gated Ca²⁺ channels. Importantly, in 2012, X-ray structure of the M₂ and M₃ subtypes has been determined.^{168, 169} Several groups have reported a selective loss of different nAChRs subtype ($\alpha 7$ or $\alpha 4\beta 2$) in AD brains.^{170, 171, 172} Moreover, also a reduction of mAChRs is thought to be involved in the development of AD. The major subtypes of mAChRs involved in cognition are the post-synaptic M₁ receptors, which mediate the effects of ACh, and the pre-synaptic M₂ receptors, which regulate ACh release. A decreased in density of M₂ in post-mortem AD brain tissue have been reported.¹⁷³ On the other hand, normal levels of M₁ receptor contrasted with its diminished activity,¹⁷⁴ suggesting that the coupling of these receptors to their G-proteins is impaired.¹⁷⁵ This finding demonstrated that the extent of reduction in M₁/G-protein coupling is correlated to the severity of cognitive symptoms in AD.¹⁷⁵ Both the amyloid and the cholinergic hypothesis of AD have been widely investigated and debated. There are various indications that a relationship exists between the two hypotheses. However, the link between them has not been established yet. The main pathways linking them are summarized below.

A Toxicity of A β on the cholinergic system

In animal models of AD, fragments of β -amyloid protein and tau protein are thought to interfere with central cholinergic transmission, specifically with synthesis and release of ACh.¹⁷⁶ In cultured rat cortical neurons, A β 40 and A β 42 decreased the cholinergic neuron number and shortened neurite outgrowth length.^{177, 178} It was further shown that neuronal nAChRs interact with A β 42 and A β 40.^{179, 180, 181} Binding studies have revealed that the affinity of A β 42 binding to $\alpha 7$ nAChRs is exceptionally higher than the affinity of A β 40. This interaction can be inhibited by $\alpha 7$ nAChR antagonists.¹⁷⁹ It has been suggested that the high-affinity binding of A β 42 to $\alpha 7$ nAChRs may be an important early step that promotes the internalization and accumulation of A β 42 in neurons of AD brains. In fact, *in vitro* and *in vivo* studies revealed a substantial intraneuronal A β 42 accumulation only in cells that express high levels of $\alpha 7$ nAChRs.^{180, 181} Moreover, A β peptides can block the interaction of ACh with their receptors on hippocampal neurons. The potential blockade of basal forebrain and hippocampal nAChRs by endogenous A β peptides promotes the cognitive decline associated with AD.

Moreover, subtoxic concentration of A β impaired the mAChR activation of G-proteins. A reduction of mAChR-stimulated phosphatidylinositol hydrolysis was found in rat primary cortical neurons exposed to A β fragments.¹⁸² Machova'et al.¹⁸³ suggested that the results point to a complex malfunction of muscarinic/G-protein coupling, rather than a depletion of a specific mAChR subtype.

B *Cholinergic regulation of APP processing*

The relation between the effects of mAChRs^{184, 185, 186} and nAChRs^{187, 188, 189} stimulation and the modulation in APP processing has been studied for a long time. Biochemical studies revealed that stimulation of α 7nAChRs can increase α APPs which might be due to an enhanced cleavage of APP by α -secretase. Galantamine has an interesting pharmacological profile as it is both a reversible acetylcholinesterase inhibitor (AChEI) and an allosteric potentiator of nAChRs.¹⁹⁰ Furthermore, it increases the release of sAPP α , promoting the non-amyloidogenic processing of APP. The action of galantamine was prevented by α -bungarotoxin, a specific antagonist for α 7nAChRs, but not atropine, a selective mAChR antagonist, suggesting the specific involvement of α 7nAChRs. Agonist induced activation of M₁ and M₃ mAChRs, which are coupled to PLC and PKC activation, stimulates sAPP α release *in vitro*.¹⁸⁵ This implicates increased α -secretase activity through mAChR activation. In fact, it is well-known that α -secretase-mediated cleavage of APP is regulated by several kinases like, for example, PKC.^{191, 192} M₂ and M₄ mAChRs are not effective in increasing sAPP α . Recent results showed that M₂ stimulation decreased the BACE-1 expression.¹⁹³ Since BACE-1 is a key enzyme in the accumulation of A β , its inhibition by a selective M₂ mAChR agonist would be an important therapeutic target.

1.3.1 *Acetylcholinesterase*

AChE is a serine protease that hydrolyzes ACh in cholinergic brain synapses. The principal biological role of AChE is termination of impulse transmission at cholinergic synapses by rapid hydrolysis of the neurotransmitter ACh.¹⁹⁴ The first X-ray crystallographic determination of AChE structure of was obtained from *Torpedo californica*.¹⁹⁵ Later, it was also obtained the crystallographic structure of the human AChE.¹⁹⁶ From crystallography, it was possible to observe at atomic resolution the protein binding pocket for ACh. It was found that the active site consists of a catalytic triad (Ser₂₀₃, His₄₄₇, Glu₃₃₄) which lies in the bottom of a deep and narrow gorge, which is delimited by the ring of 14 aromatic amino acid residues (**Fig. 12**). Despite the complexity of this array of aromatic rings, it was suggested on the basis of modeling, which involved docking of the ACh molecule, that the quaternary group of the choline moiety makes

cation- π interaction with the indole ring of Trp₈₆. At the top of the gorge, a peripheral binding site (PAS) was also identified. It is delimited by Tyr₇₂, Tyr₁₂₄, Tyr₃₄₁, Glu₂₈₅, Asp₇₄ and Trp₂₈₆. Inestrosa and co-workers^{197, 198} proved for the first time the “non cholinergic action” of AChE, suggesting that PAS is able to induce A β aggregation. Thus, the interaction of A β at the PAS of AChE catalyzes some conformational changes in A β fibrils to form the β -sheet with increased aggregating potential.^{199, 200} The high concentration of AChE observed inside A β plaques support this hypothesis.²⁰¹

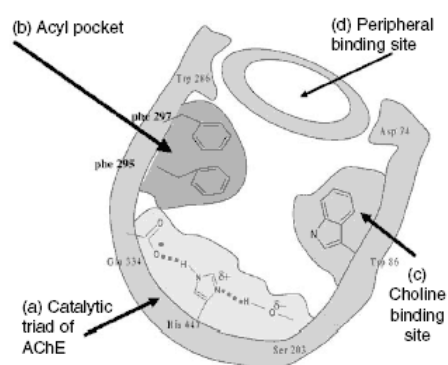


Figure 12: Active center gorge of human AChE.

In vitro and *in vivo* studies have consistently demonstrated a link between A β production and cholinergic dysfunction. Scientific efforts to target AD are based on the identification of disease-modifying compounds that are capable of affecting both cholinergic system and APP processing. However, to date, the only drugs approved by FDA for clinical use in AD are AChEI (tacrine, donepezil, rivastigmine, and galantamine, **Fig. 13**) and memantine, a NMDA antagonist (see **1.7**). Donepezil, rivastigmine and galantamine are generally preferred due to their modest risk of hepatotoxicity compared to tacrine. Tacrine, rivastigmine and galantamine interact at the catalytic site of the enzyme, while donepezil spans the whole length of the catalytic site simultaneously interacting with the tryptophan residues characteristic of the active and PAS of AChE.²⁰²

AChEIs can provide symptomatic improvements but they do not offer long term cure for this disorder. Moreover, not all AD patients are responsive to the efficacy of AChEIs and to date the differences between ‘responders’ and ‘non-responders’ remain unclear.

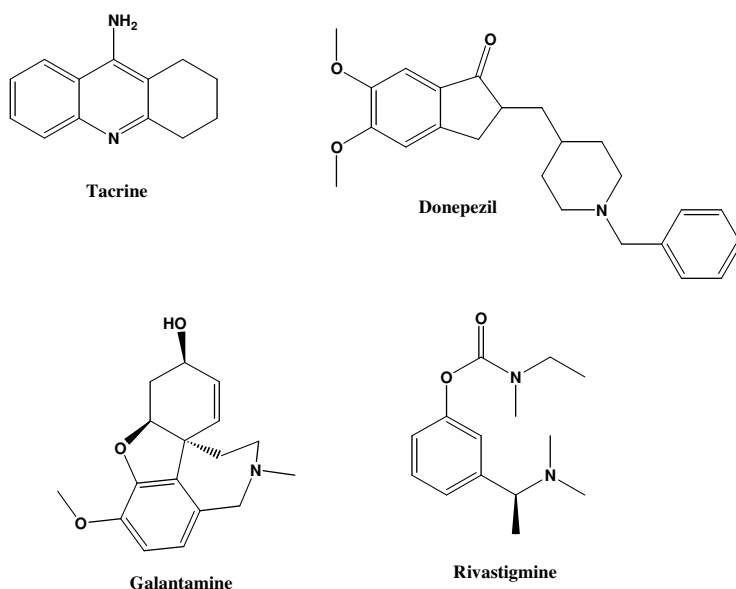


Figure 13: Molecular structure of AChEIs used in clinical practice for AD

1.4 Role of ApoE

Apolipoprotein (Apo) E is a 34kDa lipid transport protein encoded on the long arm of chromosome 19. Its amino acid sequence is essentially identical in many species, thus, it is likely to be a protein fundamental for life functions. In fact, apoE plays important roles in neurobiology;^{203, 204, 205} it is the major apolipoprotein in the CNS capable of redistributing lipids, including cholesterol, to sites of injury to repair cells. It is synthesized and secreted mainly in astrocytes but it is expressed also in some neurons in response to brain injury.²⁰⁶

In the mid-1970s, Utermann et al.²⁰⁷ found that apoE was polymorphic; the gene encodes three alleles: apoE2 (frequency in population 5-10%), apoE3 (60-70%), and apoE4 (15-20%). ApoE4 involvement in neuropathology is well documented and it is one of the genetic risk factor for sporadic and familial AD.^{208, 209, 210, 211, 212} Indeed, 40-80% of patients with AD possess at least one apoE4 allele.²¹³ Similarly, apoE4 is associated with earlier onset and severity of head trauma,^{214, 215, 216} stroke,²¹⁷ Parkinson's disease,^{218, 219, 220} amyotrophic lateral sclerosis,^{221, 222} multiple sclerosis²²³ and other severe CNS diseases. On the other hand, apoE2 seems protective relative to the prevalent apoE3.²²⁴

ApoE has two structural domains: a 22-kDa N-terminal domain, which contains the LDL receptor binding region, and a 10-kDa C-terminal domain, which contains the major lipid binding element. Interaction between the C- and N-terminal domains is a unique property of apoE4.^{225, 226} X-ray crystallography has demonstrated the structural basis of domain interaction.

In apoE4, Arg-112 allows Arg-61 to form a salt bridge with Glu-255 at the C-terminus (**Fig. 14**). Differently, apoE2 and apoE3 have a cysteine in position 112. Thus, Arg-61 has a different conformation, and domain interaction does not occur. Interestingly, only human apoE has Arg-61; the 17 other species in which the apoE gene is present all have Thr-61.²²⁷ Mutation of Arg-61 to Thr or Glu-255 to Ala in apoE4 prevents C-terminal/N-terminal interaction and makes apoE4 structurally and functionally similar to apoE3. Domain interaction between Arg-61 and Glu-255 makes apoE4 unstable and it is thought to be responsible for the detrimental effects of apoE4. Protein instability is an important component of several neurodegenerative disorders. ApoE4 is the less stable isoform. In fact, it denatures at lower concentration of guanidine-HCl and urea, and at lower temperature. This makes apoE4 more susceptible to form molten globules and to increase its propensity to proteolysis.

Small molecules that are predicted to interact with apoE4 in the region of Arg-61 would disrupt domain interaction and may convert apoE4 to an “apoE3-like” molecule (**Fig. 14**). Thus, apoE4 could be a new target for drugs development for AD.

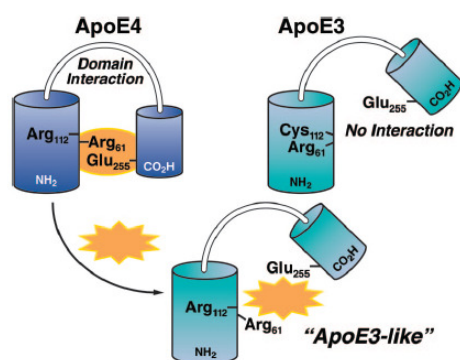


Figure 14: ApoE4 domain interaction mediated by salt bridge formation between Arg-61 and Glu-255.²²⁸

Throughout life, neurons must be remodeled and regenerated to maintain synapto-dendritic connections. Through its lipid transport function, apoE is an important factor in this process. ApoE3 and apoE2 are effective in repairing neuronal cells, but apoE4 is less so. The detrimental insults could be oxidative stress, inflammation, excess A β production and aging process itself. Although apoE4 is strongly linked to AD pathology, its exact mode of action is still unknown. Many mechanisms have been suggested and are summarized below.

A *Effects of ApoE4 on A β deposition and clearance*

Through interactions with A β , apoE4 may increase amyloid deposition, plaque formation and reduce its clearance in a mouse model of AD.^{229, 230, 231, 232} *In vitro* lipid-free apoE3 and apoE4 can form stable complex with A β peptides. However, apoE4 forms complexes more rapidly and effectively.^{233, 234} Prolonged incubation of apoE with A β peptide gives rise to insoluble, high molecular weight complexes that precipitate in fibers. Moreover, apoE4 forms a denser, more extensive matrix of amyloid monofibrils and does so more rapidly and effectively than apoE3.^{235, 236} In addition, apoE4 enhances zinc- and copper-induced A β aggregation.²³⁷ Thus, increased amyloid fibril formation caused by apoE4 might trigger or exacerbate neurodegeneration and the development of AD. However, poorly lipidated apoE3 and apoE4 yielded different results when incubated with A β peptides. It seems that apoE3 bound with a 20-fold greater affinity than apoE4 to A β . This suggests that the lipidation status of apoE modifies its ability to interact with A β peptides.^{238, 239} It is thought that the binding of apoE3 to A β , might enhance clearance of the peptide, preventing the conversion of A β into neurotoxic specie.²³⁹

B *Effects of ApoE4 on A β production.*

Many studies have been focused on the role of apoE4 in stimulating A β accumulation. However, apoE4 also enhances A β production. In rat neuroblastoma cells transfected with human wild-type APP695, lipid-poor apoE4 increased A β production more than apoE3 (60% vs. 30%).²⁴⁰ It seems that LRP, a member of the LDL receptor family,²⁴¹ may mediate the isoform-specific effects of apoE on A β release. Ye et al.²⁴⁰ suggested that the binding of apoE4 to LRP accelerates APP endocytosis and recycling and thus enhances A β production.^{242, 243, 244}

C *Effects of ApoE4 on Tau Phosphorylation*

In AD brains, tau is abnormally hyperphosphorylated and self-assembles into pathological paired helical filaments, which result in NFTs. Evidence from *in vitro* and *in vivo* studies suggests that apoE3 and apoE4 have different effects on the interaction with hyperphosphorylated tau. *In vitro*, apoE3 forms stable complex with tau, on the other hand apoE4 does not interact significantly.^{245, 246} Phosphorylation of tau inhibited the interaction of apoE3 with tau suggesting that apoE3 binds to tau and may protect it from hyperphosphorylation inducing NFTs formation.²⁴⁷ In addition, it was found that, single-nucleotide polymorphisms (SNPs) in the GRB-associated binding protein 2 (GAB2) gene in apoE4 carriers, highly increase LOAD (late-onset AD) risk. GAB2 is the main activator of phosphatidylinositol 3-kinase (PI3K). PI3K promotes cell survival by activating its downstream effector Akt kinase.²⁴⁸ Akt inactivates GSK-3 α and GSK-3 β by phosphorylating the former at Ser21 and the latter at Ser9. Thus, GAB2 might protect neurons

from tangle formation and cell death and a loss of function of GAB2 would diminish such protection. Six SNPs which reduce GAB2 function were identified and, in association of apoE4 allele increase AD genetic risk.²⁴⁹ Discovery of these LOAD susceptibility genes provides new opportunities in the scientific understanding, treatment and prevention of AD.

D *ApoE4 Fragmentation and AD*

The neuronal expression of apoE is induced to protect neurons from injury and to promote intraneuronal repair. However, when synthesized in neurons, apoE can be cleaved by proteases, and the fragments are toxic for cells leading to cell death and to the formation of cytoplasmic NFT-like inclusions in the cytoplasm and in mitochondria.²⁵⁰ ApoE4 is more susceptible to proteolytic cleavage than apoE3, when expressed in transfected neuronal cells.²⁵¹ In addition, apoE fragments are produced at higher levels in brains of AD patients than in brains of non-demented controls.

E *ApoE4 potentiation of A β -induced lysosomal leakage and apoptosis*

Internalized A β 42 is degradation resistant, and it accumulates as insoluble aggregates in endosomes and lysosomes leading to their leakage through free radicals generation. In cultured cells, apoE4 enhances A β -induced lysosomal leakage and apoptosis to a greater extent than apoE3. It is suggested that, because of its unique conformation and reactivity, apoE4 forms toxic intermediates (molten globules) and assumes detrimental activities when it reaches acidic pH in lysosomes destabilizing their membrane.

1.5 The role of metallobiology in AD

Mounting evidences support the idea that endogenous ‘biometals’, such as Cu, Fe, Zn and exogenous Al, can be involved as factors or cofactors in the etiopathogenesis of AD. In AD, the process of A β misfolding and plaque aggregation seems to be greatly influenced by alterations in the homeostasis of these metal ions. Indeed, they are found with high concentration in both the core and rim of AD senile plaques.²⁵²

In eukaryotes, Cu, Fe and Zn are the most abundant biochemically functional metals. These elements are often referred to as “trace metals”. Although they exist in a smaller amount compared to carbon, hydrogen, nitrogen, oxygen and phosphorous, they are just as essential. In fact, metals are important for enzymatic function, playing important roles in catalysis, structural stability, transport of oxygen and cellular signaling. Genetic dysfunction, environmental

exposure, ageing, inadequate dietary intake and drug interaction can all induce an alteration in their homeostasis leading to deleterious effects and neurotoxicity (**Fig. 15**).

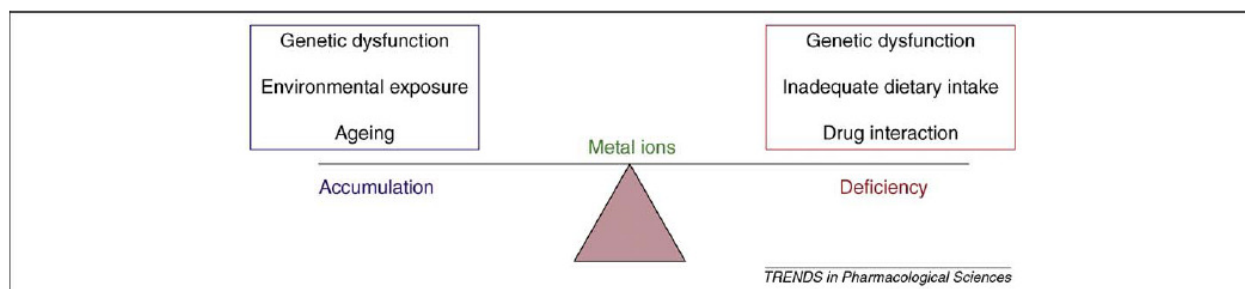


Figure 15: Schematic representation of the factors affecting the delicate balance between metal ions accumulation and deficiency.²⁵³

The “amyloid cascade theory” has dominated AD research for the past 15 years but the exact factors that drive A β accumulation remain a mystery. However, the interest for the role of metal dyshomeostasis as a pathogenic factor for AD has been strongly revived after the finding that therapeutic strategies restoring metal ion homeostasis in the brain of both AD patients and AD transgenic mice are able to reverse amyloid aggregation, dissolve amyloid plaques and delay the cognitive impairment associated to AD.^{254, 255, 256}

1.5.1 Metals in AD

Most of the glutamatergic synapses in the cerebral cortex co-release Zn with glutamate.^{257, 258, 259} This cation has been found to have a primary role in AD because of its efficacy to induce fast precipitation of A β together with its ability to build up protease resistant ‘non-structured’ aggregates.²⁶⁰ Studies on AD animal models have also revealed that genetic ablation of synaptic Zn greatly reduces the amount of amyloid plaques.²⁶¹ Moreover, several studies showed that compounds affecting Zn homeostasis can decrease A β deposition in the brain.^{262, 263} Finally, expression levels of Zn transporters (ZnT1, ZnT3,²⁶⁴ ZnT4 and ZnT6²⁶⁵), essential for loading Zn into synaptic vesicles, were discovered to be altered in the brain of individuals affected by mild cognitive impairment and AD. Zn may again be important as it has been shown to enhance the synthesis of the PS subunit of γ -secretase, altering the processing of APP to favor the amyloidogenic pathway.²⁶⁶

Like Zn, Cu is synaptically released after stimulation of the N-methyl-D-aspartate (NMDA) receptor by glutamate²⁶⁷ and it acts as a potent mediator of A β aggregation under conditions of mild acidosis.²⁶⁸ Nevertheless, Cu has the additional property of producing strong mitochondrial oxidative stress.²⁶⁹

The third transition metal found localized in human amyloid plaques is Fe. Despite having a high concentration in AD plaque,²⁷⁰ Fe ions are not likely to interact directly with A β *in vivo*. In fact, studies of various metal-ion chelators in solubilizing A β from postmortem AD-affected brain tissue have correlated the dissolution of precipitated A β with the release of Cu and Zn, but not Fe.²⁷¹ Several studies suggest that Fe homeostasis is altered in AD, however it seems a secondary effect via another process such as increased heme oxygenase activity in response to oxidative stress.²⁷²

In the context of AD-related metal dyshomeostasis, the role of Al is the subject of a controversial debate because of the paucity of reliable studies and data. Several researchers indicated that Al can contribute to both tau and A β pathology. Al, a highly reactive element, can promote tau and A β pathology as the ion can easily cross-link hyperphosphorylated proteins.²⁷³ Moreover, Drago et al,²⁷⁴ indicated that Al seems to be very effective in promoting *in vitro* ‘structured’ aggregation of A β associated with particularly high neurotoxicity.

1.5.2 A β binding to metals

Multivalent metal ions are fundamental to redox chemistry. The ability of these metal ions to occupy multiple valence states and undertake facile redox cycling, has been utilized by a variety of enzymes including ceruloplasmin,²⁷⁵ cytochrome c oxidase²⁷⁵ and amine oxidases.²⁷⁶ A β is a metalloprotein that displays high affinity binding of Cu²⁺, Zn²⁺ and Fe³⁺ ions.²⁷⁷ The metal binding site for Zn and Cu implicate three histidine residues (His₆, His₁₃, His₁₄) which coordinate the metal ions through the imidazole nitrogens. A β possesses a strong positive formal reduction potential and rapidly reduces Cu²⁺ and Fe³⁺ to Cu⁺ and Fe²⁺, respectively. Molecular oxygen is then trapped generating free radical and peroxides species via Fenton chemistry or Haber- Weiss reaction with the A β ₄₂ species exhibiting the greatest activity (**Fig. 16**).²⁷⁸

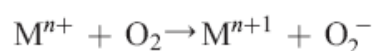
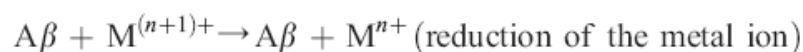


Figure 16: Redox chemistry involving A β and metals.²⁷⁹

Excessive levels of A β and metal ions may generate ROS concentration exceeding the capacity of the normal oxidation defence system. A broad range of lipid peroxidation products can evolve from the cascade of events described above. High levels of reactive electrophilic aldehydes and 4-hydroxy-2-nonenal (HNE) have been found in AD brain tissue. These aldehydes readily react with nucleophile such as DNA, protein and other lipids initiating a cascade of oxidation events leading to cellular dysfunction and ultimately death (**Fig. 17**).

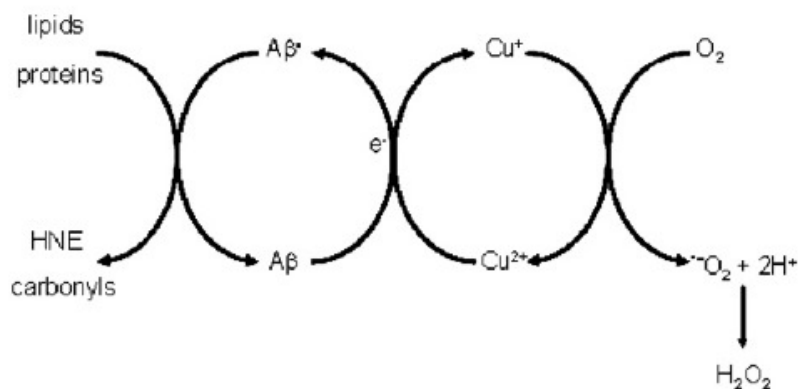


Figure 17: Redox cycle and ROS generation.²⁷⁹

Moreover, it is suggested that A β , in the presence of Cu²⁺ and H₂O₂, forms dityrosine cross-linked structures which facilitate further peptide aggregation, leading to the formation of higher ordered oligomers that accumulate in the senile plaques (**Fig. 18**).²⁸⁰

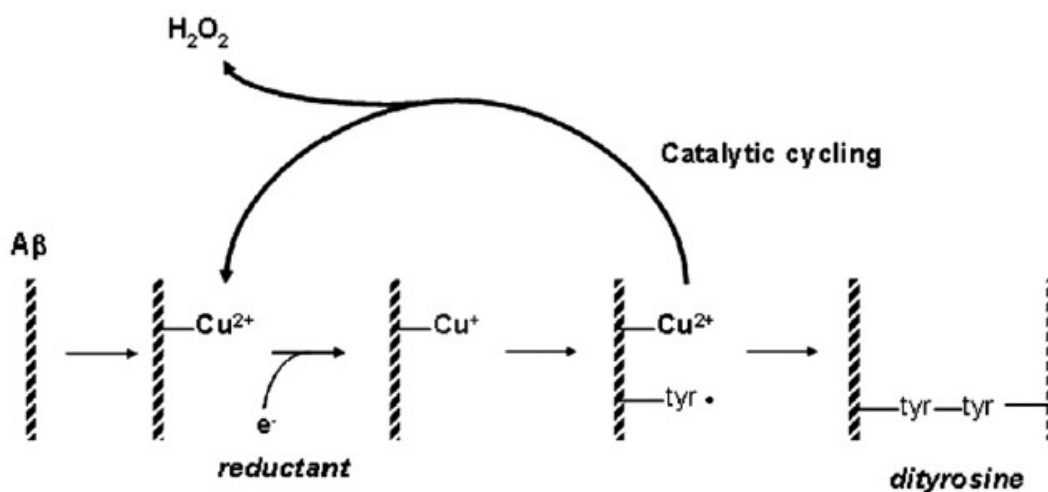


Figure 18: Generation of A β dityrosine oligomers.²⁷⁹

1.5.3 Metal homeostatic therapy

Although metal ion dyshomeostasis is certainly not the only cause of the disease, therapeutic interventions aimed at restoring metal homeostasis remain strong candidates as disease-

modifying strategies for AD treatment. 5-Chloro-7-iodo-8-hydroxyquinoline (clioquinol, CQ) has generated a great interest because of promising results *in vitro* and *in vivo*. CQ (**Fig. 19**) was produced as a topical antiseptic and sold as an oral intestinal amebicide in 1934. In the early 1970s, it was withdrawn from the market as an oral agent because of its severe side effects. CQ is currently available in some countries as a topical formulation for the treatment of skin infections. Its ability to act as a zinc and copper chelator²⁸¹ has renewed the interest of many researchers for its possible use in the treatment of AD. Prana Biotechnology has developed a new hydroxyquinoline derivative (PBT-2) with a better toxicological profile than that of CQ. PBT-2 is currently in Phase II for the treatment of AD.¹²²

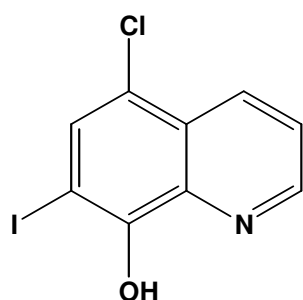


Figure 19: CQ structure.

1.6 Role of oxidative stress in AD

Oxidative stress is defined as a breaching of the antioxidant defense system. The brain is the most aerobically active organ in the body due its high metabolic requirements. The brain accounts for 2% of total body mass and it consumes 20% of total oxygen. Neurons are subject to a number of unique conditions that make them particularly vulnerable to oxidative stress. This vulnerability is a consequence of the high energy and oxygen consumption rate and the high amount of unsaturated lipid content in neuronal membrane.²⁸² Therefore, it is essential to maintain oxidative balance and control in the brain, and this is tightly regulated by antioxidants that are present in higher amounts than in any other organs. In the case of age-related neurodegeneration, like that observed in AD, this balance between oxidative radicals and antioxidant defenses is altered, resulting in various forms of cellular and molecular damage than can culminate in cell death. Although it is debatable whether oxidative stress is the cause or consequence of the disease, recent evidence suggesting that oxidative stress occurs earlier than all other known changes indicates a causative role in the pathogenesis of AD.²⁸³

1.6.1 Contribution of ROS

ROS that are generated intracellularly and extracellularly by various mechanisms are among the major intermediary risk factors that initiate and promote neurodegeneration in idiopathic AD.^{284, 285} Individuals affected by AD showed increased oxidative damage to every class of biological macromolecules, like sugars, lipids, proteins, and nucleic acids.

A schematic pathway of pathological lesions induced by oxidative stress is shown in **Figure 20**.

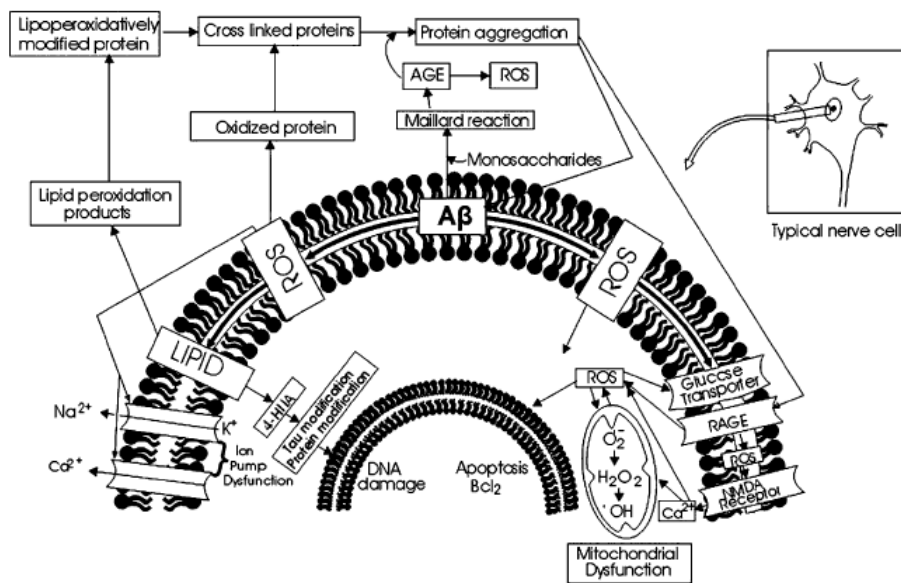


Figure 20: Schematic pathway of pathological lesions induced by oxidative stress.²⁸⁶

The vast majority of oxidative-stress-dependent protein modifications involve the adduction of products following the oxidation of carbohydrate or lipid moieties (glycoxidation and lipoxidation, respectively) and results in the formation of stable adducts called advanced glycation end products (AGEs) or advanced lipoxidation end products (ALEs).²⁸⁷ AGE modification and the resulting cross-linking of protein deposits have been shown to occur in both senile plaques and NFTs in AD. ROS cause damage to lipid by forming lipid peroxidation and products such as malonaldehyde and 4-hydroxynonenal (4-HNE). 4-HNE adducts bind directly to tau, inhibiting its dephosphorylation. Aβ generated ROS also disrupt ion homeostasis, changing the function of ion motive ATPase and promoting the activation of N-methyl-D-aspartate (NMDA) receptors which determine an increase of intercellular Ca²⁺ levels. Moreover, DNA damage induced by free radicals, in particular by hydroxyl radical ($\cdot\text{OH}$), triggers DNA damage, which may be an important factor in the progression of cell death in AD.²⁸⁸

1.6.2 Mitochondrial dysfunction

Mitochondria are dynamic organelles required for several biosynthetic processes and provide most of the cellular energy demand. Moreover, they maintain Ca^{2+} homeostasis and take part in apoptosis. They are composed by outer and inner membranes containing phospholipid bilayers and proteins (**Fig. 21**). The two membranes, however, have different properties. Because of this double-membraned organization, there are five distinct compartments within the mitochondrion. They are:

- the outer membrane
- the intermembrane space (the space between the outer and inner membranes)
- the inner membrane
- the cristae space (formed by infoldings of the inner membrane)
- the matrix (space within the inner membrane)

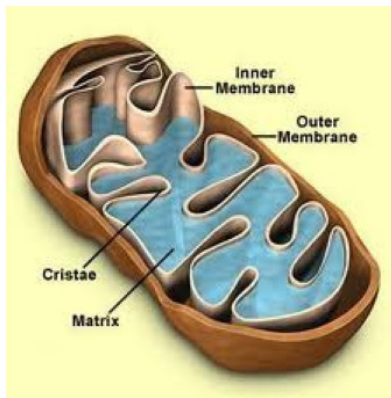


Figure 21: Mitochondrion structure.

The outer membrane, like the plasma membrane, is composed by lipid and protein in ratio of 1:1 and it does not offer a barrier to small molecules that can simply diffuse through pores in the membrane formed by a membrane spanning protein called porin. ATP synthesis occurs in the matrix space via the electronic transport chain (ETC), localized in the inner membrane, that performs the redox reactions of oxidative phosphorylation (OXPHOS). The inner membrane contains also the ATP/ADP carrier that allows ADP to cross the inner membrane while simultaneously transferring out ATP from the matrix space. The composition of the inner membrane differs from the outer in that it is more proteinacious and contains an unusual phospholipid, cardiolipin. Unlike the outer membrane, the inner membrane does not contain porins and is highly impermeable to all molecules. In fact, almost all ions and molecules require special membrane transporters to enter or exit the matrix. Perhaps, the most important function

of mitochondria is the synthesis of ATP, the most important source of energy. In fact, mitochondria are defined as “the power house” of the cell.²⁸⁹ In neurons, mitochondria are significantly localized at synapses and are essential for their normal function, supplying them with ATP for neurotransmission.²⁹⁰ The energy released by the flow of ETC is used to pump protons out of the mitochondria inner membrane through complexes I, II, III, and IV (**Fig. 22**). This generates an electrochemical gradient across the mitochondria inner membrane. The potential stored is coupled to ATP synthesis by complex V (ATP synthase).

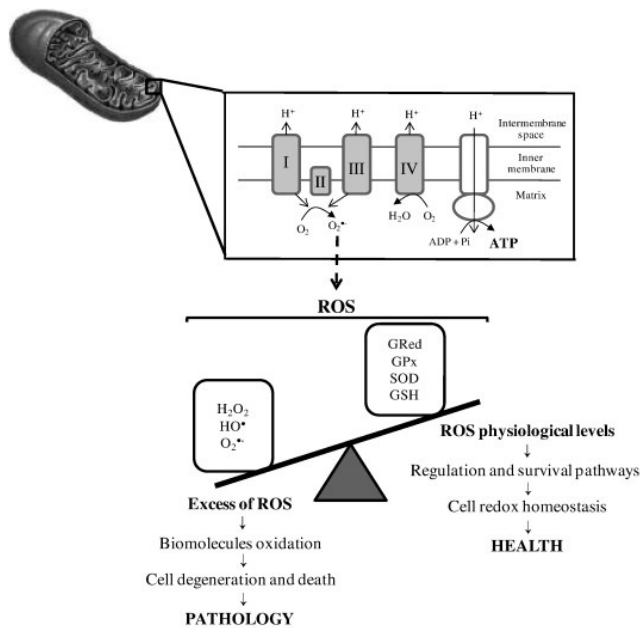


Figure 22: The two faces of mitochondria.²⁹¹

Oxygen normally serves as the ultimate electron acceptor and is reduced to water.²⁹² However, OXPHOS is a major source of toxic endogenous free radicals. In fact, when ETC is inhibited, electrons accumulate in complex I and III, where they can be donated directly to molecular oxygen to yield $O_2^{\cdot-}$ that can be further detoxified by the mitochondrial manganese superoxide dismutase producing H_2O_2 by the glutathione peroxidase. However, $O_2^{\cdot-}$ in the presence of $NO\cdot$, formed by the nitric oxide synthase, can lead to the formation of $ONOO\cdot$. Furthermore, H_2O_2 in the presence of reduced transition metals can be converted via Fenton reaction to the hydroxyl radical $OH\cdot$. Other mitochondrial enzymes can generate ROS, like α -ketoglutarate-dehydrogenase complex (KGDHC) and pyruvate-dehydrogenase complex (PDHC). KGDHC and PDHC are two enzymes of the tricarboxylic acids cycle. The reduced activity of these key enzymes favors the aberrant production of ROS, especially in the form of H_2O_2 .²⁹³

Abnormalities in the oxidative balance and the reduced rate of glucose metabolism are one of the best documented dysfunctions in AD, which precedes, rather than follows, the clinical

manifestation of the disease.²⁹⁴ If ROS levels overwhelm the defense mechanism of the cells, oxidative damage of proteins, lipid and DNA takes place, leading to cell degeneration and death (**Fig. 20**). The reduction of cerebral metabolism in AD places mitochondria at the center of the attention and indeed, several studies corroborate the idea that mitochondrial dysfunction is a hallmark of A β -induced neuronal toxicity in AD.

Many researchers showed that both APP and A β are present in mitochondria in the brains of AD patients.^{295, 296, 297} APP is imported to mitochondria and spans the mitochondrial intermembrane space with the NH₂-terminus inside the matrix and COOH-terminal fragment facing the cytosol, staying in close association with outer membrane channels. Docking APP in mitochondrial import channels has been proposed to inhibit the import of nuclear-encoded proteins, essential for mitochondrial function.^{295, 296} It appears that A β is also present in mitochondria of non-demented human brains, albeit at a lower level.²⁹⁷ Likewise, Sheng et al.²⁹⁸ demonstrated that constitutive low levels of APP are involved in maintaining mitochondrial functions. In brain specimens from AD patients, mitochondrial APP and A β induce ROS generation,²⁹⁹ decrease COX activity and ATP production.²⁹⁶ Interestingly, it was demonstrated that A β binds to alcohol dehydrogenase (ABAD). ABAD is localized in mitochondrial matrix and plays an essential role in mitochondria. The interaction of A β and ABAD inhibits ABAD activity and leads to elevated ROS production, cell death, and subsequent memory impairment in transgenic mice AD models.³⁰⁰ Furthermore, evidence indicates that γ -secretase, which is essential for A β production, is present in mitochondria.³⁰¹ Moreover, it seems that ATP synthase inhibition and COX inhibition drives APP processing towards the amyloidogenic pathway³⁰² and tau phosphorylation.³⁰³

Besides mitochondria are highly affected by oxidative damage, another key event, resulting from mitochondrial dysfunction, is the opening of the mitochondrial permeability transition pore, leading to loss of mitochondrial permeability and consequent release of cytochrome C into the cytosol.³⁰⁴ This event results in the activation of a family of cysteine protease called caspase, the intracellular executors of apoptosis, ultimately leading to the activation of caspase-dependent nucleases, which result in DNA fragmentation and cell death. Thus, considering the extreme importance of oxidative stress and mitochondria in AD, therapeutic antioxidant strategies preventing oxidative damage and targeting mitochondria are currently pursued.

1.7 Inflammation and AD

According to the inflammatory hypothesis of AD, chronic cerebral inflammation causes injury to neurons, contributing over time to cognitive decline.³⁰⁵ It is hypothesized that neuronal injury results from the direct effects of inflammatory effectors, such as cytokines or activated complement, or indirect effects, such as an increased production of neurotoxic A β in response to cytokines or other inflammatory stimuli.³⁰⁶ Microglia and astrocytes, the primary immune effector cells of the brain, are thought to be the key elements in this process. In AD, the number of reactive astrocytes and activated microglia is increased, and they are found in and around neuritic plaques.

A β is thought to be neurotoxic and to play a key role in the pathophysiology of AD. Significantly, A β induces microglia to produce many agents with the potential to injure neurons, including inflammatory and chemotactic cytokines,³⁰⁷ chemokines,³⁰⁸ NO³⁰⁹ and ROS^{310, 311} (Fig. 23)

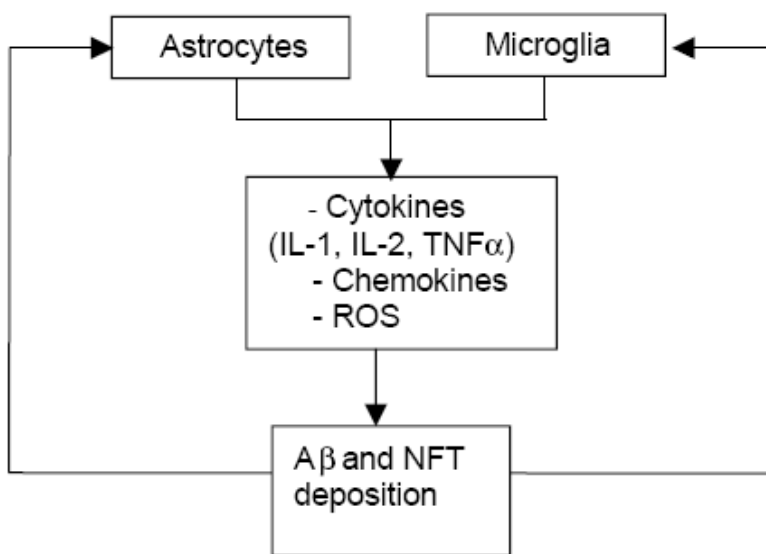


Figure 23: Schematic inflammation process in AD brains.²⁸⁶

The proinflammatory cytokine IL-1 is thought to play a critical role in neuronal injury in AD.³⁰⁸ IL-1 is increased in AD brains and is found mainly around diffuse amyloid plaques.³¹² It accounts for increasing the translation of mRNA encoding APP³¹³ and its over-expression could lead to an early onset of AD. IL-1 increases A β , then A β could induce additional IL-1 expression³¹⁴ resulting in a positive feedback loop. IL-1 also induces astrocytes and microglia proliferation.³¹⁵ Although astrocytes have neuroprotective functions, excessive astrocytic

proliferation can inhibit neurite growth, whereas microglial proliferation is associated with cytotoxic activity. Finally, IL-1 induces microglial inducible macrophage nitric oxide synthase (NOS)³¹⁶ and the release of ROS that enhance the degenerative process.³¹⁷ Although under some conditions IL-1 may be neuroprotective, existing evidence strongly suggests a negative role for IL-1 in AD.

Tumor necrosis factor (TNF)- α is thought to be involved in AD pathogenesis too. Thus, He et al.³¹⁸ showed that TNF receptor 1 knockout protects against AD-like disease in mice.

Cyclooxygenase (COX) is an enzyme that converts arachidonic acid to prostaglandin H₂ (PGH₂), the precursor of prostanoids (prostaglandins, prostacyclin and thromboxane), important biological mediators of inflammation. Although COX-1 is constitutively expressed in many cell types and tissues, COX-2 is increased during inflammation, resulting in proinflammatory prostanoids synthesis.³¹⁹ Cyclooxygenases are the key targets of non-steroidal anti-inflammatory drugs (NSAIDs). COX is strongly implicated in AD by epidemiologic studies of long term NSAIDs use. It was shown that such long term use reduced AD risk by half.³²⁰ These findings have been confirmed in a number of other studies, but did not lead to successful treatment trials yet. One possible reason for this failure may be that, like many other inflammatory mediators, prostaglandins are janus-faced, exerting beneficial or toxic functions depending on the setting. For example, COX-2, which is localized postsynaptically, is involved in modulating physiological synaptic transmission, but excessive activation in pathological conditions in transgenic mice induces neuronal apoptosis and cognitive deficits.³²¹ Thus, it was shown that transgenic over-expression of COX-2 in neurons led to a two-fold increase in A β plaque and cognitive deficits in an APP mouse model^{322 323} supporting a detrimental role for COX-2 in neurodegeneration and AD.

NSAIDs have been shown to directly affect the production of A β . For example, ibuprofen, flurbiprofen, indomethacin and sulindac sulphide were shown to decrease A β 42 peptide by up to 80% in cultured cells but this effect was not observed with naproxen, celecoxib, or aspirin.³²⁴ Since not all NSAIDs had this effect, it would seem that this effect occurs through a process that is independent of their anti-inflammatory COX inhibition.³²⁵

1.8 The glutamatergic hypothesis

Glutamatergic neurons form the major excitatory system in the brain and play a critical role in several physiological functions. The neurotransmitter glutamate activates many metabotropic receptors and three major types of ionotropic receptors; α -amino-3-hydroxy-5-methyl-4-isoxazolepropionic acid (AMPA), kainate and N-methyl-D-aspartate (NMDA). There is

increasing evidence for the involvement of glutamate-mediated neurotoxicity in the pathogenesis of AD. In particular, the overactivation of NMDA seems to be one of the major causes that mediate neurotoxicity in AD.

NMDA is a voltage-gated ion (or ionotropic) channel permeant to Ca^{2+} , Na^+ and K^+ (**Fig. 24**). It is a tetrameric hetero-oligomeric protein. Two major subunit families designated NR1, NR2 as well as a minor subunit designated NR3 have been cloned. A functional NMDA receptor is formed by one or more NR1 subunits, plus one or more NR2 subunits. NR1 contains the glycine-binding site, while NR2 expresses the glutamate recognition site.^{326, 327} Glycine is a co-agonist, necessary for NMDA activation. There are four known subtypes of NR2 (A, B, C and D) and eight splice variants of NR1. NR3 (NRL or Chi-1) seems to be expressed predominantly in the developing CNS.

The subunits are differentially expressed in the brain. For example, the NR2B subunit predominates in extrasynaptic rather than in synaptic NMDARs and it is thought that excessive stimulation of extrasynaptic receptors containing NR2B might contribute to neurotoxicity, whereas NR2A might be neuroprotective maintaining physiological synaptic activity.³²⁸

NMDA receptors can be blocked by competitive glutamate antagonists such as D-AP5 ((2*R*)-amino-5-phosphonovaleric acid)³²⁹ and glycine antagonists such as 5,7-DCKA (5,7-dichlorokynurenic acid).³³⁰ Polyamines such as spermine and spermidine are positive modulators binding to NR2B subunits but they also block the channel at higher concentrations. Ifenprodil³³¹ is the prototypic “selective“ antagonist for NR2B containing receptors, while Zn^{2+} is a potent, voltage-independent antagonist at NR2A containing receptors.

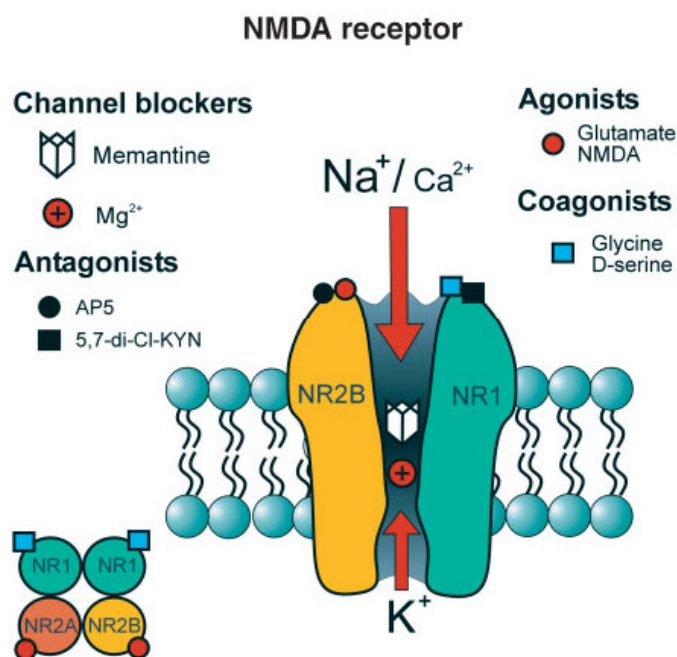


Figure 24: Scheme of the NMDA receptor.³³²

The gating of NMDA receptor involves a voltage-dependent Mg^{2+} blockade of the channel pore. When the signal arrives at the glutamatergic synapse, glutamate is released and it binds to both NMDA and AMPA receptors (**Fig. 25**). However, only the latter is activated, since Mg^{2+} blocks the NMDA channel (this ion is trapped in a narrow region of NMDA and it is attracted into the cell which has a negative membrane potential). Activation of AMPA receptors leads to a continued influx of Na^+ ions into the cell which leads to a decrease in membrane potential (partial depolarization). This depolarization removes Mg^{2+} , since the charge of the neuronal membrane is now much less negative. At this stage, Ca^{2+} ions can freely enter the cell via the NMDA receptor channel and initiate a number of enzymatic processes that are involved in the fixation of increased synaptic strength (neuronal memory formation).³³³

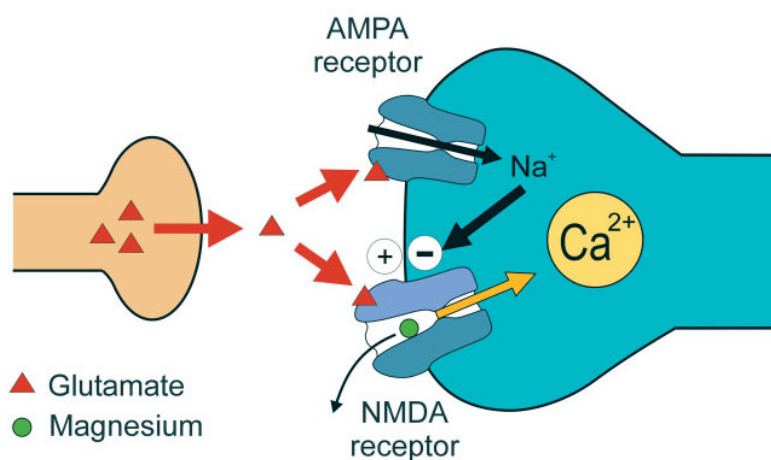


Figure 25: Activation of NMDA receptor.³³²

On the other hand, excessive activation of NMDA can also evoke neuronal dysfunction and even damage and death. This cell death caused by an excessive activation of glutamate receptors has been termed “excitotoxicity”^{334, 335} and is thought to contribute to a wide range of neurological disorders such as stroke and trauma, but also neurodegenerative diseases like AD.³³⁶ Overactivation of NMDARs results in an excessive opening of ion channels that causes an exaggerated Ca^{2+} influx, which can result in the production of damaging free radicals and activation of proteolytic processes that contribute to cell injury or death.^{337, 338, 339, 340, 341} The signaling cascade that leads to apoptosis

and cell death is summarized in **Figure 26**. The excessive Ca^{2+} influx (**a**) causes oxygen free-radical formation and activation of neuronal NOS that leads to nitric oxide ($NO\bullet$) and peroxynitrite ($ONOO^-$) production (**c**).^{342, 343, 344} Cytochrome-c is then released from mitochondria with the subsequent activation of pro-apoptotic enzyme such as caspases (**d**).^{345, 346} Moreover, NMDAR hyperactivation leads to the stimulation of the p38 mitogen-activated kinase

(MAPK)–MEF2C pathway (**b**) which activates transcription factors that can go into the nucleus to influence neuronal injury and apoptosis.³⁴⁷

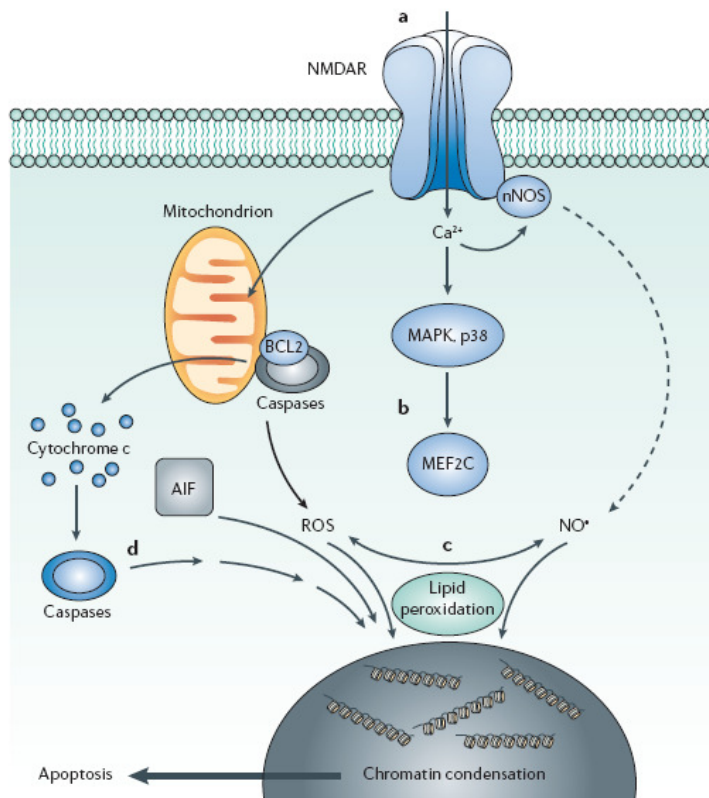


Figure 26: Scheme of the apoptotic cell injury and death pathways triggered by excessive NMDAR activity.³⁴⁸

There are several potential links between glutamate-mediated excitotoxicity and the main hallmarks of AD such as A β and hyperphosphorylated tau proteins. For example, A β destabilizes calcium homeostasis, increasing NMDA responses and therefore excitotoxicity.³⁴⁹

APP and A β have different effects on glutamatergic activity (**Fig. 27**). In fact, APP blocks NMDAR activity (**1**), and it enhances glutamate transport removing glutamate from the synaptic cleft (**2**). On the other hand, A β stimulates NMDA receptors (**3**) and it blocks glutamate uptake (**4**) thereby increasing glutamate concentrations in the synaptic cleft (**5**).^{350, 351, 352, 353, 354}

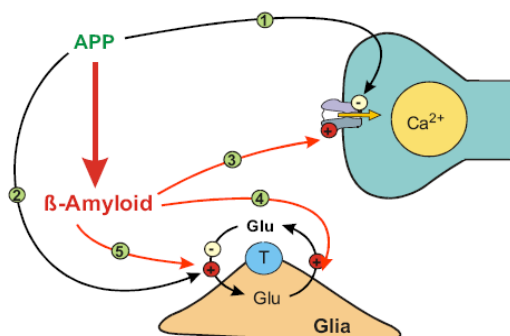


Figure 27: Effects of APP and A β on glutamatergic activity.³⁵⁵

Moreover, it was reported that glutamate transporters are down-regulated in AD and A β can either directly or indirectly inhibit glutamate reuptake or even enhance its release.³⁵⁶ Excessive NMDAR activity has also been reported to increase the hyperphosphorylation of tau, which contributes to NFTs.³⁵⁷

1.8.1 Memantine: a NMDA receptor uncompetitive fast off-rate inhibitor

Excitotoxicity represents an attractive target for neuroprotective efforts because it is involved in the pathophysiology of a wide variety of acute and chronic neurodegenerative disorders. However, the same processes that in excess lead to excitotoxic cell death, are at lower levels absolutely crucial for normal neuronal function. In fact, the blockade of NMDARs in the brainstem, an area responsible for wakefulness and attention, would cause drowsiness and even coma. It is therefore essential to preserve physiological NMDAR activity in order to maintain these normal functions and avoid intolerable clinical side effects. Consequently, to be clinically acceptable, an anti-excitotoxic therapy must block excessive activation of NMDARs while maintaining normal function intact. Drugs that simply compete with glutamate or glycine at the agonist-binding sites block normal function and therefore do not meet this requirement. Thus, they have failed in clinical trials to date, because of their severe and unacceptable side effects such as drowsiness, hallucinations and coma.^{358, 359}

Memantine (**Fig. 28**) is a drug approved by the European Union and the US FDA for the treatment of moderate-to-severe AD and since this time, it is on the market in Europe, USA and many other countries in the world.³⁶⁰

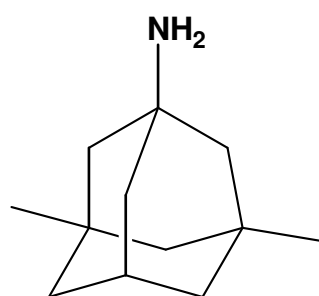


Figure 28: Memantine structure.

Memantine mechanism of action differs from that of the major therapies in AD which are all AChEIs (see 1.3.1). In fact, AChEIs offered only symptomatic relief, whereas memantine is thought to be the first neuroprotective drug that achieved clinical approval. It is a low-affinity, open-channel blocker, which is a drug that only enters the channel when it is excessively opened by agonist. Indeed, memantine blocks the excessive NMDAR activity while sparing normal

excitatory synaptic function.³⁴⁸ A low micromolar concentration of memantine blocks the effects of higher amounts of NMDAR agonist to a greater extent than the effects of lower concentration of agonist. This phenomenon can be explained by the fact that, as memantine blocks only open channels, more channels are blocked when more agonist is present. Thus, memantine is an example of a drug that has an “*uncompetitive*” mechanism of action. An *uncompetitive* antagonist can be distinguished from a *noncompetitive* antagonist. The latter is a compound that binds in a site that is different from the agonist-binding site. On the other hand, an *uncompetitive* drug is a receptor antagonist whose inhibitory action depends on prior activation of the receptor by an agonist. Memantine has also fast off-rate properties. It means that, although memantine is highly selective for the NMDAR, it has a low affinity for the receptor. It assures fast association and dissociation kinetics with the receptor during prolonged depolarization, restoring normal NMDA activity (Fig. 29). Lipton³⁴⁸ suggested that NMDAR activity can be compared to a television. The agonist sites act as the ‘on/off’ switch button of the television. Drugs that interact with agonist sites cut off all normal NMDAR functions and result in clinically unacceptable side effects. Instead, during excessive Ca²⁺ flux through the NMDAR, it would be necessary to regulate the volume control (or ‘volume’ of ion flow) of the NMDAR. Several experiments suggested that memantine possesses this mechanism of action.

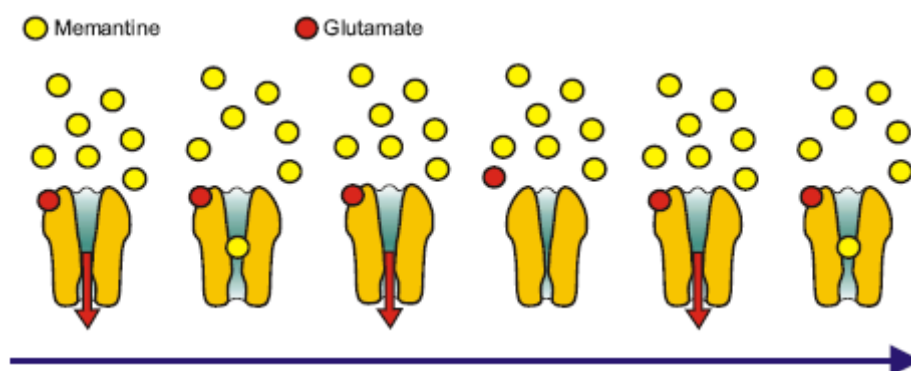


Figure 29: Fast blocking/unblocking channel properties of memantine.³⁵⁵

The **Fast Off-rate** and the **Uncompetitive** mechanism of memantine make this drug very tolerant compared to other NMDA-type receptor antagonists. Molecules that possess these both properties have been coined **UFO** drugs.

1.9 The role of G protein-coupled receptors in AD

G protein-coupled receptors (GPCRs) are the largest class of cell-surface receptors and play essential and crucial roles in every organ system.³⁶¹ GPCRs are involved in several key neurotransmitter systems in the brain that are disrupted in AD. GPCRs are membrane-bound proteins that are activated by extracellular ligands such as light, peptides, neurotransmitters and transducer intracellular signals via interactions with G proteins. The resulting change in conformation of the GPCR induced by ligand binding activates the G protein, which is composed by a heterotrimeric complex of α , β , and γ subunits. In their inactive state, G proteins are bound to guanosine 5-diphosphate (GDP). Activation of the G protein causes the exchange of guanosine 5-triphosphate (GTP) for GDP within the α subunit. Activated G protein subunits then modulate the function of various effector molecules such as enzymes, ion channels, and transcription factors. Inactivation of the G protein occurs when the bound GTP is hydrolyzed to GDP, resulting in reassembly of the heterotrimer. The most of GPCRs are often termed rhodopsin-like GPCRs and are structurally similar in that they consist of an extracellular N-terminal domain, seven transmembrane-spanning domains, and an intracellular C-terminus domain.

Current AD drugs target AChE which stimulates cholinergic system. However, neurodegeneration does not involve a specific neurotransmitter system. Glutamatergic, serotonergic, adrenergic and peptidergic neurotransmitter systems are also involved in the pathology of AD. The cleavage of APP by α -, β -, and γ -secretases, A β deposition and amyloid plaque formation are regulated by GPCRs. In this section it is discussed the involvement of GPCRs in the amyloid cascade and the pharmacological approaches to target the putative therapeutic properties of AD-associated GPCRs.

1.9.1 Metabotropic glutamate receptors

Glutamate is the transmitter of the vast majority of the fast excitatory synapses in the mammalian CNS and plays an important role in a wide variety of CNS functions.³⁶² In the past, the actions of glutamate in mammalian brain were thought to be mediated exclusively by activation of glutamate-gated cation channels termed ionotropic glutamate receptors (iGluRs). However, in the mid 1980s, it was discovered that glutamate interacts also with metabotropic glutamate receptors (mGluRs), which are coupled to effector systems through GTP-binding proteins.

mGluRs are divided into three groups: group I (mGluR1 and mGluR5), group II (mGluR2 and mGluR3) and group III (mGluR4, mGluR6, mGluR7 and mGluR8).³⁶³ In general, group I mGluRs couple to G_q and activate PLC, resulting in the hydrolysis of phosphoinositides and

generation of IP3 and DAG. This classical pathway leads to calcium mobilization and activation of PKC. They are thought to participate in the regulation of synaptic plasticity and postsynaptic glutamatergic excitability.^{364, 365} In contrast to group I mGluRs, group II and group III mGluRs are coupled to G_i proteins that inhibit adenylyl cyclase and cAMP production. It is becoming increasingly appreciated that group II and group III mGluRs also couple to other signaling pathways, including activation of MAPK and PI3K pathways.³⁶⁶ Group I mGluRs-linked PLC activity is downregulated in the cerebral cortex of AD patients.³⁶⁷ By contrast mGluR2 is overexpressed in the hippocampus of patients with AD and its activation leads to tau phosphorylation.^{368, 369} Kim et al.³⁷⁰ showed that group I mGluR stimulation leads to activation of α - and β -secretases, accumulation of C83 and C99, respectively, and increased release of A β 40 (**Figure 30**). The 40 amino acid isoform of A β seems to be antiamyloidogenic *in vivo*.¹¹⁸ Similar to group I mGluRs, group II mGluR stimulation activates the α - and β -secretases. However, group II mGluR stimulation causes the release of A β 42. On the other hand the 42 amino acid isoform of A β seems to aggregate into amyloid much more rapidly than A β 40 *in vitro*. In fact, A β 42 is the predominant isoform of A β that accumulates in the brains of patients with AD and it is essential for seeding A β deposition *in vivo*.^{371, 372}

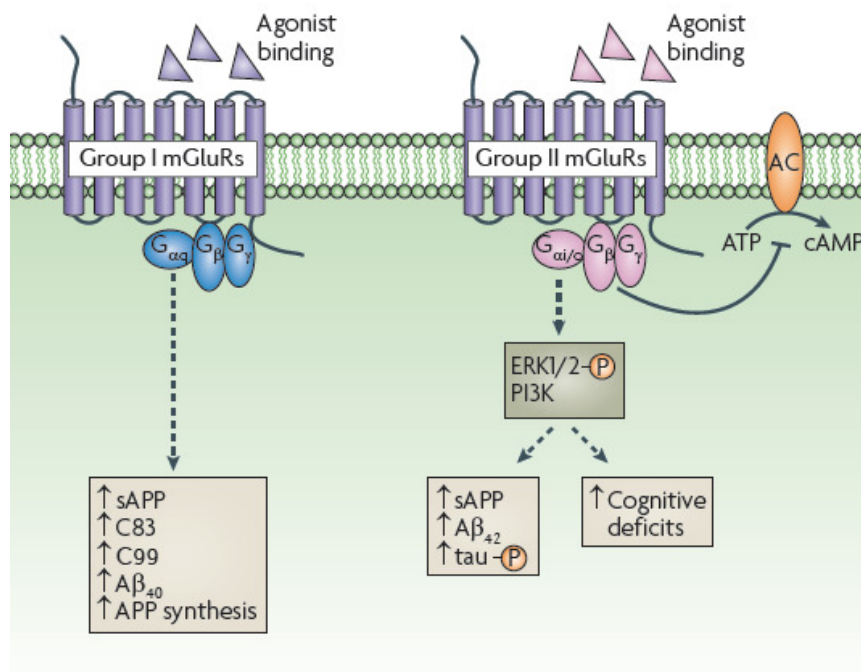


Figure 30: mGluRs signaling pathway.³⁷³

Thus, A β 42 production could be blocked with a specific group II mGluR antagonist, whereas upregulation of group I mGluR signaling may increase synaptic A β 40 generation. Moreover, group II mGluR inhibitors seem to enhance hippocampus-dependent cognitive functions in

rodents.³⁷⁴ Only two drugs are currently in development as mGluR antagonists for the treatment of AD. ADX71149 is in Phase II as an mGluR2 antagonist and BCI-838 is in preclinical phase as a mGluR2/R3 antagonist.¹²²

1.9.2 5-Hydroxytryptamine receptors

Several lines of evidence suggest that 5-hydroxytryptamine (5-HT also known as serotonin) signaling pathway is impaired in AD. Therefore, the serotonergic system appears to be a particularly attractive target, because it has been involved not only in cognitive processes but also in depression, psychosis, and aggression.³⁷⁵

5-HT₄ receptors are highly expressed in the hippocampus, basal ganglia and amygdala.³⁷⁶ Brains of AD patients display a reduction in the number of 5-HT₄, therefore they might be involved in the memory and cognition deficits in AD.³⁷⁷ It was shown that *in vitro*³⁷⁸ and *in vivo*³⁷⁹ stimulation of 5-HT₄ leads to an increase in the soluble fragment sAPP α and ACh release (**Fig. 31**). Stimulation of ACh in rat frontal cortex improves cholinergic function which is important for memory acquisition and retention. To date, it is still unclear whether the effects of 5-HT₄ receptors on APP metabolism are directly linked to an increase in the activity of the α -secretase or an effect on the trafficking of APP. Moreover, the 5-HT₆ receptor class of serotonin receptors has received the most attention in recent years because the blockade of 5-HT₆ seems to attenuate both the cognitive and the behavioral abnormalities of AD via modulation of multiple neurotransmitters and synaptic plasticity (**Fig. 31**). In particular, *in vivo* it was shown that the administration of a 5-HT₆ antagonist is able to increase ACh release.³⁸⁰ Moreover, it is reported^{381, 382} that 5-HT₆ antagonists reversed the amnesic effects of anticholinergic drugs and have been shown to be effective in diverse learning paradigms, all of which may depend on ACh transmission. Many of the findings on 5-HT₆ receptor interactions demonstrate a complex relationship with excitatory amino acids. Thus, it was shown that the blockade of 5-HT₆ increases the release of glutamate in the cortex and in the hippocampus.³⁸³ 5-HT₆ receptor antagonists are in clinical development for cognitive disorders. For example, SGS518/LuAE58054 reached with success Phase III trials and AVN-211 and Syn-120 are in Phase I.¹²²

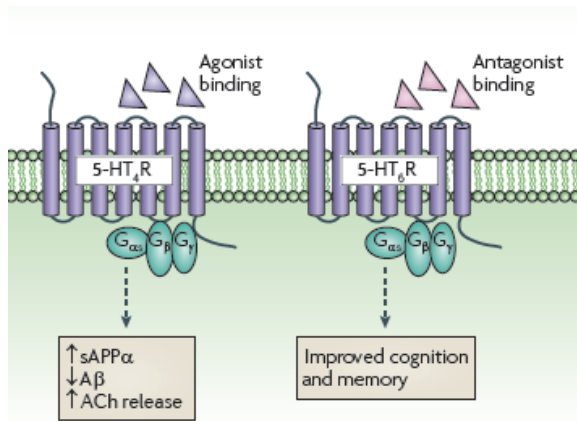


Figure 31: 5-Hydroxytryptamine signaling pathway.³⁷³

1.9.3 β_2 -adrenergic receptors

β_2 -adrenergic receptors (β_2 -ARs) are typical GPCRs, expressed in hippocampus and cortex,³⁸⁴ the main brain regions involved in AD. Activation of β_2 -ARs enhances γ -secretase activity and results in increased A β 40 and A β 42 production. Thus, *in vivo* and *in vitro*, treatment with β_2 -AR agonists increased amyloid plaque formation. On the other hand, treatment with β_2 -AR antagonists reduced A β production. The γ -secretase activity regulation by β_2 -ARs is independent of cAMP signaling pathway but correlates with receptor endocytosis. It has been suggested that β_2 -AR constitutively associates with γ -secretase by directly binding to PS1 at the plasma membrane. Once agonist treatment induces endocytosis of β_2 -ARs, endocytosis of PS1 occurs, leading to the traffic of PS1 to the late endosomes and lysosomes systems which provide an optimal environment for γ -secretase activity.³⁸⁵

It is known that environmental influences activate β_2 -ARs. Stress has been recently determined to be a risk factor for AD³⁸⁶ because can elevate the concentration of endogenous β_2 -AR ligands epinephrine and norepinephrine.³⁸⁷ The abnormal activation of β_2 -ARs, which could result from the response to stress, might contribute to A β accumulation. As β_2 -AR antagonists are widely used in the treatment of cardiovascular disease, these results suggest the use of β_2 -AR antagonists to decrease the incidence of AD pathogenesis.

1.9.4 Adenosine A_{2A} receptors

Adenosine receptors are GPCRs whose endogenous ligand is adenosine. In humans, there are four types of adenosine receptors classified as A_1 , A_{2A} , A_{2B} and A_3 . A_{2A} Rs are by far the most abundant in the mammalian brain. The interest for the A_{2A} subtype is growing because of its potential involvement in several diseases like, schizophrenia, anxiety, depression and neurodegenerative diseases. In fact, A_{2A} Rs in striatal neurons seem to control the dopaminergic

signaling.³⁸⁸ However, there is currently a major interest in the ability of A_{2A} receptors to regulate glutamate release. This makes A_{2A}Rs a good target for the modulation of synaptic plasticity at glutamatergic synapses. Thus, A_{2A}R-deficient mice display improved spatial recognition memory,³⁸⁹ whereas *in vivo* overexpression of the A_{2A}R leads to memory deficits.³⁹⁰ Caffeine is the most widely consumed psychoactive drug. Some of the most evident effects of caffeine, such as its psychomotor effects or its memory enhancing effects, are now recognized to be due to its ability to antagonize adenosine A_{2A} receptors. Interestingly, caffeine consumption has been found to reduce the incidence of AD.³⁹¹ Thus, caffeine reduces the expression of both PS1 and BACE in caffeine-treated transgenic mice accompanied by a modest reduction of Aβ₄₀ and Aβ₄₂ generation.³⁹² Furthermore, it is protective against Aβ-induced neurotoxicity in cultured neurons of rats³⁹³ and against Aβ-induced cognitive impairments in mice (**Figure 32**).³⁹⁴ Collectively, these findings suggest that the adenosinergic system is a promising therapeutic avenue to target AD.

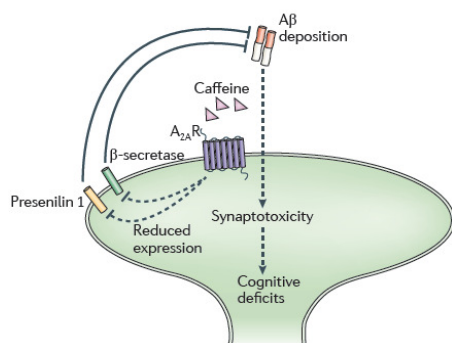


Figure 32: Adenosine A_{2A} receptor and Aβ-mediated toxicity.³⁷³

1.9.5 M₁ muscarinic receptors

Muscarinic receptors, a family of five GPCR subtypes (M₁-M₅), have been implicated in the pathophysiology of major diseases of the CNS, including AD. They are composed by seven transmembrane regions. M₁, M₃ and M₅ mAChRs activate G proteins of class G_q that activate PLC, which in turn hydrolyzes phosphatidylinositol 4,5-bisphosphate (PIP₂) to DAG and IP₃. DAG acts as a second messenger that activates PKC, while IP₃ increases the cytosolic concentration of Ca²⁺ (**Figure 33**). On the other hand, M₂ and M₄ activate G_i that inhibits adenylate cyclase activity, decreasing the production of cAMP from ATP, which, in turn, results in decreased activity of cAMP-dependent protein kinases (**Figure 33**).

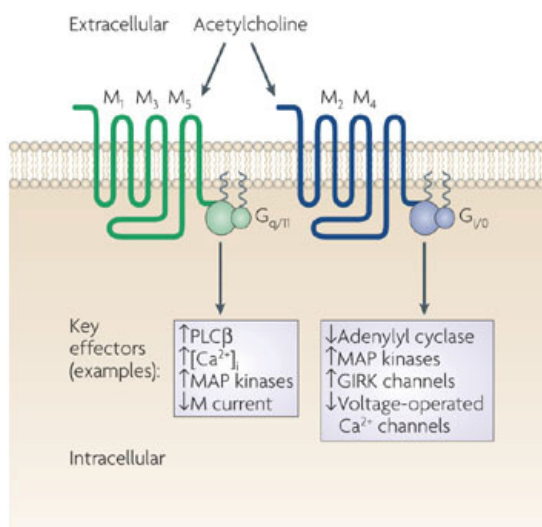


Figure 33: Intracellular signaling pathway of mAChRs.³⁹⁵

The M₁ mAChR is predominant in cerebral cortex and hippocampus, two major brain regions that develop amyloid plaques and NFTs in AD. Postsynaptic M₁ mAChRs have a major role in hippocampal-based memory and learning, regulation of cognition and psychosis and in particular in short-term memory, which is impaired in AD.^{396, 397} M₁ is a promising target because activation of this receptor seems to have beneficial effects on the three major hallmarks of AD (cholinergic hypofunction, Aβ and tau neuropathology). Therefore, M₁ stimulation might possess not only beneficial effects on memory and cognitive deficits, but also disease-modifying properties.^{398, 399} In the past, many efforts have been focused on the synthesis of highly selective mAChRs orthosteric agonists to improve cognitive impairment in AD patients. Representative chemical structures are shown in **Figure 34**. Unfortunately, all the mAChR agonists presented below exhibit nonselective profiles of binding affinities across the different mAChR subtypes, because they target the highly conserved ACh binding site. Despite they revealed good effects on cognition and memory in Phase II and III, their clinical developments have failed due to serious side effects.^{400, 401}

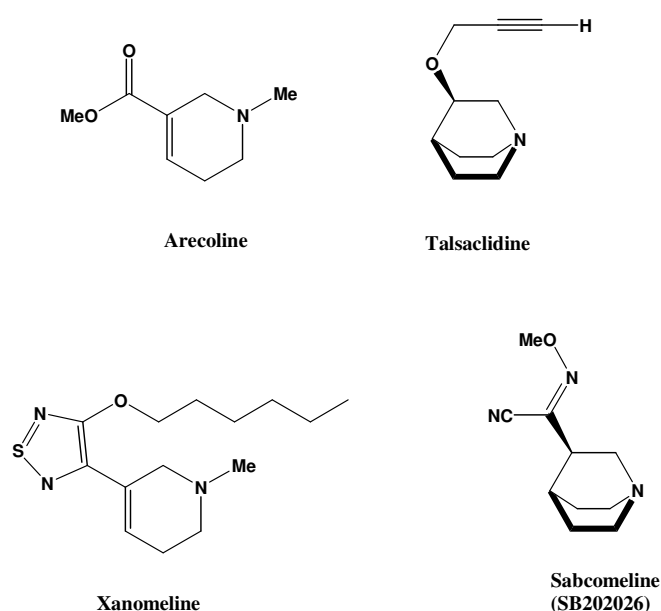


Figure 34: Representative structures of orthosteric mAChRs.

However, to date, targeting the M_1 subtype is considering an attractive tool for the treatment of AD. In this section, evidences of the linkage between M_1 , cholinergic hypofunction, amyloid aggregation and tau hyperphosphorylation are reviewed:

A Modulation of $A\beta$ levels via M_1 mAChRs

Stimulation of M_1 can increase formation of the neuroprotective and neurotrophic α -APPs, preventing the formation of $A\beta$.^{185, 402, 403} The decrease of $A\beta$ was reported in many *in vitro* systems following treatment with muscarinic agonists.^{404, 405} Stimulation of M_1 activates PKC- and MAPK- pathways that lead to activation of α -secretase,^{406, 407} the enzyme responsible of the non-amyloidogenic pathway of APP processing (**Figure 35**). The α -secretase involved in M_1 -mediated effect is ADAM17⁴⁰⁸ (or TACE) activated by PKC isoforms α and ϵ .⁴⁰⁹ Recently, also BACE-1 has been found to be regulated by M_1 mAChR. Its level was found to be elevated in sporadic AD brains. It was shown, *in vitro*⁴¹⁰ and *in vivo*,⁴¹¹ a reduction in BACE-1 activity after M_1 activation. Jiang et al.⁴¹⁰ suggested that M_1 mAChRs directly interacts with BACE-1 and thereby regulate its level through promoting the ubiquitin-proteasome degradation of BACE-1. Moreover, overexpression and downregulation of M_1 mAChRs decreases and increases the level of BACE-1 and the generation of $A\beta$, respectively.

Activation of M_3 mAChRs also elevates α -APPs secretion but M_1 stimulation is preferable to prevent peripheral side effects mediated by the M_3 subtype.¹⁸⁵ M_2 and M_4 mAChRs are not effective in elevating α -APPs and M_2 may even have an inhibitory effect on α -APPs release. This may be one of the major disadvantages of AChEIs vs direct acting M_1 agonists, since AChEIs,

due to the inhibition of AChE, elevate synaptic ACh that can activate all receptor subtypes, including the inhibitory M_2 and M_4 .¹⁸⁵ Thus, any possible elevation of α -APPs via activation of M_1 , may be inhibited by M_2 activation.

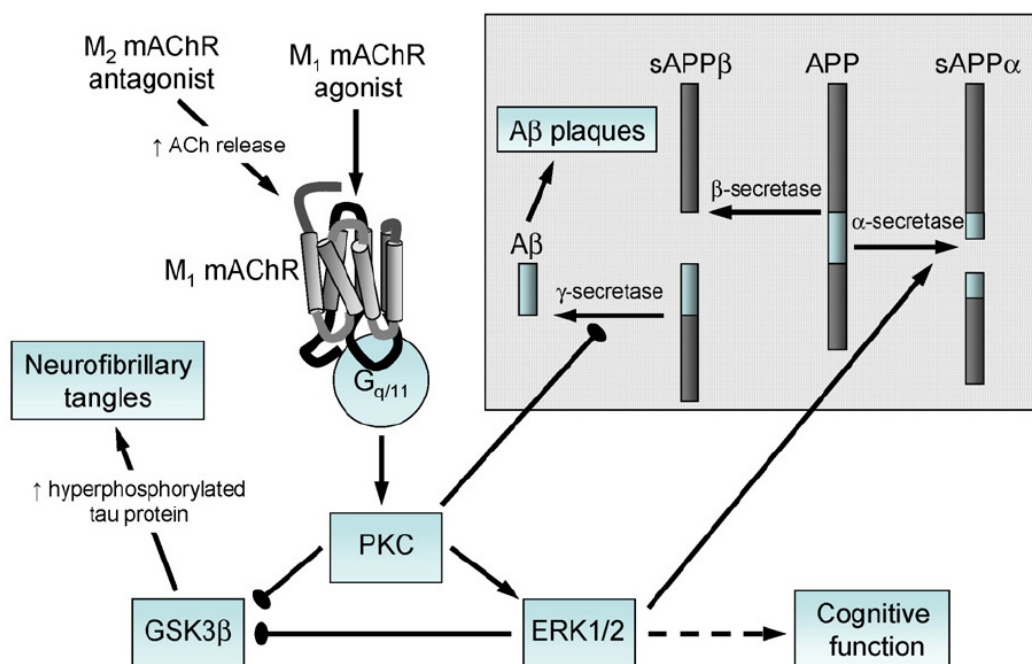


Figure 35: Various effects that can be modulated by activation of M_1 mAChRs.⁴¹²

Many efforts have been made in developing selective M_1 orthosteric agonists. However, some agonists showed disappointing clinical results in AD. This may be attributable to one or more of the followings reasons: lack of selectivity for the M_1 subtype, low bioavailability, extensive metabolism, and low safety margin.^{413, 414} In fact, selectivity for an mAChR subtype *in vitro* is not always reflected into good selectivity *in vivo* and a good bioavailability/pharmacokinetic profile. Indeed, xanomeline was highly selective *in vitro*, but it exhibited bad pharmacokinetics and poor selectivity *in vivo* with high incidence of side effects in AD patients.⁴¹⁵

Over the years selective partial M_1 orthosteric agonists were developed. These include AF102B (**Cevimeline**, **EVOXACT™**) prescribed in USA and Japan for the treatment of Sjogren's syndrome, AF150(S) and AF267B (**Figure 36**).^{415, 416}

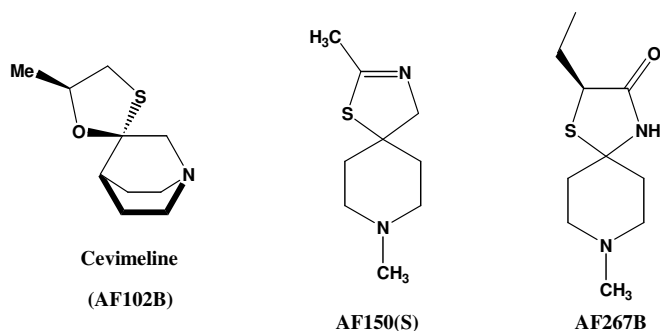


Figure 36: Structure of AF102B, AF150(S) and AF267B.

These agonists, in particular AF267B, do not cause down regulation of M_1 mAChRs following chronic administration. They penetrate the BBB restoring learning and memory impairments in several animal models. Studies *in vivo* confirm the linkage between the M_1 stimulation and A β metabolism. In rabbits, where the sequence of A β 42 is similar to humans, treatments with AF102B decreased A β 40, while AF267B and AF150(S) reduced levels of both A β 42 and A β 40 in the cerebrospinal fluid (CSF) and all three M_1 agonists decreased cortical A β 42.⁴¹⁶ Moreover, chronic treatment with AF102B significantly decreased CSF A β in AD patients.⁴¹⁷ Physostigmine (an AChEI) and hydroxychloroquine (an anti-inflammatory drug) did not reduce CSF A β levels when tested in AD patients in the same study as AF102B. Nitsch et al.⁴¹⁷ suggested that the reduction in A β production can be explained by an indirect inhibitory effect on γ -secretase via M_1 mAChR-mediated phosphorylation of PS-1. However, more studies will be required to better investigate the correlation between M_1 activation and γ -secretase.

In rat cortical and hippocampal primary cell cultures, AF150(S) and AF267B were more potent in elevating α -APPs than carbachol (CCh), oxotremorine (OXO-M) and physostigmine.⁴¹⁶ After exposure of neurons from spinal cord to muscarinic agonists, any increase in α -APPs was detected, as these neurons do not contain M_1 mAChRs. Thus, from these results we can envisage that the M_1 mAChR activation has a major role in α -APPs elevation.⁴¹⁶

In transgenic (3xTg-AD) mice, dicyclomine, a relative selective M_1 muscarinic antagonist, caused a significant increase in A β deposition, BACE-1 and GSK-3 β activity and a decrease in ADAM-17 activity. On the other hand, treatment with AF267B reduced the major hallmarks of AD. Thus, it improved the memory impairment, decreased A β 42, BACE-1 activity and tau hyperphosphorylation and increased steady-state level of ADAM17 and PKC.⁴¹¹

Taken together, these data suggest a tight correlation between the cholinergic and amyloid hypothesis. M₁ selective activation, due to its beneficial effects on the hallmarks of AD, can be considered the first disease-modifying treatment.

Great efforts have been devoted to developing β - and/or γ -secretase inhibitors as a rationale therapy in AD. However, inhibition of β - and/or γ -secretase alone, could lead to accumulation of APP or C99 if the α -secretase remained unmodified. M₁ selective agonists can prevent this drawback because of their dual properties; activation of α -secretase and inhibition of γ -secretase and BACE-1.

B *Modulation of hyperphosphorylated tau protein via M₁ mAChRs*

Activation of M₁ decreases tau phosphorylation as shown *in vitro*^{418, 419} and *in vivo*.^{420, 411} This effect is mediated via activation of PKC-pathway, leading downstream to a decrease in GSK-3 β activity. In 3xTg-AD mice with PS, APP and tau mutants, chronic administration of AF267B reduced the level of hyperphosphorylated tau. Moreover, it was found a decrease in the activity of GSK-3 β compared to the control. In contrast, dicyclomine (an M₁ antagonist) led to an increase of GSK-3 β activity and hyperphosphorylated tau.⁴¹¹

C *Modulation of cognitive impairment via M₁ mAChRs*

AF150(S) and AF267B restored memory and learning deficits in several animal models that mimic AD pathology. 3xTg-AD mice were tested in the Morris water maze after AF267B treatment. It was found that the time to reach the hidden platform was substantially reduced compared to not-treated 3xTg-AD.⁴¹¹ Moreover, ablation of M₁ mAChRs in the 3xTgAD and triple mutant APP (Tg-SwDI) mice exacerbated the cognitive impairment.⁴²¹ Medeiros et al.⁴²¹ found that deletion of M₁ mAChRs resulted in impairment of c-Fos and p-CREB signaling in AD-like mouse brain. c-Fos and p-CREB are transcriptional factors considered key mediators of stimulus-induced nuclear responses that underlie the development, function, and plasticity of the nervous system.^{422, 423}

These data confirm that M₁ mAChRs are key receptors involved in memory and learning processes.

1.9.5.1 *Allosteric ligands*

In the past, several attempts have been made to generate compounds which are selective for the M₁ subtype. However, many of these efforts have failed because these first generations of muscarinic agents bind to the highly conserved orthosteric ACh binding site. For example,

AF267B was suggested to have selective agonist activity at M₁ during its initial screening.⁴¹¹ However, when evaluated across multiple systems, AF267B was found to have activity at M₃ and M₅ receptor subtypes.⁴²⁴ Selective targeting of M₁ mAChRs for the development of novel drugs has proven challenging because the high degree of homology of the orthosteric agonist binding site among the five mAChR subtypes. Allosteric modulation of GPCRs represents a valid alternative for identifying subtype selective ligands because it is thought that allosteric binding sites are less conserved than the orthosteric binding sites (**Fig. 37**).

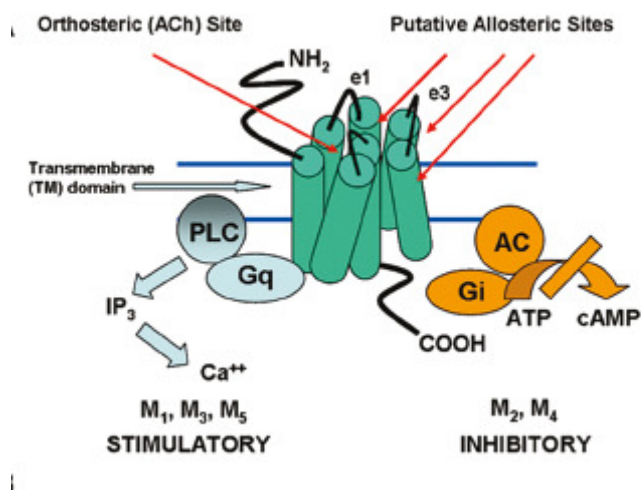


Figure 37: Schematic representation of a mAChRs showing orthosteric and putative allosteric binding sites and effector mechanisms.⁴²⁵

Recently, several allosteric compounds, both positive allosteric modulators (PAMs) and allosteric agonists, have been identified. PAMs are unable to activate receptors directly, but their binding potentiates the effect of ACh through enhancement of the affinity of ACh for its site and/or through increased coupling efficiency to the G-proteins. In contrast, allosteric mAChR agonists bind to an allosteric site on the receptor and can directly activate the receptor in the absence of ACh. They have the potential to stabilize unique receptor conformations, which may in turn cause differential activation of signal transduction pathways.

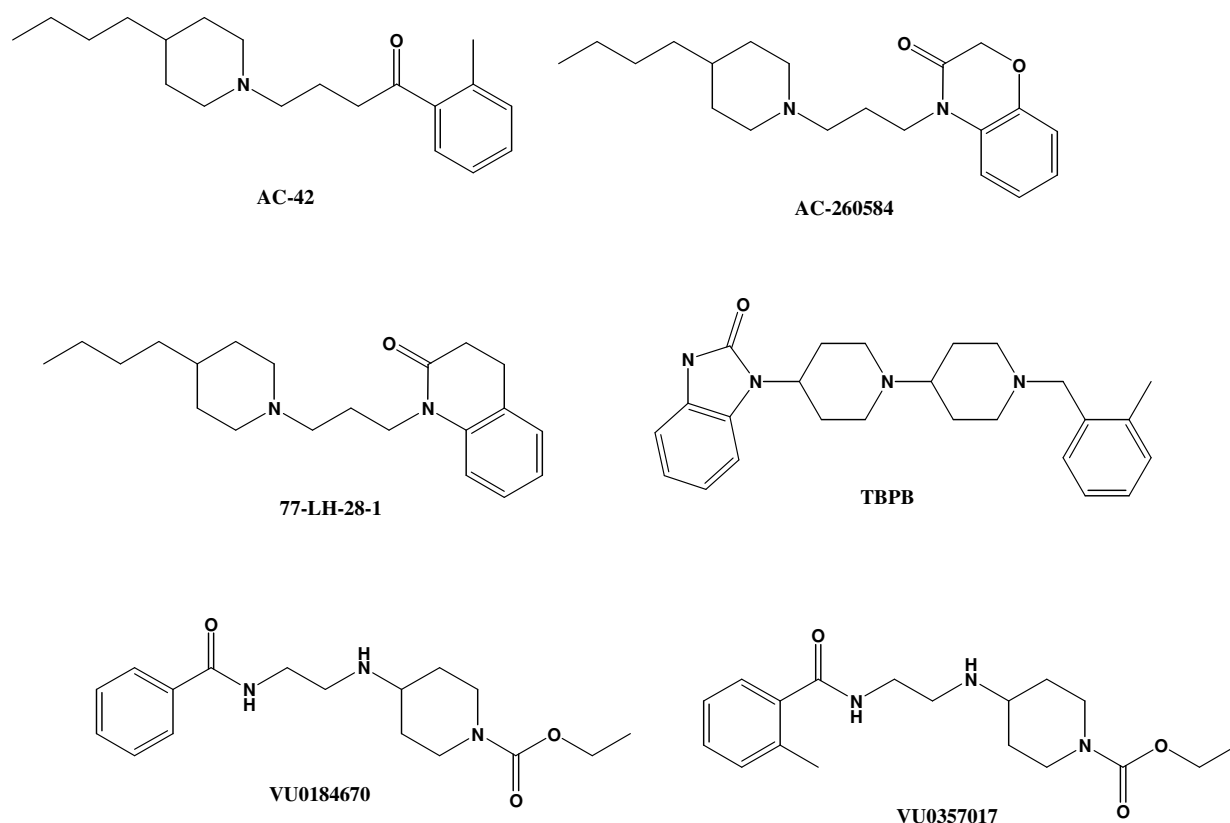


Figure 38: Structures of allosteric M₁ muscarinic agonists.

AC-42 (**Fig. 38**) was the first allosteric agonist described for the M₁ mAChRs.^{426, 427, 428} Using a series of chimeric receptors, AC-42 was shown to activate M₁ receptors at a region that is clearly distinct from the orthosteric ACh binding site and involves N terminus-TM1 and extracellular loop 3-TM7 regions.⁴²⁶ The residues in these regions are not conserved among the muscarinic subtypes, which probably accounts for the selectivity of AC-42. On the other hand, ACh interacts with the orthosteric site that is embedded in the transmembrane domains of the receptor and involves TM3, TM5 and TM6.⁴²⁹ TM3 plays a crucial role in this orthosteric site and is believed to be essential in activation mechanism of mAChRs and many other GPCRs.⁴³⁰ Moreover, ACh is thought to bind to TM3 through a binding salt bridge believed to exist between the choline head group of ACh and aspartate-105 (Asp₁₀₅). Receptor binding of classic agonists such as CCh (a nonselective muscarinic orthosteric agonist), is mediated largely through interactions with two highly conserved residues, tyrosine-381 and asparagine-382 in TM6.^{431, 432} Spalding et al.⁴²⁶ demonstrated that the potency of AC-42 was not significantly attenuated by either of the point mutations Y381A or N382A in TM6. Differently, these mutations abolished the agonist activity of CCh. This result prompted the authors to categorize AC-42 as an “ectopic” agonist, in the knowledge that its binding site is partially or totally distinct from that for CCh.

The investigation of the mode of interaction of AC-42 with various orthosteric ligands confirmed that AC-42 exhibited characteristics associated with allosteric ligands.⁴²⁷ For example, in functional assays, atropine inhibited M₁ receptor-mediated calcium mobilization in a manner completely consistent with orthosteric antagonism, when tested against the classic orthosteric agonist CCh (**Fig. 39 A**). Moreover, Schild slope was not significantly different from unity over concentrations of antagonist spanning six orders of magnitude. On the other hand, the translocation of the AC-42 concentration-response curve by atropine (**Fig. 39 B**) led to Schild slopes significantly less than unity (0.69 ± 0.01) indicating that the antagonism does not reflect a simple orthosteric interaction. Schild slopes that deviate significantly from unity reflects the saturability of negative allosteric interaction, i. e. increasing of the concentration of one ligand results in a progressive inability to further antagonize the other ligand.⁴³³

To validate this mechanism of interaction, [³H] N-methyl scopolamine ([³H]NMS) inhibition binding studies, were performed. The radioligand [³H]NMS was used as an orthosteric-site “probe”. NMS is a well-known muscarinic orthosteric antagonist. Both atropine and pirenzepine fully inhibited specific [³H]NMS binding at radioligand concentrations of either 0.2 nM or 2 nM (**Fig. 40 A**), as expected for simple orthosteric antagonism. On the other hand, AC-42 was unable to expel [³H]NMS from the orthosteric binding site. This was more marked when the concentration of radioligand was increased 10-fold (**Fig. 40 B**). This effect confirms that AC-42 interacts in a site that is different from ACh binding site. For comparison, the same experiment was also performed with the well characterized and prototypical negative mAChR allosteric modulator gallamine. As expected, gallamine also inhibited the specific binding of the radioligand [³H]NMS (**Fig. 40 B**). It is evident that the inhibition of AC-42 is more notable when the concentration of [³H]NMS was 10-fold higher. This can be explained by the fact that allosteric ligands can have effects on the binding of the orthosteric ligands. The saturability in the allosteric site becomes more evident when the concentration of orthosteric radioligand is increased.⁴³⁴

Allosteric modulators of GPCRs cause a conformational change in the receptor and they may alter the equilibrium of radioligand binding by reducing its rate of association and affecting its dissociation.⁴³⁵ An altered dissociation rate is unequivocally indicative of an allosteric action: the dissociation of a radioligand–receptor complex can only be modified by the binding of a compound to a site distinct from the radioligand binding site. Therefore, [³H]NMS dissociation binding studies were also performed to validate the allosteric character of AC-42. As shown in **Figure 41** the presence of gallamine (1 mM) produced a marked retardation of [³H]NMS dissociation. It is noteworthy that AC-42 (100 μM) also significantly slowed the rate of

[³H]NMS dissociation, although this effect was much less marked than that for gallamine. The reason of this behavior depends from the concentration used for AC-42 that is close to its solubility limits. Thus it was not possible to determine the maximum extent of its ability to retard [³H]NMS dissociation. Nonetheless, the ability of AC-42 to significantly alter the dissociation rate of [³H]NMS confirmed that it binds to a site that is topographically distinct from the orthosteric binding site. Despite these promising results, the *in vivo* use of AC-42 has remained in question.⁴³⁶

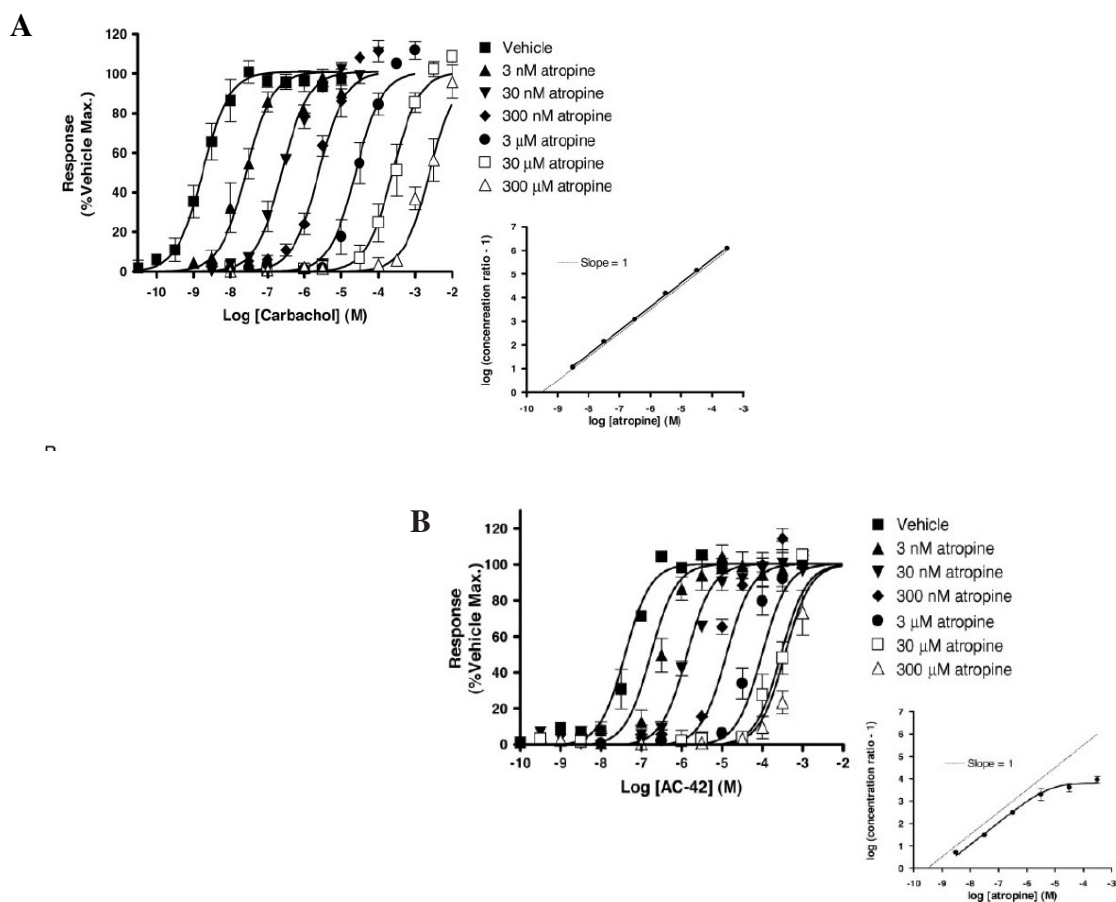


Figure 39: Concentration-dependent antagonism of CCh-stimulated (A) or AC-42-stimulated (B) calcium mobilization in CHO-hM1 cells by atropine (3 nM–300 μM) with inset Schild regressions.⁴²⁷

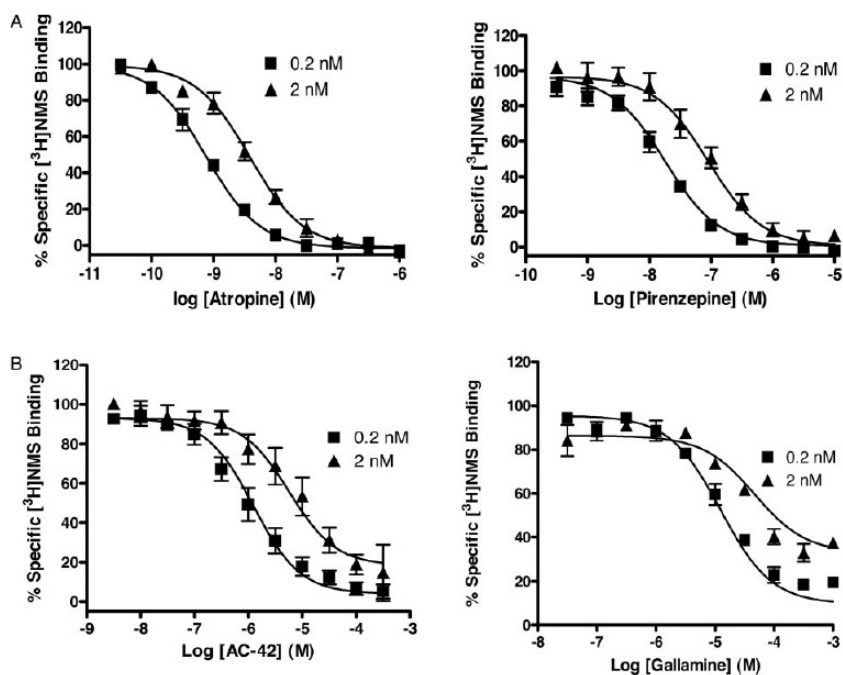


Figure 40: Inhibition of 0.2 and 2 nM $[^3\text{H}]$ NMS binding in CHO-hM1 cell membranes by atropine or pirenzepine (A) or AC-42 or gallamine (B).⁴²⁷

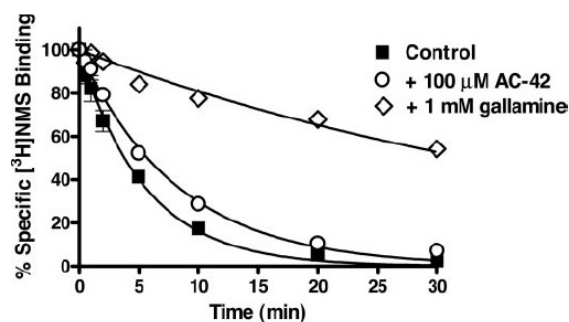


Figure 41: Effect of AC-42 (100 μM) or gallamine (1 mM) on atropine (1 μM)-induced dissociation of $[^3\text{H}]$ NMS from CHO-hM1 cell membranes.⁴²⁷

An additional structure analog of AC-42, AC-260584 (**Fig. 38**) was also recently reported as an orally bioavailable M_1 allosteric agonist with antipsychotic and cognitive enhancing effect. Acute systemic administration of AC-260584 significantly reversed amphetamine and MK-801-induced hyperlocomotion and apomorphine-induced climbing, two animal models predictive of antipsychotic efficacy.⁴³⁷ Interestingly, AC-260584 also improved the performance of mice in the Morris water maze, a measure of hippocampal-dependent spatial memory.⁴³⁸

Another active M_1 allosteric agonist, 77-LH-28-1, was discovered as a structural analog of AC-42.⁴³⁹ 77-LH-28-1 is selective for M_1 but it has also weak agonist activity at M_3 at higher concentrations. Site-directed mutagenesis studies revealed that 77-LH-28-1 acts as a *bi-topic* ligand i.e. it binds to an allosteric site that partially overlaps the orthosteric site.⁴⁴⁰ Moreover,

pharmacokinetic and *in vivo* electrophysiological studies demonstrated that 77-LH-28-1 is able to penetrate into the CNS after subcutaneous administration and it activates M₁ mAChRs to stimulate CA1 cell firing *in vivo*.⁴³⁹ Recent studies have also shown that 77-LH-28-1 can enhance NMDA-mediated neuronal excitation in the rat hippocampus.⁴⁴¹

Recently, TBPB (**Fig. 38**) was found to be a selective M₁ allosteric agonist.⁴⁴² It has high affinity on the M₁ subtype and no detectable agonist activity at other mAChR subtypes (**Fig. 42**).⁴⁴³ Jones et al.⁴⁴⁴ evaluated the effects of TBPB in a cell line expressing the M₁ receptor containing a mutation (tyrosine 381 to alanine: Y381A) in the orthosteric binding site. CCh lost completely its effect at M₁ Y381A at concentrations that fully activated the wild type (wt) M₁ receptor. In contrast, increasing concentrations of TBPB activated the mutant M₁ with an EC₅₀ similar to the wt M₁ mAChR, indicating that TBPB is not acting at a site identical to the orthosteric binding site. Using chimeric receptors, it was also established that TBPB and AC-42 share the same binding pocket adjacent to the orthosteric binding site.⁴⁴⁵

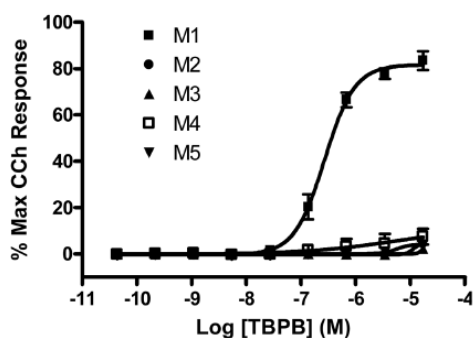


Figure 42: Concentration response curves for TBPB at M₁–M₅. M₁ EC₅₀= 289 nM, 82% CCh Max.

To further evaluate the effects of TBPB at the allosteric binding site of M₁, the effects of TBPB on M₁ activation in the presence of increasing concentrations of the nonselective orthosteric mAChR antagonist atropine were determined. As shown in **Fig. 43 A**, increasing concentrations of atropine (1-10 nM) competitively antagonized the action of CCh at the M₁ receptor. On the other hand, increasing concentrations of atropine (0.3-3.0 nM) produced a robust decrease in the maximum effect of TBPB at M₁, consistent with a noncompetitive interaction (**Fig. 43 B**).

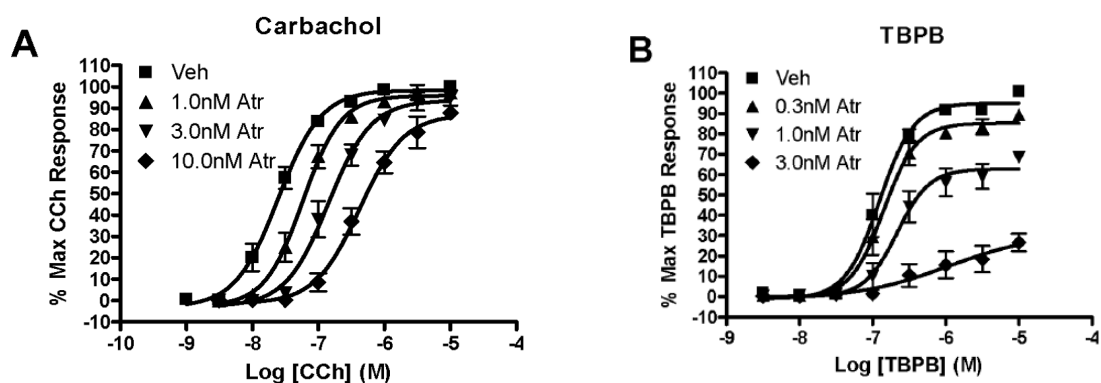


Figure 43: Effects of atropine in antagonizing CCh and TBPB at M_1 .⁴⁴⁴

Moreover, Jacobson et al.⁴⁴⁵ investigated the allosteric interactions of TBPB at the M_1 subtype through kinetic experiments of [3 H]NMS dissociation. As reported in **Figure 44**, the orthosteric ligand atropine (1 μ M) is able to displace [3 H]NMS with a $t_{1/2}$ of 12 min. In contrast, the classic muscarinic allosteric compound gallamine drastically slowed the atropine-induced dissociation of [3 H]NMS ($t_{1/2}$ = 97 min). Similarly, TBPB (100 μ M) showed a significant retardation of [3 H]NMS dissociation with a $t_{1/2}$ of 20 min.

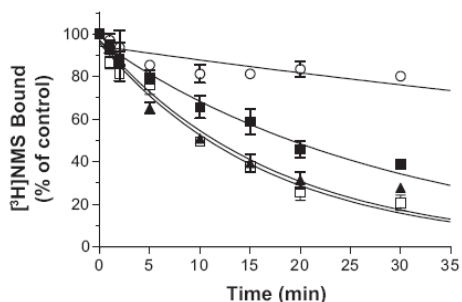


Figure 44: Effect of TBPB (100 μ M; ■), gallamine (1 mM; ○) and clozapine (10 μ M; ▲) on the atropine-induced dissociation of [3 H]NMS binding to human M_1 receptor expressed on CHO-K1 membranes. Atropine alone (1 μ M; □).⁴⁴⁵

Taken together, these findings provide support for hypothesis that TBPB is an allosteric agonist. Furthermore, recent studies revealed that TBPB increases non-amyloidogenic APP processing, reducing $A\beta$ production *in vitro*.⁴⁴⁴ Interestingly, TBPB potentiates also NMDA receptor currents in CA1 hippocampal pyramidal cells.^{444, 446} An important effect of activation of the M_1 subtype in the hippocampus and other brain regions is the potentiation of currents through the NMDA subtype of the glutamate receptor.⁴⁴⁷ Potentiation of NMDAR currents is thought to be important for both cognition and psychosis and has been postulated to play a role in the antipsychotic effects of mAChR agonists.

Finally, VU0184670 and VU0357017 (**Fig. 45**) have been recently discovered. They represent highly potent, selective and systemically M_1 allosteric agonists.⁴²⁵ These compounds are optimized analogs of M_1 allosteric agonists identified through high-throughput-screenings. They did not display any agonist or antagonist activity at M_2 - M_5 and possessed an exceptionally clean pharmacology profile when tested in a screen of sixty-eight GPCRs, ion channels and transporter targets. Mutagenesis studies revealed that the allosteric site is located in the third extracellular loop and the first turn of the seventh transmembrane span. Similar to TBPB, they potentiated NMDA current and reversed cognitive deficit *in vivo*.

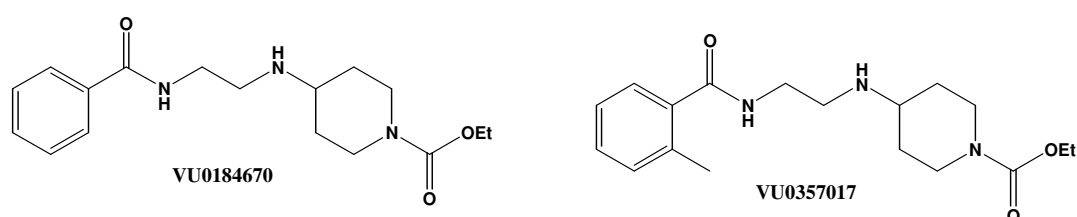


Figure 45: Chemical structures of VU0184670 and VU0357017.

In addition to the discovery of novel M_1 -selective allosteric agonists, much progress has been made in the discovery of novel M_1 PAMs that act as allosteric potentiators of this receptor. In a recent publication, researchers reported the discovery of benzyl quinolone carboxylic acid (BQCA, **Fig. 46**) as highly selective and efficacious allosteric modulator.⁴⁴⁸

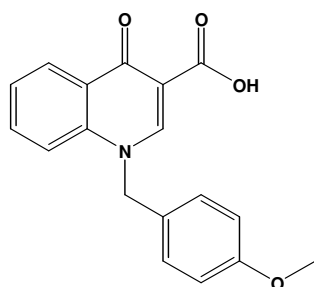


Figure 46: Chemical structure of BQCA

BQCA had no agonist activity alone, but it induced a robust leftward shift in ACh concentration-response curve. Interestingly, at 100 μ M, BQCA was able to increase ACh potency 128.8 ± 20.1 -fold (**Fig. 47**). Moreover, BQCA had no effect at the M_2 - M_5 subtypes.

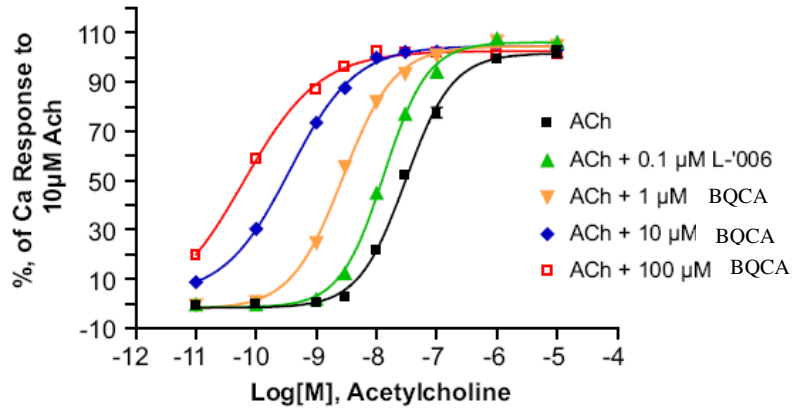


Figure 47: ACh concentration-response curve obtained with different concentrations of BQCA.⁴⁴⁸

To determine if BQCA interacts with the ACh binding site, [³H]NMS competition assays were performed. 100 µM BQCA had no effect on the binding of [³H]NMS (**Fig. 48**). Moreover, BQCA reduced the concentration of ACh required to displace [³H]-NMS 45-fold at 10 µM.

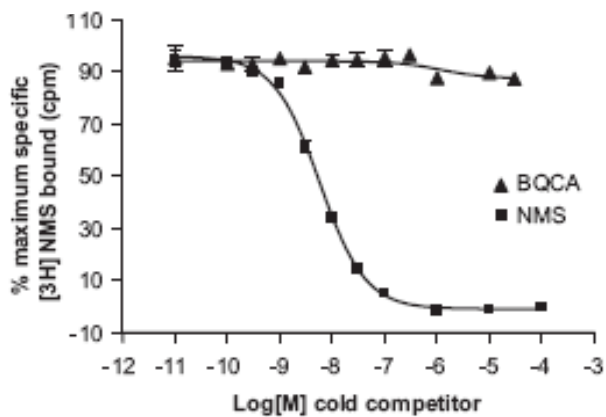


Figure 48: [³H]NMS competition assays.⁴⁴⁸

1.10 Multitarget-Directed-Ligand approach for the treatment of Alzheimer's disease.

AD constitutes an overwhelming health, social and economic problem to nations. So far, the therapeutic paradigm “one-compound-one-target” has failed. This could be due to the multiple pathogenic mechanisms involved in AD as discussed previously. However, in the last decade, new strategies have emerged to find an efficient therapy to combat multifactorial diseases like neurodegenerative diseases, cancer, depression ecc... One of these approaches is represented by the development of ligands capable to interact with multiple targets simultaneously, or the so-called “multitarget-directed ligands” (MTDLs).^{449, 450, 451, 452} However, the design of such a drug may not be easy because it could also bind targets that are not directly involved with the disease and could be responsible for side effects (Fig. 49).

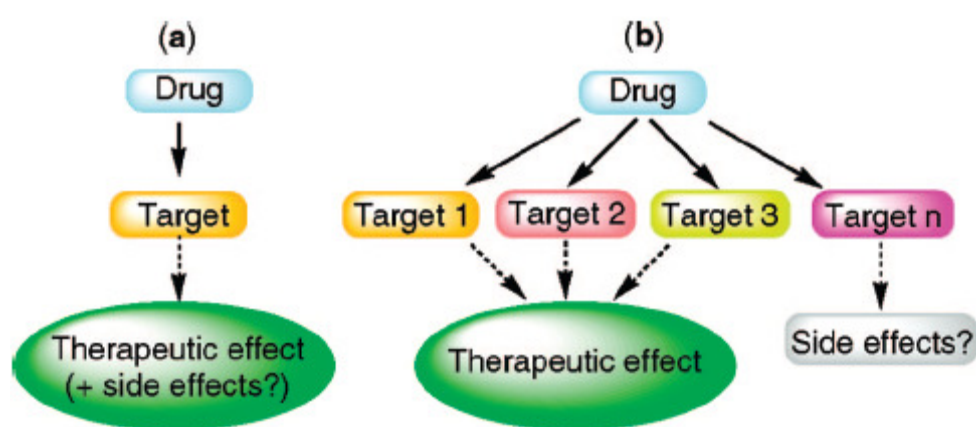


Figure 49: a) Schematic representation of the discovery approach, based on “one-molecule one-target” paradigm. b) MTDLs approach to drug discovery.⁴⁴⁹

The concept of the multitarget approach is particularly applicable to AD since the molecular basis of this disease can be considered as a complex network of pathological events (Fig. 50). However, nowadays, the drugs used in the clinical practice are based only on the cholinergic hypothesis. Cholinergic hypothesis states that the loss of cholinergic function is closely related to cognitive dysfunction of AD patients. So the primary therapeutic approach address cognitive loss associated with AD, has been the cholinergic replacement strategy. Current treatments for AD are mainly based on the inhibition of AChE. The only AChE inhibitors approved by FDA are tacrine, donepezil, galantamine and rivastigmine (see 1.3). Later on, memantine was approved for the treatment of AD. It possesses a different mechanism of action; it is an NMDAR antagonist (see 1.8). However, their clinical usefulness is limited because of the severe peripheral side effects associated to long-term therapies such as confusion, hallucinations, extreme or sudden changes in behavior, nausea, ecc.. Moreover, another limitation depends on

the fact that they have only a palliative effect and seem unable to address the molecular mechanisms that underlie the pathogenic processes. Therefore, the development of multitarget modifying molecules is an attractive approach to slow down the progression of AD. Many efforts have been made to find effective and selective MTDLs. This paragraph will focus on the recent approaches devoted to the design of multitarget ligands.

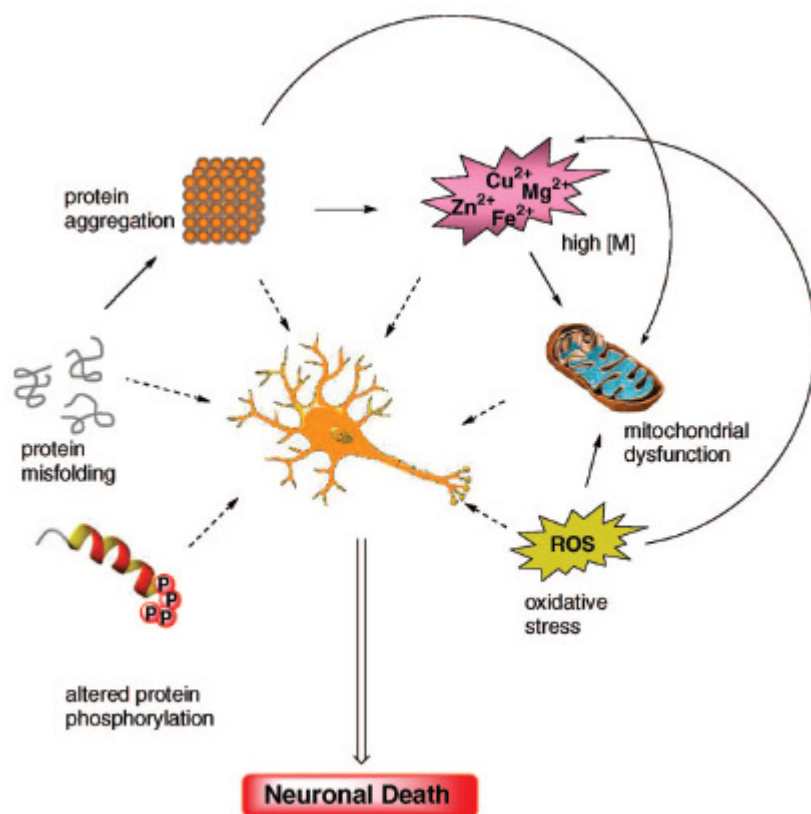


Figure 50: Representation of the interconnected pathways in AD.⁴⁴⁹

1.10.1 Dual binding site AChE inhibitors

The development of the so-called “dual binding site” AChEIs was suggested by the peculiar architecture of the enzyme, with the two target sites at the top and the bottom of a gorge.^{453, 454}

The inhibition of AChE at its catalytic site increases the concentration of ACh in the synaptic cleft, restoring central cholinergic activity. More importantly, they are able to reduce A β aggregation interacting with the PAS of AChE. The rational development of these drugs was suggested by the finding that PAS accelerates the aggregation of this toxic peptide.^{200, 201, 198, 199}

Thus, inhibitors targeting the PAS of the enzyme will decrease the aggregation rate of A β , therefore facilitating its clearance. This strategy could represent a new area of research for the AD treatment based on both the cholinergic and the amyloid hypothesis.

The observation that AChE gorge and PAS are enriched of aromatic amino acids capable of forming cation- π interactions with basic counterparts or π - π stacking, dual binding site AChEIs

were designed by linking the molecular features of well-known AChEIs through a polyamine chain. The nature and the length of the polyamine chain are critical since they play an active role in the target recognition process as postulated by the universal template design strategy.⁴⁵⁵

Bis(7)-tacrine (**Fig. 51**) was one of the first homodimers reported in the literature showing good selectivity and increased potency for AChE (AChE IC_{50} =0.4 nM vs BuChE IC_{50} = 390 nM).⁴⁵⁶

Bis(7)-tacrine seemed to increase the spontaneous quantal ACh release from peripheral cholinergic terminals in the electric organ of *Torpedo marmorata* at lower concentrations than tacrine (IC_{50} bis(7)-tacrine=100 nM vs IC_{50} tacrine= 100 μ M).⁴⁵⁷ It showed also to improve memory in rats⁴⁵⁸ and revealed an NMDAR antagonist character, with an IC_{50} of 0.76 mM preventing glutamate-induced neuronal apoptosis.⁴⁵⁹ Moreover, bis(7)-tacrine also showed neuroprotection against hydrogen peroxide-induced oxidative stress.⁴⁶⁰ Interestingly, this compound inhibited the AChE-induced A β aggregation with an IC_{50} of 41.7 mM.⁴⁶¹ Its ability to block A β assembly was demonstrated by computational and crystallographic studies^{462, 463} by its interaction with the PAS of the enzyme. Finally, Fu et al.⁴⁶⁴ reported a decrease by bis(7)-tacrine in the generation of both secreted and intracellular A β 42 (48.5% reduction at 3 mM), A β 40 (37.7% reduction at 3 mM) and the aberrant insoluble β -fragment (APP β), and an increase in the amount of soluble amyloid protein precursor α fragment (s-APP α). They demonstrated that bis(7)-tacrine is able to activate α -secretase and to inhibit BACE-1 with an IC_{50} of 7.5 mM.

In 2003, Piazzini et al.⁴⁶⁵ reported the synthesis and biological activity of AP2238 (**Fig. 51**), a dual inhibitor designed by combining in the same molecule two moieties optimal for the binding at each enzyme site and linked by an appropriate spacer. The phenyl ring in the spacer was chosen by the fact that it could favorably interact with some of the numerous aromatic residues of the AChE gorge. AP2238 is a good inhibitor of AChE (IC_{50} = 44.5 nM) and a good antiaggregating molecule (35% inhibition at 100 μ M, 1.6-fold more potent than donepezil).

Camps et al.⁴⁶⁶ developed a dual binding site inhibitor by combining the 5,6-dimethoxy-2[(4-piperidinyl)-methyl-1-indanone] moiety of donepezil with tacrine, which would thus replace the benzyl moiety of donepezil. Compound **A** (**Fig. 51**) was a subnanomolar inhibitor with an IC_{50} of 0.09 nM, more potent than all parent compounds (tacrine, 6-chlorotacrine and donepezil). Furthermore, compound **A** inhibited the AChE-induced A β aggregation up to 46.1% (at 100 μ M) presumably by interaction at the PAS of the enzyme. Thus, by molecular binding studies, it was shown that the tacrine moiety may be stacked between the aromatic rings of Trp₈₆ and Tyr₃₃₇ in the catalytic site of hAChE. The aromatic nitrogen of tacrine, protonated at physiological pH, is hydrogen-bonded to the main chain carbonyl oxygen of His₄₄₇. Finally, the indanone ring makes

π - π interactions with Trp₂₈₆ in the peripheral site of enzyme and is responsible for the inhibition of the AChE-induced A β aggregation.

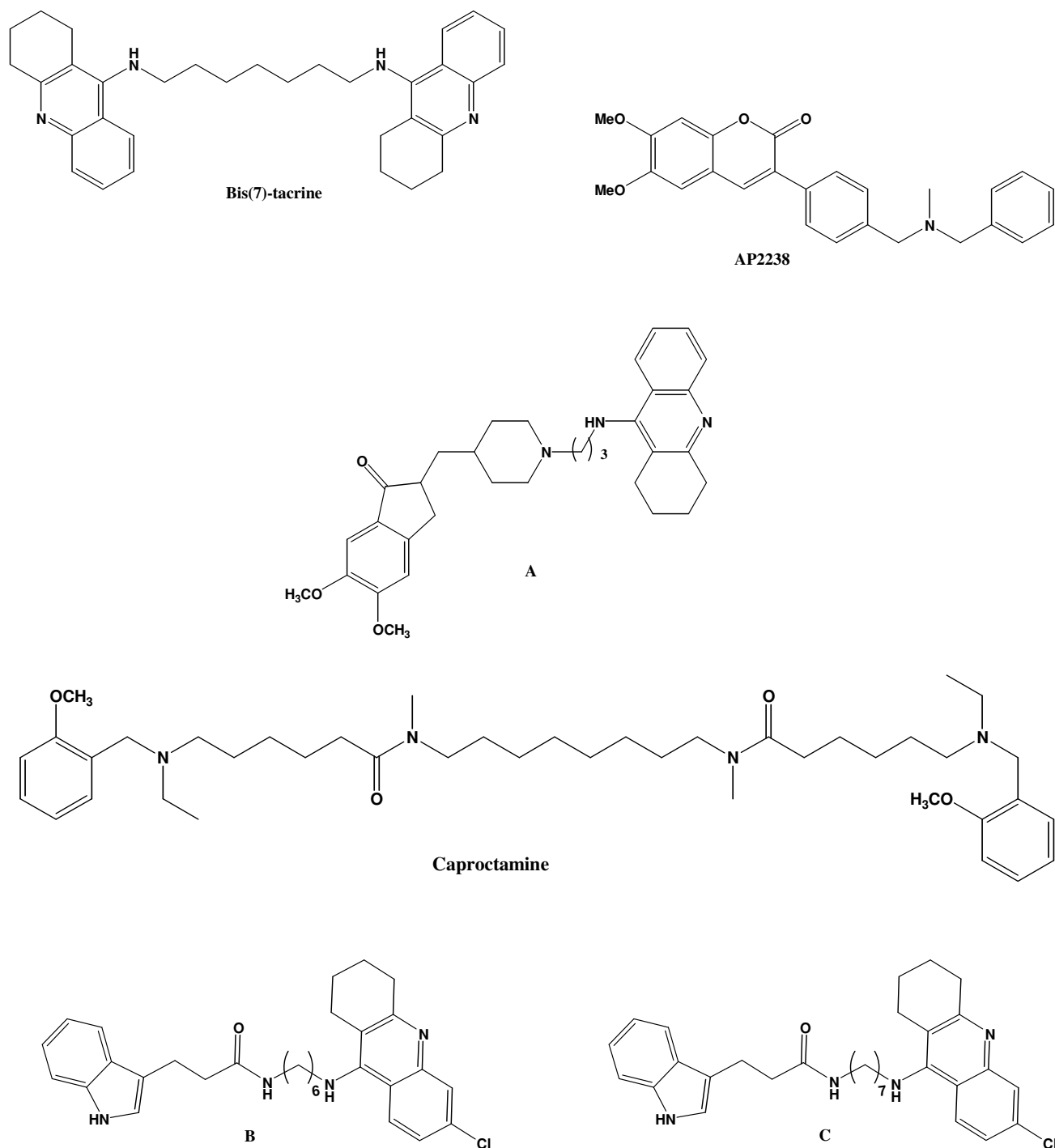


Figure 51: Chemical structures of some dual binding site AChE inhibitors.

Caproctamine (**Fig. 51**) represents one of the first examples of a successfully designed AChEI endowed with additional pharmacological effects beneficial in AD.⁴⁶⁷ Caproctamine is a polyamine-based dual inhibitor of AChE designed from benextramine using the universal template approach.⁴⁶⁸

Caproctamine was able to inhibit AChE (IC_{50} = 0.17 mM) and to block the mAChRs (M_2 K_b = 0.41 μ M). From docking studies it was shown that caproctamine was able to simultaneously contact both the active and the peripheral sites of AChE. Thus, the inhibition of AChE activity would potentiate the remaining cholinergic transmission in affected brain regions while antagonism of muscarinic M_2 autoreceptors would facilitate the release of ACh in the synapse. An improved AChE-induced $A\beta$ aggregation inhibitory profile was shown by a series of heterodimers in which a 1,2,3,4-tetrahydroacridine moiety was linked through a suitable spacer to an indole ring. The indole ring was shown to interact with the Trp₈₆ of the catalytic gorge by forming a π - π stacking. In particular, compounds **B** and **C** were the most potent AChEIs of the series; they displayed IC_{50} values of 20 and 60 pM, respectively. Moreover, they were able to inhibit the AChE-induced $A\beta$ aggregation with IC_{50} values 1 order of magnitude lower than that of propidium.⁴⁶⁹

1.10.2 AChEIs Targeting Other Neurotransmitter Systems

It is well-known that AD is caused by a decline of cholinergic and glutamatergic neurons in the brain. However, other neurotransmitter systems are involved in the neuropsychiatric abnormalities observed in AD patients. Thus, it is argued that the noradrenergic deficits of AD stem from locus ceruleus atrophy and are linked to depression,⁴⁷⁰ while the serotonergic deficits in raphe atrophy are linked to depression and psychosis.⁴⁷¹

A recent and renewed interest has regarded monoamine oxidases (MAOs) as a “druggable” target for the treatment of neurodegenerative diseases like AD, Parkinson’s disease and amyotrophic lateral sclerosis. MAOs are a family of enzymes that catalyze the oxidation of xenobiotics and endogenous amines, including monoamine neurotransmitters such as serotonin (5-HT), noradrenalin (NA), and dopamine (DA).⁴⁷² Two distinct enzymatic isoforms, namely MAO-A and MAO-B, have been isolated and studied. Both are found in neurons and astroglia, while outside the CNS, MAO-A is also present in the liver, gastrointestinal tract and placenta, and MAO-B is mostly found in blood platelets.⁴⁷³ Both enzymes oxidatively deaminate DA, whereas MAO-A preferentially deaminates 5-HT, NA and adrenaline. MAO-B metabolizes also benzylamine and phenethylamine. Moreover, another MAO activity seems to be involved in the pathogenic process of neurodegenerative diseases. In fact, MAO, during its catalytic activity of

deamination of neurotransmitters, produces H_2O_2 which is a possible source of radical ROS that can promote harmful cellular alterations in pathological conditions (**Fig. 52**)

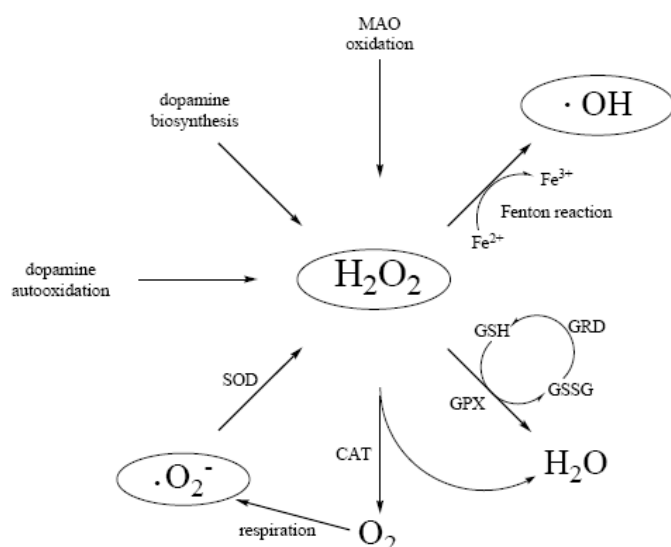


Figure 52: ROS endogenous production and monoamines metabolism.⁴⁷⁴

Within this complex scenario, MAO inhibitors (MAOIs) might play a beneficial action in AD by reducing oxidative stress conditions in the brain and increasing the activity of other neurotransmitter systems (e.g., serotonin, noradrenalin) whose levels are influenced by the catabolic action of MAOs. The initial design strategy for combined MAO/AChE agents resulted in a series of inhibitors (e.g., compound **A**, **Fig. 53**) that were designed linking the tricyclic 1,2,3,4-tetrahydrocyclopent[b]indole carbamate scaffold, inspired by the known natural AChEI physostigmine, with a propargylamino group, belonging to selegiline, a potent, selective and irreversible “suicide-type” MAO-B inhibitor. These compounds were good AChEIs, but they were still irreversible MAO inhibitors associated to severe side effects.⁴⁷⁵ More interestingly, the synthetic iminic compounds represented by the general formula **B** (**Fig. 53**), were also tested and showed from moderate to good dual inhibitory activities. Regarding MAO inhibition, most of them exhibited a reversible mechanism of action and a marked selectivity for MAO-A.⁴⁷⁵

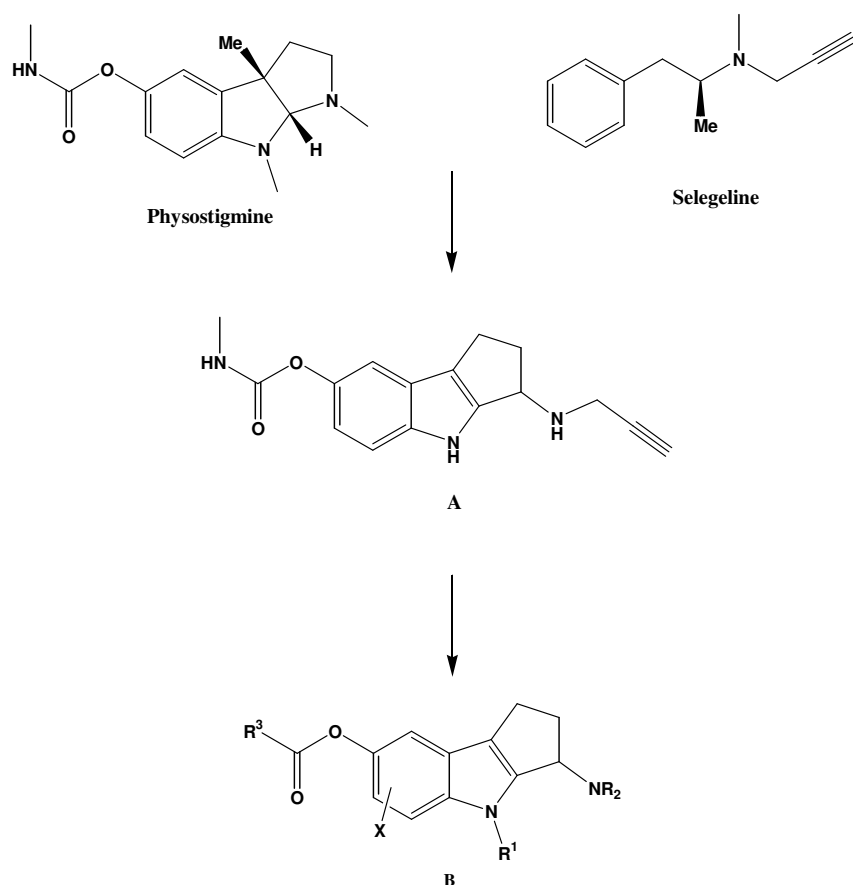


Figure 53: MAO/AChE inhibitors.

Youdim and co-workers.⁴⁷⁶ studied a large series of *N*-propargylaminoindans and *N*-propargylphenethylamines (**Fig. 54**), as dual MAO-AChE inhibitors. The molecular design was based on the combination in the same molecule of a propargylaminic fragment, characterizing well known MAOIs such as rasagiline and selegiline, with a carbamate moiety, which could add the AChE inhibitory property. In addition to AChE and MAO-B inhibition, these molecules might display a potential antidepressant action through MAO-A inhibition. The most promising compound was ladostigil (**Fig. 54**).⁴⁷⁶ Ladostigil showed to be a potent and selective AChEI. It also displayed high MAO inhibition in the CNS and low MAO inhibition in the liver and small intestine with fewer side effects. Moreover, ladostigil decreased apoptosis via prevention of caspase-3 activation through a mechanism related to regulation of the Bcl-2 family proteins. This resulted in reduced levels of Bad and Bax and increased levels of Bcl-2. It also stimulated the release of the nonamyloidogenic soluble APP via a C-MAP kinase dependent pathway. Due to its promising profile, ladostigil is currently in Phase II as a potential MTDL drug for the treatment of AD.¹²²

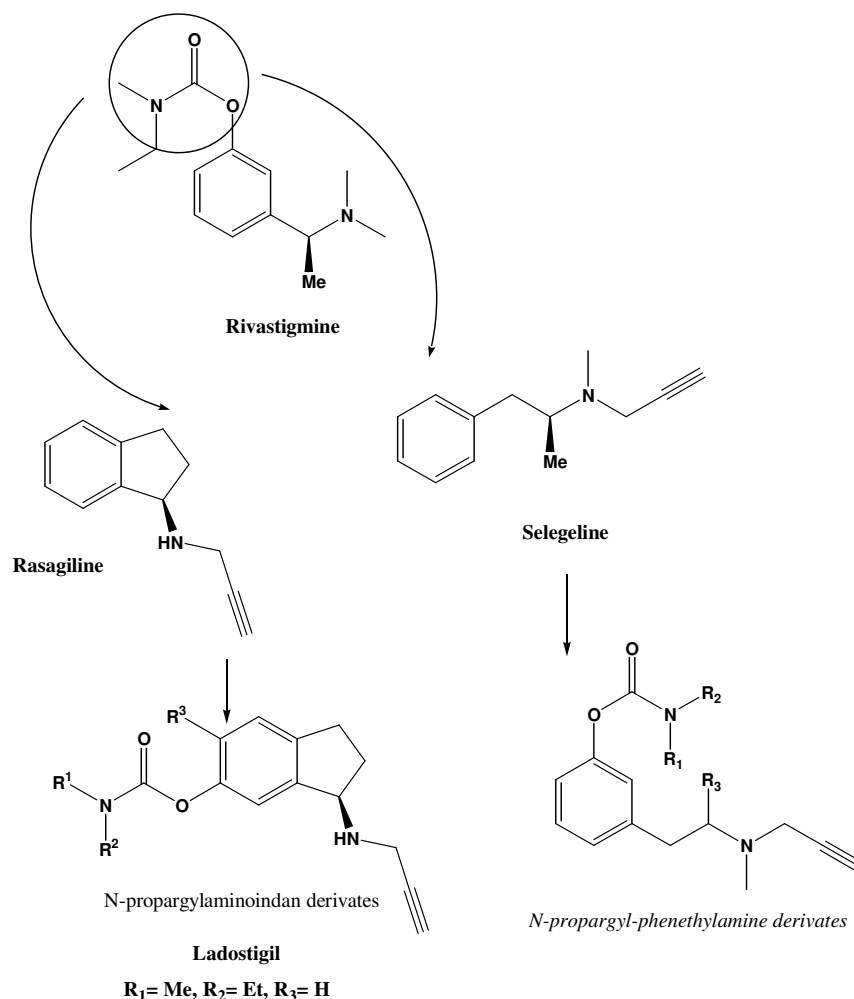


Figure 54: Other MAO/AChEI inhibitors.⁴⁷⁶

In 2012, Simoni et al.⁴⁷⁷ reported the synthesis of MTDLs obtained combining galantamine and memantine in new entities. Galantamine and memantine are two of the few approved drugs used for the treatment of AD. Galantamine is an AChEI while memantine is a NMDA antagonist. These compounds were designed using the dual target design strategy.⁴⁷⁸ Among all the compounds, memagal (**Fig. 55**) seemed to be the most promising MTDL. Thus, it was able to inhibit AChE with an IC_{50} of 1.16 nM and to interact with both the catalytic site and the PAS of the enzyme. Moreover it was found to interact with NMDAR with a K_i of 4.6 μM .

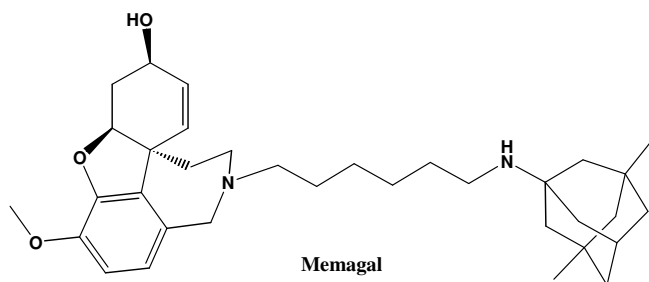


Figure 55: Molecular structure of memagal.

1.10.3 AChEIs with Antioxidant Properties

As already discussed (see **1.6**), oxidative stress is recognized as a central feature of AD pathogenesis. Oxidative stress refers to the production of high concentrations of ROS in AD patients. ROS oxidize lipids and damage membranes in the brain destabilizing several systems or equilibriums inside neurons. Free radicals can also oxidize DNA and RNA and their oxidation products were found to be elevated in vulnerable neurons in the brains of AD patients. Therefore, treatments that specifically target sources of ROS have attracted particular attention. In the search

for MTDLs, lipocrine (**Fig. 56**)⁴⁷⁹ was design combining the 1,2,3,4-tetrahydroacridine moiety of tacrine with the structure of lipoic acid (LA), an antioxidant exerting different protective effects in neurodegeneration underlying AD.⁴⁸⁰ Lipocrine is one of the most potent AChEIs ($IC_{50}= 0.25$ nM).

Kinetic studies verified that lipocrine also interacts with the AChE PAS. Furthermore, it inhibited AChE-induced A β aggregation was tested. It emerged as significantly more potent than all the other AChEIs investigated at the time. Considering its antioxidant effect, lipocrine decreased by 51% the production of ROS species at 10 μ M demonstrating a good profile as a neuroprotectant against oxidative stress.

Fang et al.⁴⁸¹ synthesized a series of tacrine–ferulic acid hybrids as MTDLs for AD. Among all the compounds, compound **A** (**Fig. 56**) was the most promising drug candidate. It inhibited AChE with high potency ($IC_{50}= 4.4$ nM) and, in experiments performed by the oxygen radical absorbance capacity method,⁴⁸² **A** showed a value of 1.5 trolox equiv. in decreasing ROS species.

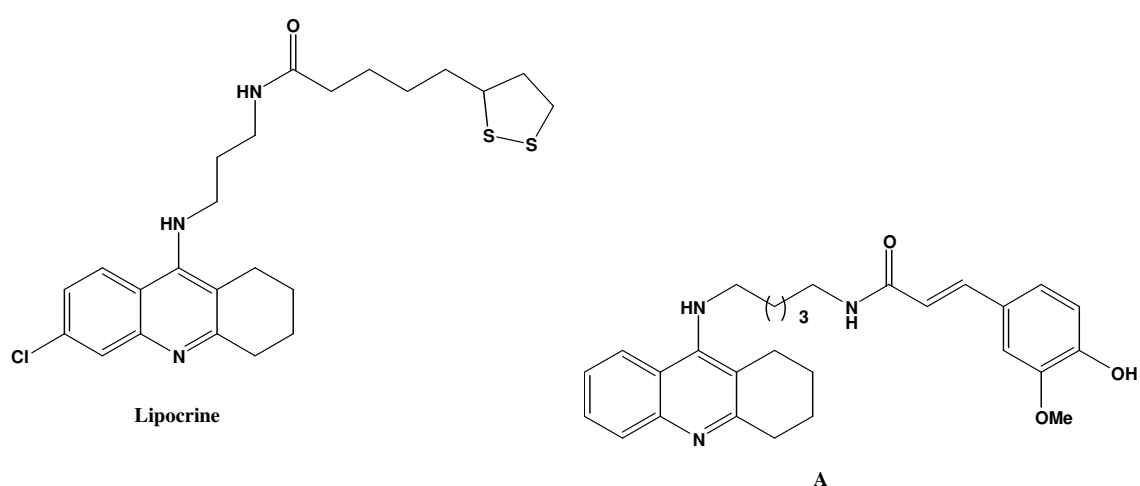


Figure 56: Molecular structures of AChEIs with antioxidant properties.

1.10.4 Development of Memoquin

Recently, a new drug candidate, memoquin (**Fig. 57**) has been identified.⁴⁸³ It possessed some of the above-mentioned activities relevant to AD, such as the ability to inhibit AChE, A β processing and aggregation, and the ability to counteract oxidative stress. It was rationally designed by replacing the linear alkyl chain of caproctamine with a radical scavenger function (**Fig. 57**). Caproctamine was chosen as the lead compound because of its well balanced affinity profile as an AChEI and a competitive M₂ mAChRs antagonist.⁴⁶⁷ Concerning the radical scavenger moiety, attention was focused on the benzoquinone moiety, the key fragment of coenzyme Q10 (CoQ10). CoQ10 is a natural antioxidant that may have potential activity against AD.⁴⁸⁴ The benzoquinone ring of memoquin is a lipophilic and planar π -system which has been recognized as an important design feature for obtaining high-binding specificity with A β and for perturbing protein-protein interactions in the fibrillogenesis process.⁴⁸⁵

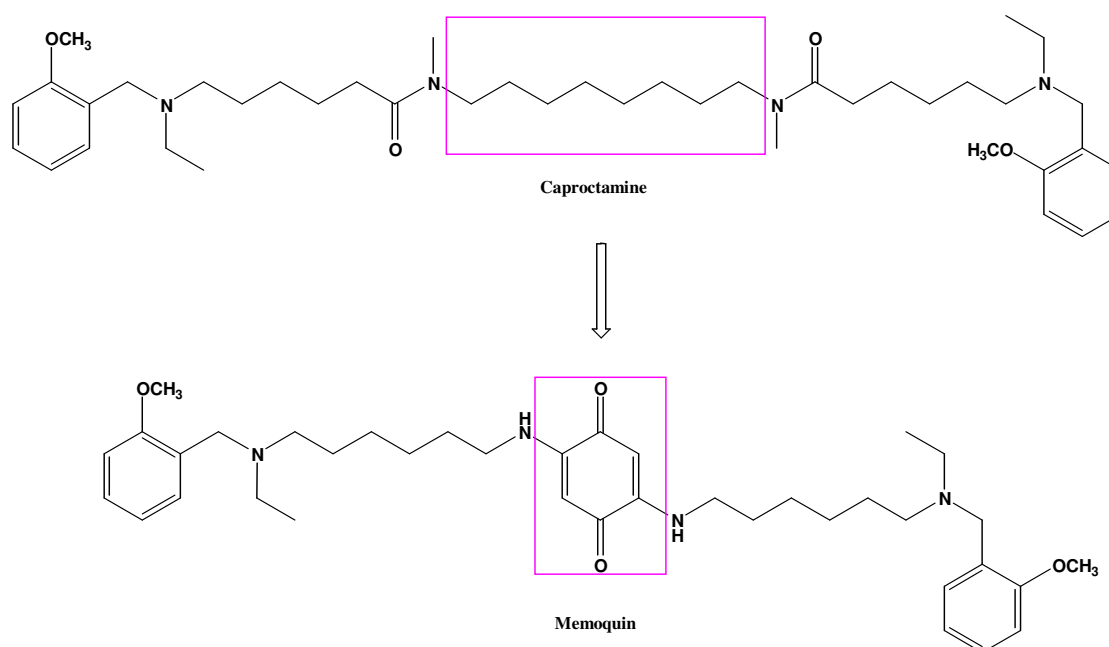


Figure 57: Design strategy leading to memoquin.

The biological profile of memoquin was then widely studied by both *in vitro* (**Fig. 58**) and *in vivo* assays. It was shown that memoquin was able to decrease the formation of free radicals with an percent inhibition 44.1 ± 3.7 , which is slightly lower than that of trolox ($57.6 \pm 0.9\%$). Moreover, memoquin was a good substrate for the enzyme NAD(P)H:quinone oxidoreductase 1 (NQO1). NQO1 activity is increased in the hippocampal pyramidal neurons of AD patients. It was demonstrated that the quinone moiety of memoquin is transformed by NQO1 into the hydroquinone form. Therefore, it was suggested that the reduced form of memoquin is the real

antioxidant specie. This molecular mechanism was also confirmed in cellular assays, using SH-SY5Y cells.⁴⁸³ Moreover, memoquin was a potent inhibitor of the activity of human AChE, with IC_{50} (1.55 nM) and K_i (2.60 nM) values 15 and 8 times lower, respectively, than those of donepezil. Kinetic measurements also revealed that the inhibition was of mixed type and this reflected the interaction of memoquin with both the catalytic site and the PAS of the enzyme. Docking simulations confirmed that memoquin was able to bind simultaneously Trp₈₆ and Trp₂₈₆ of the catalytic site and the PAS, respectively.⁴⁸³ As we have already discussed, AChE can induce A β aggregation through the PAS. So, AChEIs that bind to the PAS could block this proaggregating process. Thus, memoquin was able to inhibit the AChE-induced A β 40 aggregation with an IC_{50} of 28.3 μ M. Interestingly, among the classical AChEIs (tacrine, donepezil, galantamine, rivastigmine, propidium), only propidium, which is a specific inhibitor of PAS, displayed a comparable anti-aggregating potency.⁴⁸⁶ Memoquin also inhibited *in vitro* the self-assembly of A β 42, which is the most amyloidogenic A β form. At the concentration of 50 μ M, memoquin was able to inhibit fibril formation by (95.5 \pm 0.4)%. Finally, memoquin also inhibited BACE-1, the enzyme involved in A β production from APP, with an IC_{50} of 108 nM.

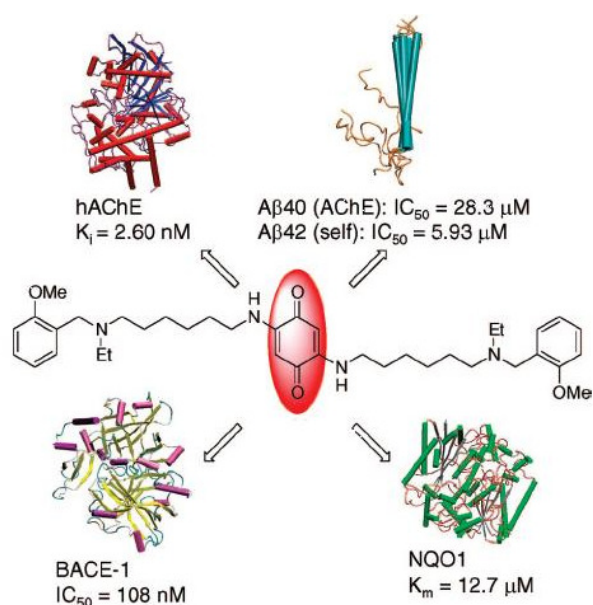


Figure 58: Memoquin activities *in vitro*.

Memoquin was then tested *in vivo*⁴⁸⁷ using the anti-NGF transgenic mouse (AD11 mouse), which is an animal model for AD.⁴⁸⁸ Memoquin was able to prevent the AD-like hallmarks at three stages (at 2, 6, and 15 months of age). At all ages, memoquin rescued the cholinergic and behavioral deficits linked to attention and memory. Moreover, it was able to prevent or rescue τ hyperphosphorylation in the cortex, and it reduced A β expression and accumulation.

2 Aim of the project

AD is an irreversible, multi-factorial neurodegenerative disorder characterized by a progressive decline in cognitive faculties.⁴⁸⁹ Several lines of evidence implicate impaired cholinergic neurotransmission in the brain as contributing to cognitive loss and neuropsychiatric symptoms of AD. The “cholinergic hypothesis” postulates that augmentation of cholinergic tonus can be achieved by enhancing activity of the neurotransmitter ACh. Two families of receptors mediate the action of ACh: nAChRs, which function as ligand-gated ion channels, and mAChRs, which are members of the GPCRs. mAChRs family is composed by five receptor subtypes. The M₁ subtype is the most abundant in the cortex and hippocampus, two regions involved in learning and memory. This suggests that M₁-selective agonists can be of therapeutic value in AD. Stimulation of M₁ mAChRs might possess not only beneficial effects on memory and cognitive deficits, but also disease-modifying properties.³⁹⁸ Thus, it is thought that activation of the M₁ subtype could reduce A β levels and hyperphosphorylated tau protein, the two major hallmarks of AD.⁴⁹⁰ Although activation of M₁ mAChRs is beneficial, many efforts have failed to produce highly selective compounds because of the highly conserved orthosteric binding site across all mAChRs. However, in recent years, the research has focused the attention on the development of allosteric ligands. They are compounds that bind the receptor in a site that is different from the orthosteric site. Allosteric ligands offer many advantages. Since allosteric binding sites are less conserved than the orthosteric sites, high subtype selectivity can be achieved. Moreover, they might be less toxic because in many cases, direct acting agonists lead to receptor desensitization, internalization or down-regulation.⁴⁹¹

The aim of this project was to synthesize multi-potent ligands, which would exploit the allosteric site on the M₁ receptors, restoring the central cholinergic deficit of AD patients. The rationale that led to the design of these new compounds was based on the structural similarity between TBPB and memoquin. TBPB is a high selective M₁ allosteric agonist.⁴²⁵ Memoquin is a MTDL bearing a benzoquinone moiety which possesses antioxidant properties.⁴⁸³ Indeed, NQO1 enzyme whose activity is increased in neurons of patients with AD, may convert the benzoquinone ring into a hydroquinone form, which can neutralize ROS. This effect could be of therapeutic value because it is well known that oxidative stress plays a significant role in the neurodegeneration of cholinergic system.²⁸³ Interestingly, idebenone, a synthetic derivative of CoQ10, had been shown in a clinical trial to improve cognitive function and behavioral deficits in patients with mild to moderate AD.⁴⁹² Moreover, the quinone ring is a privileged motif for inhibiting A β fibrils formation.^{493, 494, 495}

The first library of compounds (**1-10**) contain a benzoquinone linked to 1-(2-methoxy-benzyl)-[4,4']bipiperidinyl moiety which might mimic the bipiperidinyl group of TBPB (**Fig. 59**). The [4,4']bipiperidinyl moiety was chosen because, among several memoquin congeners with different chain lengths, the best MTDL profile was observed with an hexamethylene spacer between inner and outer nitrogen atoms.^{496, 497} Moreover, it has been shown that the 2-methoxy substituent on the aryl group was optimal for the interaction with AChE.⁴⁹⁶ On the other hand, the substituents on the benzoquinone group exploit different electronic and lipophilic properties to obtain Structure-Activity-Relationship (SAR) for M₁ receptors whose crystal structure is unknown.

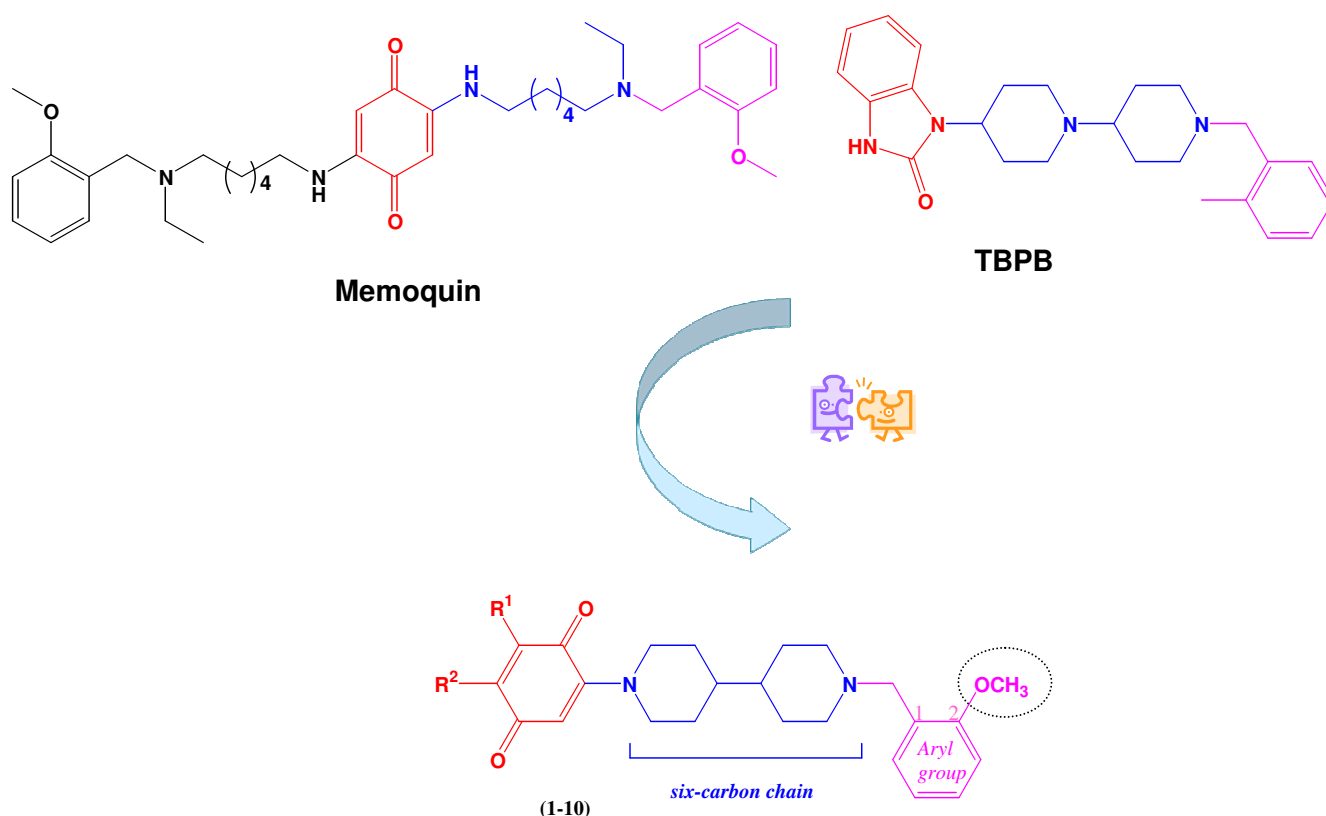


Figure 59: Design strategy for compounds **1-10**.

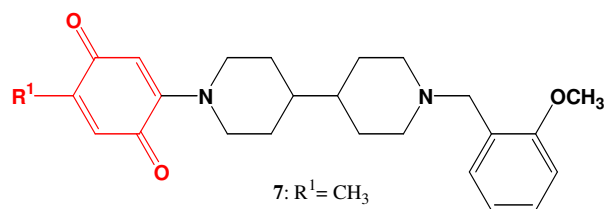
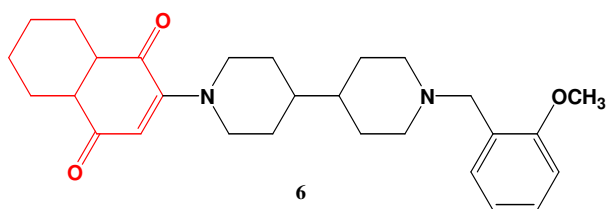
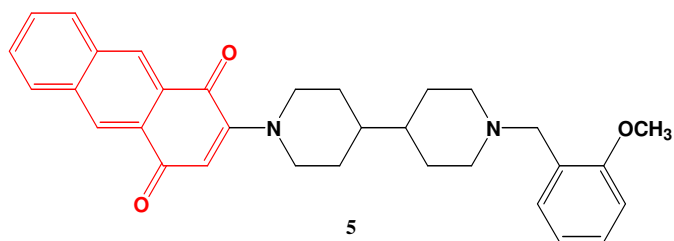
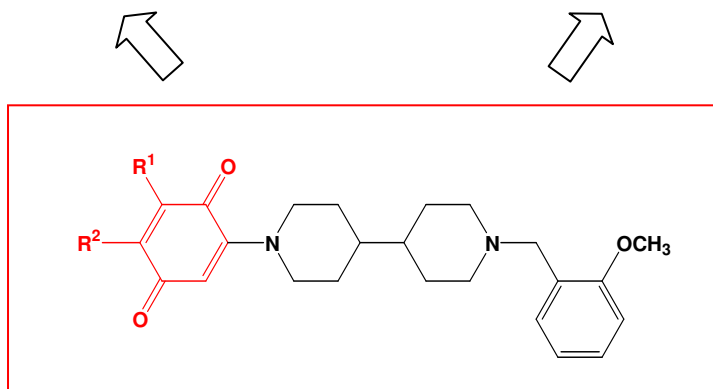
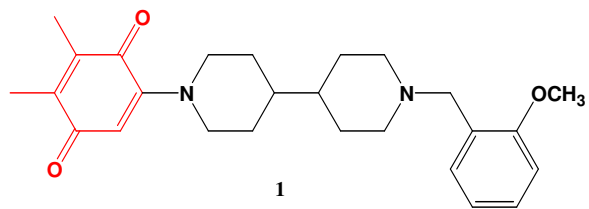
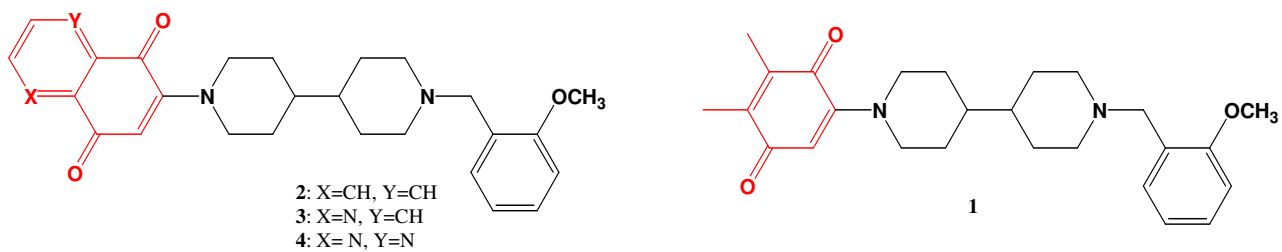


Figure 60: Design strategy for compounds 1-10.

The selected quinones are shown in **Figure 60**. The 2,3-dimethylbenzoquinone of compound **1** was replaced by a naphthoquinone affording compound **2**. The naphthoquinone is more lipophilic and bulkier than 2,3-dimethylbenzoquinone. Moreover, the planar and aromatic structure of the benzene ring allows the molecule to establish a cation- π interaction or a π - π stacking with the biological counterpart. To extend the interactions with the target, the naphthoquinone was replaced by a quinolinoquinone and a quinoxaline-5,8-dione affording compounds **3** and **4**, respectively. Thus, a nitrogen atom is able to create an H-bond interaction with the counterpart, modifying the affinity for the receptor. To increase the steric hindrance and the lipophilicity of the compound, the anthraquinone was introduced, leading to **5**. Compound **6** was designed replacing the planar and aromatic naphthoquinone of **2** with the 5,6,7,8-tetrahydro-[1,4]naphthoquinone. The latter possesses an aliphatic and less planar cycle compared to an aromatic ring. This substituent is not able to establish a cation- π interaction or a π - π stacking with the target. This allows us to obtain important information about the chemical environment of the binding site on M_1 receptors. Compounds **7-10** were designed introducing only one substituent on the quinone ring. The substituents exploit different electronic and lipophilic effects according to the Craig's diagram.⁴⁹⁸ Finally, to verify whether the benzoquinone plays a role, compounds **11** (**Fig. 61**) in which the quinone is replaced by a carbamic group was also synthesized.

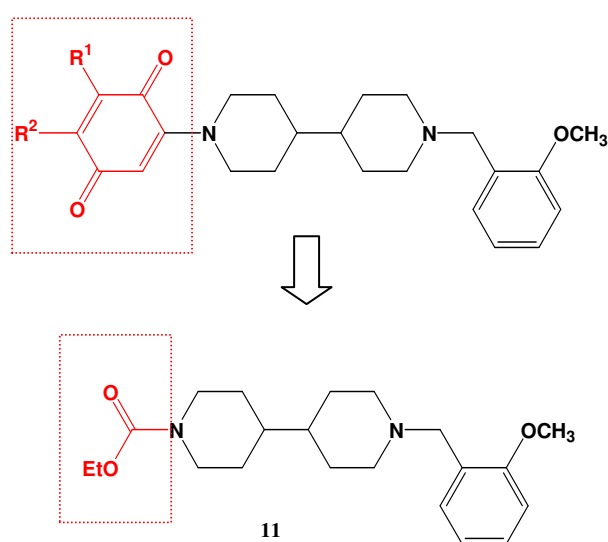


Figure 61: Design strategy for compound **11**.

To extend the SAR for the allosteric site on the M_1 subtype, other molecules were developed through chemical optimization of the lead compound VU0184670 (**Fig. 62**).⁴²⁵ In 2010, Lebois et al.⁴²⁵ reported the synthesis of a novel series of highly selective and systemically active M_1

allosteric agonists. Among all the compounds, VU0184670 showed the highest potency at M₁ mAChRs (EC₅₀= 152 nM). Moreover, it was completely inactive at M₂-M₅ up to the highest concentrations tested (30 μM). From the SAR on VU0184670 analogs, it was established that N-methylation of the secondary nitrogen atom was detrimental for the activity. Furthermore, alternate chain lengths abolished M₁ activity. We decided to introduce a cyclic constrained structure on the lead compound, through substitution of the ethyldiamine chain with a piperazine ring, to study the effect of conformationally restricted structures on biological activity. Compounds **12** and **13** (**Fig. 62**) were designed by replacing the carbamic group with a 2,3-dimethylbenzoquinone and a naphthoquinone, respectively. These two quinones were selected from the observation that, among the previous products **1-10** (**Fig. 60**), compounds **1** and **2** were the most promising.

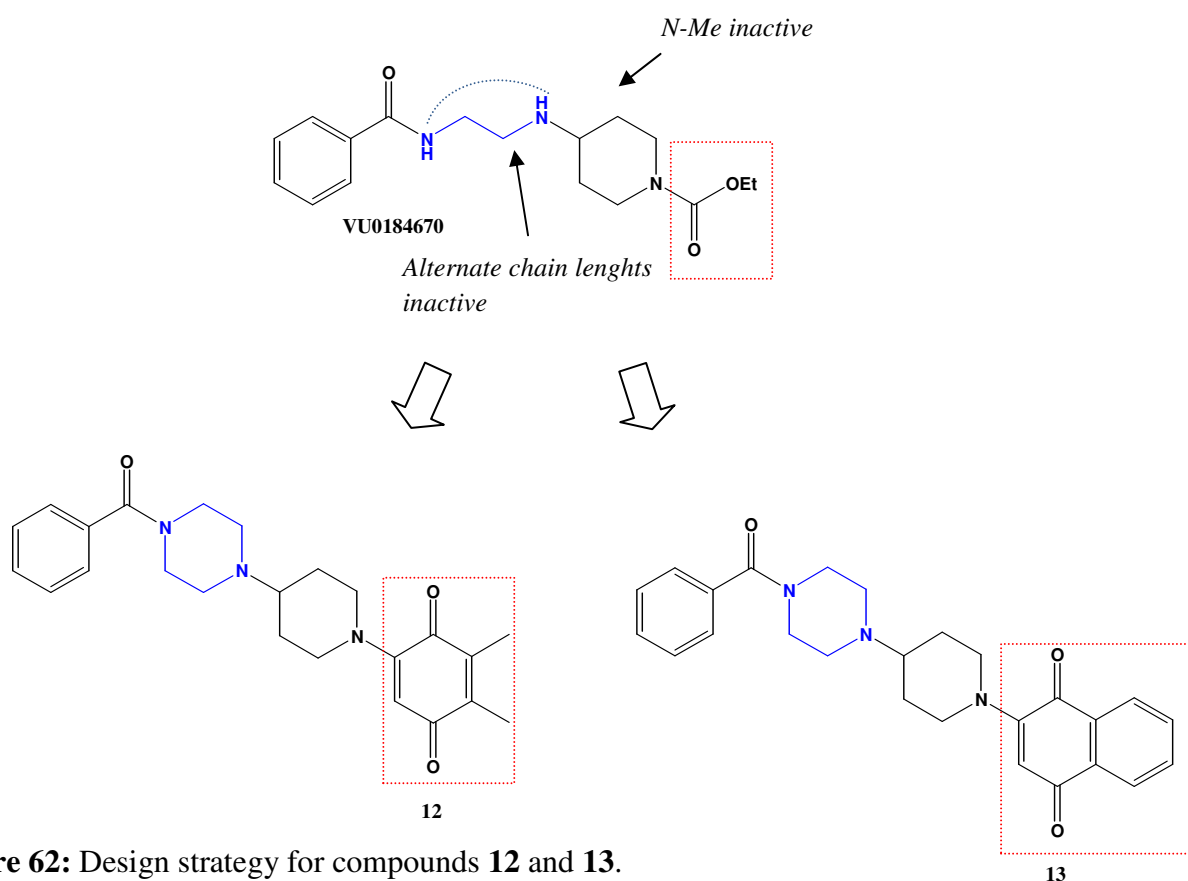


Figure 62: Design strategy for compounds **12** and **13**.

To increase the diversity of the compounds, a second library of products was designed (**14-17**, **Fig. 63**). The new molecules contain an amide group and an amine chain as in TBPB, but they are more flexible than TBPB. This property allows them to adopt a large number of different conformations and, potentially, they may interact with different targets simultaneously providing a MTDL profile. The amine chain of compounds **14-17** is the 1-(2-methoxy-benzyl)-

[4,4']bipiperidinyl moiety of compounds **1-10**. The linker between the amide and the amine chain contains an aromatic substituent to mimic the 1,3-dihydro-benzoimidazol-2-one of TBPB. The presence of a phenyl ring offers the opportunity to verify whether electronic (σ) and/or lipophilic (π) properties of substituents in the *ortho* position could extent any favorable effects on the biological profile. The substituents were selected in such a way as to have σ and π values in positive or negative direction, in all combinations.⁴⁹⁸ All the compounds were synthesized through multicomponent reaction (MCR) between an amine chain, an aromatic aldehyde, an isocyanide and trimethoxyborane. The synthesis of **14-17** allows us to apply also in medicinal chemistry, the use of isocyanide multicomponent reactions (see **Chapter 3**).

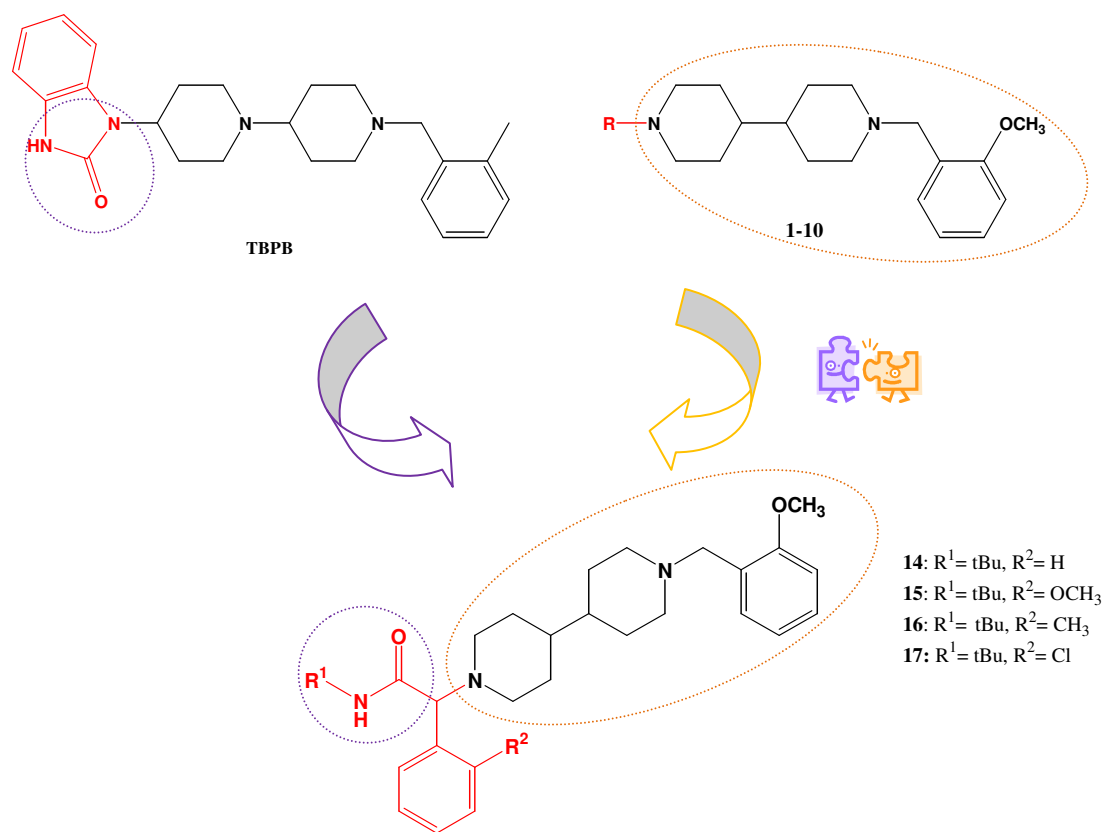


Figure 63: Design strategy for compounds **14-17**.

3 Chemistry

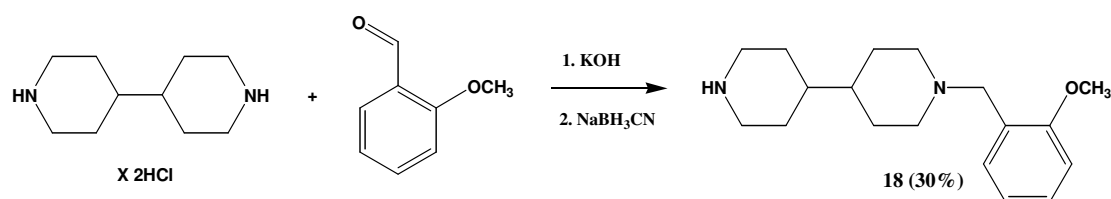
The key intermediate for the synthesis of the amino-quinones **1-10** and the derivative of carbamic acid **11** was 1-(2-methoxybenzyl)-[4-4']bipiperidine (**18**). It was synthesized through reductive amination between the commercially available 4,4'-bipiperidine and 2-methoxy-benzaldehyde (**Scheme 1**). In accordance with the widely reported reactivity of the quinone system in the 1,4-Michael addition and in substitution reactions, the amino-quinones were synthesized from the reaction between **18** and the appropriate quinone. The quinone **19**, used in the synthesis of **1** (**Scheme 3**), was obtained from oxidation of the commercially available 2,3-dimethyl-benzene-1,4-diol with MnO₂ (**Scheme 2**). The synthesis of **1** was performed at RT in a biphasic system formed by CHCl₃ and H₂O. As shown in **Scheme 4**, also compound **2** was obtained at RT, through 1,4-Michael addition between **18** and the corresponding 1,4-naphthoquinone. Quinoline-5,8-dione **20**, synthesized treating 8-hydroxyquinoline with bis(trifluoroacetoxy)iodobenzene (PIFA) (**Scheme 5**),⁴⁹⁹ was then reacted with **18** leading to the desired amino-quinone **3** (**Scheme 6**). The reaction was performed in the presence of 0.1 eq. of CeCl₃. Metal ions catalyze the amination of quinoline-5,8-dione and the amino group would be preferentially introduced onto the 6-position of the quinone.^{500, 501} The formation of a metal chelate complex, in which the nitrogen and the oxygen of the neighboring carbonyl group coordinate to the metal ion, was proposed to increase the electrophilicity of the carbon in 6-position, facilitating the amination. The regiochemistry of **6** was confirmed through HMBC and HMQC experiments. The synthesis of quinoxaline-5,8-dione **23** was performed from the commercially available 2-amino-3-nitrophenol (**Scheme 7**). Hydrogenation of the nitro group afforded the diamine derivative **21**⁵⁰² which was then condensed with sodium glyoxal bisulfate to give quinoxaline **22**⁵⁰³ in 90% yields. Oxidation of the arene with PIFA generated the quinone **23**.⁵⁰⁴ This step was followed by 1,4-Michael addition of **18** to the quinone scaffold to afford **4** (**Scheme 8**). A catalytic amount of CeCl₃ was used to improve the yield of the reaction. The synthesis of the anthraquinone derivative **5** is shown in **Scheme 9**. It was obtained in very low yield treating **18** with the corresponding 1,4-anthraquinone. The final compound **6** (**Scheme 11**) was synthesized from **18** and the quinone **25** obtained from the commercially available 5,6,7,8-tetrahydro-naphthalen-1-ol as shown in **Scheme 10**. The synthesis of the quinone **27** is described in **Scheme 12**. Addition of HCl to p-toluquinone afforded the hydroquinone **26** that was oxidized to the corresponding quinone **27** with potassium dichromate.⁵⁰⁵ Substitution reaction between **27** and the amine chain **18** in EtOH at reflux led to the desired product **7** in 54% yield (**Scheme 13**). Similarly, substitution reaction between **18** and 2,5-dimethoxy-1,4-benzoquinone and 2,5-dichloro-1,4-

benzoquinone afforded **8** (Scheme 14) and **9** (Scheme 15), respectively. In both cases, an excess of quinone (5 eq.) was used, to ensure the mono-substitution. The last amine-quinone of this series (**10**) was obtained through 1,4-Michael addition between **18** and 1,4-benzoquinone at RT. Also in this case an excess of quinone was used (Scheme 16). The synthesis of **11** is shown in Scheme 17. It contains a carbamic group instead of a quinone ring as in the previous compounds. It was synthesized in good yield, coupling **18** with ethyl chloroformate.

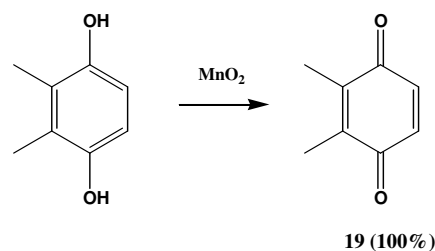
The key intermediate for the synthesis of the amino-quinones **12** and **13** was the amine **31** (Scheme 18). Its synthesis started from protection of the amine group of piperidone hydrochloride with (Boc)₂O. The reaction was performed in MeOH in the presence of triethylamine. **28** was then reacted with an excess of piperazine, sodium cyanoborohydride and acetic acid affording the intermediate **29**, which was reacted with benzoyl chloride to give **30**. Removal of the protecting Boc group gave **31** in good yield. Finally, addition of amine **31** to 2,3-dimethyl-1,4-benzoquinone (**19**) and 1,4-naphthoquinone led to **12** (Scheme 19) and **13** (Scheme 20.), respectively.

The syntheses of the compounds **14-17** through borane-mediated Ugi-type reaction are reported in Scheme 21-24. Amine **18**, tert-butyl isocyanide and aldehydes with different substituents in *ortho* position were coupled in the presence of trimethoxyborane under microwave irradiation, to give the corresponding α -amino amides. Presently, there is a great interest in using borane derivatives to generate iminium ions, which are critical intermediate in Ugi and Mannich multicomponent reactions (see Chapter 3).

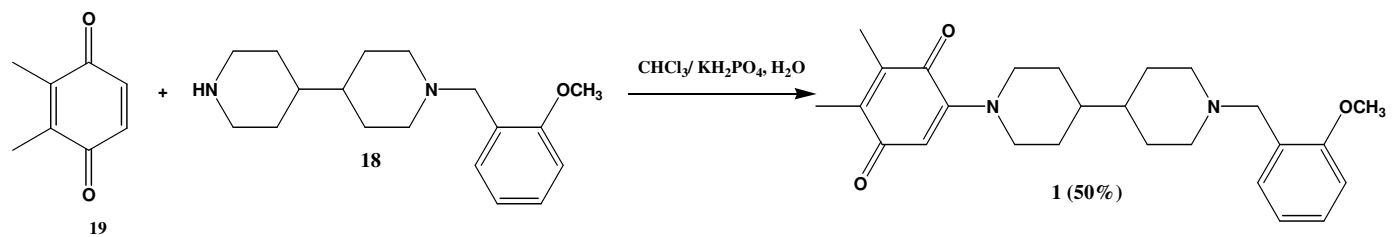
Scheme 1



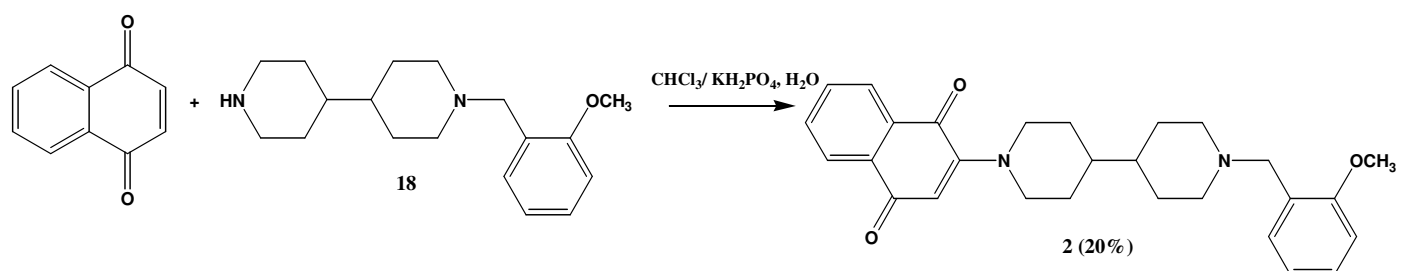
Scheme 2



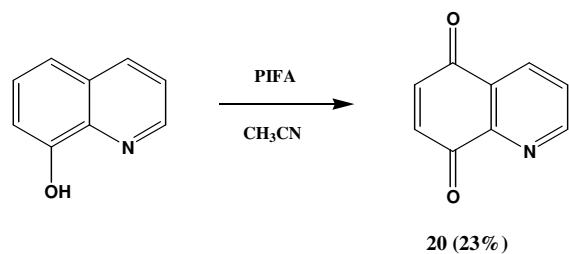
Scheme 3



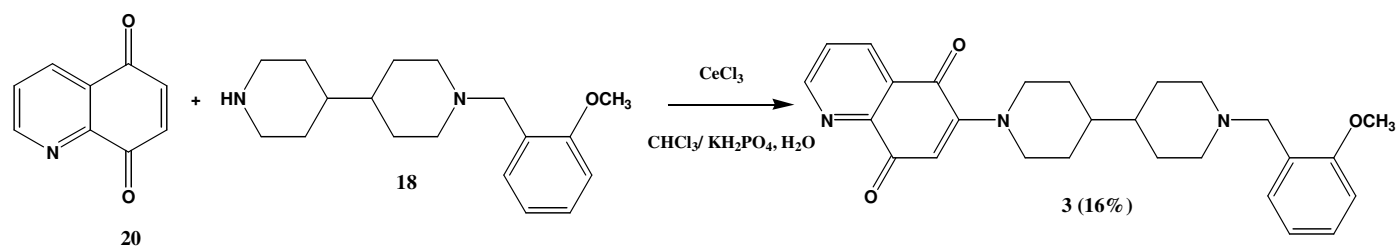
Scheme 4



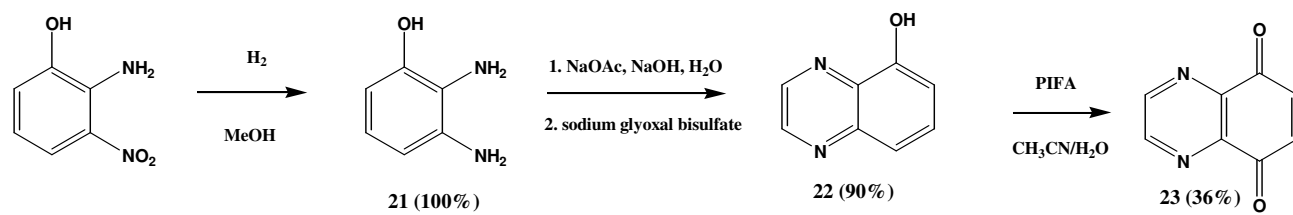
Scheme 5



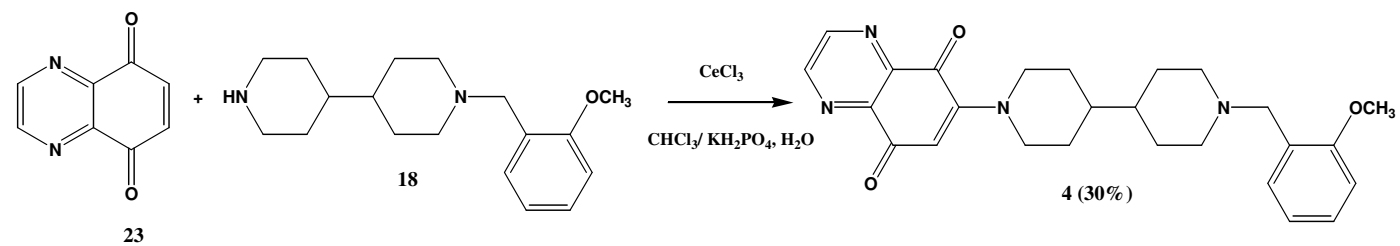
Scheme 6



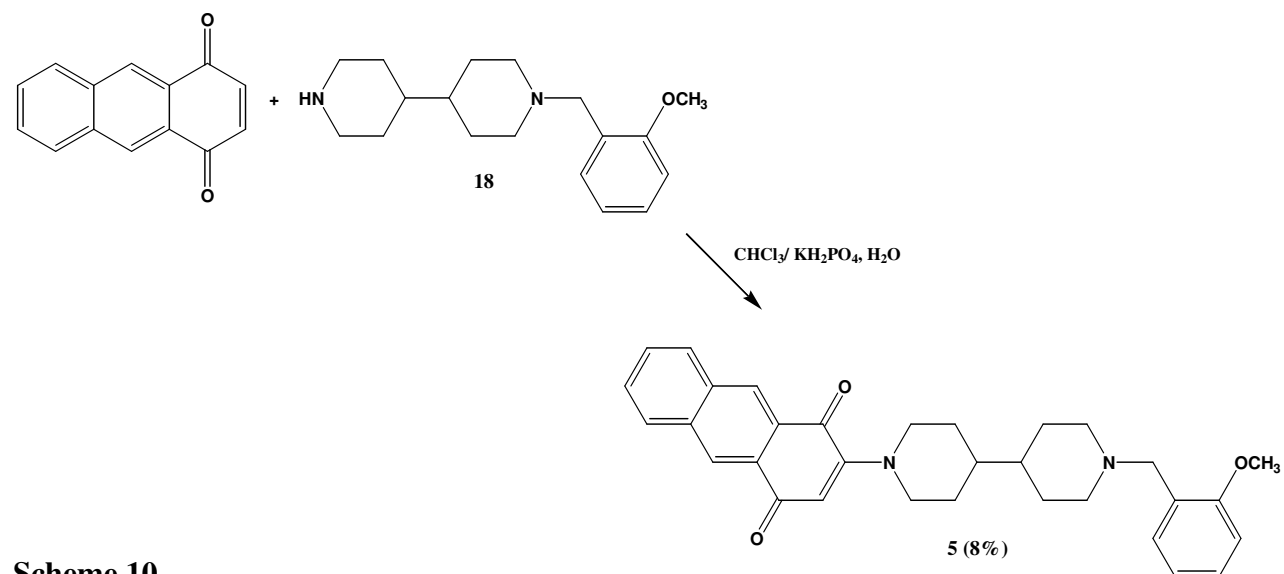
Scheme 7



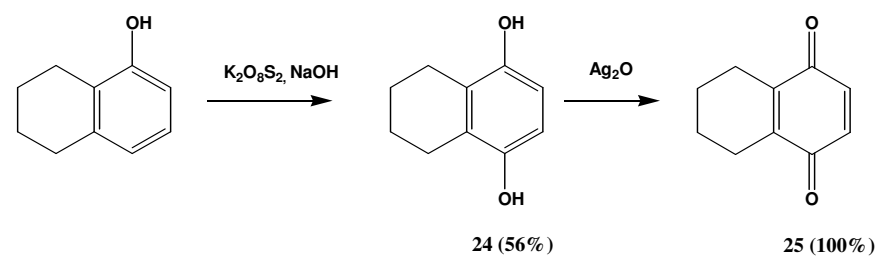
Scheme 8



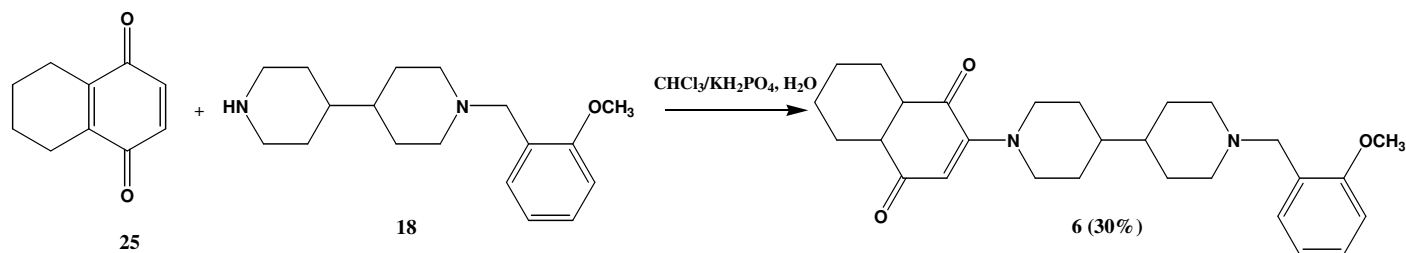
Scheme 9



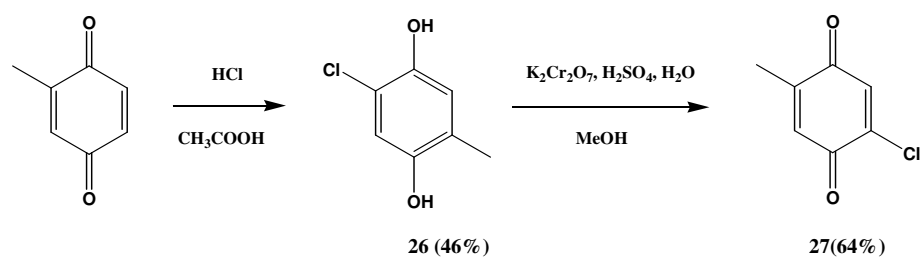
Scheme 10



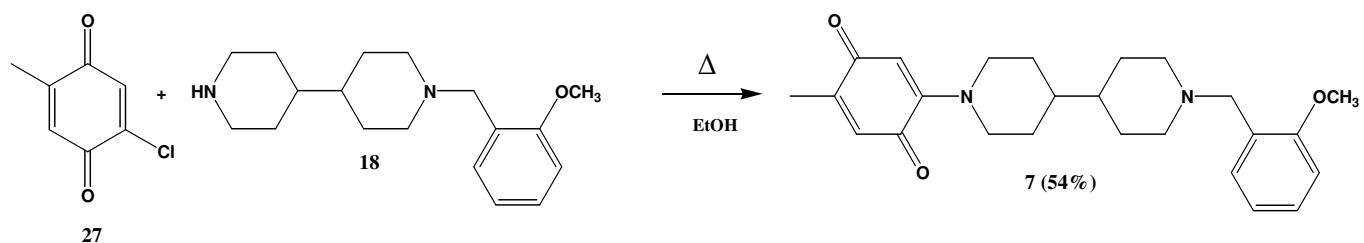
Scheme 11



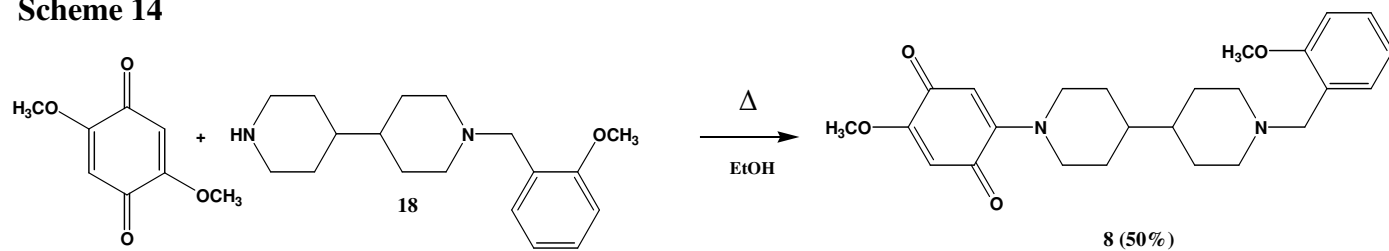
Scheme 12



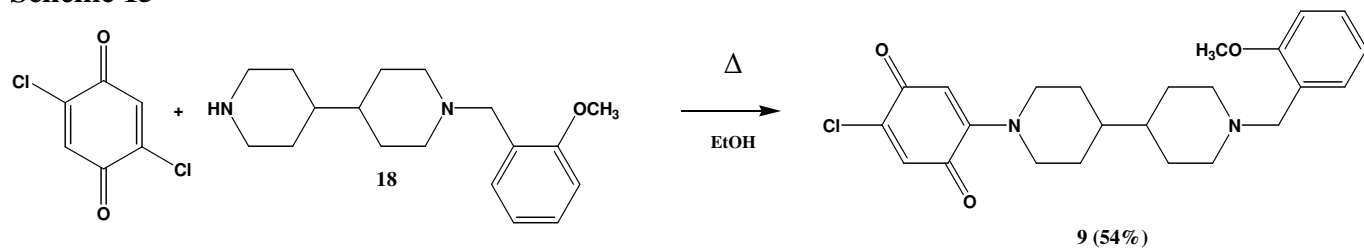
Scheme 13



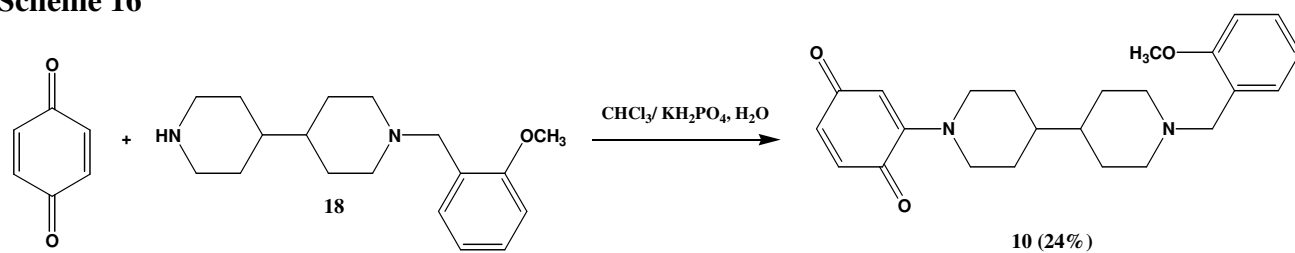
Scheme 14



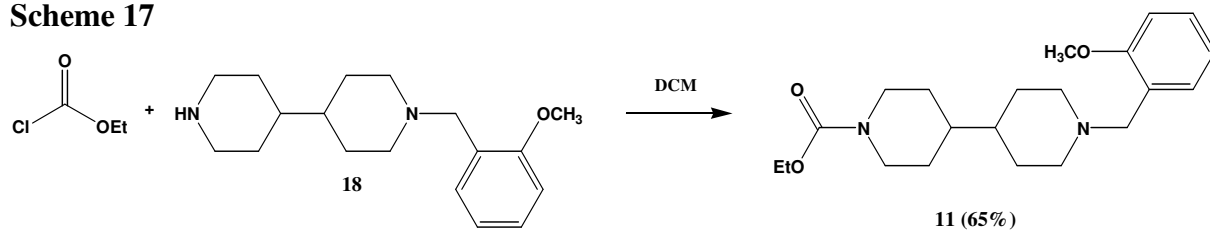
Scheme 15



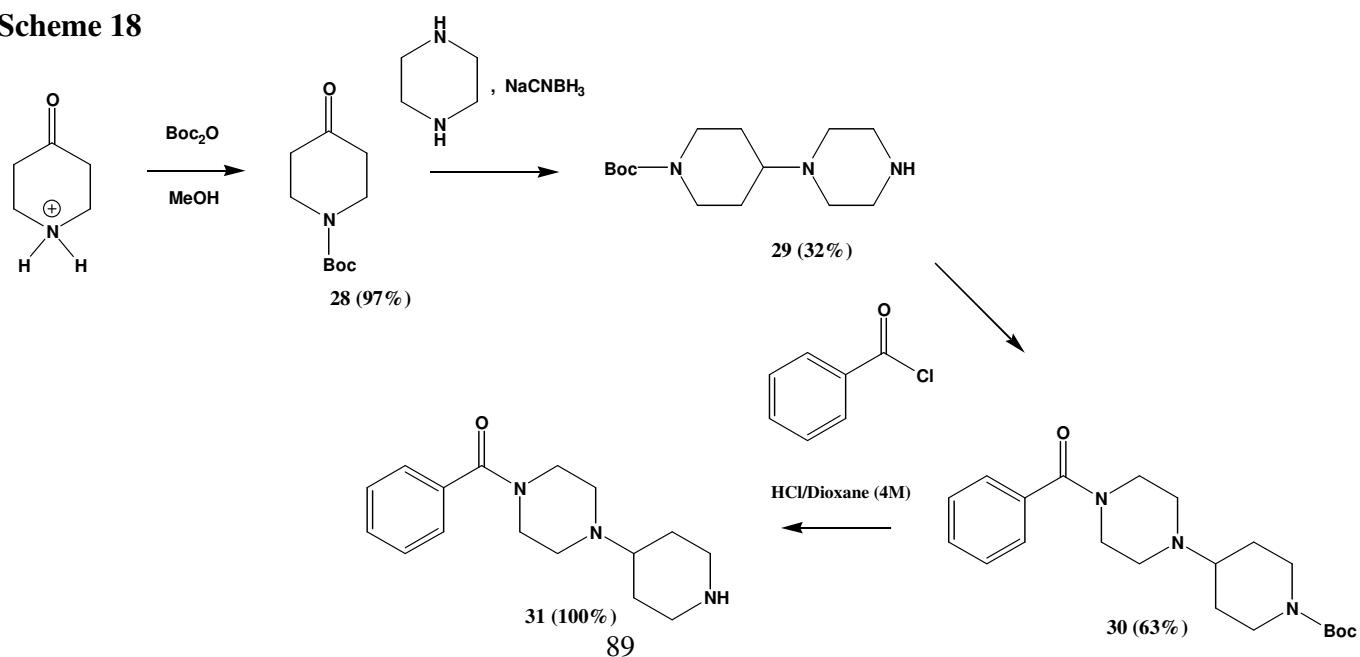
Scheme 16



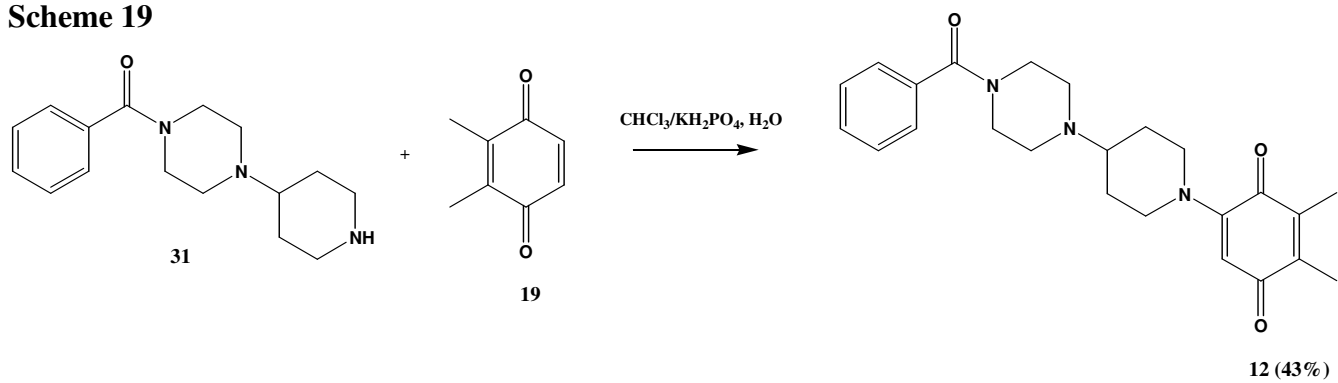
Scheme 17



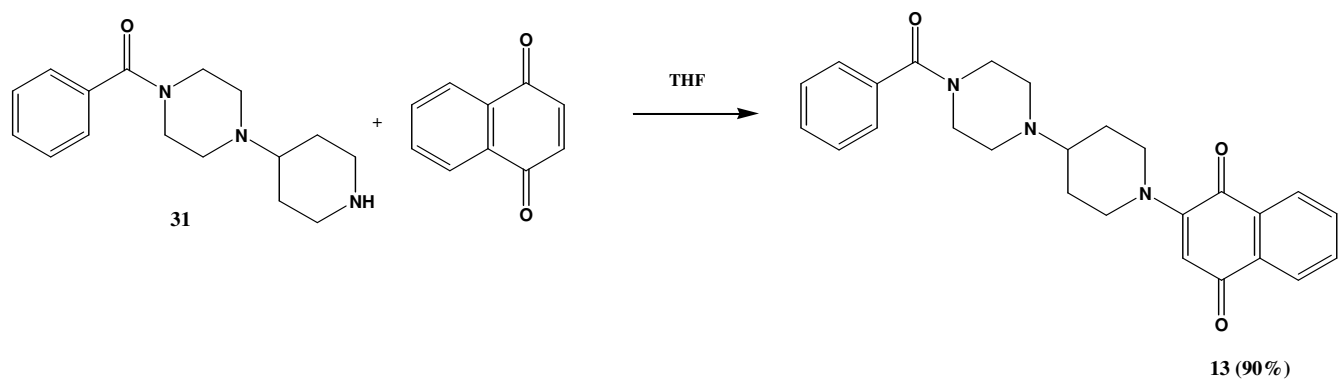
Scheme 18



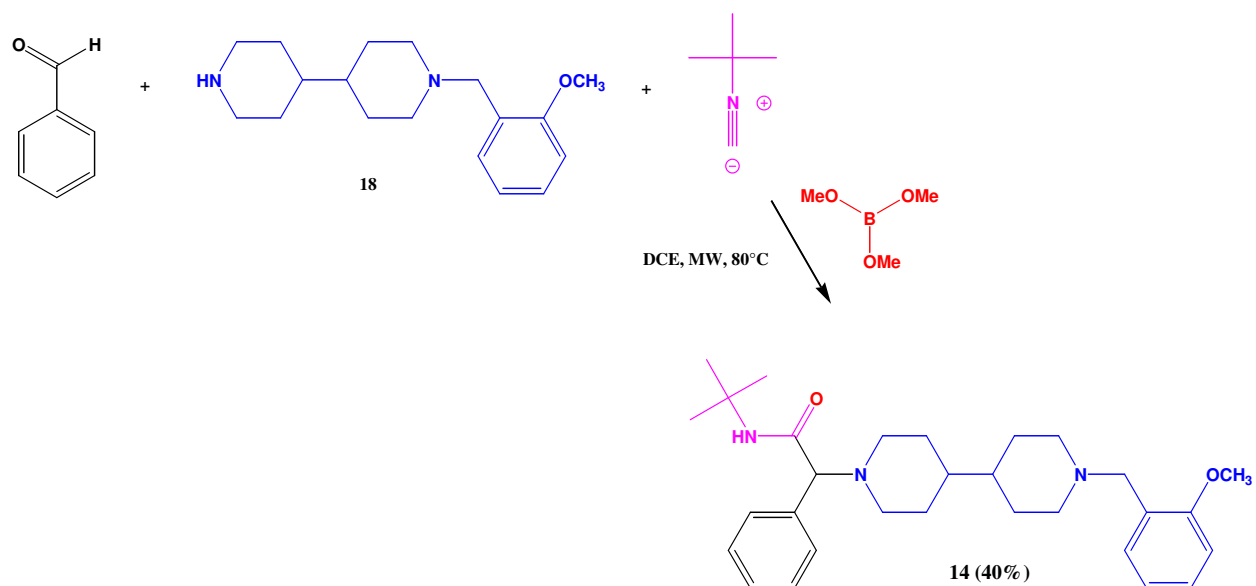
Scheme 19



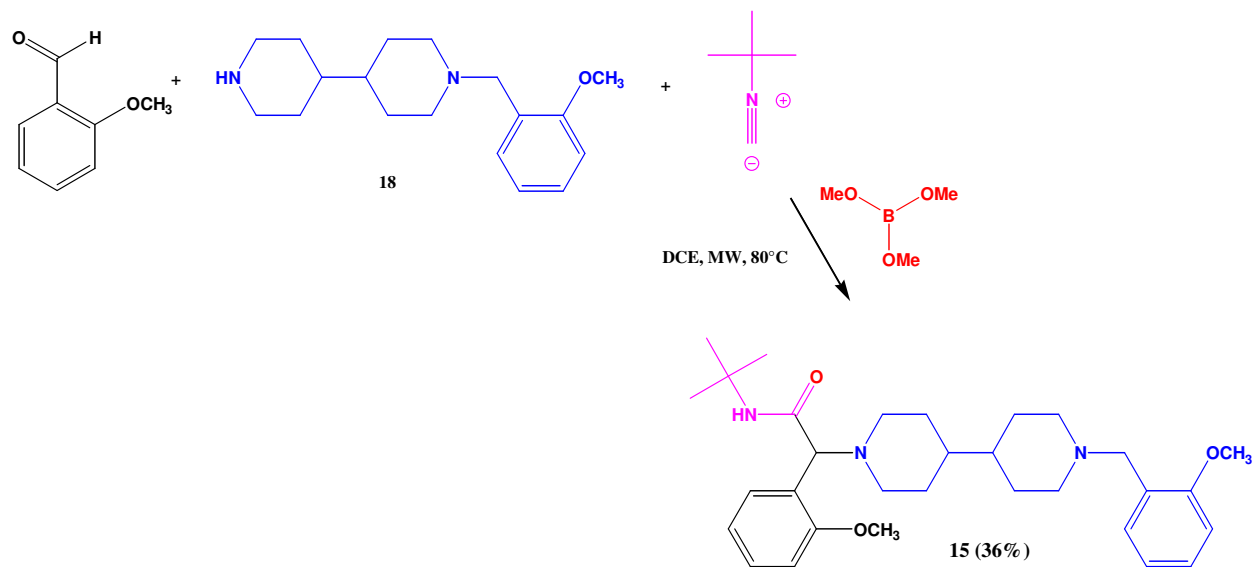
Scheme 20



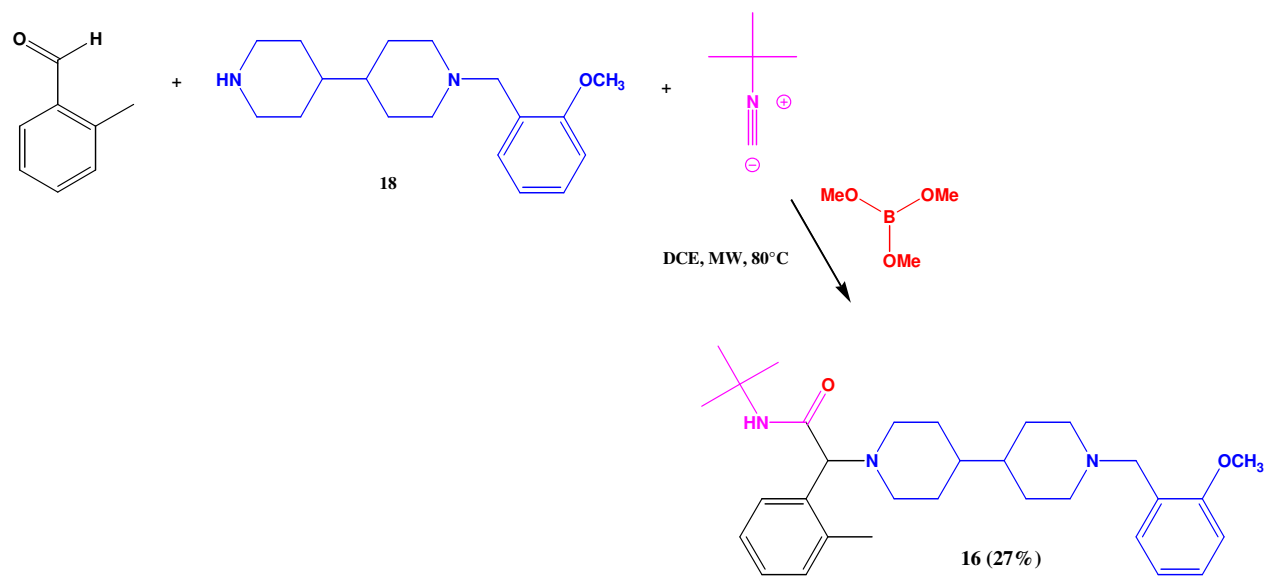
Scheme 21



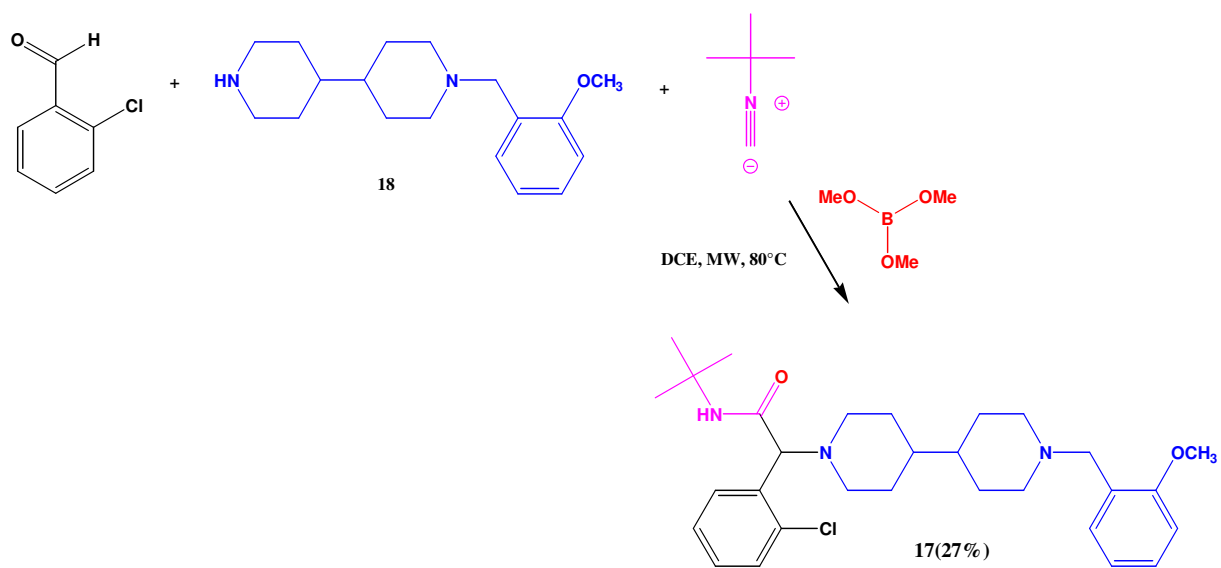
Scheme 22



Scheme 23



Scheme 24



4 Results and Discussion

4.1 Compounds 1-11

Allosteric interactions are quite complex and there are several pharmacological approaches that can be used to detect and quantify the interactions at GPCRs. These biological assays are: radioligand binding assays, functional cellular assays, dissociation binding studies and site-directed mutagenesis studies. All these approaches have been used to study the effects of compounds **1-11** on mAChRs. Moreover, **1-11** were also tested to assess their inhibition of AChE. All the results are reported and discussed below.

A Radioligand Binding Assays

Radioligand binding assays often provide the most direct way for visualizing an allosteric ligand. As we already discussed, an allosteric ligand binds to a site on the receptor that is spatially distinct from the orthosteric site to which the endogenous ligand (or another primary ligand) binds, allowing the primary and allosteric ligands to bind simultaneously and form a ternary complex with the receptor. The interaction of the orthosteric radioligand and the receptor may be modified by the presence of the allosteric ligand. Therefore, if the binding of the second ligand does not fully inhibit the radioligand binding, this effect could suggest that the second ligand might possess an allosteric behavior. Radioligand binding assays were performed by Prof. Spampinato's group using the muscarinic orthosteric antagonist [³H]NMS. The experiments were conducted in HEK293 cells transfected with M₁ and M₂ mAChRs. As expected, atropine, another muscarinic orthosteric antagonist, was able to fully displace [³H]NMS from its site as shown in the binding isotherm in **Figure 64** (bottom: 8.35% [³H]NMS bound). This behavior reflects their competitive interaction.

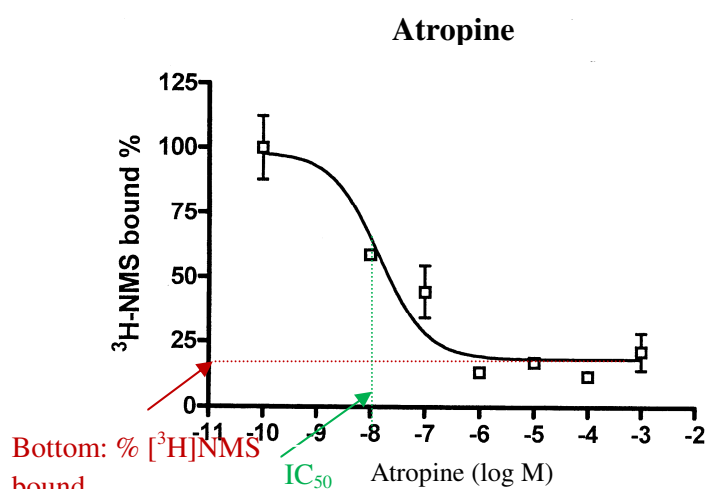
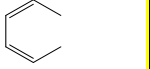
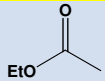


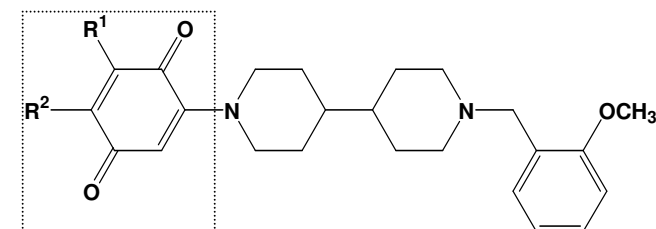
Figure 64: Atropine binding isotherm.

Compounds **1-11** were tested to firstly identify which compounds do not fully inhibit [³H]NMS binding. The results are summarized in **Table 1**. The pK_i value, the pIC₅₀, and the percent inhibition of specific [³H]NMS binding are reported for both the M₁ and the M₂ subtype. The ligand potency is expressed as IC₅₀, which represents the concentration of ligand required to decrease [³H]NMS bound by 50%. K_i is the dissociation constant of the ligand for its receptor and represents the affinity of the ligand. Among all the compounds, **1**, **2** and **11** appeared to be the most interesting because they were not able to fully displace [³H]NMS from the orthosteric binding site on M₁ mAChRs, suggesting that they might interact at a site that is distinct from ACh binding site. From these preliminary results we can also observe that the quinone ring did not seem to be essential for the interaction with the allosteric site on the M₁ subtype. In fact, **11** whose bottom value was 36.49% possesses a carbamic group instead of a quinone moiety as in **1** and **2**. Compound **1**, compared to **2** and **11**, displayed the highest affinity and the highest potency for M₁ mAChRs. Moreover, its affinity for M₁ was 1400-fold higher than that for the M₂ subtype (pK_i 9.53 vs 6.38). This selectivity for the M₁ subtype is very important because activation of muscarinic M₂ autoreceptors would inhibit the release of ACh in the synapse, contrasting the activation of M₁. An analysis of the results reported in **Table 1** reveals that the substituents on the quinone moiety markedly affected the interaction of the compounds with the allosteric site on M₁ mAChRs. It turned out that the replacement of the 2,3-dimethylbenzoquinone of **1** with a bulkier substituent as naphthoquinone in compound **2** caused a reduction in affinity, potency and percentage of [³H]NMS bound. Moreover, the introduction of an even bulkier substituent as anthraquinone (compound **5**) was detrimental for the interaction with the allosteric site on the M₁ subtype. In fact, **5** completely inhibited [³H]NMS binding (bottom: 1.84% [³H]NMS bound). The introduction of quinoline-5,8-dione and quinoxaline-5,8-dione as in **3** and **4**, respectively, generated more polar compounds. In fact, the nitrogen atom might form H-bond interactions with the biological counterpart. From the competition binding of [³H]NMS, we can observe that **4** completely displaced [³H]NMS from ACh binding site and **3** showed a bottom value of 17.85%. This might suggest that the introduction of more polar quinones may have a detrimental effect on the interaction on the allosteric site on the M₁ subtype. This effect was more marked for **4** that contains two nitrogen atoms in the quinone ring. From these results, we can envisage that the substituents on the quinone group might interact with a lipophilic pocket that is present in the allosteric site on M₁ but not on M₂ mAChRs. Thus, the introduction of polar groups like a nitrogen as in **3** and **4** might not favour the interaction with M₁ receptors. Moreover, these findings suggest that the allosteric binding site on the M₁ subtype might possess a definite binding area. Indeed, the best activity is obtained with small substituents like a methyl group as

in **1**. On the other hand, bulkier substituents may not be optimal to be embedded in the lipophilic pocket. In addition, compound **11**, which possesses a carbamic group, retained its activity on M₁ mAChRs. Its affinity and potency were even higher than those of **2**. This could suggest that a planar and less bulky structure and two oxygen groups able to form hydrogen bonds are sufficient for the interaction with the allosteric site on M₁ mAChRs.

The influence of a single substituent on the quinone ring was also exploited according to Craig diagram.⁴⁹⁸ An analysis of the results reveals that compounds **7-10** fully inhibited [³H]NMS binding and their affinities for M₁ mAChRs were lower than that of atropine. It turned out that the second substituent on the quinone ring is essential for the interaction with the allosteric binding site. Thus, compound **7** bearing only one methyl group on the quinone ring, fully inhibited [³H]NMS binding, while compound **1** caused a 47.46% inhibition of [³H]NMS binding. From the results shown in **Table 1**, we can also observe that the chemical and physical properties of the quinone moiety markedly affected the interaction with M₁ mAChRs but not with the M₂ subtype. This finding suggests that the allosteric site on M₁ mAChRs might possess a defined binding area that is marked affected by the nature of the substituents on the quinone ring.

Compound			M ₁ ^a			M ₂ ^a		
	R ¹	R ²	pK _i ^b	pIC ₅₀ ^c	Bottom ^d (% [³ H]NMS bound)	pK _i ^b	pIC ₅₀ ^c	Bottom ^d (% [³ H]NMS bound)
Atropine			8.36	7.84	8.35			
1	Me	Me	9.53	9.00	47.46	6.38	6.11	0
2			6.25	5.72	32.82	6.62	6.35	0
3			7.42	6.90	17.85	6.74	6.47	0
4			6.60	6.07	4.73	6.55	6.28	0.27
5			6.61	6.09	1.84	6.38	6.11	0
6			nt ^e	nt ^e	nt ^e	nt ^e	nt ^e	nt ^e
7	CH ₃	H	6.98	6.45	0	nt ^e	nt ^e	nt ^e
8	OCH ₃	H	6.48	5.95	0	nt ^e	nt ^e	nt ^e
9	Cl	H	6.29	5.77	0	nt ^e	nt ^e	nt ^e
10	H	H	5.59	5.07	0	nt ^e	nt ^e	nt ^e
R ³								
11			7.82	7.30	36.49	6.09	5.82	5.63



R³

Table 1: Binding constants of atropine and **1-11** at M₁ and M₂ mAChRs. ^a Assays were performed in HEK293 cells transfected with M₁ and M₂ mAChRs using [³H]NMS 1 nM. The values are the mean of two independent experiments. ^b pK_i = -log(K_i), K_i represents the dissociation constant of the ligand. ^c pIC₅₀ = -log(IC₅₀), IC₅₀ represents the concentration of ligand required to decrease [³H]NMS bound by 50%. ^d Bottom represents the lowest asymptote (basal response) of the curve. ^e nt: not tested.

B Functional Assays

Functional assays were also performed by Prof. Spampinato's group using a protocol described by Thomas et al.⁵⁰⁶ It is well known that ligands binding to M₁ mAChRs activate G_q proteins, which, in turn, activate PLC with the subsequent generation of IP₃ and DAG. However, the ability of this receptor subtype to influence additional downstream effector pathways (via distinct G protein subtypes) has also been reported. Thus, the M₁ subtype has been shown to activate also adenylyl cyclase activity via a G_s protein-dependent mechanism.⁵⁰⁷ Among a range of orthosteric muscarinic agonists, OXO-M exhibited the greatest intrinsic activity in adenylyl cyclase activation and cAMP accumulation.⁵⁰⁶ In the light of these considerations, functional assays were performed studying the effects of these new compounds on the production of cAMP induced by OXO-M. Compounds **1-11** were analyzed firstly at a concentration of 100 nM on HEK293 cells transfected with M₁ mAChRs. The results are summarized in **Table 2**. The EC₅₀ represents the concentration of a ligand required to induce a response of 50% of its maximal effect. R_{max} % is the percent of the maximal response of each compound referred to OXO-M. An analysis of the results reported in **Table 2** reveals that at 100 nM **1** and **2** caused a marked increase in cAMP production. This effect was much more marked for compound **1**. In fact, it was able to triplicate cAMP accumulation induced by OXO-M. On the other hand, compound **2** increased the production of cAMP by 189.1%. Moreover, it was shown that **11** caused a decrease in cAMP production by 62.5%. This indicates that **11**, unlike **1** and **2**, may destabilize the receptor conformation induced by OXO-M, negatively affecting the downstream signaling cascade. Functional assays performed without the orthosteric agonist OXO-M showed that **1**, **2** and **11**, alone, did not have any noteworthy effect on cAMP production (**Fig. 65**). The present finding suggests that these compounds do not possess intrinsic activity. Thus, they are not able to induce (**1** and **2**) or inhibit (**11**) G_s protein-dependent pathways.

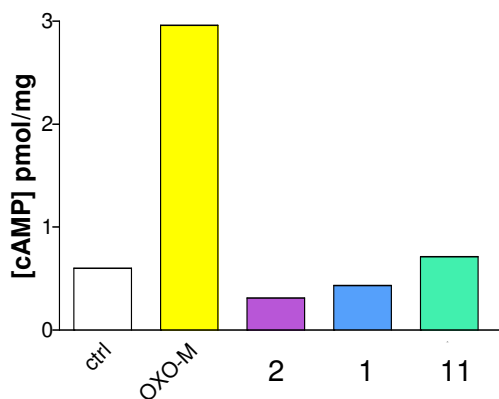


Figure 65: cAMP assays performed with **1**, **2**, and **11** without OXO-M.

Interestingly, compounds **7** and **10** were able to increase cAMP accumulation by 181.4% and 166.5%, respectively, while completely displacing [³H]NMS (**Table 1**, 0% [³H]NMS bound). Derivative **8** is probably even more interesting: it did not increase the maximal response of OXO-M but it caused a leftward shift in OXO-M concentration response curve with a significant increase of the pEC₅₀ value compared to that of OXO-M alone (7.59 vs 5.23). This suggests that a lower OXO-M concentration is required to obtain the same maximal response. This effect would be particularly useful in AD where the levels of the neurotransmitter ACh are reduced. The same behaviour was displayed by compounds **4**, **5**, and **9**. However, their effects were not so marked as for **8**.

To study the effect of different concentrations of **1** and **2** on the activation of M₁ mAChRs, functional studies were performed also at 0.01 μM and 1 μM. An analysis of the results shown in **Figure 66A** and in **Table 3** reveals that increasing concentration of **1** caused a marked increase in cAMP production induced by OXO-M. Moreover, increasing concentrations of **1** were associated with an increase in pEC₅₀ and therefore in OXO-M potency. Interestingly, the stimulation of cAMP production was more marked when the concentration was increased from 0.01 μM to 0.1 μM. Thus, the percentage of the maximal response at 0.01 μM was 63.9% and reached 327.4% when the concentration was 0.1 μM. However, when the concentration was 1 μM the maximal response was found to be 444.4%. This effect reflects the saturability of the allosteric interaction; once the allosteric sites are completely occupied, no further allosteric effect is observed.⁵⁰⁸ An analysis of the results shown in **Figure 66B** and in **Table 3** reveals that, in the presence of OXO-M, increasing concentration of **2** caused a decrease in cAMP production. This effect could be due to the fact that, at lower concentrations, **2** interacts with the allosteric site affecting positively cAMP production, whereas, at higher concentrations, after saturating the allosteric site, it might bind also to a different binding site, contrastating OXO-M effect.

Compound		pEC ₅₀ ^a	R _{max} % ^b	Effect ^c	
R ¹	R ²				
Oxotremorine		5.23	100		
1	Me	Me	6.09	327.4	↑
2			4.42	189.1	↑
3			5.20	85.1	↓
4			6.51	97.0	↔
5			6.27	71.5	↓
6		nt ^d	nt ^d	nt ^d	
7	CH ₃	H	4.45	181.4	↑
8	OCH ₃	H	7.59	93.0	↔
9	Cl	H	6.67	92.3	↔
10	H	H	3.92	166.5	↑
R ³					
11			4.43	62.5	↓

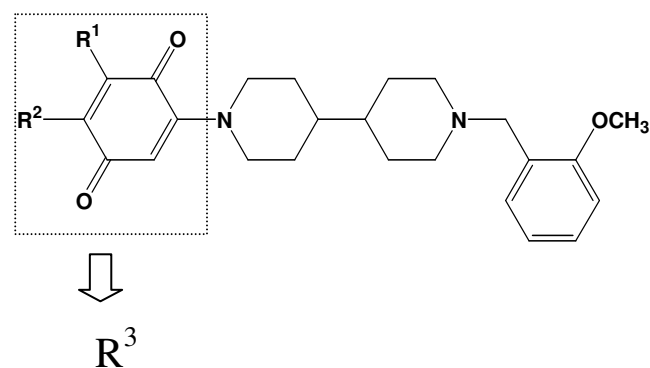
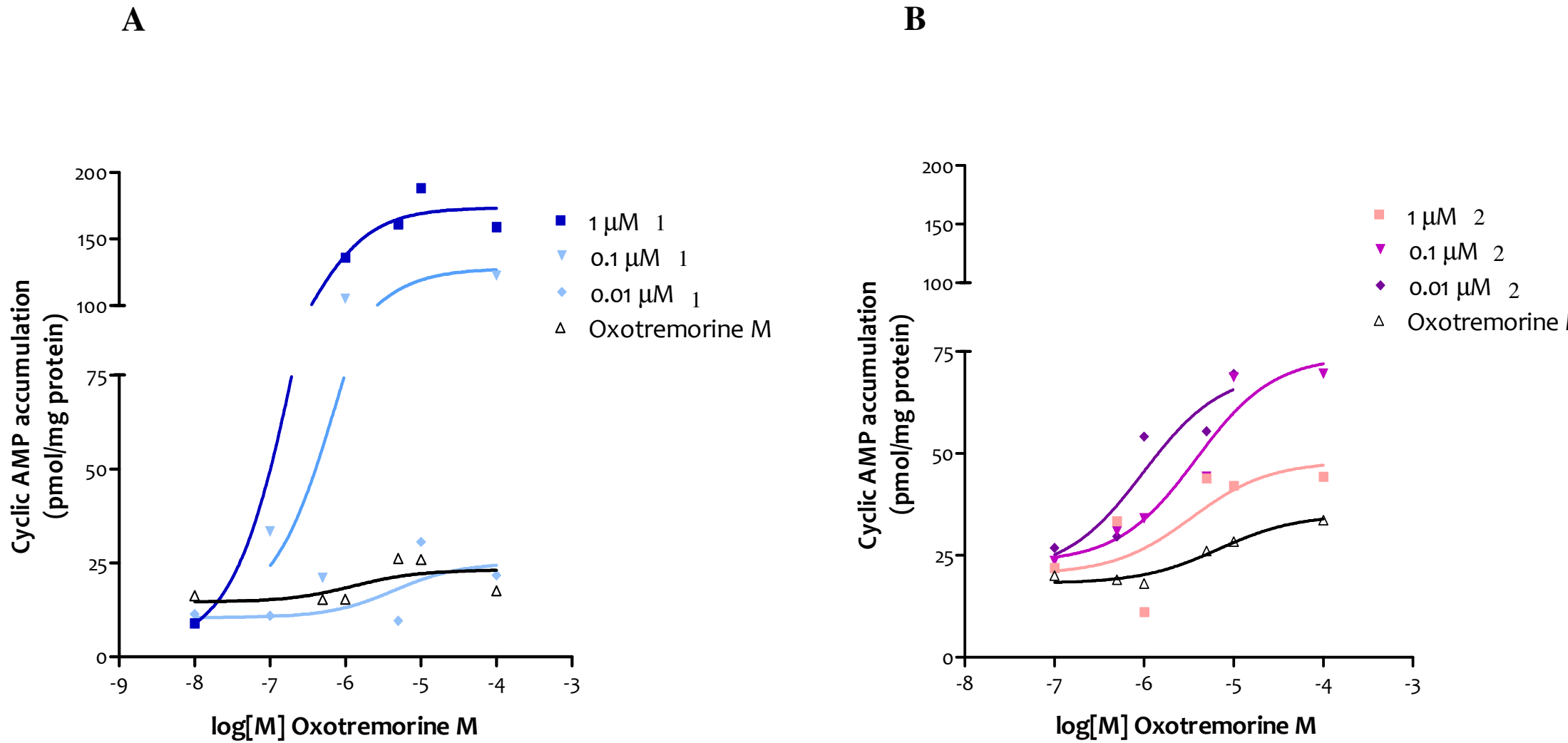


Table 2: Functional studies (cAMP assay) of compounds **1-10** were performed in HEK293 transfected with M₁ mAChRs. The values are the mean of two independent experiments. ^a pEC₅₀ = -log(EC₅₀), EC₅₀ represents the concentration of ligand required to decrease the [³H]NMS bound by 50%. ^b R_{max} % is the percentage of the maximal response using OXO-M as reference compound. ^c The effect of the compounds on the production of cAMP is summarized as:

↑ = increase in cAMP production; ↓ = reduction in cAMP production; ↔ = any effect on cAMP production. ^d nt: not tested.



Compound	Concentration	pEC ₅₀ ^a	R _{max} ^b	R _{max} % ^c
OXO-M	0,1 μM	5,23	39,04	100
OXO-M + 1	0,01 μM	5,35	24,9	63,9
	0,1 μM	6,09	127,8	327,4
	1 μM	6,58	173,5	444,4
OXO-M + 2	0,01 μM	6,01	70,06	179,5
	0,1 μM	5,42	73,83	189,1
	1 μM	5,47	47,98	122,9

Table 3: Effect of three different concentrations of **1 (A)** and **2 (B)** on cAMP production induced by OXO-M. The values are the mean of two independent experiments. ^a pEC₅₀ = -log(EC₅₀), EC₅₀ represents the concentration of a ligand required to induce a response of 50% of its maximal effect. ^b R_{max} is the maximal response of cAMP production in pmol/mg. ^c R_{max}% is the percentage of the maximal response referred to OXO-M.

C [³H]NMS Dissociation Binding Studies

Allosteric modulators cause a conformational change in the receptor that is often manifested as an alteration of the dissociation rate of a preformed orthosteric ligand-receptor complex.⁴³⁵ Hence, a change in receptor conformation induced by an allosteric agent would be expected to slow down the orthosteric ligand dissociation rate. A kinetic assay determines the ligand dissociation rate (K_{off}) as a function of time. Since kinetic studies represent the most sensitive direct measurement of allosteric interactions at GPCRs, [³H]NMS dissociation binding assays were also performed to validate the allosteric character of **1 (Figure 67)**. It was shown that **1** significantly slowed the rate of [³H]NMS dissociation induced by the orthosteric antagonist atropine (**Table 4**). In fact, atropine alone was able to displace completely [³H]NMS with an half-life of 7.9 min, whereas, in the presence of **1**, the half-life was 13.1. Thus, the ability of **1** to significantly alter the dissociation rate of [³H]NMS reinforces the hypothesis that it binds to a site topographically distinct from ACh binding site.

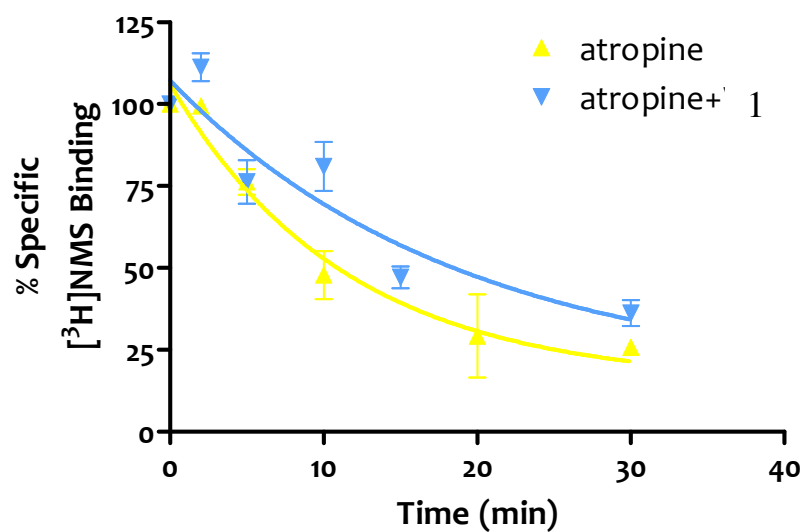


Figure 67: [³H]NMS kinetic studies in the presence of atropine alone and atropine plus **1**.

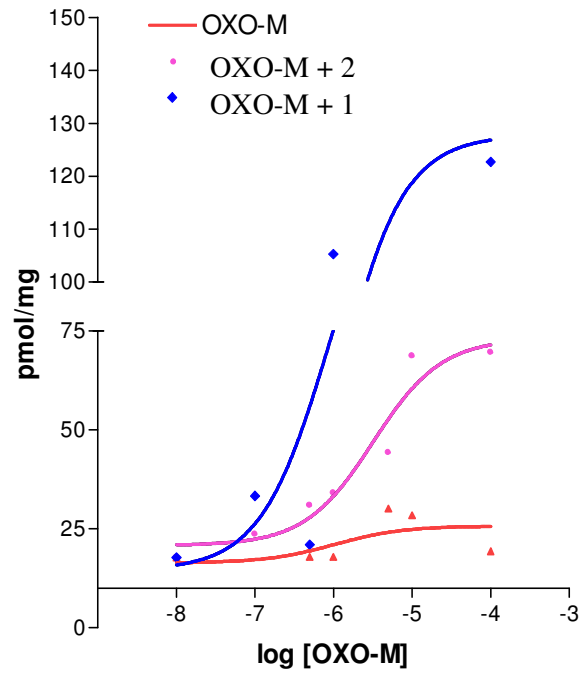
Compound ^a	K _{off} (min ⁻¹) ^b	Half-life (min) ^c
Atropine	0.088	7.9
Atropine + 1	0.053	13.1

Table 4: [³H]NMS kinetic studies in the presence of atropine and atropine plus **1**. The values are the mean of two independent experiments. ^a The concentration of atropine and **1** was 10 μM. ^b K_{off} denotes the rate constant for dissociation of the radioligand from its site. ^c Half-life is the time required to decrease the [³H]NMS bound by 50%.

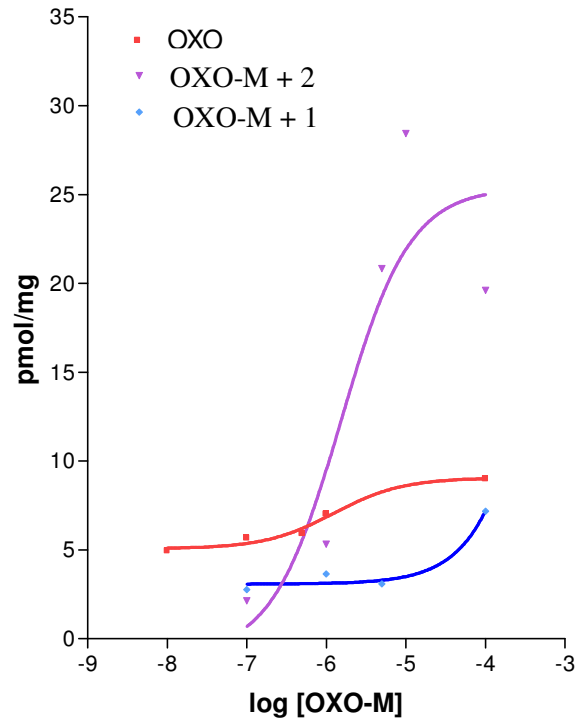
D *Mutagenesis studies*

To confirm that **1** and **2** bind at an allosteric site, mutagenesis studies were also performed. In literature, it is reported that Y381A mutation in TM6 profoundly affected the binding of the orthosteric agonist CCh. However, the allosteric agonists AC-42 and TBPB still produced a robust agonist response similar to that obtained in wt M₁ mAChRs.^{426, 444} Moreover, chimeric receptors revealed that Phe₇₇ in TM2 plays an important role for the interaction of AC-42 and TBPB with the allosteric site on the M₁ subtype.⁴⁴⁵ In the light of these considerations, functional experiments were performed on M₁ mAChRs containing Y381A and F77I mutations. The concentration of OXO-M, **1** and **2** was 100 nM. The results are shown in **Figure 68**. From the analysis of the graphs, we can observe that, as expected, OXO-M and derivatives **1** and **2** activated wild type M₁ mAChRs with the subsequent production of cAMP. Y381A mutation on the orthosteric site abrogated the effect of OXO-M and also that of **1** and **2**. In functional assays, it was observed that **1** and **2** were not able to activate the M₁ subtype in the absence of the orthosteric agonist OXO-M (**Fig. 65**). The finding on M₁ mAChRs bearing Y381A mutation confirms that, when OXO-M cannot interact with the orthosteric site, derivatives **1** and **2** lose completely their activity. Therefore, no cAMP accumulation was detected. On the other hand, F77I mutation on the allosteric site did not completely abrogate OXO-M activity, while derivative **1** was completely inactive. The present finding suggests that compound **1** might share the same binding pocket of the allosteric ligands AC-42 and TBPB. Interestingly, derivative **2** retained its activity, suggesting a possible interaction with a site different from that of **1**, explaining why F77I mutation did not affect its activity.

WT M₁ mAChRS



F77I mutation



Y381A mutation

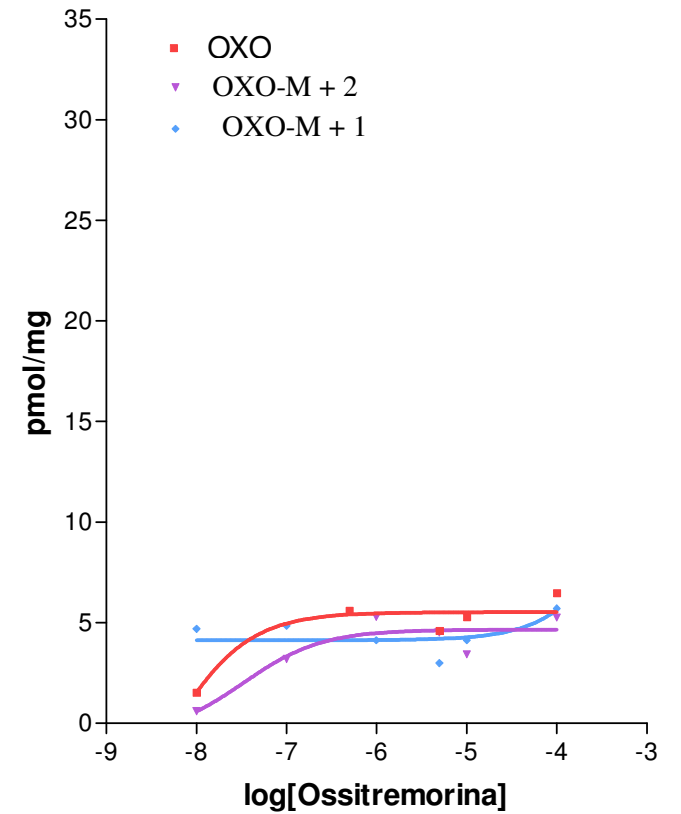
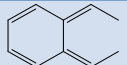
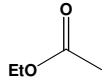


Figure 68: Effects of OXO-M and compounds **1** and **2** (100 nM) on wild type or M₁ mAChRs containing F77I and Y381A mutations.

E *AChE Inhibition*

The inhibitory effects of compounds **1-11** on human recombinant AChE and BuChE from human serum were assessed in comparison to memoquin, a dual binding AChEI, which accounts for its remarkable nanomolar activity.⁴⁸³ The experiments were performed by Dr. Bartolini's group and the results are summarized in **Table 5**. The inhibition activity is expressed as IC₅₀ value that represents the concentration of inhibitor required to decrease enzyme activity by 50%. The inhibitory potency of **1-11** was evaluated on both AChE and BuChE because selectivity for AChE over BuChE may be beneficial for AD. Thus, BuChE may have a role inverse to that of AChE in AD.⁵⁰⁹ Moreover, BuChE does not possess the PAS that is responsible for the A β assembly into amyloid fibrils.¹⁹⁸ From an analysis of the results shown in **Table 5** it turned out that **1-11** were modest AChEI. They inhibited AChE with IC₅₀ values ranging from 2.56 to 290 μ M while memoquin displayed an IC₅₀ of 1.55 nM. It is plausible that the constrained structure of **1-11** does not allow an optimal interaction with AChE gorge as already observed for other memoquin monomeric derivatives.⁵¹⁰ In previous assays, it was envisaged that the substituents on the quinone ring may give critical interactions with a lipophilic pocket in the allosteric site on the M₁ subtype. Thus, the physical and chemical properties of such substituents play an important role in driving the ligand in the allosteric site. An analysis of the results reported in **Table 5** reveals that changing the electronic and lipophilic properties of the quinone ring did not markedly affect the inhibitory potency against AChE and BuChE. Among all the compounds, the most potent AChEIs were compounds **3** and **5**. They were 6-fold and 5-fold, respectively, more selective for AChE than for BuChE. However, from studies on mAChRs, it was found that a quinoline-5,8-dione (**3**) or a bulky quinone as anthraquinone (**5**) did not display any positive effect on M₁ activation. Binding and functional assays on mAChRs revealed that compounds **1** and **2** were the most promising. In AChE inhibition assays, **1** and **2** displayed an IC₅₀ values of 12.2 and 17.0 μ M, respectively. Moreover, **2** was slightly more potent for BuChE than for AChE. Compound **11**, bearing a carbamic group, was expected to be a pseudo-irreversible AChE inhibitor. It is well known that carbamates might form a carbamoylated complex with the serine residue of the catalytic triad of AChE enzyme, which is hydrolyzed in hours. Unfortunately, the inhibitory activity of **11** resulted time-independent, suggesting that it was not an irreversible inhibitor.

Compound			IC ₅₀ AChE (μM) ^a	IC ₅₀ BuChE (μM) ^a	Selectivity AChE/BuChE
	R ¹	R ²			
Memoquin^b			0.00155±0.00011	0.144±0.100	0.011
1	Me	Me	12.2 ± 0.6	14.9 ± 0.7	0.82
2			17.0 ± 0.9	13.9 ± 0.6	1.22
3			2.56 ± 0.18	15.2 ± 0.8	0.17
4			10.8 ± 0.8	12.1 ± 1.2	0.89
5			2.64 ± 0.23	13.8 ± 0.7	0.19
6			9.53 ± 0.26	3.04 ± 0.13	3.13
7	CH ₃	H	10.1 ± 0.7	16.1 ± 1.2	0.63
8	OCH ₃	H	24.4 ± 1.4	3.58 ± 0.15	6.81
9	Cl	H	9.45 ± 0.41	21.8 ± 0.2	0.43
10	H	H	8.20 ± 0.43	30.9 ± 1.5	0.27
11			290 ± 11	102 ± 5	2.84

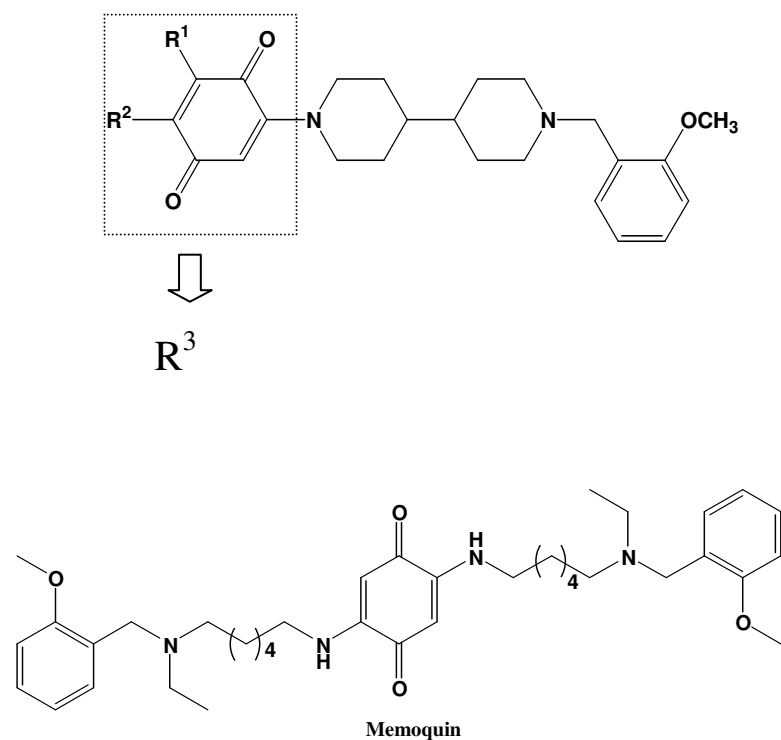


Table 5: Inhibitory activities on human AChE and BuChE of **1–11** and the reference compound memoquin. ^a Human recombinant AChE and BuChE from human serum were used. IC₅₀ represents the concentration of inhibitor required to decrease enzyme activity by 50% and is the mean of two independent measurements, each performed in duplicate. ^b Data from ref.⁵¹⁰

F Antioxidant Activity

Several studies on the antioxidant properties of 1,4-benzoquinone derivatives, such as idebenone and CoQ, have conclusively demonstrated that the antioxidant activity is due exclusively to their hydroquinone form, since the quinone, in principle, cannot scavenge radicals.⁵¹¹ Furthermore, NAD(P)H:quinone oxidoreductase 1 (NQO1, DT-diaphorase) was shown to catalyze the two-electron reduction of quinones to hydroquinones, bypassing the production of semiquinones and, consequently, preventing their participation in redox-cycling and the subsequent generation of ROS. Moreover, NQO1 was found to be increased in AD in response to the perturbation of the balance between generation and scavenging of ROS.⁵¹² In the light of these considerations, compounds **1**, **2**, and **8** were tested with respect to their ability to accept electrons from NAD(P)H via rat NQO1, in comparison with menadione as a reference compound, following the absorbance change of NAD(P)H. The results are shown in **Figure 69** and in **Table 6** and expressed in terms of variation of absorbance (Δ abs) at 340 nm per minute. High values in Δ abs/min mean that high amounts of NAD(P)H have been oxidized to reduce the quinone ring to the corresponding hydroquinone form. To study the effect of the concentration on the ability to accept electrons, the experiments were performed using three different concentrations of tested compounds (20, 40, and 80 μ M) to. Only two concentrations were used for the reference compound menadione, because the best activity was obtained at concentrations higher than 20 μ M. However, at 80 μ M, a decrease in menadione activity was observed (Δ abs/min 1.045 vs 0.630) because at higher concentrations, menadione solubility decreases slowing down the enzymatic rate. An analysis of the graph shown in **Figure 69** reveals that at 20 μ M the best substrate of NQO1 was compound **1**. Its Δ abs/min value was higher than that of menadione at 40 μ M (1.124 vs 1.045). Moreover, almost no difference was observed between Δ abs/min values obtained with the three concentrations of **1**. Compound **8** at 20 μ M was found to be a good substrate for NQO1, being not very different from menadione in terms of reduction by the enzyme (1.042 vs 1.045). We can also observe that increasing concentrations of **8** caused a decrease in Δ abs/min. This was caused by the fact that, at high concentrations, the solubility of **8** was reduced and therefore, the results obtained are not accurate.

Finally, compound **2** was completely inactive up to 80 μ M. We can envisage that the methyl groups of **1** and the methoxy group of **8**, through their electron donating effects, can stabilize the hydroquinone form and the subsequent phenoxy radicals. On the other hand, the naphthoquinone is less stable in its reduced form.

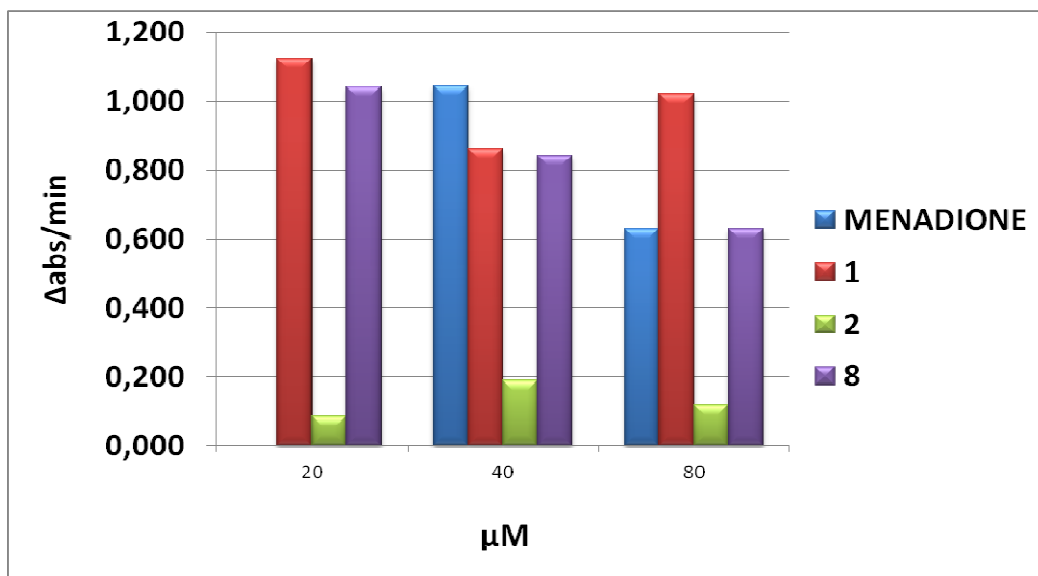


Figure 69: Ability of **1**, **2**, and **8** to accept electrons from the rat enzyme NQO1. The results are expressed in terms of variation of absorbance (Δ abs) at 340 nm per minute.

Concentration (μ M)	Menadione (Δ abs/min)	1 (Δ abs/min)	2 (Δ abs/min)	8 (Δ abs/min)
20		1.124	0.085	1.042
40	1.045	0.860	0.188	0.840
80	0.630	1.020	0.116	0.630

Table 6: Ability of **1**, **2**, and **8** to accept electrons from the rat enzyme NQO1. The results are expressed in terms of variation of absorbance (Δ abs) at 340 nm per minute.

4.2 Compounds 12 and 13

Functional and binding studies of **12** and **13** on mAChRs are in progress to verify whether they might be selective M_1 allosteric ligands. AChE inhibition assays were also performed and the results are shown below.

A AChE Inhibition

An analysis of the results shown in **Table 7** reveals that the change of position of the basic nitrogen in the amine chain is detrimental for the interaction with AChE gorge. Thus, compound **12** was 14.5-fold less potent than its homologous **1**. Furthermore, **13** was 13.4-fold less potent than **2**. These results might indicate that the structures of **13** and **14** are too constrained to create optimal interactions with AChE gorge. Moreover, since the protonable nitrogen belongs to the piperazin ring, the rotation around N-C bond is not allowed, making, perhaps, more difficult the formation of hydrogen bonds with the biological counterpart.

Compound		IC ₅₀ AChE (μ M) ^a	IC ₅₀ BuChE (μ M) ^a	Selectivity AChE/BuChE
	R ¹ R ²			
Memoquin ^b		0.00155±0.00011	0.144±0.100	0.011
12	CH ₃ CH ₃	177 ± 9	562 ± 22	0.31
13		228 ± 7	159 ± 13	1.43

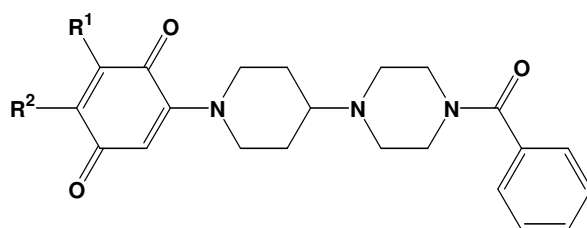


Table 7: Inhibitory activities on human AChE and BuChE of **12**, **13** and the reference compound memoquin.^a Human recombinant AChE and BuChE from human serum were used. IC₅₀ represents the concentration of inhibitor required to decrease enzyme activity by 50% and is the mean of two independent measurements, each performed in duplicate.^b Data from ref.⁵¹⁰

4.3 Compounds 14-17

Functional and binding studies of **14-17** on mAChRs are in progress to verify whether they might be promising drugs to target the neurodegeneration in AD. AChE inhibition assays were also performed and the results are shown below.

A AChE Inhibition

In the design of these compounds, we hypothesized that the two aromatic rings of **14-17** might create π - π stacking interactions with aromatic aminoacids in the gorge of AChE and with Trp₂₈₆ in the PAS of the enzyme. Surprisingly, an analysis of the results reported in **Table 8** reveals that these compounds were not good AChEIs. In fact, all the compounds showed an IC₅₀ values ranging from 71.3 to 124 μ M. Moreover, they were more selective for BuChE than for AChE.

Compound		IC ₅₀ AChE (μ M) ^a	IC ₅₀ BuChE (μ M) ^a	Selectivity AChE/BuChE
	R ¹			
Memoquin ^b		0.00155 \pm 0.00011	0.144 \pm 0.100	0.011
14	H	124 \pm 7	6.86 \pm 0.29	18.1
15	OCH ₃	122 \pm 2	6.94 \pm 0.30	17.8
16	CH ₃	77.7 \pm 5.3	8.72 \pm 0.46	8.91
17	Cl	71.3 \pm 5.5	7.47 \pm 0.39	9.54

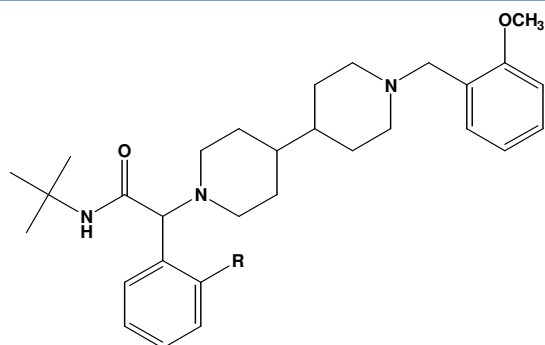


Table 8: Inhibitory activities on human AChE and BuChE of **14-17** and the reference compound memoquin. ^a Human recombinant AChE and BuChE from human serum were used. IC₅₀ represents the concentration of inhibitor required to decrease enzyme activity by 50% and is the mean of two independent measurements, each performed in duplicate. ^b Data from ref.⁵¹⁰

5 Conclusions and Future Works

A Compounds 1-11

Despite the therapeutic potential of M₁ mAChRs for the treatment of AD, high selective orthosteric ligands for the M₁ subtype have not been identified yet. However, allosteric modulation of GPCRs represents a valid alternative for identifying subtype selective ligands because it is expected that allosteric binding sites, unlike the orthosteric pockets, are less conserved among receptor subtypes. In the present thesis, we studied the effect of some quinone derivatives on M₁ mAChRs activation. The pharmacological approaches used to detect and quantify the interaction at mAChRs are radioligand binding assays, functional cellular assays, dissociation binding studies and site-direct mutagenesis studies. Among all the compounds, **1** and **2** were the most promising. In fact, from radioligand binding assays (**Table 1**) it was shown that **1** and **2** did not displace completely the orthosteric antagonist [³H]NMS, suggesting that they might interact at an allosteric site. Moreover, compound **1** was 1400-fold more selective for M₁ than for the M₂ subtype. In functional assays (**Table 2**, **Fig. 66**), **1** and **2** (100 nM) were able to increase the production of cAMP induced by the orthosteric agonist OXO-M by 327.4% and 189.1%, respectively. However, they were not able to activate M₁ mAChRs in the absence of OXO-M. Mutagenesis studies revealed that **1** loses completely its functional activity with F77I mutation in the allosteric site of the M₁ subtype, suggesting that **1** might share the same binding pocket of the allosteric agonists AC-42 and TBPB. On the other hand, compound **2** retained its activity, indicating that its binding site might be different from that of **1**. The mode of action of **1** was evaluated also in kinetic experiments. Similar to AC-42 and TBPB, **1** was able to reduce [³H]NMS dissociation rate from M₁ mAChRs (**Fig. 67**, **Table 4**). Taking together, these results suggest that **1** and **2** are positive allosteric modulators i. e., they do not have intrinsic activity but their binding potentiates the effect of orthosteric agonists such as OXO-M and ACh. From our results, also compounds **7**, **8** and **10** appear to be interesting. In fact, in functional assays, **7** and **10** (100 nM) were able to increase cAMP accumulation induced by OXO-M by 181.4% and 166.5%, respectively (**Table 2**). Mutagenesis studies are in progress to better clarify their mode of action. Regarding compound **8**, it caused a leftward shift in OXO-M response curve, without affecting cAMP production. This finding suggests that in presence of **8**, a lower OXO-M concentration is required to obtain the maximal response. This effect might be useful in AD. It is well known that in the brain of AD patients the levels of the neurotransmitter ACh are reduced. Therefore, the use of ligands that are able to induce M₁ activation also with low levels of ACh could restore the impaired signalling pathway and memory deficit. Functional experiments with different concentration of **8** and mutagenesis studies are in progress to better study the mode of

action of this interesting compound. Despite the promising results on M₁ activation, compounds **1-11** were modest AChEIs (**Table 5**). Again, the constrained structure of these derivatives might not allow an optimal binding into AChE gorge. However, their inhibitory effects were in the μM range, which might contribute to further increase ACh concentration in the synapses.

Compounds **1, 2** and **8** were also tested to determine their ability to accept electrons from NAD(P)H via NQO1, in comparison with the reference compound, menadione (**Fig. 69, Table 6**). It turned out that **1** and **8** were good substrate of NQO1 with **1**, at 20 μM, even more active than menadione.

In conclusion, we demonstrated that these quinone derivatives could be promising candidates to target M₁ mAChRs. As discussed, the activation of the M₁ subtype has the potential for positive disease-modifying treatments in a variety of psychiatric and neurological diseases such as AD. Moreover, the ability of these compounds to interact with an allosteric site could result in selective targeting of the M₁ subtype, reducing the side effects associated with activation of the other receptor subtypes. The addition of antioxidant properties could be very interesting, since it is well known that in the brain of AD patients the balance between generation and scavenging of ROS is altered.

B *Compounds 12 and 13*

Assays on mAChRs are in progress to study the mechanism of action of **12** and **13** on the M₁ subtype. Compounds **12** and **13** inhibited AChE with an IC₅₀ of 177 and 228 μM, respectively (**Table 7**). Perhaps, as for **1-11**, their structures are too constrained to penetrate into AChE gorge.

C *Compounds 14-17*

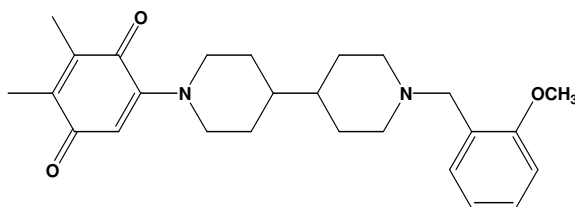
Regarding derivatives **14-17**, only AChE inhibition assays were performed. From the results shown in **Table 8**, we can observe that they were not good AChEIs. Perhaps, as for **1-13**, their structures are too constrained to fit well into AChE gorge. Assays on mAChRs are in progress to verify their activity as allosteric ligands.

6 Experimental section

6.1 Chemistry

All reactions were carried out at atmospheric pressure with stirring unless otherwise indicated. All solvents and chemicals were purchased from suppliers and used without further purification. For microwave-assisted organic synthesis a CEM Discover BenchMate reactor was used. Reaction progress was monitored by TLC plates pre-coated with silica gel 60 F₂₅₄ (Sigma Aldrich) visualized by UV (254 nm) or chemical stain (KMnO₄, bromocresol green and Ce-Mo). Flash and gravity column chromatography were performed on silica gel (particle size 40-63 μM, Merck). Melting points were determined using Büchi SMP-20 apparatus. Compounds were named relying on the naming algorithm developed by CambridgeSoft Corporation and used in Chem-BioDraw Ultra 11.0. Optical activity was determined using a Perkin Elmer instrument. ¹H-NMR and ¹³C-NMR spectra were recorded at 200-400 and 50-100 MHz, respectively, on Varian instruments. Chemical shifts were measured in ppm and are quoted as δ, relative to TMS. Multiplicities are quoted as s (singlet), d (doublet), t (triplet), q (quartet), quintet and m (multiplet), br (broad) with coupling constants defined as J given in Hz. Mass spectra were recorded on a V.G. 7070 E spectrometer or on a Waters ZQ 4000 apparatus operating in electrospray (ES) mode.

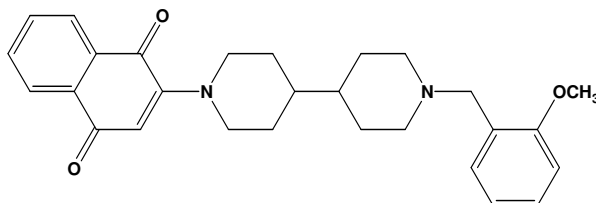
5-[1'-(2-Methoxy-benzyl)-[4,4']bipiperidiny-1-yl]-2,3-dimethyl-[1,4]benzoquinone (**1**)



A solution of **18** (200 mg, 0.70 mmol) and KH₂PO₄ (95 mg, 0.70 mmol) in H₂O (8 ml) was added dropwise to a solution of **19** (95 mg, 0.70 mmol) in CHCl₃ (2 ml). The mixture was stirred vigorously at RT for 2 h. The aqueous phase was then washed with CHCl₃ (3 x 10 ml). The combined organic extracts were dried over Na₂SO₄, filtered and concentrated *in vacuo*. The crude was purified by gravity chromatography (DCM-MeOH-aqueous 33% ammonia, 9:1:0.05) affording **1** as a purple slurry (148 mg, 0.35 mmol, 50%); ES [M+H⁺]: 423; δ_H (400 MHz, CD₃OD) 0.81-0.86 (1H, m, CH), 1.02-1.07 (5H, m, CH, 2CH₂), 1.44 (2H, d, J 13.0, CH₂), 1.51 (2H, d, J 9.4, CH₂), 1.67 (3H, s, CH₃), 1.68 (3H, s, CH₃), 1.77-1.82 (2H, m, CH₂-N), 2.55 (2H, t, J 11.8, CH₂-N), 2.72 (2H, d, J 12.2, CH₂-N), 3.31 (2H, s, CH₂-Ph), 3.54 (3H, s, OCH₃), 3.66 (2H, d, J 13.0, CH₂-N), 5.39

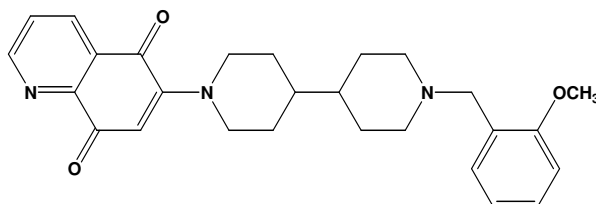
(1H, s, CH-C=O), 6.63 (1H, t, J 8.0, Ar), 6.68 (1H, d, J 8.0, Ar), 6.97-7.0 (2H, m, Ar); δ_C (100 MHz, CDCl₃) 10.83, 11.09, 28.35, 29.00, 40.21, 40.50, 49.19, 53.35, 54.33, 55.83, 105.67, 110.22, 119.77, 124.13, 128.65, 131.34, 139.15, 140.55, 153.10, 158.17, 184.89, 186.18.

2-[1'-(2-Methoxy-benzyl)-[4,4']bipiperidinyl-1-yl]-[1,4]naphthoquinone (2)



A solution of **18** (100 mg, 0.35 mmol) and KH₂PO₄ (48 mg, 0.35 mmol) in H₂O (4 ml) was added dropwise to a solution of 1,4-naphthoquinone (55 mg, 0.35 mmol) in CHCl₃ (1 ml). The mixture was stirred vigorously at RT for 2 h. The aqueous phase was then washed with CHCl₃ (3 x 10 ml). The combined organic extracts were dried over Na₂SO₄, filtered and concentrated *in vacuo*. The crude was purified by gravity chromatography (DCM-MeOH-aqueous 33% ammonia, 9:1:0.05) affording **2** as a red solid (30 mg, 0.07 mmol, 20%); mp= 53 °C; ES [M+H⁺]: 445; δ_H (400 MHz, CDCl₃) 1.09-1.15 (1H, m, CH), 1.39-1.45 (5H, m, 2CH₂, CH), 1.66 (2H, d, J 12.1, CH₂), 1.77 (2H, d, J 8.6, CH₂), 2.03 (2H, t, J 11.1, CH₂-N), 2.84 (2H, t, J 11.5, CH₂-N), 3.01 (2H, d, J 10.2, CH₂-N), 3.61 (2H, s, CH₂-Ph), 3.77 (3H, s, OCH₃), 4.02 (2H, d, J 12.1, CH₂-N), 5.96 (1H, s, CH-C=O), 6.82 (1H, d, J 7.7, Ar), 6.89 (1H, t, J 7.7, Ar), 7.20 (1H, t, J 7.7, Ar), 7.33 (1H, d, J 7.7, Ar), 7.56 (1H, t, J 7.4, Ar), 7.63 (1H, t, J 7.4, Ar), 7.93 (1H, d, J 7.4, Ar), 7.98 (1H, d, J 7.4, Ar); δ_C (100 MHz, CDCl₃) 28.92, 29.26, 40.37, 40.70, 49.76, 53.60, 55.38, 55.87, 110.42, 110.60, 120.36, 125.40, 126.55, 128.41, 131.02, 132.19, 132.50, 132.87, 132.71, 153.87, 157.82, 183.29, 183.45.

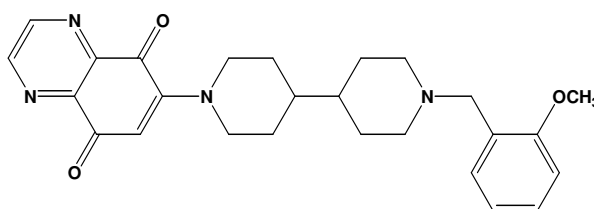
6-[1'-(2-Methoxy-benzyl)-[4,4']bipiperidinyl-1-yl]-quinoline-5,8-dione (3)



A solution of **18** (120 mg, 0.42 mmol), KH₂PO₄ (57 mg, 0.42 mmol) and CeCl₃ (10 mg, 0.04 mmol) in H₂O (4 ml) was added dropwise to a solution of **20** (67 mg, 0.42 mmol) in CHCl₃ (1 ml). The mixture was stirred vigorously at RT for 2 h. The aqueous phase was then washed with CHCl₃ (3 x 10 ml). The combined organic extracts were dried over Na₂SO₄, filtered and concentrated *in vacuo*. The crude was purified twice by gravity chromatography (DCM-MeOH-aqueous 33% ammonia,

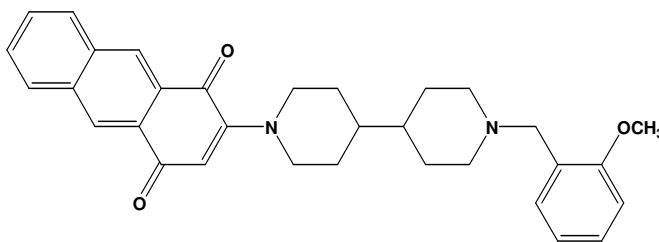
9:1:0.05) affording **3** as a purple slurry (30 mg, 0.07 mmol, 16%); ES [M+H⁺]: 446; δ_{H} (400 MHz, CD₃OD) 1.21-1.23 (1H, m, CH), 1.28-1.44 (5H, m, CH, 2CH₂), 1.79 (2H, d, J 12.6, CH₂), 1.88 (2H, d, J 12.2, CH₂), 2.25 (2H, t, J 11.8, CH₂-N), 3.01-3.11 (4H, m, CH₂-N), 3.72 (2H, s, CH₂-Ph), 3.84 (3H, s, OCH₃), 4.22 (2H, d, J 13.0, CH₂-N), 6.14 (1H, s, CH-C=O), 6.93 (1H, t, J 7.7, Ar), 6.99 (1H, d, J 7.7, Ar), 7.29-7.32 (2H, m, Ar), 7.71 (1H, dd, J 7.7, 4.7, Ar), 8.37 (1H, d, J 7.7, Ar), 8.86 (1H, d, J 4.7, Ar); δ_{C} (100 MHz, CD₃OD) 27.92, 29.14, 39.74, 40.26, 49.44, 53.15, 54.39, 55.66, 107.74, 110.35, 119.91, 122.87, 126.75, 129.23, 129.71, 131.58, 134.81, 147.67, 153.40, 153.61, 158.22, 181.51, 182.16.

-[1'-(2-Methoxy-benzyl)-[4,4']bipiperidinyl-1-yl]-quinoxaline-5,8-dione (4)



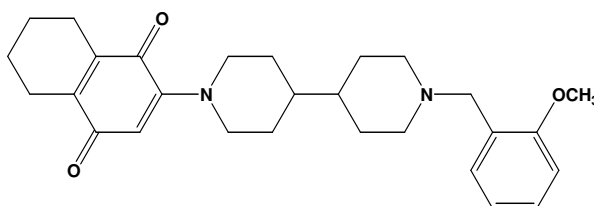
A solution of **18** (107 mg, 0.37 mmol), KH₂PO₄ (50 mg, 0.37 mmol) and CeCl₃ (9 mg, 0.04 mmol) in H₂O (4 ml) was added dropwise to a solution of **23** (67 mg, 0.42 mmol) in CHCl₃ (2 ml). The mixture was stirred vigorously at RT overnight. The aqueous phase was then washed with CHCl₃ (3 x 10 ml). The combined organic extracts were dried over Na₂SO₄, filtered and concentrated *in vacuo*. The crude was purified by gravity chromatography (DCM-MeOH-aqueous 33% ammonia 9.5:0.5:0.05) affording **4** as a red solid (50 mg, 0.11 mmol, 30%); mp= 90°C; δ_{H} (400 MHz, CD₃OD) 1.45-1.55 (6H, m 2CH, 2CH₂), 1.90 (2H, d, J 10.6, CH₂), 2.03 (2H, d, J 11.4, CH₂), 3.01 (2H, t, J 12.0, CH₂-N), 3.12 (2H, t, J 12.4, CH₂-N), 3.54 (2H, d, J 13.0, CH₂-N), 3.92 (3H, s, OCH₃), 4.26 (2H, d, J 13.8, CH₂-N), 4.30 (2H, s, CH₂-Ph), 6.24 (1H, s, CH-C=O), 7.04 (1H, t, J 7.5, Ar), 7.12 (1H, d, J 7.5, Ar), 7.41 (1H, dd, J, 7.5, 1.6, Ar), 7.49 (1H, td, J 7.5, 1.6, Ar), 8.91 (1H, s, Ar), 8.94 (1H, s, Ar); δ_{C} (100 MHz, CD₃OD) 26.38, 28.87, 37.94, 39.68, 49.34, 52.67, 54.75, 55.46, 107.37, 110.97, 117.07, 120.59, 131.89, 132.63, 147.43, 148.35, 158.44, 162.48, 180.45.

2-[1'-(2-Methoxy-benzyl)-[4,4']bipiperidinyl-1-yl]-anthracene-1,4-dione (5)



A solution of **18** (97 mg, 0.37 mmol) and KH_2PO_4 (50 mg, 0.37 mmol) in H_2O (4 ml) was added dropwise to a solution of 1,4-anthraquinone (77 mg, 0.35 mmol) in CHCl_3 (3 ml). The mixture was stirred vigorously at RT for 1 h. The aqueous phase was then washed with CHCl_3 (3 x 10 ml). The combined organic extracts were dried over Na_2SO_4 , filtered and concentrated *in vacuo*. The crude was purified twice by gravity chromatography (DCM-MeOH-aqueous 33% ammonia, 9:1:0.1) affording **5** as a red solid (14 mg, 0.03 mmol, 8%); mp= 52°C; δ_{H} (400 MHz, CD_3OD) 1.42-1.57 (6H, m, 2CH, 2CH₂), 1.86 (2H, d, J 11.0, CH₂), 2.02 (2H, d, J 11.8, CH₂), 3.00 (4H, t, J 12.2, CH₂-N), 3.52 (2H, d, J 12.6, CH₂-N), 3.92 (3H, s, OCH₃), 4.21 (2H, d, J 13.4, CH₂-N), 4.29 (2H, s, CH₂-Ph), 6.06 (1H, s, CH-C=O), 7.04 (1H, t, J 7.5, Ar), 7.12 (1H, d, J 7.5, Ar), 7.41 (1H, d, J 7.5, Ar), 7.49 (1H, td, J 7.5, 1.2, Ar), 7.63-7.69 (2H, m, Ar), 8.04 (2H, d, J 7.1, Ar), 8.40 (1H, s, Ar), 8.45 (1H, s, Ar); δ_{C} (100 MHz, CD_3OD) 26.39, 20.80, 39.80, 46.92, 49.14, 52.68, 54.75, 55.45, 109.82, 110.98, 117.06, 120.59, 126.23, 128.64, 128.73, 128.79, 129.17, 129.38, 129.61, 129.72, 131.88, 132.63, 134.32, 135.00, 155.14, 158.44, 182.22, 183.38.

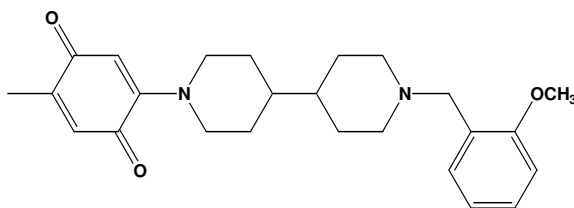
2-[1'-(2-Methoxy-benzyl)-[4,4']bipiperidiny-1-yl]-4a,5,6,7,8,8a-hexahydro-[1,4]naphthoquinone (6)



A solution of **18** (162 mg, 0.56 mmol) KH_2PO_4 (76 mg, 0.56 mmol) in H_2O (8 ml), was added dropwise to a solution of **25** (91 mg, 0.56 mmol) in CHCl_3 (2 ml). The mixture was stirred vigorously at RT for 2 h. The aqueous phase was then washed with CHCl_3 (3 x 10 ml). The combined organic extracts were dried over Na_2SO_4 , filtered and concentrated *in vacuo*. The crude was purified by flash chromatography (EtOAc-MeOH, 9:1) affording **6** as a purple slurry (80 mg, 0.71 mmol, 30%); δ_{H} (400 MHz, CDCl_3) 1.07-1.11 (1H, m, CH [amine chain]), 1.31-1.43 (5H, m, 2CH₂, CH [amine chain]), 1.64-1.69 (6H, m, 2CH₂ [tetrahydro-naphthalene ring], CH₂ [amine chain]), 1.76 (2H, d, J 9.8, CH₂ [amine chain]), 2.07-2.1 (2H, m CH₂-N), 2.35-2.41 (4H, m, 2CH₂ [tetrahydro-naphthalene ring]), 2.76 (2H, t, J 11.7, CH₂-N), 3.01 (2H, d, J 11.7, CH₂-N), 3.61 (2H, s, CH₂-Ph), 3.81 (3H, s, OCH₃), 3.89 (2H, d, J 12.5, CH₂-N), 5.68 (1H, s, CH-C=O), 6.86 (1H, d, J 7.8, Ar), 6.93 (1H, td, J 7.8, 1.6, Ar), 7.23 (1H, td 7.8, 1.6, Ar), 7.35 (1H, dd, J 7.8, 1.6, Ar); δ_{C} (100

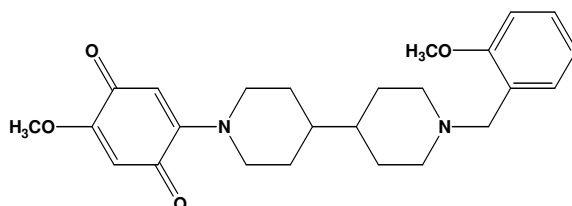
MHz, CDCl₃) 21.08, 21.37, 22.64, 29.05, 29.16, 40.48, 40.73, 49.67, 53.70, 55.38, 55.98, 108.18, 110.42, 120.31, 128.27, 130.92, 140.48, 142.79, 152.57, 157.83, 185.27, 186.25.

2-[1'-(2-Methoxy-benzyl)-[4,4']bipiperidiny-1-yl]-5-methyl-[1,4]benzoquinone (7)



A solution of **18** (200 mg, 0.69 mmol) in EtOH (5 ml) was added dropwise to a solution of **27** (216 mg, 1.38 mmol) in EtOH (10 ml) at 78 °C. The mixture was stirred at reflux for 3 h. The solvent was then evaporated under reduced pressure and the crude was purified by flash chromatography (Et₂O-MeOH, 7:3) affording **7** as a purple solid (150 mg, 0.37 mmol, 54%); mp= 98°C; ES [M+H⁺]: 409; δ_H (400 MHz, CDCl₃) 1.05-1.12 (1H, m, CH), 1.34-1.41 (5H, m, CH, 2CH₂), 1.68 (2H, d, J 12.6, CH₂), 1.78 (2H, d, J 9.0, CH₂), 1.99-2.04 (2H, m, CH₂-N), 2.01 (3H, d, J 1.2, CH₃), 2.81 (2H, t, J 11.8, CH₂-N), 3.01 (2H, d, J 11.4, CH₂-N), 3.59 (2H, s, CH₂-Ph), 3.82 (3H, s, OCH₃), 3.98 (2H, d, J 12.6, CH₂-N), 5.74 (1H, s, CH-C=O), 6.38 (1H, d, J 1.2, CH-C=O), 6.87 (1H, t, J 7.5, Ar) 6.94 (1H, t, 7.5, Ar), 7.24 (1H, td, J 7.5, 1.4, Ar), 7.36 (1H, dd, J 7.5, 1.4, Ar); δ_C (100 MHz, CDCl₃) 15.64, 29.16, 29.21, 40.52, 40.74, 49.57, 53.80, 55.39, 56.11, 108.00, 110.41, 120.28, 128.16, 130.82, 131.85, 146.65, 152.16, 157.82, 185.23, 186. 24.

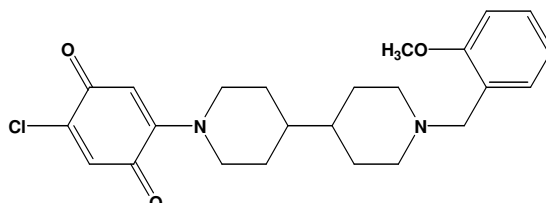
2-Methoxy-5-[1'-(2-methoxy-benzyl)-[4,4']bipiperidiny-1-yl]-[1,4]benzoquinone (8)



A solution of **18** (218 mg, 0.75 mmol) in EtOH (5 ml) was added dropwise to a solution of 2,5-dimethoxy-1,4-benzoquinone (480 mg, 3.75 mmol) in EtOH (20 ml) at 78 °C. The mixture was stirred at reflux for 3 h and then at RT overnight. The solvent was then evaporated under reduced pressure and the crude was purified by flash chromatography (DCM-MeOH-aqueous 33% ammonia, 9.5:0.5:0.03, then 9.5:0.5:0.05) affording **8** as a pink solid (160 mg, 0.38 mmol, 50%); mp=153°C; ES [M+H⁺]: 425; δ_H (400 MHz, CDCl₃) 1.10-1.14 (1H, m, CH), 1.28-1.39 (3H, m, CH, CH₂), 1.46-1.55 (2H, m, CH₂), 1.70 (2H, d, J 12.6, CH₂), 1.79 (2H, d, J 10.6, CH₂), 2.14, (2H, t, J 11.4, CH₂-N), 2.88 (2H, t, J 12.2, CH₂-N) 3.1 (2H, d, J 11.4, CH₂-N), 3.72 (2H, s, CH₂-Ph), 3.79

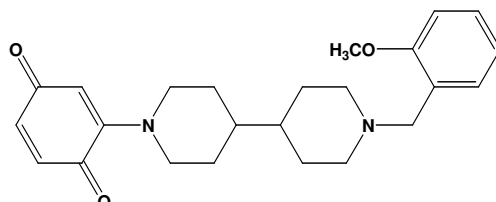
(3H, s, OCH₃), 3.82 (3H, s, OCH₃), 4.08 (2H, d, J 13.0, CH₂-N), 5.66 (1H, s, CH-C=O), 5.69 (1H, s, CH-C=O), 6.87 (1H, d, J 7.4, Ar), 6.94 (1H, t, J 7.4, Ar), 7.24-7.28 (1H, m, Ar), 7.41 6.87 (1H, d, J 7.4, Ar); δ_C (100 MHz, CDCl₃) 28.54, 29.34, 40.08, 40.49, 49.86, 53.32, 55.44, 55.58, 56.25, 104.95, 105.79, 110.52, 120.51, 128.94, 131.46, 152.58, 157.90, 159.94, 179.77, 184.74.

2-Chloro-5-[1'-(2-methoxy-benzyl)-[4,4']bipiperidinyl-1-yl]-[1,4]benzoquinone (9)



A solution of **18** (162 mg, 0.56 mmol) in EtOH (5 ml) was added dropwise to a solution of 2,5-dichloro-1,4-benzoquinone (496 mg, 2.80 mmol) in EtOH (20 ml) and THF (2 ml) at 78 °C. The mixture was stirred at reflux for 15 min. The solvent was then evaporated under reduced pressure and the crude was purified by flash chromatography (DCM-MeOH-aqueous 33% ammonia, 9.5:0.5:0.03, then 9.5:0.5:0.1) affording **9** as a purple solid (140 mg, 0.30 mmol, 50%); mp=166°C; ES [M+H⁺]: 429; δ_H (400 MHz, CDCl₃) 1.12-1.17 (1H, m, CH), 1.26-1.42 (3H, m, CH, CH₂), 1.51-1.59 (2H, m, CH₂), 1.71, (2H, d, J 12.6, CH₂), 1.81 (2H, d, J 11.4, CH₂), 2.19 (2H, t, J 11.4, CH₂-N), 2.89 (2H, t, J 12.2, CH₂-N), 3.13 (2H, d, J 11.0, CH₂-N), 3.76 (2H, s, CH₂-Ph), 3.83 (3H, s, OCH₃), 4.02 (2H, d, J 13.0, CH₂-N), 5.83 (1H, s, CH-C=O), 6.76 (1H, s, CH-C=O), 6.89 (1H, d, J 7.4, Ar), 6.96 (1H, t, J 7.4, Ar), 7.26-7.30 (1H, m, Ar), 7.44 (1H, d, J 7.4, Ar); δ_C (100 MHz, CDCl₃) 28.37, 29.25, 39.94, 40.38, 49.70, 53.19, 55.44, 106.16, 110.54, 120.56, 129.12, 131.60, 131.75, 145.60, 151.77, 157.92, 177.43, 182.60.

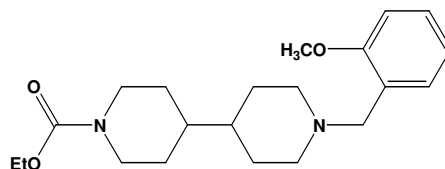
2-[1'-(2-Methoxy-benzyl)-[4,4']bipiperidinyl-1-yl]-[1,4]benzoquinone (10)



A solution of **18** (140 mg, 0.49 mmol) and KH₂PO₄ (67 mg, 0.49 mmol) in H₂O (5 ml) was added dropwise over a period of 2 h to a solution of 1,4-benzoquinone (265 mg, 2.45 mmol) in CHCl₃ (5 ml) and THF (1 ml) at 30-40 °C. The excess of 1,4-benzoquinone was then filtered and the residue was portioned between CHCl₃ and water. The aqueous phase was separated and the organic phase

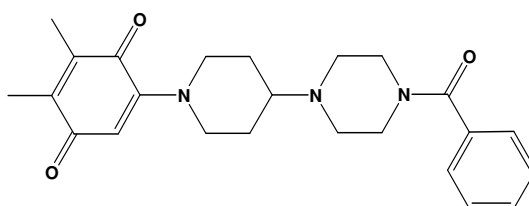
was washed with H₂O (3 x 20 ml). The combined organic extracts were dried over Na₂SO₄, filtered and concentrated *in vacuo*. The crude was purified by flash chromatography (DCM-MeOH-aqueous 33% ammonia, 9.5:0.5:0.05) affording **10** as a dark purple solid (45 mg, 0.11 mmol, 24%); mp= 123°C; δ_{H} (400 MHz, CDCl₃) 1.08-1.11 (1H, m, CH), 1.25-1.37 (5H, m, CH, CH₂, CH₂), 1.66 (2H, d, J 12.6, CH₂), 1.80 (2H, d, J 9.4, CH₂), 1.97 (2H, td, J 11.8, 2.0, CH₂-N), 2.83 (2H, t, J 12.2, CH₂-N), 2.97 (2H, d, J 11.8, CH₂-N), 3.48 (2H, s, CH₂-Ph), 3.55 (3H, s, OCH₃), 3.96 (2H, d, J 12.6, CH₂-N), 5.75 (1H, d, J 2.4, CH-C=O), 6.53 (1H, d, J 10.0, CH-C=O), 6.58 (1H, dd J 10.0 2.4, CH-C=O), 6.86 (1H, d, J 7.5, Ar), 6.93 (1H, td, J 7.5, 1.4, Ar), 7.22 (1H, td, J 7.5, 2.0, Ar), 7.34 (1H, dd, J 7.5, 1.4, Ar); δ_{C} (100 MHz, CDCl₃) 29.23, 29.31, 40.61, 40.76, 49.57, 53.91, 55.37, 56.26, 108.037, 110.39, 116.33, 120.22, 127.97, 130.66, 134.99, 137.30, 151.90, 157.80, 185.00, 186.06.

1'-(2-Methoxy-benzyl)-[4,4']bipiperidinyl-1-carboxylic acid ethyl ester (11)



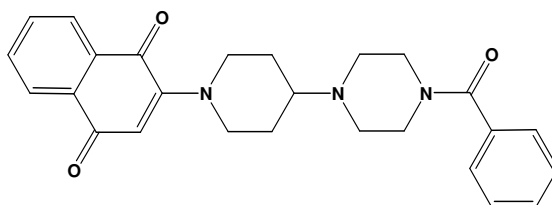
Ethyl chloroformate (14 mg, 0.13 mmol) and **18** (38 mg, 0.13 mmol) were dissolved in DCM (10 ml). The mixture was stirred at RT for 18 h. The solvent was evaporated under reduced pressure and the crude was purified by flash chromatography (DCM-MeOH, 9:1) affording **11** as a pale yellow oil (31 mg, 0.08 mmol, 65%); ES [M+H⁺]⁺: 361; δ_{H} (400 MHz, CDCl₃) 1.04-1.14 (3H, m, CH, CH₂), 1.23 (3H, t 7.1, OCH₂CH₃), 1.24-1.31 (1H, m, CH), 1.60-1.74 (6H, m, 3CH₂), 2.27 (2H, t, J 11.2, CH₂-N), 2.66 (2H, t, J 12.3, CH₂-N), 3.18 (2H, d, J 11.8, CH₂-N), 3.82 (3H, s, OCH₃), 3.84 (2H, s, CH₂-Ph), 4.10 (2H, q, J 7.1, OCH₂CH₃), 4.14-4.16 (2H, br m, CH₂-N), 6.88 (1H, d, J 7.5, Ar), 6.96 (1H, td, J 7.5, 1.2, Ar), 7.29 (1H td, J 7.5, 1.6, Ar), 7.49 (1H, dd, J,7.5, 1.2, Ar); δ_{C} (100 MHz, CDCl₃) 12.65, 27.90, 29.15, 39.84, 40.54, 44.07, 52.94, 55.05, 55.49, 61.10, 110.59, 120.72, 129.64, 132.18, 155.47, 158.00.

5-[4-(4-Benzoyl-piperazin-1-yl)-piperidin-1-yl]-2,3-dimethyl-[1,4]benzoquinone (12)



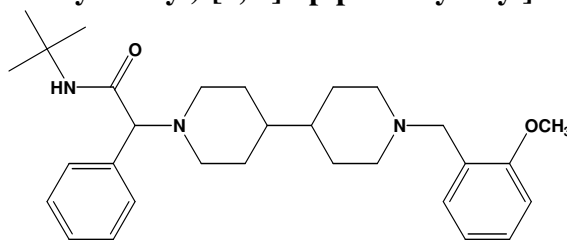
A solution of **31** (154 mg, 0.57 mmol) and KH_2PO_4 (78 mg, 0.57 mmol) in H_2O (8 ml) was added dropwise to a solution of **19** (77 mg, 0.57 mmol) in CHCl_3 (2 ml). The mixture was stirred vigorously at RT for 4 h. The aqueous phase was then washed with CHCl_3 (3 x 10 ml). The combined organic extracts were dried over Na_2SO_4 , filtered and concentrated *in vacuo*. The crude was purified by flash chromatography (Et_2O - MeOH , 8.5:1.5) affording **12** as a purple slurry (100 mg, 0.24 mmol, 43%); δ_{H} (400 MHz, CDCl_3) 1.64 (2H, ddd, J 23.9, 12.4, 3.7, CH_2), 1.87 (2H, d, J 11.7, CH_2), 1.97 (6H, s, 2CH_3), 1.49-1.64 (5H, m, $2\text{CH}_2\text{-N}$, CH), 2.83 (2H, td, J 12.4, 2.0, $\text{CH}_2\text{-N}$), 3.42-3.44 (2H, m, $\text{CH}_2\text{-N}$), 3.77-3.80 (2H, m, $\text{CH}_2\text{-N}$), 3.89 (2H, d, J 12.9, $\text{CH}_2\text{-N}$), 7.52 (1H, s, CH-C=O), 7.72-7.73 (5H, m, Ar); δ_{C} (100 MHz, CDCl_3) 12.28, 12.45, 27.86, 42.37, 48.47, 49.18, 61.37, 108.87, 127.04, 128.44, 129.67, 135.69, 139.10, 141.16, 152.24, 170.16, 185.13, 186.10.

2-[4-(4-Benzoyl-piperazin-1-yl)-piperidin-1-yl]-[1,4]naphthoquinone (13)



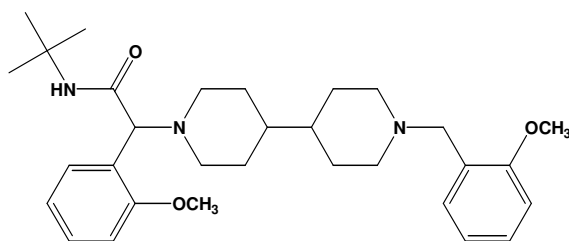
A solution of **31** (179 mg, 0.65 mmol) in THF (2 ml) was added dropwise to a solution of naphthoquinone (104 mg, 0.65 mmol) in THF (1 ml). The mixture was stirred vigorously at RT for 1 h. The solvent was evaporated under reduced pressure and the crude was purified by flash chromatography (EtOAc - MeOH , 9:1) affording **13** as a red slurry (250 mg, 0.58 mmol, 90%); δ_{H} (400 MHz, CDCl_3) 1.62 (2H, ddd, J 23.10, 11.7, 3.4, CH_2), 1.85 (2H, ddd, J 11.9, CH_2), 2.46-2.57 (5H, m, $2\text{CH}_2\text{-N}$, CH), 2.88 (2H, t, J 11.9, $\text{CH}_2\text{-N}$), 3.34-3.36 (2H, m, $\text{CH}_2\text{-N}$), 3.70-3.72 (2H, m, $\text{CH}_2\text{-N}$), 4.01 (2H, d, J 12.9, $\text{CH}_2\text{-N}$), 5.93 (1H, s, CH-C=O), 3.72-3.73 (5H, m, Ar), 7.53 (1H, td, J 7.4, 1.2, Ar), 7.59 (1H, td, J 7.4, 1.2, Ar), 7.89 (1H, d, J 7.4, Ar), 7.93 (1H, d, J 7.4, Ar); δ_{C} (100 MHz, CDCl_3) 27.99, 42.35, 48.51, 49.31, 61.20, 111.08, 125.39, 126.57, 127.00, 128.41, 129.66, 132.34, 132.73, 133.79, 135.64, 153.53, 170.14, 183.04, 183.45.

N-tert-Butyl-2-[1'-(2-methoxy-benzyl)-[4,4']bipiperidinyl-1-yl]-2-phenyl-acetamide (14)



18 (100 mg, 0.35 mmol), benzaldehyde (55 mg, 0.52 mmol), tert-butyl isocyanide (43 mg, 0.52 mmol) and trimethoxyborane (109 mg, 1.05 mmol) were dissolved in DCE (1 ml). The mixture was stirred under microwave irradiation at 80 °C for 20 min. After evaporating the solvent under reduced pressure, the crude was purified by flash chromatography (CHCl₃-MeOH-aqueous 33% ammonia, 9.5:0.5:0.03) affording **14** as a yellow oil (65 mg, 0.14 mmol, 40%); ES [M+H⁺]: 478; δ_H (400 MHz, CDCl₃) 1.03-1.05 (2H, m, 2CH), 1.15-1.20 (1H, m, CHH), 1.24-1.32 (3H, m, CHH, CH₂), 1.35 (9H, s, tBu), 1.60-1.67 (4H, m, 2CH₂), 1.72-1.75 (1H, m, CHH-N), 1.97 (2H, t, J 11.6, CH₂-N), 2.02-2.07 (1H, m, CHH-N), 2.6 (1H, dd, J 11.2, 2, CHH-N), 2.95-3.02 (3H, m, CH₂-N, CHH-N), 3.55 (2H, s, CH₂-Ph), 3.69 (1H, s, CH-C=O), 3.80 (3H, s, OCH₃), 6.84 (1H, d, J 7.6, Ar), 6.92 (1H, t, J 7.6, Ar), 7.18-7.32 (6H, m, Ar), 7.34 (1H, dd, J 7.5, 1.6, Ar); δ_C (100 MHz, CDCl₃) 28.70, 29.40, 29.82, 30.00, 40.62, 40.75, 50.44, 54.04, 54.15, 55.38, 56.22, 110.37, 120.24, 126.23, 127.72, 127.91, 128.27, 128.90, 130.56, 136.44, 157.76, 170.89.

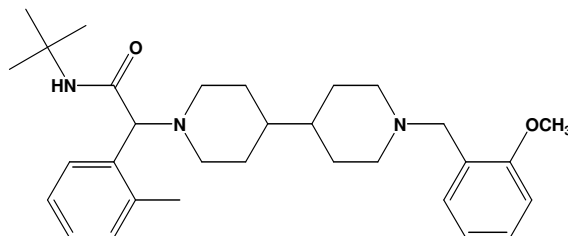
N-tert-Butyl-2-[1'-(2-methoxy-benzyl)-[4,4']bipiperidiny-1-yl]-2-(2-methoxy-phenyl)-acetamide (15)



18 (150 mg, 0.52 mmol), 2-methoxybenzaldehyde (106 mg, 0.78 mmol), tert-butyl isocyanide (65 mg, 0.78 mmol) and trimethoxyborane (162 mg, 1.56 mmol) were dissolved in DCE (1.3 ml). The mixture was stirred under microwave irradiation at 80 °C for 20 min. After evaporating the solvent under reduced pressure, the crude was purified by flash chromatography (CHCl₃-MeOH then CHCl₃-MeOH-aqueous 33% ammonia, 9.5:0.5 then 9.5:0.5:0.05) affording **15** as a yellow oil (98 mg, 0.19 mmol, 36%); δ_H (400 MHz, CDCl₃) 0.98-1.05 (2H, m, 2CH), 1.07-1.16 (1H, m, CHH), 1.23 (1H, ddd, J 23.2, 11.8, 3.5, CHH), 1.33-1.43 (2H, m, CH₂), 1.37 (9H, s, tBu), 1.59-1.69 (4H, m, 2CH₂), 1.72-1.78 (1H, m, CHH-N), 2.07 (2H, t, J 11.4, CH₂-N), 2.15 (1H, td, J 11.8, 2, CHH-N), 2.62 (1H, dd, J 11.4, 1.2, CHH-N), 2.98-3.03 (3H, m, CH₂-N, CHH-N), 3.64 (2H, s, CH₂-Ph), 3.79 (3H, s, OCH₃), 3.81 (3H, s, OCH₃), 4.39 (1H, s, CH-C=O), 6.87-6.88 (2H, m, Ar), 6.90-6.95 (2H, m, Ar), 7.16 (1H, dd, J 7.5, 1.2, Ar), 7.20-7.24 (2H, m, Ar), 7.39 (1H, d, J 7.1, Ar); δ_C (100 MHz, CDCl₃) 28.75, 28.93, 30.10, 30.28, 40.44, 40.49, 49.18, 50.32, 53.71, 54.08, 55.41, 55.44, 55.86,

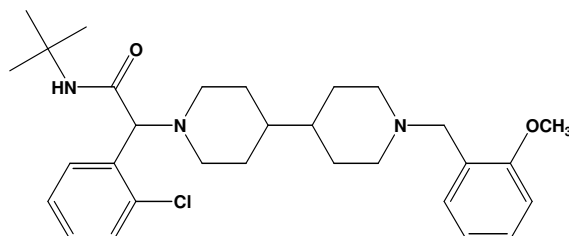
67.67, 110.42, 110.98, 120.29, 120.38, 124.39, 128.43, 128.67, 130.10, 131.07, 157.83, 158.18, 171.19.

N-tert-Butyl-2-[1'-(2-methoxy-benzyl)-[4,4']bipiperidiny-1-yl]-2-o-tolyl-acetamide (16)



18 (150 mg, 0.52 mmol), 2-methylbenzaldehyde (94 mg, 0.78 mmol), tert-butyl isocyanide (65 mg, 0.78 mmol) and trimethoxyborane (162 mg, 1.56 mmol) were dissolved in DCE (1.3 ml). The mixture was stirred under microwave irradiation at 80 °C for 20 min. After evaporating the solvent under reduced pressure, the crude was purified by flash chromatography (CHCl₃-MeOH then CHCl₃-MeOH-aqueous 33% ammonia, 9.5:0.5 then 9.5:0.5:0.03) affording **16** as a yellow oil (68 mg, 0.14 mmol, 27%); δ_{H} (400 MHz, CDCl₃) 1.05-1.11 (2H, m, 2CH), 1.14-1.26 (2H, m, CH₂), 1.33-1.38 (2H, m, CH₂), 1.33 (9H, s, tBu), 1.57-1.70 (3H, m, CH₂, CHH), 1.73-1.78 (2H, m, CHH, CHH-N), 2.02 (2H, t, J, 11.8, CH₂-N), 2.10 (1H, td, J 11.8, 2, CHH-N), 2.43 (3H, s, CH₃), 2.64 (1H, dd, J 11.4, 2.4, CHH-N), 2.99 (2H, d, J 9.0, CH₂-N), 3.06-3.09 (1H, m, CHH-N), 3.58 (2H, s, CH₂-Ph), 3.80 (3H, s, OCH₃), 4.00 (1H, s, CH-C=O), 6.86 (1H, d, J 7.6, Ar), 6.93 (1H, t, J 7.6, Ar), 7.12-7.17 (3H, m, Ar), 7.23 (1H, td, J 7.6, 2, Ar), 7.24-7.28 (1H, m, Ar), 7.37 (1H, dd, J 7.6, 1.2, Ar); δ_{C} (100 MHz, CDCl₃) 19.51, 27.66, 28.22, 28.90, 29.03, 39.64, 39.74, 49.22, 49.44, 52.89, 53.46, 54.39, 55.07, 70.47, 109.40, 119.31, 124.93, 126.27, 127.13, 129.79, 134.62, 136.49, 156.79, 170.49

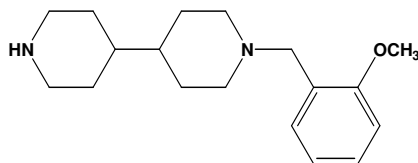
N-tert-Butyl-2-(2-chloro-phenyl)-2-[1'-(2-methoxy-benzyl)-[4,4']bipiperidiny-1-yl]-acetamide (17)



18 (150 mg, 0.52 mmol), 2-chlorobenzaldehyde (110 mg, 0.78 mmol), tert-butyl isocyanide (65 mg, 0.78 mmol) and trimethoxyborane (162 mg, 1.56 mmol) were dissolved in DCE (1.3 ml). The

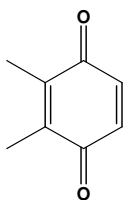
mixture was stirred under microwave irradiation at 80 °C for 20 min. After evaporating the solvent under reduced pressure, the crude was purified by flash chromatography (CHCl₃-MeOH then CHCl₃-MeOH-aqueous 33% ammonia, 9.5:0.5 then 9.5:0.5:0.03) affording **17** as a yellow oil (70 mg, 0.14 mmol, 27%); δ_{H} (400 MHz, CDCl₃) 1.04-1.09 (2H, m, 2CH), 1.11-1.18 (1H, m, CHH), 1.20-1.29 (1H, m, CHH), 1.32-1.42 (2H, m, CH₂), 1.37 (9H, s, tBu), 1.62-1.65 (3H, m, CH₂, CHH), 1.72-1.76 (1H, m, CHH), 1.86 (1H, td, J 11.4, 2.4, CHH-N), 2.05 (2H, t, J 11.4, CH₂-N), 2.22 (1H, td, J 11.8, 2.0, CHH-N), 2.58 (1H dd, J 11.4, 2.0, CHH-N), 3.01 (2H, d, J 11.0, CH₂-N), 3.08 (1H, dd J 11.3, 1.7, CHH-N), 3.62 (2H, s, CH₂-Ph), 3.81 (3H, s, OCH₃), 4.52 (1H, s, CH-C=O), 6.86 (1H, d, J 7.6, Ar), 6.93 (1H, t, J 7.6, Ar), 7.16-7.26 (3H, m, Ar), 7.30 (1H, dd, J 7.6, 1.8, Ar), 7.35-7.39 (2H, m, Ar); δ_{C} (100 MHz, CDCl₃) 28.69, 29.00, 29.98, 30.15, 30.89, 40.38, 40.47, 49.46, 50.63, 53.74, 54.00, 55.39, 55.92, 70.40, 110.42, 120.35, 126.53, 128.34, 128.78, 129.76, 130.29, 130.97, 133.89, 135.57, 157.80, 170.14.

1-(2-Methoxy-benzyl)-[4,4']bipiperidinyl (18)



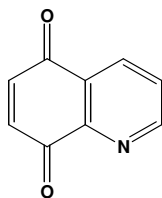
4,4'-Bipiperidyl dihydrochloride (2.3 g, 9.40 mmol) and KOH (140 mg, 2.55 mmol) were dissolved in MeOH (50 ml). 2-Methoxybenzaldehyde (980 mg, 7.20 mmol) was added and the mixture was stirred at reflux for 3 h. After cooling at 0 °C, NaBH₃CN (180 mg, 2.90 mmol) was added slowly and the mixture was stirred at RT overnight. After evaporating the solvent, the reaction was quenched at 0 °C by dropwise addition of water (40 ml). The aqueous phase was acidified with 6N HCl and extracted with Et₂O (3 x 20 ml). The aqueous phase was then basified with 40% NaOH and extracted with CHCl₃ (3 x 40 ml). The combined organic extracts were dried over Na₂SO₄, filtered and concentrated *in vacuo*. The crude was purified by flash chromatography (DCM-MeOH-aqueous 33% ammonia, 6.5:3.5:0.35) affording **18** as a white solid (600 mg, 2.10 mmol, 30%); δ_{H} (400 MHz, CDCl₃) 1.03-1.15 (4H, m, 2CH, CH₂), 1.25-1.35 (2H, m, CH₂), 1.64-1.68 (4H, m, 2CH₂), 1.88 (1H, br s, NH), 1.96 (2H, td, J 11.9, 2.1, CH₂-N), 2.55 (2H, t, J 11.8, CH₂-N), 2.96 (2H, d, J 11.6, CH₂-N), 3.07 (2H, d, J 12.1, CH₂-N), 3.54 (2H, s, CH₂-Ph), 3.81 (3H, s, OCH₃), 6.82 (1H, d, J 7.5, Ar), 6.92 (1H, t, J 7.5, Ar), 7.22 (1H, t, J 7.5, Ar), 7.35 (1H, d, J 7.5, Ar); δ_{C} (100 MHz, CDCl₃) 29.30, 29.65, 40.83, 41.01, 46.38, 54.06, 55.35, 55.37, 56.39, 110.34, 120.19, 126.45, 127.81, 130.53, 157.76.

2,3-Dimethyl-[1,4]benzoquinone (**19**)



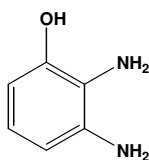
MnO₂ (2.5 g, 29 mmol) was added to a solution of 2,3-dimethyl-benzene-1,4-diol (500 mg, 3.62 mmol) in anhydrous Et₂O (50 ml). The mixture was stirred at RT for 4 h and then filtered through Celite. The solvent was evaporated under reduced pressure affording **19** as a yellow solid (500 mg, 3.62 mmol, 100%); δ_{H} (400 MHz, CDCl₃) 2.04 (3H, s, CH₃), 2.05 (3H, s, CH₃), 6.72 (1H, s, Ar), 6.73 (1H, s, Ar).

Quinoline-5,8-dione (**20**)⁴⁹⁹



Water (1 ml) was added to a solution of bis(trifluoroacetoxy)iodobenzene (1.4 g, 3.22 mmol) in acetonitrile (2.5 ml). After cooling at 0 °C, 8-hydroxyquinoline (400 mg, 2.80 mmol) was added portionwise and the cooling bath was removed. The resulting mixture was stirred for 3 h at RT. The solvent was evaporated under reduced pressure and the crude was purified by flash chromatography (DCM-EtOAc, 6:4) affording **20** as an orange solid (100 mg, 0.64 mmol, 23%); δ_{H} (200 MHz, CDCl₃) 7.16 (1H, d, J 11.0, CH-C=O), 7.17 (1H, d, J 11.0, CH-C=O), 7.86 (1H, dd, J 7.8, 4.5, Ar), 8.37 (1H, dd, J 7.8, 1.6, Ar), 9.03 (1H, dd, J 4.5, 1.6, Ar).

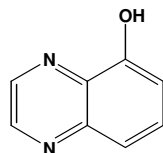
2,3-Diamino-phenol (**21**)⁵⁰²



2-Amino-3-nitrophenol (500 mg, 3.20 mmol) was dissolved in MeOH (30 ml) and 10% Pd/C was added. The reaction mixture was allowed to stir under H₂ (1 atm) for 4 h, monitoring the consumption of starting material by TLC. The reaction mixture was filtered through Celite and concentrated *in vacuo* to yield a brown solid (397 mg, 3.20 mmol, 100%), which was used in the

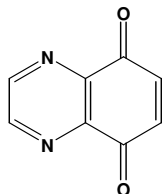
next step without further purification; δ_{H} (200 MHz, CDCl_3) 6.37 (2H, m, Ar), 6.67 (1H, t, J 8.0, Ar).

Quinoxalin-5-ol (22)⁵⁰³



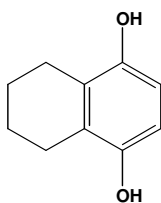
2,3-Diamino-phenol **21** (150 mg, 1.21 mmol) was dissolved in a mixture of 4 M NaOAc (1.5 ml) and 2 M AcOH (2.3 ml) and heated to 60 °C. In a separate flask, sodium glyoxal bisulfite (338 mg, 1.27 mmol) was dissolved in H_2O (9 ml) and heated to 60 °C. When both solutions reached ~60 °C, the solution of **21** was transferred by pipette to the sodium glyoxal bisulfite solution. The reaction mixture was allowed to stir at 60 °C for 1 h. After cooling the mixture to RT, the pH was adjusted to ~8 using 1N NaOH. The resulting aqueous solution was extracted with EtOAc (8 x 100 ml), dried over Na_2SO_4 , filtered, and concentrated *in vacuo*. The crude material was purified by flash chromatography (petrol-EtOAc, 5:5) to yield **22** as a yellow solid (160 mg, 1.09 mmol, 90%); δ_{H} (400 MHz, CDCl_3) 7.26 (1H, dd, J 7.5, 1.2, Ar), 7.67 (1H, dd, J 8.5, 1.2, Ar), 7.72 (1H, dd, J 8.5, 7.5, Ar), 7.84 (1H, br s, OH), 8.73 (1H, d, J 2.0, Ar), 8.92 (1H, d, J 2.0, Ar).

Quinoxaline-5,8-dione (23)⁵⁰⁴



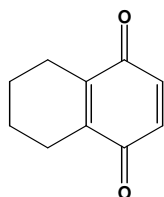
Quinoxalin-5-ol **22** (150 mg, 1.03 mmol) was dissolved in CH_3CN (3 ml) and H_2O (1.5 ml) and cooled in an ice bath. In a separate flask, bis(trifluoroacetoxy)iodobenzene (976 mg, 2.27 mmol) was dissolved in CH_3CN (3 ml) and H_2O (1.5 ml) and added dropwise to the solution containing **22** at 0 °C. The reaction mixture was allowed to stir at RT for 4 h, then diluted with H_2O (10 ml). The aqueous solution was extracted with EtOAc (3 x 20 ml), dried over Na_2SO_4 , filtered, and concentrated *in vacuo*. The crude was purified by flash chromatography (DCM-EtOAc, 3:7) to afford **23** as a yellow solid (60 mg, 0.37 mmol, 36%); δ_{H} (400 MHz, CDCl_3) 7.26 (2H, s, Ar), 9.07 (2H, s, Ar).

5,6,7,8-Tetrahydro-naphthalene-1,4-diol (**24**)



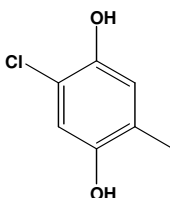
A solution of potassium persulphate (1.8 g, 6.74 mmol) in H₂O (13 ml) was added dropwise over a period of 3-4 h, to a solution of 5,6,7,8-tetrahydro-naphthalen-1-ol (500 mg, 3.37 mmol) and NaOH (3 g, 74.11 mmol). Stirring was continued overnight at RT. The reaction mixture was then acidified to pH 3-4, filtered and extracted with ethyl acetate (3 x 100 ml). The aqueous solution was acidified with an excess of 37% HCl and heated for 30 min. After cooling, the solution was extracted with Et₂O (3 x 100 ml). The dried ether extracts were evaporated under reduced pressure affording **24** as a brown solid (310 mg, 1.89 mmol, 56%); δ_{H} (400 MHz, (CD₃)₂CO) 1.79-1.82 (4H, m, 2CH₂), 2.68-2.71 (4H, m, 2CH₂), 6.55 (2H, s, Ar), 7.41 (1H, br s, OH); δ_{C} (100 MHz, (CD₃)₂CO) 22.36, 23.42, 111.21, 124.68, 147.73.

5,6,7,8-Tetrahydro-[1,4]naphthoquinone (**25**)



Ag₂O (741 mg, 3.20 mmol) and Na₂SO₄ (200 mg) were added to a solution of **24** (105 mg, 0.64 mmol) in dry toluene (7 ml). The mixture was stirred at RT overnight and then filtered through Celite. The solvent was evaporated under reduced pressure affording **25** as a brown solid (103 mg, 0.60 mmol, 100%); δ_{H} (400 MHz, (CD₃)₂CO) 2.48-2.52 (4H, m, 2CH₂), 3.21-3.24 (4H, m, 2CH₂), 7.49 (2H, s, Ar);

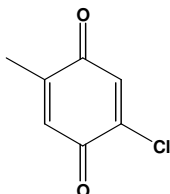
2-Chloro-5-methyl-benzene-1,4-diol (**26**)⁵⁰⁵



p-Toluquinone (2 g, 16.30 mmol) was dissolved in CH₃COOH (10 ml). Concentrated HCl (6 ml) was added dropwise at 0 °C. The mixture was stirred at RT for 4 h. The solvent was then

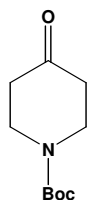
evaporated under reduced pressure and the crude was purified by flash chromatography (petrol-EtOAc, 8:2) affording **26** as a purple solid (1.2 g, 7.44 mmol, 46%); δ_{H} (400 MHz, CD_3OD) 2.10 (3H, s, CH_3), 6.65 (1H, s, Ar), 6.68 (1H, s, Ar); δ_{C} (100 MHz, CD_3OD) 14.50, 115.04, 116.80, 118.12, 124.29, 145.22, 148.39.

2-Chloro-5-methyl-[1,4]benzoquinone (27)⁵⁰⁵



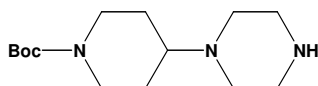
A solution of **26** (1.2 g, 7.44 mmol) in MeOH was added dropwise at 0 °C to a solution of $\text{K}_2\text{Cr}_2\text{O}_7$ (4.4 g, 14.88 mmol) and H_2SO_4 (3 ml) in H_2O (60 ml). The mixture was stirred at 0 °C for 4 h and then filtered. The filtrate was concentrated and the residue portioned between DMC and water. The organic layer was separated and the aqueous phase extracted with DCM (3 x 500 ml). The combined organic extracts were dried over Na_2SO_4 , filtered and concentrated *in vacuo* affording **27** as a yellow solid (750 mg, 4.80 mmol, 64%); δ_{H} (400 MHz, CDCl_3) 2.10 (3H, s, CH_3) 6.77 (1H, s, Ar), 7.01 (1H, s, Ar).

4-Oxo-piperidine-1-carboxylic acid tert-butyl ester (28)



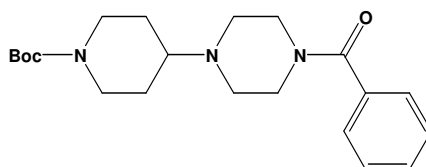
Di-*tert*-butyl dicarbonate (4 g, 19 mmol) was added dropwise at 0 °C to a solution of 4-piperidone monohydrate hydrochloride (2 g, 13 mmol) in 10% NEt_3 (4 equiv.)/MeOH. The mixture was stirred at RT overnight. The solvent was then evaporated under reduced pressure and the crude was purified by flash chromatography (petrol-EtOAc, 7:3) affording **28** as a white solid (2.5 g, 12.60 mmol, 97%); δ_{H} (400 MHz, CDCl_3) 1.42 (9H, s, OtBu), 2.36 (4H, t, J 6.2, $2\text{CH}_2\text{-C=O}$), 3.64 (4H, t, J 6.2, $2\text{CH}_2\text{-N}$); δ_{C} (100 MHz, CDCl_3) 28.26, 41.04, 42.89, 80.26, 154.35, 207.56.

4-Piperazin-1-yl-piperidine-1-carboxylic acid tert-butyl ester (29)



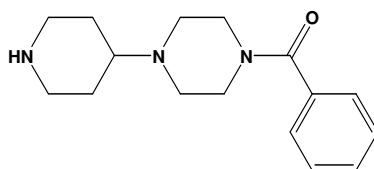
28 (2 g, 10.60 mmol) and piperazine (4.6 g, 53 mmol) were dissolved in MeOH (42 mmol). Acetic acid was added until pH 6-7, followed by the addition of sodium cyanoborohydride (1.7 g, 26.50 mmol) at 0 °C. The mixture was stirred at RT for 24 h. The solvent was evaporated under reduced pressure and excess sodium cyanoborohydride was quenched by careful addition of a solution of Na₂CO₃ (20 ml). The aqueous phase was extracted with EtOAc (3 x 20 ml) and the combined organic extracts were dried over Na₂SO₄, filtered and concentrated *in vacuo*. The crude was purified by flash chromatography (DCM-MeOH-aqueous 33% ammonia, 9:1:0.1) affording **29** as a transparent oil (910 mg, 3.40 mmol, 32%); δ_{H} (400 MHz, CDCl₃) 1.28-1.32 (2H, m, CH₂), 1.35 (9H, s, OtBu), 1.74 (2H, d, J 11.3, CH₂), 2.48-2.53 (1H, m, CH), 2.66 (2H, t, J 11.5, CH₂-N), 2.79-2.81 (4H, m, 2CH₂-N), 3.14-3.16 (4H, m, 2CH₂-N), 4.00 (2H, d, J 12.9, CH₂-N); δ_{C} (100 MHz, CDCl₃) 27.74, 28.34, 43.00, 44.27, 45.86, 61.53, 80.00, 154.81.

4-(4-Benzoyl-piperazin-1-yl)-piperidine-1-carboxylic acid tert-butyl ester (**30**)



Benzoyl chloride (950 mg, 6.76 mmol) was added dropwise at 0 °C to a solution of **29** (910 mg, 3.38 mmol) and NEt₃ (684 mg, 6.76 mmol) in DCM (12 ml). The mixture was stirred at RT for 4h. The solvent was evaporated under reduced pressure and the crude was purified by flash chromatography (DCM-MeOH, 9.5:0.5) affording **30** as a yellow oil (800 mg, 3.40 mmol, 63%); δ_{H} (400 MHz, CDCl₃) 1.28 (2H, ddd, J 24.0, 11.9, 4.0, CH₂), 1.33 (9H, s, OtBu), 1.64-1.67 (2H, m, CH₂), 1.28-1.61 (7H, m, 3CH₂-N, CH), 3.29-3.31 (2H, m, CH₂-N), 3.65-3.67 (2H, m, CH₂), 3.96-4.01 (2H, m, CH₂), 7.27-7.28 (5H, m, Ar).

Phenyl-(4-piperidin-4-yl-piperazin-1-yl)-methanone (**31**)



A solution of HCl in dioxane (18 ml) was added dropwise at 0 °C to a solution of **30** (800 mg, 2.14 mmol) in MeOH (3 ml). The mixture was stirred at RT overnight. The solvent was then evaporated under reduce pressure and the residue was basified with 4N NaOH. The aqueous layer was

extracted with DCM (2 x 20 ml). The combined organic extracts were dried over Na₂SO₄, filtered and concentrated *in vacuo* affording **31** and a yellow oil (582 mg, 2.14 mmol, 100%); δ_{H} (400 MHz, CDCl₃) 1.23 (2H, ddd, J 23.9, 12.1, 3.7, CH₂), 1.61 (2H, m, CH₂), 2.20 (1H, tt, J 11.5, 3.7, CH), 2.30-2.32 (2H, m, CH₂-N), 2.39 (2H, t, 12.1, CH₂-NH), 2.44-2.45 (2H, m, CH₂-N), 2.93-2.96 (2H, t, 12.1, CH₂-NH), 3.23-3.25 (2H, m, CH₂-N), 3.59-3.61 (2H, m, CH₂-N), 7.21-7.22 (5H, m, Ar).

6.2 Biology

A *Methods for assays at mAChRs*

- **cDNA constructs**

cDNA encoding the human M₁ and M₂ mAChRs were obtained from Missouri University of Science and Technology cDNA resource Center (Rolla, MO). Single point mutations of M₁ receptor (F77I and Y381A) were introduced with the Stratagene Quick-Change Kit (La Jolla, CA) and confirmed by sequencing. Wild type plasmids were transfected with Lipofectamine 2000 (Life Technologies) into HEK293 cells and stable clones were selected in 1mg/ml G418. Mutated plasmids were transiently transfected in HEK293 cells with polyethylenimine and analyzed 48 h after transfection.

- **Cell Membrane preparation.**

Cell membrane preparation was performed using a method described by Thomas et al.⁵⁰⁶ Confluent monolayers of HEK293-M₁ cells were rapidly washed with 10 mM HEPES, 0.9% NaCl, and 0.2% EDTA, pH 7.4 (HBS-EDTA) before incubation with HBS-EDTA for 15 min to lift cells. Cells were centrifuged (400g, 4 min), and the pellet was resuspended in 10 mM HEPES and 10 mM EDTA, pH 7.4, homogenized using a tissue grinder and centrifuged (40,000g, 15 min, 4°C). The cell pellet was resuspended in 10 mM HEPES and 0.1 mM EDTA, pH 7.4, and rehomogenized and centrifuged as described above. The final pellet was resuspended in the 10mM HEPES and 10 mM EDTA, pH 7.4, buffer either used immediately or snap-frozen and stored at -80°C. Protein concentration was determined by BCA Protein Assay (Pierce).

- **Radioligand binding assays**

Radioligand binding studies were performed by incubating HEK293-M₁ or M₂ cell membranes (70 μ g of protein/tube) with [³H]NMS (1 nM) and a range of concentrations of the tested compounds at RT for 2 h in buffer containing 25 mM sodium phosphate, 5 mM MgCl₂, 0.1% bovine serum albumin (BSA), pH 7.4 (binding buffer). The final assay volume was 1 ml. Compounds were serially diluted in binding buffer to generate eight different test concentrations over a 4 log unit

range. Nonspecific binding was defined as that remaining in the presence of 30 μM atropine. The reaction was terminated by rapid filtration through GF/C filter mates presoaked in 0.3% polyethylenimine, followed by four washes with ice-cold wash buffer (25 mM sodium phosphate, pH 7.4); filters were allowed to dry before bound radioactivity was measured using liquid scintillation counting. Binding data represent the mean of two determinations and were analyzed by nonlinear regression analysis with the use of Prism software (GraphPad Software, Inc., San Diego, CA). Receptor expression levels for M_1 and M_2 cell lines were 213 ± 25 and 5940 ± 50 fmol/mg, respectively.

- **Functional assays**

Functional assays were performed using a method described by Thomas et al.⁵⁰⁶ HEK293 cells seeded at 40,000 cells/well in 24-well plates were transfected with M_1 receptor 2 days before assay, then the cells were washed twice with 450 μl of Ca^{2+} -free KHB containing 100 μM EGTA. Cells were incubated at 37°C with tested compounds for 5 min, then with OXO-M for 10 min and then with forskolin 1 μM for 10 min, before termination by aspiration of buffer and addition of 0.1 M HCl for 20 min. cAMP concentrations were determined using Cyclic AMP EIA kit (Cayman) following manufacturer's instruction.

- **Kinetic studies**

For dissociation studies, HEK293- M_1 cell membranes (70 μg of protein/tube) were preincubated with [^3H]NMS (1 nM) and either binding buffer or atropine (1 μM final) for 60 min to achieve equilibrium. Triplicate determinations of total and nonspecific binding of [^3H]NMS, as defined above, were then measured at 2, 5, 10, 15, 20, and 30 min after the addition of atropine (1 μM final) either in the presence or absence of **1** (1 μM final). Buffer composition, reaction termination, and radioactivity determination were all as for HEK293- M_1 inhibition binding. The amount of specific [^3H]NMS bound was calculated and analyzed by Prism using the one-phase exponential decay equation.

- **Western blot analysis**

The proteins were extracted as previously described in Cell Membrane Preparation. Proteins were denatured at 95 °C for 3 min, then loaded and separated by sodium dodecyl sulfate-polyacrylamide gel electrophoresis. MagicMark™ XP Western Standard (Invitrogen) served as a molecular weight standard. Proteins were transferred to Protran™ nitrocellulose membranes, which were blocked with 5% non-fat milk in Tris buffered saline (10 mM Tris-HCl, pH 8), containing 150 mM NaCl plus 0.1% Tween-20 for 1.5 h at RT (25 °C). The blots were probed overnight at 4 °C with rabbit anti- M_1 muscarinic acetylcholine receptor affinity purified polyclonal antibody, diluted 1:1000 in

Tris buffered saline containing 0.1% Tween-20, 5% non-fat milk. The membranes were incubated with peroxidase conjugated secondary antibodies at a dilution of 1:8000. Blots were finally developed with SuperSignal West Pico chemiluminescent substrate for 3 min. The substrate was prepared by mixing the SuperSignal West Pico Stable Peroxidase Solution and the SuperSignal West Pico Luminol/Enhancer Solution at a ratio of 1:1. After drainage of the solutions, chemiluminescence was detected using a luminescent image analyzer LAS-3000 (Fujifilm, Tokyo, Japan).

B *Inhibition of AChE and BuChE activities*

The method of Ellman et al. was followed.⁵¹³ Five different concentrations of each compound were selected in order to obtain inhibition of AChE or BuChE activities comprised between 20 and 80%. The assay solution consisted of 0.1 M potassium phosphate buffer pH 8.0, with the addition of 340 μ M 5,5'-dithio-bis(2-nitrobenzoic acid), 0.02 unit/mm of human recombinant AChE or BuChE from human serum (Sigma Chemical) and 550 μ M of substrate (acetylthiocholine iodide or butyrylthiocholine iodide, respectively). Tested compounds were added to the assay solution and preincubated at 37 °C with the enzyme for 20 min before the addition of substrate. Enzyme reaction was followed at 412 nm for five min by a double beam spectrophotometer (Jasco V-530). Assays were carried out with a blank containing all components except AChE or BuChE in order to account for non-enzymatic reaction. The reaction rates were compared, and the percent inhibition due to the presence of tested compounds was calculated. Each concentration was analyzed in triplicate, and IC₅₀ values were determined graphically from inhibition curves (percent inhibition vs log inhibitor concentration).

C *Substrate specificity for NQO1*

1, **2**, and **8** were tested with respect to their ability to accept electrons from NADH via rat NQO1 (Sigma), by following the absorbance change of NADH. Menadione was used as a reference compound. Briefly, each reaction consisted of NADH, NQO1, and the tested compounds in a final volume of Tris-HCl buffer containing bovine serum albumin (0.07%). Reactions were started by the addition of NADH. The time course of the reaction was followed by monitoring the absorbance decrease of NADH at 340 nm, using an extinction coefficient of 6.22 mM⁻¹ cm⁻¹ in a Jasco 7850 double-beam spectrophotometer. The extent of nonenzymatic quinone reduction by NADH was determined in all cases either in the absence of the enzyme or in the presence of 20 μ M dicoumarol. The results are expressed in terms of variation of optical density per minute at 340 nm (Δ abs/min).

Chapter 2

DESIGN AND SYNTHESIS OF QUINAZOLINE DERIVATIVES AS NOVEL AND MULTIPOTENT DRUGS FOR THE TREATMENT OF BENIGN PROSTATIC HYPERPLASIA (BPH)

OUTLINES

Chapter 2	132
1 Introduction	133
1.1 α_1 -Adrenoreceptor antagonists	134
1.1.1 Quinazolines	135
1.1.2 Phenylethylamines	145
1.1.3 Piperidines	147
1.2 5α -reductase inhibitors	150
2 Aim of the project	153
3 Chemistry	159
4 Results and Discussion	164
5 Conclusions and Future Works	170
6 Experimental section	171
6.1 Chemistry	171
6.2 Biology	181

1 Introduction

Benign prostatic hyperplasia (BPH) describes a proliferative process of both stromal and epithelial elements of the prostate. BPH leads to a progressive enlargement of the prostate gland that affects the patient's quality of life.⁵¹⁴ The incidence of BPH increases from approximately 50% at 60 years to 90% in men older than 85 years.⁵¹⁵ The clinical manifestation of BPH includes lower urinary tract symptoms (LUTS) represented by incomplete bladder emptying, urinary tract infection, acute and chronic urinary retention, urosepsis, chronic renal insufficiency, and hematuria.

In the past, age, genetics, and testosterone were regarded as the primary causes of prostate enlargement, but the exact cause of BPH is still unknown. Recently, various etiological hypotheses for BPH have been formulated and they are summarized below.

A *Metabolic syndrome*

Metabolic syndrome (MetS) represents a group of medical disorders that increase the risk of developing cardiovascular diseases like stroke and diabetes. Obesity, high triglyceride level, low HDL cholesterol level, and high blood pressure are the main metabolic risk factors. MetS is increasing in countries with Western lifestyles, and in particular in the United States. The association between MetS and BPH has been investigated in the past decades in several studies. In fact, increased insulin level and type 2 diabetes, increased body weight and body mass index, hypertension, and lower high-density lipoprotein were confirmed to be important risk factors of prostate enlargement, and patients with MetS had a higher annual growth rate of the prostate.^{516, 517, 518} Moreover, Vikram et al.⁵¹⁹ reported an overgrowth of prostate volume in hyperinsulinemic rats induced by a high-fat diet. The hypothetical link between hyperinsulinemia and BPH was suggested as follows: an increased insulin level, a compensatory phenomenon by insulin resistance, causes an increased density of growth hormone receptors in the liver and then results in an increased hepatic production of insulin-like growth factor 1, a mitogen for prostate epithelial cells which promotes the proliferation of prostate cells.^{520, 521}

B *Lifestyle, food, and exercise*

According to a study carried out by the Prostate Cancer Prevention Trial, high consumption of red meat and a high-fat diet were suggested to increase the risk of BPH, whereas high consumption of vegetables was associated with a reduced risk of BPH.⁵²² Physical activities were also shown to reduce the possibility of prostate enlargement, LUTS, and LUTS-related surgery.⁵²³

C *Inflammation*

It was also suggested a correlation between inflammation and BPH. In fact, the severity of LUTS and the intensity of inflammation are related.⁵²⁴ Moreover, inflammation in the prostate increased significantly with the increase in prostate volume.⁵²⁵ A large number of inflammatory cells and cytokines may be involved in the proliferation of the prostate. It was found that T-lymphocytes, B-lymphocytes, and macrophages are chronically activated in BPH. They produce IL 2, interferon gamma (IFN γ), and transforming growth factor- β (TGF- β), which result in fibromuscular growth of the prostate.⁵²⁶

In the past, the choice of treatment for BPH was the transurethral resection of the prostate (TURP) or open prostatectomy. Although surgery remains the most effective treatment for complicated or severe BPH, its invasive nature and its potential side effects have led to the search for nonsurgical and less invasive treatments. Nowadays, the pharmacotherapy of BPH is based on two classes of compounds: α_1 -adrenoreceptor (α_1 -AR) antagonists and 5α -reductase (5α -R) inhibitors. α_1 -AR antagonists are used to treat the dynamic component of BPH through the inhibition of sympathetic tone of the prostate. Conversely, 5α -R inhibitors are administered to reduce the prostatic mass through suppression of androgen stimulation of prostatic growth.

1.1 α_1 -Adrenoreceptor antagonists

Initially developed as antihypertensive agents, α_1 -AR antagonists exert their effect by blocking sympathetic adrenergic receptors-mediated contraction of the prostatic smooth muscle cells and bladder neck. α -ARs are a class of metabotropic GCPRs that are targeted by catecholamines, i. e. norepinephrine (noradrenalin) and epinephrine (adrenaline). α -ARs are divided in two subtypes: α_1 and α_2 . α_1 couples to Gq, which results in increased intracellular Ca^{2+} and in smooth muscle contraction. In smooth muscle of blood vessels the principal effect of α_1 activation is represented by vasoconstriction with the subsequent increase of blood pressure. α_1 activation causes also contraction of smooth muscle of the urinary system, like prostate, bladder, ureter etc. α_2 , on the other hand, couples to Gi, which causes a decrease of cAMP activity. They are mostly localized in pre-synaptic nerve terminals where they decrease the release of neurotransmitters.

To date, α_1 -AR has been characterized as α_{1A} , α_{1B} , α_{1D} and α_{1L} but the role of the α_{1L} subtype has not to be established yet.^{527, 528} α_{1A} -AR subtypes are predominant in human prostate and urethra,^{529, 530, 531, 532} while α_{1B} -ARs seem to play a role in the regulation of blood pressure.⁵³³ α_{1D} -ARs seem to

be predominant in the destruktor muscle. Therefore, their relevant role in the control of the symptoms associated with BPH is also postulated.^{534, 535}

During the last decade a large number of α_1 selective antagonists were synthesized for the treatment of BPH, but none of those used in clinical practice displays selectivity for the α_{1A} subtype. Presumably, some of the adverse side effects associated with non-selective α_{1A} blockade are mediated by the activation of α_{1B} -ARs. In the present section, the main classes of α_1 selective antagonists potentially useful for BPH are reviewed.

1.1.1 Quinazolines

Quinazoline derivatives are exemplified by prazosin, doxazosin, terazosin and alfuzosin. They are the oldest α_1 selective antagonists used in clinical practice. The structure of these compounds differs for the fragment attached to the quinazoline 2-side chain (**Fig. 1**).

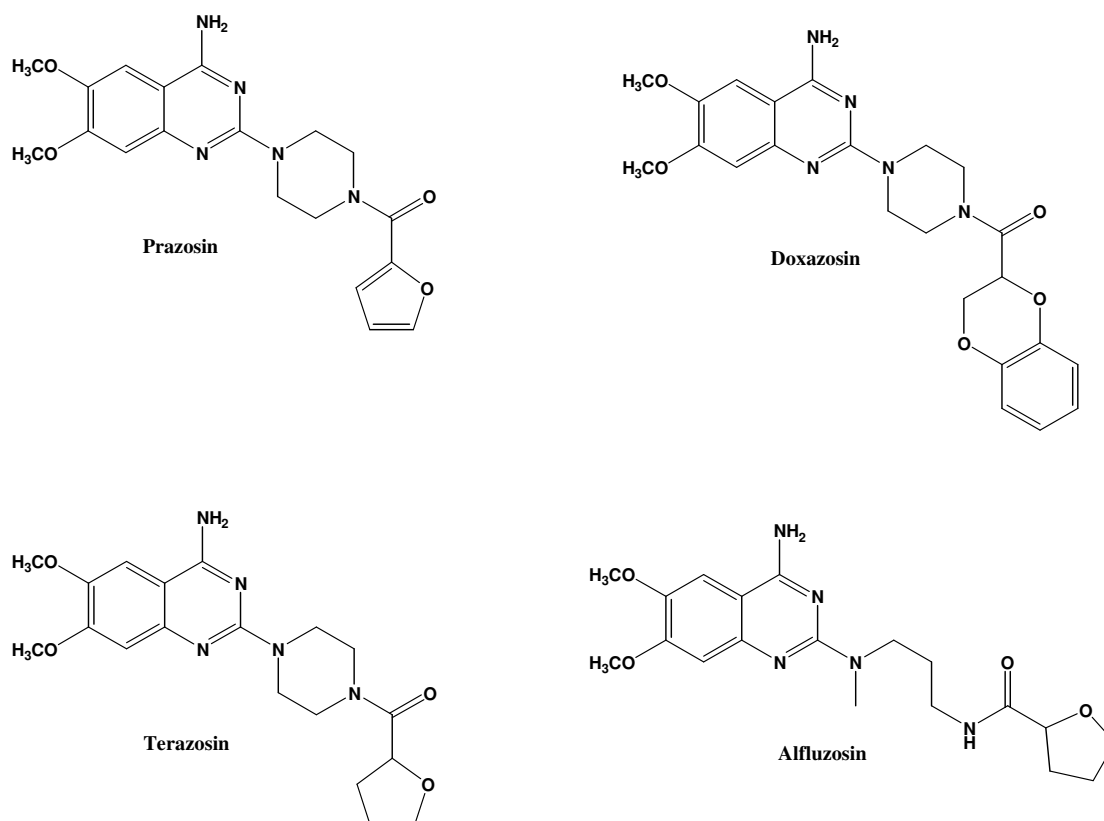


Figure 1: Chemical structures of quinazoline derivatives used in clinical practice.

Prazosin is the prototype α_1 -AR antagonist. It does not distinguish between α_1 -AR subtypes [pK_i 9.7 (α_{1A}), 9.6 (α_{1B}) and 9.5 (α_{1D})]. Because of its relatively short half-life, this compound has to be administered twice a day, which is not ideal for BPH, where long-term sustained effects are required. Moreover, being non-selective for α_1 -AR subtypes, prazosin may also induce orthostatic

hypotension by antagonizing vascular α_{1B} -ARs. However, the influence of prazosin on α_{1B} -ARs may prove beneficial in patients suffering from both hypertension and BPH.⁵³⁶ Like prazosin, doxazosin [pK_i 8.5 (α_{1A}), 9.0 (α_{1B}) and 8.4 (α_{1D})] and terazosin [pK_i 8.2 (α_{1A}), 8.7 (α_{1B}) and 8.6 (α_{1D})] are non-selective α_{1A-D} -AR antagonists, so they may cause orthostatic hypotension. In contrast to prazosin, doxazosin and terazosin are longer-acting, with elimination half-lives of 12–20 h. Alfuzosin is the fourth α_1 selective blocker approved by FDA for the treatment of symptomatic BPH. Like the previous compounds, it is a non-selective α_{1A-D} -AR antagonist [pK_i 8.0 (α_{1A}), 8.0 (α_{1B}) and 8.5 (α_{1D})]. However, its excellent tolerance has been attributed to its slow release formulation.

In the past, efforts have been made to synthesized prazosin-related compounds that can distinguish between the α_1 -AR subtypes. For example, Melchiorre and co-workers^{537, 538} found that the replacement of both piperidine and furan rings of prazosin may afford antagonists that are able to differentiate among α_1 -AR subtypes.

For example, the replacement of the furan ring of prazosin by various substituted phenyl groups has yielded several active compounds (**Fig. 2**).⁵³⁷ The nature of the substituent affected the affinity and subsequently the selectivity for the α_1 -AR subtypes. Any substituent (CHO, Me, OMe and CF₃) at position 2 caused a decrease in potency compared to prazosin and to the unsubstituted phenyl ring. However, they were more selective for α_{1A} - and α_{1D} -subtypes than prazosin. Interestingly, the 2-trifluoromethyl substituted derivative was markedly selective for α_{1D} -ARs. The insertion of the same substituents at position 3 does not cause a significant modification of the selectivity profile. The only exception is represented by the 3-OMe derivatives that turned out to be slightly more potent at both α_{1A} - and α_{1B} -ARs. All these compounds are less potent than prazosin at α_1 -AR subtypes. The only exception is represented by 3-Me derivative that displayed a potency value at α_{1D} comparable to that of prazosin.

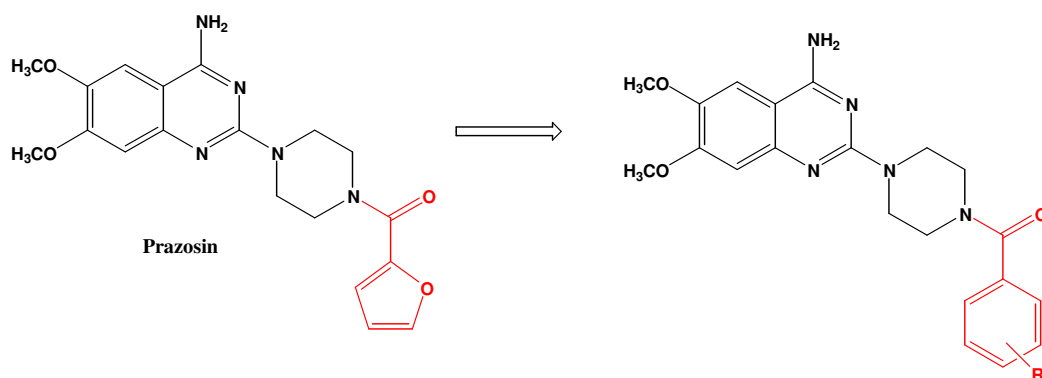


Figure 2: Replacement of the furan ring of prazosin with a substituted phenyl ring.

It was also found that the piperidine ring of prazosin is not essential for the activity and can be replaced by an α,ω -alkanediamine.^{539, 540} Based on these investigations, several hybrid structures which combine both prazosin and benextramine were synthesized in an attempt to improve the selectivity (**Fig. 3**).^{537, 538} Benextramine is the prototype of tetramine disulfides, which inhibits α_1 -ARs by an irreversible mechanism of action.⁵⁴¹

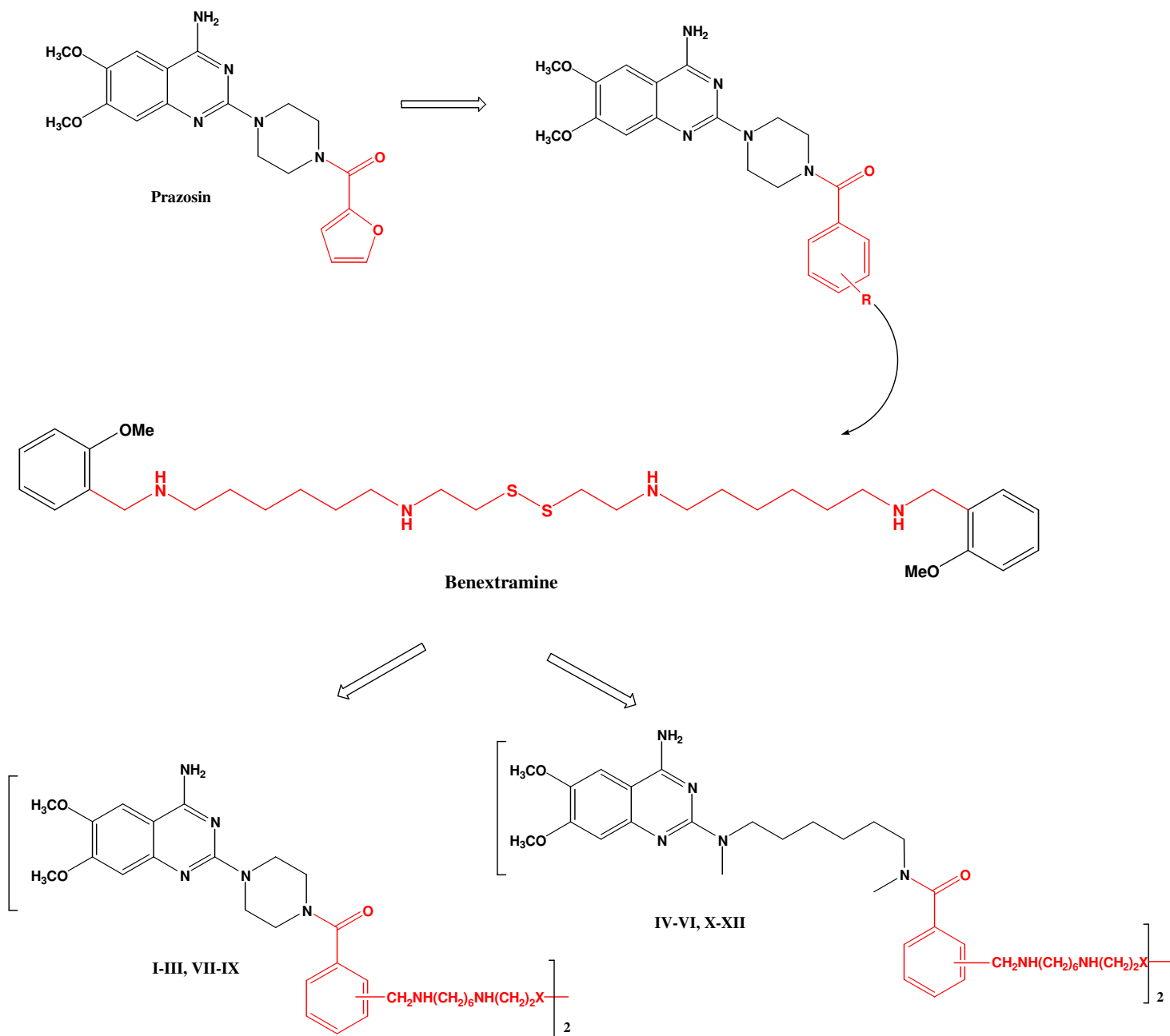


Figure 3: Hybrids prazosin-benextramine.

As shown in **Table 1** functional studies revealed that all quinazolines lacking the disulfide bridge (X= CH₂, **VII-XII**) behaved like prazosin as competitive antagonists. In contrast, all polyamine disulfides (X= S, **I-VI**) displayed a nonhomogeneous mechanism of inhibition at the three receptor subtypes. They seem to be irreversible antagonists at the α_{1A} and α_{1B} subtypes like benextramine, and competitive antagonists at the α_{1D} subtype like prazosin. This means that in the active site of α_{1A} and α_{1B} there is a thiol function that would make an interchange reaction with the disulfide moiety of the antagonist leading to an irreversible blockade. On the other hand, this thiol function might be absent in the α_{1D} subtype.

no.	position	X	pK _b (pIC ₅₀)		
			α_{1A}	α_{1B}	α_{1D}
prazosin			8.99±0.01	8.74±0.01	9.71±0.17
benextramine			(4.79±0.01)	(4.17±0.03)	(5.30±0.01)
I	2	S	(5.30±0.01)	(5.29±0.03)	7.57±0.06
II	3	S	(5.41±0.02)	(4.26±0.05)	7.09±0.02
III	4	S	(5.70±0.11)	(4.38±0.06)	7.61±0.14
IV	2	S	(5.73±0.01)	(5.73±0.05)	8.05±0.15
V	3	S	(5.70±0.11)	(4.38±0.06)	7.61±0.14
VI	4	S	(5.33±0.03)	(5.67±0.01)	8.50±0.14
VII	2	CH ₂	7.74±0.18	6.80±0.12	7.94±0.22
VIII	3	CH ₂	7.29±0.03	6.50±0.12	7.43±0.14
IX	4	CH ₂	6.97±0.04	7.26±0.21	7.47±0.13
X	2	CH ₂	8.17±0.08	7.22±0.10	8.47±0.13
XI	3	CH ₂	8.48±0.13	7.41±0.15	9.30±0.21
XII	4	CH ₂	8.53±0.20	7.56±0.19	7.90±0.14

Table 1: Selectivity of **I-XII** (see **Fig. 3**) for α_1 -ARs.⁵³⁷

All disulfide-bearing compounds were more potent than benextramine at the α_{1A} subtype. At the α_{1B} subtype **I** and **IV-VI** are more potent, while **II** and **III** are as potent as benextramine. Interestingly **V**, in which the piperidine ring is replaced by an open amine chain, was 355-fold more potent than benextramine at the α_{1A} subtype and it also possessed selectivity for α_{1A} and α_{1D} . As discussed above, the carbon analogues **VII-XII** displayed a competitive interaction at all α_1 -ARs like prazosin

1. They are less potent than prazosin, but in contrast to prazosin, they showed different selectivity among the α_1 -AR subtypes. In particular, compound **XI** was 7- and 78-fold more potent at α_{1D} adrenoreceptors than at α_{1A} and α_{1B} , respectively.

In order to obtain compounds endowed with both α_1 -AR antagonist and antioxidant properties the furo moiety of prazosin was replaced with lipoyl fragments of lipoic acid, its lower homologues or naphthoquinone.⁵⁴² The choice of lipoic acid and its homologues was dictated by the observation that lipoic acid is known as a universal antioxidant. Among the synthesized compounds, the derivative in which the 1,2-dithiolane ring was directly connected to its carbonyl group is the most interesting (**A**, **Fig. 4**). It showed high potency among all the α_1 -AR subtypes but it was 20-fold more selective for α_{1D} -ARs than for α_{1A} -ARs. A comparable biological activity and selectivity profile was displayed by naphthoquinone derivative (**B**, **Fig. 4**) and additionally, it showed the highest antiproliferative and antioxidant effects.

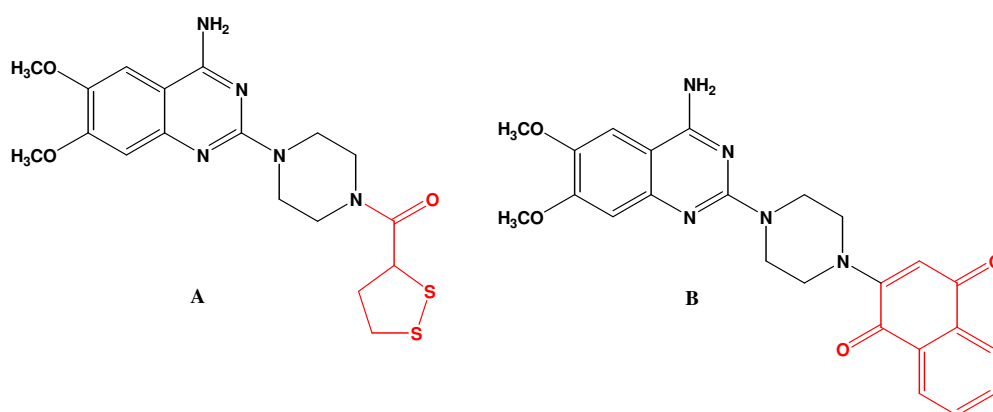


Figure 4: Prazosin-derivatives with antioxidant properties.

As discussed above, changing the amine chain attached to the quinazoline ring and the carbonyl group is possible to modify the affinity and the selectivity for the three α_1 -AR subtypes. On the other hand, the quinazoline seems to be essential for the interaction. Thus, Campbell et al.⁵⁴³ suggested that an essential role for the interactions of the 2,4-diamino-6,7-dimethoxyquinazoline derivatives is the protonated N1 of the quinazoline system. The role of the N1 in receptor binding was also confirmed through the synthesis of a series of isoquinoline derivatives in which the lack of this nitrogen atom resulted in no significant affinity for α_1 -ARs.⁵⁴⁴ Moreover, Ishiguro et al.⁵⁴⁵ suggested a possible binding site for prazosin through molecular modeling (**Fig. 5**). They found that the 4-amino group and 1-nitrogen atom on quinazoline ring possibly interact with the carboxyl group of Asp₁₀₆(α_{1A}), 125(α_{1B}), 176(α_{1D}) in TM3 and the hydroxyl group of Ser₁₈₈(α_{1A}), 207(α_{1B}),

²⁵⁸(α_{1D}) in TM5 by hydrogen bonds. Two methoxy groups of quinazoline ring may also interact with hydroxyl group of Thr₁₁₁(α_{1A}), ₁₃₀(α_{1B}), ₁₈₁(α_{1D}) in TM3 and the hydroxyl group of Ser₁₉₂(α_{1A}), ₂₁₁(α_{1B}), ₂₆₂(α_{1D}) in TM5 and the carbonyl group between the piperidine and furan ring is thought to form a hydrogen bond with Ser₂₉₆ (α_{1A}), ₃₁₈(α_{1B}), ₃₇₂(α_{1D}) in TM6. These results showed that the aminoacids involved in the interaction of prazosin are the same in all receptor subtypes. This may account for the nonselectivity of prazosin to all α_1 -ARs.

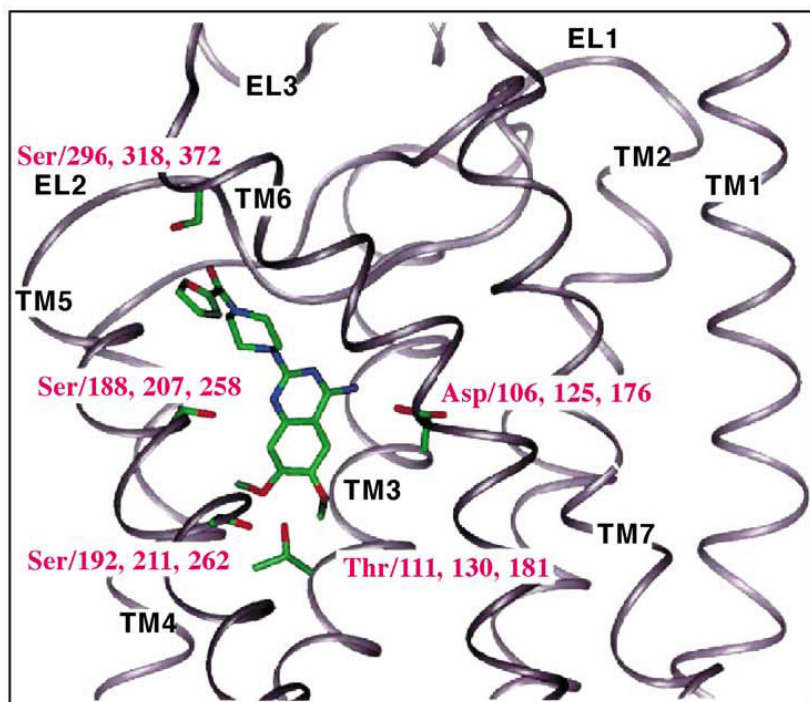


Figure 5: Complex of prazosin at the ligand binding site at α_{1A} -, α_{1B} -, α_{1D} -ARs.⁵⁴⁵

Several evidences suggest that the quinazoline-based α_1 -adrenoceptor antagonists, doxazosin and terazosin, exhibit a potent apoptotic effect against prostate tumor epithelial cells.^{546, 547, 548, 549} This activity seems to be dependent from the quinazoline ring since tamsulosin, a sulphonamide-based α_1 -adrenoceptor antagonist, does not have this effect.⁵⁴⁷ To identify the precise molecular mechanism underlying this apoptosis induction, *in vitro* experiments were performed in three types of cellular lines; DU-145 (that lack α_1 -adrenoceptors), PC3 (androgen-independent prostate cancer cells) and LnCaP (androgen-sensitive prostate cancer cells). It was observed that the apoptotic effect against prostate cancer cells was independent from the ability of the two α_1 -adrenoceptor antagonists to antagonize the α_1 -adrenoceptors. Thus, the irreversible α_1 -adrenoceptor inhibitor phenoxybenzamine does not inhibit the apoptotic effect of doxazosin or terazosin against prostate

cancer cells and smooth muscle cells. Doxazosin and terazosin also reduced the viability of PC-3 prostate cancer cells by inducing apoptosis in a dose-dependent manner after 2 days of treatment. This effect is more significant for doxazosin. In contrast, tamsulosin had no effect on PC-3 prostate cancer cell viability (Fig. 6).⁵⁴⁷

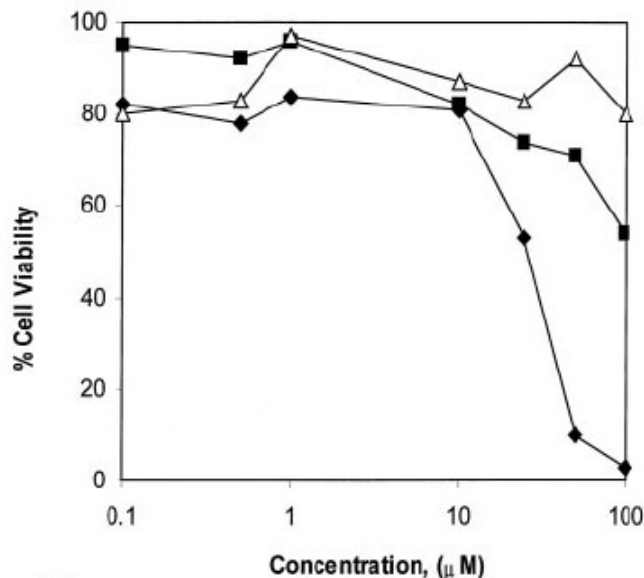


Figure 6: Effect of α_1 -adrenoceptor antagonists on cell viability PC-3 prostate cancer cells. Cells were exposed to increasing concentrations of doxazosin, terazosin, and tamsulosin (0, 0.1, 0.5, 1, 5, 10, 25, 50, and 100 mM). ♦: doxazosin, ■: terazosin, tamsulosin.⁵⁴⁷

Furthermore, *in vivo* trials showed that doxazosin administration (at tolerated pharmacologically relevant doses) in mice bearing PC-3 prostate cancer xenografts resulted in a significant inhibition of tumor growth. Mice were treated with increased oral doses of doxazosin (0, 3, 10 or 100 mg/kg). 3 mg/kg of doxazosin resulted in a significant decrease in tumor volume of prostate cancer xenografts compared with untreated controls. Higher doses of doxazosin did not cause further tumor suppression.⁵⁴⁷

Interestingly, the two quinazoline based α_1 -adrenoceptor antagonists also induce apoptosis in the androgen-sensitive prostate cancer cells LNCaP. In **Table 2**, the effect of doxazosin, terazosin, and tamsulosin (25 μ M) on apoptosis in LNCaP prostate cancer cells are reported. Doxazosin and terazosin caused an increase in the number of apoptotic cells (14 and 13%, respectively), while tamsulosin treatment had no apoptotic effect against LNCaP cells (1.2%) compared with the control (1.1%).⁵⁴⁸

Treatment	LNCaP (% apoptotic cells)	Normal prostate cells (PrEC) (% apoptotic cells)
Control	1.1 ± 0.2%	2 ± 0.7%
Doxazosin (25 μM)	14 ± 0.8%	5 ± 1.1%
Terazosin (25 μM)	13 ± 1.2%	1 ± 0.3%
Tamsulosin (25 μM)	1.2 ± 0.3%	ND

Table 2: Percentage of apoptosis in normal (PrEC) and malignant prostate epithelial cells (LNCaP) in response to α_1 -adrenoceptor antagonists.⁵⁴⁸

To determine whether androgens have the ability to modify the apoptotic response of prostate cancer cells to the quinazoline-based α_1 -antagonists, the effect of 5 α -dihydrotestosterone on doxazosin-induced cell death in LNCaP cells was examined. The decrease of cell viability with increasing concentration of doxazosin in the absence of DHT was comparable to that obtained in the presence of DHT. Therefore, DHT had no protective effect on doxazosin-mediated apoptosis. Moreover, cells were treated with doxazosin alone (25 μM), doxazosin in the presence of DHT, or DHT alone (1 nM). As shown in **Figure 7**, the percentage of apoptotic cells induced by doxazosin was similar to that obtained in the presence of DHT, whereas DHT alone caused a basal apoptosis level, comparable with the values observed for untreated cultures (control). The results suggest that the apoptotic activity of doxazosin and terazosin against prostate cancer cells is independent from the hormone sensitivity status of the cells.

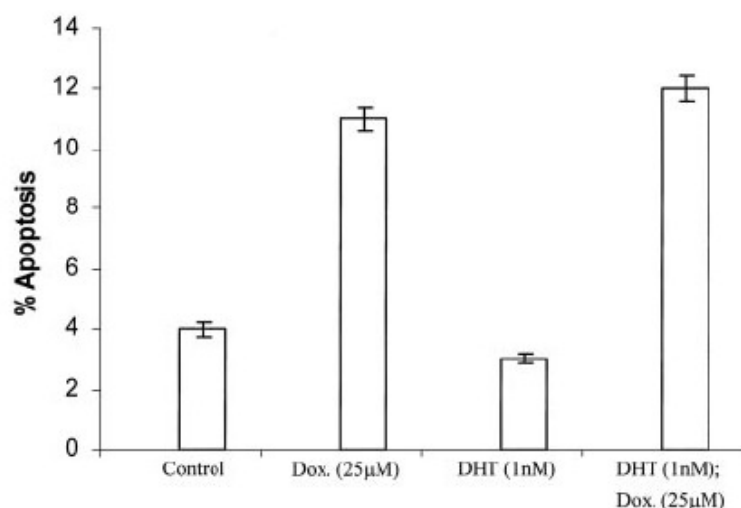


Figure 7: Effect of androgens on sensitivity of LNCaP cells to doxazosin-induced apoptosis.⁵⁴⁸

Finally, it was shown that these α_1 -AR antagonists do not have any effect on cell cycle progression in LNCaP prostate cancer cells. In fact, after two days of treatment with drugs at 25 μM, the

percentage of relative distribution of the prostate cancer cells in each phase of the cell cycle remained very similar to the untreated cells. There was not a significant increase in the number of cells in the G₂-M phase, suggesting that the prostate antigrowth effect of the quinazolines results from targeting the apoptotic pathway without an antiproliferative activity.

The potential signaling pathways that may underlie the apoptotic effect mediated by the quinazoline-based α_1 -AR antagonists in prostate tumor cells seems to be mediated by the TGF- β signal transduction pathway. TGF- β is a multifunctional cytokine which regulates cell proliferation, extracellular matrix production and degradation, differentiation and modulation of apoptosis.⁵⁵⁰ TGF- β is a physiological regulator of prostatic growth.^{551, 552} Thus, it inhibits prostate epithelial cell proliferation and activates apoptosis in the presence of physiological levels of androgens. Several evidence^{553, 554} suggested that there was a significant increase in TGF- β expression in the prostates of patients treated with terazosin and doxazosin. The apoptotic process initiated by TGF- β , is mediated by complex downstream signaling events that lead finally to nuclear gene expression and activation of apoptotic events. Moreover, it seems that quinazoline-based compounds are able to reduce tumor growth by targeting their invasion and migration potential. Anoikis is a form of programmed cell death which is induced by anchorage-dependent cells detaching from the surrounding extracellular matrix (ECM). Cells stay close to the tissue to which they belong since the communication between proximal cells as well as between cells and ECM provides essential signals for growth or survival. When cells are detached from the ECM, they may undergo anoikis. However, metastatic tumor cells may escape from anoikis and invade other organs. It was shown that some quinazoline-based compounds are able to induce anoikis phenomenon in prostate cancer cells. This effect is mediated by reduction in integrin β_1 surface expression that mediates cell adhesion through collagen and fibronectin.⁵⁵⁵

All these results suggest that quinazoline derivatives may have important therapeutic significance in the treatment of not only androgen-dependent prostate cancer, but also for androgen-independent human prostate cancer.

In the continuing search for quinazoline-based α_1 -AR antagonists, Melchiorre and co-workers⁵⁵⁶ developed cyclazosin (**Fig. 8**), a compound known to possess high antagonist affinity and selectivity for α_{1D} - and α_{1B} -ARs relative to the α_{1A} subtype. To further study the effects of doxazosin-related compounds on prostate cancer cells, derivatives of cyclazosin were synthesized, through replacement of 2-furoyl ring of cyclazosin with the 2,3-dihydro-1,4-benzodioxine-2-carbonyl moiety.⁵⁵⁷ The novel cyclazosin analogues are **XIII** (*cis*, cyclodoxazosin), **XIV** (*trans*,

cyclodoxazosin) and **XV** (*cis*, 4a*S*,8a*R*) a couple of the four stereoisomers of **XIII** (**Fig. 8**). An open analog of doxazosin **XVI**, was also tested. In functional assays **XVI** (**Table 3**) was more potent than **XIII** and **XIV** at all α_1 -AR subtypes with the exception of **XIII** at the α_{1B} -subtype. The replacement of piperidine with a *cis*- and *trans*-decahydroquinoxaline nucleus to give **XIII** and **XIV**, respectively, is detrimental for the affinity at α_1 -adrenoceptors. However, the *cis* isomer **XIII** was more potent than the *trans* **XIV** at all the subtypes. Interestingly, in binding assays, the affinity of **XIII-XVI** and cyclazosin at α_1 -AR subtypes did not reflect the affinity observed in functional experiments as already found for a number of other prazosin-related compounds.⁵⁴²

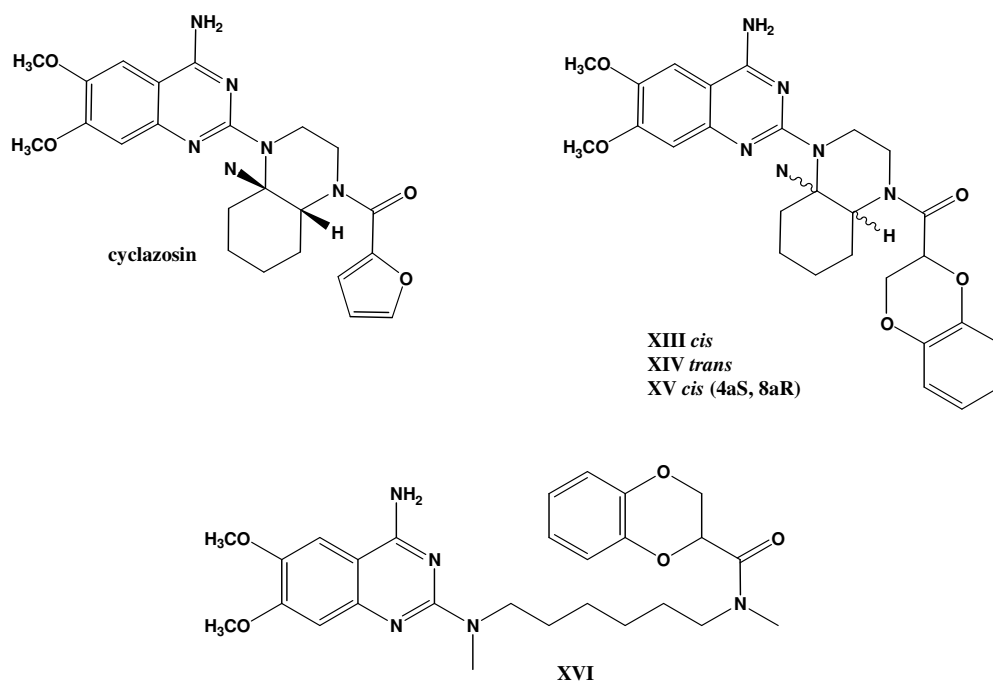


Figure 8: Molecular structure of cyclazosin, **XIII-XVI**.

no.	p <i>K</i> _i ^a			pA ₂ ^b or p <i>K</i> _B ^c			IC ₅₀ (μM) ^d			
	α _{1a}	α _{1b}	α _{1d}	α _{1A}	α _{1B}	α _{1D}	PC-3	DU-145	LNCaP	NHDF
XIII	8.55	9.38	9.77	7.21 ± 0.07 ^e	8.30 ± 0.05 ^e	7.39 ± 0.06 ^b	0.85	0.96	0.57	1.46
XV	8.47	8.85	9.31				1.02			
XIV	7.09	7.65	7.58	5.88 ± 0.18 ^e	7.14 ± 0.07 ^e	6.88 ± 0.10 ^e	> 10 ^g	> 10 ^g	9.75	> 10 ^g
XVI	8.73	9.03	8.80	8.51 ± 0.07 ^e	8.35 ± 0.10 ^e	8.64 ± 0.13 ^e	8.40	9.25	4.61	9.80
cyclazosin	8.26 ^e	9.49 ^e	9.77 ^e	8.91 ± 0.04 ^b	9.18 ± 0.03 ^b	9.21 ± 0.02 ^b				
doxazosin	9.27 ^f	9.09 ^f	9.09 ^f	8.69 ± 0.70 ^{b,f}	9.51 ± 0.41 ^{b,f}	8.97 ± 0.23 ^{b,f}	38.60	37.44	28.11	43.00

Table 3: Binding (p*K*_i) and functional affinity (pA₂ or p*K*_B) constants and *in vitro* antiproliferative activity (IC₅₀) of **XIII-XVI**, cyclazosin, and doxazosin at cloned human α_1 -AR.⁵⁵⁶

The cytotoxic activity of **XIII-XVI** and doxazosin were evaluated *in vitro* in PC-3, DU-145, and LNCaP human prostate cancer cells as well as in normal human dermal fibroblasts. As shown in **Table 3**, compounds **XIII** and **XVI** were significantly more potent than doxazosin in all tested

cells. In particular, **XIII** exhibited the highest effect, whereas **XVI** was about 10-fold less potent than **1**. The trans isomer **XIV** was 17-fold less potent than **XIII** at LNCaP cells, and no effect was observed in the other cells up to the maximal tested concentration (10 μ M). This suggests that the stereochemistry may not have a relevant role in the antiproliferative activity in LNCaP cells.

1.1.2 Phenylethylamines

Phenylethylamines can be identified, from a structural point of view, as the most closely related compounds to the endogenous agonist noradrenalin. Tamsulosin and silodosin are the most important phenylethylamines used in clinical practice (**Fig. 9**).

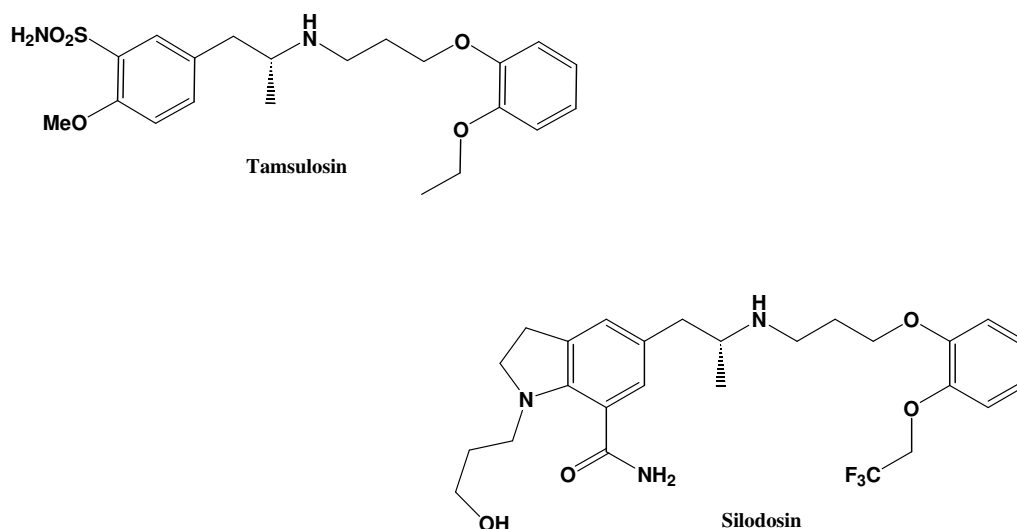


Figure 9: Chemical structures of tamsulosin and silodosin.

Tamsulosin shows selectivity for α_{1A} -ARs and α_{1D} -ARs over α_{1B} ARs [pK_i 9.70 (α_{1A}), 8.90 (α_{1B}) and 9.80(α_{1D})]. However, clinical advantages attributed to pharmacological selectivity require receptor selectivity more than 10-fold, as observed with tamsulosin. Therefore, the slight receptor selectivity of tamsulosin is not sufficient to ensure a clinically advantage. Tamsulosin is a chiral compound and it was found that stereochemistry at the methyl-bearing carbon atom is critical on its pharmacological profile. (S)(+)-tamsulosin displays a greater subtype selectivity, albeit with at least 10-fold reduction in potency compared with its (R)(-)-tamsulosin.⁵³⁶

Silodosin (KMD-3213) is a recent α_1 -AR antagonist approved in 2008 by FDA. Silodosin is 162 times more selective for α_{1A} than for α_{1B} , and is 55 times more selective for α_{1A} than for α_{1D} .⁵⁵⁸ The unique receptor selectivity profile overcomes the common side effect associated with α_1 -AR antagonists. Silodosin possesses cardiac and blood pressure-related safety profile, and data have demonstrated that it does not promote QT-interval prolongation.⁵⁵⁹

In the attempt to search for new α_{1A} -AR antagonists among phenylethylamines, several compounds have been synthesized. Related compounds are shown in **Figure 10**, where the linker between the aromatic ring and the basic amine is truncated (JHT-601)⁵⁶⁰ or extended (WB-4101).⁵⁶¹ They maintain excellent levels of binding selectivity.

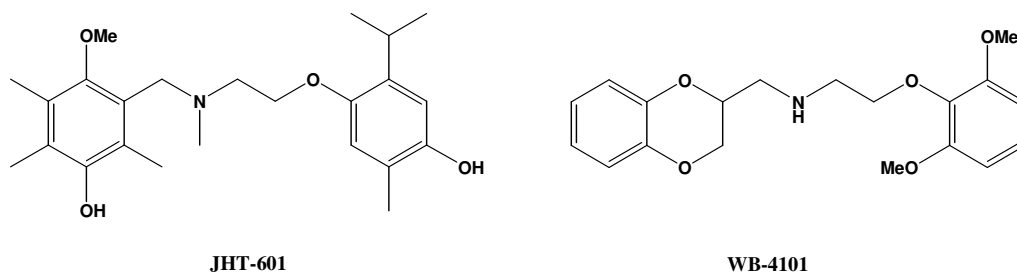


Figure 10: Chemical structures of JHT-601 and WB-4101.

WB-4101 is the prototype of α_1 -AR antagonists bearing a benzodioxan moiety. It became a lead molecule and the subject of intensive investigations aimed at improving its affinity and selectivity. As a result, a variety of analogues have been studied and characterized for their affinity for cloned human α_1 -AR subtypes. Data showed that the two oxygen atoms at positions 1 and 4 might have a different role in receptor binding.^{562, 563} The oxygen atom at position 4 of WB-4101 is not essential for the interaction in fact it could be replaced by a sulfur atom or a methylene unit without affecting potency. Differently, the oxygen atom at position 1 seems to contribute to receptor binding. Moreover, the insertion of a phenyl ring or a *p*-tolyl moiety at the 3-position having a *trans* relationship with the 2-side chain afforded phendioxan **A** and **B**, respectively (**Fig. 11**), that displayed the highest affinity for native α_{1A} -ARs relative to both α_{1B} and α_{1D} subtypes.

Starting from this observation, Melchiorre and co-workers⁵⁶⁴ expanded the study of another aspect of SAR leading to several compounds in which the oxygen atom at position 4 of benzodioxan was replaced by a phenylmethine group, and the resulting compound was the subject of further modifications, such as the exchange of the oxygen atom at position 1 with a sulfur atom, a carbonyl group or a methylene unit. In functional assays, compound **C** was the most potent at α_{1D} -ARs, while the prototypes WB-4101 and **A** are more potent at α_{1A} -ARs. Compound **D**, bearing a carbonyl moiety at position 1, was the most potent at α_{1A} -ARs like the prototypes. Replacing the oxygen with a sulfur atom retained the activity. However, the stereochemistry of the substituent in 4- and 2-position is essential for the activity. In fact, a *trans* relationship between the 2-side chain and the 4-phenyl group is detrimental for binding at α_1 -ARs as revealed by a comparison between the *trans* and the *cis* isomers **E** and **F**. *Cis* isomer **F** was significantly more potent than the *trans* isomer **E** at α_{1A} -ARs, while it was, however, only slightly more potent at both α_{1B} - and α_{1D} -ARs.

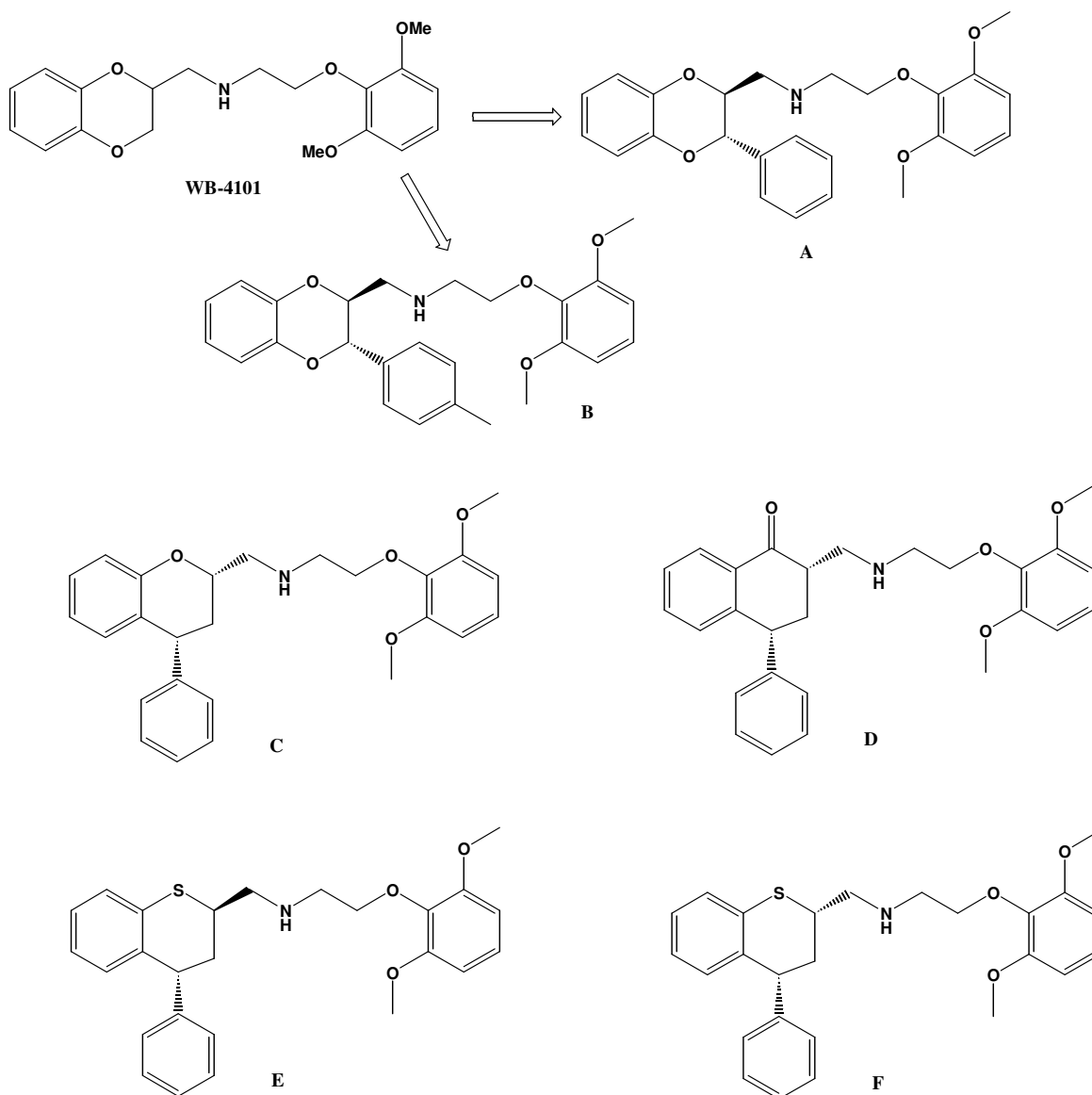


Figure 11: Further modification on the lead compound WB-4101.

1.1.3 Piperidines

Indoramin (**Fig. 12**) is the first compound of piperidine-based α_1 -selective antagonists used in BPH.⁵⁶⁵ A significant drawback with indoramin, however, is its poor selectivity. Thus, indoramin interacts with other receptors, such as 5-HT and histamine, leading to sedation and to several side effects. The major challenge within this class of compounds has been to increase α_1 subtype selectivity while reducing its polypharmacology. The replacement of the terminal indole group of indoramin by a phenyl ketone yielded the second-generation compound SNAP-1069 (**Fig. 12**). SNAP-1069 displayed a 10-fold increase in selectivity for α_{1A} -ARs over α_{1B} -ARs and α_{1D} -ARs but it still suffers, however, from a broad spectrum of activities.⁵⁶⁶

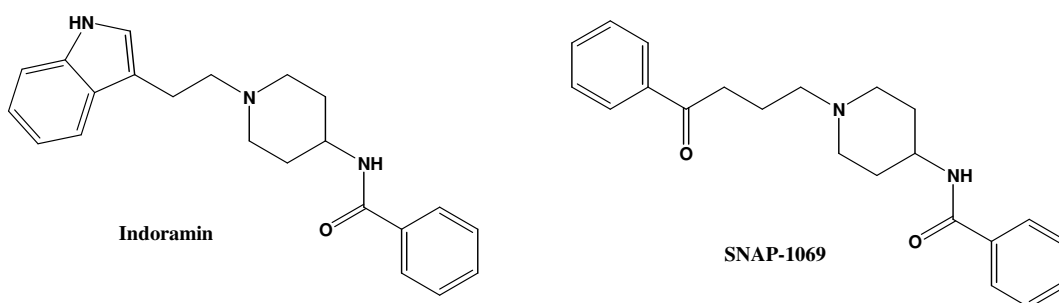


Figure 12: Chemical structures of indoramin and SNAP-1069.

Further work was inspired by the discovery of dihydropyridine (DHP) calcium channel blocker used for the treatment of hypertension. The first compound was (S)(+)-niguldipine (**Fig. 13**).

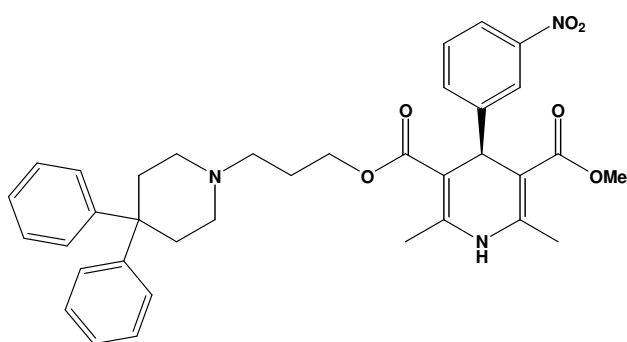


Figure 13: Chemical structure of (S)-niguldipine.

Niguldipine is a potent α_1 -AR antagonist for. In fact, it displays a 100-fold selectivity increase for α_{1A} -AR versus the other α_1 -ARs subtypes [pK_i 9.8 (α_{1A}), 7.26 (α_{1B}) and 7.00 (α_{1D})]. Structural modifications of the DHP skeleton led to SNAP 5089⁵⁶⁷ and SNAP 5540⁵⁶⁸ (**Fig. 14**), which maintained potency and selectivity for the α_{1A} subtype, but they had attenuated or no calcium channel activity. Some of the compounds that belong to this class, however, had poor oral bioavailability in rats which may be due to the oxidative metabolic conversion of the dihydropyridine moiety into a pyridine.

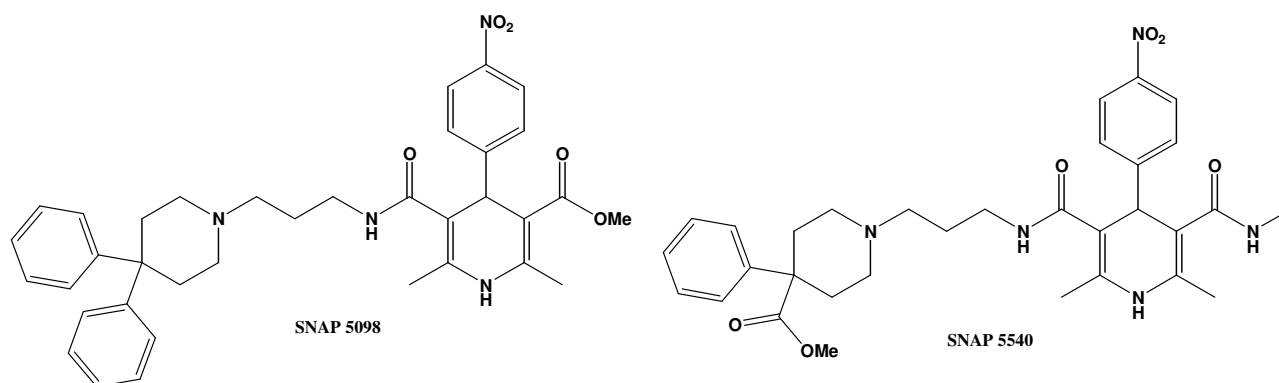


Figure 14: Molecular structure of SNAP 5098 and SNAP 5540.

In a further modification, the DHP core was replaced by a dihydropyrimidinone scaffold, as in SNAP 6201 (**Fig. 15**), in order to avoid pharmacokinetic problems. The difluoro analog SNAP 6201 showed good binding affinity for the α_{1A} receptor, no cardiovascular effects and a good pharmacokinetic profile.⁵⁶⁹ However, *in vitro* and *in vivo* evaluation of SNAP 6201 showed that its major metabolite, 4-methoxycarbonyl-4-phenylpiperidine, is a potent μ -opioid agonist.

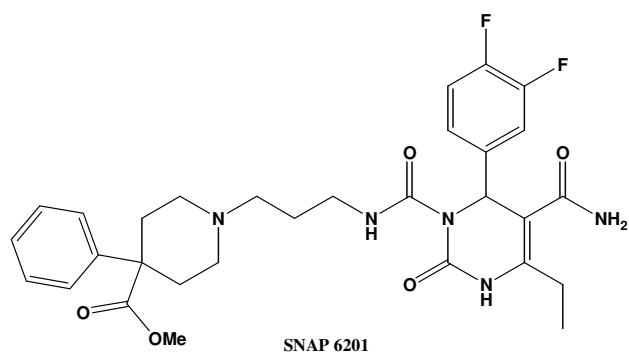


Figure 15: Molecular structure of SNAP 6201.

Modification of the linker in SNAP 6201 gave several compounds with good α_{1A} binding affinity and selectivity. One of the most promising molecules is the compound shown in **Figure 16**, where the 4-methyl-4-phenylpiperidine core was essentially inactive at the μ -opioid receptor. Moreover, it did not display affinity for other GPCRs.

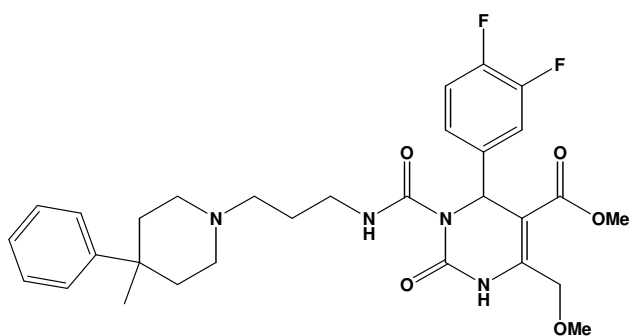


Figure 16: Further modifications of SNAP 6201.

1.2 5 α -reductase inhibitors

BPH is often correlated to an abnormal production of 5 α -dihydrotestosterone (5 α -DHT). 5 α -DHT is synthesized from testosterone by the enzyme 5 α -R in the prostate (**Fig. 17**). Two 5 α -R isoforms have been cloned: 5 α_1 -R and 5 α_2 -R. The type 2 isozyme have been found mainly in the prostate, genital skin, seminal vesicles and in the dermal papilla, while the type 1 isozyme have been found in non-genital skin and hair follicles. Therefore, inhibitors of 5 α_2 -R are useful drugs to lower the DHT level in the prostate. This might be a promising strategy for the treatment of prostate diseases.

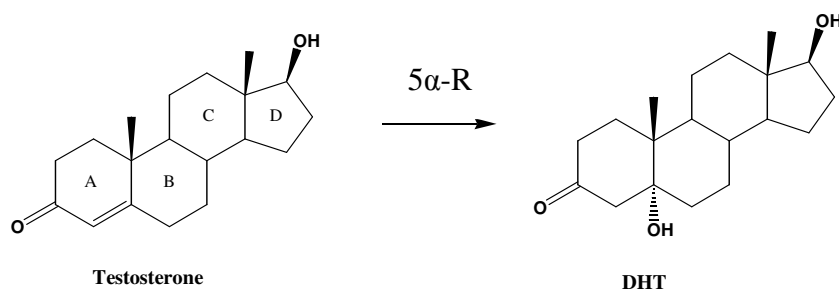


Figure 17: Conversion of testosterone to DHT.

The mechanism of testosterone reduction is shown in **Figure 18**. It involves the formation of a ternary complex between the enzyme, NADPH and the substrate testosterone. When testosterone enters into the active site of the enzyme, a complex is formed through the activation of the enone system by a strong interaction with an electrophilic residue present in the active site. The delocalized carbocation is then reduced selectively at C-5 by a direct hydride transfer from NADPH, leading to the formation of the enolate of DHT. This intermediate is presumably coordinated with NADP⁺ giving the ternary complex E–NADP⁺–DHT. Then, the departure of DHT gives the binary NADP⁺–enzyme complex, and finally the release of NADP⁺ leaves the enzyme free for further catalytic cycles.

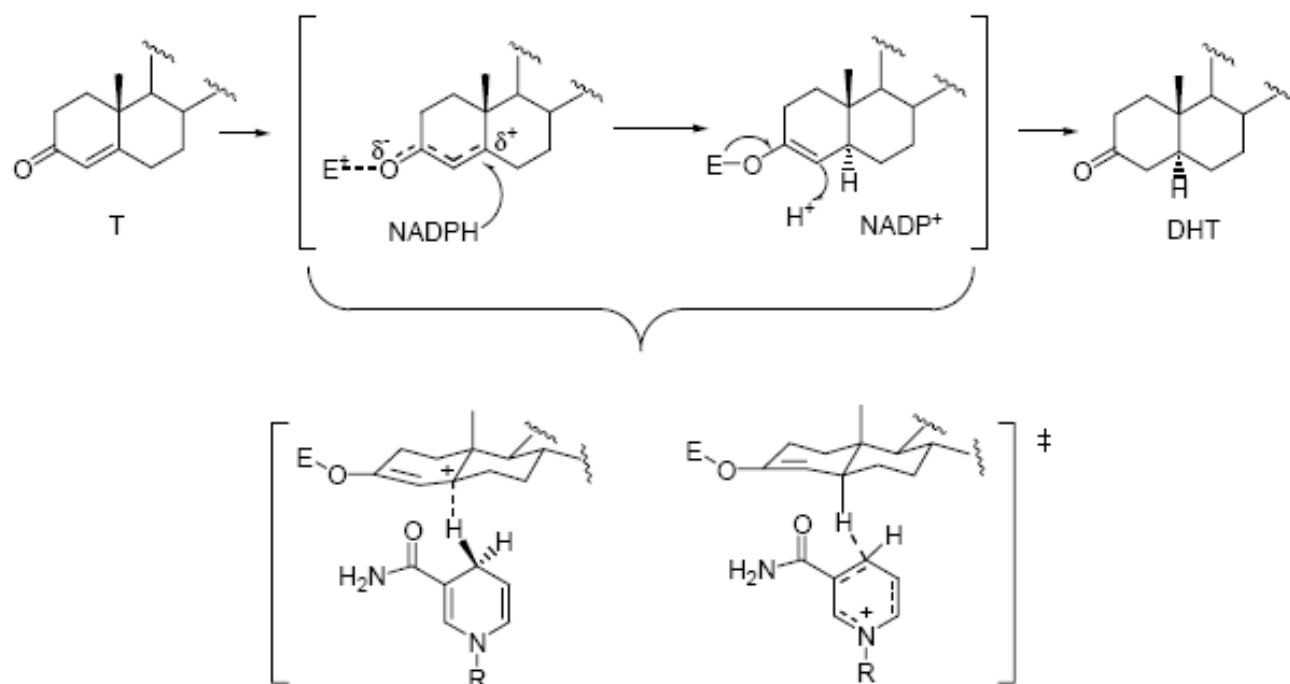


Figure 18: Reduction mechanism of testosterone to DHT.⁵⁷⁰

5 α -R inhibitors have been studied for over 25 years as potential drugs for the treatment of diseases where DHT is implicated.⁵⁷¹ These compounds can be classified into two groups: steroidal and non-steroidal inhibitors. The steroidal inhibitors are the most important class of compounds since they are used in clinical practice. The structure of steroidal inhibitors was based on the testosterone skeleton, which has been modified:

- by the introduction of a nitrogen atom in the A ring (4-azasteroids), in the B ring (6-azasteroids), and at position 10 (10-azasteroids).
- by the introduction of a double bond into the above described structures.

In the 4-azasteroid series, the first potent inhibitor of human 5 α -R used in clinical practice is finasteride (**Fig. 19**).

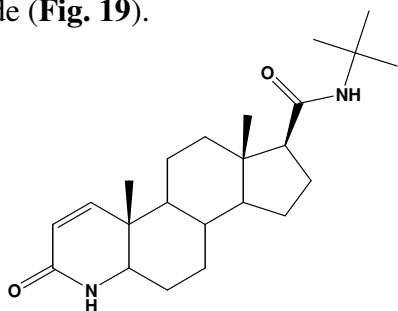


Figure 19: Molecular structure of finasteride.

Finasteride and other close structural analogs are slow-offset, essentially irreversible inhibitors. The conversion of the carbonyl in the A-ring of finasteride to an enolate and the subsequent alkylation by NADP⁺ leads to the formation of a very stable and potent enzyme-NADP-dihydrofinasteride adduct (**Fig. 20**).

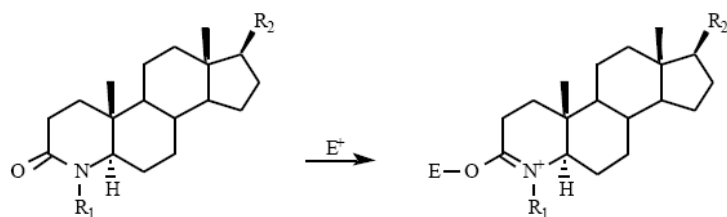


Figure 20: Formation of the enzyme-NADP-dihydrofinasteride adduct.⁵⁷⁰

Finasteride is a potent inhibitor of 5 α -R of type 2 with only weak *in vitro* activity versus the 5 α -R type 1 isozyme.⁵⁷² Finasteride (5 mg per die) is able to reduce about 70% of the serum DHT concentration, to reduce the total gland size of 15–25% and to ameliorate the severe symptoms associated to BPH. Later studies indicated the presence of a small amount of 5 α ₁-R in the prostate gland, and therefore, the use of dual inhibitors was developed as a new hypothesis for improving the reduction of DHT levels. This led to the discovery and market introduction of a new, very potent dual inhibitor, dutasteride, which was approved by FDA in 2002 for the treatment of BPH.⁵⁷³ Dutasteride (**Fig. 21**), like finasteride, is a 4-azasteroidal derivative with the more lipophilic 2,5-difluorophenyl substituent in the amide. This drug reduces the serum DHT concentration by about 90% and the total gland size by 25%.⁵⁷⁴

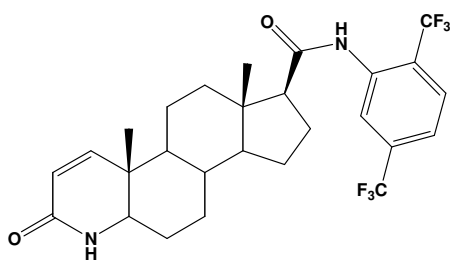


Figure 21: Molecular structure of dutasteride.

2 Aim of the project

BPH, the nonmalignant enlargement of the prostate caused by increased cellular growth, commonly affects elderly men. The incidence of BPH is increasing along with increasing average life expectancy.⁵⁷⁵ BPH causes severe LUTS such as nocturia, incomplete bladder emptying, urgency, incontinence, bladder pain, urinary hesitancy, weak stream and straining to void. These symptomatic urinary dysfunctions have a significant impact on the lifestyle of older men.⁵⁷⁶ Therapeutic approaches for treating BPH aim to decrease symptoms as well as improve the urinary flow rate. TURP is the most effective surgical therapy for this disease but it is not without any negative aspects. In fact, TURP can cause retrograde ejaculation, impotence, postoperative urinary tract infections and urinary incontinence. For these reasons, an increasing number of patients prefer conservative and less invasive therapies.

5 α -R inhibitors and α_1 -AR antagonists are the two main categories of drugs currently available for BPH.⁵⁷⁷ 5 α -R inhibitors inhibit 5 α -R, the enzyme that converts testosterone to its active metabolite 5 α -DHT, reducing prostatic cellular growth.⁵⁷⁸ Initially developed as antihypertensive agents, α_1 -AR antagonists exert their effect by blocking ARs that mediate contraction of the prostatic smooth muscle cells and bladder neck, producing lower urinary tract symptoms.⁵⁷⁹ α -ARs are a class of GPCRs belonging to the sympathetic nervous system. α -ARs are divided into two subtypes: α_1 and α_2 . The α_1 subtype is predominant in the prostate capsule and mediates smooth muscle tone.⁵⁸⁰ Blockade of α_1 -ARs is the predominant form of medical therapy for the treatment of urinary tract obstruction due to BPH, as it targets the neural elements which contribute to the symptoms of the disease. Several studies indicate that α_1 -ARs can be classified into at least three subtypes, i.e. $\alpha_{1A/1a}$, $\alpha_{1B/1b}$ and $\alpha_{1D/1d}$.⁵⁸¹ It has been shown that the α_{1A} -AR subtype is the predominant receptor involved in human prostate physiology, while α_{1B} -AR seems to play a role in the regulation of blood pressure. A potential therapeutic use for the α_{1D} -AR subtype has not been firmly established but α_{1D} -ARs are predominant in the destrusor muscle and they seem to be upregulated in the destrusor of obstructed rats.⁵³⁴ This suggests a relevant role for this subtype also in the control of the symptoms associated with BPH.

A great deal of interest now lies in the development of α -blockers which target only one receptor subtype while not affecting the others. Furthermore, the different localization of these receptor subtypes suggests the possibility of designing drugs that interact with a particular subtype in an effort to limit the adverse effect profile and improve efficacy. However, the design of an ideal selective ligand, which recognizes only one among many receptor subtypes, remains a critical challenge in medicinal chemistry.

Our research group has long been involved in designing new α_1 -AR antagonists structurally related to prazosin (**Fig. 1**)^{537, 538, 539, 540, 541, 542, 582, 583, 584} Prazosin is one of the oldest α_1 -AR antagonists and the prototype of quinazoline-bearing compounds widely used in the management of hypertension. Its congeners, terazosin, doxazosin (**Fig. 1**) and tamsulosin offer a similar pharmacology with a longer duration of action. Furthermore, prazosin and its congeners represent the most used approach in treating LUTS associated with BPH.⁵³⁶

The aim of the project was to synthesize new quinazoline derivatives in an attempt to improve affinity and selectivity for the α_1 -subtypes. We wanted also to exploit the antiproliferative activity of these compounds against prostate cancer, since it has been reported that some quinazoline-derived α_1 -AR antagonists exert apoptotic activity via an action independent from activation of α_1 -ARs and through a mechanism independent from androgens.^{547, 548} The design strategy of prazosin-related compounds was based on the observation that the piperidine ring of prazosin is not essential for the activity.^{585, 586} Furthermore, modifying the piperidine and/or the furan unit may afford antagonists that are able to differentiate among α_1 -AR subtypes.^{537, 538, 587, 588} On the other hand, the quinazoline unit of prazosin is essential for the high affinity toward α_1 -ARs. In fact, Campbell et al.⁵⁴³ suggested that an essential role for the interactions of the 2,4-diamino-6,7-dimethoxyquinazoline derivatives is the protonated N1 of the quinazoline system. The role of the N1 in receptor binding was also confirmed through the synthesis of a series of isoquinoline derivatives in which the lack of this nitrogen atom resulted in no significant affinity for α_1 -AR.⁵⁴⁴ More recently, the importance of 2,4-diamino-6,7-dimethoxyquinazoline moiety for the interaction with α_1 -AR was also confirmed by Ishiguro and co-workers by molecular modeling.⁵⁴⁵ Furthermore, the quinazoline ring seems to be essential for the apoptotic activity of some prazosin-related compounds because tamsulosin, that lacks the quinazoline moiety, is devoid of this important effect.⁵⁴⁷

In the light of these considerations, compounds **1** and **2** (**Fig. 22**) were designed maintaining the quinazoline moiety and replacing the piperidine ring with a 3-aminopiperidine unit. The free amine function can be protonated at physiological pH giving rise to a possible additional interaction with a complementary receptor group, which would increase the possibility to achieve receptor subtype selectivity. To investigate the effect of the stereochemistry in biological activity, both enantiomers at the 3-position of the aminopiperidine were synthesized. It is well-known that stereochemistry in drug discovery is very important. In fact several drugs introduced to the market are single enantiomers. The enantiomers of a chiral drug present unique chemical and pharmacological

behaviors in a chiral environment, such as the human body, in which the stereochemistry of chiral drugs determines their pharmacokinetic, pharmacodynamic, and toxicological actions.

Compounds **3** and **4** (**Fig. 22**) were obtained inserting into compound **1** and **2**, respectively, the furan-2-carbonyl group as in prazosin. Compounds **5** and **6** (**Fig. 22**) were obtained coupling the amine group of **1** and **2**, respectively, with a quinone ring to have in the same molecule multiple biological activities. Thus, replacing the furoyl moiety of **3** and **4** with a 1,4-naphthoquinone might lead to derivatives endowed with both α_1 -AR antagonism and antioxidant properties observed in previous studies with a prazosin-related compound bearing the naphthoquinone moiety.⁵⁴²

Compounds **7-10** (**Fig. 23**) were designed combining compounds **1** and **2** and the 1,4-benzodioxane-2-carbonyl group of doxazosin. The introduction of a second chiral center in the molecule results in additional structural elements that might affect activity and affinity for α -ARs and display also antiproliferative properties. Since these molecules contain two chiral center, all the four diastereoisomers were synthesized.

Although bearing a chiral center, doxazosin is used in clinical practise as a racemic mixture. In the literature there is a debate about the stereochemical specificity of doxazosin for α_1 -ARs.^{589, 590, 591} Thus, the two enantiomers of doxazosin (**11-12**, **Fig. 24**) were also synthesized to compare the activity of the new molecules with a commercially available drug.

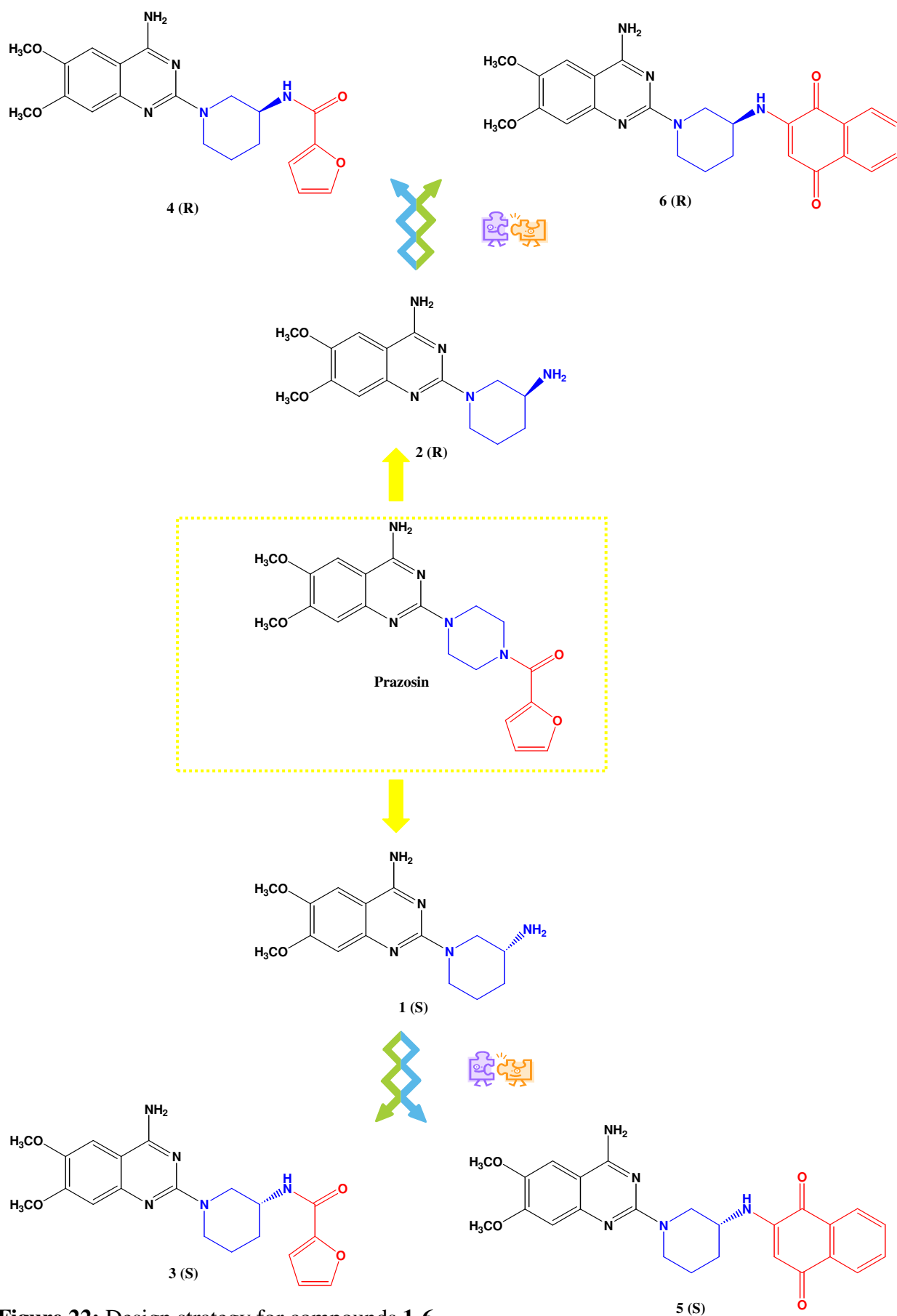


Figure 22: Design strategy for compounds 1-6.

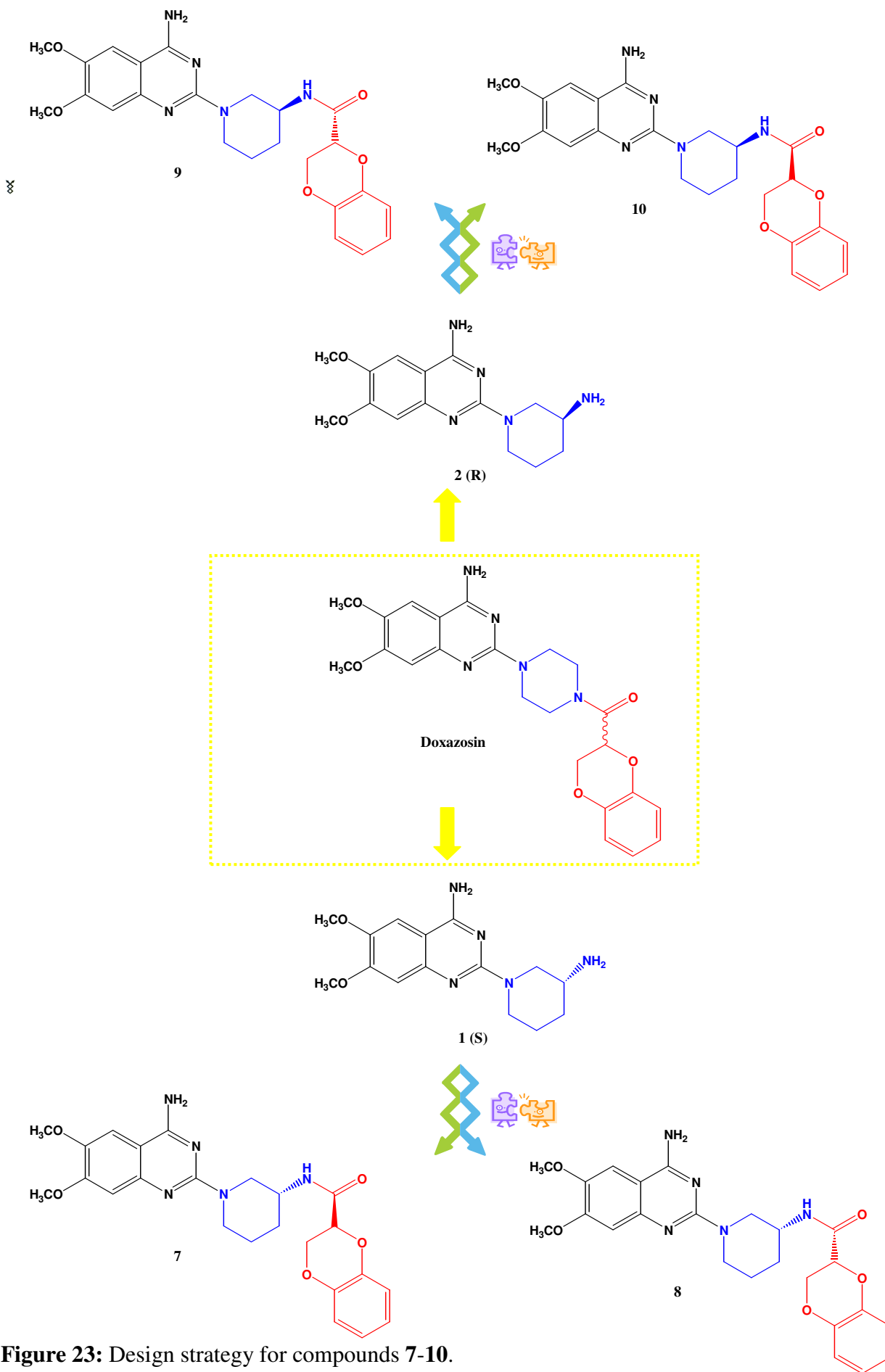


Figure 23: Design strategy for compounds 7-10.

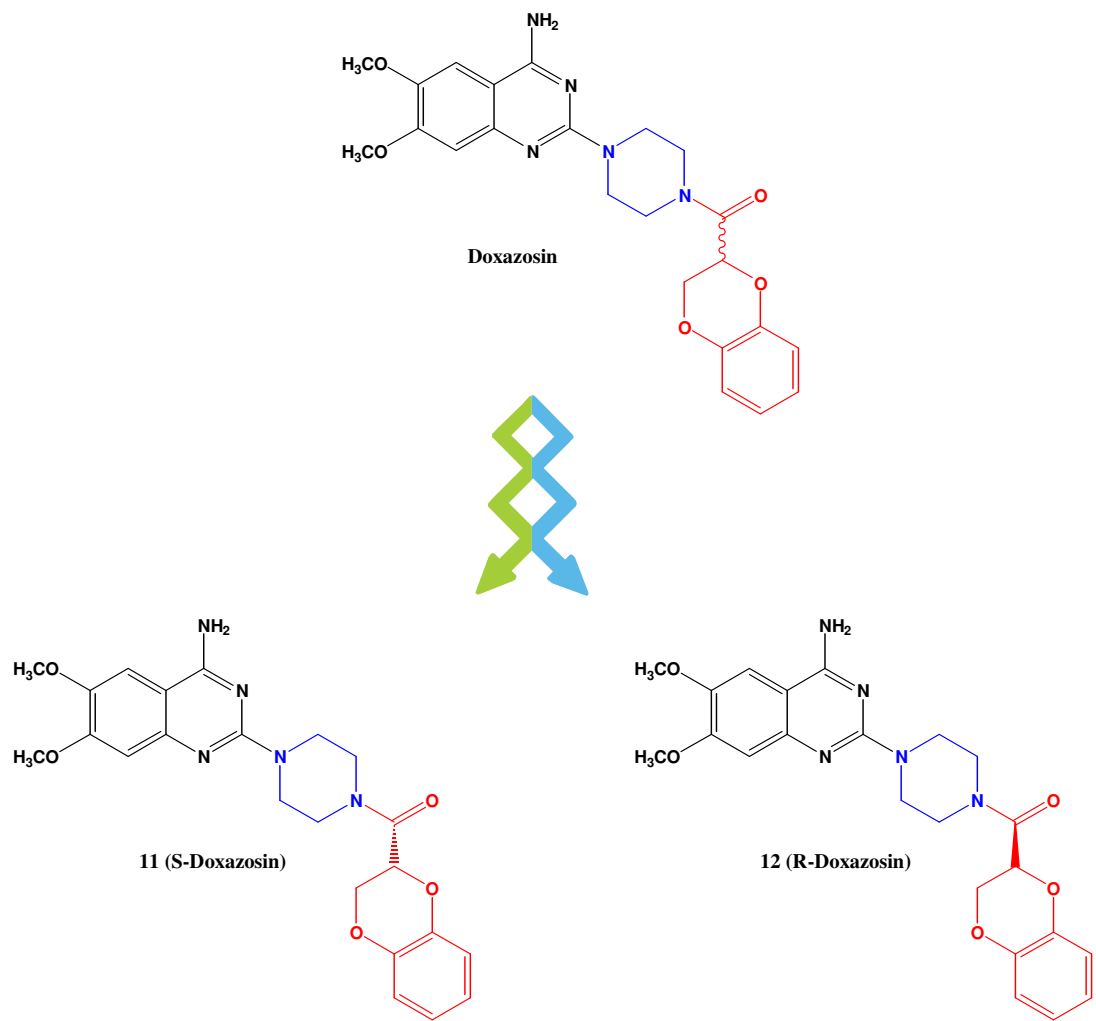
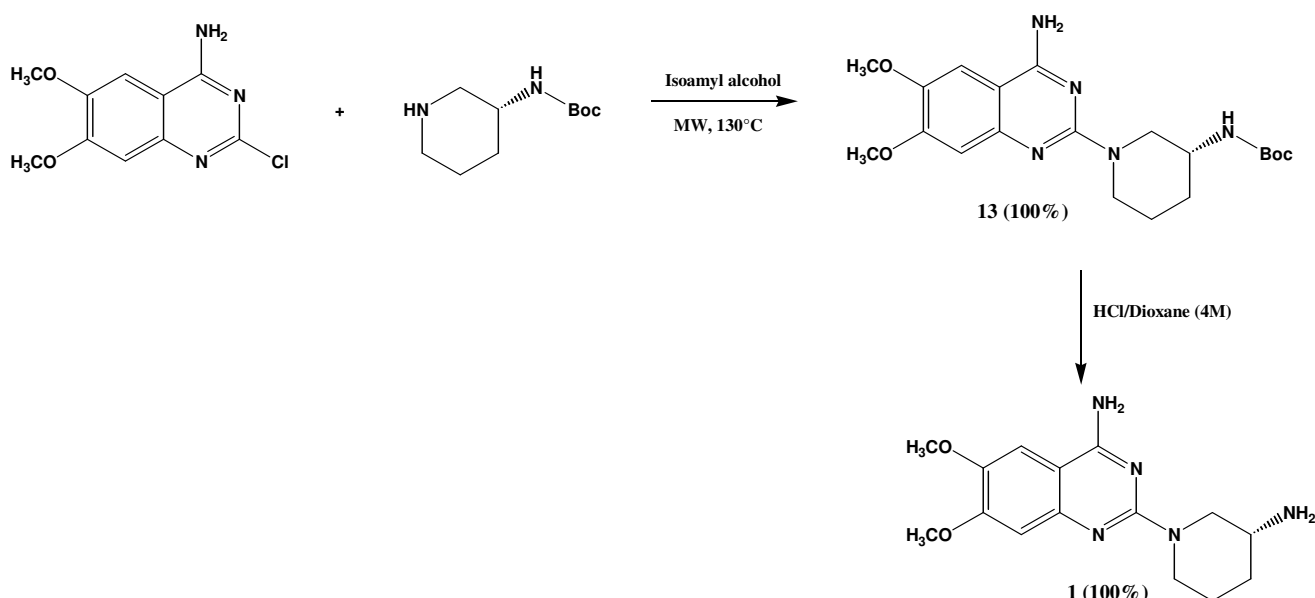


Figure 24: Molecular structures of S- and R-doxazosin.

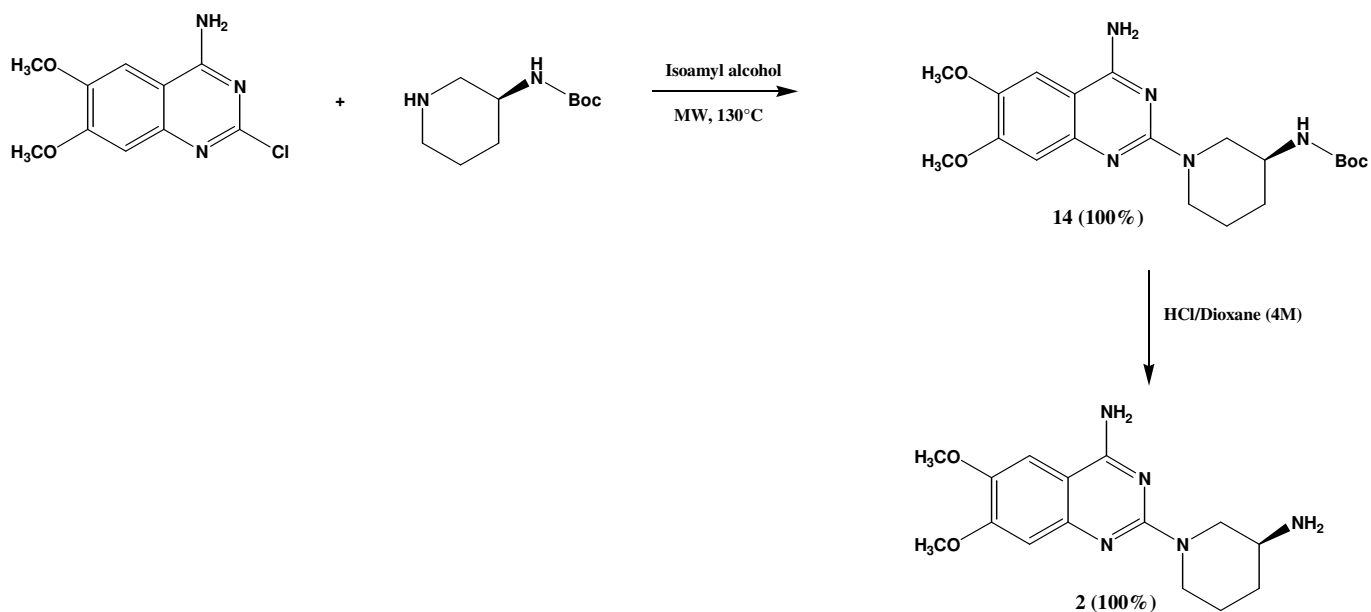
3 Chemistry

The synthesis of the new quinazoline derivatives are described in **Scheme 1-10**. Intermediates **13** (**Scheme 1**) and **14** (**Scheme 2**) were obtained through aromatic nucleophilic substitution of (S)-3-(boc-amino)piperidine and (R)-3-(boc-amino)piperidine, respectively, on 4-amino-2-chloro-6,7-dimethoxyquinazoline. The syntheses were performed by following an adapted procedure described by Althuis et al.⁵⁹² The reaction required high temperature and long time. To short the reaction time, reactions were performed under microwave irradiation. It was found that they were complete after 50 min at 130 °C. Boc-deprotection with 4M HCl in dioxane led to the primary amines **1** (**Scheme 1**) and **2** (**Scheme 2**). Then, amidation of **1** and **2** with 2-furoyl chloride afforded **3** (**Scheme 3**) and **4** (**Scheme 4**), respectively, in good yields. Moreover, addition reaction between **1** and **2** with 1,4-naphthoquinone led to the quinazoline-quinones **5** (**Scheme 5**) and **6** (**Scheme 6**). In **Schemes 9** and **10** it is shown the coupling between amines **1** and **2** and 2,3-dihydro-benzo[1,4]dioxine-2-carbonyl chloride **15** and **16**, synthesized from their respective carboxylic acids with thionyl dichloride (**Scheme 7** and **8**). Finally, R- and S-doxazosin were also synthesized as described in **Scheme 11**. The intermediate **17** was obtained through aromatic nucleophilic substitution of piperazine on 4-amino-2-chloro-6,7-dimethoxyquinazoline under microwave irradiation. Piperazine was used in excess (6 equiv.) to avoid the formation of N,N-disubstituted bisquinazolin-piperazines. Then, amidation of **17** with the acyl chlorides **15** and **16** afforded S- and R-doxazosin, respectively.

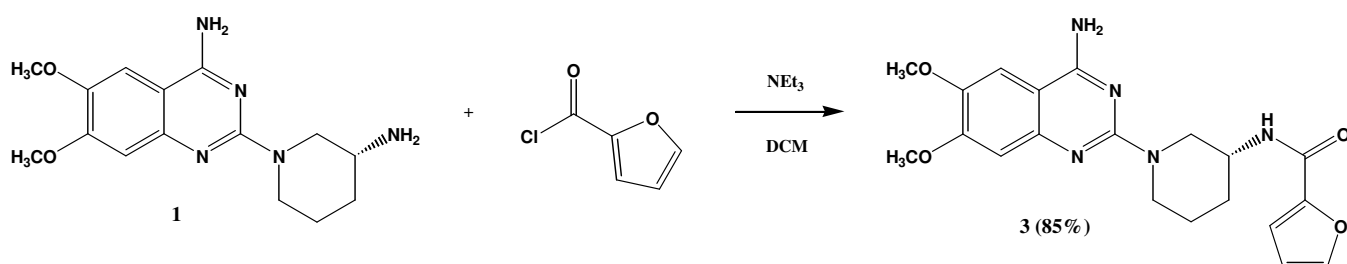
Scheme 1



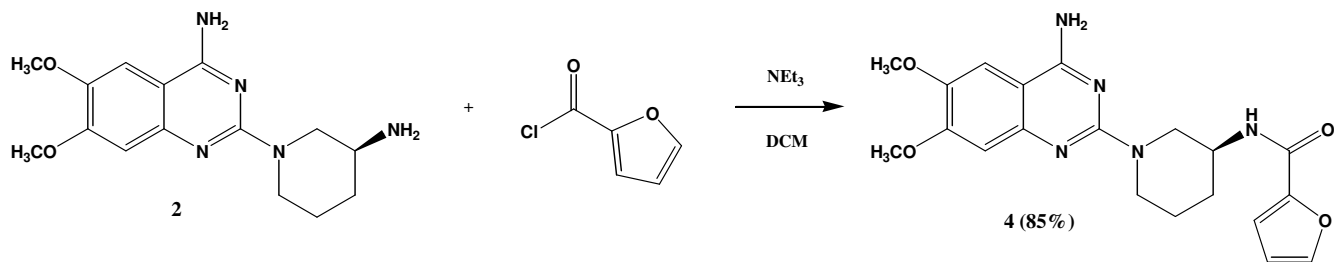
Scheme 2



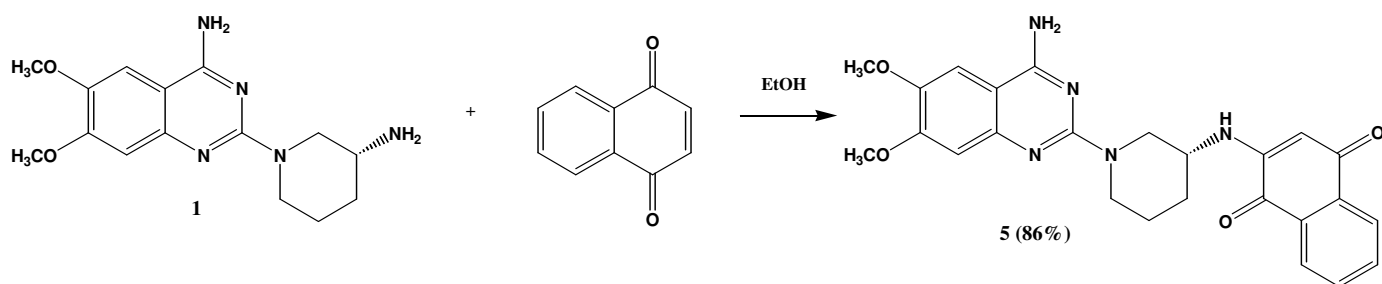
Scheme 3



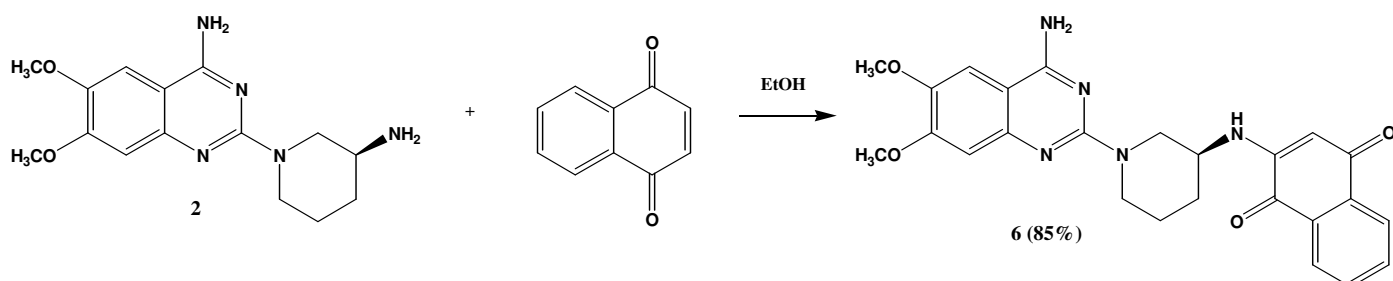
Scheme 4



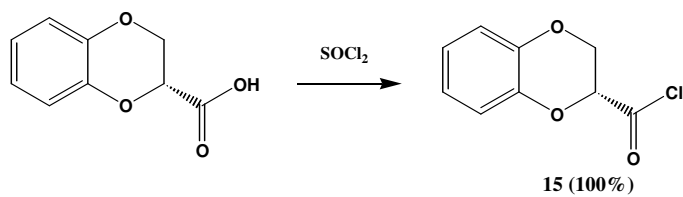
Scheme 5



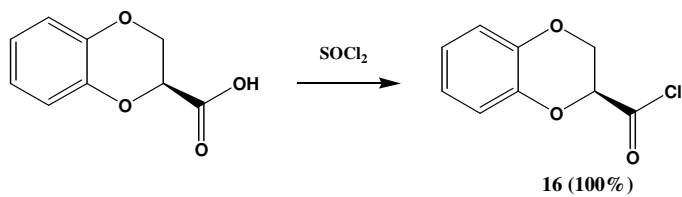
Scheme 6



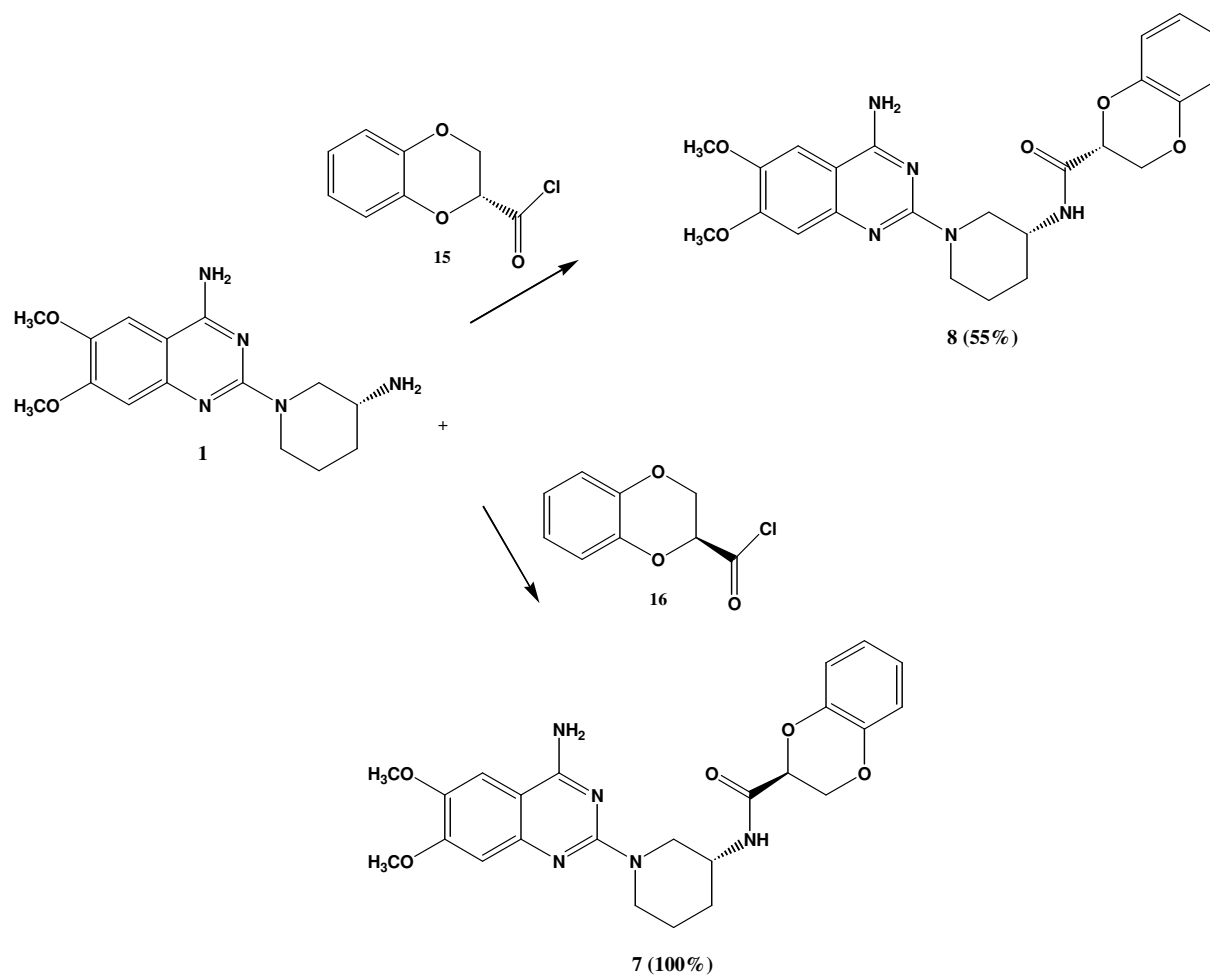
Scheme 7



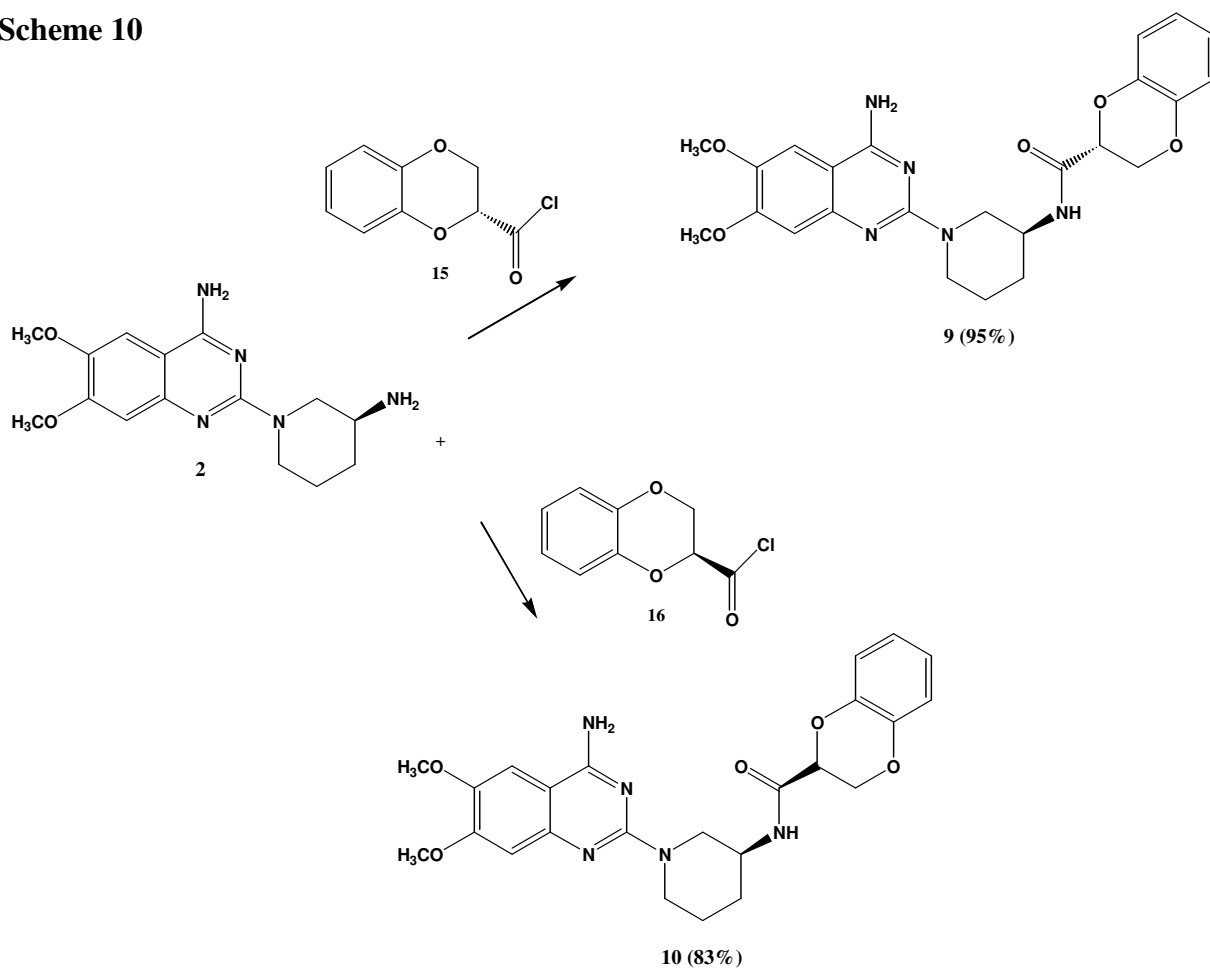
Scheme 8



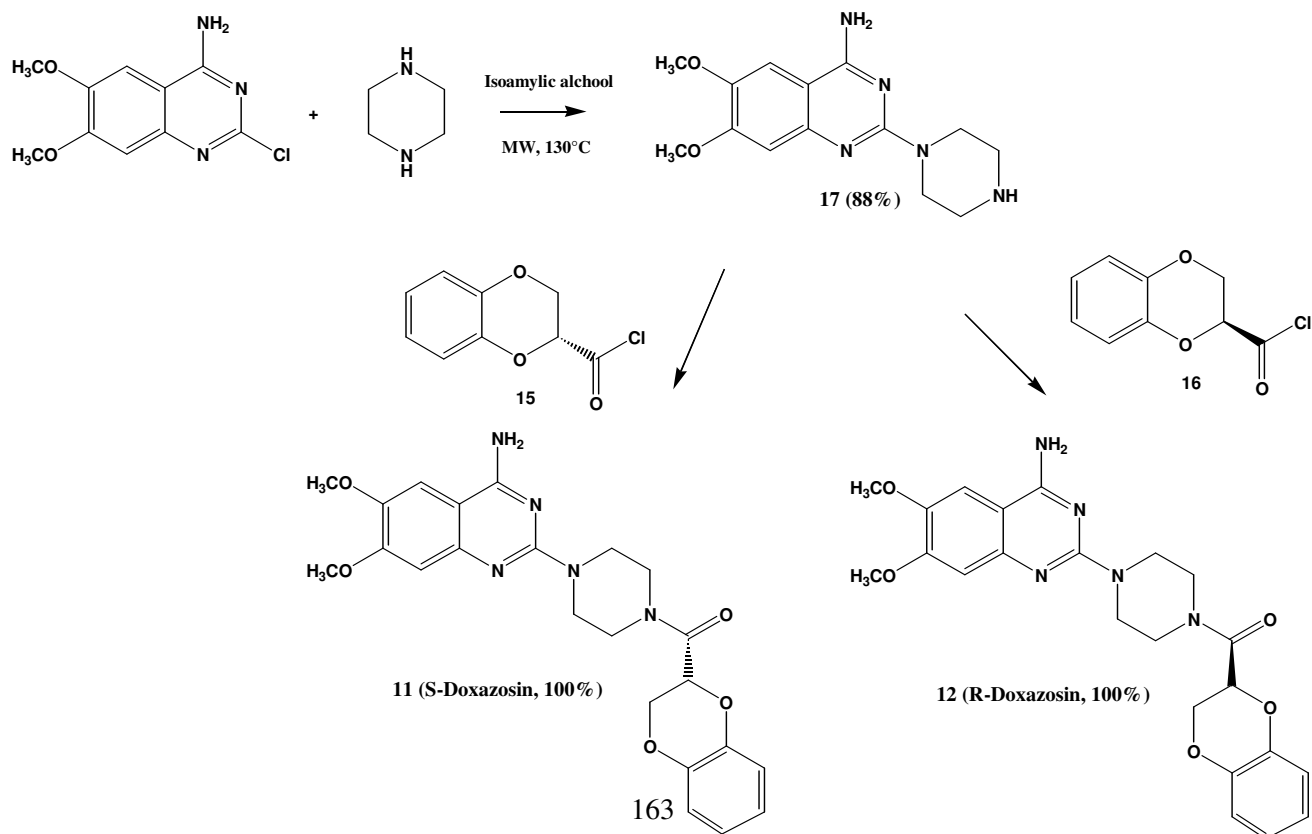
Scheme 9



Scheme 10



Scheme 11



4 Results and Discussion

A Radioligand binding assays

The affinity profile of **1-12** was evaluated in radioreceptor binding assays on membranes of Chinese hamster ovary (CHO) cells expressing human α_1 -AR subtypes. Binding assays were performed by Recordati S.p.A. Binding affinities were expressed as pK_i values derived using the Cheng-Prusoff equation. The results are reported in **Table 4**. S- and R- doxazosin (**11** and **12**) and prazosin were also included as reference compounds. An analysis of the results reveals that these compounds did not display a noteworthy affinity enhancement toward all α_1 -AR subtypes compared to doxazosin and prazosin. However, the stereochemistry at the 3-C position of the piperidine ring plays an important role for the binding at α_1 -ARs. Thus, we can observe that **3** possessed an affinity for all α_1 -AR subtypes that is more than 100-fold higher compared to its enantiomer **4**. The same observation applies to **5** vs its enantiomer **6** even though the differences in binding affinity were not so marked as between **3** and **4**. Moreover, compound **5** seemed to be 13-fold and 4-fold more selective for the α_{1B} -AR than for α_{1A} - and α_{1D} -ARs, respectively. The incorporation of an additional basic center (**1** and **2**) was detrimental for the activity. The present finding was in good agreement with a study conducted by Campbell et al.⁵⁹³ on quinazoline-related compounds. They found that the prazosin derivative lacking the furoyl moiety displayed a low affinity for α_1 -ARs. It derives that the substituent on the amine group is important for the interaction with α_1 -ARs. However, compound **1** displayed a higher affinity for all three α_1 -AR subtypes than its enantiomer **2**. Derivative **1** is slightly more selective for the α_{1D} - relative to the α_{1B} -AR. This finding is interesting because also α_{1D} -ARs are thought to have a relevant role in the control of the symptoms associated with BPH, while α_{1B} subtype is responsible for the regulation of blood pressure.^{534, 535, 533} In conclusion, the S configuration at the 3-C position of the piperidine ring is an important feature that drives the interaction with α_1 -ARs.

Doxazosin possesses a chiral center but it is used in clinical practice as a racemic mixture. In the literature there is a debate about the stereochemical specificity of doxazosin for the three α_1 -AR subtypes.^{589, 590, 591} From our results we can observe that **11** and **12** did not display a noteworthy difference in affinity toward all α_1 -AR subtypes. Therefore, it derives that the stereochemistry at the benzodioxole ring does not influence α_1 -AR subtype selectivity as also observed for doxazosin derivatives **7-10**. A marked difference in affinity was observed between **7** and the two stereoisomers **9** and **10**. Changing the S into the R configuration at the 3-C position of the piperidine ring of **7**, as in **9** and **10**, was detrimental for the affinity. This effect was more evident for the α_{1A} - and α_{1D} -AR subtypes. On the other hand, changing the stereochemistry at the benzodioxole ring did not

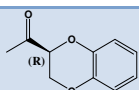
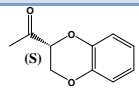
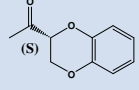
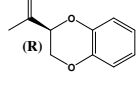
markedly affect the affinity for the α_1 -AR subtypes. Thus, **7** displayed the same biological profile of **8**, whose affinity for α_{1B} -ARs was, however, 8-fold higher than that of **7**. Similarly, **9** and **10** possessed the same biological profile. They were both more selective for the α_{1B} -AR, but **10** displayed a 6-fold increase in affinity for α_{1B} -ARs compared to **9**.

B *Antiproliferative activities*

It is well known that some quinazoline-based α_1 -AR antagonists possess apoptotic effect against prostate tumor cells.^{547, 548} Therefore, antiproliferative activities of compounds **1-12** were also evaluated *in vitro* by National Cancer Institute (NCI), Bethesda, USA. Compounds were tested at a concentration of 10 μ M on sixty different human tumor cell lines, representing leukemia, melanoma and cancers of the lung, colon, brain, ovary, breast, prostate, and kidney. The aim is to prioritize for further evaluation of compounds showing selective growth inhibition or cell killing of particular tumor cell lines. If the results obtained meet selection criteria, then the compounds are studied again in all sixty cell lines in a 5-dose testing to obtain the IC₅₀ value. Among all the compounds, **5** and **6** were found to be the most promising in the 1-dose assays. 5-dose assays for **5** and **6** are in progress to better investigate their antiproliferative profile. The results regarding the single dose screen of derivatives **5** and **6** are reported in **Table 5**. The numbers reported for the one-dose assay is growth relative to the no-drug control, and relative to the time zero number of cells. This allows detection of both growth inhibition (values between 0 and 100) and lethality (values less than 0). For example, a value of 100 means no growth inhibition. A value of 40 would mean 60% growth inhibition. A value of 0 means no net growth over the course of the experiment. A value of -40 would mean 40% lethality. A value of -100 means all cells are dead.

An analysis of the results shown in **Table 5** revealed that **5** and **6** possessed an antiproliferative activity that is more marked for particular cell lines. They were very potent antitumor agent against CNS cancer where they caused a lethality that is almost 100%. The only exception is represented by SF-268 cell line where **5** and **6** caused a lethality of 47.42% and 52.29%, respectively. There was not a noteworthy change in activity between the two enantiomers. This finding is in contrast with radioligand binding assays where it was found that the stereochemistry at the 3-C position of the piperidine ring was critical for the interaction with α_1 -ARs. In lung cancer, **5** and **6** seemed to be inactive on NCI-H226 cells. In HOP-62, HOP-92 and NCI-H522 cell lines they inhibited cellular growth, even though less than 40%. Interestingly, in NCI-H322M and NCI-H460 they were able to induce a marked level of lethality. Therefore, these derivatives could be promising drugs for the treatment of a particular type of lung cancer. Regarding colon cancer, **5** and **6** were quite potent

anticancer agents. In fact, it was found that the percent lethality was more than 60% in all cell lines. The only exception is represented by HCC-2998 cells, where they were completely inactive, and by KM12 cells, where the lethality was 35.24% and 39.21% for **5** and **6**, respectively. There was not a noteworthy difference in antiproliferative activity between the two enantiomers. Interestingly, in melanoma the stereochemistry was an important feature. Compound **6** was completely inactive in all cells lines except in LOX IMVI. On the other hand, its enantiomer **5** was found to be a potent antiproliferative drug with a lethality value more than 80%. However, in M14, SK-MEL-2 and UACC-257 cell lines it was inactive. Regarding ovarian cancer, in OVCAR-4 and NCI/ADR-RES cells the stereochemistry seemed to be important. Derivates **6** caused 88% of lethality in the first cell line and inhibited 71% of growth in the latter. In contrast, compound **5** was inactive. In renal tumor compound **6**, compared to **5**, was found to be the most promising. It caused cell death in a range between 57% and 100%, while in A498 cells was completely inactive. In breast cancer derivates **5** and **6** were quite good antiproliferative agents with **6** slightly more potent. Regarding leukemia, these derivates caused lethality in all cell lines but, however, they were not as potent as for CNS tumor cells. They caused a lethality lower than 50%. The only exception was represented by HL-60(TB) cells where the value was about 60%. In this case, the stereochemistry did not seem to be critical. Finally, in DU-145 (that lack α_1 -AR) prostate cancer cells they caused 54% of cell death. In PC-3 (androgen-independent) cells **5** and **6** inhibited cellular growth by 77.05% and 45.51%, respectively. Therefore, compound **5** seemed to be most promising for the treatment of BPH.

Compound		pK _i ^a		
	R	α _{1a}	α _{1b}	α _{1d}
1	H	6.72	7.26	7.55
2	H	<6	6.75	6.99
3		9.20	9.55	9.48
4		6.96	7.37	7.43
5		8.15	9.28	8.67
6		6.92	7.60	7.47
7		7.74	7.20	7.31
8		7.48	8.13	7.88
9		<6	6.50	<6
10		<6	7.33	6.53
11		9.11	9.20	9.49
12		8.55	9.00	9.06
Prazosin^c		9.23	9.39	9.65

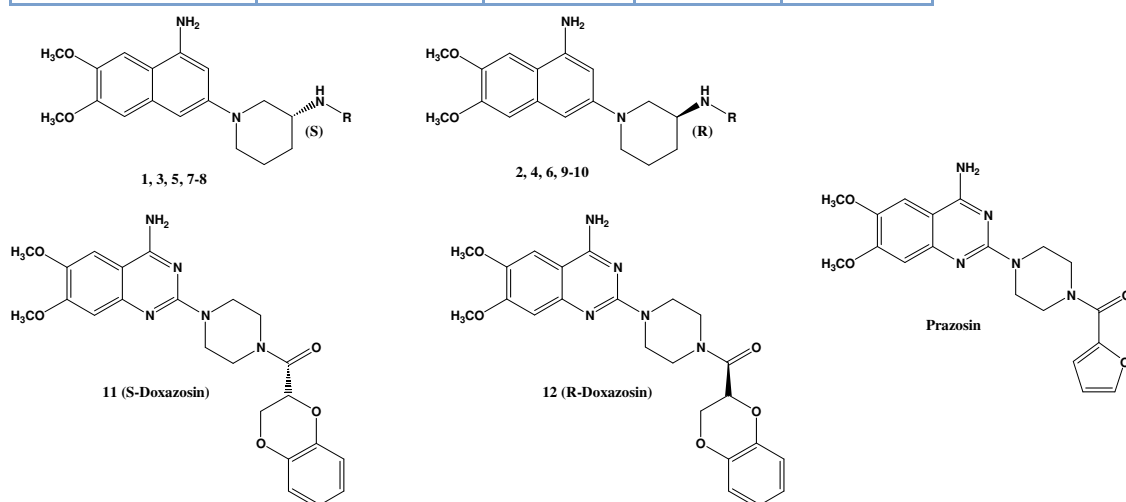


Table 4: Affinity constants expressed as pK_i (CHO cells) values at human recombinant α₁-AR subtypes. ^a Equilibrium dissociation constants (K_i) were derived from IC₅₀ values using the Cheng-Prusoff equation.⁵⁹⁴ K_i values were from two to three experiments, which agreed within ±20%. ^c Data from ref.⁵³⁸

	Compound 5 (Growth Percent)^a	Compound 6 (Growth Percent)^a
Cell lines		
Leukemia		
CCRF-CEM	-20.94	-23.52
HL-60(TB)	-60.35	-64.56
K-562	-47.09	-48.45
MOLT-4	-37.07	-41.30
RPMI-8226	-44.06	-50.10
SR-11	-11.33	-20.07
Non-Small Cell Lung Cancer		
A549/ATCC	-74.61	-80.59
HOP-62	94.54	64.04
HOP-92	84.75	75.81
NCI-H226	113.31	107.33
NCI-H23	87.23	nt ^b
NCI-H322M	-65.33	-72.21
NCI-H460	-72.92	-65.70
NCI-H522	94.29	74.42
Colon Cancer		
COLO 205	-71.76	-79.56
HCC-2998	106.36	92.94
HCT-116	-83.60	-85.26
HCT-15	-67.17	-63.47
HT29	-59.81	-69.15
KM12	-35.24	-39.21
SW-620	-60.62	-45.07
CNS Cancer		
SF-268	-47.42	-52.29
SF-295	-88.95	-96.84
SF-539	-99.88	-100.00
SNB-19	-49.73	-74.71
SNB-75	-92.32	-83.53
U251	-89.35	-90.22
Melanoma		
LOX IMVI	-65.26	-82.93
MALME-3M	94.75	-81.28
M14	96.32	96.18
MDA-MB-435	64.65	-96.09
SK-MEL-2	109.29	110.80
SK-MEL-28	109.41	-85.25
SK-MEL-5	93.98	nt ^b

UACC-257	95.26	97.68
UACC-62	87.80	-87.86
Ovarian Cancer		
IGROV1	-82.33	-81.57
OVCAR-3	-69.49	57.72
OVCAR-4	81.54	-88.02
OVCAR-5	109.78	125.27
OVCAR-8	-41.17	-57.22
NCI/ADR-RES	98.99	29.40
SK-OV-3	112.2	115.99
Renal Cancer		
786-0	94.75	-92.66
A498	107.38	93.00
ACHN	72.00	-100.00
CAKI-1	64.86	-56.61
RXF 393	-76.33	-76.65
SN12C	95.91	65.40
TK-10	-49.30	-72.60
UO-31	46.03	-76.10
Prostate Cancer		
PC-3	22.97	54.49
DU-145	-53.84	-54.06
Breast Cancer		
MCF7	-63.30	-77.35
MDA-MB-231/ATCC	-71.23	-86.77
BT-549	118.22	105.35
T-47D	-40.89	-56.23
MDA-MB-468	-51.31	-55.85
HS 578T	nt ^b	-49.14

Table 5: Antiproliferative activity in one-dose (10 μ M) assays of compounds **5** and **6**. ^a Growth percent: cell growth relative to the no-drug control. Growth inhibition (values between 0 and 100) and lethality (values less than 0). ^b nt: not tested.

5 Conclusions and Future Works

BPH is a common disease that affects elderly. It is well-known that among α_1 -ARs, the α_{1A} - and the α_{1B} -AR subtypes seem to be involved in the symptoms of BPH. Nowadays, there are no selective antagonists for these α_1 -AR subtypes. In the present thesis, we studied the effect of stereochemistry on α_1 -ARs inhibition by quinazoline-bearing compounds related to prazosin and doxazosin. We found that the S configuration at the 3-C position of the piperidine ring increases the affinity of the compounds at all three α_1 -AR subtypes. We also demonstrated that the stereochemistry at the benzodioxole ring of doxazosin did not markedly influence the affinity and the selectivity for α_1 -ARs. In conclusion, the present investigation has shown that the pharmacophore represented by compound **1** can be considered as a useful starting point for the synthesis of enantioselective drugs for α_1 -AR subtypes.

The antiproliferative activity of **1-12** was also evaluated on sixty different cancer cell lines by NCI at the preliminary concentration of 10 μ M. Among all the compounds, **5** and **6** were the most interesting. Moreover, their activity is more marked for particular cell lines. They were potent agents against CNS and colon cancers. It turned out that the stereochemistry is an important feature for their antiproliferative activity on some cell lines. Thus, derivative **6**, compared to **5**, was more potent against melanoma, renal and breast cancers. However, derivative **5** seemed to be more promising for prostate cancer.

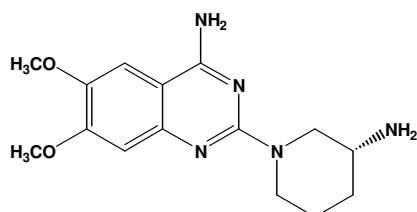
The antiproliferative studies conducted by NCI were performed at 10 μ M. However, in literature, it is reported that the apoptotic activity of doxazosin and related compounds was observed at higher concentrations.⁵⁴⁸ For this reason, further studies are in progress to evaluate the activity of **1-12** against PC-3, DU-145 and LnCap (androgen-sensitive) cells and to clarify the mechanisms underlying their apoptotic effect.

6 Experimental section

6.1 Chemistry

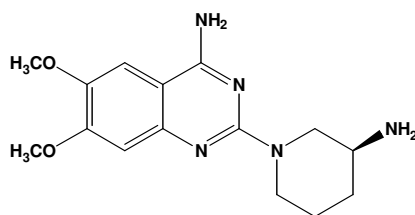
All reactions were carried out at atmospheric pressure with stirring unless otherwise indicated. All solvents and chemicals were purchased from suppliers and used without further purification. For microwave-assisted organic synthesis a CEM Discover BenchMate reactor was used. Reaction progress was monitored by TLC plates pre-coated with silica gel 60 F₂₅₄ (Sigma Aldrich) visualized by UV (254 nm) or chemical stain (KMnO₄, bromocresol green and Ce-Mo). Flash and gravity column chromatography were performed on silica gel (particle size 40-63 μM, Merck). Melting points were determined using Büchi SMP-20 apparatus. Compounds were named relying on the naming algorithm developed by CambridgeSoft Corporation and used in Chem-BioDraw Ultra 11.0. Optical activity was determined using a Perkin Elmer instrument. ¹H-NMR and ¹³C-NMR spectra were recorded at 200-400 and 50-100 MHz, respectively, on Varian instruments. Chemical shifts were measured in ppm and are quoted as δ, relative to TMS. Multiplicities are quoted as s (singlet), d (doublet), t (triplet), q (quartet), quintet and m (multiplet), br (broad) with coupling constants defined as J given in Hz. Mass spectra were recorded on a V.G. 7070 E spectrometer or on a Waters ZQ 4000 apparatus operating in electrospray (ES) mode.

(S)-2-(3-Amino-piperidin-1-yl)-6,7-dimethoxy-quinazolin-4-ylamine (1)



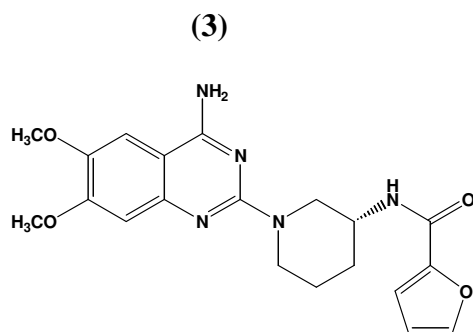
A solution of HCl in dioxane (25 ml) was added dropwise at 0 °C to a solution of **13** (1.2 g, 3 mmol) in MeOH (3 ml). The mixture was stirred at RT overnight. The solvent was then evaporated under reduce pressure and the residue was basified with 4N NaOH. The aqueous layer was saturated with NaCl and extracted with EtOAc (10 x 30 ml). The combined organic phases were dried over Na₂SO₄ and evaporated to dryness affording **1** as a white solid (910 mg, 3 mmol, 100%). **1** was then converted into its dihydrochloride salt; mp (salt)= 240 °C; [α]_D²⁰ = +49.03; δ_H (free base, 400 MHz, CD₃OD) 1.29-1.38 (1H, m, CHH), 1.46-1.57 (1H, m, CHH), 1.69-1.76 (1H, m, CHH), 1.94-1.98 (1H, m, CHH), 2.72-2.81 (2H, m, CHH-N, CH-NH₂), 2.97 (1H, ddd, J 12.9, 11.0, 3.1, CHH-N), 3.84 (3H, s, OCH₃), 3.88 (3H, s, OCH₃), 4.39 (1H, dd, J 9.4, 3.9, CHH-N), 4.49-4.56 (1H, m, CHH-N), 6.83 (1H, s, Ar), 7.27 (1H, s, Ar); δ_C (free base, 100 MHz, CD₃OD) 23.53, 32.98, 44.04, 47.31, 51.49, 54.78, 55.24, 102.84, 102.93, 104.20, 145.56, 148.84, 154.86, 159.03, 161.73.

(R)-2-(3-Amino-piperidin-1-yl)-6,7-dimethoxy-quinazolin-4-ylamine (2)



A solution of HCl in dioxane (25 ml) was added dropwise at 0°C to a solution of **14** (1.3 g, 3.30 mmol) in MeOH (3 ml). The mixture was stirred at RT overnight. The solvent was then evaporated under reduce pressure and the residue was basified with 4N NaOH. The aqueous layer was saturated with NaCl and extracted with EtOAc (10 x 30 ml). The combined organic phases were dried over Na₂SO₄ and evaporated to dryness affording **2** as a white solid (1 g, 3.3 mmol, 100%). **2** was then converted into its dihydrochloride salt; mp (salt)= 240°C; ES [M+H⁺]: 304; [α]_D²⁰ = -49.99; δ_H (free base, 400 MHz, CD₃OD) 1.23-1.33 (1H, m, CHH), 1.43-1.54 (1H, m, CHH), 1.69 (1H, dt, J 13.3, 3.9, CHH), 1.90-1.94 (1H, m, CHH), 2.67-2.75 (2H, m, CHH-N, CH-NH₂), 2.92 (1H, ddd, J 12.9, 11.3, 3.1, CHH-N), 3.81 (3H, s, OCH₃), 3.86 (3H, s, OCH₃), 4.38-4.32 (1H, m, CHH-N), 4.54 (1H, dd, J 17.6, 9.0, CHH-N), 6.82 (1H, s, Ar), 7.24 (1H, s, Ar); δ_C (free base, 100 MHz, CD₃OD) 23.65, 33.26, 44.04, 47.37, 51.74, 54.80, 55.24, 102.86, 102.90, 104.29, 145.50, 148.96, 154.81, 159.07, 161.70; Anal. Calcd for C₁₅H₂₉Cl₂N₅O₅: C 41.87, H 6.79, N 16.27, found C 42.12, H 6.65, N 15.94.

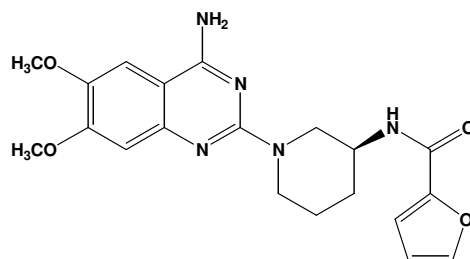
(S)-Furan-2-carboxylic acid [1-(4-amino-6,7-dimethoxy-quinazolin-2-yl)-piperidin-3-yl]-amide (3)



A solution of 2-furoyl chloride (77 mg, 0.59 mmol) in DCM (2 ml) was added dropwise at 0 °C to a solution of **1** (178 mg, 0.59 mmol) and NEt₃ (69 mg, 0.59 mmol) in DCM (4 ml). The mixture was stirred at RT for 2 h. The solvent was evaporated under reduced pressure and the crude was purified by flash chromatography (CHCl₃-MeOH, 9:1) affording **3** as a white solid (200 mg, 0.50 mmol, 85%). **3** was then converted into its hydrochloride salt; mp (salt)= 226°C; [α]_D²⁰ = +96.54; δ_H (free base, 400 MHz, CDCl₃) 1.60-1.66 (1H, m, piperidine ring), 1.72-1.82 (1H, m, piperidine ring), 1.85-1.95 (2H, m, piperidine ring), 3.69-3.75 (1H, m, piperidine ring), 3.90-3.96 (3H, m, piperidine ring), 3.90 (3H, s, OCH₃), 3.93 (3H, s, OCH₃), 4.16-4.23 (1H, m, piperidine ring), 5.82 (2H, br s, NH₂), 6.41 (1H, dd, J 3.6, 1.7, Ar), 6.94 (1H, s, Ar), 7.02 (1H, d, J 3.6, Ar), 7.07 (1H, s, Ar), 7.14

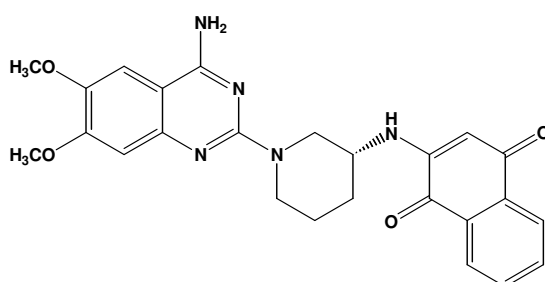
(1H, d, J 7.1, NH-C=O), 7.28-7.29 (1H, m, Ar); δ_C (100 MHz, CD₃OD) 23.49, 29.49, 45.03, 45.76, 48.59, 55.79, 55.85, 98.24, 101.13, 103.70, 111.70, 114.38, 135.55, 145.31, 147.12, 147.19, 150.86, 155.57, 158.95, 161.36.

(R)-Furan-2-carboxylic acid [1-(4-amino-6,7-dimethoxy-quinazolin-2-yl)-piperidin-3-yl]-amide (4)



A solution of 2-furoyl chloride (70 mg, 0.54 mmol) in DCM (2 ml) was added dropwise at 0 °C to a solution of **2** (163 mg, 0.54 mmol) and NEt₃ (55 mg, 0.54 mmol) in DCM (4 ml). The mixture was stirred at RT for 2 h. The solvent was evaporated under reduced pressure and the crude was purified by flash chromatography (CHCl₃-MeOH, 9:1) affording **4** as a white solid (200 mg, 0.50 mmol, 85%). **4** was then converted into its hydrochloride salt; mp (salt)= 226°C; ES [M+H⁺]: 398; $[\alpha]_D^{20} = -96.87$; δ_H (free base, 400 MHz, CDCl₃) 1.58-1.66 (1H, m, piperidine ring), 1.73-1.83 (1H, m, piperidine ring), 1.86-1.95 (2H, m, piperidine ring), 3.68-3.75 (1H, m, piperidine ring), 3.91-3.99 (3H, m, piperidine ring), 3.91 (3H, s, OCH₃), 3.94 (3H, s, OCH₃), 4.17-4.24 (1H, m, piperidine ring), 5.76 (2H, br s, NH₂), 6.42 (1H, dd, J 3.5, 2.0, Ar), 6.94 (1H, s, Ar), 7.02 (1H, d, J 3.5, Ar), 7.06 (1H, s, Ar), 7.14 (1H, d, J 7.0, NH-C=O), 7.29-7.30 (1H, m, Ar); δ_C (free base, 100 MHz, CD₃OD) 23.39, 29.41, 44.95, 45.72, 48.58, 55.62, 55.68, 98.22, 101.27, 103.75, 111.61, 114.26, 135.69, 145.13, 147.28, 151.06, 155.78, 158.97, 161.57.

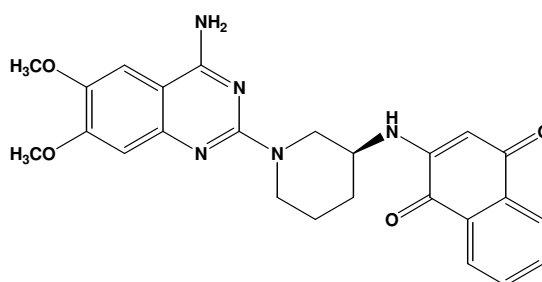
(S)-2-[1-(4-Amino-6,7-dimethoxy-quinazolin-2-yl)-piperidin-3-ylamino]-[1,4]naphthoquinone (5)



A solution of 1,4-naphthoquinone (88 mg, 0.56 mmol) in EtOH (3 ml) was added dropwise to a solution of **1** (171 mg, 0.56 mmol) in EtOH (1 ml). The mixture was stirred at RT for 8 h. The

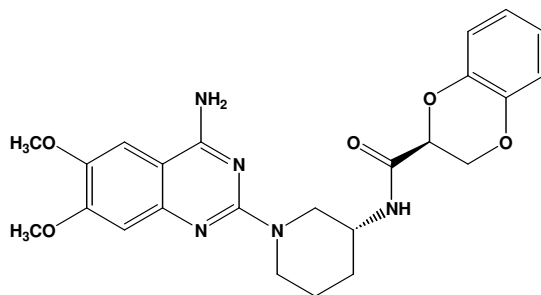
solvent was evaporated under reduced pressure and the crude was purified by flash chromatography (CHCl₃-MeOH, 9.5:0.5) affording **5** as a red solid (220 mg, 0.48 mmol, 86%). **5** was then converted into its hydrochloride salt; mp (salt) > 250° C; ES [M+H⁺]: 460; [α]_D²⁰ = +93.51; δ_H (free base, 400 MHz, CDCl₃) 1.59-1.70 (1H, m, CHH), 1.74-1.85 (2H, m, CH₂), 2.02-2.06 (1H, m, CHH), 3.15 (1H, dd, J 12.9, 8.2, CHH-N), 3.37-3.47 (2H, m, CHH-N, CH), 3.90 (3H, s, OCH₃), 4.00 (3H, s, OCH₃), 4.32-4.35 (1H, m, CHH-N), 4.61 (1H, d, J 12.9, CHH-N), 5.69 (2H, br s, NH₂), 6.14 (1H, d, J 7.0, NH-Ar), 6.59 (1H, s, Ar), 6.88 (1H, s, Ar), 7.03 (1H, s, Ar), 7.58 (1H, td, J 7.6, 1.2, Ar), 7.69 (1H, td, J 7.6, 1.2, Ar), 8.00 (1H, dd, J 7.6, 0.8, Ar), 8.07 (1H, dd, J 7.6, 0.8, Ar); δ_C (free base, 100 MHz, CDCl₃) 23.48, 29.99, 45.45, 48.30, 48.90, 56.09, 56.16, 101.27, 102.49, 102.91, 105.93, 125.91, 126.21, 130.68, 131.89, 133.54, 134.57, 145.88, 147.23, 155.07, 160.93, 181.91, 182.45; Anal. Calcd for C₂₅H₂₈ClN₅O₅: C 58.42, H 5.49, N 13.63, found C 58.46, H 5.29, N 13.21.

(R)-2-[1-(4-Amino-6,7-dimethoxy-quinazolin-2-yl)-piperidin-3-ylamino]-[1,4]naphthoquinone
(6)



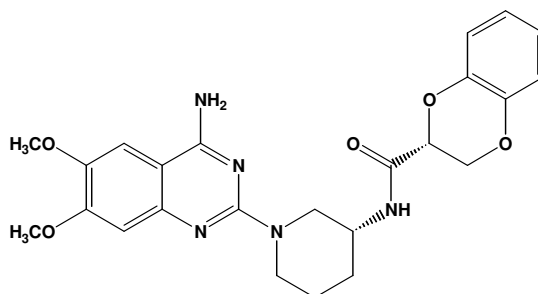
A solution of naphthoquinone (85 mg, 0.54 mmol) in EtOH (3 ml) was added dropwise to a solution of **2** (163 mg, 0.54 mmol) in EtOH (1 ml). The mixture was stirred at RT for 8 h. The solvent was evaporated under reduced pressure and the crude was purified by flash chromatography (CHCl₃-MeOH, 9.5:0.5) affording **6** as a red solid (210 mg, 0.46 mmol, 85%). **6** was then converted into its hydrochloride salt; mp (salt) > 250°C; [α]_D²⁰ = -94.46; δ_H (free base 400 MHz, CDCl₃) 1.59-1.69 (1H, m, CHH), 1.75-1.84 (2H, m, CH₂), 2.02-2.06 (1H, m, CHH), 3.13 (1H, dd, J 12.9, 8.6, CHH-N), 3.35-3.48 (2H, m, CH, CHH-N), 3.89 (3H, s, OCH₃), 4.00 (3H, s, OCH₃), 4.32-4.36 (1H, m, CHH-N), 4.61 (1H, d, J 12.9, CHH-N), 5.73 (2H, s, NH₂), 6.14 (1H, d, J 7.0, NH-Ar), 6.58 (1H, s, Ar), 6.88 (1H, s, Ar), 7.04 (1H, s, Ar), 7.58 (1H, td, J 7.7, 1.2, Ar), 7.69 (1H, td 7.7, 1.2, Ar), 8.00 (1H, dd, J 7.7, 1.0, Ar), 8.07 (1H, dd, J 7.7, 1.0, Ar); δ_C (free base, 100 MHz, CDCl₃) 23.49, 30.00, 45.50, 48.33, 48.91, 56.10, 56.17, 101.34, 102.49, 102.92, 105.87, 125.93, 126.23, 130.69, 131.90, 133.55, 134.59, 145.93, 147.24, 155.10, 160.97, 181.89, 183.48.

(R, S)-2,3-Dihydro-benzo[1,4]dioxine-2-carboxylic acid [1-(4-amino-6,7-dimethoxy-quinazolin-2-yl)-piperidin-3-yl]-amide (7)



A solution of **16** (41 mg, 0.21 mmol) in DCM (2 ml) was added dropwise at 0 °C to a solution of **1** (63 mg, 0.21 mmol) and NEt₃ (21 mg, 0.21 mmol) in DCM (2 ml). The mixture was stirred at RT for 2 h. The solvent was evaporated under reduced pressure and the crude was purified by flash chromatography (CHCl₃-MeOH, 9.5:0.5) affording **7** as a white solid (98 mg, 0.21 mmol, 100%). **7** was then converted into its hydrochloride salt; mp (salt)= 223 °C; [α]_D²⁰ = +89.71; δ_H (free base, 400 MHz, CDCl₃) 1.59-1.65 (1H, m, piperidine ring), 1.71-1.81 (1H, m, piperidine ring), 1.83-1.91 (2H, m, piperidine ring), 3.63-3.70 (1H, m, piperidine ring), 3.81 (3H, s, OCH₃), 3.89 (3H, s, OCH₃), 3.91-3.99 (3H, m, piperidine ring), 4.04-4.09 (1H, m, piperidine ring), 4.09 (1H, dd, J 11.3, 7.8, CHH-O), 4.52 (1H, dd, J 11.3, 2.7, CHH-O), 4.58 (1H, dd, J 7.8, 2.7, CH-C=O), 5.66 (2H, br s, NH₂), 6.52 (1H, d, J 8.2, Ar), 6.67 (1H, td, J 8.2, 1.6, Ar), 6.76 (1H, td, J 8.2, 1.6, Ar), 6.81 (1H, dd, J 8.2, 1.6, Ar), 6.84 (1H, s, Ar), 6.97 (1H, s, Ar), 7.17 (1H, d, J 7.0, NH-C=O); δ_C (free base, 100 MHz, CDCl₃) 22.26, 29.71, 44.66, 46.14, 48.30, 55.88, 56.11, 65.58, 73.09, 101.69, 102.87, 105.61, 117.10, 117.28, 121.63, 122.21, 141.41, 142.96, 145.81, 154.98, 160.87, 166.76.

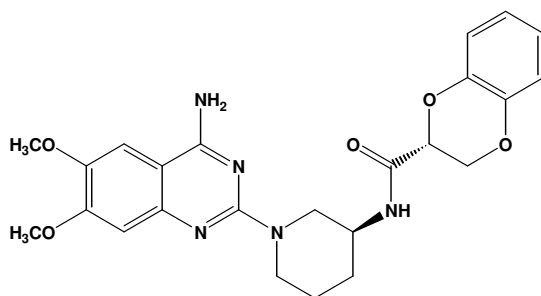
(S, S)-2,3-Dihydro-benzo[1,4]dioxine-2-carboxylic acid [1-(4-amino-6,7-dimethoxy-quinazolin-2-yl)-piperidin-3-yl]-amide (8)



A solution of **15** (40 mg, 0.20 mmol) in DCM (2 ml) was added dropwise at 0 °C to a solution of **1** (61 mg, 0.20 mmol) and NEt₃ (20 mg, 0.20 mmol) in DCM (2 ml). The mixture was stirred at RT for 2 h. The solvent was evaporated under reduced pressure and the crude was purified by flash chromatography (CHCl₃-MeOH, 9.5:0.5) affording **8** as a white solid (51 mg, 0.11 mmol, 55%). **8**

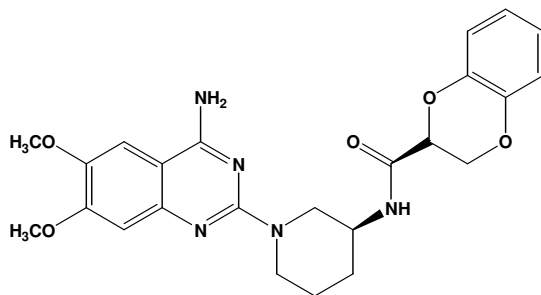
was then converted into its hydrochloride salt; mp (salt)= 221 °C; $[\alpha]_D^{20} = +20.46$; δ_H (free base, 400 MHz, CDCl₃) 1.46-1.53 (2H, m, piperidine ring), 1.77-1.81 (2H, m, piperidine ring), 3.55-3.61 (1H, m, piperidine ring), 3.78 (1H, dd, J 12.9, 2.7, piperidine ring), 3.93 (3H, s, OCH₃), 3.97 (3H, s, OCH₃), 3.97-4.07 (3H, m, piperidine ring), 4.23 (1H, dd, J 11.3, 6.7, CHH-O), 4.42 (1H, dd, J 11.3, 2.7, CHH-O), 4.64 (1H, dd J 6.7, 2.7, CH-C=O), 5.57 (2H, br s, NH₂), 6.44 (1H, d, J 8.2, 1.2, Ar), 6.63 (1H, ddd, J 8.2, 7.0, 2.0), 6.79 (1H, td, J 7.0, 1.2, Ar), 6.84 (1H, dd, J 8.2, 2.0), 6.94 (1H, s, Ar), 6.96 (1H, s, Ar), 7.0 (1H, d, J 7.0, NH-C=O); δ_C (free base, 100 MHz, CDCl₃) 21.90, 29.72, 44.63, 46.13, 48.12, 56.07, 56.18, 65.22, 73.19, 101.60, 102.88, 105.62, 116.90, 117.38, 121.67, 122.18, 141.39, 143.17, 145.87, 155.13, 160.78, 166.89.

(S, R)-2,3-Dihydro-benzo[1,4]dioxine-2-carboxylic acid [1-(4-amino-6,7-dimethoxy-quinazolin-2-yl)-piperidin-3-yl]-amide (9)



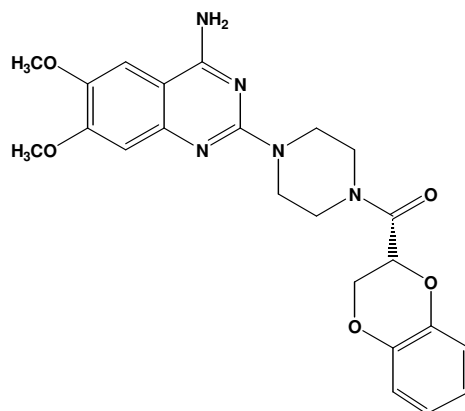
A solution of **15** (40 mg, 0.20 mmol) in DCM (2 ml) was added dropwise at 0 °C to a solution of **2** (61 mg, 0.20 mmol) and NEt₃ (20 mg, 0.20 mmol) in DCM (2 ml). The mixture was stirred at RT for 2 h. The solvent was evaporated under reduced pressure and the crude was purified by flash chromatography (CHCl₃-MeOH, 9.5:0.5) affording **9** as a white solid (87 mg, 0.19 mmol, 95%). **9** was then converted into its hydrochloride salt; mp (salt)= 223 °C; ES [M+H⁺]: 466; $[\alpha]_D^{20} = -89.68$; δ_H (free base, 400 MHz, CDCl₃) 1.60-1.65 (1H, m, piperidine ring), 1.73-1.81 (1H, m, piperidine ring), 1.87-1.92 (2H, m, piperidine ring), 3.62-3.68 (1H, m, piperidine ring), 3.77 (1H, d, J 12.9, piperidine ring), 3.83 (3H, s, OCH₃), 3.91 (3H, s, OCH₃), 3.95 (1H, dd, J 12.9, 4.7, piperidine ring), 4.01-4.06 (1H, m, piperidine ring), 4.07-4.10 (1H, m, piperidine ring), 4.10 (1H, dd, J 11.3, 7.8, CHH-O), 4.54 (1H, dd, J 2.7, 11.3, CHH-O), 4.59 (1H, dd, J 7.8, 2.7, CH-C=O), 5.53 (2H, br s, NH₂), 6.51 (1H, d, J 7.8, Ar), 6.68 (1H, td, J 7.8, 1.6, Ar), 6.77 (1H, t, J 7.8, Ar), 6.83 (1H, dd, J 7.8, 1.6, Ar), 6.85 (1H, br s, Ar), 6.93 (1H, s, Ar), 7.18 (1H, d, J 7.0, NH-C=O); δ_C (free base, 100 MHz, CDCl₃) 22.20, 29.68, 44.72, 46.12, 48.28, 55.91, 56.13, 65.61, 73.08, 101.56, 102.81, 105.62, 117.11, 117.28, 121.62, 122.20, 141.42, 142.98, 145.85, 155.04, 160.78, 166.71.

(R,R)-2,3-Dihydro-benzo[1,4]dioxine-2-carboxylic acid [1-(4-amino-6,7-dimethoxy-quinazolin-2-yl)-piperidin-3-yl]-amide (10)



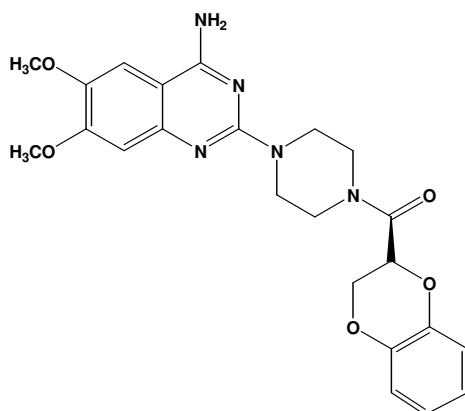
A solution of **16** (46 mg, 0.23 mmol) in DCM (2 ml) was added dropwise at 0 °C to a solution of **2** (70 mg, 0.23 mmol) and NEt₃ (23 mg, 0.23 mmol) in DCM (2 ml). The mixture was stirred at RT for 2 h. The solvent was evaporated under reduced pressure and the crude was purified by flash chromatography (CHCl₃-MeOH, 9.5:0.5) affording **10** as a white solid (89 mg, 0.19 mmol, 83%). **10** was then converted into its hydrochloride salt; mp (salt)= 221 °C; [α]_D²⁰ = -20.66; δ _H (free base, 400 MHz, CDCl₃) 1.43-1.49 (2H, m, piperidine ring), 1.75-1.79 (2H, m, piperidine ring), 3.54-3.60 (1H, m, piperidine ring), 3.80 (1H, dd, J 12.9, 2.7, piperidine ring), 3.91 (3H, s, OCH₃), 3.91-3.95 (1H, m, piperidine ring) 3.95 (3H, s, OCH₃), 4.01 (1H, dd, J 13.3, 5.9, piperidine ring), 4.05-4.10 (1H, m, piperidine ring), 4.22 (1H, dd, J 11.3, 6.4, CHH-O), 4.42 (1H, dd, J 11.3, 2.7, CHH-O), 4.63 (1H, dd, J 6.4, 2.7, CH-C=O), 5.60 (2H, br s, NH₂), 6.44 (1H, dd, J 8.2, 1.2, Ar), 6.63 (1H, td J 8.2, 2.0, Ar), 6.79 (1H, td, J 7.0, 1.2, Ar), 6.83 (1H, dd, J 8.2, 2.0, Ar), 6.96 (2H, s, Ar), 7.03 (1H, d, J 7.0, NH-C=O); δ _C (free base, 100 MHz, CDCl₃) 21.90, 29.72, 44.62, 46.14, 48.12, 56.07, 56.17, 65.21, 73.19, 101.65, 102.90, 105.59, 116.90, 117.38, 121.68, 122.18, 141.38, 143.16, 145.86, 155.13, 160.

(S)-[4-(4-Amino-6,7-dimethoxy-quinazolin-2-yl)-piperazin-1-yl]-(2,3-dihydro-benzo[1,4]dioxin-2-yl)-methanone (11)



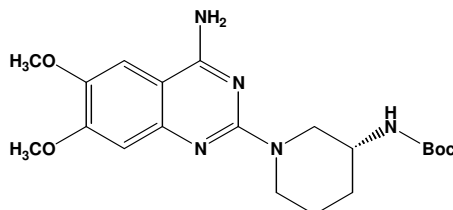
A solution of **15** (58 mg, 0.29 mmol) in DCM (2 ml) was added dropwise at 0 °C to a solution of **17** (84 mg, 0.29 mmol) and NEt₃ (29 mg, 0.29 mmol) in DCM (2 ml). The mixture was stirred at RT for 2 h. The solvent was evaporated under reduced pressure and the crude was purified by flash chromatography (CHCl₃-MeOH, 9.5:0.5) affording **11** as a white solid (131 mg, 0.29 mmol, 100%). **11** was then converted into its hydrochloride salt; mp (salt)= 228°C; ES [M+H⁺]: 452; [α]_D²⁰ = +90.91; δ_H (free base, 400 MHz, CDCl₃) 3.55-3.65 (2H, m, piperazine ring), 3.72-3.77 (1H, m, piperazine ring), 3.86-3.89 (3H, m, piperazine ring), 3.92 (3H, s, OCH₃), 3.97 (3H, s, OCH₃), 4.02-4.09 (2H, m, piperazine ring), 4.36 (1H, dd, J 11.7, 8, CHH-O), 4.52 (1H, dd, J 11.7, 1.8, CHH-O), 4.88 (1H, dd, J 8, 1.8, CH-C=O), 5.33 (2H, br s, NH₂), 6.86-6.95 (6H, m, Ar); δ_C (free base, 100 MHz, CDCl₃) 42.23, 43.79, 44.40, 45.84, 56.08, 56.14, 65.19, 70.67, 101.31, 102.92, 105.65, 117.29, 117.37, 121.53, 122.24, 142.50, 143.27, 146.07, 155.22, 160.63, 165.08.

(R)-[4-(4-Amino-6,7-dimethoxy-quinazolin-2-yl)-piperazin-1-yl]-(2,3-dihydro-benzo[1,4]dioxin-2-yl)-methanone (12)



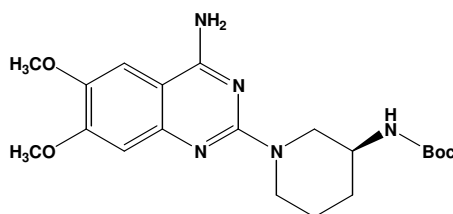
A solution of **16** (66 mg, 0.33 mmol) in DCM (2 ml) was added dropwise at 0 °C to a solution of **17** (95 mg, 0.33 mmol) and NEt₃ (33 mg, 0.33 mmol) in DCM (2 ml). The mixture was stirred at RT for 2 h. The solvent was evaporated under reduced pressure and the crude was purified by flash chromatography (CHCl₃-MeOH, 9.5:0.5) affording **12** as a white solid (149 mg, 0.33 mmol, 100%). **12** was then converted into its hydrochloride salt; mp (salt)= 228°C; [α]_D²⁰ = -90.30; δ_H (free base, 400 MHz, CDCl₃) 3.56-3.65 (2H, m, piperazine ring), 3.71-3.79 (1H, m, piperazine ring), 3.86-3.91 (3H, m, piperazine ring), 3.93 (3H, s, OCH₃), 3.97 (3H, s, OCH₃), 4.03-4.10 (2H, m, piperazine ring), 4.36 (1H, dd, J 11.7, 8, CHH-O), 4.52 (1H, dd, J 11.7, 2.3, CHH-O), 4.89 (1H, dd, J 8, 2.3, CH-C=O), 5.38 (2H, br s, NH₂), 6.84-6.94 (6H, m, Ar); δ_C (free base, 100 MHz, CDCl₃) 42.25, 43.79, 44.43, 45.84, 56.11, 56.15, 65.17, 70.67, 101.41, 102.93, 105.61, 117.29, 117.37, 121.55, 122.24, 142.48, 143.26, 146.06, 155.20, 160.67, 165.10.

(S)-[1-(4-Amino-6,7-dimethoxy-quinazolin-2-yl)-piperidin-3-yl]-carbamic acid tert-butyl ester
(13)



4-Amino-2-chloro-6,7-dimethoxyquinazoline (600 mg, 2.5 mmol) and (S)-3-(Boc-amino)piperidine (1 g, 5 mmol) were dissolved in isoamylic alcohol (20 ml). The mixture was stirred under microwave irradiation at 130 °C for 50 min. After evaporating the solvent under reduced pressure, the crude was purified by flash chromatography (petrol-EtOAc-CHCl₃-MeOH, 3:2:4:1) affording **13** as a white solid (1 g, 2.5 mmol, 100%); δ_{H} (400 MHz, CDCl₃) 1.26 (9H, s, OtBu), 1.36-1.38 (2H, m, piperidine ring), 1.52-1.58 (1H, m, piperidine ring), 1.67-1.72 (1H, m, piperidine ring), 3.23-3.32 (2H, m, piperidine ring), 3.54-3.57 (1H, br m, piperidine ring), 3.61 (3H, s, OCH₃), 3.69 (3H, s, OCH₃), 3.80-3.84 (1H, m, piperidine ring), 4.00-4.03 (1H, br m, piperidine ring), 5.09 (1H, br s, NH-C=O), 6.15 (2H, s, NH₂), 6.76 (1H, s, Ar), 7.00 (1H, s, Ar); δ_{C} (100 MHz, CDCl₃) 22.74, 28.20, 30.47, 44.15, 46.62, 49.08, 55.54, 55.70, 78.90, 102.34, 102.90, 105.03, 145.27, 148.93, 154.50, 155.33, 158.69, 160.99.

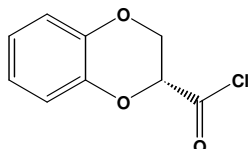
(R)-[1-(4-Amino-6,7-dimethoxy-quinazolin-2-yl)-piperidin-3-yl]-carbamic acid tert-butyl ester
(14)



4-Amino-2-chloro-6,7-dimethoxyquinazoline (600 mg, 2.5 mmol) and (R)-3-(Boc-amino)piperidine (1 g, 5 mmol) were dissolved in isoamylic alcohol (20 ml). The mixture was stirred under microwave irradiation at 130 °C for 50 min. After evaporating the solvent under reduced pressure, the crude was purified by flash chromatography (petrol-EtOAc-CHCl₃-MeOH, 3:2:4:1) affording **14** as a white solid (1 g, 2.5 mmol, 100%); δ_{H} (400 MHz, CDCl₃) 1.41 (9H, s, OtBu), 1.56-1.63 (2H, m, piperidine ring), 1.70-1.77 (1H, m, piperidine ring), 1.84-1.89 (1H, m, piperidine ring), 3.53 (1H, dd, J 12.7, 6.8, piperidine ring), 3.63-3.73 (2H, m, piperidine ring), 3.83 (1H, dd, J 7.0, 2.7, piperidine ring), 3.87 (3H, s, OCH₃), 3.92 (3H, s, OCH₃), 4.02 (1H dd, J 12.8, 2.7, piperidine

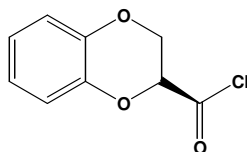
ring), 4.91 (1H, d, J 6.7, NH-C=O), 5.69 (2H, s, NH₂), 6.91 (1H, s, Ar), 6.95 (1H, s, Ar); δ_C (100 MHz, CDCl₃) 22.67, 28.41, 30.61, 44.40, 46.70, 49.21, 55.96, 56.10, 79.21, 101.83, 102.91, 105.47, 145.66, 154.93, 155.38, 158.88, 160.80

(S)-2,3-Dihydro-benzo[1,4]dioxine-2-carbonyl chloride (15)



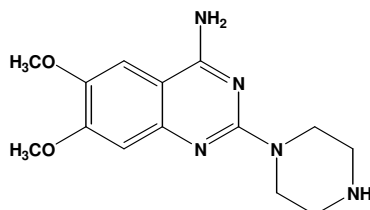
Thionyl dichloride (256 mg, 2.15 mmol) was added dropwise at 0 °C to a solution of (S)-2,3-dihydro-benzo[1,4]dioxine-2-carboxylic acid (97 mg, 0.54 mmol) in toluene (2 ml). The mixture was stirred at reflux for 4 h. The solvent was then evaporated to dryness affording **15** as a yellow oil (107 mg, 0.54 mmol, 100%); δ_H (400 MHz, CDCl₃) 4.35 (1H, dd, J 11.8, 2.7, CHH-O), 4.75 (1H, dd, J 11.8, 2.7, CHH-O), 5.10 (1H, t, J 2.7, CH-C=O), 6.91-6.98 (3H, m, Ar), 7.02-7.04 (1H, m, Ar); δ_C (100 MHz, CDCl₃) 63.77, 78.58, 117.27, 117.58, 122.47, 122.74, 141.39, 142.82, 170.26.

(R)-2,3-Dihydro-benzo[1,4]dioxine-2-carbonyl chloride (16)



Thionyl dichloride (400 mg, 3.36 mmol) was added dropwise at 0 °C to a solution of (R)-2,3-dihydro-benzo[1,4]dioxine-2-carboxylic acid (202 mg, 1.12 mmol) in toluene (4 ml). The mixture was stirred at reflux for 4 h. The solvent was then evaporated to dryness affording **16** as a yellow oil (222 mg, 1.12 mmol, 100%); δ_H (200 MHz, CDCl₃) 4.34 (1H, dd, J 12.0, 2.8, CHH-O), 4.76 (1H, dd, J 12.0, 2.8, CHH-O), 5.10 (1H, t, 2.8, CH-C=O), 6.93-7.09 (4H, m, Ar); δ_C (50 MHz, CDCl₃) 63.87, 78.70, 117.40, 117.72, 122.61, 122.89, 142.54, 142.99, 170.44.

6,7-Dimethoxy-2-piperazin-1-yl-quinazolin-4-ylamine (17)



4-Amino-2-chloro-6,7-dimethoxyquinazoline (300 mg, 1.25 mmol) and piperazine (646 mg, 7.5 mmol) were dissolved in isoamyl alcohol (10 ml). The mixture was stirred under microwave

irradiation at 130 °C for 50 min. After evaporating the solvent under reduced pressure, the crude was purified by flash chromatography (DCM-MeOH-aqueous 33% ammonia, 8:2:0.1) affording **17** as a pale yellow solid (320 g, 1.1 mmol, 88%); δ_{H} (400 MHz, CDCl_3) 2.95 (4H, t, J 4.9, piperazine ring), 3.92 (4H, t, J 4.9, piperazine ring), 3.93 (3H, s, OCH_3), 3.97 (3H, s, OCH_3), 5.12 (2H, br s, NH_2), 6.79 (1H, s, Ar), 6.92 (1H, s, Ar).

6.2 Biology

A *Radioligand Binding Assays*

Binding to cloned human $\alpha 1$ -AR subtypes was performed in membranes from CHO cells transfected by electroporation with DNA expressing the gene encoding each $\alpha 1$ -AR subtype. Cloning and stable expression of the human $\alpha 1$ -AR gene was performed as previously described.⁵⁹⁵ CHO cell membranes (30 μg proteins) were incubated in 50 mM Tris-HCl (pH 7.4) with 0.2 nM [^3H]prazosin, in a final volume of 1.02 ml for 30 min at 25 °C, in absence or presence of competing drugs (1 pM to 10 μM). Non-specific binding was determined in the presence of 10 μM phentolamine. The incubation was stopped by addition of ice-cold Tris-HCl buffer and rapid filtration through 0.2% polyethylenimine pretreated Whatman GF/B or Schleicher & Schuell GF52 filters. Binding data were analyzed using the non-linear curve-fitting program Allfit.⁵⁹⁶ Equilibrium inhibition constants (K_i) were derived from the Cheng–Prusoff equation,⁵⁹⁴ $K_i = \text{IC}_{50}/(1 + L/K_d)$, where L and K_d are the concentration and the equilibrium dissociation constant of the radioligand. $\text{p}K_i$ values are the mean \pm SE of 2-3 separate experiments performed in triplicate.

B *Antiproliferative activity*

The human tumor cell lines of the cancer screening panel are grown in RPMI 1640 medium containing 5% fetal bovine serum and 2 mM L-glutamine. For a typical screening experiment, cells are inoculated into 96 well microtiter plates in 100 μl at plating densities ranging from 5000 to 40000 cells/well depending on the doubling time of individual cell lines. After cell inoculation, the microtiter plates are incubated at 37° C, 5% CO_2 , 95% air and 100% relative humidity for 24 h prior to addition of experimental drugs. After 24 h, two plates of each cell line are fixed in situ with TCA, to represent a measurement of the cell population for each cell line at the time of drug addition (T_z). Experimental drugs are solubilized in dimethyl sulfoxide at 400-fold the desired final maximum test concentration and stored frozen prior to use. At the time of drug addition, an aliquot of frozen concentrate is thawed and diluted to twice the desired final maximum test concentration with complete medium containing 50 $\mu\text{g}/\text{ml}$ gentamicin. Additional four, 10-fold or $\frac{1}{2}$ log serial dilutions are made to provide a total of five drug concentrations plus control. Aliquots of 100 μl of

these different drug dilutions are added to the appropriate microtiter wells already containing 100 µl of medium, resulting in the required final drug concentrations.

Following drug addition, the plates are incubated for an additional 48 h at 37°C, 5% CO₂, 95% air, and 100% relative humidity. For adherent cells, the assay is terminated by the addition of cold TCA. Cells are fixed in situ by the gentle addition of 50 µl of cold 50% (w/v) TCA (final concentration, 10% TCA) and incubated for 60 min at 4°C. The supernatant is discarded, and the plates are washed five times with tap water and air dried. Sulforhodamine B (SRB) solution (100 µl) at 0.4% (w/v) in 1% acetic acid is added to each well, and plates are incubated for 10 min at RT. After staining, unbound dye is removed by washing five times with 1% acetic acid and the plates are air dried. Bound stain is subsequently solubilized with 10 mM trizma base, and the absorbance is read on an automated plate reader at a wavelength of 515 nm. For suspension cells, the methodology is the same except that the assay is terminated by fixing settled cells at the bottom of the wells by gently adding 50 µl of 80% TCA (final concentration, 16% TCA). Using the seven absorbance measurements [time zero, (Tz), control growth, (C), and test growth in the presence of drug at the five concentration levels (Ti)], the percentage growth is calculated at each of the drug concentrations levels. Percentage growth inhibition is calculated as:

$[(Ti - Tz) / (C - Tz)] \times 100$ for concentrations for which $Ti \geq Tz$

$[(Ti - Tz) / Tz] \times 100$ for concentrations for which $Ti < Tz$.

Three dose response parameters are calculated for each experimental agent. Growth inhibition of 50% (GI₅₀) is calculated from $[(Ti - Tz) / (C - Tz)] \times 100 = 50$, which is the drug concentration resulting in a 50% reduction in the net protein increase (as measured by SRB staining) in control cells during the drug incubation. The drug concentration resulting in total growth inhibition (TGI) is calculated from $Ti = Tz$. The LC₅₀ (concentration of drug resulting in a 50% reduction in the measured protein at the end of the drug treatment as compared to that at the beginning) indicating a net loss of cells following treatment is calculated from $[(Ti - Tz) / Tz] \times 100 = -50$. Values are calculated for each of these three parameters if the level of activity is reached; however, if the effect is not reached or is exceeded, the value for that parameter is expressed as greater or less than the maximum or minimum concentration tested.

Chapter 3

DEVELOPMENT OF NEW ISOCYANIDE-BASED MULTICOMPONENT REACTIONS

OUTLINES

1	Introduction.....	184
1.1	History of MCRs	184
1.2	Isocyanides	197
1.3	MCRs in Drug Discovery.....	201
1.3.1	Tubulin Inhibitors	201
1.3.2	Phosphatase Inhibitors	201
1.3.3	GPCR Ligands	203
1.3.4	Aspartyl Protease Inhibitors.....	204
1.3.5	Protein-Protein Interaction Inhibitors	206
2	Research project.....	208
2.1	Hydroxy-carbonyl compounds in multicomponent reactions	208
2.2	Aminoalcohols in multicomponent reactions.....	209
2.3	Carbonyl-carboxylic substrates in multicomponent reactions	210
3	Results and Discussion	211
3.1	Hydroxy-carbonyl products.....	211
3.2	Aminoalcohols.....	218
3.2.1	Synthesis of aminoalcohols.....	218
3.2.2	Multicomponent reactions with aminoalcohol 8.....	221
3.2.3	Multicomponent reactions with aminoalcohol 7.....	225
3.2.4	Multicomponent reactions with aminoalcohol 6.....	226
3.2.5	Multicomponent reactions with aminoalcohol 9.....	228
3.2.6	Multicomponent reactions with carbonyl-carboxylic compounds 35 and 35'	229
4	Conclusions and Future Works.....	233
5	Experimental section	234

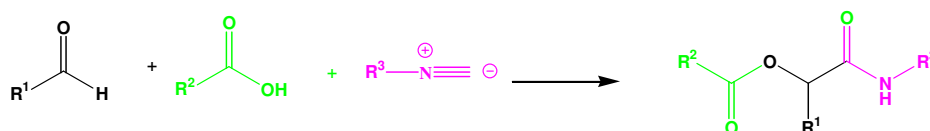
1 Introduction

Multicomponent reactions (MCRs) are defined as reaction in which three or more components condense to give a single product.⁵⁹⁷ They are highly atom efficient methods in which relatively complex molecules can be obtained in a *one-pot* reaction from simple starting materials. Thus, they exemplify many of the desired features of an “ideal synthesis”. They are a very useful tool for the generation of compound libraries for drug discovery.

1.1 History of MCRs

Despite having received much attention over the last few decades, isocyanide-based multi-component reactions (IMCRs) have a long history which dates back to the publication of the Passerini three-component reaction (P-3CR) in 1921.^{598, 599}

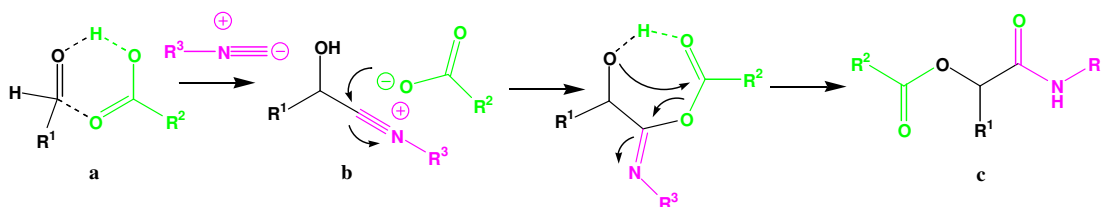
The P-3CR involves the condensation of an aldehyde, an isocyanide and a carboxylic acid to give highly functionalized α -carboxamide (**Scheme 1**).



Scheme 1

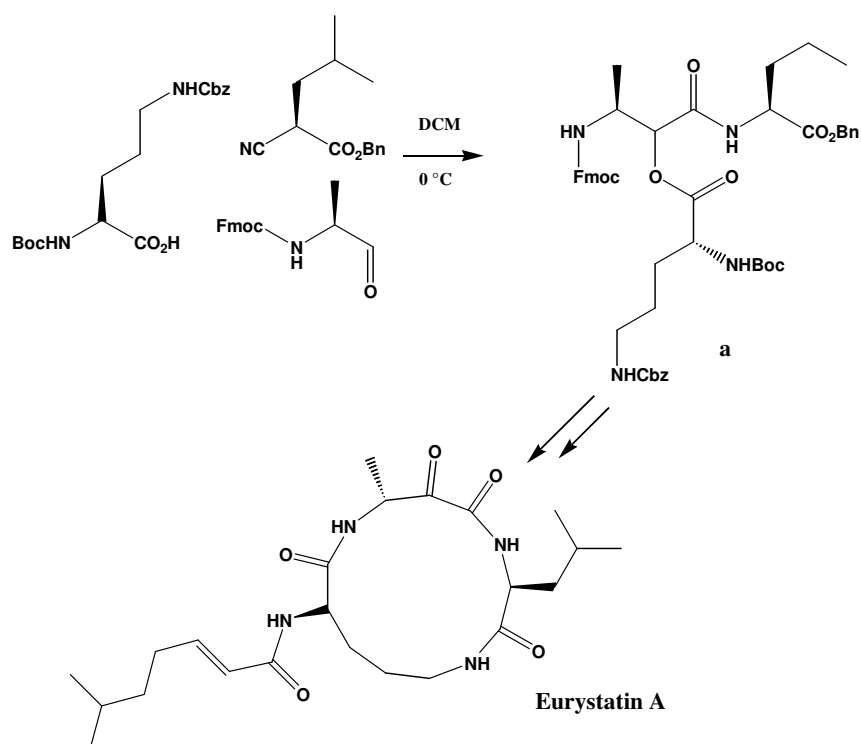
This reaction exploits the ambiphilic nature of the isocyanide moiety, which is able to act as both a nucleophile and an electrophile sequentially at the same carbon atom.

The isocyanide inserts into the acid-activated aldehyde **a** to give nitrilium ion **b**, which is in turn attacked by the resultant carboxylate. An O-O' acyl transfer then takes place leading the final product **c** (**Scheme 2**).



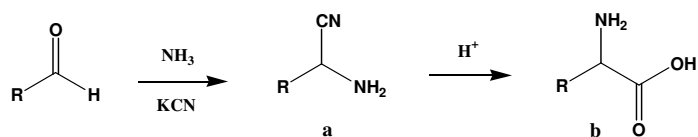
Scheme 2

Sample et al.⁶⁰⁰ recently put this reaction to excellent use in the total synthesis of eurystatin A (**Scheme 3**). A P-3CR reaction led to the intermediate **a** in good yield (75%), which was then elaborated in just six steps to give the natural product.



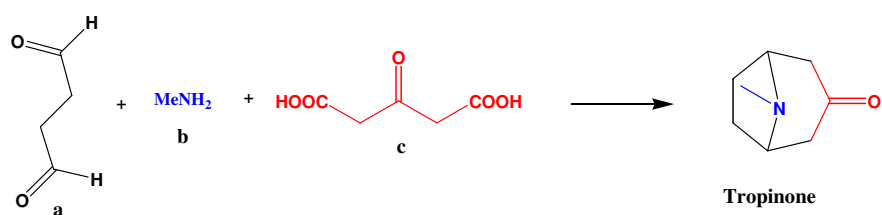
Scheme 3

The Strecker synthesis of α -aminoacids via α -amino-cyanide was first published in 1850 and it is generally considered to be the first MCR.⁶⁰¹ Strecker reaction involves the reaction between an aldehyde, ammonia and potassium cyanide to give an α -amino-cyanide **a** which is subsequently hydrolyzed to give the amino-acid **b** (**Scheme 4**).



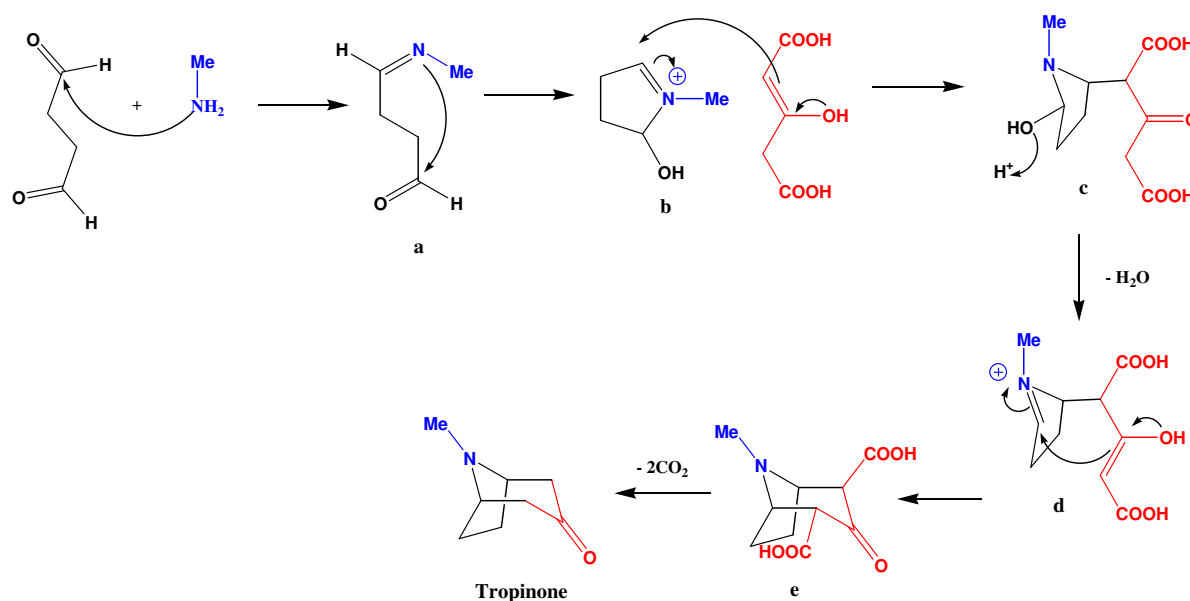
Scheme 4

Robinson's synthesis of the alkaloid Tropinone (**Scheme 5**) from succinic dialdehyde **a**, methylamine **b** and acetonedicarboxylic acid **c**, carried out in 1917, is the first important application of MCRs in natural product synthesis.⁶⁰²



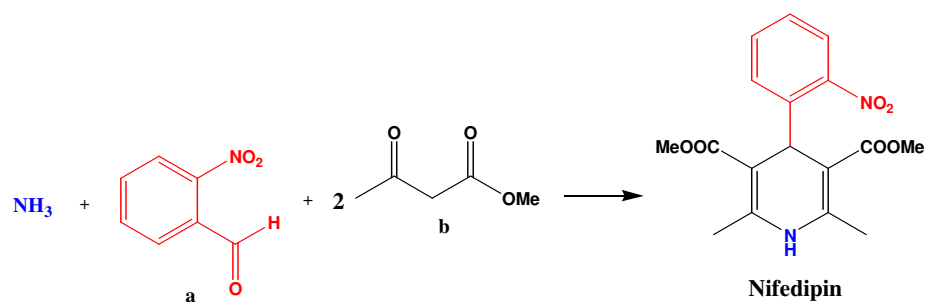
Scheme 5

The mechanism⁶⁰³ starts with the formation of an imine **a** between methylamine and succinaldehyde (**Scheme 6**). Then intramolecular addition of the imine to the second aldehyde unit and ring closure leads to the intermediate **b**. Intermolecular Mannich reaction between **b** and the enolate of acetoacetic acid gives **c**, which, following loss of water, affords **d**. Second Mannich reaction between the imine function and the enolate of acetoacetic acid of **d**, followed by ring closure, gives **e**, which is converted into Tropinone by warming.



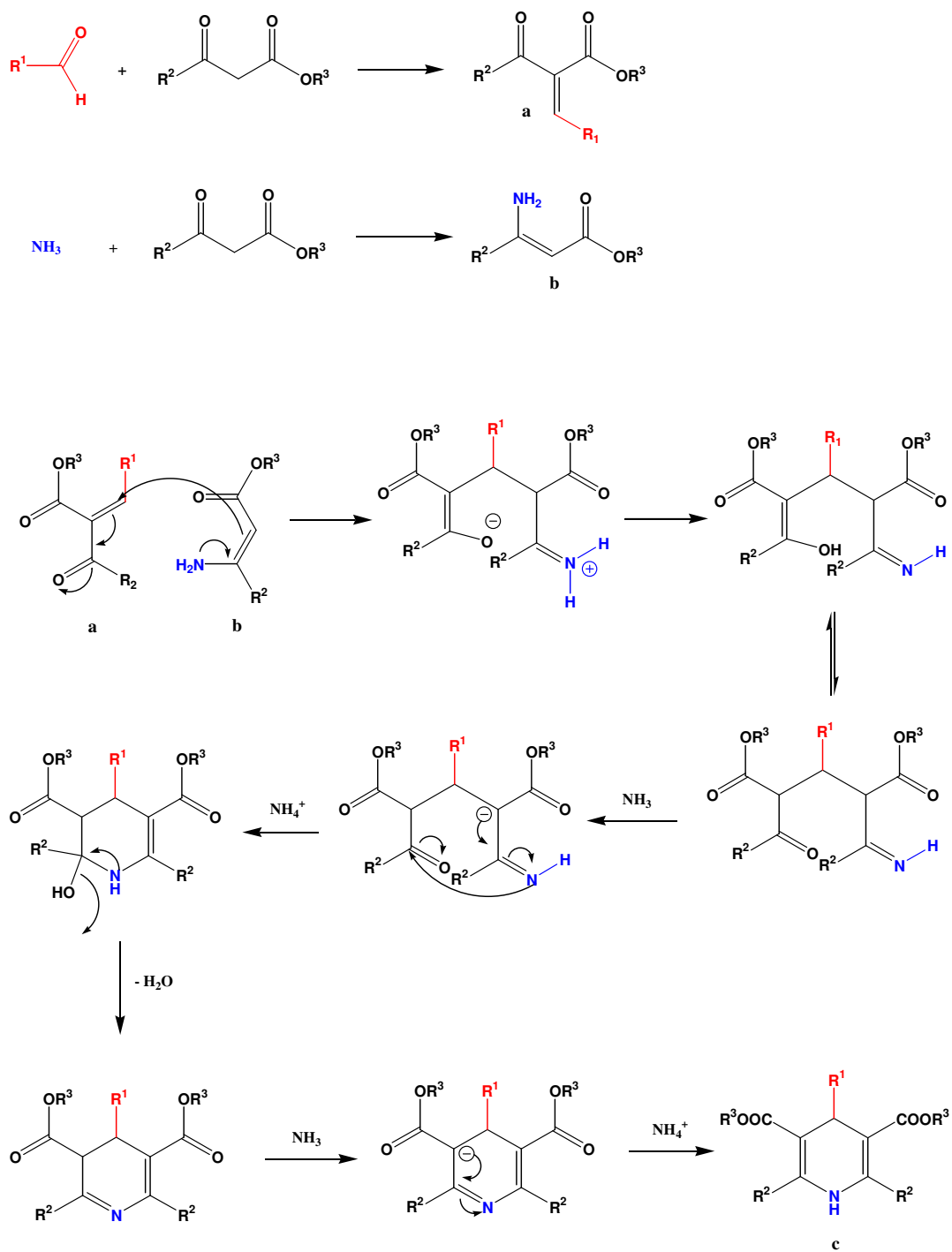
Scheme 6

Many important heterocycle syntheses are MCRs. 1,4-Dihydropyridines such as Nifedipin (an antihypertensive) were first synthesized in a four-component reaction by Hantzsch (H-4CR),⁶⁰⁴ from ammonia, aldehyde **a**, and two molecules of acetoacetic ester **b** (**Scheme 7**) in 1882.



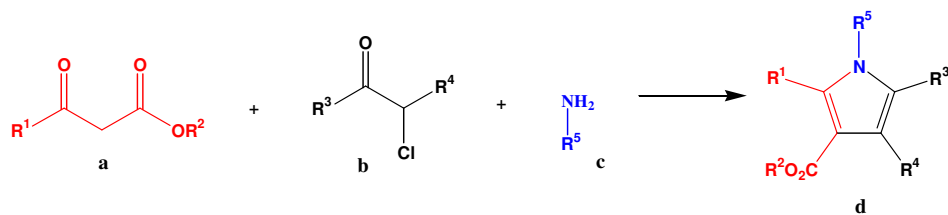
Scheme 7

The mechanism of the H-4CR is shown in **Scheme 8**. The reaction starts with a Knoevenagel condensation between the aldehyde and the first molecule of acetoacetic ester leading to **a**. A second key intermediate is the ester enamine **b**, which is produced by condensation of the second equivalent of the β -ketoester with ammonia. Further condensation between these two molecules gives the dihydropyridine derivative **c**.



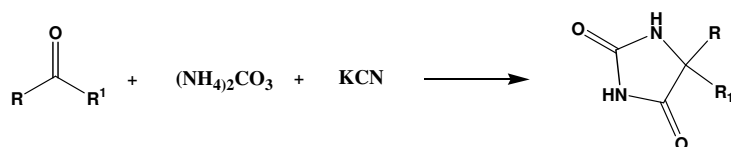
Scheme 8

Later in 1890, Hantzsch discovered the synthesis of substituted pyrroles **d** from β -ketoesters **a**, α -haloketones **b** and primary amines **c** (**Scheme 9**).



Scheme 9

A further important MCR is the Bucherer-Bergs reaction (BB-4CR)⁶⁰⁵ discovered in 1941. It can be understood as an extension of the Strecker reaction by one component (CO_2). The BB-4CR allows the synthesis of hydantoin derivatives from a ketone, potassium cyanide and ammonium carbonate (**Scheme 10**). Whereas the Strecker three-component reaction is an equilibrium reaction and often delivers the products in unsatisfactory yields, the BB-4CR is practically irreversible upon addition of CO_2 . It still is an important method for the synthesis of unnatural α -amino acids.



Scheme 10

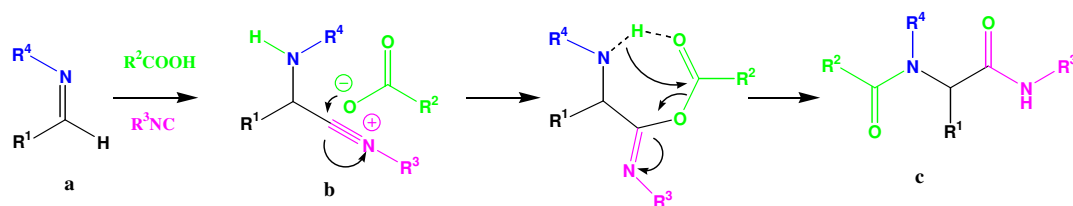
Since its discovery in the late 1950s,^{606, 607} the Ugi four-component reaction (U-4CR) has become one of the most important and widely used of all MCRs.^{608, 609}

As with the P-3CR, the U-4CR also employs the unique reactivity of isocyanides in their condensation with an aldehyde, a primary amine and a carboxylic acid (**Scheme 11**).



Scheme 11

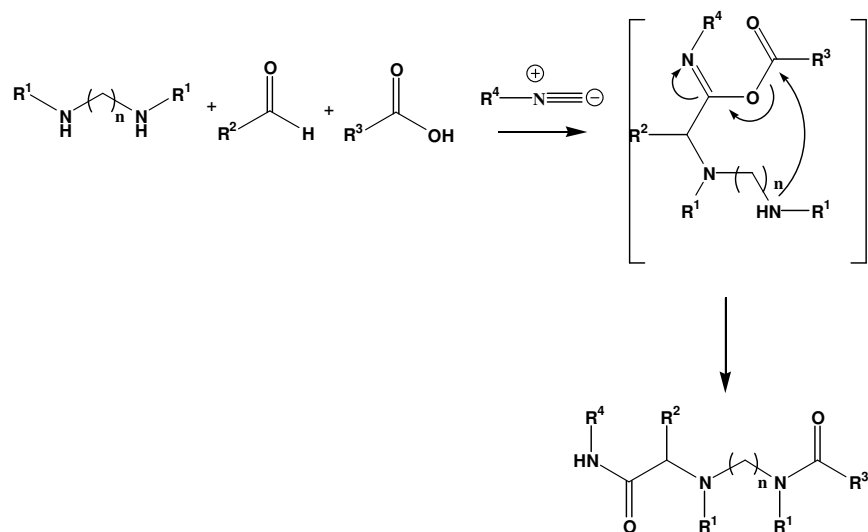
Imine **a**, formed upon condensation of the primary amine and aldehyde, is protonated by the carboxylic acid and attacked by the isocyanide to give nitrilium ion **b**. Attack by the carboxylate followed by Mumm rearrangement⁶¹⁰ (O-N acyl transfer) then gives the α -amidoamide product **c** (**Scheme 12**).



Scheme 12

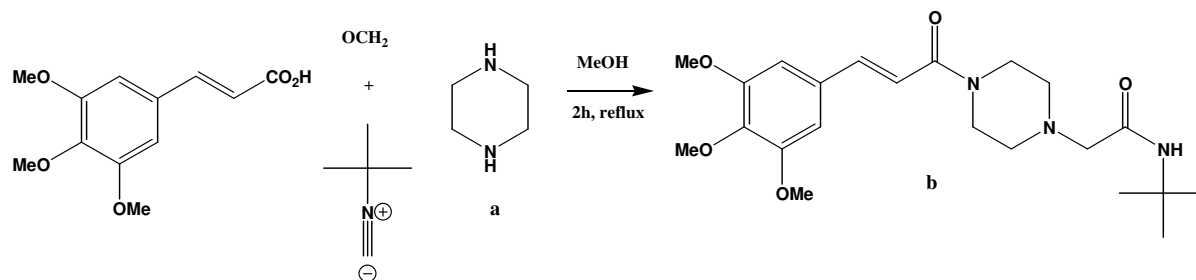
Since its discovery, the reaction has been studied extensively and has seen a great number of extensions and developments. Several modifications of U-4CR have been described. These modifications involve the variation of one of the components or the introduction of a linkage between two of them, which leads to interesting potentially drug-like derivatives of the original α -acylamino amide product.^{611, 612, 613}

Giovenzana recently reported a modified U-4CR,⁶¹⁴ which involves the use of bis-secondary diamines as mimics for the primary amine. The bis-diamine splits the N-alkylation and N-acylation steps between two different nitrogen atoms, giving even more highly functionalized products in excellent yield (**Scheme 13**).



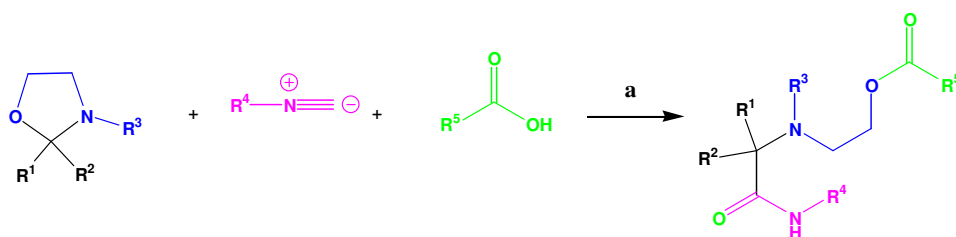
Scheme 13

The synthetic utility of this reaction was elegantly demonstrated in the one step synthesis of vasodilator **b** from piperazine **a** (**Scheme 14**). This route is both higher yielding than the previous synthesis,⁶¹⁵ as well as being far more atom efficient, clearly proving this to be a powerful synthetic transformation.



Scheme 14

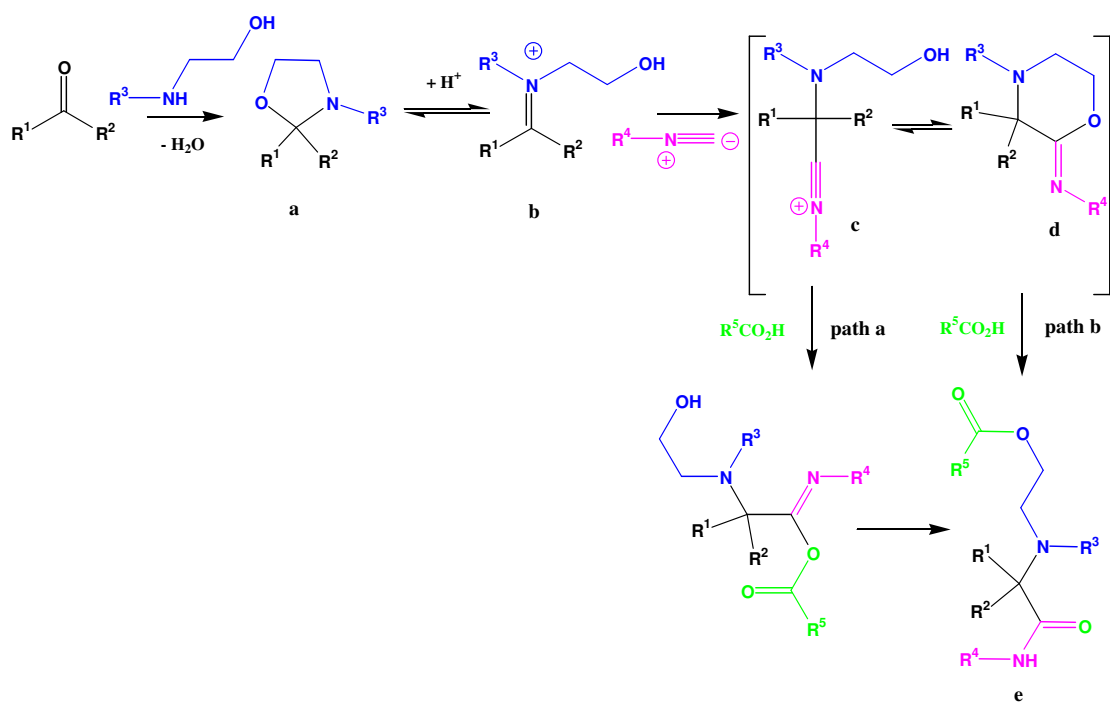
In the same year, Motherwell⁶¹⁶ reported the IMCRs of oxazolidines with carboxylic acids to give ethanolamine derivative (**Scheme 15**).



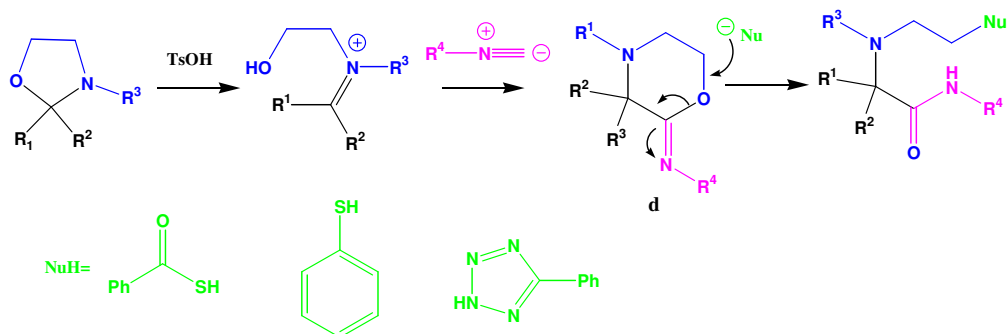
Reaction conditions: a) TsOH (10%), MeCN, 18-24 h reflux.

Scheme 15

The acid-catalyzed ring opening of the oxazolidine **a** (readily formed from an aminoalcohol and a carbonyl compound) gives the iminium species **b**, which is attacked by isocyanide to give nitrilium ion **c** (**Scheme 16**). Two plausible mechanisms can be envisaged from this intermediate. The carboxylic acid could form the α -adduct and undergo the acyl migration to the desired product **e** (*path a*). Alternatively, the hydroxyl group could trap the nitrilium ion and form the six-membered intermediate **d**, which could be attacked by the carboxylic acid at the β -carbon and form the same multicomponent product **e** (*path b*). ¹⁸O-labelled acetic acid later confirmed that the reaction does indeed proceed via *path a*.⁶¹⁷ The intermediate **d** could be trapped with various nucleophiles as shown in **Scheme 17**. Indeed S_N2 reactions at the β -carbon were found to work with 5-phenyl-1H-tetrazole, thiobenzoic acid and thiophenol, forming new C-S and C-N bonds while increasing the complexity of the final product.

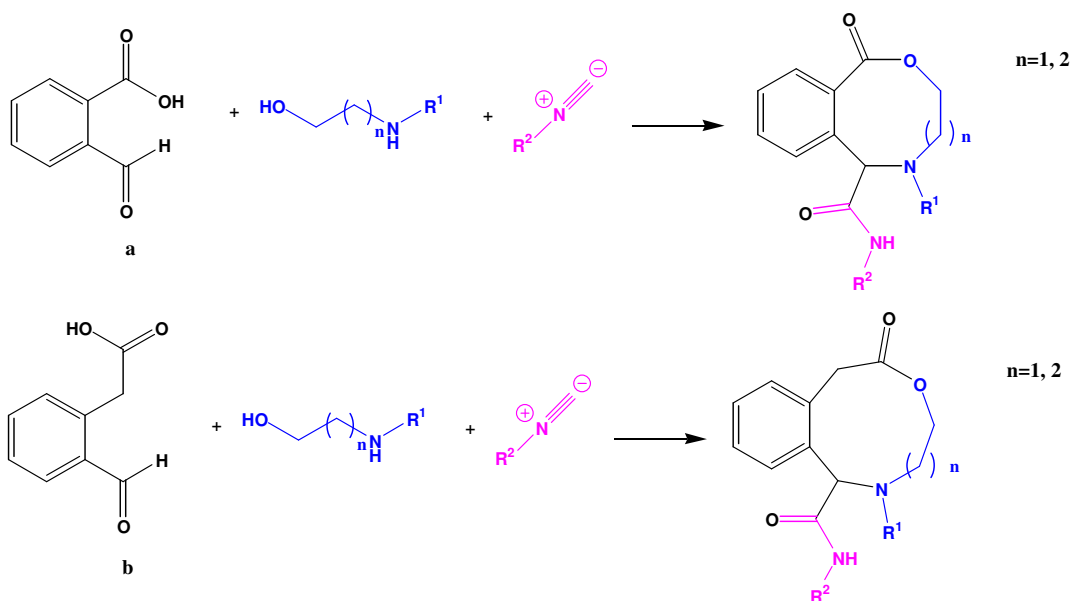


Scheme 16



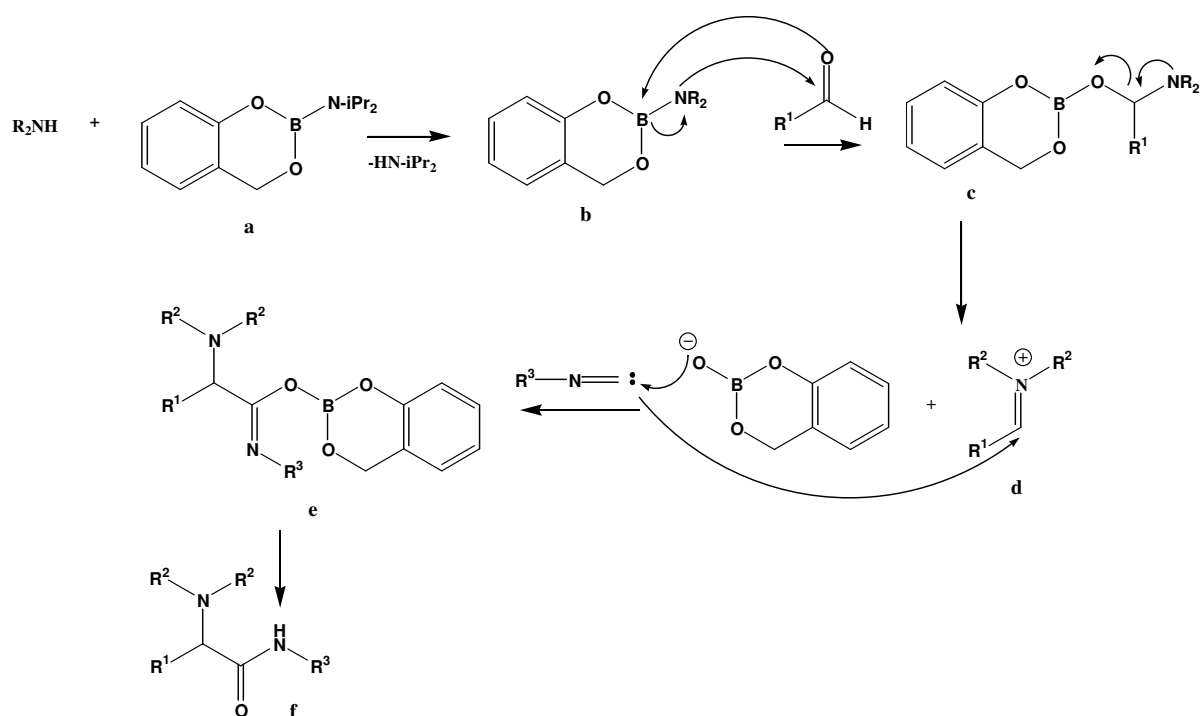
Scheme 17

Moreover combining the aldehyde and carboxylic acid components in bifunctional substrates **a** and **b** allowed the synthesis of eight, nine and ten-membered lactones (**Scheme 18**).⁶¹⁸ Sheppard and co-workers optimized reaction conditions in microwave, reducing reaction times and increasing the yield.



Scheme 18

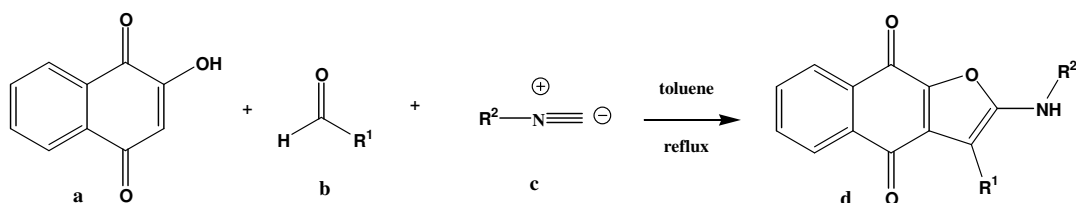
In 2007, the use of aminoboranes as an “iminium ion” generators was reported for Ugi-type reactions for secondary amines, aldehydes and isocyanides without a carboxylic acid component.⁶¹⁹ One of the possible mechanisms is shown in **Scheme 19**. The aminoborane **b** is generated from the free amine and **a**. The intermediate **b** then reacts with the aldehyde through nucleophilic attack of its amino group to the carbonyl group and the subsequent B-O formation giving the intermediate **c**. The cleavage of the C-O bond in **c** leads to the formation of the iminium ion **d** which reacts with the isocyanide, giving the Ugi-product **f** through **e**. More recently, the same properties were described for the cheap and readily available trimethoxyborane.⁶²⁰



Scheme 19

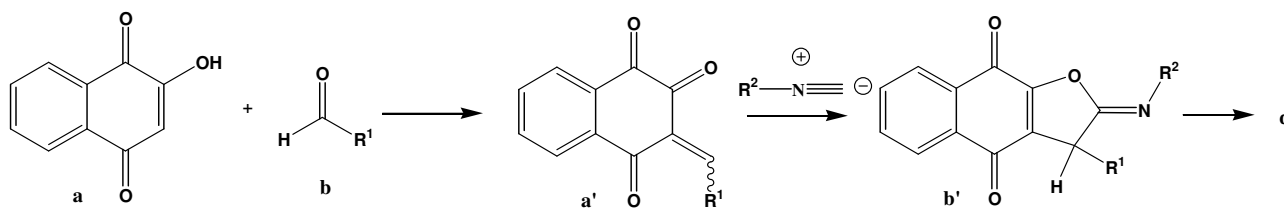
An interesting application of MCRs is in the one-pot three-component regioselective synthesis of linear naphtho[2,3-*b*]-furan-4,9-diones.⁶²¹ Among the class of heterocyclic quinones, naphthofuroquinones have attracted a big interest because of their presence in natural products, and for their pharmacological activities. A great number of naphthofuroquinones are natural products exhibiting a broad spectrum of biological activity. For example, some naphthofuroquinone derivatives as avicequinones⁶²² and maturinones⁶²³ have shown a diversity of biological activities of medical importance, such as anticancer, antibacterial, and anti-inflammatory activities.⁶²⁴

The one-pot three-component condensation reactions (**Scheme 20**) of 2-hydroxy-1,4-naphthoquinone **a** with various aldehydes **b** in the presence of alkyl isocyanides **c** proceeded rapidly in refluxing toluene and were complete after 4 h to afford 2-(alkylamino)-3-alkyl or aryl naphtho[2,3-*b*]furan-4,9-diones **d** in good yields.



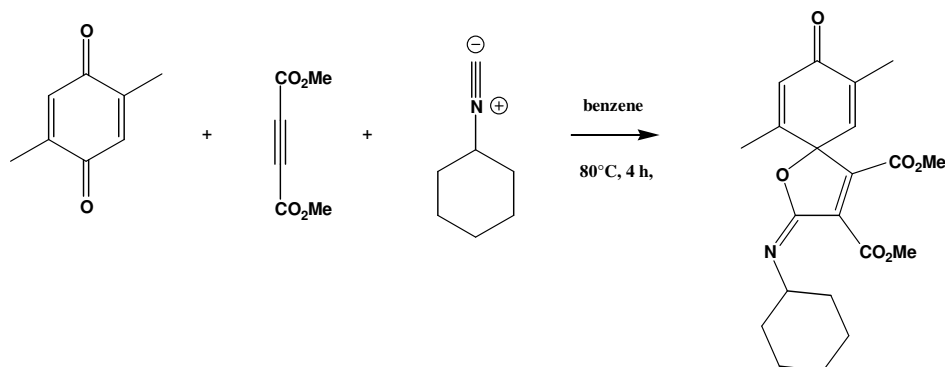
Scheme 20

Although the mechanism of this reaction have not been established, the authors suggested that the synthesis of naphtho[2,3-b]-furan-4,9-dione derivatives **d**, can be rationalized by initial formation of a conjugated electron-deficient enone **a'** (**Scheme 21**) by a Knoevenagel condensation of the cyclic 2-hydroxy-1,4-naphthoquinone **a** and the aldehyde **b**. The next step of this mechanism could involve a [4+1] cycloaddition reaction of the electron-deficient heterodyne moiety of adduct **a'** with the isocyanide to afford an iminolactone intermediate **b'**. The subsequent isomerization of iminolactone **b'** leads to formation of product **d**.



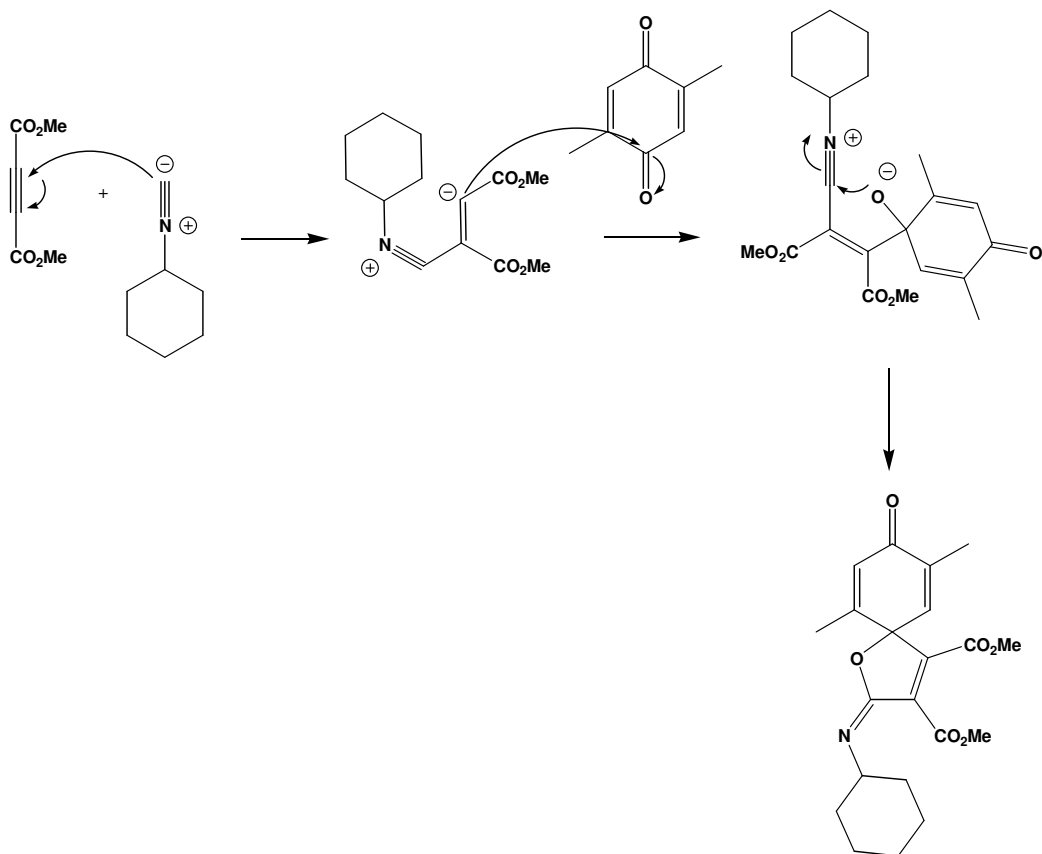
Scheme 21

Moreover, Nair et al.⁶²⁵ reported a novel synthesis of iminolactones based on the reaction between cyclohexyl isocyanide and dimethyl acetylenedicarboxylate with o- and p-quinones (**Scheme 22**).



Scheme 22

In **Scheme 22** the reaction with 2,5-dimethyl p-benzoquinone is shown but, similar reactivity was also observed with 1,2-benzoquinones and with a large number of other quinones. The formation of the product can be rationalized as shown in **Scheme 23**.



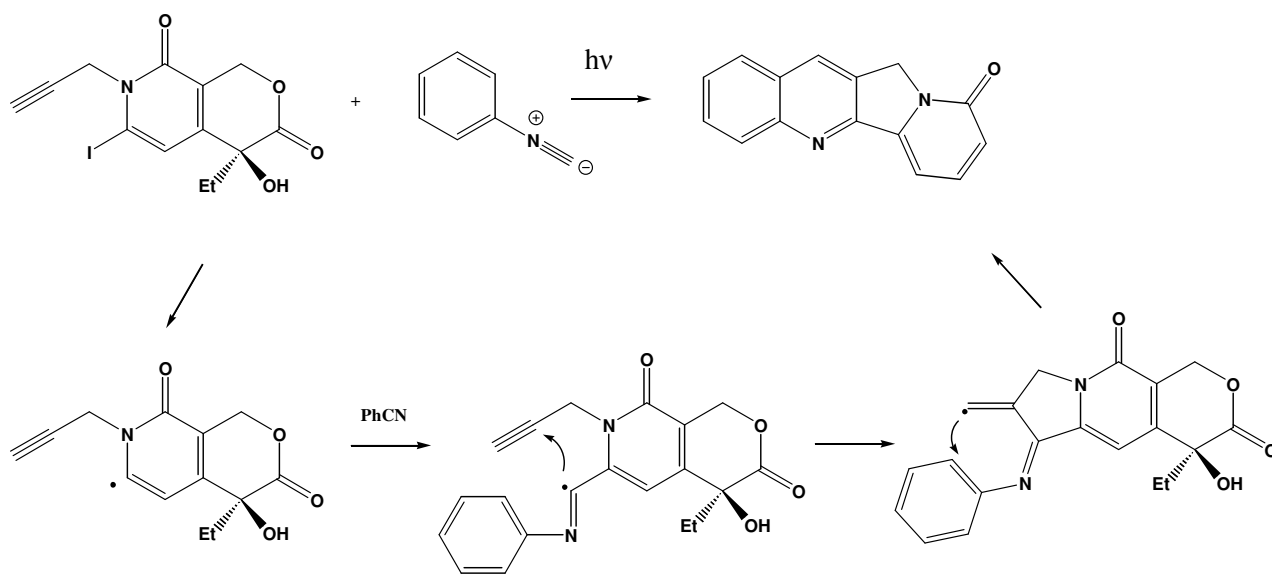
Scheme 23

1.2 Isocyanides

Isocyanides, formerly known as isonitriles, are compounds with an extraordinary functional group. The chemistry of isocyanides is characterized by three properties: α -acidity, α -addition and the easy formation of radicals.

A Formation of radicals

Isocyanides and in particular phenyl isocyanide are substrates for radical-induced cyclization. A famous example is the synthesis of the ABCD ring moiety of the topoisomerase II inhibitor camptothecin by Curran et al. (Scheme 24).⁶²⁶



Scheme 24

B α -Acidity

The α -acidity is increased by electron-withdrawing substituents in the α -position like carboxylic esters, nitriles, phosphonic esters or sulfonyl groups. This property is displayed by R-substituted tosylmethyl isocyanides (TOSMIC) used in the van Leusen multicomponent reaction (vL-3CR).⁶²⁷ TOSMIC (Fig. 1) represents a densely functionalized building block with three important groups contributing to a multitude of reactions: the isocyano function undergoes typical α -addition reactions, the acidic α -carbon atom, and the sulphonyl group in the α -position that has two functions, acting both as a sulphinyl leaving group and further enhancing the acidity of the α -carbon.

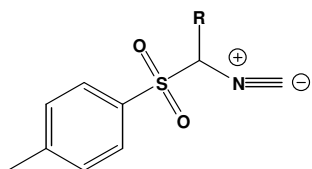
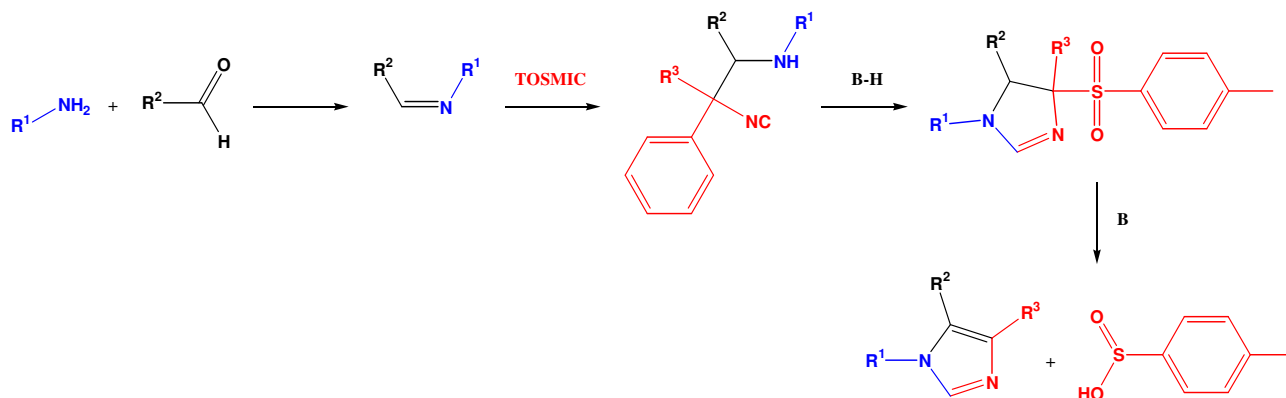


Figure 1: TOSMIC structure.

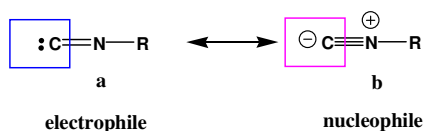
The vL-3CR constitutes an important application of isocyanides in MCR to obtain 1,4,5-trisubstituted imidazoles which are otherwise not easily accessible. It is a reaction between an aldehyde, a primary amine and TOSMIC. The mechanism shown in **Scheme 25** involves the nucleophilic attack of the α -acidic carbon of TOSMIC to a Schiff base followed by cyclization with loss of tosylsulphinic acid.



Scheme 25

C α -Addition

The synthetically most important property of isocyanides is the reaction with nucleophile and electrophile at the isocyanide carbon. In fact, they have two resonance structures **a** and **b** (**Scheme 26**), and their characteristic IR absorption at ca. 2000 cm^{-1} indicates that **b** resonance structure gives more contribution.



Scheme 26

In the isocyanide group both N and C atoms assume sp hybrid states as shown in **Figure 2**.

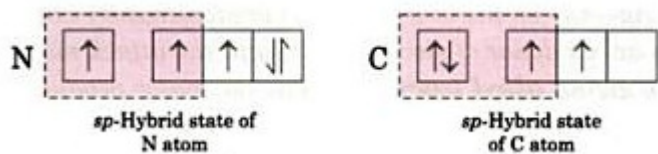


Figure 2: Hybrid states of isocyanide.

One of the hybrid orbitals of nitrogen is used to form a sigma bond with the hydrocarbon part while the other hybrid orbital is used to form an $sp-sp$ σ bond with the C atom. One of the unhybridised p orbitals of the N atom forms a $p\pi-p\pi$ bond with a similar orbital on the C atom. The other unhybridised p orbital of the nitrogen atom, containing a lone pair of electrons, overlaps with an empty p -orbital on the carbon atom to form another π -bond as shown in **Figure 3**.

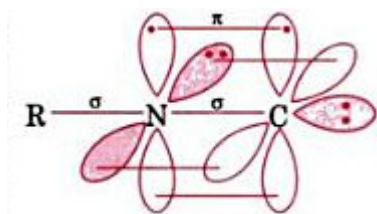
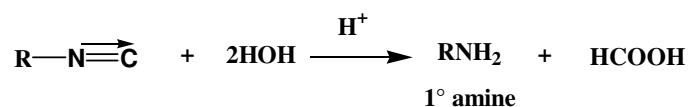


Figure 3: Orbital structure of R-NC.

Isocyanides undergo hydrolysis in acid medium to form formic acid and primary amines (**Scheme 27**).



Scheme 27

The present work was carried out using *tert*-butyl-isocyanide (tBu N=C) because it is a readily available and highly nucleophilic isocyanide as shown in **Figure 4**.

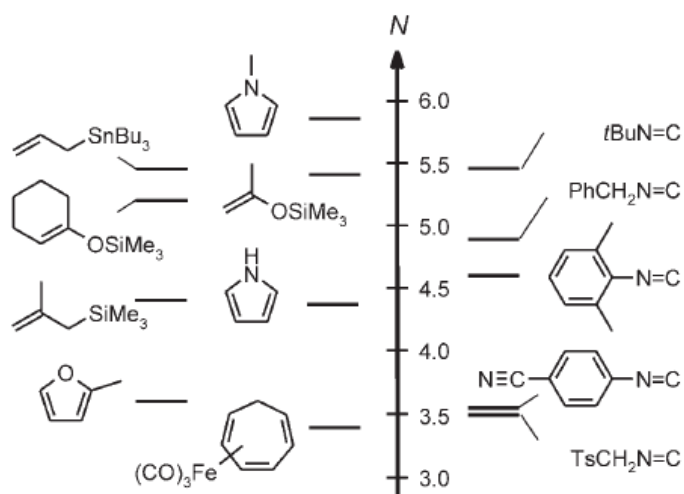


Figure 4: Comparison of the nucleophilicities of isocyanides and other C nucleophiles.⁶²⁸

Hundreds of isocyano group containing natural products were isolated, mainly from marine species. Moreover, many natural isocyanides show a strong antibiotic, fungicidal, or antineoplastic effect.⁶²⁹ Examples of bioactive natural products that contain an isocyano group are shown in **Figure 5**.

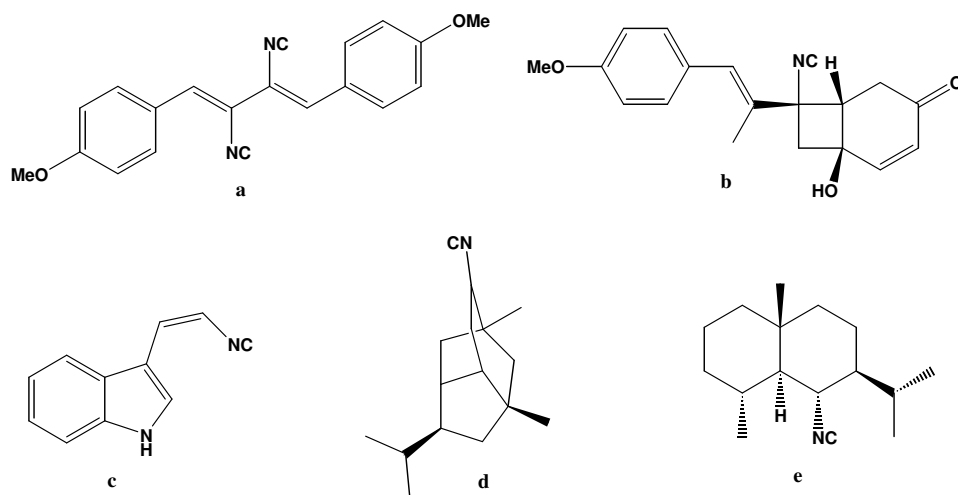


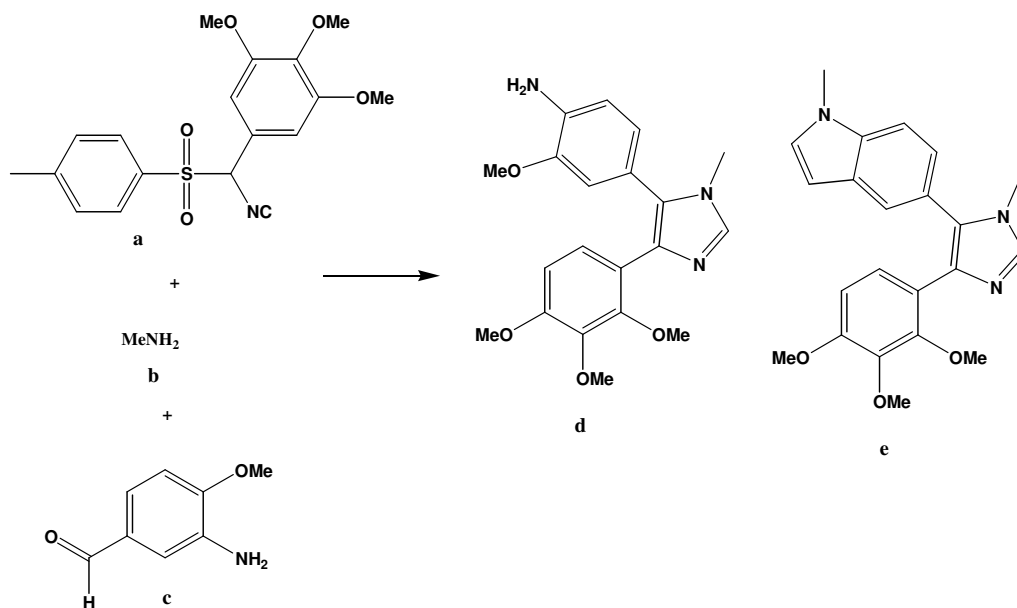
Figure 5: Examples of naturally occurring isocyanides: a) the antibiotic xanthocillin, b) leptocillin from *Penicillium chrysogenum*, c) the antimalarial kalihinol A from *Pseudomonas* sp., d) isocyanopupukean from *Pyrenochaeta spaeropsidales*, d) acenthellin-1 from *Chromobacterium spec.*

1.3 MCRs in Drug Discovery

By far, most applications of IMCRs described until today arise from the area of drug discovery. Potentially, the ease of performance, the time-saving aspect, the versatility and diversity of scaffolds, and the very large chemical space will attract chemists in pharmaceutical companies to use MCRs for their projects. Another interesting aspect of MCRs in the context of drug discovery is the effective assembly of scaffolds out of smaller fragments. The following overview describes examples of MCRs used in drug discovery, taken from recent patent and journal literature.

1.3.1 Tubulin Inhibitors

Potent, orally available tubulin inhibitors have potential applications in cancer therapy. The imidazole MCR of van Leussen was used for this purpose.⁶³⁰ Herein, R-substituted TOSMIC **a** reacts with primary amines **b** and aldehydes **c** to form 1,4,5-trisubstituted imidazoles **d** and **e** (**Scheme 28**). Thus, **d** and **e** show IC₅₀ values of 170 and 32 nM in the cancer cell line NCI-H460 and oral bioavailabilities of 82 and 36%, respectively. Moreover, mice xenograft models revealed that both have remarkable oral efficacy against the solid murine M5076 reticulum sarcoma cell line.

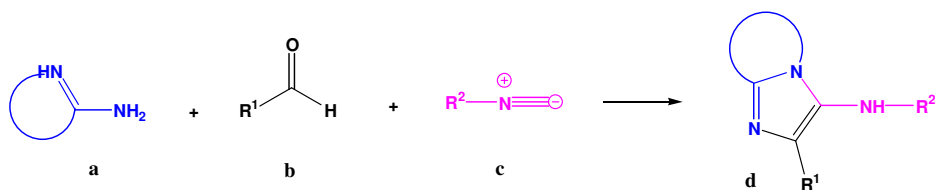


Scheme 28

1.3.2 Phosphatase Inhibitors

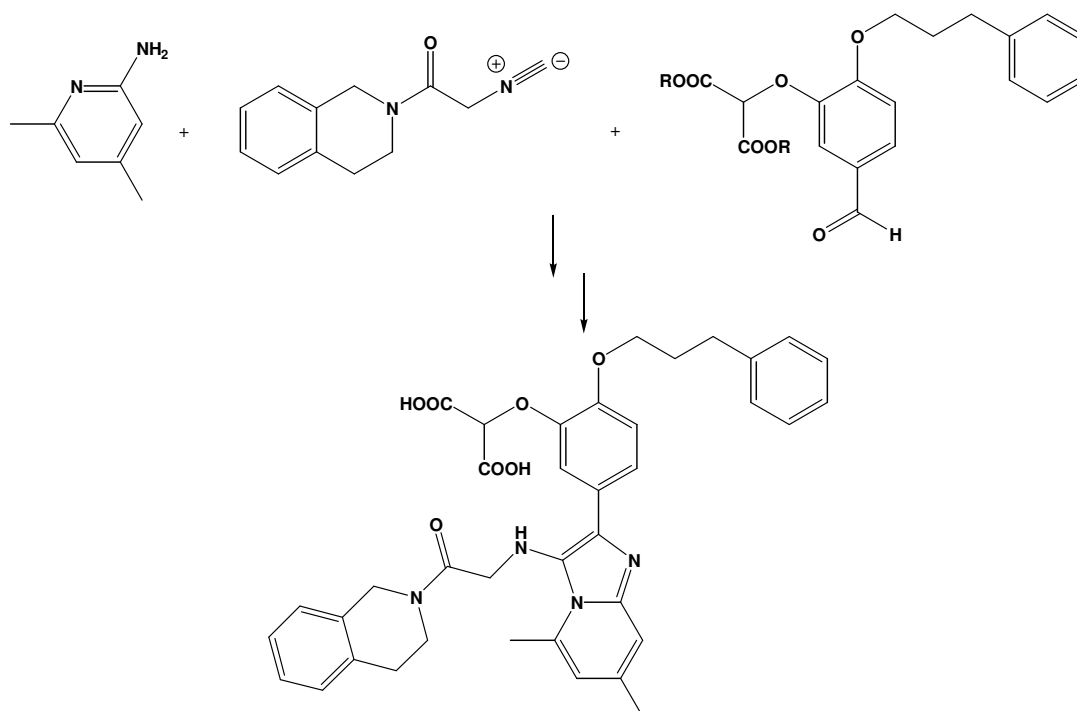
Morphochem workers used the Groebcke MCR to prepare a new class of specific PTP1B inhibitors. Groebcke reaction is a three-component reaction to obtain fused 3-aminoimidazoles **d** from aromatic heterocyclic 2-aminoazines **a**, aldehydes **b**, and isocyanides **c** in the presence of a variety of Lewis acids or Brønsted acids (**Scheme 29**). The relevance of this powerful 3-component

transformation is significant because imidazo[1,2-*a*]heterocycles of this nature have received a great deal of attention in drug discovery. Imidazopyridines, imidazopyrazines, and imidazopyrimidines, in particular, have been the focus of pharmaceutical investigations across a broad range of therapeutic areas.



Scheme 29

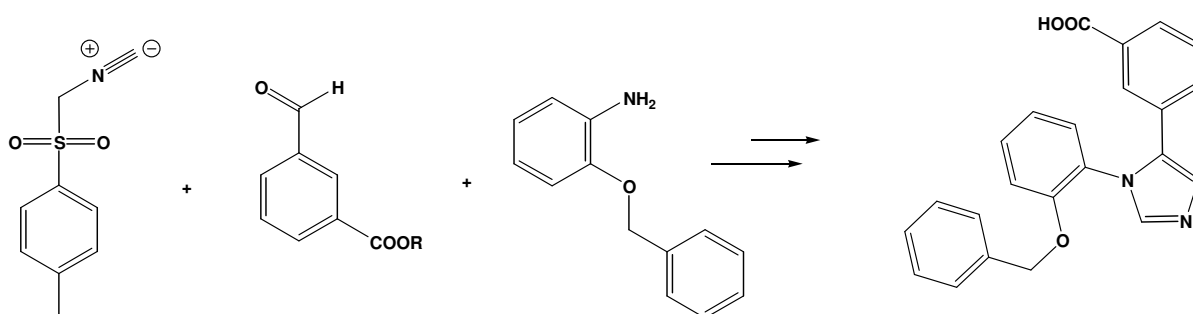
PTP1B also known as protein-tyrosine phosphatase 1B is an enzyme that is the founding member of the protein tyrosine phosphatase (PTP) family. PTP1B is a negative regulator of the insulin signaling pathway and is considered a promising potential therapeutic target, in particular for treatment of type 2 diabetes. Several inhibitors exhibited low micromolar activity and remarkable selectivity versus similar phosphatase. An example of a novel PTP1B inhibitor, synthesized by one-pot Groebcke MCR, is shown in **Scheme 30**.



Scheme 30

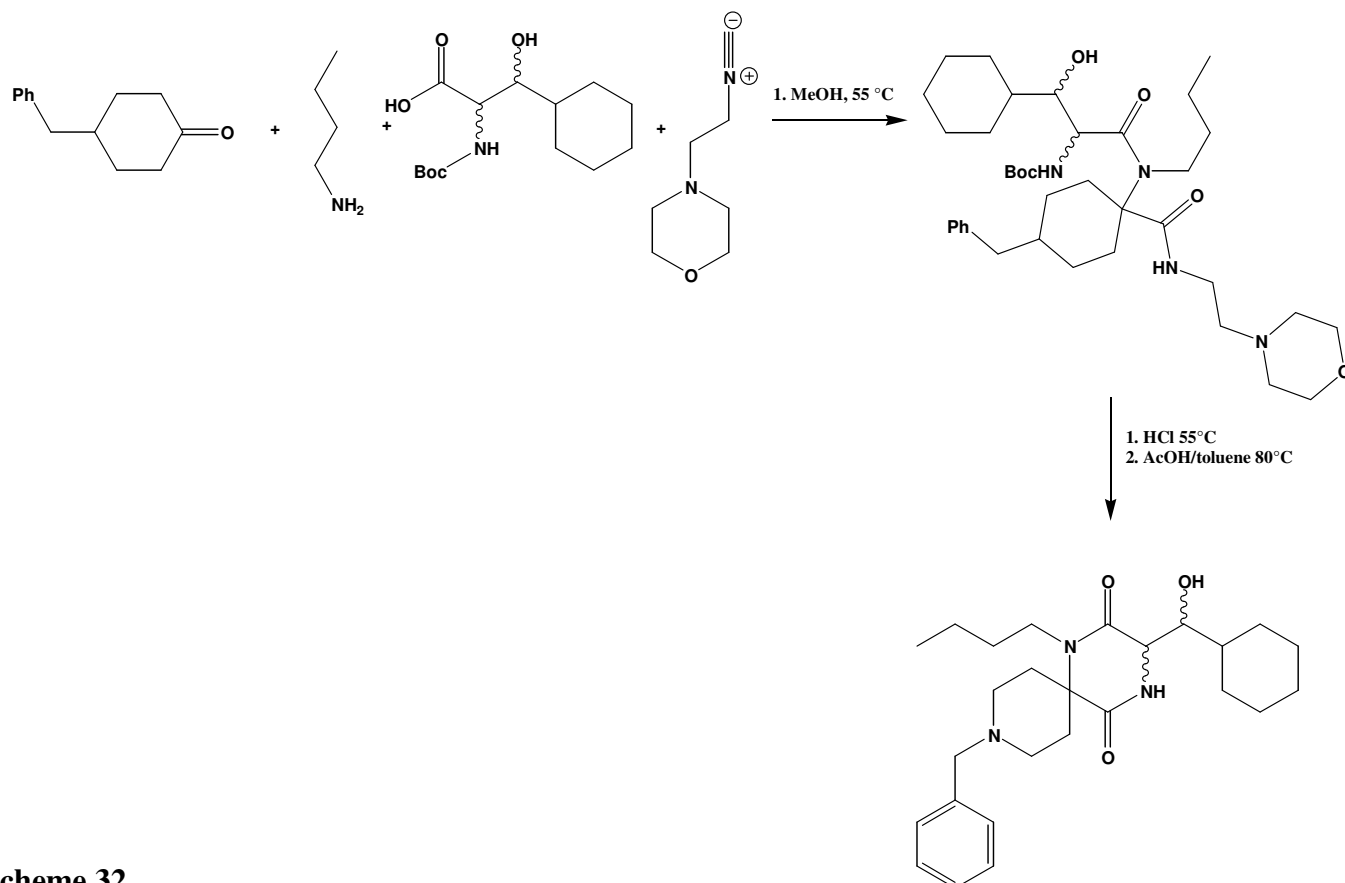
1.3.3 GPCR Ligands

G-protein coupled receptors are by far the most important drug discovery target of the past, present, and foreseeable future. Because of the rareness of biostructural information in the GPCR field, however, the most common way to initiate chemistry programs is via high-throughput screening (HTS). GSK scientists discovered compounds which bind to the 7-transmembrane receptor EP1 (whose natural ligand is prostaglandin PGE₂) with high affinities. The EP1 receptor is associated with smooth muscle contraction, pain, inflammation, allergic activities, renal regulation, and gastric or enteric mucus secretion. A series of EP1 receptor antagonists have been synthesized by the vL3-CR of TOSMIC, 2-*O*-benzyl anilines and *m*-formylbenzoic acid esters after subsequent saponification.⁶³¹ An example is shown in **Scheme 31**.



Scheme 31

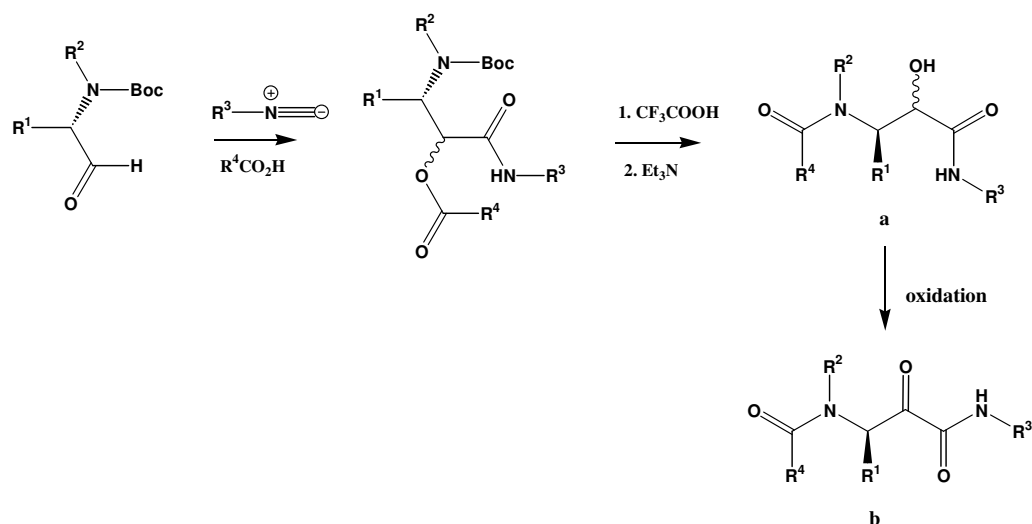
An U-4CR was used to prepare nitrogen-containing heterocyclic derivatives as chemokine receptor CCR5 antagonists⁶³² Chemokines are a family of small cytokines, or proteins secreted by cells. These proteins exert their biological effects by interacting with G protein-linked transmembrane receptors called chemokine receptors, which are selectively found on the surfaces of their target cells. Some chemokines are considered pro-inflammatory and can be induced during an immune response to recruit cells of the immune system to a site of infection. An example of these new CCR5 antagonists synthesized by a U-4CR is shown in **Scheme 32**.



Scheme 32

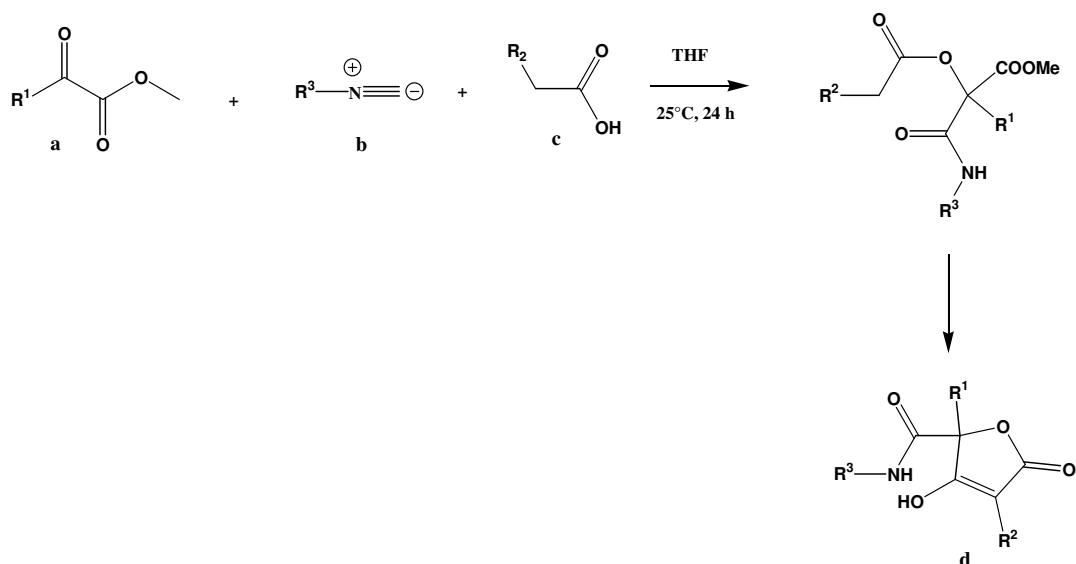
1.3.4 Aspartyl Protease Inhibitors

Several aspartyl proteases are important human disease targets. These involve α -secretase (Alzheimer and other neurodegenerative diseases), HIV protease (AIDS), cathepsin D (malaria), and renin (cardiovascular diseases). Banfi et al.⁶³³ and Sample et al.⁶³⁴ reported the P-3CR with isocyanides, carboxylic acids, and *N*-Boc-protected aldehydes yielding after Boc-deprotection and rearrangement, a multitude of complex peptide-like substances **a** possessing a central α -hydroxy- β -amino acid unit (**Scheme 33**). This type of monomer has been widely used in the synthesis of enzyme inhibitors.⁶³⁵ Moreover, a simple oxidation will produce oligopeptides **b** containing an α -oxo- β -amino acid unit, which is an even more attractive structure, thanks to its similarity with protease transition state.⁶³⁶



Scheme 33

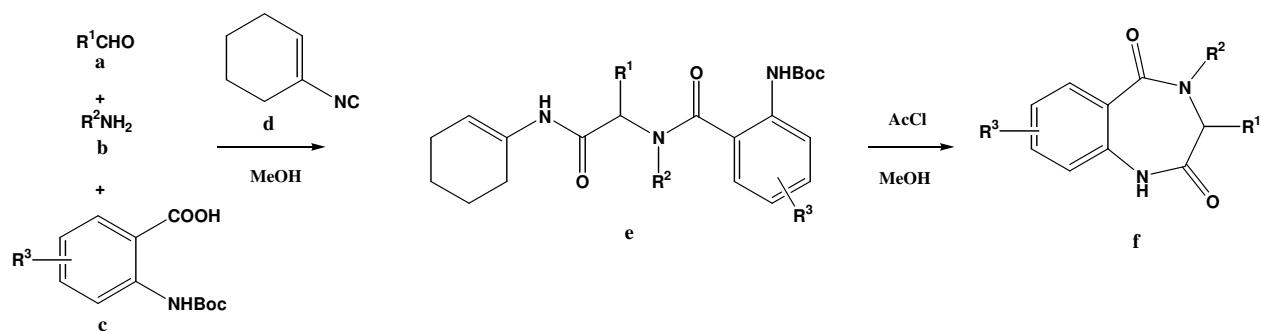
Aspartyl proteases inhibitors are also useful for treating the HIV infection that causes AIDS. HIV is a virus that contains an aspartyl protease (HIV-PR) that is essential for the life-cycle of HIV. HIV-PR cleaves newly synthesized polyproteins at the appropriate places to create the mature protein components of an infectious HIV virion. Without effective HIV-PR, HIV virions remain uninfected. The cost of HIV protease inhibitors is highly dependent on the complexity of the synthesis. Unfortunately, all currently available HIV protease inhibitors are made by very long and costly sequential syntheses. Recently, a novel sequence of P-3CR of R-ketocarboxylic acid esters **a**, isocyanides **b**, and substituted acetic acids **c** and a subsequent Dieckmann ring closing reaction were used to construct five-membered acid amides **d** (**Scheme 34**).⁶³⁷ The particular chemistry can be performed in a one-pot manner in 96-well plates. A big library of new compounds was synthesized and revealed several low micromolar to nanomolar inhibitors. They represent a starting point for novel HIV protease inhibitors synthesized by a much shorter route. This example nicely presents the advantages of MCR chemistry. All currently available HIV protease inhibitors are synthesized via linear syntheses of 15 steps or more. In contrast, these inhibitors are synthesized by a sequence of only two steps.



Scheme 34

1.3.5 Protein-Protein Interaction Inhibitors

The p53 gene has been the subject of intense study, since it was discovered that more than 50% of human cancers are caused by mutations in p53 gene. The hdm2 oncogene product suppresses the transcriptional activity of p53 by direct binding to the *N*-terminal transactivation domain of p53. It has been recently revealed by an X-ray structure that the protein-protein interaction between hdm2 and p53 is mediated by a small piece of an R-helix. From the crystal structure and mutational studies, it is evident that three hydrophobic pockets occupied by Phe₁₉, Trp₂₃, and Leu₂₆ of p53 gene are crucial for this interaction. The discovery and optimization of a series of 1,4-benzodiazepine-2,5-diones (BDPs) that act as potent antagonists of the HDM2-p53 interaction has been reported.⁶³⁸ The library was synthesized utilizing the highly efficient and versatile U-4CR: an anthranilic acid **c**, an amine **b**, an aldehyde **a**, and isocyanocyclohexene **d** were combined, followed by acid catalyzed cyclization of the intermediate **e**, producing the desired BDPs **f** in good yield and purity (**Scheme 35**).



Scheme 35

Twenty-two thousand BDPs were produced in this way. Compound **a'** (**Fig. 6**) showed a potent K_i of 67 nM. This is surprising, taking into account the relatively small size of these molecules as compared to the p53 binding. In **Fig. 6** the interaction between **a'** and p53-hdm2 is shown.⁶³⁹ In yellow are the side chains of F19, W23, L26 of the R-helical amphiphatic p53 peptide. In blue is the superimposed benzodiazepine. The green surface represents the acceptor protein mdm2. A nice spatial overlap of the *p*-chlorophenyl and the second *p*-chlorophenyl substituents with Phe and Ile, respectively, and of the *p*-iodophenyl with the indole side chain is observed.

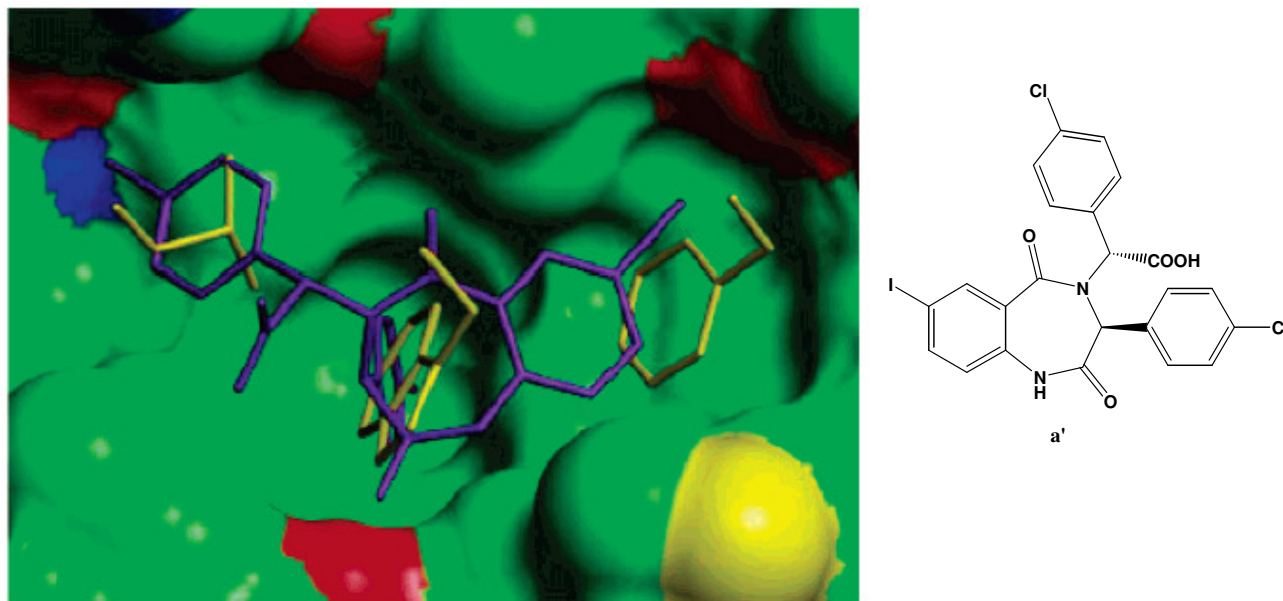


Figure 6: X-ray structure of compound **a'** and p53-hdm2.⁶³⁹

2 Research project

2.1 Hydroxy-carbonyl compounds in multicomponent reactions

In an attempt to expand upon the methodologies being developed in the Sheppard group, the aim of this project was to extend MCRs to a wide range of molecules for example the aldol products **1** and **2** and 5-hydroxy-2-pentanone shown in **Figure 7**.

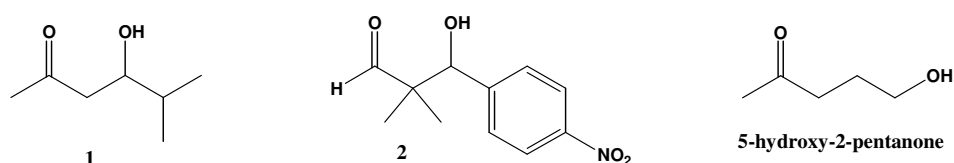
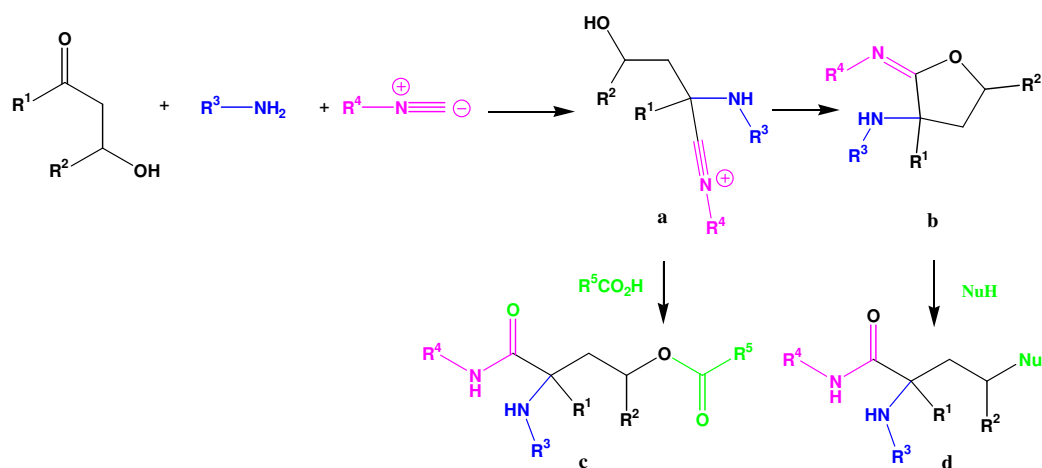


Figure 7: Chemical structures of **1**, **2** and 5-hydroxy-2-pentanone.

The aldol reaction is amongst the most widely used carbon carbon bond forming reactions and therefore the starting β -hydroxy ketones or β -hydroxy aldehydes are readily available. By analogy to the above reactions, it is hypothesized that an isocyanide and an amine could react with an aldol product to form the nitrilium ion **a** (**Scheme 36**), which could again react with carboxylic acids and undergo an acyl migration to one of the hydroxyl group to give **c**, or alternatively, be trapped by the nearby hydroxyl group to form the cyclic intermediate **b**. It can be envisaged that the formation of an amide bond would drive nucleophiles to open in an S_N2 reaction to give the product **d**.



Scheme 36

2.2 Aminoalcohols in multicomponent reactions

We were interested in exploring new MCRs using aminoalcohols that have a three-carbon chain containing a substituent, such as a methyl group (**6**, **7** and **8**) or an allyl group (**9**), to see how the substituent can modify the reactivity and whether it provides any stereoselectivity in the reaction. We would also explore how the aminoalcohol carbon chain inserted in a bulky cycle like a benzene (**10**) can change the chemical reactivity. Examples of aminoalcohols used are shown in **Figure 8**.

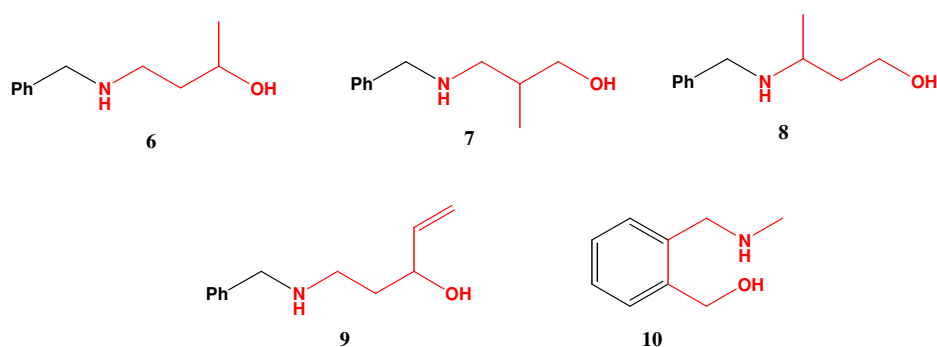
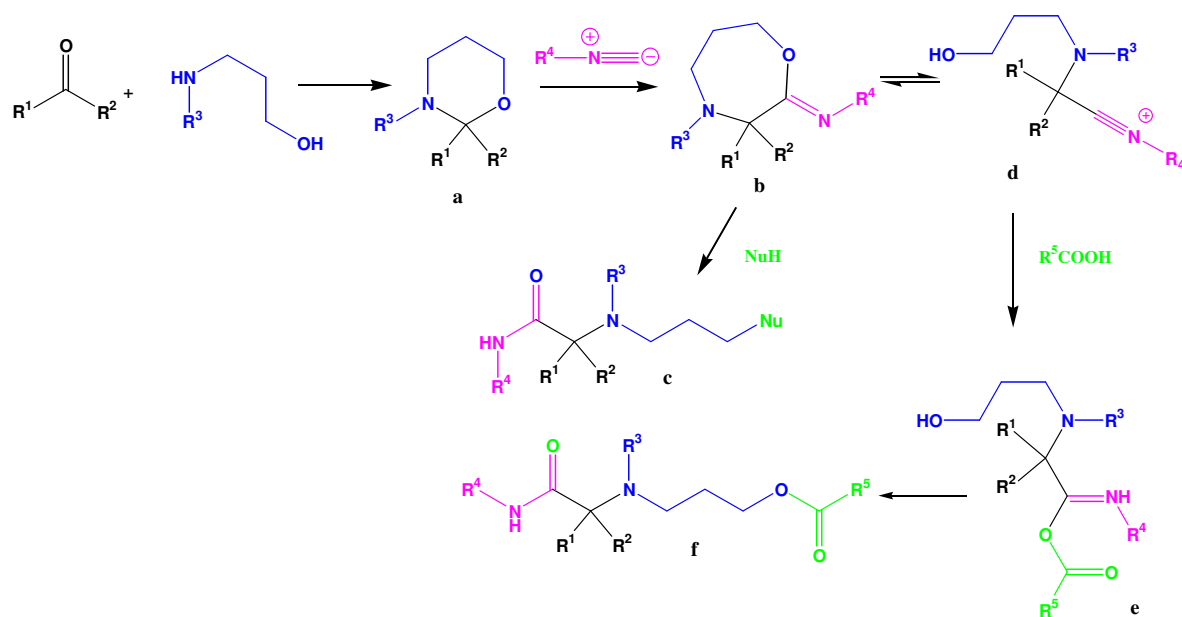


Figure 8: Examples of aminoalcohols used in MCRs.

By analogy to the above reactions, it was hypothesized that the reaction between the aminoalcohol and the carbonyl compound makes the intermediate **a** (**Scheme 37**), which is attacked by the isocyanide to give the seven-membered intermediate **b**. Then, **b** can be opened by a nucleophile in an S_N2 reaction to give the final product **c**. Alternatively, the intermediate **b**, which is in equilibrium with the nitrilium ion **d**, can react with a carboxylic acid to give the intermediate **e**, and after acyl transfer the final product **f**.



Scheme 37

2.3 Carbonyl-carboxylic substrates in multicomponent reactions

Moreover, to increase molecular diversity and to give access to novel drug-like structures, we were interested in trying MCRs between aminoalcohols and molecules that contain both the carbonyl group and the carboxylic moiety. Examples are shown in **Figure 9**.

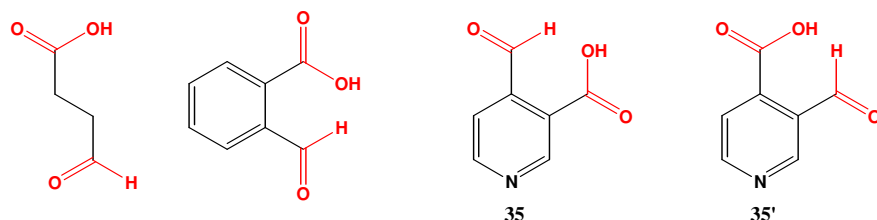
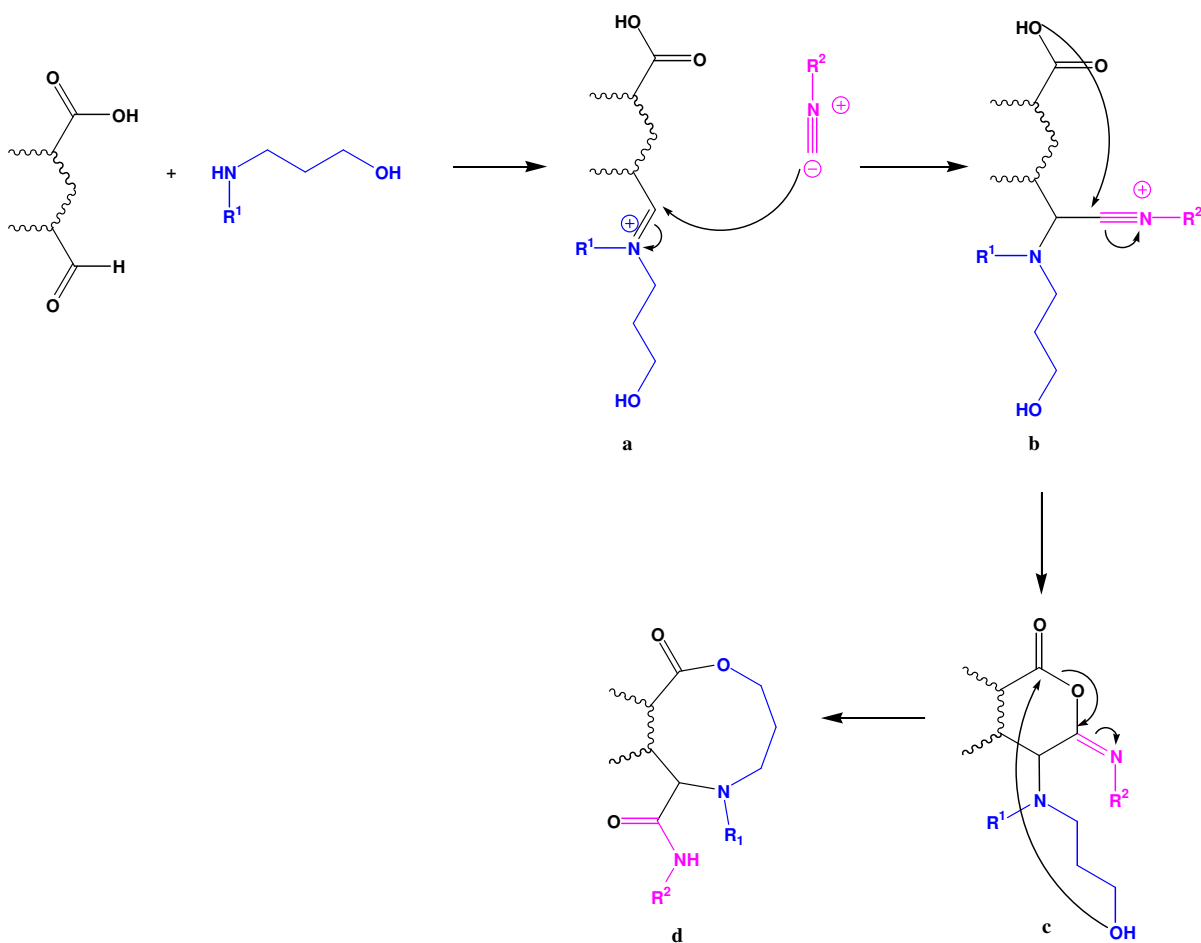


Figure 9: Molecules that contain both the carbonyl group and the carboxylic moiety.

These molecules allow the synthesis of medium-ring heterocycles. The proposed mechanism is shown in **Scheme 38**. The iminium ion **a**, formed upon condensation of the secondary amine and aldehyde, is attacked by the isocyanide to give nitrilium ion **b**. Attack by the carboxylate gave the intermediate **c**, which leads to the medium-ring **d** after rearrangement. The synthesis of medium rings is often difficult due to the unfavorable thermodynamics of the ring closing process.⁶⁴⁰



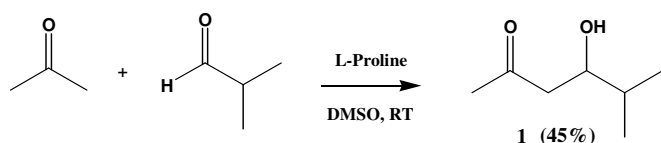
Scheme 38

3 Results and Discussion

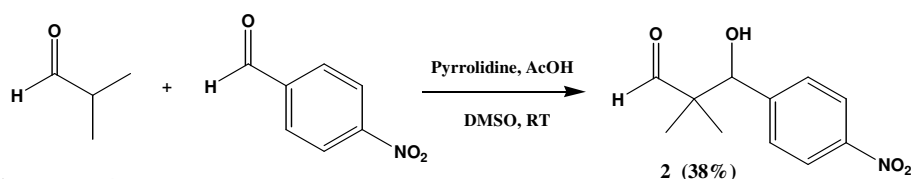
The following section will be divided into two parts. MCRs of aldol products will be presented first, followed by reactions of aminoalcohols.

3.1 Hydroxy-carbonyl products

To test if simple aldol products can participate in an IMCR as shown above in **Scheme 36**, a β -hydroxy ketone **1** (**Scheme 39**) and a β -hydroxy aldehyde **2** (**Scheme 40**) were synthesized using a protocol developed by List⁶⁴¹ and Mase⁶⁴² respectively.

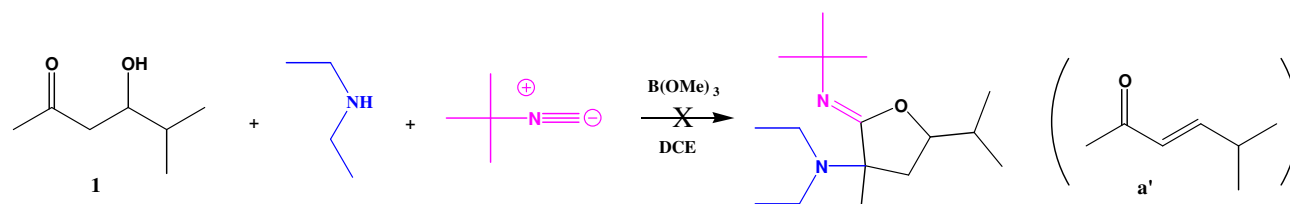


Scheme 39



Scheme 40

1 was then reacted with tert-butyl isocyanide, diethylamine and trimethoxyborane (**Scheme 41**).



Reaction conditions: β -hydroxy ketone **1** (1 equiv.), amine (1.5 equiv.), isocyanide (1.5 equiv.), $B(OMe)_3$ (3 equiv.), DCE, RT, 2 days or 83°C, 4h.

Scheme 41

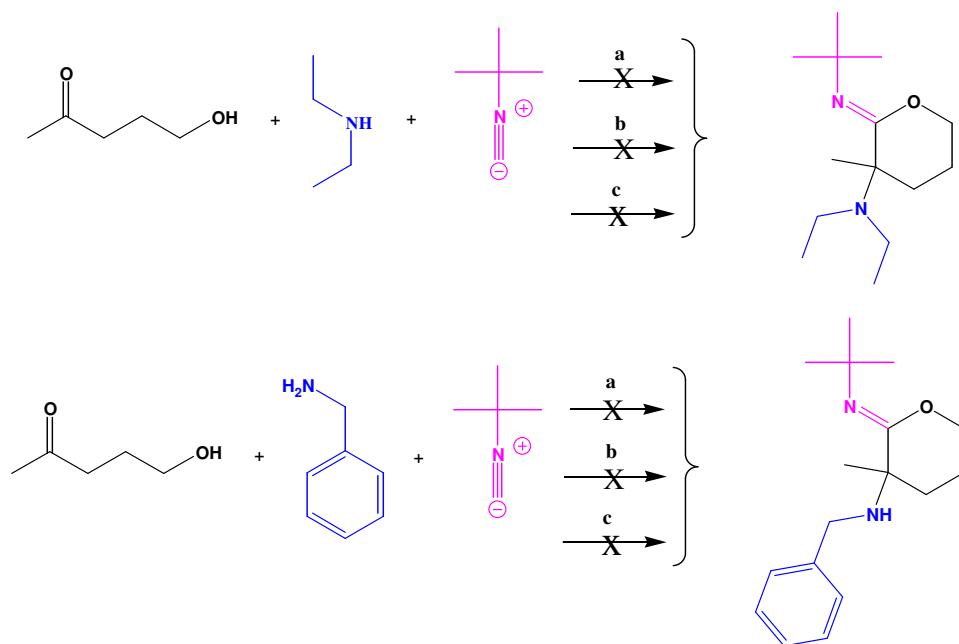
We envisaged that, in the presence of trimethoxyborane, the reaction between β -hydroxy ketone, secondary amine and isocyanide will form the nitrilium ion **a** and, after cyclization, the imino lactone **b** (**Scheme 36**). Different reaction conditions were tried out (RT for 2 days and reflux 4h,) but the enone **a'** (**Scheme 41**) was observed.

Since the reaction with a β -hydroxy ketone did not work, we decided to use 5-hydroxy-2-pentanone, a more stable hydroxy ketone. We tried out both three-component and four-component

reactions. All the reactions were performed in the microwave for 15 minutes. The three-component reactions (**Scheme 42**) involved the reaction between 5-hydroxy-2-pentanone, a secondary (diethylamine) or a primary (benzylamine) amine and tert-butyl isocyanide. Each reaction was performed with and without the catalyst trimethoxyborane. The reaction with the boron derivative was performed in 1,2-dichloroethane, (*reaction conditions a*). Instead methanol was used for reactions without catalyst (*reaction conditions b*). No reaction gave the desired product. From crude $^1\text{H-NMR}$ we could see only starting materials.

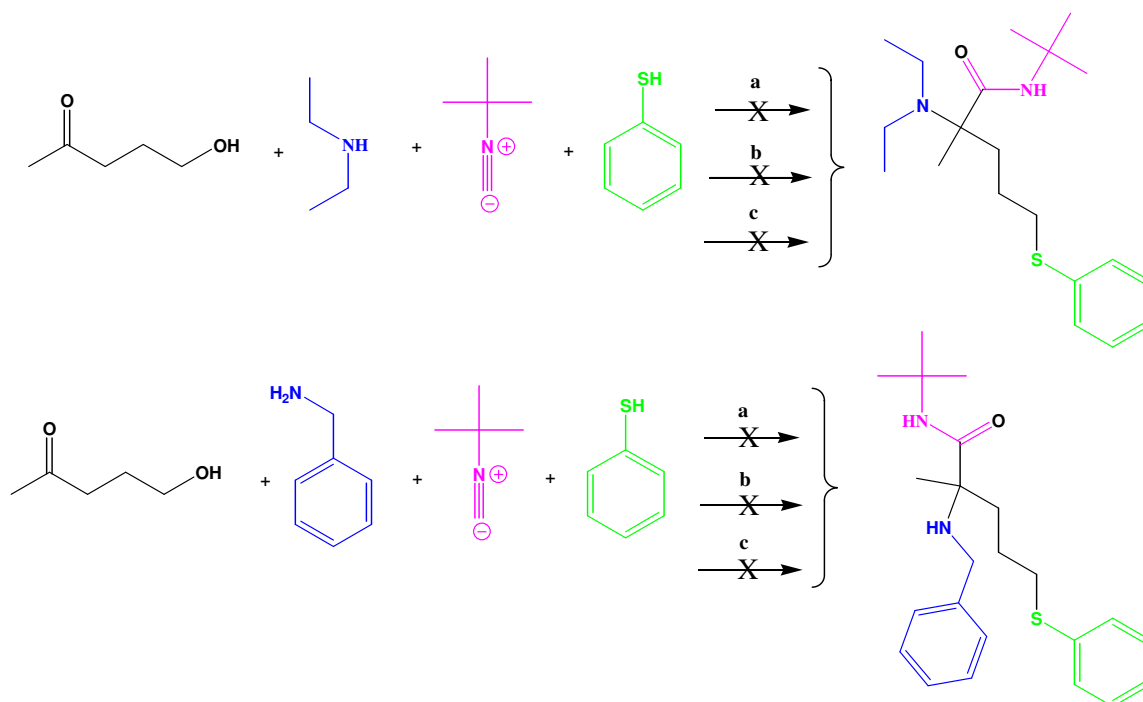
Four-component reactions were also performed in the same way as the three-component reactions, but with the addition of a nucleophile i.e. thiophenol (**Scheme 43**, *reaction condition a and b*). In this case, we wanted to see if the imino lactone intermediate, formed from the reaction between ketone, amine and isocyanide, can be opened by a nucleophile to give the multicomponent products (**Scheme 36**). Also in this case, no reaction worked.

Finally, we performed three-component (**Scheme 42**, *reaction conditions c*) and four-component reactions (**Scheme 43**, *reaction conditions c*) using tris(2,2,2-trifluoroethyl) borate ($\text{B}(\text{OCH}_2\text{CF}_3)_3$) as catalyst. $\text{B}(\text{OCH}_2\text{CF}_3)_3$ is more electrophile than $\text{B}(\text{OMe})_3$ so the formation of the iminium ion could be more favorable. All the reactions were performed in MeCN but, again, no reaction worked.



Reaction conditions: a) hydroxy ketone (1 equiv.), amine (1.5 equiv.), isocyanide (1.5 equiv.), $\text{B}(\text{OMe})_3$ (3 equiv.), DCE, microwave 83 °C, 15 min., b) hydroxy ketone (1 equiv.), amine (1.5 equiv.), isocyanide (1.5 equiv.), MeOH, microwave 65°C, 15 min., c) hydroxy ketone (1 equiv.), amine (1 equiv.), isocyanide (1 equiv.), $\text{B}(\text{OCH}_2\text{CF}_3)_3$ (2 equiv.), CH_3CN , microwave 82 °C, 15 min.

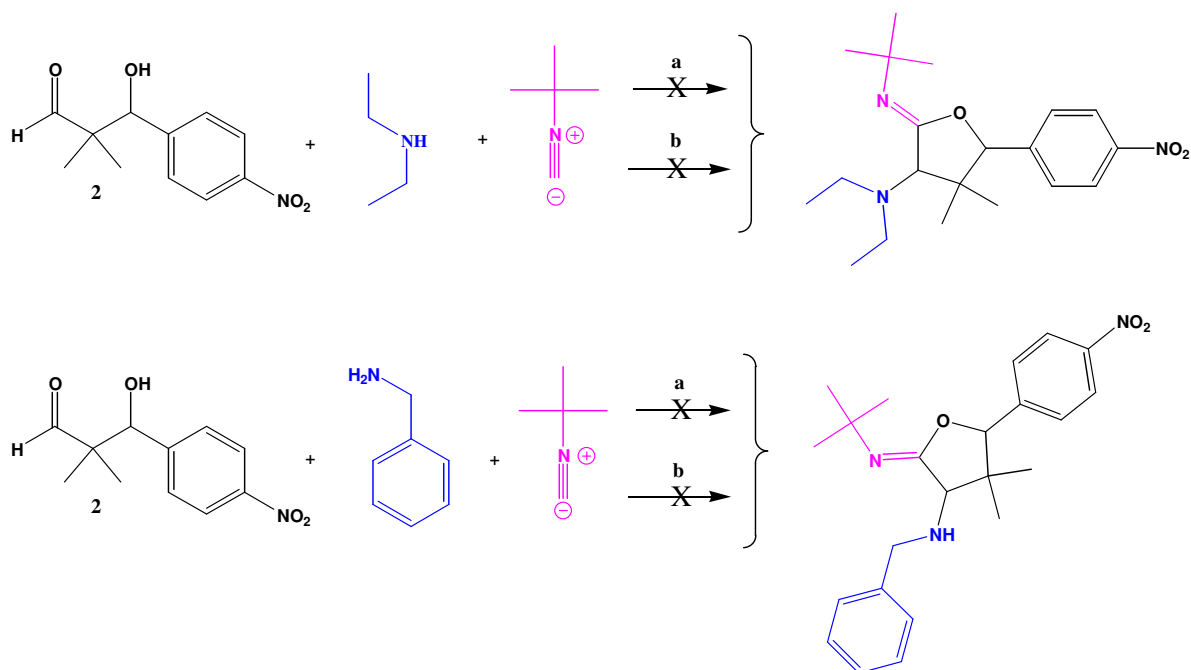
Scheme 42



Reaction conditions: a) hydroxy ketone (1 equiv.), amine (1.5 equiv.), isocyanide (1.5 equiv.), thiophenol (1.5 equiv.), B(OMe)₃ (3 equiv.), DCE, microwave 83 °C, 15 min., b) hydroxy ketone (1 equiv.), amine (1.5 equiv.), isocyanide (1.5 equiv.), thiophenol (1.5 equiv.), MeOH, microwave 65°C, 15 min., c) hydroxy ketone (1 equiv.), amine (1 equiv.), isocyanide (1 equiv.), thiophenol (1 equiv.), B(OCH₂CF₃)₃ (2 equiv.), CH₃CN, microwave 82 °C, 15 min.

Scheme 43

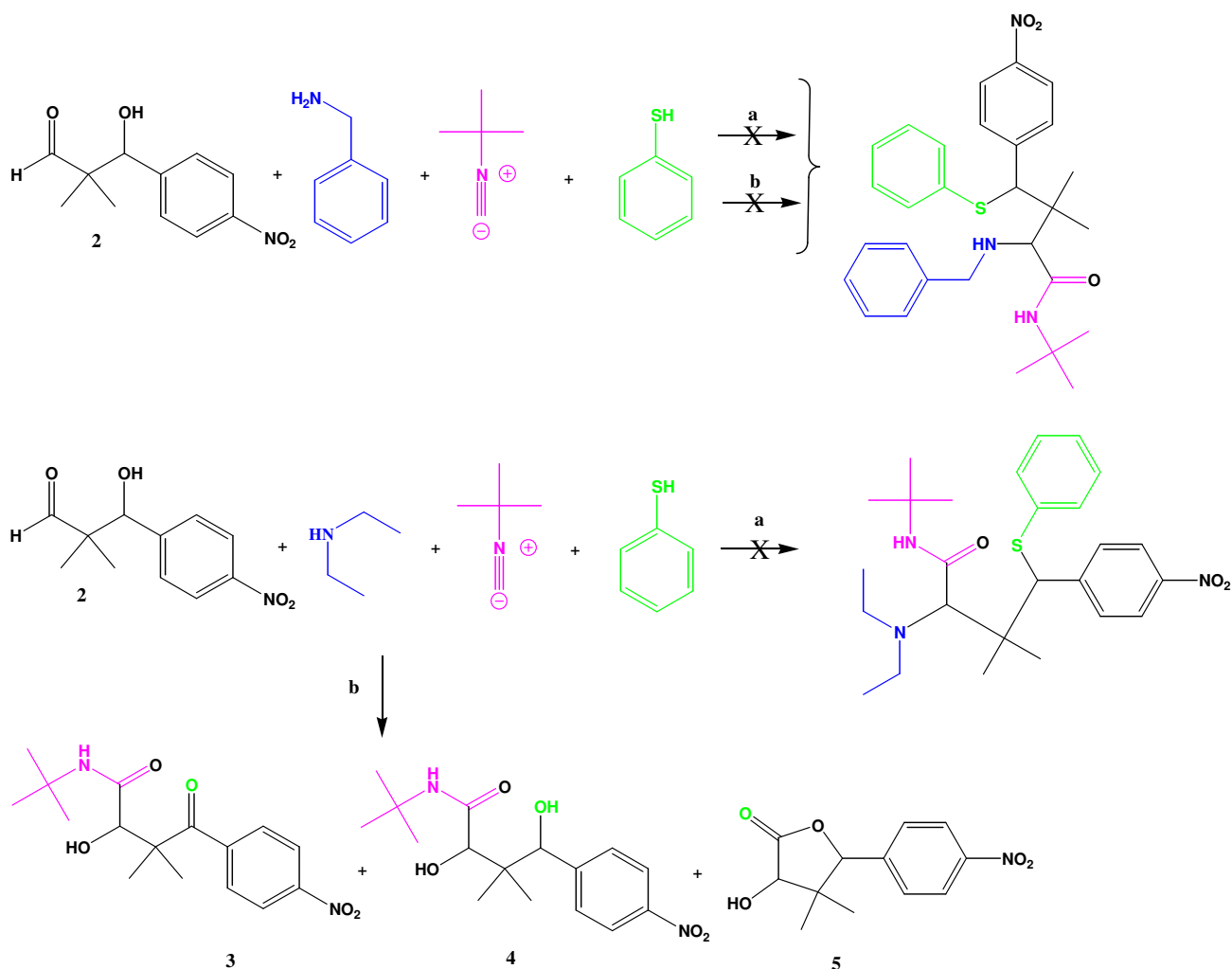
Since the reactions with hydroxy ketones did not work, we tried MCRs using the β -hydroxy aldehyde **2**. As for 5-hydroxy-2-pentanone, we performed three-component and four-component reactions. All the reactions were performed in the microwave for 15 minutes. The three-component reactions (**Scheme 44**) involved the reaction between the β -hydroxy aldehyde **2**, a secondary (diethylamine) or a primary (benzylamine) amine and tert-butyl isocyanide. Each reaction was performed with and without the catalyst trimethoxyborane. The reaction with the boron derivative was performed in 1,2-dichloroethane. Instead methanol was used for reactions without catalyst. No reaction gave the desired product. From crude ¹H-NMR we could see only starting materials.



Reaction conditions: β-hydroxy aldehyde (1 equiv.), amine (1.5 equiv.), isocyanide (1.5 equiv.), *a*) $\text{B}(\text{OMe})_3$ (3 equiv.), DCE, microwave 83 °C, 15 min., *b*) MeOH, microwave 65°C, 15 min.

Scheme 44

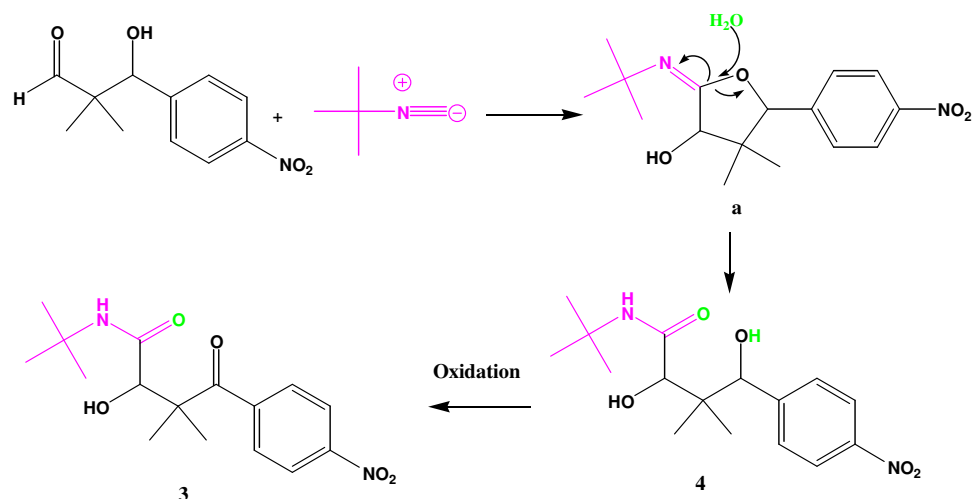
Four-component reactions were performed in the same way as three-component reactions but with the addition of the nucleophile thiophenol (**Scheme 45**). The reaction between the β-hydroxy aldehyde **2**, benzylamine, tert-butyl isocyanide and thiophenol, with and without the catalyst $\text{B}(\text{OMe})_3$ did not work. Replacing benzylamine with diethylamine gave an unsuspected result; the reaction with $\text{B}(\text{OMe})_3$, did not work, but the reaction without catalyst gave the products **3**, **4** and **5** as shown in **Scheme 45**.



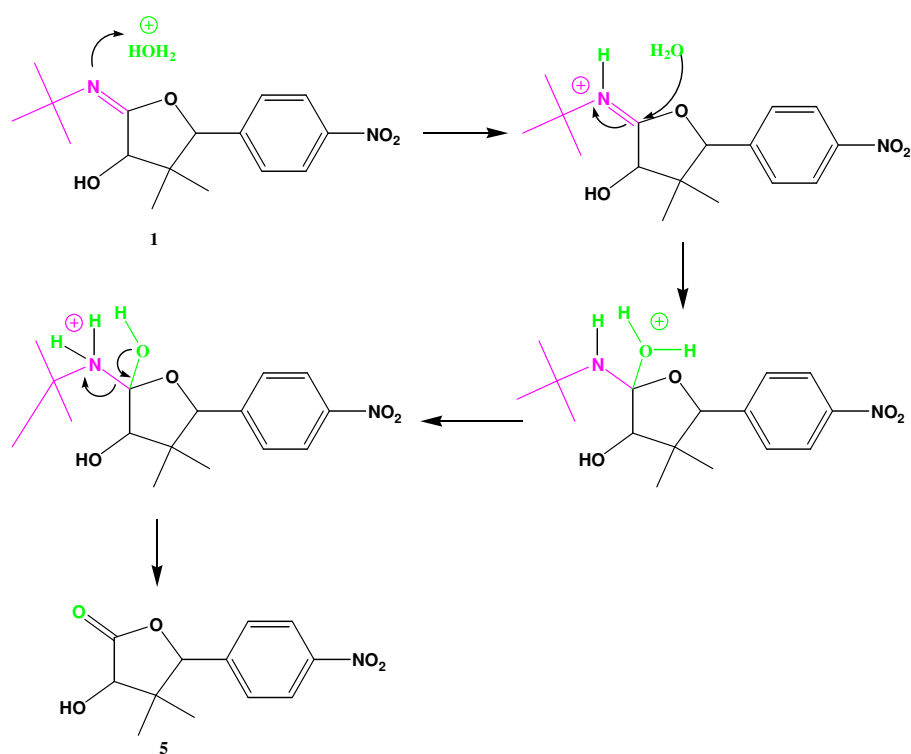
Reaction conditions: β -hydroxy aldehyde (1 equiv.), amine (1.5 equiv.), isocyanide (1.5 equiv.), thiophenol (1.5 equiv.), *a*) $B(OMe)_3$ (3 equiv.), DCE, microwave $83^\circ C$, 15 min., *b*) MeOH, microwave $65^\circ C$, 15 min.

Scheme 45

To explain the formation of **3**, **4** and **5** we have envisaged that the cyclic intermediate **a** is formed from the reaction between the β -hydroxy aldehyde and tert-butyl isocyanide (**Scheme 46**). Then water acts as a nucleophile opening **a** and leading to the formation of **4**. Finally, compound **3** is formed by oxidation of **4**. Alternatively the imino group of the intermediate **a** can be hydrolyzed by water giving the lactone **5** (**Scheme 47**).

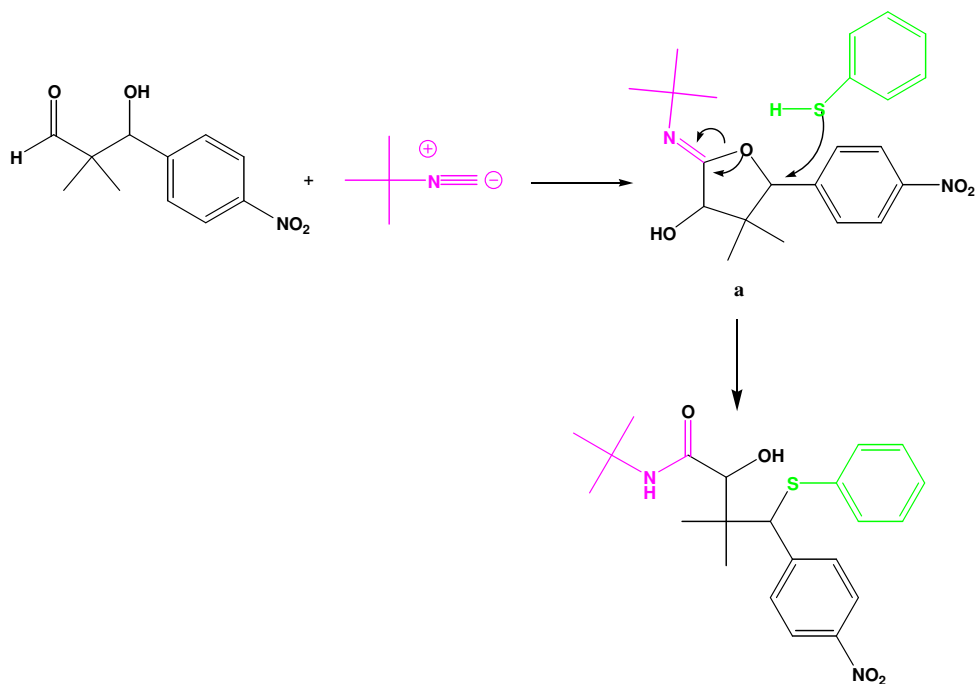


Scheme 46



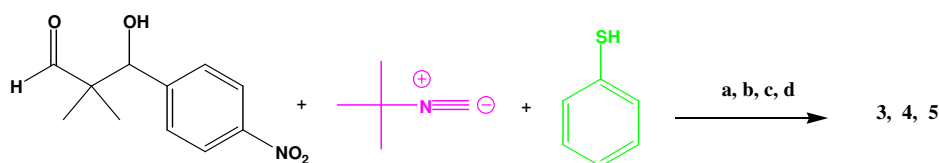
Scheme 47

To confirm this hypothesis, we repeated the reaction, in different conditions, between the aldehyde **2**, tert-butyl isocyanide and the nucleophile thiophenol. We hoped that, once the imino lactone **a** is formed, thiophenol instead of water, can open **a** in an $\text{S}_{\text{N}}2$ process giving three-component product as shown in **Scheme 48**.



Scheme 48

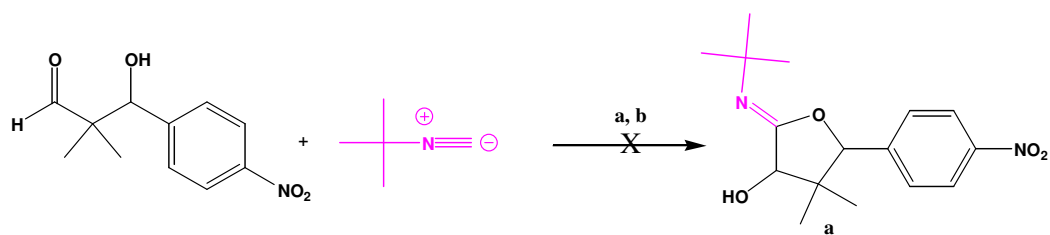
The following conditions were tried out to lead to the formation of the desired products. We performed the reaction in different solvents and we found out that the reaction in DMSO, acetonitrile, and isopropanol did not work. We tried also to use dry MeOH and the drying agent trimethyl orthoformate to reduce water in the reaction mixture but, in both cases, we noticed from $^1\text{H-NMR}$ the formations of **3**, **4** and **5**. Also the addition of $\text{B}(\text{OMe})_3$ led to the formation of the same products (**Scheme 49**).



Reaction conditions: β -hydroxy aldehyde (1 equiv.), isocyanide (1 equiv.), thiophenol (1 equiv.), *a*) $\text{B}(\text{OMe})_3$ (2 equiv.), DCE, microwave 83°C, 15 min., *b*) MeOH, microwave 65°C, 15 min., *c*) dry MeOH, microwave 65°C, 15 min., *d*) trimethyl orthoformate (1 equiv.), dry MeOH, microwave 65°C, 15 min.

Scheme 49

Finally we performed the reaction between only the aldehyde **2** and tert-butyl isocyanide to see if the desired imino lactone **a** is formed (**Scheme 50**). Then, if the reaction works, we hypothesized that **a** can be opened by thiophenol, giving the multicomponent product as shown in **Scheme 48**. Also this last attempt was unsuccessful.



Reaction conditions: a) aldehyde (1 equiv.), isocyanide (2 equiv.), MeOH, microwave 65°C, 15 min. b) aldehyde (2 equiv.), isocyanide (1 equiv.), MeOH, microwave 65°C, 15 min.

Scheme 50

3.2 Aminoalcohols

The amino alcohols used for MCRs are shown in **Figure 10**.

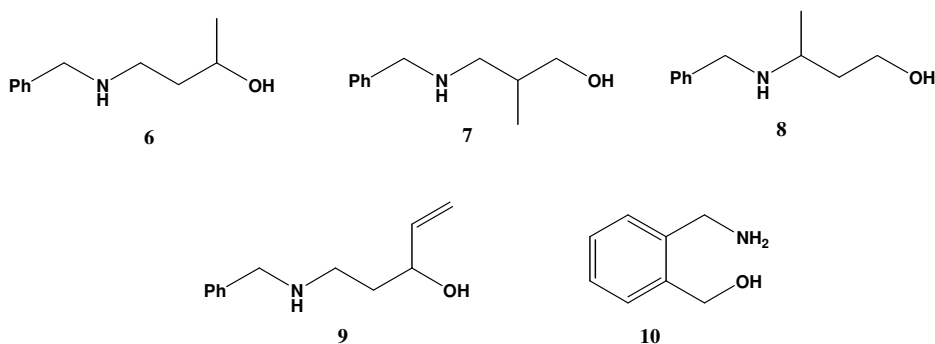
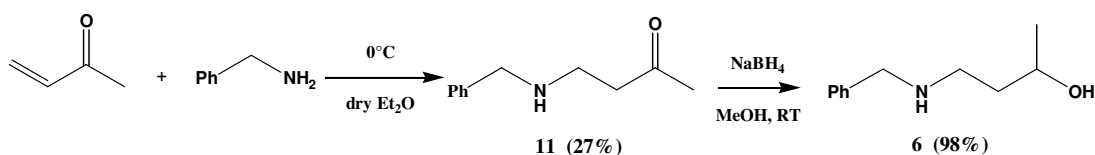


Figure 10: Aminoalcohols used for MCRs.

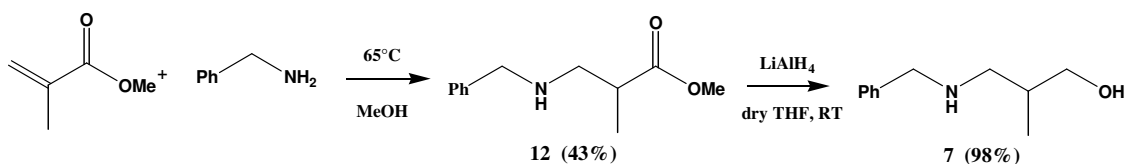
3.2.1 Synthesis of aminoalcohols

Compound **6** was synthesized from methyl-vinyl ketone and benzylamine. Michael addition of the amine to the double bond⁶⁴³ gave the intermediate **11**, and after reduction of the carbonyl group with NaBH₄, the aminoalcohol **6** is formed (**Scheme 51**).



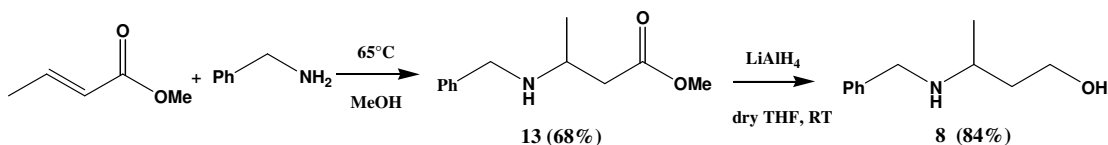
Scheme 51

Compound **7** was synthesized from methyl methacrylate and benzylamine. Michael addition of the amine to the double bond,⁶⁴³ gave the intermediate **12**. Reduction of the carbonyl group with LiAlH₄ afforded the aminoalcohol **7** (**Scheme 52**).



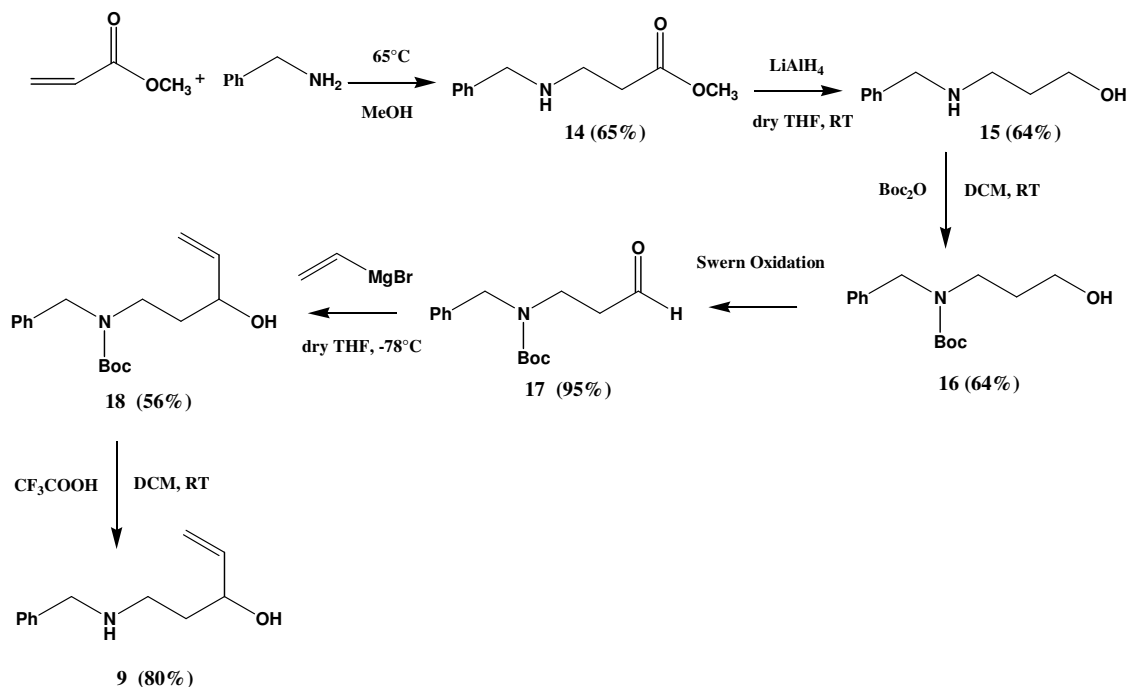
Scheme 52

The synthesis of aminoalcohol **8** is shown in **Scheme 53**. After reaction between methyl crotonate and benzylamine,⁶⁴³ the carbonyl group of intermediate **13** was reduced to alcohol giving the compound **8**.



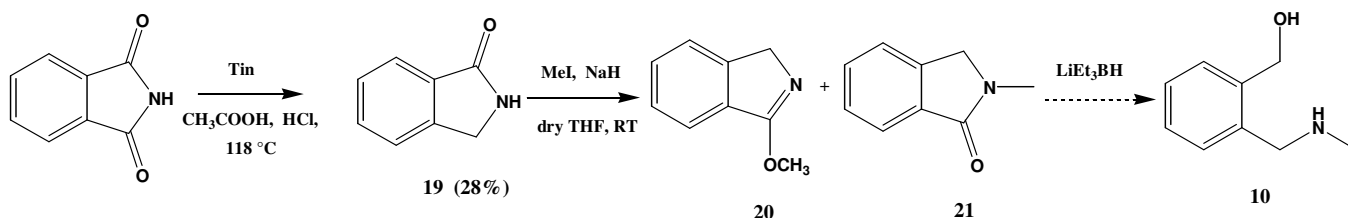
Scheme 53

The synthesis of aminoalcohol **9** is shown in **Scheme 54**. Michael addition between benzylamine and methyl acrylate⁶⁴³ gave the intermediate **14**. Reduction of the carbonyl group with LiAlH₄ afforded the aminoalcohol **15** which was treated with di-*t*-Butyl dicarbonate leading to the *N*-protected aminoalcohol **16**. The hydroxyl group was subsequently oxidized to aldehyde affording **17**. Reaction with vinyl magnesium bromide (**18**) and deprotection with trifluoroacetic acid gave the final aminoalcohol **9**.



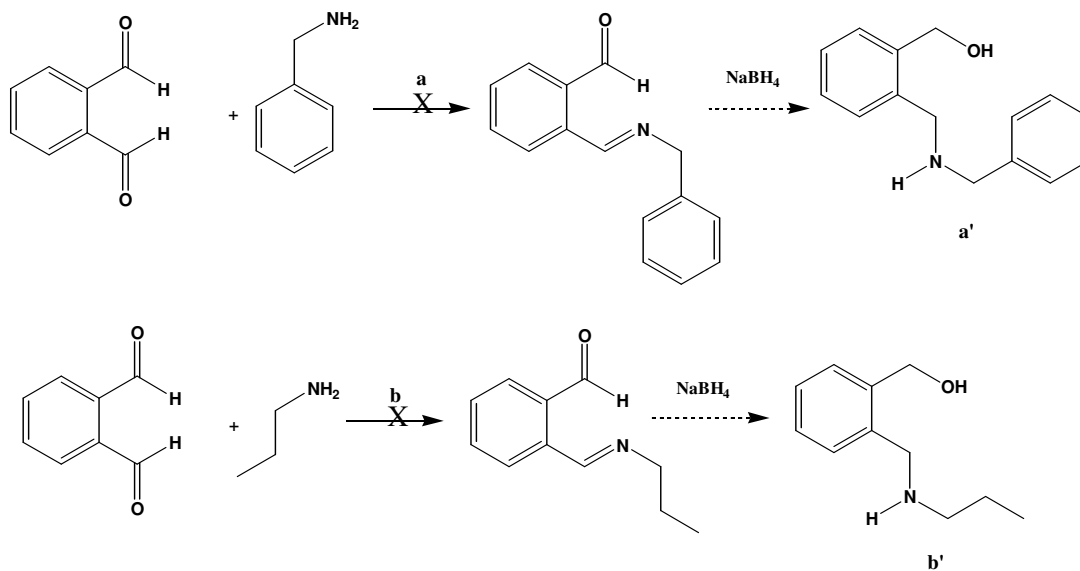
Scheme 54

For the synthesis of **10** several ways were tried out. The first attempt is shown in **Scheme 55**. Phthalimide was reduced with tin in glacial acetic acid and HCl affording 2,3-dihydro-isoindol-1-one **19**.⁶⁴⁴ Methylation of **19** (Method A) gave a mixture of two compounds. The major compound was **20** while the desired **21** was the minor. If the methylation would have given **21** in good yield, we could have tried the reduction with LiEt₃BH.



Scheme 55

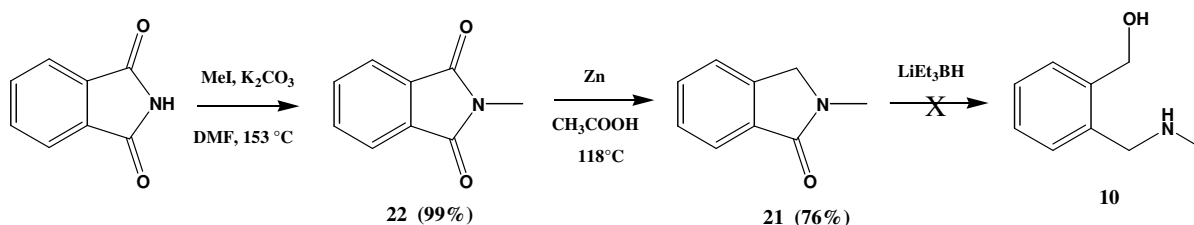
The second way is shown in **Scheme 56**. We performed the reaction between phthaldialdehyde, benzylamine or propylamine. We hoped that, if an imine is formed, reduction of the imine gives the aminoalcohols **a'** and **b'** shown below. We tried the reaction at reflux in toluene with Dean- Stark apparatus, or at RT in methanol but all attempts did not give a successful result. The crude ¹H-NMR revealed the imine was not formed.



Reaction conditions: Phthaldialdehyde (3 equiv.), amine (1 equiv.), a) toluene, reflux with Dean-Stark apparatus, 4 h, b) dry MeOH, RT overnight.

Scheme 56

The last attempt is shown in **Scheme 57**. Methylation of phthalimide gave the intermediate **22** which was reduced to **21** with zinc in acetic acid (Method B).⁶⁴⁵ Reduction of **21** with an excess (5 equiv.) of LiEt_3BH ⁶⁴⁶ produced many side products and none of them could be isolated. On the other hand, reduction with 2 equivalents of LiEt_3BH did not work. From crude $^1\text{H-NMR}$ we could observe only starting materials.

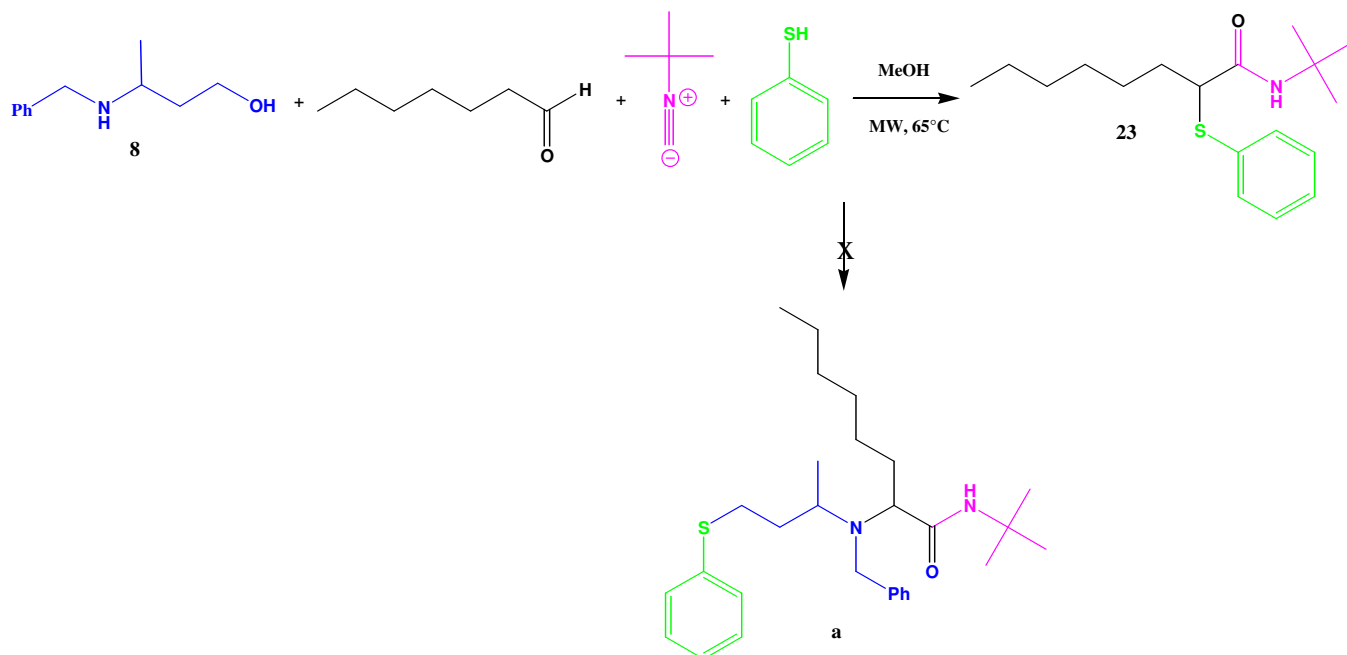


Scheme 57

3.2.2 Multicomponent reactions with aminoalcohol **8**

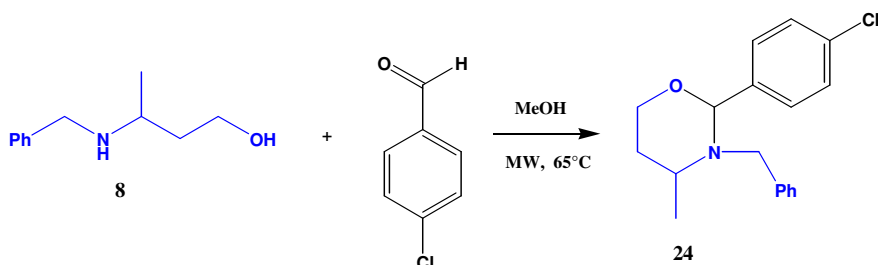
As described in the introduction, the four-component reaction between N-alkylamino alcohols, aldehydes, isocyanides and carboxylic acids leads to N-acyloxy amides **e** (**Scheme 16**). Replacing carboxylic acids with general nucleophiles leads to multicomponent products (**Scheme 17**).

The first attempt was to try a four-component reaction between the aminoalcohol **8**, pentanal, tert-butyl isocyanide and the nucleophile thiophenol (**Scheme 58**). Surprisingly the reaction did not give the desired product **a**. New products were observed and the main product could be identified as **23**.



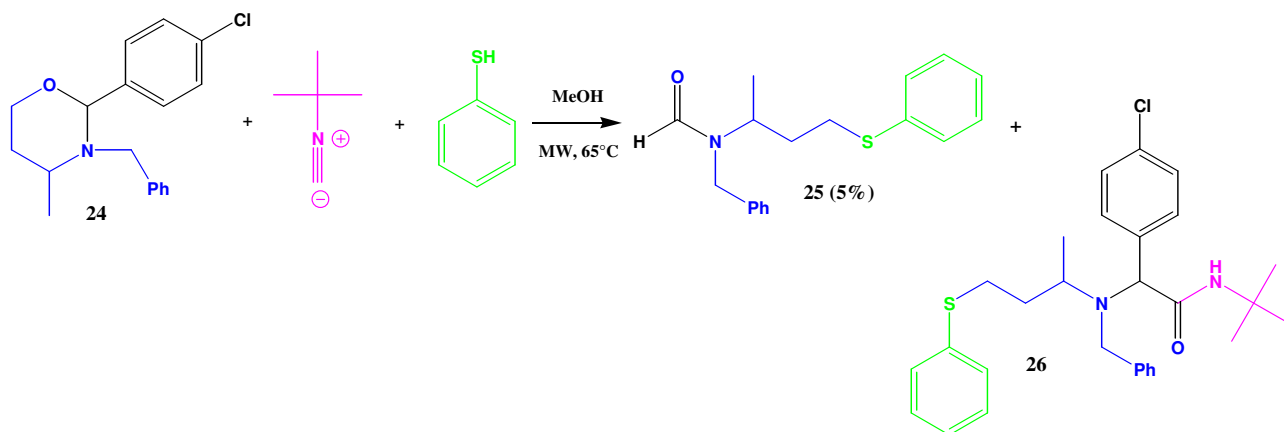
Scheme 58

We therefore decided to synthesize at first the N-O cyclic acetal **a** shown above in **Scheme 37**. We hypothesized the isocyanide and thiophenol could react easier with this intermediate leading to the formation of the desired product. The synthesis of the intermediate is shown in **Scheme 59**. The reaction between **8** and para-chlorobenzaldehyde gave the intermediate **24** which was used without further purification in the next step.



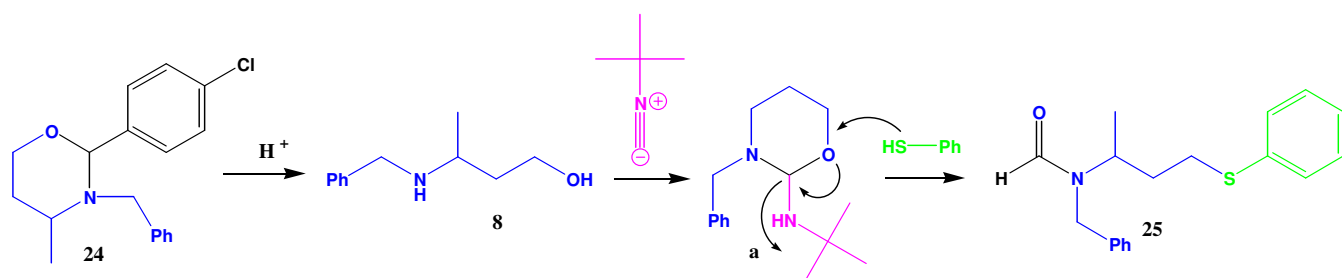
Scheme 59

It was found that, from the reaction between **24**, tert-butyl isocyanide and thiophenol, the main product was **25** (**Scheme 60**). From crude $^1\text{H-NMR}$ and $^{13}\text{C-NMR}$ we could see that also the desired **26** is formed, but the conversion is too low and it could not be fully isolated.



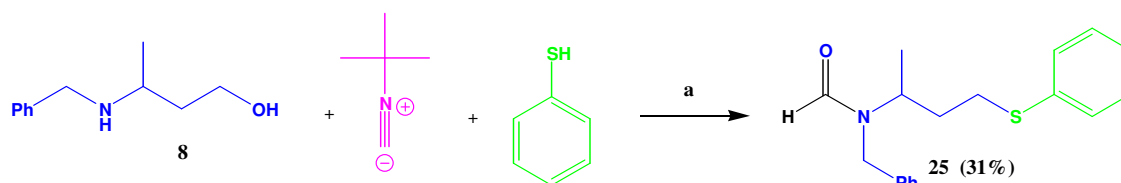
Scheme 60

To explain why **25** is formed, it is thought that the acidity of thiophenol causes the hydrolysis of the N-O acetal **24** and the release of the aminoalcohol **8** which can react with tert-butyl isocyanide giving the cyclic intermediate **a** (**Scheme 61**). Then, thiophenol opens the cycle in a $\text{S}_{\text{N}}2$ with liberation of the tert-butylamino group, giving the product **25**.



Scheme 61

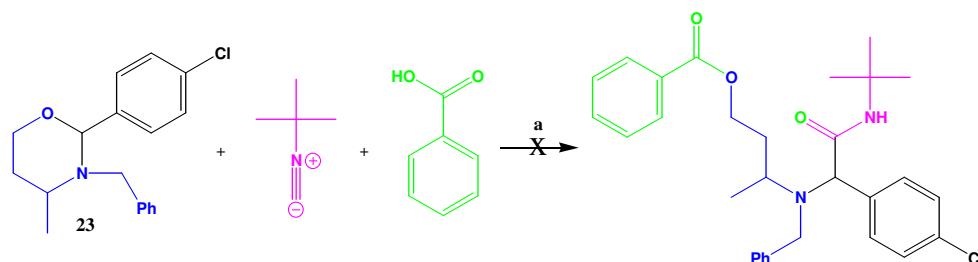
To confirm this hypothesis, the reaction between **8**, tert-butyl isocyanide and thiophenol was performed leading to **25** in 31% yield (**Scheme 62**).



Reaction conditions: **8** (1 equiv.), tert-butyl isocyanide (1 equiv.), thiophenol (1 equiv.), *a*) MeOH, microwave 65 °C, 15 min.

Scheme 62

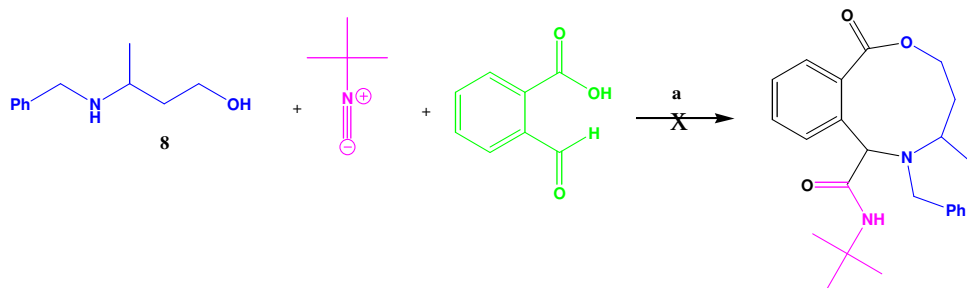
Since the reaction with thiophenol did not give the desired product in good yield, we decided to attempt the reaction using another nucleophile like benzoic acid. From the mechanism discussed above (**Scheme 37**), the reaction should give the product shown in **Scheme 63**. From crude $^1\text{H-NMR}$ we could see new products but none of them could be fully isolated and identified.



Reaction conditions: **23** (1 equiv.), tert-butyl isocyanide (1 equiv.), benzoic acid (1 equiv.) para-toluenesulphonic acid (10%), *a*) isopropanol, microwave 82 °C, 15 min.

Scheme 63

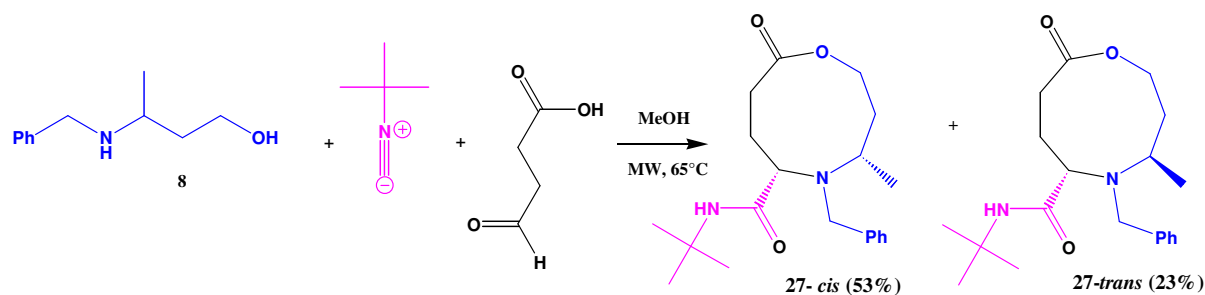
We were moreover interested in reactions between an aminoalcohol and a bifunctional substrate that contains the aldehyde group and the carboxylic acid to allow the synthesis of medium ring heterocycles. The first attempt was to try a MCR between 2-carboxy-benzaldehyde, aminoalcohol **8** and tert-butyl isocyanide. The reaction did not give the desired nine-membered ring shown in **Scheme 64**.



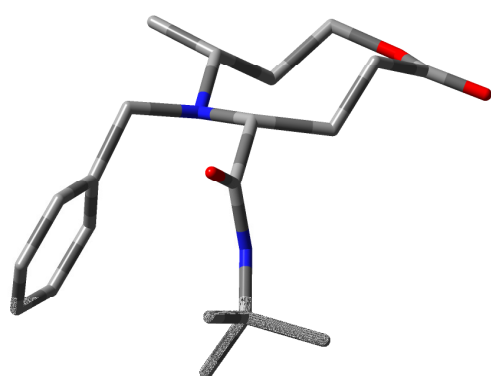
Reaction conditions: **8** (1 equiv.), tert-butyl isocyanide (1 equiv.), 2-carboxy-benzaldehyde (1 equiv.), a) MeOH, microwave 65 °C, 15 min.

Scheme 64

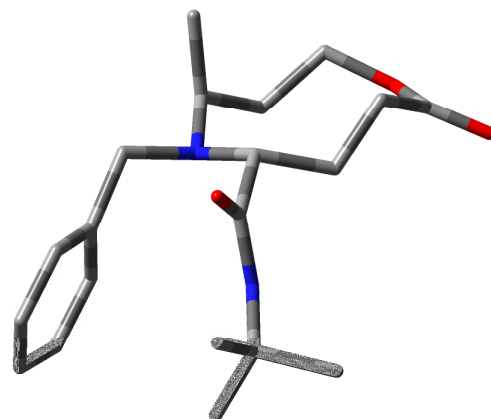
We therefore turned our attention to another bifunctional substrate, 4-oxo-butyric acid. The reaction between **8**, 4-oxo-butyric acid and tert-butyl isocyanide gave the products shown in **Scheme 65**. It was possible to separate the two diastereoisomers and from the comparison of J-couplings and from NOESY experiments we could state that the major compound (53% yield) is the *cis* isomer while the minor compound (23% yield) is the *trans* (**Fig. 11**).



Scheme 65



27-cis

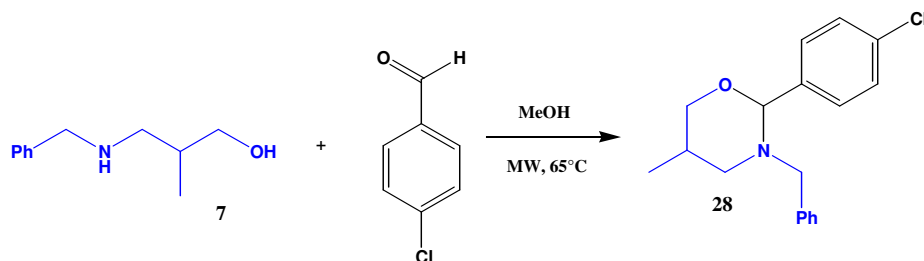


27-trans

Figure 11: Nine membered-ring heterocycles **27**.

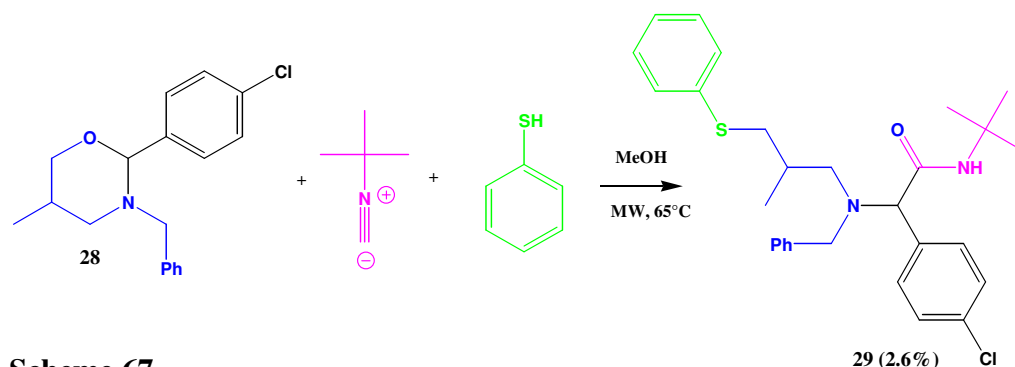
3.2.3 Multicomponent reactions with aminoalcohol 7

Then we decided to investigate MCRs with another aminoalcohol (**7**). As we did for the aminoalcohol **8**, at first, the reaction between **7** and para-chlorobenzaldehyde was performed to obtain the intermediate **28** (Scheme 66).



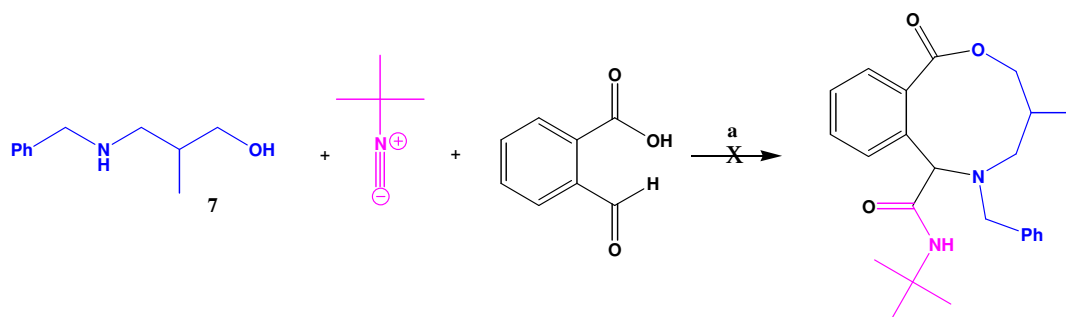
Scheme 66

The intermediate **28** was then used in the three-component reaction with tert-butyl isocyanide and thiophenol (Scheme 67). The reaction gave **29** in 2.6% yield. To increase the yield of this product, different conditions were tried out. We repeated the reaction at RT and 40 °C and with more equivalents of nucleophile and isocyanide but none led to a more successful result.



Scheme 67

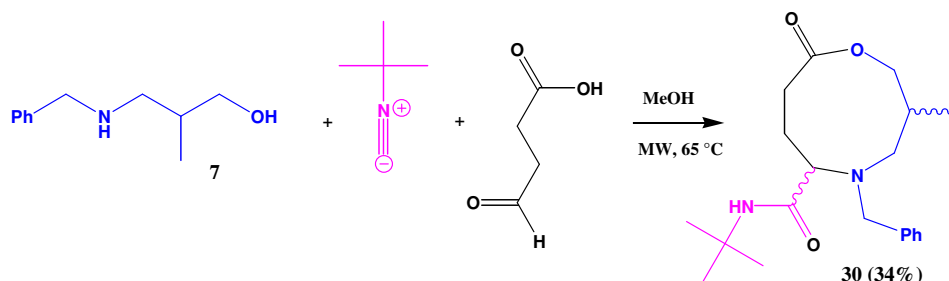
The reaction between **7** and the bifunctional substrate 2-carboxy benzaldehyde should give the product shown in Scheme 68 but the reaction did not work.



Reaction conditions: **7** (1 equiv.), tert-butyl isocyanide (1 equiv.), 2-carboxy-benzaldehyde (1 equiv.), a) MeOH, microwave 65 °C, 15 min.

Scheme 68

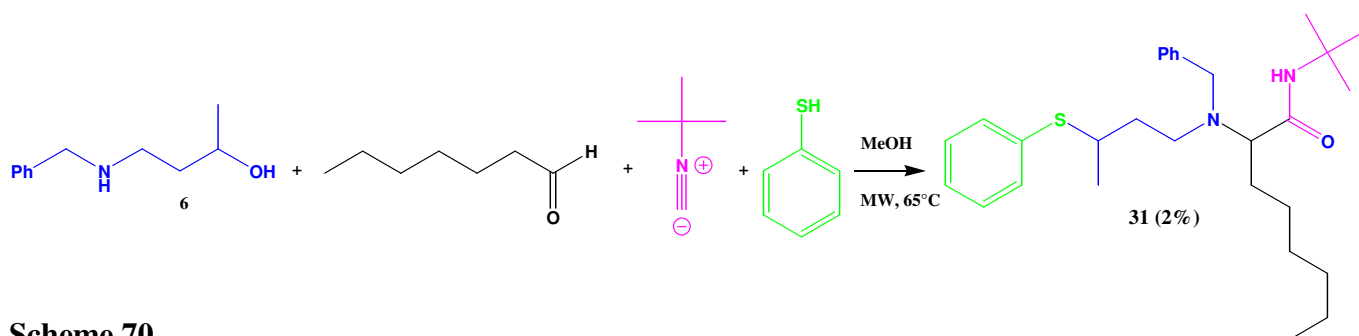
On the other hand the reaction between **7** and 4-oxo-butyric acid gave the nine-membered ring **30** (Scheme 69). The $^1\text{H-NMR}$ and $^{13}\text{C-NMR}$ revealed a mixture of *cis* and *trans* products, but it was not possible to separate the two diastereoisomers by flash chromatography. The two diastereoisomers are in a ratio of 1:1.1.



Scheme 69

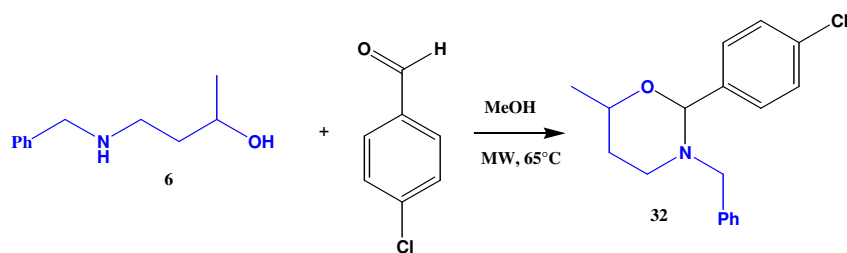
3.2.4 Multicomponent reactions with aminoalcohol **6**

We decided to turn our attention to the aminoalcohol **6**. At first, we tried the four-component reaction between **6**, pentanal, tert-butyl isocyanide and thiophenol. The reaction gave the desired compound **31** (Scheme 70) but the yield was very low (2%). Only one of the two possible diastereoisomers was isolated.



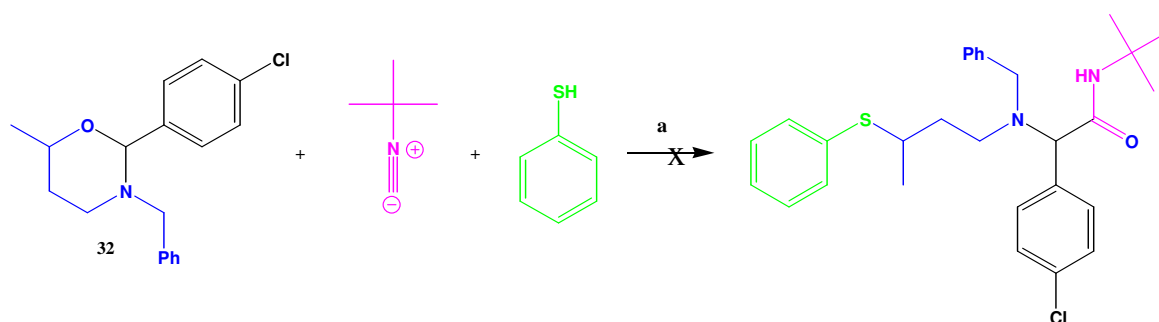
Scheme 70

In order to increase the yield, we decided firstly to synthesize the cyclic intermediate **32** (Scheme 71), as we did for the aminoalcohols **7** and **8**. **32** was formed from the reaction between **6** and para-chlorobenzaldehyde.



Scheme 71

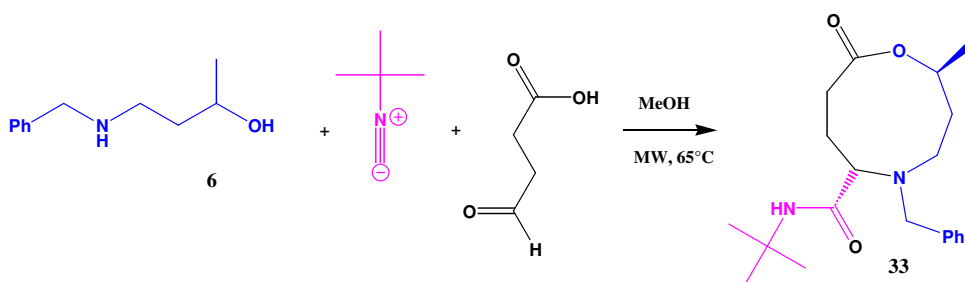
The intermediate **32** was then used in the three-component reaction with tert-butyl isocyanide and thiophenol. The reaction should give the product shown in **Scheme 72**. From crude $^1\text{H-NMR}$ we could still observe starting materials and, unfortunately, the desired product could not be isolated and characterized. It is possible that the intermediate **32** is very stable, and it cannot be easily opened by a nucleophile as thiophenol to give the desired multicomponent product.



Reaction conditions: **32** (1 equiv.), tert-butyl isocyanide (1 equiv.), thiophenol (1 equiv.), a) MeOH, microwave 65 °C, 15 min.

Scheme 72

The reaction between the aminoalcohol **6** and the bifunctional substrate 4-oxo-butyric gave the nine-membered heterocycle **33** (**Scheme 73**). Only one of the two diastereoisomers could be isolated and from NOESY experiment and from comparison of J-couplings it was possible to identify the diastereoisomer as *trans* (**Fig. 12**). From crude $^1\text{H-NMR}$ it was not possible to observe the *cis* diastereoisomer because the crude $^1\text{H-NMR}$ was very complex.



Scheme 73

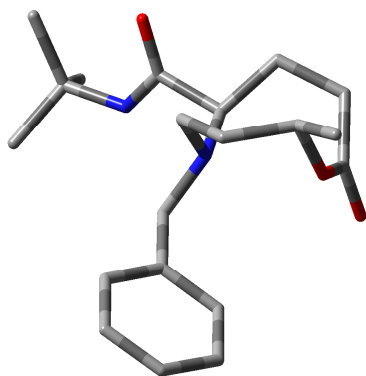
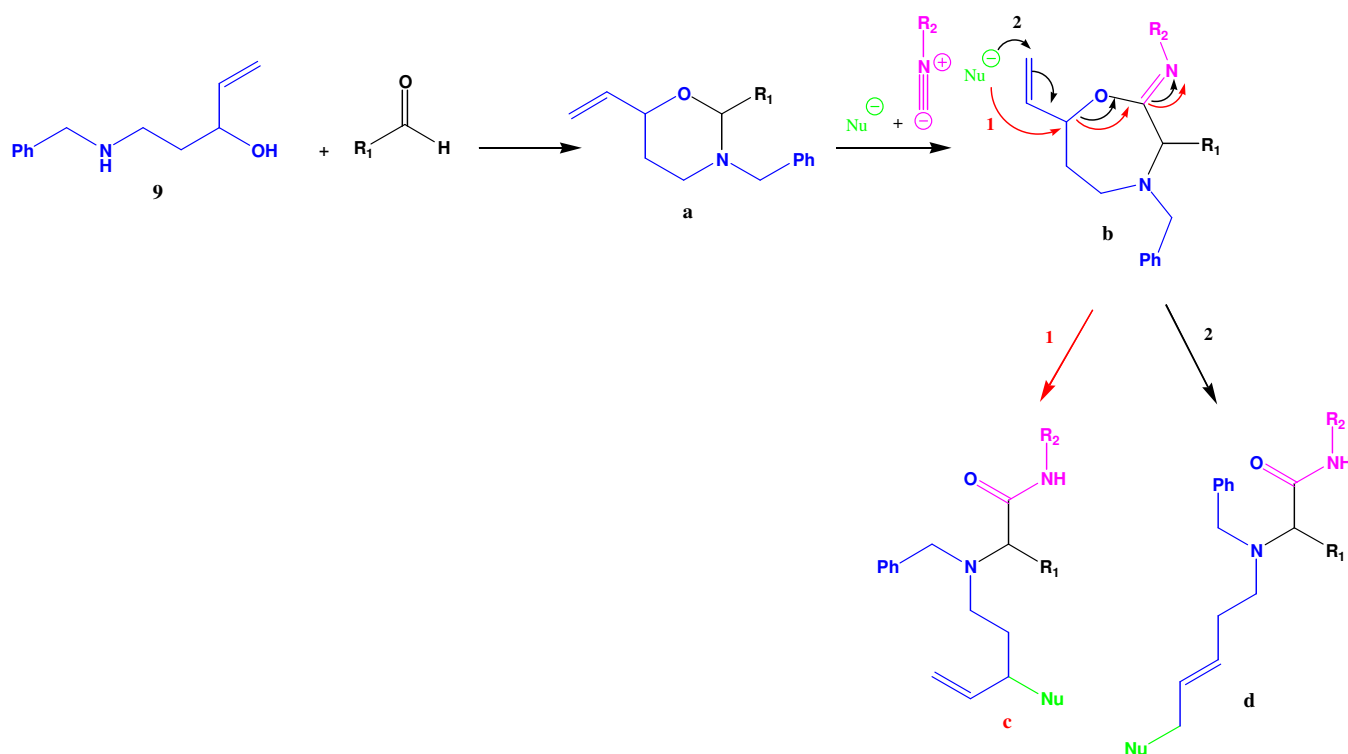


Figure 12: Nine membered- ring heterocycles **33** (*trans*).

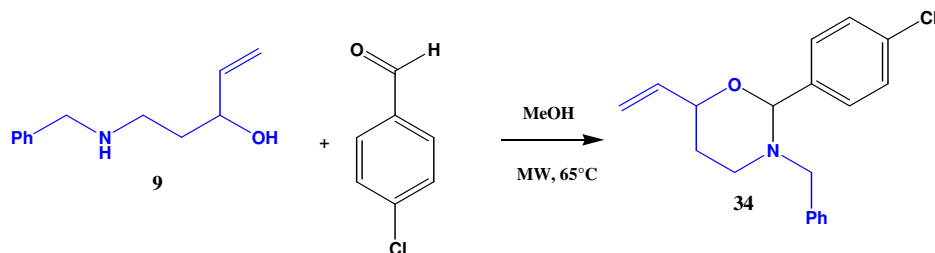
3.2.5 Multicomponent reactions with aminoalcohol **9**

We then decided to turn our attention to the aminoalcohol **9**. Two plausible mechanisms can be envisaged for this aminoalcohol (**Scheme 74**). First of all the reaction between **9** and an aldehyde could give the intermediate **a**, which reacts with an isocyanide to form the seven-membered ring intermediate **b**. As we observed with the other aminoalcohols, the nucleophile could open the cycle with a S_N2 reaction affording the product **c**. Alternatively, the nucleophile could attack the double bond giving the final product **d**.



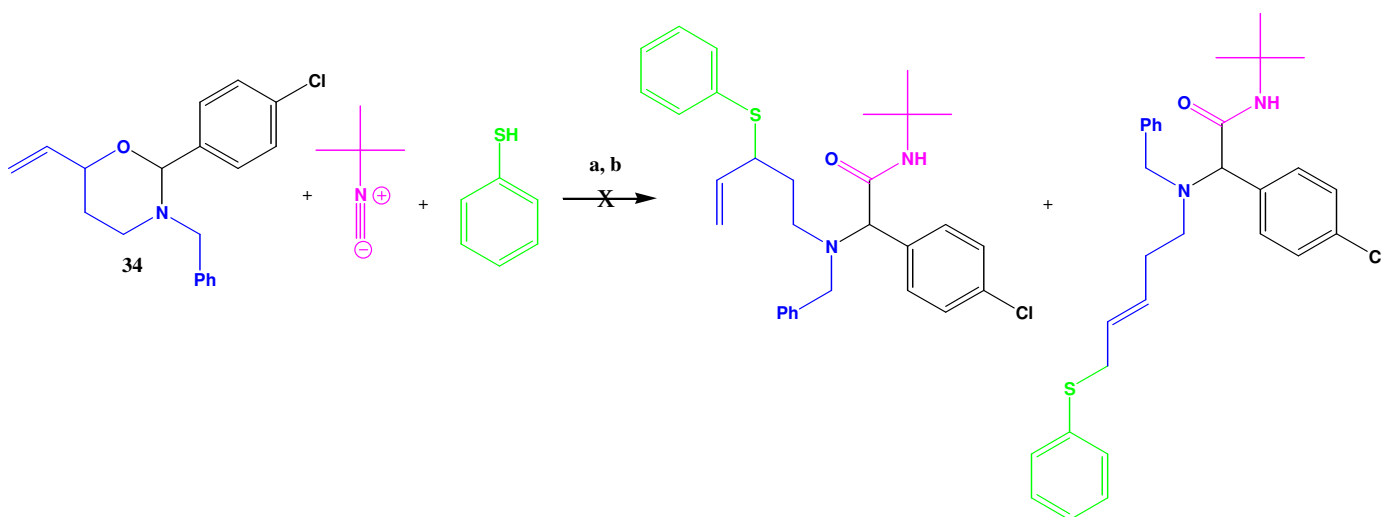
Scheme 74

To study this mechanism, the reaction between **9** and para-chloro benzaldehyde was performed at first, affording the intermediate **34** (**Scheme 75**).



Scheme 75

The intermediate **34** was then allowed to react with tert-butyl isocyanide and the nucleophile thiophenol as shown in **Scheme 76**. Analysis by TLC and ¹H-NMR revealed a complex mixture of products. None was fully isolated and characterized but none of the desired products was present.



Reaction conditions: **34** (1 equiv.), tert-butyl isocyanide (1 equiv.), 2-carboxy-benzaldehyde (1 equiv.), a) MeOH, microwave 65 °C, 15 min., b) MeOH, RT, 8 h.

Scheme 76

3.2.6 Multicomponent reactions with carbonyl-carboxylic compounds **35** and **35'**

Finally, we decided to investigate MCRs using others bifunctional substrates like the pyridine derivatives shown in **Figure 13**.

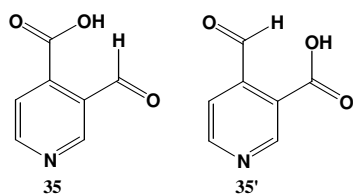
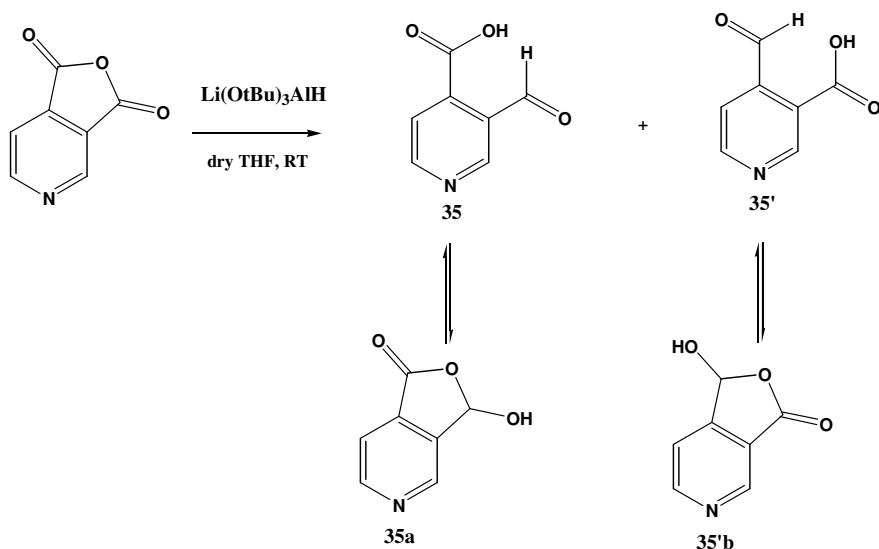


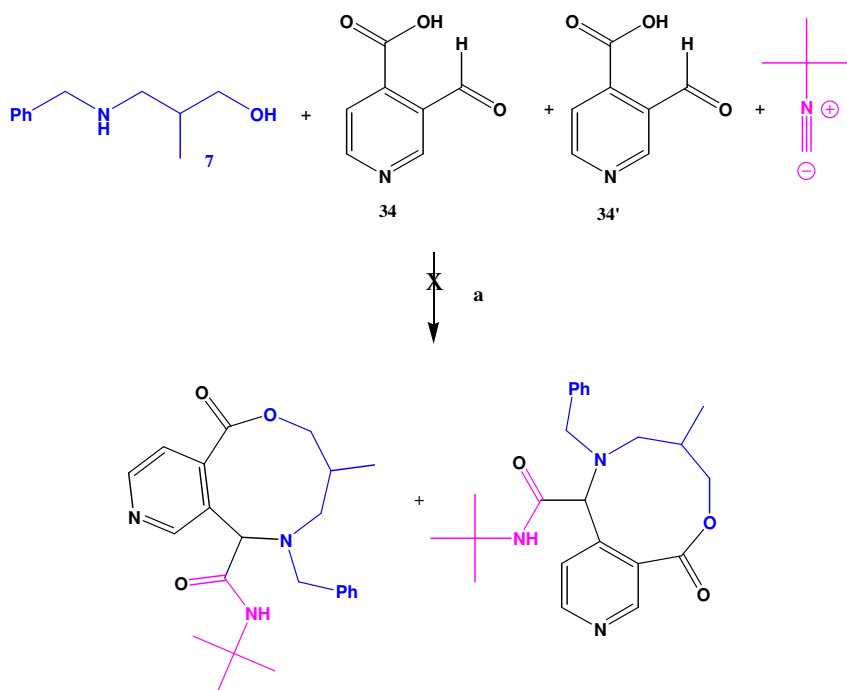
Figure 13: Pyridine derivatives used in MCRs.

Compounds **35** (3-Formyl-isonicotinic acid) and **35'** (4-Formyl-nicotinic acid) were synthesized from reduction of 3,4-pyridinedicarboxylic anhydride with $\text{Li}(\text{OtBu})_3\text{AlH}$ (**Scheme 77**).⁶⁴⁷ From $^1\text{H-NMR}$ and $^{13}\text{C-NMR}$ it was possible to observe that **35** and **35'** are in equilibrium with the hydroxyphthalide form **35a** and **35'b**, respectively. It was not possible to purify and separate **35** and **35'** because these pyridine derivatives are not very soluble in most organic solvents.



Scheme 77

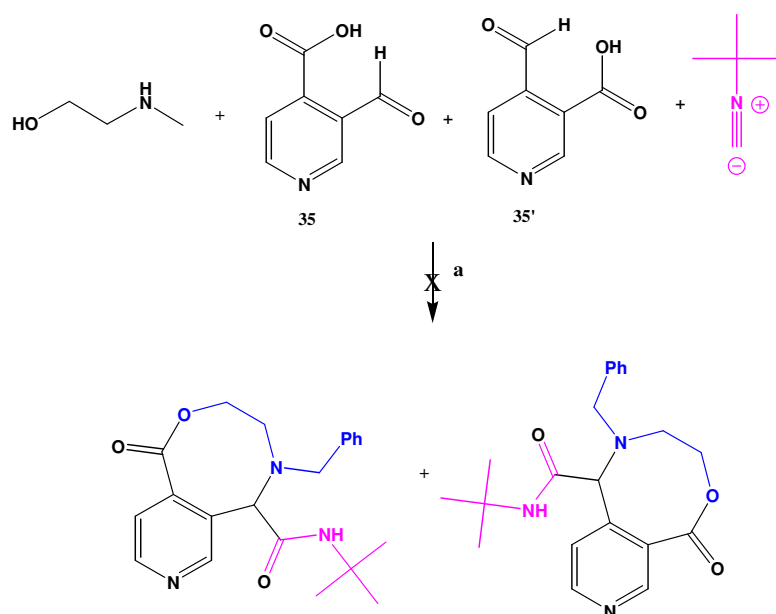
The mixture of **35** and **35'** was used in a three-component reaction with the aminoalcohol **7** and tert-butyl isocyanide (**Scheme 78**). By analogy to the mechanism envisaged in **Scheme 38**, the reaction should give the products shown in **Scheme 78**. From crude $^1\text{H-NMR}$ we could observe only starting materials



Reaction conditions: **35-35'** (1 equiv.), **7** (1 equiv.), tert-butyl isocyanide (1 equiv.), *a*) MeOH microwave 65 °C, 15 min.

Scheme 78

Finally, the mixture of **35** and **35'** was reacted with a simpler aminoalcohol, 2-methylamino-ethanol (**Scheme 79**).



Reaction conditions: **35-35'** (1 equiv.), 2-methylamino-ethanol (1 equiv.), tert-butyl isocyanide (1 equiv.), *a*) MeOH microwave 65 °C, 15 min.

Scheme 79

Also in this case, from crude $^1\text{H-NMR}$ we could observe only starting materials. We can envisage that hydroxyphthalide form **35a** and **35'b** are more stable than the form with free carboxylic and aldehyde group. So these functional groups are not able to interact with the aminoalcohol and isocyanide and lead to the synthesis of medium ring heterocycles.

4 Conclusions and Future Works

We explored MCRs of aldol products like **1** and **2** and a hydroxy ketone like 5-hydroxy-2-pentanone. We tried out three-component reactions (Scheme **41**, **42** and **44**) between these bifunctional molecules, tert-butyl isocyanide and a primary or secondary amine. None of the reactions gave the desired imino lactone. We also tried four-component reactions, adding the nucleophile thiophenol, (Scheme **43** and **45**) but all attempts to synthesize the desired Ugi-type products were unsuccessful. It was only possible to identify the side products **3**, **4** and **5**.

We also investigated new isocyanide-based MCRs using three-carbon chain aminoalcohols that contain a methyl substituent. We demonstrated that the reaction between an aminoalcohol, an aldehyde, tert-butyl isocyanide and thiophenol gave amide products in low yield. We can envisage that, the cyclic *N,O*-acetal obtained from the reaction between the aminoalcohol and the aldehyde (Scheme **37**), is very stable and cannot easily be opened by a nucleophile. All attempts to increase the yield were unsuccessful. Moreover, increasing the temperature or increasing the reaction time did not improve the yield but sometimes increased the amount of side products.

Reactions between the new aminoalcohols **6**, **7** and **8** and the bifunctional substrate 2-carboxy benzaldehyde did not work but surprisingly with 4-oxo-butyric acid the nine-membered ring heterocycles were obtained in moderate yields. The synthesis of medium rings is often difficult due to the unfavorable thermodynamics of the ring closing process, so these reactions are valuable as they offer a one-pot route to synthesize functionalized medium ring systems from readily available starting materials.

In the future it would be interesting focus on the optimization of the reaction conditions to improve the yields of these nine-membered ring heterocycles. Moreover if the work was carried on, we would investigate the synthesis of a more diverse range of aminoalcohols and other bifunctional substrates for the synthesis of nine, ten, eleven-membered ring products.

Finally different reaction conditions for 5-benzylamino-pent-1-en-3-ol (aminoalcohol **9**) would be explored because it would be interesting study the chemistry of an aminoalcohol which has a reactive group like a double bond.

5 Experimental section

All reactions were carried out at atmospheric pressure with stirring unless otherwise indicated. All solvents and chemicals were purchased from suppliers and used without further purification.

Reactions were monitored by TLC and $^1\text{H-NMR}$. TLC plates pre-coated with silica gel 60 F₂₅₄ on aluminium (Merk KGaA) were used, being visualized by UV (254 or 365 nm) or chemical stain (KMnO_4 , and phosphomolybdic acid). Normal phase silica gel (DBH, 40-63 μm) was used for flash column chromatography.

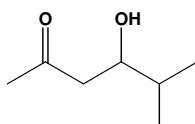
Melting points were determined using Reichert hot-stage apparatus and are uncorrected. Infrared (IR) spectra were recorded on a Perkin-Elmer spectrum 100 FT-IR spectrometer as thin film.

$^1\text{H-NMR}$ spectra were recorded at 300 MHz, 500 MHz, and 400 MHz on a Bruker Avance spectrometers or at 600 MHz on a AMX600 spectrometer. Chemical shifts were measured in ppm and are quoted as δ , relative to TMS. Multiplicities are quoted as s (singlet), d (doublet), t (triplet), q (quartet), quintet and m (multiplet), br (broad) with coupling constants defined as J given in Hz.

$^{13}\text{C-NMR}$ was recorded at 75 MHz, 100 MHz and 125 MHz, on a 300 MHz, 400 MHz, and 500 MHz Bruker Avance spectrometers respectively, and at 150 MHz on a AMX600 spectrometer.

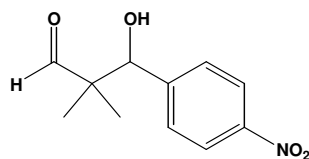
High and low resolution mass spectra were recorded by Dr. Lisa Haigh using a VG70 SE instrument operating in modes CI, EI, ES, and FAB.

4-Hydroxy-5-methyl-hexan-2-one (1)⁶⁴¹



L-Proline (144 mg, 1.25 mmol) was stirred in a mixture of acetone (8 ml) and DMSO (33 ml) at RT for 15 min. Isobutyraldehyde was added (300 mg, 4.16 mmol) and the mixture was stirred at RT for 3 days. After evaporating the solvent, ammonium chloride (10 ml) was added and then extracted with ethyl acetate (2 x 10 ml). The combined organic layers were washed with brine (10 ml), dried over MgSO_4 and concentrated *in vacuo*. The residue was purified by flash chromatography (ethyl acetate-petrol, 8:2) to give the hydroxy ketone as a yellow oil (243 mg, 1.87 mmol, 45%); ν_{max} (film/ cm^{-1}) 3434, 2961, 2877, 1705; δ_{H} (500 MHz, CDCl_3) 0.90 (3H, d, J 6.8, CH_3) 0.93 (3H, d, J 6.8, CH_3), 1.63-1.73 (1H, m, $\text{CH}-(\text{CH}_3)_2$), 2.20 (3H, s, $\text{CH}_3-\text{C}=\text{O}$), 2.53 (1H, dd, J 9.6, 17.5, $\text{CHH}-\text{C}=\text{O}$), 2.62 (1H, dd, J 17.5, 2.5, $\text{CHH}-\text{C}=\text{O}$), 3.79-3.83 (1H, ddd, J 9.6, 5.8, 2.5, $\text{CH}-\text{OH}$); δ_{C} (125 MHz, CDCl_3) 17.8, 18.4, 30.9, 33.1, 47.0, 72.3, 210.4.

3-Hydroxy-2,2-dimethyl-3-(4-nitro-phenyl)-propionaldehyde (**2**)⁶⁴²

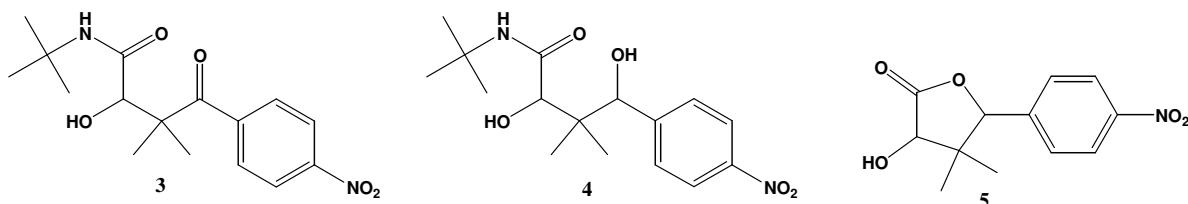


p-Nitrobenzaldehyde (1 g, 6.6 mmol) was dissolved in anhydrous DMSO (7 ml) and isobutyraldehyde (571 mg, 7.92 mmol) was added. To the mixture, acetic acid (1.65 mmol) and pyrrolidine (0.33 mmol) were added. After stirring for 2 h at RT, the reaction mixture was directly purified by flash chromatography (petrol-ethyl acetate, 8:2) affording the aldol product as a white solid (563 mg, 2.5 mmol, 38%); ES $[M+H^+]$: 224, $C_{11}H_{14}NO_4$; δ_H (500 MHz, $CDCl_3$) 0.98 (3H, s, CH_3), 1.06 (3H, s, CH_3), 5.04 (1H, s, $CH-OH$), 7.50 (2H, d, J 8.4, Ar), 8.21 (2H, d, J 8.4, Ar), 9.61 (1H, s, $HC=O$); δ_C (125 MHz, $CDCl_3$) 15.68, 19.96, 50.86, 76.23, 123.19, 128.49, 146.94, 147.67, 205.91.

N-tert-Butyl-2-hydroxy-3,3-dimethyl-4-(4-nitro-phenyl)-4-oxo-butyramide (**3**)

N-tert-Butyl-2,4-dihydroxy-3,3-dimethyl-4-(4-nitro-phenyl)-butyramide (**4**)

3-Hydroxy-4,4-dimethyl-5-(4-nitro-phenyl)-dihydro-furan-2-one (**5**)



Aldehyde **2** (75 mg, 0.34 mmol), diethylamine (37 mg, 0.50 mmol), tert-butyl isocyanide (42 mg, 0.50 mmol) and thiophenol (56 mg, 0.50 mmol) were dissolved in MeOH (0.85 ml). The mixture was stirred under microwave irradiation at 65°C for 15 min. The solvent was evaporated under reduced pressure and the crude was purified by flash chromatography (petrol-ethyl acetate, 7:3) affording a mixture of **3** and **4** as a transparent oil in a ratio of 1:1.5, respectively (18.3 mg).

3 and **4**: ν_{max} (film/ cm^{-1}) 3360, 2972, 1642, 1605, 1518, 1350, 851, 733.

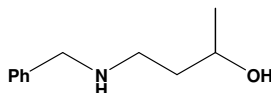
3: δ_H (600 MHz, $CDCl_3$) 1.17 (3H, s, CH_3), 1.19 (3H, s, CH_3), 1.39 (9H, s, tBu), 3.79 (1H, d, J 5.8, OH), 4.22 (1H, d, J 5.8, $CH-OH$), 6.43 (1H, br s, NH), 7.38 (2H, d, J 8.8, Ar), 8.29 (2H, d, J 8.8, Ar); δ_C (150 MHz, $CDCl_3$) 22.39, 23.06, 28.92, 44.90, 51.44, 78.84, 123.53, 129.07, 139.80, 147.83, 164.42, 170.68.

4: δ_H (600 MHz, $CDCl_3$) 0.85 (3H, s, CH_3), 0.89 (3H, s, CH_3), 1.41 (9H, s, tBu), 3.06 (1H, d, J 4.5, OH), 4.22 (1H, d, J 4.5, $CH-OH$), 4.63 (1H, d, J 3.9, OH), 4.69 (1H, d, J 3.9, $CH-OH$), 6.50 (1H, br

s, NH), 7.53 (2H, d, J 8.8, Ar), 8.18 (2H, d, J 8.8, Ar); δ_C (150 MHz, $CDCl_3$) 18.93, 19.77, 28.86, 43.20, 51.69, 75.60, 76.85, 122.89, 129.07, 147.30, 148.66, 172.12.

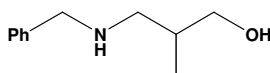
5 (not isolated): δ_H (500 MHz, $CDCl_3$) 0.62 (3H, s, CH_3), 1.35 (3H, s, CH_3), 4.37 (1H, s, $CH-OH$), 5.20 (1H, s, $CH-COO$), 7.49 (2H, d, J 8.7, Ar), 8.28 (2H, d, J 8.7, Ar); δ_C (125 MHz, $CDCl_3$) 14.75, 22.56, 46.49, 76.90, 84.59, 123.76, 126.85, 141.23, 142.76, 175.73.

4-Benzylamino-butan-2-ol (**6**)



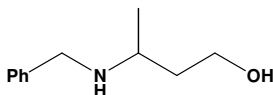
11 (676 mg, 3.81 mmol) was dissolved in MeOH (5 ml) and $NaBH_4$ (288 mg, 7.62 mmol) was added carefully at 0°C. The mixture was stirred at RT for 15 min. After evaporating the solvent, $NaBH_4$ in excess was quenched at 0°C with 2M HCl. The aqueous phase was washed with DCM (2 x 20 ml), basified with 1M NaOH, and then extracted with DCM (3 x 20 ml). The combined organic layers were dried over $MgSO_4$ and concentrated *in vacuo* affording **6** as an orange oil (668 mg, 3.73 mmol, 98%); ν_{max} (film/ cm^{-1}) 3295, 3062, 3027, 2963, 2924, 2832, 1494, 1453, 733; δ_H (500 MHz, $CDCl_3$) 1.17 (3H, d, J 6.2, CH_3), 1.60-1.64 (1H, m, CHH), 1.48-1.55 (1H, m, CHH), 2.78 (1H, td, J 10.9, 3.4, $CHH-N$), 3.01 (1H, ddd, J 12.0, 4.8, 3.4, $CHH-N$) 3.74 (1H, d, J 13.1, $CHH-Ph$), 3.82 (1H, d, J 13.1, $CHH-Ph$), 3.99 (1H, m, $CH-CH_3$), 7.27-7.34 (5H, m, Ar); δ_C (125 MHz, $CDCl_3$) 23.71, 37.11, 48.09, 53.84, 69.13, 127.17, 128.21, 128.51, 139.65.

3-Benzylamino-2-methyl-propan-1-ol (**7**)



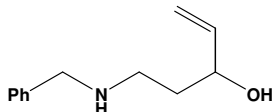
A solution of **12** (500 mg, 2.40 mmol) in anhydrous THF (5 ml) was added carefully at 0 °C and under an argon atmosphere, to a suspension of $LiAlH_4$ (137 mg, 3.60 mmol) in anhydrous THF. The mixture was warmed at RT and then stirred for 2 h. The reaction was quenched at 0 °C by dropwise addition of water (0.1 ml), followed by 1N NaOH (0.4 ml) and water (0.3 ml). Then, the mixture was filtered, dried over $MgSO_4$ and concentrated *in vacuo* affording **7** as a yellow oil (421 mg, 2.35 mmol, 98%); ν_{max} (film/ cm^{-1}) 3303, 2954, 2832, 1495, 1453, 1041, 740; δ_H (300 MHz, $CDCl_3$) 0.76 (3H, d, J 6.9, CH_3), 1.82-1.91 (1H, m, $CH-CH_3$), 2.53 (1H, dd J 11.7, 2.0, $CHH-N$), 2.72-2.77 (1H, m, $CHH-N$), 3.46 (1H, dd J 10.7, 1.9, $CHH-OH$), 3.57-3.62 (1H, m, $CHH-OH$), 3.65 (1H, d, J 13.2, $CHH-Ph$), 3.74 (1H, d, J 13.2, $CHH-Ph$), 7.18-7.30 (5H, m, Ar); δ_C (125 MHz, $CDCl_3$) 15.04, 34.48, 54.16, 56.62, 70.48, 127.26, 128.23, 128.58, 139.31.

3-Benzylamino-butan-1-ol (8)



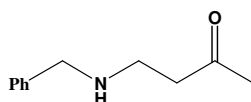
A solution of **13** (504 mg, 2.87 mmol) in anhydrous THF (5 ml) was added carefully at 0 °C and under an argon atmosphere to a suspension of LiAlH₄ (163 mg, 4.30 mmol) in anhydrous THF. The mixture was warmed at RT and then stirred for 2 h. The reaction was quenched at 0 °C by dropwise addition of water (0.2 ml), followed by 1N NaOH (0.5 ml) and water (0.6 ml). Then, the mixture was filtered, dried over MgSO₄ and concentrated *in vacuo* affording **8** as a yellow oil (430 mg, 3.40 mmol, 84%); ν_{\max} (film/cm⁻¹) 3294, 1453, 1085, 906, 698; δ_{H} (500 MHz, CDCl₃) 1.21 (3H, d, J 6.6, CH₃), 1.57 (1H, dtd, J 14.5, 8.5, 3.5, CHH), 1.74 (1H, dtd J 14.5, 6.2, 3.1, CHH), 2.98-3.04 (1H, m, CH-CH₃), 3.78, (1H, ddd, J 10.7, 8.5, 3.1, CHH-OH), 3.79 (1H, d, J 12.8, CHH-Ph), 3.84-3.88 (1H, m, CHH-OH), 3.89 (1H, d, J 12.8, CHH-Ph), 7.24-7.27 (3H, m, Ar), 7.30-7.33 (2H, m, Ar); δ_{C} (125 MHz, CDCl₃) 20.32, 37.30, 51.20, 53.51, 62.09, 127.19, 128.28, 128.57, 139.85.

5-Benzylamino-pent-1-en-3-ol (9)



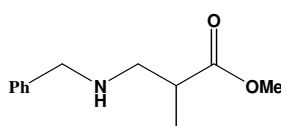
Trifluoroacetic acid (103 mg, 0.90 mmol) was added dropwise at 0° C to a solution of **18** (44 mg, 0.15 mmol) in DCM (1 ml). The mixture was stirred at RT for 2 h after which it was quenched with water. The aqueous layer was washed with DCM (3 x 10 ml), basified with 1N NaOH and then extracted with DCM (3 x 10 ml). The combined organic phases were dried over MgSO₄ and evaporated to dryness affording **9** as a yellow-orange oil (22 mg, 0.11 mmol, 80%); ν_{\max} (film/cm⁻¹) 3457, 3021, 2970, 2947, 1437; δ_{H} (400 MHz, CDCl₃) 1.58-1.67 (1H, m, CHH), 1.79 (1H, dddd, J 14.6, 9.4, 6.4, 3.1, CHH), 2.85 (1H, ddd J 12.0, 9.4, 3.4, CHH-N), 3.03 (1H, ddd, J 12.0, 6.4, 3.5 CHH-N), 3.77 (1H, d, J 13.0, CHH-Ph), 3.83 (1H, d, J 13.0, CHH-Ph), 4.36-4.40 (1H, m, CH-OH), 5.12 (1H, dd, J 10.5, 1.7, HCH=CH), 5.30 (1H, ddd, J 17.3, 1.7, HCH=CH), 5.88 (1H, ddd, J 17.3, 10.5, 5.1, CH₂=CH), 7.26-7.37 (5H, m, Ar); δ_{C} (100 MHz, CDCl₃) 34.78, 47.56, 53.78, 74.01, 113.80, 127.28, 128.23, 128.54, 139.20, 140.97.

4-Benzylamino-butan-2-one (11)⁶⁴³



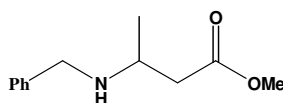
Methyl vinyl ketone (1 g, 14.30 mmol), dissolved in anhydrous Et₂O (3.6 ml), was added at 0 °C over a period of 3 h to a solution of benzylamine (3 g, 28.60 mmol) dissolved in anhydrous Et₂O (7 ml). The solvent was evaporated under reduced pressure and the crude was purified by flash chromatography (petrol-DCM-ethanol, 1:8.5:0.5) affording **11** as a yellow oil (676 mg, 3.81 mmol, 27%); ν_{\max} (film/cm⁻¹) 3320, 3062, 3028, 2923, 2824, 1715, 1603, 1494, 735, 699; δ_{H} (500 MHz, CDCl₃) 1.97 (3H, s, CH₃), 2.47 (2H, t, J 6.4, CH₂-C=O), 2.71 (2H, t, J 6.4, CH₂-N), 3.65 (2H, s, CH₂-Ph), 7.10-7.16 (2H, m, Ar), 7.19-7.21 (3H, m, Ar); δ_{C} (125 MHz, CDCl₃) 30.03, 43.71, 43.88, 53.98, 126.91, 128.09, 128.38, 140.36, 208.20.

3-Benzylamino-2-methyl-propionic acid methyl ester (**12**)⁶⁴³



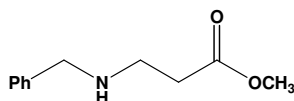
A mixture of methyl methacrylate (10 g, 0.10 mol) and benzylamine (11 g, 0.10 mol) in MeOH (50 ml) was stirred at reflux for 20 h. After evaporating the solvent, the crude was purified by flash chromatography (petrol-ethyl acetate, 8:2) affording **12** as a yellow oil (9 g, 0.04 mol, 43%); ν_{\max} (film/cm⁻¹) 3328, 2921, 2841, 1730, 1453, 1436, 1169, 735, 697; δ_{H} (300 MHz, CDCl₃) 1.12 (3H, d, J 6.9, CH₃), 2.57-2.68 (2H, m, CH₂), 2.78-2.87 (1H, m, CH-CH₃), 3.61 (3H, s, OCH₃), 3.73 (2H, s, CH₂-Ph), 7.15-7.27 (5H, m, Ar); δ_{C} (125 MHz, CDCl₃) 15.28, 40.04, 51.54, 52.12, 53.73, 126.91, 128.04, 128.36, 140.35.

3-Benzylamino-butyric acid methyl ester (**13**)⁶⁴³



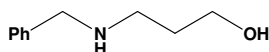
A mixture of methyl crotonate (10 g, 0.10 mol) and benzylamine (11 g, 0.10 mol) in MeOH (50 ml) was stirred at reflux for 20 h. After evaporating the solvent, the crude was purified by flash chromatography (petrol-ethyl acetate, 8:2) affording **13** as a yellow oil (13 g, 0.07 mol, 68%); ν_{\max} (film/cm⁻¹) 3318, 2955, 2870, 1731, 1453, 1436, 1174, 732; δ_{H} (500 MHz, CDCl₃) 1.07 (3H, d, J 6.3, CH₃), 2.29 (1H, dd, J 15.0, 5.7, CHH-COO), 2.40 (1H, dd, J 15.0, 6.8, CHH-COO), 3.05-3.11 (1H, m, CH-CH₃), 3.56 (3H, s, OCH₃), 3.65 (1H, d, J 13.4, CHH-Ph), 3.74 (1H, d, J 13.4, CHH-Ph), 7.13-7.16 (1H, m, Ar), 7.22 (2H, t, J 7.5, Ar), 7.26 (2H, t, J 7.5, Ar); δ_{C} (150 MHz, CDCl₃) 20.16, 41.10, 49.54, 51.02, 51.38, 126.95, 128.13, 128.39, 140.11, 172.67.

3-Benzylamino-propionic acid methyl ester (**14**)⁶⁴³



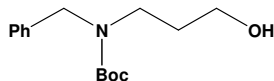
A mixture of methyl acrylate (10 g, 0.12 mol) and benzylamine (13 g, 0.12 mol) in MeOH (50 ml) was stirred at reflux for 20 h. After evaporating the solvent, the crude was purified by flash chromatography (petrol-ethyl acetate, 8:2) affording **14** as a yellow oil (15 g, 0.08 mol, 65%); ν_{\max} (film/cm⁻¹) 3328, 2951, 2841, 1730, 1453, 1436, 1169, 734, 697; δ_{H} (300 MHz, CDCl₃) 2.42 (2H, t, J 6.5 CH₂-COO), 2.78 (2H, t, J 6.5 CH₂-N), 3.55 (3H, s, OCH₃), 3.69 (2H, s, CH₂-Ph), 7.23-7.11 (5H, m, Ar); δ_{H} (75 MHz, CDCl₃) 34.38, 44.47, 51.36, 53.65, 126.86, 128.02, 128.32, 140.34, 172.98.

3-Benzylamino-propan-1-ol (**15**)



A solution of **14** (5 g, 28.30 mmol) in anhydrous THF (10 ml) was added carefully at 0 °C and under an argon atmosphere, to a suspension of LiAlH₄ (1 g, 28.30 mmol) in anhydrous THF. The mixture was warmed at RT and then stirred for 2 h. The reaction was quenched at 0 °C by dropwise addition of water (1 ml), followed by 1N NaOH (2.5 ml) and water (3 ml). Then, the mixture was filtered, dried over MgSO₄, and concentrated *in vacuo* affording **15** as a yellow oil (3 g, 18 mmol, 64%); ν_{\max} (film/cm⁻¹) 3291, 2930, 2840, 1494, 1453, 1068, 732, 697; δ_{H} (500 MHz, CDCl₃) 1.64-1.69 (2H, m, CH₂), 2.88 (2H, t, J 5.8 CH₂-N), 3.77 (2H, s, CH₂-Ph), 3.79 (2H, t, J 5.4, CH₂-OH), 7.24-7.34 (5H, m, Ar); δ_{C} (125 MHz, CDCl₃) 30.91, 49.26, 54.04, 64.16, 127.24, 128.23, 128.58, 139.60.

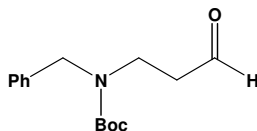
Benzyl-(3-hydroxy-propyl)-carbamic acid tert-butyl ester (**16**)



Boc₂O (201 mg, 0.92 mmol) was added at 0 °C to a solution of **15** (160 mg, 0.97 mmol) in DCM (1 ml). The mixture was stirred at RT for 1 h. The solvent was evaporated under reduced pressure and the crude was purified by flash chromatography (petrol-ethyl acetate, 7:3) affording **16** as a yellow oil (169 mg, 0.64 mmol, 64%); ν_{\max} (film/cm⁻¹) 3451, 2970, 2943, 1740, 1666, 1415, 1160, 733, 698; δ_{H} (400 MHz, CDCl₃, 58 °C) 1.50 (9H, s, OtBu), 1.66-1.72 (2H, m, CH₂), 3.39 (2H, t, J 6.1,

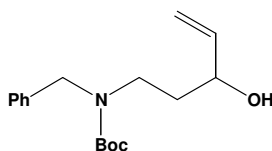
CH₂-N), 3.60 (2H, br m, CH₂-OH), 4.43 (2H, s, CH₂-Ph), 7.24-7.36 (5H, m, Ar); δ_C (125 MHz, CDCl₃) 28.44, 30.25, 42.26, 50.54, 58.47, 80.62, 127.29, 127.38, 128.61, 138.19, 157.17

Benzyl-(3-oxo-propyl)-carbamic acid tert-butyl ester (**17**)



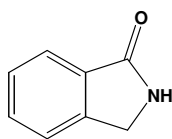
Oxalyl chloride (53 mg, 0.42 mmol) was added dropwise to a solution of DMSO (65 mg, 0.83 mmol) in dry CH₂Cl₂ (4 ml) cooled to -78 °C. The solution was stirred at this temperature for 15 min., after which **16** (85 mg, 0.32 mmol) was added. The resulting mixture was stirred for 1 h at -78°C, then NEt₃ (162 mg, 1.6 mmol) was added and the mixture was stirred at RT for 4 h. The reaction was quenched with water and the phases were separated. The organic layer was washed with brine, dried over MgSO₄, filtered and evaporated to dryness. The crude was purified by flash chromatography (petrol-ethyl acetate, 9:1) affording **17** as an orange oil (80 mg, 0.64 mmol, 95%); v_{\max} (film/cm⁻¹) 2971, 1728, 1737, 1688, 1453, 1414, 1162, 734, 699, δ_H (400 MHz, CDCl₃) 1.44 (9H, s, OtBu), 2.55 (2H, td, J 6.7, 1.4, CH₂-C=O), 3.48 (2H, t, J 6.7, CH₂-N), 4.41 (2H, s, CH₂-Ph), 7.19-7.29 (5H, m, Ar), 9.67 (1H, t, J 1.4, HC=O); δ_C (100 MHz, CDCl₃) 28.30, 40.80, 43.11, 50.99, 80.03, 127.22, 127.42, 128.47, 138.25, 155.41, 200.14.

Benzyl-(3-hydroxy-pent-4-enyl)-carbamic acid tert-butyl ester (**18**)



A solution of vinyl magnesium bromide (383 mg, 2.92 mmol) in anhydrous THF was added slowly at -78°C to a solution of **17** (192 mg, 0.73 mmol) in anhydrous THF (2 ml). The mixture was stirred at -78°C for 3 h. The reaction was quenched with a solution of NH₄Cl (40 ml). The aqueous phase was extracted with Et₂O (3 x 10 ml). The combined organic layers were dried over MgSO₄, filtered and evaporated to dryness affording **18** as a orange oil (119 mg, 0.41 mmol, 56%); v_{\max} (film/cm⁻¹) 3449, 2971, 1739, 1690, 1416, 1163, 699; δ_H (400 MHz, DMSO, 100°C) 1.43 (9H, s, OtBu), 1.58-1.73 (2H, m, CH₂), 3.25 (2H, ddd, J 8.1, 6.6, 3.6, CH₂-N), 3.96 (1H, br m, CH-OH), 4.34 (1H, br s, OH), 4.40 (2H, s, CH₂-Ph), 4.99 (1H, dd, J 10.5, 1.7, HCH=CH), 5.15 (1H, dd, J 17.2, 1.7, HCH=CH), 5.83, (1H, ddd, J 17.2, 10.5, 5.5, CH₂=CH), 5.35-5.32 (2H, m, Ar), 7.27-7-23 (3H, m, Ar); δ_C (125 MHz, DMSO) 28.03, 35.28 (br), 43.35, 59.75 (br), 68.94, 78.70, 113.17, 126.94, 127.10, 128.39, 138.78 (br), 142.07, 170.33.

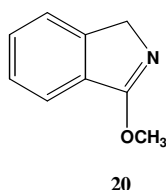
2,3-Dihydro-isoindol-1-one (**19**)⁶⁴⁵



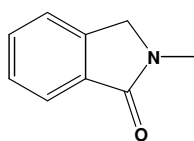
Tin powder (13 g, 10.7 mmol) was added to a vigorously stirred suspension of phthalimide (6 g, 41 mmol) in a mixture of glacial acetic acid (5 ml) and concentrated HCl (2.5 ml). The reaction mixture was heated at reflux for 2 h and then filtered hot. The filtrate was concentrated and the residue portioned between DMC and water. The organic layer was separated and the aqueous phase extracted with DCM (3 x 20 ml). The combined organic extracts were dried over MgSO₄, filtered and concentrated *in vacuo*. The crude was purified by flash chromatography (petrol-ethyl acetate, 1:9) affording **19** as a white solid (1.53 g, 11.00 mmol, 28%); mp= 150 °C; δ_{H} (300 MHz, CDCl₃) 4.44, (2H, s, CH₂), 7.44-7.48 (2H, m, Ar), 7.51 (1H, d, J 8.0, Ar), 7.83, (1H, t, J 8.0, Ar); δ_{C} (100 MHz, CDCl₃), δ_{c} (125MHz, CDCl₃) 45.91, 123.25, 123.70, 128.03, 131.75, 132.36, 143.42, 172.45,

3-Methoxy-1H-isoindole (**20**)

2-Methyl-2,3-dihydro-isoindol-1-one (**21**)



20



21

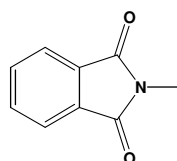
Method A: **19** (1.8 g, 13.40 mmol) was added under argon to a suspension of NaH (643 mg, 26.80 mmol) in anhydrous THF (15 ml). After 30 min, MeI (3 g, 20.10 mmol) was added and the mixture was stirred at RT for 18 h. The solvent was evaporated, water (15 ml) was added and the aqueous layer neutralized with 10% HCl. After extraction with ethyl acetate (3 x 15 ml) and evaporation of the solvent, the crude was purified by flash chromatography (petrol-ethyl acetate, 2:8) affording a mixture of **20** and **21** as a white solid in a ratio of 2:1, respectively (500 mg).

Method B⁶⁴⁵: A solution of N-methyl phthalimide (1.57 g, 13.50 mmol) in acetic acid (32 ml) was heated to 60 °C and Zn dust was added at once with mechanical stirring. The reaction mixture was heated at reflux with stirring for 4 h and then filtered hot on a sintered Buchner-type funnel. The filter cake was washed with acetic acid (3 x 10 ml). The filtrate was evaporated to a small volume under reduced pressure. Saturated solution of NaHCO₃ was added and the mixture was extracted with CHCl₃ (3 x 20 ml). The combined extracts were washed once with water and dried over MgSO₄. Evaporation of the solvent under reduced pressure afforded **21** as a white solid (1.50 g, 10.20 mmol, 76%).

20 (not isolated): δ_{H} (500 MHz, CDCl_3) 1.61 (2H, s, CH_2), 2.95 (3H, s, CH_3), 7.37 (2H, m, Ar), 7.48 (1H, t, J 7.8, Ar), 7.73 (1H, d, J 7.8, Ar); δ_{C} (75 MHz, CDCl_3 , mixture of two rotamers) 23.22, 23.35, 88.30, 88.67, 119.82, 121.64, 123.12, 123.19, 129.48, 129.66, 130.48, 131.89, 132.27, 136.20, 143.02, 140.12, 166.65, 167.25.

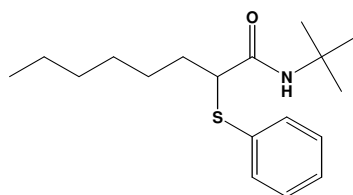
21: mp= 114 °C; δ_{H} (500 MHz, CDCl_3) 3.19 (3H, s, CH_3), 4.37 (2H, s, CH_2), 7.42-7.46 (2H, m, Ar), 7.52 (1H, t, J 7.6, Ar), 7.79 (1H, d, J 7.6, Ar); δ_{C} (75MHz, CDCl_3) 29.33, 51.91, 122.58, 123.33, 127.86, 131.07, 132.77, 140.98, 168.51.

2-Methyl-isoindole-1,3-dione (**22**)



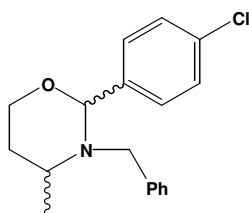
Phthalimide (2 g, 13.60 mmol) and K_2CO_3 are dissolved in DMF (20 ml). After 15 min, MeI was added and the mixture was stirred at reflux for 3 h after which water (120 ml) was added and the aqueous phase was extracted with EtOAc (3 x 20 ml). The combined organic phases were washed with a solution of LiCl, dried over MgSO_4 , filtered and evaporated to dryness affording **22** as a yellow solid (1.57 g, 13.50 mmol, 99%); mp= 135 °C; δ_{H} (500 MHz, CDCl_3) 3.14 (3H, s, CH_3), 7.67 (2H, dd, J 5.4, 3.0, Ar), 7.79 (2H, dd, J 5.4, 3.0, Ar); δ_{C} (125 MHz, CDCl_3) 23.97, 123.19, 132.27, 133.91, 168.49.

2-Phenylsulfanyl-octanoic acid tert-butylamide (**23**)



8 (158 mg, 0.88 mmol), pentanal (101 mg, 0.88 mmol), tert-butyl isocyanide (73 mg, 0.88 mmol) and thiophenol (97 mg, 0.88 mmol) were dissolved in MeOH (1 ml). The mixture was stirred under microwave irradiation at 65°C for 15 min. Evaporation of the solvent under reduced pressure afforded **23** (100 mg, not isolated); δ_{H} (600 MHz, CDCl_3) 0.67-0.69 (1H, br m, CHH), 0.85 (3H, t, CH_3), 0.99-1.04 (2H, br m, CHH , CHH), 1.12-1.17 (2H, m, CH_2), 1.19-1.28 (4H, CH_2 , CHH , CHH), 1.40 (9H, s, tBu), 1.44-1.50 (1H, br m, CHH), 2.86 (1H, d, J 9.2, CH-C=O), 7.40 (2H, d, J 6.0 Ar), 7.57-7.59 (3H, m, Ar); δ_{H} (150 MHz, CDCl_3) 14.24, 22.78, 26.41, 29.31, 29.34, 32.08, 37.52, 55.85, 56.30, 129.29, 129.38, 131.07, 136.72, 160.77.

3-Benzyl-2-(4-chloro-phenyl)-4-methyl-[1,3]oxazinane (24)



Para-chlorobenzaldehyde (235 mg, 1.67 mmol) and **8** (200 mg, 1.11 mmol) were dissolved in MeOH (1 ml). The mixture was stirred under microwave irradiation at 65°C for 15 min. Evaporation of the solvent under reduced pressure affording **24** as a mixture of two diastereoisomers in a ratio of 1:1.4 (220 mg, not isolated).

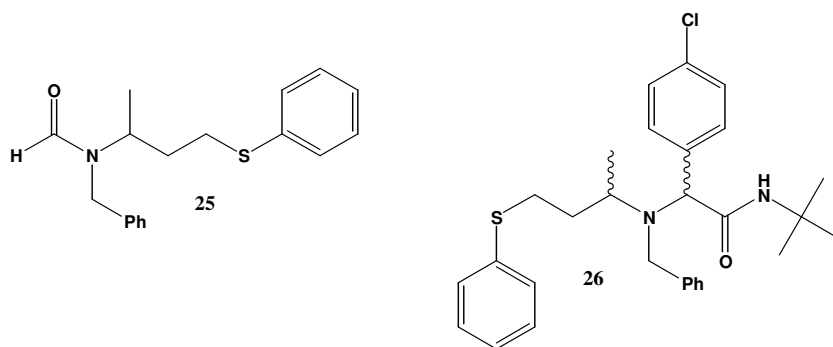
Diastereoisomer A (major): δ_{H} (500 MHz, CDCl_3) 1.34 (3H, d, J 7.3, CH_3), 1.32-1.40 (2H, m, CH_2), 3.16-3.22 (1H, m, CH-CH_3). 3.77 (1H, d, J 14.6, CHH-Ph), 3.83, (1H, d, J 14.6, CHH-Ph), 4.06 (2H, dd, J 7.1, 4.2, CH_2O), 5.61 (1H, s, CH), 7.22 (2H, d, J 8.6, Ar), 7.30-7.37 (5H, m, Ar), 7.34 (2H, d, J 8.6, Ar).

Diastereoisomer B (minor): δ_{H} (500 MHz, CDCl_3) 1.06 (3H, J 6.7, CH_3), 1.99 (1H, ddd, J 25.4, 12.2, 5.0, CHH), 2.04-2.10 (1H, m, CHH), 3.29-3.36 (1H, m, CH-CH_3), 3.63 (1H, d, J 16.1, CHH-Ph), 3.68 (1H, d, J 16.1, CHH-Ph), 3.85 (1H, td J 12.0, 2.7, CHH-O), 4.26 (1H, ddd, J 12.0, 5.0, 1.0, CHH-O), 5.27 (1H, s, CH-Ph), 7.11-7.14 (1H, m, Ar), 7.19-7.25 (4H, m, Ar), 7.47 (2H, d, J 8.3, Ar), 7.50 (2H, d, J 8.3, Ar);

δ_{C} (150 MHz, CDCl_3 , mixture of two diastereoisomers) 18.41, 21.71, 25.07, 29.17, 47.32, 47.80, 49.44, 57.31, 63.24, 68.19, 86.33, 94.17, 126.10, 126.89, 127.43, 127.93, 128.20, 128.23, 128.40, 128.45, 128.58, 128.74, 133.27, 133.62, 138.53, 138.65, 140.50, 142.41.

N-(1-Methyl-3-phenylsulfanyl-propyl)-formamide (25)

2-[Benzyl-(1-methyl-3-phenylsulfanyl-propyl)-amino]-N-tert-butyl-2-(4-chloro-phenyl)-acetamide (26)



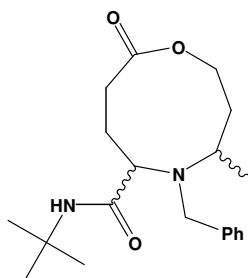
24 (310 mg, 1.03 mmol), tert-butyl isocyanide (86 mg, 1.03 mmol) and thiophenol (113 mg, 1.03 mmol) were dissolved in MeOH (1 ml). The mixture was stirred under microwave irradiation at 65°C for 15 min. After evaporating the solvent, the crude was purified by flash chromatography (DCM-ether, 9.5:0.5) affording **25** as colorless oil (15 mg, 0.05 mmol, 5%); ν_{\max} (film/cm⁻¹) 3460, 3058, 3027, 2970, 2933, 1740, 1665, 1437, 1419, 738, 688; ES [M+H⁺]: 300.1418, C₁₈H₂₁NOS; δ_{H} (500 MHz, CDCl₃ mixture of two rotamers) 1.09 (3H, d, J 6.7, CH₃), 1.16 (3H, d, J 6.7, CH₃), 1.65-1.75 (2H, m, CH₂), 1.81-1.87 (1H, m, CHH), 1.94-2.01 (1H, m, CHH), 2.64 (1H, dt, J 7.4, 12.9, CHH-S), 2.72-2.82 (3H, m, CHH-S, CH₂-S), 3.78-3.84 (1H, m, CH-CH₃), 2.25-2.29 (1H, m, CH-CH₃), 4.45 (1H, d, J 15.2, CHH-Ph), 4.49 (1H, d, J 15.2, CHH-Ph), 4.30 (1H, d, J 15.2, CHH-Ph), 4.33 (1H, d, J 15.2, CHH-Ph), 7.18-7.34 (20H, m, Ar), 8.30 (2H, s, HC=O); δ_{C} (150 MHz, CDCl₃, mixture of two rotamers) 18.53, 20.78, 30.53, 30.88, 33.52, 34.29, 44.16, 49.31, 49.75, 53.06, 126.59, 127.55, 128.07, 128.71, 129.71, 129.88, 135.48, 138.07; 163.16, 163.75.

26 (not isolated, two diastereoisomers in a ratio of 1:1.5):

Diastereoisomer A (major): δ_{H} (600 MHz, CDCl₃) 1.10 (3H, d, J 6.5, CH₃), 1.21-1.29 (1H, m, CHH), 1.39-1.46 (1H, m; CHH), 1.57 (9H, s, tBu), 2.96-3.02 (1H, m, CH-CH₃), 3.24 (1H, br m, CHH-S), 3.42 (1H, br m, CHH-S), 3.70 (1H, d, J 14.7, CHH-Ph), 3.91 (1H, d, J 14.7, CHH-Ph), 4.49 (1H, s, CH-C=O), 6.89 (2H, d, J 6.7, Ar), 6.94 (2H, d, J 8.2, Ar), 7.04 (2H, d, J 7.5, Ar), 7.15 (2H, d, J 7.5, Ar), 7.12-7.19 (5H, m, Ar), 7.28 (1H, t, J 7.6, Ar); δ_{C} (150 MHz, CDCl₃) 17.51, 29.37, 36.98, 51.38, 52.67, 57.46, 61.31, 64.98, 126.65, 128.09, 128.17, 128.70, 129.06, 129.18, 130.86, 131.59, 133.30, 136.17, 137.86, 141.44, 155.38.

Diastereoisomer B (minor): δ_{H} (600 MHz, CDCl₃) 0.41 (3H, d, J 6.1, CH₃), 1.39-1.46 (1H, m, CHH), 1.58 (9H, s, tBu), 1.68-1.75 (1H, m, CHH), 3.24 (1H, br m, CH-CH₃), 3.34 (1H, d, J 13.9 CHH-Ph), 3.58-3.62 (1H, m, CHH-S), 3.73 (1H, br m, CHH-S), 4.01 (1H, d, J 13.9, CHH-Ph), 4.55 (1H, s, CH-C=O), 6.74 (2H, d, J 7.5, Ar), 6.89 (2H, d, J 6.7, Ar), 6.94 (2H, d, J 8.2, Ar), 7.04 (2H, d, J 7.5 Ar), 7.12-7.19 (6H, m, Ar); δ_{C} (150 MHz, CDCl₃) 17.51, 29.37, 36.98, 51.38, 53.57, 57.46, 61.60, 65.51, 126.65, 128.09, 128.17, 128.70, 129.06, 129.18, 130.86, 131.59, 133.30, 136.17, 137.86, 141.44, 155.38.

5-Benzyl-4-methyl-9-oxo-[1,5]oxazonane-6-carboxylic acid tert-butylamide (**27**)

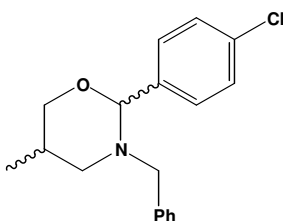


8 (114 mg, 0.64 mmol), 4-oxo-butyrac acid (65 mg, 0.64 mmol) and tert-butyl isocyanide (53 mg, 0.64 mmol) were dissolved in MeOH (1 ml). The mixture was stirred under microwave irradiation at 65°C for 15 min. After evaporating the solvent, the crude was purified by flash chromatography (petrol-ethyl acetate, 8:2) affording **27-cis** as a white solid (119 mg, 0.34 mmol, 53%) and **27-trans** as a colorless oil (52 mg, 0.15 mmol, 23%); ν_{\max} (film/cm⁻¹) 3364, 2965, 2930, 1735, 1669, 1515, 1453, 1238, 755, 703.

27-cis: mp= 107 °C; EI [M]⁺: 346.22521, C₂₀H₃₀N₂O₃; δ_{H} (400 MHz, DMSO, 110°C) 1.23 (9H, s, tBu), 1.26-1.28 (1H, m, CHH-CH₂O), 1.34 (3H, d, J 7.5, CH₃), 1.99-2.09 (1H, m, CHH-CH₂O), 2.12-2.23 (1H, m, CHH-CH₂COO), 2.38-2.51 (3H, m, CH₂-COO, CHH-CH₂COO), 3.17-3.25 (1H, m, CH-CH₃), 3.48 (1H, dd, J 8.8, 1.7, CH-C=O), 3.69 (1H, d, J 14.7, CHH-Ph), 3.77 (1H, d, J 14.7, CHH-Ph), 3.91 (1H, td J 10.8, 5.8, CHH-O), 4.67 (1H, ddd, J 10.8, 6.6, 2.8, CHH-O), 6.41 (1H, br s, NH), (1H, tt J 7.4, 1.6, Ar), 7.30 (2H, t, J 7.4, Ar), 7.34 (2H, d, J 7.4); δ_{C} (100MHz, DMSO, 110°C) 22.53, 23.18, 28.46, 30.97, 33.60, 47.58, 50.68, 60.55, 62.82, 70.20, 127.00, 128.35, 129.61, 140.08, 172.20, 173.72; Anal. Calcd for C₂₀H₃₀N₂O₃: C 69.33, H 8.73, N 8.09, found C 69.04, H 8.82, N 7.90.

27-trans: ES [M+H⁺]: 347.23405, C₂₀H₃₁N₂O₃; δ_{H} (400 MHz, DMSO, 110°C) 1.04 (3H, d, J 6.5, CH₃), 1.31 (9H, s, tBu), 1.37-1.44 (1H, m, CHH-CH₂O), 1.45-1.52 (1H, m, CHH-CH₂O), 1.86-1.96 (1H, m, CHH-CH₂COO), 2.03-2.12 (1H, m, CHH-CH₂COO), 2.29-2.37 (2H, m, CH₂-COO), 3.27 (1H, dd, J 10.6, 2, CH-C=O), 3.32-3.37 (1H, m, CH-CH₃), 3.70 (1H, d, J 14.1, CHH-Ph), 3.98 (1H, d, J 14.1, CHH-Ph), 4.07 (1H, td, J 10.2, 4.8 CHH-O), 4.27-4.32 (1H, m, CHH-O), 6.52 (1H, br s, NH), 7.22 (1H, t, J 7.3 Ar), 7.29 (2H, t, J 7.3, Ar), 7.39 (2H, d, J 7.3); δ_{C} (100MHz, CDCl₃) 18.07, 25.41, 28.94, 30.73, 33.21, 47.13, 50.27, 51.34, 61.28, 61.35, 127.58, 128.95, 130.07, 138.91, 171.27, 73.83.

3-Benzyl-2-(4-chloro-phenyl)-5-methyl-[1,3]oxazinane (**28**)



Para-chlorobenzaldehyde (350 mg, 2.49 mmol) and **7** (298 mg, 1.66 mmol) were dissolved in MeOH (1.5 ml). The mixture was stirred under microwave irradiation at 65°C for 15 min.

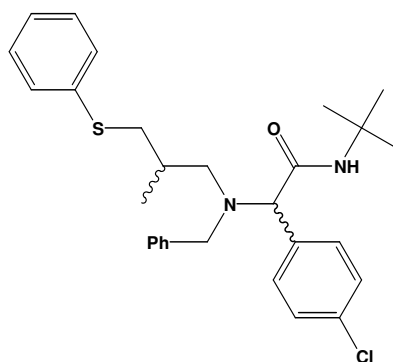
Evaporation of the solvent under reduced pressure afforded **28** as a mixture of two diastereoisomers in a ratio of 1:4.5 (301 mg, not isolated).

Diastereoisomer A (major): δ_{H} (500 MHz, CDCl_3) 0.74 (3H, d, J 6.4, CH_3), 2.25-2.31 (1H, m, CH-CH_3), 2.35 (1H, t, J 11.8, CHH-N), 3.06-3.09 (1H, m, CHH-N), 3.29 (1H, d, J 14.0, CHH-Ph), 3.38 (1H, t, J 11.0, CHH-O), 3.66 (1H, d, J 14.0, CHH-Ph), 4.21 (1H, ddd, J 11.0, 4.4, 2.1, CHH-O), 5.05 (1H, s, CH-Ph), 7.29-7.35 (5H, m, Ar), 7.39 (2H, J 8.5, Ar), 7.59 (2H, J 8.5, Ar).

Diastereoisomer B (minor): δ_{H} (500MHz, CDCl_3) 0.88 (3H, d, J 6.7 CH_3), 2.11-2.17 (1H, m, CH-CH_3), 2.63 (1H, dd J 13.1, 3.6, CHH-N), 2.77 (1H, dd, J 13.1, 8.3, CHH-N), 3.54 (1H, dd, J 11.2, 7.6, CHH-O), 3.70 (1H, d, J 13.6, CHH-Ph), 3.82 (1H, ddd, J 11.2, 3.9, 1.0, CHH-O), 4.08 (1H, d, J 13.6, CHH-Ph), 5.11 (1H, s, CH-Ph), 7.25-7.28 (2H, m, Ar), 7.36-7.41 (3H, m, Ar), 7.43 (2H, J 8.3, Ar), 7.62 (2H, J 8.3, Ar).

δ_{C} (125 MHz, CDCl_3 , mixture of two diastereoisomers) 14.46, 15.56, 25.89, 52.38, 53.03, 57.01, 57.17, 69.46, 74.80, 90.61, 93.81, 126.97, 127.15, 128.36, 128.45, 128.50, 128.57, 128.64, 128.76, 128.80, 129.42, 133.74, 134.04, 138.23, 138.30, 139.12, 139.29.

2-[Benzyl-(2-methyl-3-phenylsulfanyl-propyl)-amino]-N-tert-butyl-2-(4-chloro-phenyl)-acetamide (**29**)



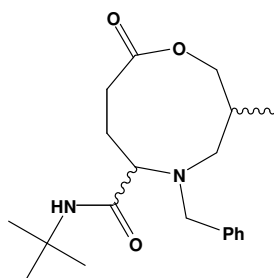
28 (605 mg, 2.00 mmol), tert-butyl isocyanide (166 mg, 2.00 mmol) and thiophenol (220 mg, 2.00 mmol) were dissolved in MeOH (2 ml). The mixture was stirred under microwave irradiation at 65°C for 15 min. After evaporating the solvent, the crude was purified by flash chromatography (DCM-ether, 9:1) affording **29** as a yellow solid and as a mixture of two diastereoisomers in a ratio of 0.7:1 (25 mg, 0.51 mmol, 3%); ν_{max} (film/ cm^{-1}) 3155, 2926, 2854, 1640, 1468, 1384, 911, 740, 651; ES $[\text{M}+\text{H}^+]$: 495.2215, $\text{C}_{29}\text{H}_{36}\text{N}_2\text{OSCl}$; Anal. Calcd for $\text{C}_{29}\text{H}_{37}\text{ClN}_2\text{O}_2\text{S}$: C 67.88, H 7.27, N 5.26, found C 67.33, H 6.94, N 5.19.

Diastereoisomer A (major): δ_{H} (600 MHz, CDCl_3) 0.56 (3H, d, J 6.7, CH_3), 1.58 (9H, s, tBu), 1.76 (1H, m, CH-CH_3), 2.07 (1H, dd, J 12.4, 2.3, CHH-N), 2.54 (1H, t, J 12.4, CHH-N), 2.91 (1H, d, J

13.4, *CHH*-Ph), 3.30 (1H, t, J 9.7, *CHH*-S), 3.54 (1H, d, J 9.7, *CHH*-S), 4.14 (1H, d, J 13.4, *CHH*-Ph), 4.53 (1H, s, CH-Ph), 4.94 (1H, br s, NH), 6.73 (2H, d, J 8.2, Ar), 6.76 (2H, d, J 7.6, Ar), 6.99 (2H, t, J 7.6, Ar), 7.16-7.19 (1H, m, Ar), 7.20 (2H, d, J 8.2, Ar), 7.30-7.35 (5H, m, Ar); δ_c (150 MHz, CDCl_3) 15.23, 29.53, 32.13, 56.21, 57.31, 57.59, 66.12, 69.09, 127.27, 128.07, 128.59, 128.63, 128.85, 129.18, 130.69, 131.52, 133.47, 133.93, 135.56, 139.29, 155.02.

Diastereoisomer B (minor): δ_H (600 MHz, CDCl_3) 0.84 (3H, d, J 6.7, CH_3), 1.58 (9H, s, tBu), 1.86 (1H, br m, CH- CH_3), 2.54 (1H, t, J 12.4, *CHH*-N), 2.68 (1H, t, J 9.8, *CHH*-S), 3.04-3.07 (1H, m, *CHH*-N), 3.26 (1H, br m, *CHH*-S), 3.82 (1H, d, J 13.0, *CHH*-Ph), 4.03 (1H, d, J 13.0, *CHH*-Ph), 4.40 (1H, s, CH-Ph), 4.94 (1H, br s, NH), 6.57 (2H, d, J 7.5 Ar), 6.83-6.86 (4H, m, Ar), 7.08 (1H, t, J 7.5, Ar), 7.23 (2H, d, J 7.2, Ar), 7.30-7.35 (5H, m, Ar); δ_c (150 MHz, CDCl_3) 15.11, 29.67, 31.73, 55.94, 57.31, 57.71, 65.99, 69.90, 127.27, 128.30, 128.59, 128.63, 128.85, 129.48, 130.69, 131.45, 133.47, 133.93, 135.86, 139.29, 155.02.

5-Benzyl-3-methyl-9-oxo-[1,5]oxazonane-6-carboxylic acid tert-butylamide (**30**)



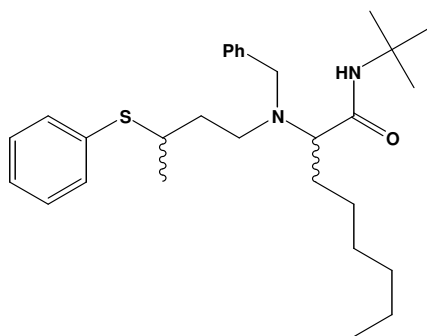
7 (108 mg, 0.61 mmol), 4-oxo-butyrac acid (62 mg, 0.61 mmol) and tert-butyl isocyanide (51 mg, 0.61 mmol) were dissolved in MeOH (1 ml). The mixture was stirred under microwave irradiation at 65°C for 15 min. After evaporating the solvent, the crude was purified by flash chromatography (petrol-ethyl acetate, 8:2) affording **30** as a colorless oil and as a mixture of two diastereoisomers in a ratio of 1:1.1 (175 mg 0.22 mmol, 34%); ν_{max} (film/ cm^{-1}) 3365, 3058, 2965, 1730, 1669, 1507, 1454, 1265, 732, 700; ES $[\text{M}+\text{H}^+]$: 347.23301, $\text{C}_{20}\text{H}_{31}\text{O}_3\text{N}_2$.

Diastereoisomer A (major): δ_H (600 MHz, CDCl_3) 0.88 (3H, d, J 7.2, CH_3), 1.40 (9H, s, tBu), 2.05-2.14 (1H, m, *CHH*- CH_2COO), 2.18-2.29 (2H, m, *CHH*- CH_2COO , CH- CH_3), 2.20 (1H, dd, J 14.0, 1.2, *CHH*-N), 2.36 (1H, ddd, J 12.7, 10.1, 6.3, *CHH*-COO), 2.42-2.45 (1H, m, *CHH*-COO), 3.29 (1H, dd, J 14.0, 9.8, *CHH*-N), 3.35-3.46 (2H, m, CH-C=O, *CHH*-O), 3.42 (1H, d, J 13.3, *CHH*-Ph), 3.91 (1H, d, J 13.3, *CHH*-Ph), 4.92 (1H, dd, J 10.8, 7.4, *CHH*-O), 7.24-7.28 (1H, m, Ar), 7.23-7.35 (4H, m, Ar).

Diastereoisomer B (minor): δ_{H} (600 MHz, CDCl_3) 0.57 (3H, d, J 7.0, CH_3), 1.34 (9H, s, tBu), 1.46-1.51 (1H, m, $\text{CHH-CH}_2\text{COO}$), 1.75-1.83 (1H, m, CH-CH_3), 1.97 (1H, ddd, J 15.0, 13.3, 3, CHH-COO), 2.46-2.48 (1H, m, CHH-COO), 2.51-2.62 (1H, m, $\text{CHH-CH}_2\text{COO}$), 2.70 (1H, dd, J 14.5, 8.8, CHH-O), 2.84-2.88 (1H, m, CHH-O), 2.87 (1H, dd, J 12.2, 4.1, CH-C=O), 3.35-3.46 (1H, m, CHH-N), 3.49 (1H, d, J 13.6, CHH-Ph), 3.90 (1H, d, J 13.6, CHH-Ph), 4.54 (1H, dd, J 10.9, 6.5, CHH-N), 7.24-7.32 (5H, Ar).

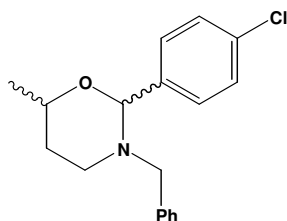
δ_{C} (150 MHz, CDCl_3 , mixture of two diastereoisomers) 15.78, 17.05, 24.45, 25.99, 28.35, 28.89, 29.72, 33.05, 33.36, 51.22, 51.34, 53.26, 56.00, 57.83, 62.60, 67.82, 68.87, 127.28, 127.42, 128.22, 128.63, 129.57, 129.61, 138.42, 138.50, 170.18, 171.37, 173.09, 173.66.

2-[Benzyl-(3-phenylsulfanyl-butyl)-amino]-octanoic acid tert-butylamide (31)



6 (187 mg, 1.04 mmol), pentanal (119 mg, 1.04 mmol) and tert-butyl isocyanide (87 mg, 1.04 mmol) were dissolved in MeOH (1 ml). The mixture was stirred under microwave irradiation at 65°C for 15 min. After evaporating the solvent, the crude was purified by flash chromatography (DCM-ether, 9.5:0.5) affording **31** as a colorless oil (10 mg, 0.02 mmol, 2%); ν_{max} (film/ cm^{-1}) 3461, 2970, 2927, 2855, 1738, 1455; ES $[\text{M}+\text{H}]^+$: 469.3247, $\text{C}_{29}\text{H}_{45}\text{N}_2\text{OS}$; δ_{H} (600 MHz, CDCl_3) 0.82-0.86 (2H, m, CH_2), 0.87 (3H, t, J 6.7, CH_3), 1.05 (3H, d, J 6.1, CH_3), 1.15-1.19 (2H, m, CH_2), 1.22-1.28 (5H, m, 2CH_2 , CHH), 1.38-1.45 (2H, m, CH_2), 1.47 (9H, s, tBu), 1.78 (1H, m, CHH), 2.54 (1H, dt, J 13.3, 4.2, CHH-N), 3.03 (1H, ddd, J 13.3, 10.8, 3.5, CHH-N), 3.27 (1H, J 9.2, 4.4, CH-C=O), 3.40 (1H, d, J 13.3, CHH-Ph), 3.70 (1H, m, CH-CH_3), 3.78 (1H, d, J 13.3, CHH-Ph), 7.14 (2H, d, J 7.2, Ar), 7.16-7.23 (6H, m, Ar), 7.24 (2H, d, J 7.2, Ar); δ_{C} (150 MHz, CDCl_3) 14.22, 22.69, 23.47, 25.88, 26.35, 29.41, 29.74, 31.76, 35.04, 47.97, 54.83, 56.95, 62.84, 69.04, 127.16, 127.99, 128.42, 129.06, 129.77, 132.50, 134.49, 139.27, 153.92.

3-Benzyl-6-methyl-2-phenyl-[1,3]oxazinane (32)

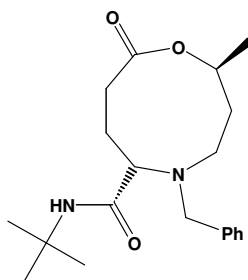


Para-chlorobenzaldehyde (140 mg, 0.42 mmol) and **6** (63 mg, 0.35 mmol) were dissolved in MeOH (0.5 ml). The mixture was stirred under microwave irradiation at 65°C for 15 min. Evaporation of the solvent under reduced pressure afforded **32** as a mixture of two diastereoisomers in a ratio of 1:6.7 (100 mg, not isolated).

Diastereoisomer A (major): δ_{H} (600 MHz, CDCl_3) 1.30 (3H, d, J 6.2, CH_3), 1.37 (1H, m, CHH), 1.74-1.81 (1H, m, CHH), 2.69 (1H, td, J 12.8, 3.0, CHH-N), 3.03 (1H, ddd, J 12.8, 4.3, 2.0, CHH-N), 3.18 (1H, J 13.9, CHH-Ph), 3.56 (1H, J 13.9, CHH-Ph), 3.80 (1H, m, CH-CH_3), 5.07 (1H, s, CH-Ph), 7.20-7.28 (5H, m, Ar), 7.34 (2H, d, J 8.6, Ar), 7.50 (2H, d, J 8.6, Ar); δ_{C} (150 MHz, CDCl_3) 22.13, 29.43, 49.29, 51.93, 74.35, 93.85, 126.96, 128.36, 128.59, 128.64, 128.85, 133.94, 138.65, 139.29.

Diastereoisomer B (minor): peaks too broad. Not distinctly observed.

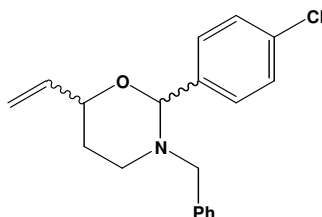
5-Benzyl-2-methyl-9-oxo-[1,5]oxazonane-6-carboxylic acid tert-butylamide (33)



6 (65 mg, 0.36 mmol), 4-oxo-butyric acid (102 mg, 0.36 mmol) and tert-butyl isocyanide (30 mg, 0.36 mmol) were dissolved in MeOH (0.5 ml). The mixture was stirred under microwave irradiation at 65°C for 15 min. After evaporating the solvent, the crude was purified by flash chromatography (petrol-ethyl acetate, 8:2) affording **33** as a pale yellow solid (13 mg, 0.04 mmol, 12%); mp= 142 °C; ν_{max} (film/ cm^{-1}) 3359, 3026, 2971, 2929, 1730, 1667, 1498, 1456, 1116, 731. 700.4; ES $[\text{M}+\text{Na}^+]$: 369.2145, $\text{C}_{20}\text{H}_{30}\text{N}_2\text{O}_3\text{Na}$; δ_{H} (600 MHz, CDCl_3) 1.29 (3H, d, J 6.6, CH_3), 1.32-1.35 (1H, m, $\text{CHH-CH}_2\text{N}$), 1.33 (9H, s, tBu), 1.42-1.46 (1H, m, $\text{CHH-CH}_2\text{COO}$), 1.95 (1H, ddd, J 15.4, 13.3, 3.0, CHH-COO), 2.14-2.19 (1H, m, $\text{CHH-CH}_2\text{N}$), 2.27 (1H, dd, J 4.8, 1.7, CHH-N), 2.46 (1H, dt, J 15.4, 3.8, CHH-COO), 2.53-2.60 (1H, m, $\text{CHH-CH}_2\text{COO}$), 2.79 (1H, dd, J 12.3, 4, CH-C=O), 3.39

(1H, d, J 13.5, *CHH*-Ph), 3.43 (1H, dd, J 11.5, 1.7, *CHH*-N), 3.93 (1H, d, J 13.5, *CHH*-Ph), 4.96 (1H, br s, NH), 5.18 (1H, dqd, J 7.6, 6.6, 2.5, CH-CH₃), 7.28 (1H, t, J 7.3, Ar), 7.37 (2H, t, J 7.3, Ar), 7.42 (2H, d, J 7.3, Ar); δ_c (150 MHz, CDCl₃) 21.30, 25.80, 29.08, 29.78, 33.78, 43.54, 51.56, 57.48, 62.48, 67.31, 127.63, 128.95, 129.65, 138.55, 170.19, 173.66.

3-Benzyl-2-(4-chloro-phenyl)-6-vinyl-[1,3]oxazinane (34)



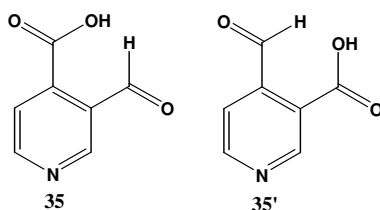
9 (22 mg, 0.11 mmol) and para-chloro benzaldehyde (31 mg, 0.22 mmol) were dissolved in MeOH (0.5 ml). The mixture was stirred under microwave irradiation at 65°C for 15 min. Evaporation of the solvent under reduced pressure afforded **34** as a mixture of two diastereoisomers in a ratio of 1:9 (31 mg, not isolated).

Diastereoisomer A (major): δ_H (500 MHz, CDCl₃) 1.40-1.44 (1H, m, *CHH*), 1.84-1.93 (1H, m, *CHH*), 2.78 (1H, td, J 12.8, 2.9, *CHH*-N), 3.06 (1H, ddd J 13.2, 4.3, 2.0, *CHH*-N), 3.21 (1H, d, J 13.9, *CHH*-Ph), 3.55 (1H, d, J 13.9, *CHH*-Ph), 4.16-4.21 (1H, m, CH-CH=CH₂), 5.15 (1H, dd, J 10.6, 1.3, CHC=CHH), 5.18 (1H, s, CH-Ph), 5.31 (1H, dd, J 17.4, 1.3, CHC=CHH), 5.94 (1H, ddd, J 17.4, 10.6, 5.3, CH=CH₂), 7.19 (2H, d, J 7.1, Ar), 7.24 (2H, t, J 7.1, Ar), 7.29-7.32 (1H, m, Ar), 7.31 (2H, d, J 8.3, Ar), 7.52 (2H, d, J 8.3, Ar); δ_c (150 MHz, CDCl₃) 27.09, 28.48, 48.78, 51.28, 78.48, 93.41, 115.04, 126.92, 128.30, 128.48, 128.51, 128.71, 133.88, 138.62, 139.16.

Diastereoisomer B (minor): peaks too broad. Not distinctly observed.

3-Formyl-isonicotinic acid (35)⁶⁴⁷

4-Formyl-nicotinic acid (35')⁶⁴⁷



A solution of tert-butyl alcohol (556 mg, 7.50 mmol) was added carefully at 0 °C and under an argon atmosphere to a suspension of LiAlH₄ (95 mg, 2.50 mmol) in anhydrous THF. The mixture was stirred at 0 °C for 30 min. A white suspension of Li(OtBu)₃AlH was formed. The solution of

Li(OtBu)₃AlH (341 mg, 1.34 mmol) previously prepared, was added slowly at 0 °C and under an argon atmosphere, to a solution of 3,4-pyridinedicarboxylic anhydride (200 mg, 1.34 mmol) dissolved in anhydrous THF (1 ml). The mixture was stirred for 2 h at RT, after which it was quenched with water (10 ml). The aqueous phase was extracted with EtOAc (3 x 3 ml). Evaporation of the aqueous phase afforded a mixture of **35** and **35'** as a white solid (44 mg, 0.29 mmol, 22%, not isolated); δ_{H} (600 MHz, CDCl₃) 5.85 (1H, s, CH-OH, hydroxyphthalide form), 5.90 (1H, s, CH-OH, hydroxyphthalide form), 7.50 (1H, d, J 4.9, Ar) 7.57 (1H, d, J 5.10, Ar), 7.62 (1H, d, J 4.7), 7.74 (1H, d, J 4.9), 8.52 (1H, d, J 4.7, Ar), 8.54 (1H, d, J 5.10, Ar), 8.60 (1H, d, J 4.9, Ar), 8.67 (1H, s, Ar), 8.74 (1H, d, J 4.9), 8.83 (1H, s, Ar), 8.88 (1H, s, Ar), 8.89 (1H, s, Ar), 10.60 (1H, s, HC=O), 10.73 (1H, s, HC=O); δ_{C} (150 MHz, CDCl₃) 97.54, 97.75, 122.64, 123.12, 124.35, 124.60, 131.05, 133.39, 135.53, 146.94, 148.67, 149.59, 150.16, 150.54, 151.01, 151.48, 152.74, 154.30, 172.88, 175.49, 193.72, 193.80.

Acknowledgements

Un sincero ringraziamento va a tutti coloro che, in momenti diversi e in vari modi, mi hanno accompagnato in questo percorso di vita e mi hanno prestato il loro aiuto nella realizzazione di questo lavoro.

In primo luogo ringrazio di cuore il mio relatore, il prof. C. Melchiorre, per essere stato un ottimo tutor sia dal punto di vista umano che da quello professionale. Grazie per i consigli, per tutto il sapere e l'amore per la ricerca che mi ha trasmesso. Grazie anche per la pazienza avuta nel leggere e soprattutto correggere questa enciclopedia.

Vorrei ringraziare anche le prof.sse A. Minarini e ML Bolognesi per avere creduto in me e per il loro appoggio in questi primi passi nel mondo del lavoro. Grazie a tutto il lab. Melchiorre, a Michela, Andrea e Chiara. Un grazie particolare va anche a Elena e Federica, per i nostri pranzi in mensa e per le chiacchierate tra una colonna e l'altra.

Vorrei ringraziare anche il Dr. T. Sheppard per avermi permesso di svolgere il periodo all'estero presso il suo laboratorio. Grazie anche a tutti i PhD students del Sheppard's lab, per avermi accolto con affetto e per avermi fatto sentire come a casa. In particolare, ricordo con affetto Cristina, Lourdes, Marialuisa, Giulia, Daniela, Filippo, Silvia e John per avermi accompagnato nella mia avventura e per aver fatto scaturire la Londoner che c'è in me. Quando penso a quel periodo mi rendo conto che ogni persona che ho incontrato mi ha arricchita e ha cambiato la mia visione di vedere il mondo.

Ringrazio anche tutti coloro che mi hanno permesso di completare questo lavoro di dottorato: Manuela, Gioia e Monica per il loro impegno, pazienza e le loro utili spiegazioni.

Last but not least, vorrei ringraziare di cuore i miei genitori e il mio fidanzato Dave. Grazie per le vostre infusioni di ottimismo e di fiducia. Grazie per aver creduto sempre in me!

Infine, vorrei ringraziare tutti miei amici e quelle persone che forse ho dimenticato di nominare, ma che ho comunque nel cuore...

References

-
- ¹Minati L.; Edginton T.; Bruzzone M. G.; Giaccone G., *Am. J. Alzheimers Dis.*, **2009**, *24*, 95.
- ² Alzheimer's Disease International, World Alzheimer Report. <http://www.alz.co.uk/research/files/WorldAlzheimerReport2010ExecutiveSummary.pdf>
- ³Alzheimer A., *Allg Z Psychiatr.* **1907**, *64*, 146.
- ⁴Torreilles F., *Prog. Neurobiol.* **2002**, *66*, 191.
- ⁵Braak H.; Braak E., *Acta Neuropathol.* **1991**, *82*, 239.
- ⁶Price D.L.; Sisodia S.S., *Annu. Rev. Neurosci.* **1998**, *2*, 479.
- ⁷Selkoe D. J., *Science* **2002**, *298*, 789.
- ⁸Hardy J.; Allsop D., *Trends Pharmacol. Sci.* **1991**, *12*, 38.
- ⁹Kang J.; Lemaire H. G.; Unterbeck A.; Salbaum J. M.; Masters C. L.; Grzeschik K. H.; Multhaup G.; Beyreuther K.; Muller-Hill B., *Nature* **1987**, 325.
- ¹⁰Sabbagh M. N.; Fleisher A.; Chen K.; Rogers J.; Berk C., et al., *Archives of Neurobiology* **2011**, *68*, 1461.
- ¹¹Turner P. R.; O'Conner K.; Tate W. P.; Abraham W. L., *Prog. Neurobiol.* **2003**, *70*, 1.
- ¹²Selkoe D. J.; Podlisny M. B.; Joachim C. L.; Vickers E. A.; Le G.; Fritz L. C.; Oltersdorf T., *Proc. Natl. Acad. Sci. U.S.A.* **1988**, *85*, 7341.
- ¹³Tanaka S.; Shiojiri, S.; Takahashi Y.; Kitaguchi N.; Ito H.; Kameyama M.; Kimura J.; Ueda K., *Biochem. Biophys. Res. Commun.* **1989**, *165*, 1406.
- ¹⁴Sisodia S. S.; Koo E. H.; Hoffman P. N.; Perry G.; Price D. L., *J. Neurosci.* **1993**, *13*, 3136.
- ¹⁵Mattson M. P., *Physiol Rev.* **1997**, *77*, 1081.
- ¹⁶Reinhard C.; Hebert S. S.; De Strooper B., *Embo J.* **2005**, *24*, 3996.
- ¹⁷Priller C.; Bauer T.; Mitteregger G.; Krebs B.; Kretschmar H. A.; Herms J., *J. Neurosci.* **2006**, *26*, 7212.
- ¹⁸Zheng H.; Koo E. H.; *Mol. Neurodegener.* **2006**, *3*, 1.
- ¹⁹De Strooper B.; Annaert W., *J. Cell Science* **2000**, *113*, 1875.
- ²⁰Esler W. P.; Wolfe M. S., *Science* **2001**, *293*, 1449.
- ²¹Bandyopadhyay S.; Goldstein L. E.; Lahiri D. K.; Rogers J. T., *Curr. Med. Chem.* **2007**, *14*, 2848.
- ²²Nikolaie A.; McLaughlin T.; O'Leary D. D.; Tessier-Lavigne M., *Nature* **2009**, *457*, 981.
- ²³Citron M., *Mol. Med. Today* **2000**, *6*, 392.
- ²⁴a) Jarrett J. T.; Berger E. P.; Lansbury P. T., *Ann N Y Acad. Sci.* **1993**, *695*, 144.
b) Pitschke, M.; Prior, R.; Haupt M.; Riesner D., *Nat. Med.* **1998**, *4*, 832–834.

-
- ²⁵ Torreilles F.; Jacques Touchon J., *Progress in Neurobiology* **2002**, *66*, 191.
- ²⁶ Bartolini M.; Andrisano V., *ChemBioChem* **2010**, *11*, 1018 .
- ²⁷ Kaye R.; Sokolov Y.; Edmonds B.; MacIntire T. M.; Milton S. C.; Cotman C. W., et al., *Science* **2003**, *300*, 486.
- ²⁸ Kirschner D. A.; Abraham C.; Selkoe D. J., *Proc. Natl. Acad. Sci. USA* **1987**, *84*, 6953.
- ²⁹ Loo D. T.; Copani A.; Pike C. J.; Whittemore E. R.; Walencewicz A. J.; Cotman C. W., *Proc. Natl. Acad. Sci. USA* **1993**, *90*, 7951.
- ³⁰ Estus S.; Tucker H. M.; van Rooyen C.; Wright S.; Brigham E. F.; Wogulis M.; et al., *J. Neurosci.*, 1997, *17*, 7736.
- ³¹ Troy C. M.; Rabacchi S. A.; Friedman W. J.; Frappier T. F.; Brown K.; Shelanski M. L., *J. Neurosci.* **2000**, *20*, 1386.
- ³² Nakagawa T.; Zhu H.; Morishima N.; Li E., Xu J.; Yankner B. A.; Yuan J., *Nature* **2000**, *403*, 98–103.
- ³³ Uetsuki T.; Takemoto K.; Nishimura I.; Okamoto M.; Niinobe M.; Momoi T., et al., *J. Neurosci.* **1999**, *19*, 6955.
- ³⁴ Morishima Y.; Gotoh Y.; Zieg J.; Barrett T.; Takano H.; Flavell R.; Davis R. J.; Shirasaki Y.; Greenberg M. E., *J. Neurosci.* **2001**, *21*, 7551.
- ³⁵ De Strooper B., *Physiol. Rev.* **2010**, *90*, 465
- ³⁶ Mattson M. P., *Ann. NY Acad. Sci.* **1994**, *747*, 50.
- ³⁷ Mattson M. P.; Cheng b., Davis D., Bryant K.; Lieberburg I.; Rydel R. E., *J. Neurosci.* **1992**, *12*, 376.
- ³⁸ Schubert D.; Behl C.; Lesley R.; Brack A.; Dargusch R.; Sagara Y., et al., *Proc Natl Acad Sci USA* **1995**, *92* 1989.
- ³⁹ Mattson M. P., *Neurobiol. Aging*, **1995**, *16*, 447 (discussion pp. 458–463).
- ⁴⁰ Saitoh T.; Horsburgh K.; Masliah E., *Ann. NY Acad. Sci.* **1993**, *695*, 34.
- ⁴¹ Shoffner J. M., *Neurogenetics*, **1997**, *1*, 13.
- ⁴² Brookes P. S.; Yoon Y.; Robotham J. L.; Anders M. W., Sheu S. S., *Am. J. Physiol. Cell. Physiol.* **2004**, *287*, C817.
- ⁴³ Cataldo A. M.; Harper J. D.; Lansbury Jr P. T., *J. Neuroscience* **1996**, *267*, 546.
- ⁴⁴ Cuervo A. M., *Trends Cell. Biol.* **2004**, *14*, 70.
- ⁴⁵ Glabe C. G., *Neurobiology of Aging* **2006**, *27*, 570.
- ⁴⁶ Yankner B. A.; Duffy L. K.; Kirschner D. A., *Science* **1990**, *250*, 279.
- ⁴⁷ Seubert P.; Vigo-Pelfrey C.; Esch F.; Lee M.; Dovey H.; Davis D.; A.; Sinha S.; Schlossmacher M.; Whaley J.; Swindlehurst C., et al., *Nature* **1992**, *359*, 325.
- ⁴⁸ Haass C.; Schlossmacher M. G.; Hung A. Y.; Vigo-Pelfrey C.; Mellon A.; et al., *Nature* **1992**, *359*, 322.

-
- ⁴⁹ Kamenetz F.; Tomita T.; Hsieh H.; Seabrook G.; Borchelt D.; Iwatsubo T.; Sisodia S.; Malinow R., *Neuron* **2003**, *37*, 925.
- ⁵⁰ Shen J.; Bronson R. T.; Chen D. F.; Xia W.; Selkoe D. J.; Tonegawa S., *Cell* **1997**, *89*, 629.
- ⁵¹ Wong P. C.; Zheng H.; Chen H.; Becher M. W.; Sirinathsinghji D. J.; Trumbauer M. E., et al., *Nature* **1997**, *387*, 288.
- ⁵² Peschon J. J.; Slack J. L.; Reddy P.; Stocking K. L.; Sunnarborg S. W.; Lee D. C., et al., *Science* **1998**, *282*, 1281.
- ⁵³ Dominguez D. I.; De Strooper B.; Annaert W., *Amyloid* **2001**, *8*, 124.
- ⁵⁴ Selkoe D. J., *Physiol. Rev.* **2001**, *81*, 741.
- ⁵⁵ Mike Mullan M.; Crawford F.; Axelma K.; Houlden H.; Lilius L.; Winblad B.; Lannfelt L., *Nature Genet.* **1992**, *1*, 345.
- ⁵⁶ Citron M.; Oltersdorf T.; Haass C.; McConlogue I.; Hung A. Y.; Seubert P.; Viho-Pelfrey C.; Lieberburg I.; Selkoe D.J., *Nature* **1992**, *360*, 672.
- ⁵⁷ Hutton M.; Perez-Tur J.; Hardy J., *Essays Biochem.* **1998**, *33*, 117.
- ⁵⁸ Lin L.; Georgievska B.; Mattsson A.; Isacson O., *Proc. Natl. Acad. Sci. USA* **1999**, *96*, 12108.
- ⁵⁹ Postina R., et al., *J. Clin. Invest.* **2008**, *320*, 520.
- ⁶⁰ Peschon J. J., et al., *Science* **1998**, *282*, 1281.
- ⁶¹ Seubert P.; Vigo-Pelfrey C.; Esch F.; Lee M.; Dovey H.; Davis D.; Sinha S.; Schlossmacher M.; Whaley J.; Swindlehurst C., et al., *Nature* **1992**, *359*, 325.
- ⁶² Shoji M.; Golde t. E.; Ghiso J.; Cheung T. T.; Estus S.; Shaffer L. M.; Cai X. D.; McKay D. M.; Tintner R.; Frangione B., et al., *Science* **1992**, *258*, 126.
- ⁶³ Lin X.; Koelsch G.; Wu S.; Downs D.; Dashti A.; Tang J., *Proc. Natl. Acad. Sci. USA* **2000**, *97*, 1456.
- ⁶⁴ Vassar R.; Bennett B. D.; Babu-Khan S.; Kahn S.; Mendiaz E. A.; Denis P.; Teplow D. B.; Ross S.; Amarante P.; Loeloff R.; Luo Y.; Fisher S.; Fuller J.; Edenson S.; Lile J.; Jarosinski M. A.; Biere A. L.; Curran E.; Burgess T.; Louis J. C.; Collins F.; Treanor J.; Rogers G.; Citron M., *Science* **1999**, *286*, 735.
- ⁶⁵ Yan R.; Bienkowski M. J.; Shuck M. E.; Miao H.; Tory M. C.; Pauley A. M.; Brashlerk J. R.; Stratman N. C.; Mathews W. R.; Buhlk A. E.; Carter D. B.; Tomasselli A. G.; Parodi L. A.; Heinrikson R. L.; Gurney M. E., *Nature* **1999**, *402*, 533.
- ⁶⁶ L. Hong, G. Koelsch, X. Lin, S. Wu, S. Terzyan, A.K. Ghosh, X.C. Zhang, J. Tang, *Science* **2000**, *290*, 150.
- ⁶⁷ Laird F. M.; Cai H.; Savonenko A. V.; Farah M. H.; He K.; Melnikova T.; Wen H.; Chiang H. C.; Xu G.; Koliatsos V. E.; Borchelt D. R.; Price D. L.; Lee H. K.; Wong P. C., *J. Neurosci.* **2005**, *25*, 11693.
- ⁶⁸ Luo Y.; Bolon B.; Kahn S.; Bennett B. D.; Babu-Khan S.; Denis P.; Fan W.; Kha H.; Zhang J.; Gong Y.; Martin L.; Louis J. C.; Yan Q.; Richards W. G.; Citron M.; Vassar R., *Nat. Neurosci.* **2001**, *4*, 231.
- ⁶⁹ McConlogue L.; Buttini M.; Anderson J. P.; Brigham E. F.; Chen K. S.; Freedman S. B.; Games D.; Johnson-Wood K.; Lee M.; Zeller M.; Liu W.; Motter R.; Sinha S., *J. Biol. Chem.* **2007**, *282*, 26326.

-
- ⁷⁰ Ohno M.; Sametsky E. A.; Younkin L. H.; Oakley H.; Younkin S. G.; Citron M.; Vassar R.; Disterhoft J. F., *Neuron* **2004**, *41*, 27.
- ⁷¹ Tamagno E.; Bardini P.; Obbili A.; Vitali A.; Borghi R.; Zaccheo D.; Prozato M. A.; Danni O.; Smith M. A.; Perry G.; Tabaton M., *Neurobiol. Dis.* **2002**, *10*, 279.
- ⁷² Wen Y.; Onyewuchi O.; Yang S.; Liu R.; Simpkins J. W., *Brain Res.* **2004**, *1009*, 1.
- ⁷³ Zhang X.; Zhou K.; Wang R.; Cui J.; Lipton S. A.; Liao F. F.; Xu H.; Zhang Y. W., *J. Biol. Chem.* **2007**, *282*, 10873.
- ⁷⁴ Blasko I.; Beer R.; Bigl M.; Apelt J.; Franz G.; Rudzki D.; Ransmayr G.; Kampfl A.; Schliebs R., *J. Neural. Transm.* **2004**, *111*, 523.
- ⁷⁵ Sambamurti K.; Kinsey R.; Maloney B.; Ge Y. W.; Lahiri D. K., *FASEB J.* **2004**, *18*, 1034.
- ⁷⁶ Bourne K. Z.; Ferrari D. C.; Lange-Dohna C.; Roßner S.; Wood T. G.; Perez-Polo J. R., *J. Neuroscience Research* **2007**, *85*, 1194.
- ⁷⁷ Bales K. R.; Verina T.; Cummins D. J.; Du Y.; Dodel R. C.; Saura J.; Fishman C. E.; DeLong C. A.; Piccardo P.; Petegnief V.; Ghetti B.; Paul S. M., *Proc. Natl. Acad. Sci.* **1999**, *96*, 15233.
- ⁷⁸ Bales K. R.; Du Y.; Holtzman D.; Cordell B.; Paul S. M., *Neurobiol Aging* **2000**, *21*, 427.
- ⁷⁹ Toliver-Kinsky T.; Rassin D.; Perez-Polo J. R., *Neurobiol Aging* **2002**, *23*, 899.
- ⁸⁰ Saunders A. J.; Kim T.-W.; Tanzi R. E.; Fan W.; Bennett B. D.; Babu-Khan S., et al., *Science* **1999**, *286*, 1255.
- ⁸¹ Acquati F.; Accarino M.; Nucci C.; Fumagalli P.; Jovine L.; Ottolenghi S.; Taramelli R., *FEBS Lett.* **2000**, *468*, 59.
- ⁸² Farzan M.; Schnitzler C. E.; Vasilieva N.; Leung D.; Choe H., *Proc. Natl. Acad. Sci. USA* **2000**, *97*, 9712.
- ⁸³ Hussain I.; Powell D. J.; Howlett D. R.; Chapman G. A.; Gilmour L.; Murdock P. R., et al., *Mol. Cell. Neurosci.* **2000**, *16*, 609.
- ⁸⁴ Fluhner R.; Capell A.; Westemeyer G.; Willem M.; Hartung B.; Condrón M. M.; Teplon D. B.; Haas C.; Walter J., *J. Neurochem.* **2004**, *279*, 3685.
- ⁸⁵ Haas C.; Selkoe D. J., *Cell* **1993**, *75*, 1039.
- ⁸⁶ Herreman A.; Serneels L.; Annaert W.; Collen D.; Schoonjans L.; De Strooper B., *Nat. Cell. Biol.* **2000**, *2*, 461.
- ⁸⁷ Li X.; Greenwald I., *Proc. Natl. Acad. Sci. USA* **1998**, *95*, 7109.
- ⁸⁸ De Strooper B.; Saftig P.; Craessaerts K.; Vanderstichele H.; Guhde G.; Annaert W.; Von Figura K.; Van Leuven F., *Nature* **1998**, *391*, 387.
- ⁸⁹ Wolfe M. S.; Xia W.; Ostaszewski B. L.; Diehl T. S.; Kimberly W. T.; Selkoe D. J., *Nature* **1999**, *398*, 513.
- ⁹⁰ Shah S.; Lee S. F.; Tabuchi K.; Hao Y. H.; Yu C.; Laplant Q.; Ball H.; Dann C. E.; Sudhof T.; Yu G., *Cell* **2005**, *122*, 435.

-
- ⁹¹ Serneels L. et al., *Proc Natl Acad Sci USA* **2005**, *102*, 1719.
- ⁹² Osenkowski P.; Li H.; Ye W.; Li D.; Aeschbach L.; Fraering P. C.; Wolfe M. S.; Selkoe D. J.; Li H., *J. Mol. Biol.* **2009**, *385*: 642.
- ⁹³ Sato C.; Morohashi Y.; Tomita T.; Iwatsubo T., *J Neurosci.* **2006**, *26*, 12081.
- ⁹⁴ <http://molgen-www.uia.ac.be/ADmutations/>
- ⁹⁵ Herreman A.; Hartmann D.; Annaert W.; Saftig P.; Craessaerts K.; Serneels L.; Umans L.; Schrijvers V.; Checler F.; Vanderstichele H.; Baekelandt V.; Dressel R.; Cupers P.; Huylebroeck D.; Zwijsen A.; Van Leuven F.; De Strooper B., *Proc. Natl. Acad. Sci. USA* **1999**, *96*, 11872.
- ⁹⁶ Thinakaran G.; Borchelt D. R.; Lee M. K.; Slunt H. H.; Spitzer L.; Kim G.; Ratovitsky T.; Davenport F.; Nordstedt C.; Seeger M.; et al., *Neuron* **1996**, *17*, 181.
- ⁹⁷ De Strooper B., *EMBO Rep.* **2007**, *8*, 141.
- ⁹⁸ Wolfe M. S., *EMBO Rep.* **2007**, *8*, 136.
- ⁹⁹ De Strooper B.; Annaert W.; Cupers P.; Saftig P.; Craessaerts K.; Mumm J. S.; Schroeter E. H.; Schrijvers V.; Wolfe M. S.; Ray W. J.; Goate A.; Kopan R., *Nature* **1999**, *398*, 518.
- ¹⁰⁰ Ikeuchi T.; Sisodi S. S., *J. Biol. Chem.* **2003**, *278*, 7751.
- ¹⁰¹ Ni C.-Y.; Murphy M. P.; Golde T. E.; Carpenter G., *Science* **2001**, *294*, 2179.
- ¹⁰² Lammich S.; Okochi M.; Takeda M.; Kaether C.; Capell A.; Zimmer A. K.; Edbauer D.; Walter J.; Steiner H.; Haass C., *J. Biol. Chem.* **2002**, *277*, 44754.
- ¹⁰³ Marambaud P.; Shioi J.; Serban G.; Georgakopoulos A.; Sarner S.; Nagy V.; Baki L.; Wen P.; Efthimiopoulos S.; Shao Z.; Wisniewski T.; Robakis N. K., *EMBO J.* **2002**, *21*, 1948.
- ¹⁰⁴ Pan D.; Rubin G. M., *Cell* **1997**, *90*, 271.
- ¹⁰⁵ Brou C.; Logeat F.; Gupta N.; Bessia C.; LeBail O.; Doedens J. R.; et al., *Mol. Cell.* **2000**, *5*, 207.
- ¹⁰⁶ Mumm J. S.; Schroeter E. H.; Saxena M. T.; Griesemer A.; Tian X.; Pan D. J., et al., *Mol. Cell.* **2000**, *5*, 197.
- ¹⁰⁷ Ohishi K.; Varnum-Finney B.; Flowers D.; Anasetti C.; Myerson D.; Bernstein I. D., *Blood* **2002**, *95*, 2847.
- ¹⁰⁸ Brou C.; Logeat F.; Gupta N.; Bessia C.; LeBail O.; Doedens J. R., et al., *Mol. Cell.* **2000**, *5*, 207.
- ¹⁰⁹ Wong P. C.; Zheng H.; Chen H.; Becher M. W.; Sirinathsingji D. J.; Trumbauer M. E., et al. *Nature* **1997**, *387*, 288.
- ¹¹⁰ Shen J.; Bronson R. T.; Chen D. F.; Xia W.; Selkoe D. J.; Tonegawa S., *Cell* **1997**, *89*, 629.
- ¹¹¹ Josien H., *Curr. Opin. Drug Discovery Dev.* **2002**, *5*, 513.
- ¹¹² Wong G. T.; Manfra D.; Poulet F. M.; Zhang Q.; Josien H.; Bara T.; Engstrom L.; Pinzon-Ortiz M.; Fine J. S.; Lee H.-J. J.; Zhang L.; Higgins G. A.; Parker E. M., *J. Biol. Chem.* **2004**, *279*, 12876.

-
- ¹¹³ Searfoss G. H.; Jordan W. H.; Calligaro D. O.; Galbreath E. J.; Schirtzinger L. M.; Berridge B. R.; Gao H.; Higgins M. A.; May P. C.; Ryan T. P., *J Biol. Chem.* **2003**, 278, 46107.
- ¹¹⁴ Tucker H. M.; Kihiko M.; Caldwell J. N.; Wright S.; Kawarabayashi T.; Price D.; Walker D.; Scheff S.; McGillis J. P.; Rydel R. E.; Estus S., *J. Neurosci.* **2000**, 20, 3937.
- ¹¹⁵ Hadland B. K.; Manley N. R.; Su D.; Longmore G. D.; Moore C. L.; Wolfe M. S.; Schroeter E. H.; Kopan R., *Proc Natl Acad Sci USA* **2001**, 98, 7487.
- ¹¹⁶ Tournoy J.; Bossuyt X.; Snellinx A.; Regent M.; Garmyn M.; Serneels L.; Saftig P.; Craessaerts K.; De Strooper B.; Hartmann D., *Hum. Mol. Genet.* **2004**, 13, 1321.
- ¹¹⁷ Chumsri S.; Matsui W.; Burger A. M., *Clinical Cancer Research* **2007**, 13, 6549.
- ¹¹⁸ Kim J., et al., *J. Neurosci.* **2007**, 27, 627.
- ¹¹⁹ Weggen S.; Eriksen J. L.; Das P.; Sagi S. A.; Wang R.; Pietrzik C. U.; Kirk A. Findlay K. A.; Smith T. E.; Murphy M. P.; Bulter T.; Kang D. E.; Marquez-Sterling N.; Todd E. Golde T. E.; Koo E. H., *Nature* **2001**, 4141, 212.
- ¹²⁰ Netzer W. J.; Dou F.; Cai D.; Veach D.; Jean S.; Li Y.; William G. Bornmann W. G.; Clarkson B.; Huaxi Xu H.; Greengard P., *PNAS* **2003**, 14, 12444.
- ¹²¹ Gianni D.; Zambrano N.; Bimonte M.; Minopoli G.; Mercken L.; Talamo F.; Scaloni A.; Russo T., *J. Biol. Chem.* **2003**, 278, 9290.
- ¹²² NeuroPerspective-NeuroInvestment, **September 2012**, n° 205, ISSN 1537-6346
- ¹²³ Thathiah A.; Spittaels K.; Hoffmann M.; Staes M.; Cohen A.; Horre K.; Vanbrabant M.; Coun F.; Baekelandt V.; Delacourte A.; Fischer D. F.; Pollet D.; De Strooper B.; Merchiers P., *Science* **2009**, 323, 946.
- ¹²⁴ Geula C.; Wu C. K.; Saroff D.; Lorenzo A.; Yuan M.; Yankher B. A., *Nature Med.* **1998**, 4, 827.
- ¹²⁵ Flament S.; Delacourte A.; Hemon B.; De´fossez A., *Acad. Sci. III.* **1989**, 308, 77.
- ¹²⁶ Grundke-Iqbal, K.; Iqbal Y. C.; Tung M.; Quinlan H. M., *Proc. Natl. Acad. Sci. USA* **1986**, 83 4913.
- ¹²⁷ Ihara Y.; Nukina N.; Miura R.; Ogawara M., *J. Biochem.* **1986**, 99, 1807.
- ¹²⁸ Gong C. X.; Liu F.; Grunfke-Iqbal I.; Iqbal K., *J. Neural. Transm.* **2005**, 112, 813.
- ¹²⁹ Asai M.; Hattori C.; Szabo B.; sasagawa N.; Maruyama K.; Tanuma S.; Ishiura S., *Biochem. Biophys. Res. Commun.* **2003**, 301, 231.
- ¹³⁰ Gomez-Isla T.; Hollister R.; West H.; Mui S.; Growdon J. H.; Petersen R. C.; Parisi J. E.; Hyman B. T., *Ann. Neurol.* **1997**, 41, 17.
- ¹³¹ Nacharaju P.; Lewis J.; Easson C.; Yen S.; Hackett J.; Hutton M.; Yen S. H., *FEBS Lett.*, **1999**, 447, 195.
- ¹³² Gamblin T. C.; King M. E.; Kuret J.; Berry R. W.; Binder L. I., *Biochemistry* **2000**, 39, 14203.
- ¹³³ Goedert M.; Jakes R.; Spillantini M. G.; Hasegawa M.; Smith M. J.; Crowther R. A., *Nature* **1996**, 383, 550.
- ¹³⁴ Kampers T.; Friedhoff P.; Biernat J.; Mandelkow E. M.; Mandelkow E., *FEBS Lett.* **1996**, 399, 344.

-
- ¹³⁵ Hasegawa M.; Smith M. J.; Goedert M., *FEBS Lett.* **1998**, 437, 207.
- ¹³⁶ Barghorn S.; Zheng-Fischhöfer Q.; Ackmann M.; Biernat J.; von Bergen M.; Mandelkow E. M.; Mandelkow E.; *Biochemistry* **2000**, 39, 11714.
- ¹³⁷ Zilka N.; Filipcik P.; Koson P.; Fialova L.; Skrabana R.; Zilkova M.; Rolkova G.; Kontsekova E.; Novak M., *FEBS Lett.* **2006**, 580, 3582.
- ¹³⁸ Yin H.; Kuret J., *FEBS Lett.* **2006**, 580, 211.
- ¹³⁹ Jeganathan S.; von Bergen M.; Brutlach H.; Steinhoff H. J.; Mandelkov E., *Biochemistry* **2006**, 45, 2283.
- ¹⁴⁰ Von Bergen M.; Friedhoff P.; Biernat J.; Heberle J.; Mandelkow E. M.; Mandelkow E., *Proc. Natl. Acad. Sci. USA* **2000**, 97, 5129.
- ¹⁴¹ Wang Y. P.; Biernat J.; Pickhardt M.; Mandelakow E.; Mandelkow E. M., *Proc. Natl. Acad. Sci. USA* **2007**, 104, 10252.
- ¹⁴² Liu S.J.; Zhang J.Y.; Li H.L.; Fang Z.Y.; Wang Q.; Deng H. M.; Gong C. X.; Grundke-Iqbal I.; Iqbal K.; Wang J.Z., *J. Biol. Chem.* **2004**, 279, 50078.
- ¹⁴³ Xiao J.; Perry G.; Troncoso J.; Monteiro M. J., *J. Neuropathol. Exp. Neurol.* **1996**, 55, 954.
- ¹⁴⁴ Yamaguchi H.; Ishiguro K.; Uchida T.; Takashima A.; Lemere C. A.; Imahori K., *Acta Neuropathol.(Berl)* **1996**, 92, 232.
- ¹⁴⁵ Pei J. J.; Tanaka T.; Tung Y. C.; Braak E.; Iqbal K.; Grundke-Iqbal I., *J. Neuropathol. Exp. Neurol.* **1997**, 56, 70.
- ¹⁴⁶ Pei J.J.; Braak E.; Braak H.; Grundke-Iqbal I.; Iqbal K.; Winblad B.; Cowburn R. F., *J. Neuropathol. Exp. Neurol.* **1999**, 58, 1010.
- ¹⁴⁷ Embi N.; Rylatt D. B.; Cohen P., *Eur. J. Biochem.* **1980**, 107, 519.
- ¹⁴⁸ Dierick H.; Bejsovec A., *Curr. Top. Dev. Biol.* **1999**, 43, 153.
- ¹⁴⁹ Forde J. E.; Dale T. C., *Cell Mol. Life Sci.* **2007**, 64, 1930.
- ¹⁵⁰ Phiel C. J.; Wilson C. A.; Lee V. M.; Klein P. S., *Nature* **2003**, 423, 435.
- ¹⁵¹ Muyliaert D.; Kremer A.; Jaworski T.; Borghgraef P.; Devijver H.; et al., *Genes Brain Behav.* 7 Suppl. **2008**, 1, 57.
- ¹⁵² Lochhead P. A.; Kinstrie R.; Sibbet G.; Rawjee T.; Morrice N., et al., *Mol. Cell.* **2006**, 24, 627.
- ¹⁵³ Wang Z. F.; Li H. L.; Li X. C.; Zhang Q.; Tian Q.; Wang Q.; Xu H.; Wang J. Z., *J. Neurochem.* **2006**, 98, 1167.
- ¹⁵⁴ Klein P. S.; Melton D. A., *Proc. Natl. Acad. Sci. USA* **1996**, 93, 8455.
- ¹⁵⁵ Killick R.; Scales G.; Leroy K.; Causevic M.; Hooper C., et al., *Biochem. Biophys. Res. Commun.* **2009**, 386, 257.
- ¹⁵⁶ Ho L.; Qin W.; Pompl P. N.; Xiang Z.; Wang J.; et al., *Faseb J.* **2004**, 18, 902.
- ¹⁵⁷ Bartus R.T.; Dean III R.L.; Beer B.; Lippa A.S., *Science* **1982**, 217, 408.

-
- ¹⁵⁸ Whitehouse P. J.; Price D. L.; Struble R. G., et al., *Science* **1982**, 215, 1237.
- ¹⁵⁹ Morrison J. H.; Hof P. R., *Science* **1997**, 278, 412.
- ¹⁶⁰ Araujo D. M.; Lapchak P. A.; Robitaille Y.; Gauthier S.; Quirion R., *J. Neurochem.* **1988**, 50, 1914.
- ¹⁶¹ Geula C.; Mesulam M. M., *Alzheimer Disease*. Eds R. D. Terry; R. Katzman; K. L. Bick. Raven Press: New York, pp. 263.
- ¹⁶² Hardy J.; Adolfsson R.; Alafuzoff I.; Bucht G.; Marcusson J.; Nyberg P.; Per Dahl E.; Wester P.; Winblad B.; *Neurochem. Int.* **7** **1985**, 545.
- ¹⁶³ Terry A. V.; Buccafusco J. J., *J. Pharm. Exp. Ther.* **2003**, 306, 821.
- ¹⁶⁴ Bowen D. M.; Smith C. B.; White P.; Davison A. N., *Brain* **1976**, 99, 459.
- ¹⁶⁵ Bowen D. M.; White P.; Spillane J. A.; Goodhardt M. J.; Curzon G.; Iwangoff P.; Meier-Ruge W.; Davison A.N., *Lancet* **1979**, 11-14
- ¹⁶⁶ Davies P.; Maloney A. J. F., *Lancet* **1976**, 1403.
- ¹⁶⁷ Whitehouse P. J.; Price D. L.; Clark A. W.; Coyle J. T.; de Long M. R., *Ann. Neurol.* **1981**, 10, 122.
- ¹⁶⁸ Haga K., et al., *Nature* **2012**, 482, 547.
- ¹⁶⁹ Kruse A. C., et al., *Nature* **2012**, 482, 552
- ¹⁷⁰ Teaktong T.; Graham A.J.; Court J.A.; Perry R.H.; Jaros E.; Johnson M.; Hall R.; Perry E.K., *J. Neurol. Sci.*, **2004**, 225, 39.
- ¹⁷¹ Nordberg A., *Neurochem. Int.*, **1994**, 25, 93.
- ¹⁷² Martin-Ruiz C.M.; Court J.A.; Molnar E.; Lee M.; Gotti C.; Mamalaki A.; Tsouloufifis T.; Tzartos S.; Ballard C.; Perry R.H.; Perry E.K., *J. Neurochem.* **1999**, 73, 1635.
- ¹⁷³ Mash D.C.; Flynn D.D.; Potter L.T., *Science* **1985**, 228, 1115.
- ¹⁷⁴ Flynn D. D.; Ferrari-DiLeo G.; Levey A. I.; Mash D. C., *Life Sci.* **1995**, 56, 869.
- ¹⁷⁵ Tsang S. W.; Lai M. K.; Kirvell S.; Francis P. T.; Esiri M. M.; Hope T.; Chen C. P.; Wong P. T., *Neurobiol. Aging* **2006**, 27, 1216.
- ¹⁷⁶ Auld D.S.; Kar S.; Quirion R., *Trends Neurosci.* **1998**, 21, 43.
- ¹⁷⁷ Harkany T.; De Jong G. I.; Soo's K.; Penke B.; Luiten P. G.; Gulya K., *Brain Res.* **1995**, 698, 270.
- ¹⁷⁸ Boncristiano S.; Calhoun M. E.; Kelly P. H.; Pfeifer M.; Bondolfi L.; Stalder M.; Phinney A. L.; Abramowski D.; Sturchler-Pierrat C.; Enz A.; Sommer B.; Staufenbiel M.; Jucker M., *J. Neurosci.*, **2002**, 22, 3234.
- ¹⁷⁹ Wang H. Y.; Lee D. H.; D'Andrea M. R.; Peterson P. A.; Shank R. P.; Reitz A. B., *J. Biol. Chem.* **2000**, 275, 5626.
- ¹⁸⁰ Nagele R. G.; D'Andrea M. R.; Anderson W. J., Wang H. Y. *Neuroscience* **2002**, 110, 199.

-
- ¹⁸¹ Oddo S.; Caccamo A.; Green K. N.; Liang K.; Tran L.; Chen Y.; Leslie F. M.; LaFerla F. M., *Pros. Natl. Acad. Sci. U.S.A.* **2005**, *102*, 3046.
- ¹⁸² Kelly J. F.; Furukawa K.; Barger S. W.; Rengen M. R.; Mark R. J.; Blanc E. M.; Roth G. S.; Mattson M. P.; *Proc. Natl. Acad. Sci. U.S.A.* **1996**, *93*, 6753.
- ¹⁸³ Machova´ E.; Jakubi´k J.; Michal P.; Oksman M.; Iivonen H.; Tanila H.; Dolez´al V., *Neurobiol. Aging* **2008**, *29*, 368.
- ¹⁸⁴ Buxbaum J. D.; Oishi M.; Chen H. I.; Pinkas-Kramarski R.; Jaffe E. A.; Gandy S. E.; Greengard, P., *Proc. Natl. Acad. Sci. U.S.A.* **1992**, *89*, 10075.
- ¹⁸⁵ Nitsch R. M.; Slack B. E.; Wurtman R. J.; Growdon J. H., *Science* **1992**, *258*, 304.
- ¹⁸⁶ Schaeffer E. L.; Gattaz, W. F., *Psychopharmacology (Berl)* **2008**, *198*, 1.
- ¹⁸⁷ Kim S. H.; Kim Y. K.; Jeong, S. J.; Haass C.; Kim Y. H.; Suh Y. H., *Mol. Pharmacol.* **1997**, *52*, 430.
- ¹⁸⁸ Qi X.L.; Nordberg A.; Xiu J.; Guan Z. Z., *Neurochem. Int.* **2007**, *51*, 377.
- ¹⁸⁹ Roensch J.; Crisby M.; Nordberg A.; Xiao Y.; Zhang L. J.; Guan Z. Z., *Neurochem. Int.* **2007**, *50*, 800.
- ¹⁹⁰ Samochocki M.; Hoffle A.; Fehrenbacher A.; Jostock R.; Ludwig J.; Christner C.; Radina M.; Zerlin M.; Ullmer C.; Pereira E. F.; Lubbert H.; Albuquerque E. X.; Maelicke A., *J. Pharmacol. Exp. Ther.* **2003**, *305*, 1024–1036.
- ¹⁹¹ Buxbaum J. D., et al., *Proc. Natl Acad. Sci. USA* **1990**, *87*, 6003.
- ¹⁹² Caporaso G. L.; Gandy S. E.; Buxbaum J. D.; Ramabhadran T. V.; Greengard P., *Proc. Natl Acad. Sci. US*, **1992**, *89*, 3055.
- ¹⁹³ Zuchner T.; Perez-Polo J. R.; Schliebs R., *J. Neurosci. Res.* **2004**, *77*, 250.
- ¹⁹⁴ Barnard E. A.; *The Peripheral Nervous System*, Plenum Press, New York, **1974**, pp. 201–224.
- ¹⁹⁵ Sussman J. L., et al., *Science* **1991**, *253*, 872-9.
- ¹⁹⁶ Kryger G.; Harel M.; Giles K.; Toker L.; Velan B.; Lazar A.; Kronman C.; Barak D.; Ariel N.; Shafferman A.; Silman I.; Sussman J. L., *Acta Crystallogr. Sect. D: Biol. Crystallogr.* **2000**, *56*, 1385–1394
- ¹⁹⁷ Alvarez A.; Bronfman F.; Perez C. A.; Vicente M.; Garrido J.; Inestrosa N. C., *Neurosci. Lett.* **1995**, *201*, 49.
- ¹⁹⁸ Inestrosa N. C.; Alvarez A.; Calderon F., *Mol. Psychiatry* **1996**, *1*, 359–361.
- ¹⁹⁹ De Ferrari G. V.; Canales M. A.; Shin I.; Weiner L. M.; Silman I.; Inestrosa N. C., *Biochemistry* **2001**, *40*, 10447–10457.
- ²⁰⁰ Bartolini M.; Bertucci C.; Cavrini V.; Andrisano V., *Biochem. Pharmacol.* **2003**, *65*, 407–416.
- ²⁰¹ Alvarez A.; Alarcon R.; Opazo C.; Campos E. O.; Munoz F. Y.; Calderon F. H., et al., *J. Neurosc.*, **1998**, *18*, 3213.
- ²⁰² Munoz- Torrero D., *Current Med. Chem.* **2008**, *15*, 2433.

-
- ²⁰³ Mahley R. W., *Science* **1988**, 240, 622.
- ²⁰⁴ Weisgraber K. H., *Adv. Protein, Chem.* **1994**, 45, 249.
- ²⁰⁵ Mahley R. W.; Rall S. C., *Annu. Rev. Genomics Hum. Genet.* **2000**, 1, 507.
- ²⁰⁶ Boschert U.; Merlo-Pich E.; Higgins G.; Roses A. D.; Catsicas S., *Neurobiol. Dis.* **1999**, 6, 508.
- ²⁰⁷ Utermann G.; Hees M.; Steinmetz A., *Nature* **1977**, 269, 604.
- ²⁰⁸ Corder E. H.; Saunders A. M.; Risch N. J.; Strittmatter W. J.; Schmechel D. E.; Gaskell P. C.; Jr. Rimmler J. B.; Locke P. A.; Conneally P. M.; Schmechel K. E., et al., *Nat. Genet.* **1994**, 7, 180.
- ²⁰⁹ Strittmatter W. J.; Saunders A. M.; Schmechel D.; et al., *Proc. Natl. Acad. Sci. USA*, **1993**, 90, 1977.
- ²¹⁰ Poirier J.; Davignon J.; Bouthillier D.; Kogan S.; Bertrand P.; Gauthier S., *Lancet* **1993**, 342, 697.
- ²¹¹ Mayeux R.; Stern Y.; Ottman R., et al., *Ann. Neurol.* **1993**, 34, 752.
- ²¹² Brousseau T.; Legrain S.; Berr C.; Gourlet V.; Vidal O.; Amouyel P., *Neurology* **1994**, 44, 342.
- ²¹³ Farrer L. A.; Cupples L. A.; Haines J. L.; Hyman B.; Kukull W. A.; Mayeux R.; Myers R. H.; Pericak-Vance M. A.; Risch N.; Van Duijn C. M., *J. Am. Med. Assoc.* **1997**, 278, 1349.
- ²¹⁴ Nicoll J. A. R.; Roberts G. W.; Graham D. I., *Ann. N.Y. Acad. Sci.* **1996**, 777, 271.
- ²¹⁵ Teasdale G. M.; Nicoll J. A. R.; Murray G.; Fiddes M., *Lancet* **1997**, 350, 1069.
- ²¹⁶ Jordan B. D.; Relkin N. R.; Ravdin L. D.; Jacobs A. R.; Bennett A.; Gandy S., *J. Am. Med. Assoc.* **1997**, 278, 136.
- ²¹⁷ Alberts M. J.; Graffagnino C.; McClenny C.; DeLong D.; Strittmatter W.; Saunders A. M.; Roses A. D., *Lancet* **1995**, 346, 575.
- ²¹⁸ Harhangi B. S.; De Rijk M. C.; van Duijn C. M.; Van Broeckhoven C.; Hofman A.; Breteler M. M. B., *Neurology* **2000**, 54, 1272.
- ²¹⁹ Parsian A.; Racette B.; Goldsmith L. J.; Perlmutter J. S., *Genomics* **2002**, 79, 458.
- ²²⁰ Li Y. J.; Hauser M. A.; Scott W. K.; Martin E. R.; Booze M. W.; Qin, X. J.; Walter J. W.; Nance M. A.; Hubble J. P.; Koller W. C., et al., *Neurology* **2004**, 62, 2005.
- ²²¹ Al-Chalabi A.; Enayat Z. E.; Bakker M. C.; Sham P. C.; Ball D. M.; Shaw C. E.; Lloyd C. M.; Powell J. F.; Leigh P. N., *Lancet* **1996**, 347, 159.
- ²²² Moulard B.; Sefiani A.; Laamri A.; Malafosse A.; Camu W., *J. Neurol. Sci.* **1996**, 139 Suppl., 34.
- ²²³ Fazekas F.; Strasser-Fuchs S.; Kollegger H.; Berger T.; Kristoferitsch W.; Schmidt H.; Enzinger C.; Schiefermeier M.; Schwarz C.; Kornek B., et al., *Neurology* **2001**, 57, 853.
- ²²⁴ Corder E. H.; Saunders A. M.; Strittmatter W. J.; Schmechel D. E.; Gaskell P. C.; Small G. W.; Roses A. D.; Haines J. L.; Pericak-Vance M. A., *Science* **1993**, 261, 921.
- ²²⁵ Dong L. M.; Wilson C.; Wardell M. R.; Simmons T.; Mahley R. W.; Weisgraber K. H., et al., *J. Biol. Chem.* **1994**, 269, 22358.

-
- ²²⁶ Dong L.-M.; Weisgraber K. H., *J. Biol. Chem.* **1996**, *271*, 19053.
- ²²⁷ Weisgraber K. H., *Adv. Protein Chem.* **1994**, *45*, 249.
- ²²⁸ Mahley R. W.; Weisgraber K. H.; Huang Y, *PNAS* **2006**, *11*, 5644.
- ²²⁹ Holtzman D. M.; Pitas R. E.; Kilbridge J.; Nathan B.; Mahley R. W.; Bu G.; et al., *Proc. Natl. Acad. Sci. USA* **1995**, *92*, 9480.
- ²³⁰ Bales K. R.; Verina T.; Cummins D. J.; Du Y.; Dodel R. C.; Saura J.; et al., *Proc. Natl. Acad. Sci. USA* **1999**, *96*, 15233.
- ²³¹ Irizarry M. C.; Cheung B. S.; Rebeck G. W.; Paul S. M.; Bales K. R.; and Hyman B. T., *Acta Neuropathol.* **2000**, *100*, 451.
- ²³² Castellano J. M.; Kim J.; Stewart F. R.; DeMattos R. B.; Patterson B. W.; Fagan A. M.; Morris J. C.; Mawuenyega K. G.; Paul S. M.; Bateman R. J.; et al., *Sci. Transl. Med.* **2011**, *3*, 89ra57
- ²³³ Strittmatter W. J.; Saunders A. M.; Schmechel D.; Pericak-Vance M.; Enghild J.; Salvesen G. S.; et. al., *Proc. Natl. Acad. Sci. USA* **1993a**, *90*, 1977.
- ²³⁴ Cho H. S.; Hyman B. T.; Greenberg S. M.; and Rebeck G. W., *J. Neuropathol. Exp. Neurol.* **2001**, *60*, 342.
- ²³⁵ Ma J.; Yee A.; Brewer H. B. Jr.; Das S.; Potter H., *Nature* **1994**, *372*, 92.
- ²³⁶ Sanan D. A.; Weisgraber K. H.; Russell S. J.; Mahley R. W.; Huang D.; Saunders A.; et al., *J. Clin. Invest.* **1994**, *94*, 860.
- ²³⁷ Moir R. D.; Atwood C. S.; Romano D. M.; Laurans M. H.; Huang X.; Bush A. I.; et al., *Biochemistry* **1999**, *38*, 4595.
- ²³⁸ LaDu M. J.; Falduto M. T.; Manelli A. M.; Reardon C. A.; Getz G. S.; Frail D. E., *J. Biol. Chem.* **1994**, *269*, 23403.
- ²³⁹ LaDu M. J.; Pederson T. M.; Frail D. E.; Reardon C. A.; Getz G. S.; Falduto M. T., *J. Biol. Chem.* **1995**, *270*, 9039.
- ²⁴⁰ Ye S.; Huang, Y.; Mullendorff K.; Dong L.; Giedt G.; Meng E. C.; Cohen F. E.; Kuntz I. D.; Weisgraber K. H.; Mahley R. W., *Proc. Natl. Acad. Sci. USA* **2005**, *102*, 18700.
- ²⁴¹ Herz J.; Beffert U.; *Nat. Rev. Neurosci.* **2000**, *1*, 51.
- ²⁴² Koo E. H.; Squazzo, S. L., *J. Biol. Chem.* **1994**, *269*, 17386.
- ²⁴³ Perez R. G.; Soriano S.; Hayes J. D.; Ostaszewski B.; Xia W.; Selkoe D. J.; Chen X.; Stokin G. B.; Koo E. H., *J. Biol. Chem.* **1999**, *274*, 18851.
- ²⁴⁴ Ulery P. G.; Beers J.; Mikhailenko I.; Tanzi R. E.; Rebecki G. W.; Hymani B. T.; Strickland D. K., *J. Biolog. Chem.* **2000**, *275*, 7410.
- ²⁴⁵ Strittmatter W. J.; Saunders A. M.; Goedert M.; Weisgraber K. H.; Dong L.-M.; Jakes R.; et al., *Proc. Natl. Acad. Sci. USA* **1994**, *91*, 11183.
- ²⁴⁶ Strittmatter W. J.; Weisgraber K. H.; Goedert M.; Saunders A. M.; Huang D.; Corder E. H.; et al., *Exp. Neurol.* **1994**, *125*, 163.

-
- ²⁴⁷ Tesseur I.; Van Dorpe J.; Spittaels K.; Van den Haute C.; Moechars D.; Van Leuven F., *Am. J. Pathol.* **2000**, *156*, 951.
- ²⁴⁸ Brunet A.; Datta S. R.; Greenberg M. E., *Curr. Opin. Neurobiol.* **2001**, *11*, 297.
- ²⁴⁹ Reiman E. M.; Webster J. A.; et al., *Neuron* **2007**, *54*, 713.
- ²⁵⁰ Harris F. M.; Brecht W. J.; Xu Q.; Tesseur I.; Kekonius L.; Wyss-Coray T.; Fish J. D.; Masliah E.; Hopkins P. C.; Scarce-Levie K.; et al., *Proc. Natl. Acad. Sci. USA* **2003**, *100*, 10966.
- ²⁵¹ Huang Y.; Liu X. Q.; Wyss-Coray T.; Brecht W. J.; Sanan D. A.; Mahley R. W., *Proc. Natl. Acad. Sci. USA* **2001**, *98*, 8838–8843.
- ²⁵² Lovell M. A., et al., *J. Neurol. Sci.* **1998**, *158*, 47.
- ²⁵³ Zatta P.; Drago D.; Bolognin S.; Sensi S. L., *Trends in Pharmacological Sciences* **2009**, *30*, 346.
- ²⁵⁴ Adlard P., A. et al., *Neuron* **2008**, *59*, 43.
- ²⁵⁵ Cherny R. A., et al., *Neuron* **2001**, *30*, 665.
- ²⁵⁶ Opazo C. et al., *Biometals* **2003**, *16*, 91.
- ²⁵⁷ Frederickson C. J.; Moncrieff D.W., *Biol. Signals* **1994**, *3*, 127.
- ²⁵⁸ Frederickson C. J., et al., *J. Chem. Neuroanat.* **1992**, *5*, 521.
- ²⁵⁹ Sindreu C. B., et al., *Cereb. Cortex* **2003**, *13*, 823.
- ²⁶⁰ Bush A. I., *Trends Neurosci.* **2003**, *26*, 207.
- ²⁶¹ Lee J. Y. et al., *Proc. Natl. Acad. Sci. U. S. A.* **2002**, *99*, 7705.
- ²⁶² Adlard P.A., et al., *Neuron* **2008**, *59*, 43.
- ²⁶³ Cherny R. A., et al, *Neuron* **2001**, *30*, 665.
- ²⁶⁴ Lee J.-Y.; Cole T. B.; Palmiter R. D.; Suh S. W.; Koh J.-Y., *Proc. Natl Acad. Sci. USA* **2002**, *99*, 7705.
- ²⁶⁵ Lovell M. A., et al., *J. Neuropathol. Exp. Neurol.* **2006**, *65*, 489.
- ²⁶⁶ Park I. H.; Jung M. W.; Mori H.; Mook-Jung I., *Biochem. Biophys. Res. Commun.* **2001**, *285*, 680.
- ²⁶⁷ Schlieff M .L., et al., *J. Neurosci.* **2005**, *25*, 239.
- ²⁶⁸ Atwood C. S., et al., *J. Neurochem.* **2000**, *75*, 1219.
- ²⁶⁹ Crouch P. J., et al., *Int. J. Biochem. Cell Biol.* **2008**, *40*, 181.
- ²⁷⁰ Lovell M. A.; Robertson J. D.; Teesdale W. J.; Campbell J. L.; Markesbery W.R., *J. Neurol. Sci.* **1999**, *158*, 47.
- ²⁷¹ Cherny R. A., et al., *J. Biol. Chem.* **1999**, *274*, 23223.
- ²⁷² Schipper H. M., *Free Radic. Biol. Med.* **2004**, *37*, 1995

-
- ²⁷³ Perl D. P.; Moalem S., *J. Alzheimers Dis.* **2006**, *9*, 291.
- ²⁷⁴ Drago D., et al., *Int. J. Biochem. Cell Biol.* **2008**, *40*, 731.
- ²⁷⁵ Arrendondo M.; Nunez M. T., *Mol. Aspects Med.* **2005**, *26*, 313.
- ²⁷⁶ Floris G.; Agro A. F., "Amine Oxidases" in Lennarz W. J.; Lane M. D., (Eds.) *Encyclopedia of Biological Chemistry*, vol. 1, Elsevier Inc., **2004**, pp. 85-89.
- ²⁷⁷ Bolognin S.; Messori L.; Drago D.; Gabbiani C.; Cendron L.; Zatta P., *Int. J. Biochem. Cell Biol.* **2011**, *43*, 877.
- ²⁷⁸ Huang, X., et al., *J. Biol. Chem.* **1999**, *274*, 37111.
- ²⁷⁹ Smith D. G.; Cappai R.; Barnham K., *J. Biochim. Biophys. Acta* **2007**, *1768*, 1976.
- ²⁸⁰ Barnham K. J.; Haeffner F.; Ciccotosto G. D.; Curtain C. C.; Tew D.; Mavros C.; Beyreuther K.; Carrington D.; Masters C. L.; Cherny R. A.; Cappai R.; Bush A. I., *FASEB J.* **2004**, *18*, 1427.
- ²⁸¹ Cuajungo M. P.; Faget K. Y.; Huang X.; Tanzi R. E.; Bush A. I., *Ann. N Y Acad. Sci.* **2000**, *920*, 292.
- ²⁸² Joseph J.; Shukitt-Hale B.; Denisova N. A.; et al., *Neurobiol. Aging* **2001**, *22*, 131.
- ²⁸³ Smith M. A.; Zhu X.; Tabaton M.; Liu G.; McKeel Jr D. W.; Cohen M. L.; et al., *J. Alzheimers Dis.* **2010**, *19*, 363.
- ²⁸⁴ Multhaup G.; Ruppert T.; Schlicksupp A.; Hesse L.; Behr D.; Masters C. L.; Beyreuther K., *Biochem. Pharmacol.* **1997**, *54*, 533.
- ²⁸⁵ Perry G.; Taddeo M. A.; Nunomura A.; Zhu X.; Zenteno-Savin T.; Drew K. L.; Shimohama S.; Avila J.; Castellani R. J.; Smith M. A., *Comp. Biochem. Physiol.* **2002**, *133*, 507.
- ²⁸⁶ Parihar M. S.; Hemnani T., *J. Clinical Neurosci.* **2004**, *11*, 456.
- ²⁸⁷ Sayre L. M.; Smith M. A.; Perry G., *Curr. Med. Chem.* **2001**, *8*, 721.
- ²⁸⁸ Dizdaroglu M., *Mutat Res.* **1992**, *275*, 331.
- ²⁸⁹ Weissig V.; Cheng S. M.; Souza G. G., *Mitochondrion* **2004**, *3*, 229.
- ²⁹⁰ Chang D. T.; Reynolds I. J., *Prog. Neurobiol.* **2006**, *80*, 241.
- ²⁹¹ Moreira P. I.; Zhu X.; Wang X.; Lee H-G.; Nunomura A.; Petersen R. B.; Perry G.; Smith M. A., *Biochimica and Biophysica Acta* **2010**, *1802*, 212.
- ²⁹² Turens J. F., *Biosci. Rep.* **1997**, *17*, 3.
- ²⁹³ Tretter L.; Adam-Vizi V., *J Neurosci.* **2004**, *24*, 7771.
- ²⁹⁴ Ibanez V.; Pietrini P.; Alexander G. E., et al., *Neurology* **1998**, *50*, 1585.
- ²⁹⁵ Anandatheerthavarada H. K.; Biswas G.; Robin M. A.; Avadhani N. G., *J. Cell Biol.* **2003**, *161*, 41.
- ²⁹⁶ Devi L.; Prabhu B. M.; Galati D. F.; Avadhani N. G.; Anandatheerthavarada H. K., *J. Neurosci.* **2006**, *26*, 9057.

-
- ²⁹⁷ Hansson Petersen C. A.; Alikhani N.; Behbahani H.; Wiehager B.; Pavlov P. F.; Alafuzoff I., et al., *Proc. Natl. Acad. Sci. USA* **2008**, *105*, 13145.
- ²⁹⁸ Sheng B. Y, Ying N.; Hui Z., JiaXin Y.; NanMing Z.; XiuFang Z.; et al., *Chin. Sci. Bull.* **2009**, *54*, 1725.
- ²⁹⁹ Caspersen C.; Wang N.; Yao J.; Sosunov A.; Chen X.; Lustbader J. W.; et al., *FASEB J.* **2005**, *19*, 2040.
- ³⁰⁰ Lustbader J. W.; Cirilli M.; Lin C.; Xu H. W.; Takuma K.; Wang N.; et al., *Science* **2004**, *304*, 448.
- ³⁰¹ Hansson C. A.; Frykman S.; Farmery M. r.; Tjernberg L. O.; Nilberth C.; Pursglove S. E.; et al., *J. Biol. Chem.* **2004**, *279*, 51654.
- ³⁰² Webster M. T.; Pearce B. R.; Bowen D. M.; Francis P. T., *J. Neural. Transm.* **1998**, *105*, 839.
- ³⁰³ Swerdlow R. H.; Khan S. M., *Exp. Neurol.* **2009**, *218*, 308.
- ³⁰⁴ Mancuso M.; Coppedè F.; Murri L.; Siciliano G., *Antiox. Redox Signal.* **2007**, *9*, 1631.
- ³⁰⁵ Murphy M. Greer. Jr., *Dialogues Clin. Neurosci.* **2000**, *2*, 233.
- ³⁰⁶ Rogers J.; Webster S.; Lue L. F.; et al., *Neurobiol. Aging* **1996**, *17*, 681.
- ³⁰⁷ Meda L.; Bernasconi S.; Bonaiuto C., et al., *J. Immunol.* **1996**, *157*, 1213.
- ³⁰⁸ Griffin W. S., Stanley L. C., Ling C.; White I.; MacLeod V.; Perrot L. J.; White C. L.; Araoz C., *Proc. Natl. Acad. Sci. USA* **1989**, *86*, 7611.
- ³⁰⁹ Goodwin J. L.; Uemura E.; Cunnick J. E., *Brain Res.* **1995**, *692*, 207.
- ³¹⁰ Van Muiswinkel F. L.; Veerhuis R.; Eikelenboom P., *J. Neurochem.* **1996**, *66*, 2468.
- ³¹¹ Klegeris A.; Walker D. G.; McGeer P. L., *Biochem. Biophys. Res. Commun.* **1994**, *199*, 984.
- ³¹² Sheng J. G.; Mrak R. E.; Griffin W. S., *Acta Neuropathol. (Berl)* **1997**, *94*, 1.
- ³¹³ Colton C. A.; Snell J.; Chernyshev O.; Gilbert D. L.; *Ann. N. Y. Acad. Sci.* **1994**, *738*, 54.
- ³¹⁴ Araujo D. M.; Cotman C. W., *Brain Res.* **1992**, *569*, 141.
- ³¹⁵ Merrill J. E., *Dev. Neurosci.* **1991**, *13*, 130.
- ³¹⁶ Szabo C.; Thiemermann C., *Adv. Pharmacol.* **1995**, *34*, 113.
- ³¹⁷ Suzuki Y. J.; Forman H. J.; Sevanian A., *Free Radic. Biol. Med.* **1997**, *22*, 269.
- ³¹⁸ He P.; Zhong Z.; Lindholm K.; Berning L.; Lee W.; Lemere C.; Staufenbiel M.; Li R.; Shen Y., *J. Cell Biol.* **2007**, *178*, 829.
- ³¹⁹ Warner T. D.; Mitchell J. A., *FASEB J.* **2004**, *18*, 790.
- ³²⁰ McGeer P. L.; Schulzer M.; McGeer E. G., *Neurology* **1996**, *47*, 425.
- ³²¹ Andreasson K. I.; Savonenko A.; Vidensky S.; Goellner J. J.; Zhang Y.; Shaffer A.; Kaufmann W. E.; Worley P. F.; Isakson P.; Markowska A. L., *J. Neurosci.* **2001**, *21*, 8198.

-
- ³²² Xiang Z.; Ho L.; Yemul S.; Zhao Z.; Qing W.; Pompl P.; Kelley K.; Dang A.; Teplow D.; Pasinetti G. M., *Gene Expr.* **2002**, *10*, 271.
- ³²³ Melnikova T.; Savonenko A.; Wang Q.; Liang X.; Hand T.; Wu L.; Kaufmann W. E.; Vehmas A.; Andreasson K. I., *Neurosci.* **2006**, *141*, 1149.
- ³²⁴ Yan Q.; Zhang J.; H. H., et al., *J. Neurosci.* **2003**, *23*, 7504.
- ³²⁵ Weggen S.; Eriksen J. L., et al., *Nature* **2001**, *414*, 212
- ³²⁶ Hirai H.; Kirsch J.; Laube B.; Betz H.; Kuhse J., *Proc. Natl. Acad. Sci. U.S.A.* **1996**, *93*, 6031.
- ³²⁷ Laube B.; Hirai H.; Sturgess M.; Betz H.; Kuhse J. *Neuron* **1997**, *18*, 493.
- ³²⁸ Hardingham G. E.; Fukunaga Y.; Bading H., *Nature Neurosci.* **2002**, *5*, 405.
- ³²⁹ Morris R. G., *J. Neurosci.* **1989**, *9*, 3040.
- ³³⁰ McNamara D.; Smith E. C.; Calligaro D. O.; O'Malley P. J.; McQuaid L. A.; Dingledine R., *Neurosci. Letters* **1990**, *120*, 17.
- ³³¹ Reynolds I. J.; Miller R. *J. Mol. Pharmacol.* **1989**, *36*, 758.
- ³³² Danysz W.; Parsons C. G., *Int. J. Geriatr. Psychiatry* **2003**, *18*, 23.
- ³³³ Husi H.; Grant S. G., *Trends Neurosci.* **2001**, *24*, 259.
- ³³⁴ Olney J. W., *J. Neuropathol. Exp. Neurol.* **1969**, *28*, 455.
- ³³⁵ Olney J. W.; & Ho, O. L., *Nature* **1970**, *227*, 609–611.
- ³³⁶ Lipton S. A.; Gu Z.; Nakamura T., *Int. Rev. Neurobiol.* **2007**, *82*, 1.
- ³³⁷ Lipton S. A.; Rosenberg P. A., *N. Engl. J. Med.* **1994**, *330*, 613.
- ³³⁸ Lipton S. A.; Nicotera P., *Cell Calcium* **1998**, *23*, 165.
- ³³⁹ Choi D. W., *Neuron*, **1988** *1*, 623.
- ³⁴⁰ Meldrum B.; Garthwaite J., *Trends Pharmacol. Sci.* **1990**, *11*, 379.
- ³⁴¹ Rothman S. M.; Olney J. W., *Ann Neurol.* **1986**, *19*, 105-11
- ³⁴² Dawson V. L.; Dawson T. M.; London E. D.; Bredt D. S.; Snyder S. H., *Proc. Natl. Acad. Sci. U.S.A.* **1991**, *88*, 6368.
- ³⁴³ Lipton S. A., et al., *Nature* **1993**, *364*, 626.
- ³⁴⁴ Nakamura T., Lipton S. A., *Cell Death and Differentiation* **2011**, *18*, 1478.
- ³⁴⁵ Tenneti L.; D'Emilia D. M.; Troy C. M.; Lipton S. A., *J. Neurochem.* **1998**, *71*, 946.
- ³⁴⁶ Budd S. L.; Tenneti L.; Lishnak T.; Lipton S. A., *Proc. Natl. Acad. Sci. U. S. A.* **2000**, *97*, 6161.
- ³⁴⁷ Okamoto S., et al., *Proc. Natl. Acad. Sci. U. S. A* **2002**, *99*, 3974.

-
- ³⁴⁸ Lipton S. A., *Nature* **2006**, 5, 160
- ³⁴⁹ Mattson M. P., et al., *J. Neurosci.* **1992**, 12, 376.
- ³⁵⁰ Furukawa K.; Mattson M. P., *Neuroscience* **1998**, 83, 429.
- ³⁵¹ Masliah E.; Raber J.; Alford M.; Mallory M.; Mattson M. P.; Yang D.; Wong D.; Mucke L., *J. Biol. Chem.* **1998**, 273, 12548.
- ³⁵² Wu J. Q.; Anwyl R.; Rowan M., *J. Neuroreport* **1995**, 6, 2409.
- ³⁵³ Harris M. E.; Wang Y. N.; Pedigo N. W.; Hensley K.; Butterfield D. A.; Carney J. M., *J. Neurochem.* **1996**, 67, 277.
- ³⁵⁴ Noda M.; Nakanishi H.; Akaike N., *Neurosci.* **1999**, 92, 1465.
- ³⁵⁵ Parsons C. G.; Stoffler A.; Danysz W., *Neuropharmacology* **2007**, 53 699.
- ³⁵⁶ Harkany T., et al., *Eur. J. Neurosci.* **2000**, 12, 2735.
- ³⁵⁷ Couratier P., et al., *Mol. Chem. Neuropathol.* **1996**, 27, 259.
- ³⁵⁸ Rogawski M. A., *Amino Acids* **2000**, 19, 133.
- ³⁵⁹ Palmer G. C., *Curr. Drug Targets* **2001**, 2, 241.
- ³⁶⁰ Reisberg B., et al., *N. Engl. J. Med.* **2003**, 348, 1333.
- ³⁶¹ George, S. R., O'Dowd, B. F. Lee, S. P., *Nature Rev. Drug Discov.* **2002**, 1, 808.
- ³⁶² Hollmann M.; Heinemann S., *Annu. Rev. Neurosci.* **1994**, 17, 31.
- ³⁶³ Conn P. J.; Pin J. P., *Annu. Rev. Pharmacol. Toxicol.* **1997**, 37, 205.
- ³⁶⁴ Pinheiro P. S., Mutle C., *Nature Neurosci.*, **2008**, 9, 423.
- ³⁶⁵ Schoepp D. D., *J. Pharmacol. Exp. Ther.* **2001**, 299, 12.
- ³⁶⁶ Iacovelli L.; Bruno V.; Salvatore L.; Melchiorri D.; Gradini R.; et al., *J. Neurochem.* **2002**, 82, 216.
- ³⁶⁷ Albasanz J. L.; Dalfo E.; Ferrer I.; Martin M., *Neurobiol. Dis.* **2005**, 20, 685.
- ³⁶⁸ Lee H. G.; et al., *Acta Neuropathol.* **2010**, 107, 365.
- ³⁶⁹ Lee H. G.; et al., *Brain Res.* **2009**, 1249, 244.
- ³⁷⁰ Kim S. H., et al., *J. Neurosci.* **2010**, 30, 3870.
- ³⁷¹ Younkin S. G., *J. Physiol. Paris* **1998**, 92, 289.
- ³⁷² Fryer J. D.; Holtzman D. M., *Neuron* **2005**, 47, 167.
- ³⁷³ Thathiah A.; De Strooper B., *Nature* **2011**, 12, 73.
- ³⁷⁴ Higgins G. A., et al., *Neuropharmacology* **2004**, 46, 907.

-
- ³⁷⁵ Ramirez M. J.; Aisa B.; Garcia-Alloza M.; Gil-Bea F. J.; Marcos B., *Curr. Psychiatry Rev.* **2005**, *1*, 337.
- ³⁷⁶ Medhurst A. D.; Lezoualc'h F.; Fischmeister R.; Middlemiss D. N.; Sanger G. J., *Brain Res. Mol. Brain Res.* **2001**, *90*, 125.
- ³⁷⁷ Reynolds, G. P., et al., *Br. J. Pharmacol.* **1995**, *114*, 993.
- ³⁷⁸ Robert S. J.; Zugaza J. L.; Fischmeister R.; Gardier A. M.; Lezoualc'h, F., *J. Biol. Chem.* **2001**, *276*, 44881.
- ³⁷⁹ Cachard-Chastel M., et al., *Br. J. Pharmacol.* **2007**, *150*, 883.
- ³⁸⁰ Bourson A.; Borroni E.; Austin R. H.; Monsma F. J.; Sleight A. J.; *J. Pharmacol. Exp. Ther.*, **1995**, *274*, 173.
- ³⁸¹ Meneses A., *Drug News Perspect* **2010**, *14*, 396.
- ³⁸² Hirst W. D.; Abrahamsen B.; Blaney F. E.; Calver A. R.; Aloj L.; Price G. W.; et al., *Mol. Pharmacol.* **2003**, *64*, 1295–1308.
- ³⁸³ Dawson L. A.; Nguyen H. Q.; Li P., *Br. J. Pharmacol.* **2000**, *130*, 2.
- ³⁸⁴ Russo-Neustadt A.; Cotman C. W., *J. Neurosci.* **1997**, *17*, 5573
- ³⁸⁵ Y. N.; Zhao X.; Bao G.; Zou L.; Teng L.; Wang Z.; Song M.; Xiong J.; Bai Y.; Pei G., *Nature* **2006**, *12*, 1390.
- ³⁸⁶ Wilson R. S.; et al., *Neurology* **2003**, *61*, 1479.
- ³⁸⁷ Ferry B.; Roozendaal B.; McGaugh J. L., *Psychiatry* **1999**, *46*, 1140.
- ³⁸⁸ Fuxe K.; Ferré S.; Genedani S.; Franco R.; Luigi F. Agnati L. F., *Physiology & Behavior* **2007**, *92*, 210.
- ³⁸⁹ Wang J. H.; Ma Y. Y. Van den Buuse M., *Exp. Neurol.* **2006**, *199*, 438.
- ³⁹⁰ Gimenez-Lort L.; et al., *Neurobiol. Learn. Mem.*, **2007**, *87*, 42.
- ³⁹¹ Maia L.; de Mendonça, A., *Eur J. Neurol.* **2002**, *9*, 377.
- ³⁹² Aredash G. W.; et al., *Neurosci.*, **2006**, *142*, 941.
- ³⁹³ Dall'Igna O. P.; Porciuncula L. O.; Souza D. O.; Cunha R. A.; Lara D. R., *Br. J. Pharmacol.* **2003**, *138*, 1207.
- ³⁹⁴ Dall'Igna O. P.; et al., *Exp. Neurol.* **2007**, *203*, 241.
- ³⁹⁵ *Nature Reviews-Drug Discovery*, **2007**, *6*, 692.
- ³⁹⁶ Anagnostaras S. G.; Murphy G. G.; Hamilton S. E.; Mitchell S. L.; Rahnama N. P.; Nathanson N. M.; Silva A. J., *Nat. Neurosci.* **2003**, *6*, 51.
- ³⁹⁷ Wess J., Eglen R. M. and Gautam D. *Nat. Rev. Drug Discov.* **2007**, *6*, 721.
- ³⁹⁸ C.J. Langmead, J. Watson, C. Reavill, *Pharmacol. Ther.* **2008**, *117*, 232-243.

-
- ³⁹⁹ Fisher A.; et al., *J. Molecular Neurosci.* **2003**, *20*, 349.
- ⁴⁰⁰ Heinrich J. N. et al., *Eur. J. Pharmacol.* **2009**, *605*, 53.
- ⁴⁰¹ Mirza N. R.; Peters D.; Sparks R. G., *CNS Drug Rev.* **2003**, *9*, 159.
- ⁴⁰² Eckols K.; Bymaster F. P.; Mitch C. H.; Shannon H. E.; Ward J. S.; Delapp N. W., *Life Sci.* **1995**, *57*, 1183.
- ⁴⁰³ Muller D. M.; Mendla K.; Farber S. A.; Nitsch R. M., *Life Sci.* **1997**, *60*, 985.
- ⁴⁰⁴ Hung A. Y.; Haass C.; Nitsch R.; Qiu W. Q.; Citron M.; Wurtmann R. J., *J. Biol. Chem.* **1993**, *268*, 22959.
- ⁴⁰⁵ Wolf B. A.; Wertkin A. M.; Jolly Y. C.; Yasuda R. O.; Wolfe B. B.; Konrad R. J. et al., *J. Biol. Chem.*, **1995**, *270*, 4916.
- ⁴⁰⁶ Haring R.; Fisher A.; Marciano D.; Pittel Z.; Kloog Y.; Zuckerman A.; et al., *J. Neurochem.* **1998**, *71*, 2094.
- ⁴⁰⁷ Buxbaum J.; Liu K. N.; Luo Y., Slack J.L.; Stocking K .L.; Peschon J. J.; Johnson R. S.; Castner B. J.; Cerretti D. P.; Black R. A., *Biol. Chem.* **1998**, *273*, 27765.
- ⁴⁰⁸ Vincent B.; Checler F., *Curr. Alzheimer Res.* **2012**, *9*, 140.
- ⁴⁰⁹ Cisse M.; et al., *Molecular and Cellular Neuroscience* **2011**, *47*, 223.
- ⁴¹⁰ Jiang S.; Wang Y.; Ma Q.; Zhou A.; Zhang X.; Zhang Y., *Neuroscience Letters* **2012**, *515*, 125.
- ⁴¹¹ Caccamo A.; Oddo S.; Billings L. M.; Green K. M.; Martinez-Coria H.; Fisher A.; LaFerla F. M., *Neuron* **2006**, *49*, 671.
- ⁴¹² Langmead C. J.; Watson J.; Reavill C., *Pharmacology & Therapeutics* **2008**, *117*, 232.
- ⁴¹³ Fisher A., *Exp. Opin. Invest. Drugs* **1997**, *6*, 1395.
- ⁴¹⁴ Fisher A., *CNS Drugs* **1999**, *12*, 197.
- ⁴¹⁵ Fisher A., *Neurotherapeutics* **2008**, *5*, 433.
- ⁴¹⁶ Fisher A., Brandeis R., Bar-Ner N., Kliger-Spatz M., Natan N., Sonogo H., Marcovitch I. Pittel Z., *J. Mol. Neurosci.* **2002**, *19*, 145.
- ⁴¹⁷ Nitsch R. M.; Deng M.; Tennis M.; Schoenfield D.; Growdon J. H., *Ann. Neurol.* **2000**, *48*, 913.
- ⁴¹⁸ Sadot E.; Gurwitz D.; Barg J.; Behar R.; Ginzburg I.; Fisher A., *J. Neurochem.* **1996**, *66*, 877.
- ⁴¹⁹ Forlenza O. V.; Spink J. M.; Dayanandan R.; Anderton B. H.; Olesen O. F.; Lovestone S., *J. Neural Transm.* **2000**, *107*, 1201.
- ⁴²⁰ Genis I.; Fisher A.; Michaelson D. M., *J. Neurochem.* **1999**, *12*, 206.
- ⁴²¹ Medeiros R.; Kitazawa M.; Caccamo A.; Baglietto-Vargas D.; Estrada-Hernandez T.; Cribbs D. H.; Fisher A.; Laferla F. M., *Am. J. Pathol.* **2011**, *179*, 980.
- ⁴²² Stork O.; Weizi H., *Cell Mol. Life Sci.* **1999**, *55*, 575.

-
- ⁴²³ Bonnie E. L.; David D. G., *Neuron* **2002**, *35*, 605.
- ⁴²⁴ Jones C. K., et al., *J. Neurosci.* **2008**, *28*, 10422.
- ⁴²⁵ Lebois E. P. et al., *ACS Chem. Neurosci.* **2010**, *1*, 104.
- ⁴²⁶ Spalding T.A.; Trotter C.; Skjaerbaek N.; Messier T. L.; Currier E. A.; Burstein E. S.; Li D.; Hacksell U.; Brann M.R., *Mol. Pharmacol.* **2002**, *61*, 1297.
- ⁴²⁷ Langmead C. J.; Fry V. A. H.; Forbes I. T.; Branch C. L.; Christopoulos A., Wood M. D.; Herdon H. J., *Mol. Pharmacol.* **2006**, *69*, 236.
- ⁴²⁸ Spaldin T. A. et al., *Mol. Pharmacol.* **2006**, *70*, 1974.
- ⁴²⁹ Hulme E. C.; Lu Z. L.; Bee M. S., *Receptors Channels* **2003**, *9*, 215.
- ⁴³⁰ Gether U., *Endocr. Rev.* **2000**, *21*, 90.
- ⁴³¹ Ward S. D.; Curtis C. A.; and Hulme E. C. *Mol. Pharmacol.* **1999**, *56*, 1031.
- ⁴³² Lu Z-L.; Saldanha J. W.; Hulme E. C., *J. Biol. Chem.* **2001**, *276*, 34098.
- ⁴³³ Christopoulos A.; Kenakin T., *Pharmacol. Rev.* **2002**, *54*, 323.
- ⁴³⁴ Christopoulos A., *Nat. Drug Rew.* **2002**, *1*, 198.
- ⁴³⁵ Kostenis E.; Mohr K., *Trends Pharmacol. Sci.* **1996**, *17*, 280.
- ⁴³⁶ Langmead C. J., et al., *Br. J. Pharmacol.* **2008**, *154*, 1104.
- ⁴³⁷ Vanover K. E.; Veinbergs I.; Davis R. E., *Behav. Neurosci.* **2008**, *122*, 570
- ⁴³⁸ Bradley S. R., et al., *Neuropharmacology* **2010**, *58*, 365.
- ⁴³⁹ Langmead C. J., et al., *Br. J. Pharmacol.* **2008**, *154*, 1104.
- ⁴⁴⁰ Avlani V. A.; Langmead C. J.; Guida E.; Wood M. D.; Tehan B. G.; Herdon H. J.M; Watson J. M.; Sexton P. M.; Christopoulos A.; *Mol. Pharmacol.* **2010**, *78*, 94.
- ⁴⁴¹ Langmead C. J.; Austin N. E.; Branch C. L.; Brown J. T.; Buchanan K. A.; Davies C. H.; Forbes I. T.; Fry V. A.; Hagan J. J., Herdon H. J.; Jones G. A.; Jeggo R.; Kew J. N., Mazzali A.; Melarange R.; Patel N.; Pardoe J.; Randall A. D.; Roberts C.; Roopun A., Starr K. R.; Teriakidis A.; Wood M. D.; Whittington M.; Wu Z.; Watson J., *Br. J. Pharmacol.* **2008**, *154*,
- ⁴⁴² Jones C. K. et al., *J. Neurosci.* **2006**, *31*, S116.
- ⁴⁴³ Bridges T. M.; Brady A. E.; Kennedy J. P.; Daniels R. N.; Millera N. R.; Kimc K.; Breiningera M. L.; Gentrya P. R.; Brogan J. T.; Jones C. K.; Conna P. J.; Lindsleya C. W., *Bioorg. Med. Chem. Lett.* **2008**, *18*, 5439.
- ⁴⁴⁴ Jones C. K., et al., *J Neurosci.* **2008**, *28*, 10422.
- ⁴⁴⁵ Jacobson M. A.; Kreatsoulas C.; Pascarella D. M.; O'Brien J. A.; Sur C., *Mol. Pharmacol.*, **2010**, *78*, 648.
- ⁴⁴⁶ Jacobson M. A.; Kreatsoulas C.; Pascarella D. M.; O'Brien J. A.; Sur C., *Mol. Pharmacol.*, **2010**, *78*, 648.

-
- ⁴⁴⁷ Marino M. J.; Rouse S. T.; Levey A. I.; Potter L. T.; Conn P. J., *Proc. Natl. Acad. Sci. U S A*, **1998**, *95*, 11465.
- ⁴⁴⁸ Ma L. et al., *PNAS*, **2009**, *15*, 15950.
- ⁴⁴⁹ Cavalli A.; Bolognesi M. L.; Minarini A.; Rosini M.; Tumiatti V.; Recanatini M.; Melchiorre C., *J. Med. Chem.* **2008**, *51*, 347.
- ⁴⁵⁰ Zimmermann G. R.; Lehar J.; Keith C. T., *Drug Discovery Today* **2007**, *12*, 34.
- ⁴⁵¹ Morphy R.; Rankovic Z., *Drug Discovery Today* **2007**, *12*, 156.
- ⁴⁵² Hopkins A. L., *Nat. Chem. Biol.* **2008**, *4*, 682.
- ⁴⁵³ Du D. M.; Carlier P. R. *Curr. Pharm. Des.* **2004** *10*, 3141–3156.
- ⁴⁵⁴ Munoz-Torrero, D.; Camps, P., *Curr. Med. Chem.* **2006**, *13*, 399–422.
- ⁴⁵⁵ Bolognesi, M. L.; Minarini, A.; Budriesi, R.; Cacciaguerra, S.; Chiarini, A.; Spampinato, S.; Tumiatti, V.; Melchiorre, C. *J. Med. Chem.* **1998**, *41*, 4150–4160.
- ⁴⁵⁶ Pang Y. P.; Quiram P.; Jelacic T.; Hong F.; Brimijoin S., *J. Biol. Chem.* **1996**, *271*, 23646.
- ⁴⁵⁷ Ros E.; Aleu J.; Gomez de Aranda I.; Canti C.; Pang Y. P.; Marsal J.; Solsona C., *J. Neurophysiol.* **2001**, *86*, 183.
- ⁴⁵⁸ Liu J.; Ho W.; Lee N. T.; Carlier P. R.; Pang Y.; Han Y., *Neurosci. Lett.* **2000**, *282*, 165.
- ⁴⁵⁹ Li W.; Pi R.; Chan H. H.; Fu H.; Lee N. T.; Tsang H. W.; Pu Y.; Chang D. C.; Li C.; Luo J.; Xiong K.; Li Z.; Xue H.; Carlier P. R.; Pang Y.; Tsim K. W.; Li M.; Han Y., *J. Biol. Chem.* **2005**, *280*, 18179.
- ⁴⁶⁰ Xiao X. Q.; Lee N. T.; Carlier P. R.; Pang Y.; Han Y. F., *Neurosci. Lett.* **2000**, *290*, 197.
- ⁴⁶¹ Bolognesi M. L.; Cavalli A.; Valgimigli L.; Bartolini M.; Rosini M.; Andrisano V.; Recanatini M.; Melchiorre C., *J. Med. Chem.* **2007**, *50*, 6446.
- ⁴⁶² Pang, Y. P.; Quiram, P.; Jelacic, T.; Hong, F.; Brimijoin, S. *J. Biol. Chem.* **1996**, *271*, 23646.
- ⁴⁶³ Rydberg, E. H.; Brumshtein, B.; Greenblatt, H. M.; Wong, D. M.; Shaya, D.; Williams, L. D.; Carlier, P. R.; Pang, Y. P.; Silman, I.; Sussman, J. L., *J. Med. Chem.* **2006**, *49*, 5491.
- ⁴⁶⁴ Fu H.; Li W.; Luo J.; Lee N. T.; Li M.; Tsim K. W.; Pang Y.; Youdim M. B.; Han Y., *Biochem. Biophys. Res. Commun.* **2008**, *366*, 631.
- ⁴⁶⁵ Piazzzi L.; Rampa A.; Bisi A.; Gobbi S.; Belluti F.; Cavalli A.; Bartolini M.; Andrisano V.; Valenti P.; Recanatini M., *J. Med. Chem.* **2003**, *46*, 2279.
- ⁴⁶⁶ Camps P.; Formosa X.; Galdeano C.; Gomez T.; Munoz-Torrero D.; Scarpellini M.; Viayna E.; Badia A.; Clos M. V.; Camins A.; Pallas M.; Bartolini M.; Mancini F.; Andrisano V.; Estelrich J.; Lizondo M.; Bidon-Chanal A.; Luque F. J., *J. Med. Chem.* **2008**, *51*, 3588–3598.
- ⁴⁶⁷ Melchiorre C.; Andrisano V.; Bolognesi M. L.; Budriesi R.; Cavalli A.; Cavrini V.; Rosini M.; Tumiatti V.; Recanatini M., *J. Med. Chem.* **1998**, *41*, 4186.
- ⁴⁶⁸ Melchiorre C.; Antonello A.; Banzi R.; Bolognesi M. L.; Minarini A.; Rosini M.; Tumiatti V., *Med. Res. Rev.*, **2003**, *23*, 200.

-
- ⁴⁶⁹ Munoz-Ruiz P., et al., *J. Med. Chem.* **2005**, *48*, 7223.
- ⁴⁷⁰ Gottfries C. G., *J. Neurosci. Res.* **1990**, *27*, 541.
- ⁴⁷¹ Meltzer C. C.; Smith G.; DeKosky S. T.; Pollock B. G.; Mathis C. A.; Moore R. Y.; Kupfer D. J.; Reynolds, C. F., *Neuropsychopharmacology* **1998**, *18*, 407.
- ⁴⁷² Edmondson D. E.; Mattevi A.; Binda C.; Li M.; Hubalek F., *Curr. Med. Chem.* **2004**, *11*, 1983.
- ⁴⁷³ Shih J. C.; Chen K., *Curr. Med. Chem.* **2004**, *11*, 1995.
- ⁴⁷⁴ Pisani L.; Catto M.; Leonetti F.; Nicolotti O.; Stefanachi A.; Campagna F.; Carotti A., *Current Medicinal Chemistry* **2011**, *18*, 4568.
- ⁴⁷⁵ Fink D. M.; Palermo M. G.; Bores G. M.; Huger F. P.; Kurys B. E.; Merriman M. C.; Olsen G. E.; Petko W.; O'Malley G. J. *Bioorg. Med. Chem. Lett.* **1996**, *6*, 625.
- ⁴⁷⁶ Sterling, J., et al., *J. Med. Chem.* **2002**, *45*, 5260.
- ⁴⁷⁷ Simoni E.; Daniele S.; Bottegoni G.; Pizzirani D.; Trincavelli M. L.; Goldoni L.; Tarozzo G.; Reggiani A.; Martini C.; Piomelli D.; Melchiorre C.; Rosini M.; Cavalli A., *J. Med. Chem.*, **2012**, *55*, 9708.
- ⁴⁷⁸ Bottegoni G.; Favia A. D.; Recanatini M.; Cavalli A., *Drug Discovery Today* **2012**, *17*, 23.
- ⁴⁷⁹ Rosini M.; Andrisano V.; Bartolini M.; Bolognesi M. L.; Hrelia P.; Minarini A.; Tarozzi A.; Melchiorre C., *J. Med. Chem.* **2005**, *48*, 1360.
- ⁴⁸⁰ Holmquist L.; Stuchbury G.; Berbaum K.; Muscat S.; Young S.; Hager K.; Engel J.; Munch G., *Pharmacol. Ther.* **2007**, *113*, 154–164.
- ⁴⁸¹ Fang L.; Kraus B.; Lehmann J.; Heilmann J.; Zhang Y.; Decker M., *Bioorg. Med. Chem. Lett.* **2008**, *18*, 2905.
- ⁴⁸² Davalos A.; Gomez-Cordoves C.; Bartolome B., *J. Agric. Food Chem.* **2004**, *52*, 48.
- ⁴⁸³ Cavalli A.; Bolognesi M. L.; Capsoni S.; Andrisano V.; Bartolini M.; Margotti E.; Cattaneo A.; Recanatini M.; Melchiorre C., *Angew. Chem., Int. Ed.* **2007**, *46*, 3689.
- ⁴⁸⁴ Pappu A. S.; Woltjer R. L.; Quinn J. F., *J. Alzheimer's Dis.* **2008**, *14*, 225.
- ⁴⁸⁵ Nesterov E. E.; Skoch J.; Hyman B. T.; Klunk W. E.; Bacskai B. J.; Swager T. M., *Angew. Chem. Int. Ed. Engl.*, **2005**, *44*, 5452.
- ⁴⁸⁶ Bolognesi M. L.; Andrisano V.; Bartolini M.; Banzi R.; Melchiorre C., *J. Med. Chem.* **2005**, *48*, 24.
- ⁴⁸⁷ Bolognesi M. L.; Cavalli A.; Melchiorre C., *Neurotherapeutics* **2009**, *6*, 152.
- ⁴⁸⁸ Capsoni S., Cattaneo A., *Cell. Mol. Neurobiol.* **2006**, *26*, 617.
- ⁴⁸⁹ Blennow K., et al., *Lancet* **2006**, *368*, 387.
- ⁴⁹⁰ Fisher A., *J. Neurochem.* **2012**, *120*, 22.
- ⁴⁹¹ Conn P. J.; Christopoulos A.; Lindsley C. W., *Nat. Rev. Drug Discov.* **2009**, *8*, 41.
- ⁴⁹² Gutzmann H.; Hadler D., *J. Neural. Transm. Suppl.* **1998**, *54*, 301.

-
- ⁴⁹³ Ono K.; Hasegawa K.; Naiki H.; Yamada M. *Biochem. Biophys. Res. Commun.* **2005**, *330*, 111.
- ⁴⁹⁴ Tomiyama T.; Shoji A.; Kataoka K.; Suwa Y.; Asano S.; Kaneko H.; Endo N., *J. Biol. Chem.* **1996**, *271*, 6839.
- ⁴⁹⁵ Bermejo-Bescos P.; Martin-Aragon S.; Jimenez-Aliaga K. L.; Ortega A.; Molina M. T.; Buxaderas E.; Orellana G.; Csaky A. G., *Biophys. Res. Commun.* **2010**, *400*, 169.
- ⁴⁹⁶ Bolognesi M. L.; Banzi R.; Bartolini M.; Cavalli A.; Tarozzi A.; Andrisano V.; Minarini A.; Rosini M.; Tumiatti V.; Bergamini C.; Fato R.; Lenaz G.; Hrelia P.; Cattaneo A.; Recanatini M.; Melchiorre C., *J. Med. Chem.* **2007**, *50*, 4882.
- ⁴⁹⁷ Bolognesi M. L.; Chiriano G.; Bartolini M.; Mancini F.; Bottegoni G.; Maestri V.; Czvitkovich S.; Windisch M.; Cavalli A.; Minarini A.; Rosini M.; Tumiatti V.; Andrisano V.; Melchiorre C., *J. Med. Chem.* **2011**, *54*, 8299.
- ⁴⁹⁸ Craig P. N., *J. Med. Chem.* **1971**, *14*, 680.
- ⁴⁹⁹ Morin C.; Besset T Moutet J.; Fayolle M.; Bruckner M.; Limosin D.; Becker K.; Davioud-Charvet E., *Org. Biomol. Chem.* **2008**, *6*, 2731.
- ⁵⁰⁰ Yoshida K.; Ishiguro M., Honda H.; Yamamoto M.; Kubo Y.; *Bull. Chem. Soc. Jpn.* **1988**, *61*, 4335.
- ⁵⁰¹ Y. T. Pratt, *J. Org. Chem.* **1962**, *27*, 3905.
- ⁵⁰² Schmidt A.; Shilabin A. G.; Nieger M., *Org. Biomol. Chem.* **2003**, *1*, 4342.
- ⁵⁰³ Freeman S. K.; Spoerri P. E., *J. Org. Chem.* **1951**, *16*, 438.
- ⁵⁰⁴ Kitahara Y.; Nakahara S.; Tanaka Y.; Kubo A., *Heterocycles* **1992**, *34*, 1623.
- ⁵⁰⁵ Andrews K. J. M.; Marrian D. H.; Maxwell D. R., *J. Chem. Soc.* **1956**, 1844.
- ⁵⁰⁶ Thomas R. L., Mistry R., , Langmead C. J.; Wood M. D.; Challiss R. A. *The Journal of Pharmacology and Experimental Therapeutics*, **2008**, *327*, 365.
- ⁵⁰⁷ Burford N. T.; Nahorski S. R., *Biochem. J.*, **1996**, *315*, 883.
- ⁵⁰⁸ Christopoulos A.; Kenakin T., *Pharmacological Review*, **2002**, *54*, 323.
- ⁵⁰⁹ Diamant S.; Podoly E.; Friedler A.; Ligumsky H.; Livnah O.; Sore Q., *Proc. Natl. Acad. Sci. U.S.A.*, **2006**, *103*, 8628.
- ⁵¹⁰ Bolognesi M. L.; Chiriano G.; Bartolini M.; Mancini F.; Bottegoni G.; Maestri V.; Czvitkovich S.; Windisch M.; Cavalli A.; Minarini A.; Rosini M.; Tumiatti V.; Andrisano V.; Melchiorre C., *J. Med. Chem.*, **2011**, *54*, 8299.
- ⁵¹¹ Mordente, A.; Martorana, G. E.; Minotti, G.; Giardina, B., *Chem. Res. Toxicol.* **1998**, *11*, 54-63.
- ⁵¹² Moreira P. I.; Siedlak S. L.; Aliev G.; Zhu X., Cash A. D., Smith M. A., et al., *J. Neural. Transm.* **2005**, *112*, 921-932.
- ⁵¹³ Ellman, G. L.; Courtney, K. D.; Andres, V., Jr.; Feather-Stone, R. M. *Biochem. Pharmacol.* **1961**, *7*, 88-95

-
- ⁵¹⁴ McNeal J. G., *Monogr. Urol.* **1983**, 4, 3.
- ⁵¹⁵ Wasserman N. F., *Radiol. Clin. North Am.* **2006**, 44, 689.
- ⁵¹⁶ Ochiai A.; Fritsche H. A.; Babaian R. J., *Urology* **2005**, 66, 819.
- ⁵¹⁷ Parsons J. K.; Carter H. B.; Partin A. W.; Windham B. G.; Metter E. J.; Ferrucci L.; et al., *J. Clin. Endocrinol. Metab.* **2006**, 91, 2562.
- ⁵¹⁸ Ozden C.; Ozdal O. L., Urgancioglu G.; Koyuncu H.; Gokkaya S.; Memis A., *Eur. Urol.* **2007**, 51, 199.
- ⁵¹⁹ Vikram A.; Jena G. B.; Ramarao P., *Prostate* **2010**, 70, 79.
- ⁵²⁰ Chan J. M.; Stampfer M. J.; Giovannucci E.; Gann P. H.; Ma J.; Wilkinson P., et al., *Science* **1998**, 279, 563.
- ⁵²¹ Barnard R. J, Aronson W. J.; Tymchuk C. N.; Ngo T. H., *Obes. Rev.* **2002**, 3, 303.
- ⁵²² Kristal A. R.; Arnold K. B.; Schenk J. M.; Neuhouser M. L.; Goodman P.; Penson D. F.; et al., *Am. J. Epidemiol.* **2008**, 167, 925.
- ⁵²³ Platz E. A.; Kawachi I.; Rimm E. B.; Colditz G. A.; Stampfer M. J.; Willett W. C.; et al., *Arch. Intern. Med.* **1998**, 158, 2349.
- ⁵²⁴ Nickel J. C.; Roehrborn C. G.; O'leary M. P.; Bostwick D. G.; Somerville M. C.; Rittmaster R. S., *J. Urol.* **2008**, 54, 1379.
- ⁵²⁵ Di Silverio F.; Gentile V.; De Matteis A.; Mariotti G., Giuseppe V., Luigi P. A., et al., *Eur. Urol.* **2003**, 43, 164.
- ⁵²⁶ Kramer G.; Steiner G. E.; Handisurya A., Stix U.; Haitel A.; Knerer B., et al., *Prostate* **2002**, 52, 43.
- ⁵²⁷ Schwinn D. A.; Roehrborn C. G., *Int. J. Urol.* **2008**;15, 193.
- ⁵²⁸ Murata S.; Taniguchi T.; Takahashi M.; Okada K.; Akiyama K.; Muramatsu I., *J. Urol.* **2000**, 164, 578.
- ⁵²⁹ Matyus P.; Horvath, K.; *Med. Res. Rev.* **1997**, 17, 523-535.
- ⁵³⁰ Cooper K. L.; McKiernan J. M.; Kaplan S. A., *Drugs* **1999**, 57, 9-17.
- ⁵³¹ Lepor H.; Tang R.; Meretyk S.; Shapiro E., *J. Urol.* **1993**, 149, 640.
- ⁵³² Forray C.; Bard J. A.; Wetzel J. M., et al., *Mol. Pharmacol.* **1994**, 45, 703–708.
- ⁵³³ Cavalli A. et al., *Proc. Natl. Acad. Sci. U.S.A.* **1997**, 94, 11589-94
- ⁵³⁴ Andersson, K.-E., *World J. Urolog.* **2002**, 19, 390.
- ⁵³⁵ Thiyagarajan M., *Pharmacology* **2002**, 65, 119.
- ⁵³⁶ Lepor H.; Kazzazi A.; Djavan B., *Curr. Opin. Urol.*, **2012**, 22, 7.
- ⁵³⁷ Bolognesi, M. L.; Marucci G.; Angeli P.; Buccioni M.; Minarini A.; Rosini M.; Tumiatti V.; Melchiorre C., *J. Med. Chem.* **2001**, 44, 362.

-
- ⁵³⁸ Bolognesi M. L.; Budriesi R.; Chiarini A.; Poggesi E.; Leonardi A.; Melchiorre C., *J. Med. Chem.* **1998**, *41*, 4844.
- ⁵³⁹ Giardina` D.; Brasili L.; Gregori M.; Massi M.; Picchio M. T.; Quaglia W.; Melchiorre C., *J. Med. Chem.* **1989**, *32*, 690.
- ⁵⁴⁰ Giardina` D.; Giulini U.; Massi M.; Piloni M. G.; Pompei P.; Rafaiiani G.; Melchiorre C., *J. Med. Chem.* **1993**, *36*, 50-55.
- ⁵⁴¹ Melchiorre C., *Trends Pharmacol. Sci.* **1981**, *2*, 209.
- ⁵⁴² Antonello A.; Hrelia P.; Leonardi A.; Marucci G.; Rosini M.; Tarozzi A.; Tumiatti V.; Melchiorre C., *J. Med. Chem.* **2005**, *48*, 28-31.
- ⁵⁴³ Campbell S. F.; Davey M. J.; Hardstone J. D.; Lewis B. N.; Palmer M. J., *J. Med. Chem.* **1987**, *30*, 49-57.
- ⁵⁴⁴ Bordner J.; Campbell S. F.; Palmer M. J.; Tute M. S., *J. Med. Chem.* **1988**, *31*, 1036-39.
- ⁵⁴⁵ Ishiguro M., et al., *Life Science* **2002**, *71*, 2531.
- ⁵⁴⁶ Hu Z. W.; Shi X. Y.; Hoffman B. B., *J. Cardiovasc. Pharmacol.* **1998**, *31*, 833.
- ⁵⁴⁷ Kyprianou N.; Benning C. M., *Cancer Res.* **2000**, *60*, 4550.
- ⁵⁴⁸ Benning C. M.; Kyprianou N., *Cancer Res.* **2002**, *62*, 597.
- ⁵⁴⁹ Kyprianou N., *The Journal of Urology* **2003**, *169*, 1520.
- ⁵⁵⁰ Wrana J. L., et al., *Nature* **1994**, *370*, 341.
- ⁵⁵¹ Kyprianou N.; Isaacs J. T., *Mol. Endocrinol.* **1989**, *3*, 1515.
- ⁵⁵² Martikainen P.; Kyprianou N.; Isaacs J. T., *Endocrinology* **1990**, *127*, 2963.
- ⁵⁵³ Anglin I. E.; D. T. Glassman D. T.; Kyprianou N., *Prostate Cancer and Prostatic Diseases* **2002**, *5*, 88.
- ⁵⁵⁴ Glassman D. T., et al., *The Prostate* **2001**, *46*, 45.
- ⁵⁵⁵ Garrison J. B.; Shaw Y.-J.; Chen C.-S.; Kyprianou N., *Cancer Res.* **2007**, *67*, 11344.
- ⁵⁵⁶ Giardinà D.; Crucianelli M.; Melchiorre C.; Taddei C.; Testa R., *Eur. J. Pharmacol.* **1995**, *287*, 13.
- ⁵⁵⁷ Giardinà D.; Martarelli D.; Sagratini G.; Angeli P.; Ballinari D.; Gulini G.; Melchiorre C.; Poggesi E.; Pompei P., *J. Med. Chem.* **2009**, *52*, 4951.
- ⁵⁵⁸ Tatemichi S.; Kobayashi K.; Maezawa A. et al., *Yakugaku Zasshi.* **2006**, *126*, 209–216.
- ⁵⁵⁹ Lopor H.; Hill L. A., *Pharmacotherapy*, **2010**, *30*, 1303.
- ⁵⁶⁰ Muramatsu I.; Takita M.; Suzuki F.; Miyamoto S.; Sakamoto S.; Ohmura T., *Eur. J. Pharmacol.*, **1996**, *300*, 155.
- ⁵⁶¹ Melchiorre C.; Belleau B. *Adrenoceptors and Catecholamine Action*, Part A; Kunos, G., Ed.; Wiley: New York, **1981**; pp 131-179.
- ⁵⁶² Melchiorre C.; Brasili L.; Giardina` D.; Pigni M.; Strappaghetti G., *J. Med. Chem.* **1984**, *27*, 1535.

-
- ⁵⁶³ Pignini M.; Brasili L.; Giannella M.; Giardina` D.; Gulini U.; Quaglia W.; Melchiorre C., *J. Med. Chem.* **1988**, *31*, 2300.
- ⁵⁶⁴ Quaglia W.; Pignini M.; Piergentili A.; Giannella M.; Gentili F.; Marucci G.; Carrieri A.; Carotti A.; Poggesi E.; Leonardi A.; Melchiorre C., *J. Med. Chem.* **2002**, *45*, 1633.
- ⁵⁶⁵ Archibald J. L.; Alps B. J.; Cavalla J. F.; Jackson J. L., *J. Med. Chem.* **1971**, *14*, 1054.
- ⁵⁶⁶ Kenny B.; Ballard S.; Blagg J.; Fox D., *J. Med. Chem.* **1997**, *40*, 1298.
- ⁵⁶⁷ Wetzel J. M.; Miao S. W.; Forray C.; Borden L. A.; Branchek T. A.; Gluchowski C., *J. Med. Chem.* **1995**, *38*, 1579.
- ⁵⁶⁸ Nagarathnam D.; Wetzel J. M.; Miao S. W.; Marzabadi M. R.; Chiu G.; Wong W. C.; Hong X.; Fang J.; Forray C.; Branchek T. A.; Heydorn W. E.; Chang R. S. L.; Broten T.; Schorn T.; Gluchowski C., *J. Med. Chem.* **1998**, *41*, 5320.
- ⁵⁶⁹ Nagarathnam D., *J. Med. Chem.* **1999**, *42*, 4764.
- ⁵⁷⁰ Kulig K.; Malawska B., *Current Medicinal Chemistry* **2006**, *13*, 3395.
- ⁵⁷¹ Doggrel S.A., *Drugs Fut.*, **2002**, *27*, 973.
- ⁵⁷² Tian G.; Mook R.A. Jr.; Moss M. L.; Frye, S. V., *Biochemistry* **1995**, *34*, 13453.
- ⁵⁷³ Rabasseda X. *rugs Today* **2004**, *40*, 649.
- ⁵⁷⁴ Roehrborn C.G.; Boyle P.; Nickel J. C.; Hoefner K.; Andriole G. *Urology* **2002**, *60*, 434
- ⁵⁷⁵ Ziada A.; Rosenblum M.; Crawford E. D., *Urology* **1999**, *53*, 1.
- ⁵⁷⁶ Lepor H. In: Lepor H, editor. Prostatic diseases. Philadelphia, PA:WB Saunders; **2000**. pp. 163–196.
- ⁵⁷⁷ Sarma A. V.; Wei J. T., *N. Engl. J. Med.* **2012**, *367*, 248-57.
- ⁵⁷⁸ Marberger M., *Nature Reviews Urology* **2006**, *3*, 495.
- ⁵⁷⁹ Lepor H. In Lepor H, editor. Prostatic diseases. Philadelphia, PA:WB Saunders; 2000. pp. 297–307.
- ⁵⁸⁰ Eri L. M.; Tveter J. K., *J. Urol.* **1995**, *154*, 923-3.
- ⁵⁸¹ Hieble J. P., *Pharm. Acta Helv*, **2000**, *74*, 163-171.
- ⁵⁸² Bolognesi M. L.; Marucci G.; Angeli P.; Buccioni M.; Minarini A.; Rosini M.; Tumiatti V.; Melchiorre C., *J. Med. Chem.* **2001**, *44*, 362-71.
- ⁵⁸³ Rosini M.; Antonello A.; Cavalli A.; Bolognesi M. L.; Minarini A.; Marucci G.; Poggesi, E.; Leonardi A.; Melchiorre C., *J. Med. Chem.*, **2003**, *46*, 4895-4903.
- ⁵⁸⁴ Minarini A.; Budriesi R.; Chiarini A.; Leonardi A.; Melchiorre C., *Bioorg. Med. Chem. Lett.* **1998**, *8*, 1353-58
- ⁵⁸⁵ Giardina` D.; Brasili L.; Gregori M.; Massi M.; Picchio M. T.; Quaglia W.; Melchiorre C., *J. Med. Chem.*, **1989**, *32*, 50-55.

-
- ⁵⁸⁶ Giardina` D.; Gulini U.; Massi M.; Piloni M. G.; Pompei P.; Rafaiani G.; Melchiorre C. *J. Med. Chem.*, **1993**, 36, 690.
- ⁵⁸⁷ Giardina` D.; Crucianelli M.; Melchiorre C.; Taddei C.; Testa, R. *Eur. J. Pharmacol.* **1995**, 287, 13.
- ⁵⁸⁸ Giardina` D.; Crucianelli M.; Romanelli R.; Leonardi A.; Poggesi E.; Melchiorre C., *J. Med. Chem.* **1996**, 39, 4602-4607.
- ⁵⁸⁹ Tian H.-L.; Zhao D.; Ren L.-M.; Su X.-H.; Kang Y.-H., *The American Journal of the Medical Sciences* **2009**, 338, 196.
- ⁵⁹⁰ Hatano A.; Tang R., Walden P. D., Lepor H., *European Journal of Pharmacology*, **1996**, 313, 135.
- ⁵⁹¹ Ma S.-P.; Ren L.-M.; Zhao D.; Zhu Z.-N.; Wang M.; Lu H.-G.; Duan L.-H., *Acta Pharmacologica Sinica* **2006**, 27, 1423.
- ⁵⁹² Althuis T. H.; Hess H. J., *J. Med. Chem.* **1977**, 20, 146.
- ⁵⁹³ . Campbell S. F.; Hardstone J. D.; Palmer M. J.; *J. Med. Chem.*, **1988**, 31, 1031.
- ⁵⁹⁴ Cheng Y. C.; Prusoff W. H., *Biochem. Pharmacol.* **1973**, 22, 3099-3108.
- ⁵⁹⁵ Testa R.; Taddei C.; Poggesi E.; Destefani C.; Cotecchia S.; Hieble J. P.; Sulpizio A. C.; Naselsky D.; Bergsma D.; Ellis S.; Swift A.; Ganguly S.; Ruffolo R. R.; Leonardi A., *Pharmacol. Comm.* **1995**, 6, 79.
- ⁵⁹⁶ DeLean A.; Munson, P. J.; Rodbard D., *Am. J. Physiol.* **1978**, 235, E97-102.
- ⁵⁹⁷ Hulme, C. in *Multicomponent Reaction*, Zhu J.; Bienaymè H., Eds.; Wiley-VCH: Weinheim **2005**
- ⁵⁹⁸ M. Passerini, *Gazz. Chim. Ital.* **1922**, 51, 755
- ⁵⁹⁹ M. Passerini, *Gazz. Chim. Ital.* **1921**, 51, 181
- ⁶⁰⁰ Owens T. D.; Araldi G. L.; Nutt R. F. Semple, J. E., *Tetrahedon Lett.* **2001**, 42, 6271.
- ⁶⁰¹ A. Strecker, *Liebigs Ann. Chem.* **1850**, 75, 27.
- ⁶⁰² Robinson R., *J. Chem. Soc. (London)* **1917**, 111, 876.
- ⁶⁰³ Mondal N.; Mandal S. C.; Das C. K.; Mukherjee S., *J. Chem. Research* **2003**, 580.
- ⁶⁰⁴ A. Hantzsch, *Justus Liebigs Ann. Chem.* **1882**, 215, 1.
- ⁶⁰⁵ a) Bergs H., DE-B 566,094 **1929**
- b) Bucherer T.; Barsch H., *J. Prakt. Chem.* **1934**, 140, 151.
- ⁶⁰⁶ Ugi I., *Angew. Chem. Int. Ed.* **1962**, 74, 9.
- ⁶⁰⁷ Ugi I.; Werner B.; Dominglo A., *Molecules* **2003**, 8, 53.
- ⁶⁰⁸ Ugi, I., *Pure & Appl. Chem.* **2001**, 73, 187.
- ⁶⁰⁹ Ugi I.; Heck S., *Comb. Chem. High T. Scr.* **2001**, 4, 1.
- ⁶¹⁰ Mumm O., *Chem. Dstch. Chem. Ges.* **1910**, 43, 886.

-
- ⁶¹¹ Armstrong R. W.; Combs A. P.; Tempest P. A.; Brown S. D.; Keating T.A., *Acc. Chem. Res.* **1996**, *29*, 123.
- ⁶¹² Weber L., *Curr. Med. Chem.* **2002**, *9*, 1241.
- ⁶¹³ Hulme C.; Gore V., *Curr. Med. Chem.* **2003**, *10*, 51.
- ⁶¹⁴ Giovenzana G. B.; Tron G. C.; Di Paola S.; Menegotto I. G.; Pirali T., *Angew. Chem. Int. Ed.* **2006**, *45*, 1099.
- ⁶¹⁵ Itho Y.; Kato H.; Oshinaka E. K.; Ogawa N.; Urata S. K.; Yamagishi K., US 4478838, **1984**.
- ⁶¹⁶ Diorazio L. J.; Motherwell W. B.; Sheppard T. D.; Waller R. W., *Synlett* **2006**, *14*, 2281-2283
- ⁶¹⁷ Waller R. W.; Diorazio L. J.; Taylor B. A.; Motherwell, W. B.; Sheppard T. D., *Tetrahedron* **2010**, *66*, 6496.
- ⁶¹⁸ Bachman M.; Mann S. E.; Sheppard T. D., *Organic Biomolecular Chemistry* **2012**, *10*, 162.
- ⁶¹⁹ Tanaka Y.; Tomoaki A.; Sugimone M., *Org. Lett.* **2007**, *22*, 4407.
- ⁶²⁰ Tanaka Y.; Hidaka K.; Hasui T.; Suginome M., *Eur. J. Org. Chem.* **2009**, 2009, 1148.
- ⁶²¹ Teimouri M. B.; Khavasi H. R., *Tetrahedron* **2007**, *63*, 1026.
- ⁶²² a) Tisler, M. *Advances in Heterocyclic Chemistry*; Katritzky, A. R., Ed.; *Heterocyclic Quinones*; Academic: London, **1989**; Vol. 45, p 37.
- b) Ito C.; Katsuno S.; Kondo Y.; Tan H. T.-W.; Furukawa H., *Chem. Pharm. Bull.* **2000**, *48*, 3331.
- ⁶²³ a) Rom, J.; Joseph-Nathan, P., *Tetrahedron* **1964**, *20*, 2331.
- b) Correa J.; Romo J., *Tetrahedron*, **1966**, *22*, 685.
- c) Kakisawa H.; Inouye Y.; Romo J., *Tetrahedron Lett.* **1969**, *10*, 1929..
- ⁶²⁴ Thomson R. H., *Naturally Occurring Quinones III: Recent Advances*; Chapman and Hall: London, New York, NY, **1987**.
- ⁶²⁵ Nair V.; Vinod A. U.; Nair J. S.; Sreekanth A. R.; Nigam P. N. P., *Tetrahedron Letters* **2000**, *41*, 6675.
- ⁶²⁶ Josien H.; Ko S. B.; Bom D.; Curran D. P., *Chem Eur. J.* **1998**, *4*, 67
- ⁶²⁷ van Leusen. *Org. React.* **2003**, *7*.
- ⁶²⁸ Tumanov V. V.; Tishkov A. A.; Mayr H., *Angew. Chem. Int. Ed.* **2007**, *46*, 3563.
- ⁶²⁹ Scheuer, P. J., *Acc. Chem. Res.* **1992**, *25*, 433
- ⁶³⁰ van Leusen; van Leusen. *Org. React.* **2003**, *7*.
- ⁶³¹ Giblin, G. M. P.; Hall, A.; Lewell, X. Q.; Miller, N. D WO 2004083185.
- ⁶³² Nishizawa R.; Takaoka Y.; Shibayama S., WO 2004080966.
- ⁶³³ Banfi L.; Guanti G; Riva R. *Chem. Commun.* **2000**, 985.

-
- ⁶³⁴ Semple E.; Owens T. D.; Nguyen K.; Levy O. E., *Org. Lett.* **2000**, 2, 2769.
- ⁶³⁵ a) Evans B. E.; Rittle K. E.; Bock M. G.; Bennett C. D.; DiPardo R. M.; Boger J.; Poe M.; Ulm E. H.; LaMont B. I.; Blaine E. H.; Fanelli G. M.; Stabilito I. I; Veber D. F., *J. Med. Chem.* **1985**, 28, 1756,
- b) Mimoto T.; Imai J.; Tanaka S.; Hattori N.; Kisanuki S.; Akaji K.; Kiso Y, *Chem. Pharm. Bull.*, **1991**, 39, 3088.
- ⁶³⁶ a) Li Z.; Ortega-Vilain A. C.; Patil G. S.; Chu D. L.; Foreman J. E.; Eveleth D. D.; Powers J. C., *J. Med. Chem.* **1996**, 39, 4089.
- b) Cacciola J.; Alexander R. S.; Fevig J. M.; Stouten P. F. W., *Tetrahedron Lett.* **1997**, 38, 5741.
- c) Harbeson S. L.; Abelleira S. M.; Akiyama A.; Barrett R.; Carroll R. M.; Straub J. A.; Tkacz J. N.; Wu C.; Musso G. F., *J. Med. Chem.*, **1994**, 37, 2918
- ⁶³⁷ Yehia, N. A. M.; Antuch, W.; Beck, B.; Hess, S.; Schauer- Vukasinovic, V.; Almstetter, M.; Furer, P.; Herdtweck, E.; Domling, A., *Bioorg. Med. Chem. Lett.* **2004**, 14, 3121.
- ⁶³⁸ a) Parks D. J.; LaFrance L. V.; Calvo R. R.; Milkiewicz, K. L.; Gupta V.; Lattanze J.; Ramachandren K.; Carver T. E.; Petrella E. C.; Cummings M. D.; Maguire, D.; Grasberger B. L.; Lu, T., *Bioorg. Med. Chem. Lett.* **2005**, 15, 765.
- b) Grasberger B. L.; Lu, T.; Schubert C.; Parks D. J.; Carver T. E.; Koblisch H. K.; Cummings M. D.; LaFrance L. V.; Milkiewicz K. L.; Calvo R. R.; Maguire D.; Lattanze J.; Franks C. F.; Zhao S.; Ramachandren K.; Bylebyl G. R.; Zhang M.; Manthey C. L.; Petrella E. C.; Pantoliano M. W.; Deckman I. C.; Spurlino J. C.; Maroney A. C.; Tomczuk B. E.; Molloy C. J.; Bone R. F. *J. Med. Chem.* **2005**, 48, 909.
- ⁶³⁹ Parks, D. J.; LaFrance, L. V.; Calvo, R. R.; Milkiewicz, K. L.; Gupta, V.; Lattanze, J.; Ramachandren, K.; Carver, T. E.; Petrella, E. C.; Cummings, M. D.; Maguire, D.; Grasberger, B. L.; Lu, T. *Bioorg. Med. Chem. Lett.* **2005**, 15, 765
- ⁶⁴⁰ a) Allinger N. L.; Tribble M. T. ; Miller M. A.; Wertz D. H., *J Am. Chem Soc.* **1971**, 93, 1637.
- b) Galli C.; Mandolini L., *Eur. J. Org. Chem.* **2000**, 3117.
- c) Illuminati G.; Mandolini L., *Acc. Chem. Res.* **1981**, 14, 95.
- d) Molander G. A., *Acc. Chem. Res.*, **1998**, 31, 603.
- ⁶⁴¹ List B.; Pojarliev P.; Castello C., *Org. Lett.* **2000**, 122, 2395.
- ⁶⁴² Mase N.; Tanaka F.; Barbas C. F., *Org. Lett.* **2008**, 23, 4369.
- ⁶⁴³ Escalante J.; Carillo-Morales M.; Linzaga I., *Molecules* **2008**, 13, 340.
- ⁶⁴⁴ Zhou Y.; Xiao Y.; Li D.; Fu M.; Qian X., *J. Org. Chem.* **2008**, 73, 1571.
- ⁶⁴⁵ Berube D.; Lessard J., *Canadian Journal of Chemistry* **1982**, 60, 1127.
- ⁶⁴⁶ Motherwell A. B.; Bégis G.; Cladingboel D. E.; Jerome L.; Sheppard T. D., *Tetrahedron* **2007**, 63, 6462.
- ⁶⁴⁷ Taub D.; Girotra N. N.; Hoffsommer R. D. ; Kuo C.H.; Slates H. L.; Weber S.; Wendler N. L.; *Tetrahedron*, **1068**, 24, 2443.